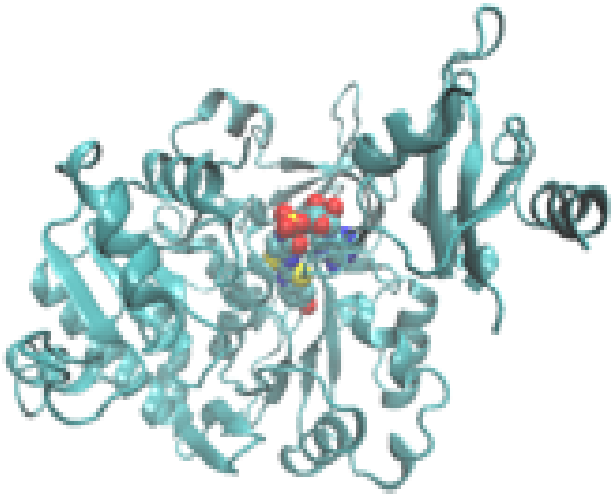

Investigation of the Firefly Bioluminescent System for the Development of *in vivo* and *in vitro* Applications

Luís Pinto da Silva
Programa Doutoral em Química
Departamento de Química e Bioquímica
2016

Orientador
Joaquim C.G. Esteves da Silva, Professor Catedrático, Faculdade de Ciências

This work was supported by a Ph.D. scholarship with the reference SFRH/BD/76612/2011, co-funded by the European Social Fund (*Fundo Social Europeu*, FSE), through *Programa Operacional Potencial Humano – Quadro de Referência Estratégico Nacional (POPH – QREN*), and by national funds from the Ministry of Education and Science through the Portuguese *Fundação para a Ciência e a Tecnologia, I.P.* (FCT).

Agradecimentos

A realização dos trabalhos que levaram a esta tese de doutoramento não teria sido possível sem a colaboração e o apoio de várias pessoas e instituições. Desta forma gostaria de expressar o meu sincero agradecimento:

Ao meu orientador Professor Doutor Joaquim C.G. Esteves da Silva, pela oportunidade, pelo apoio e por todo o conhecimento que me transmitiu, não só durante o doutoramento mas desde 2008 (quando no seu grupo comecei o meu estágio de licenciatura).

A todos os colegas do laboratório 2.30 agradeço a ajuda, e especialmente, o ótimo ambiente que se viveu nestes últimos anos. Diana Crista, Paulo Oliveira, Bruno Campos, João Vieira, Joel Santos, Dilson Pereira, Pedro Araújo, Teresa Castro, Mariana Sá e Margarida Miranda, a todos um muito obrigado.

Ao Professor Doutor Dan Huppert e seu grupo de investigação, da Universidade de Telavive, pela muito interessante colaboração e por nos ter aberto a porta ao fascinante mundo dos fotoácidos.

À Faculdade de Ciências da Universidade do Porto, em especial ao Departamento de Química e Bioquímica, assim como ao Centro de Investigação em Química (CIQUP) por serem responsáveis pelo meu crescimento científico e académico.

À Fundação para a Ciência e Tecnologia (FCT) pelo apoio financeiro concedido através de uma bolsa de doutoramento (SFRH/BD/76612/2011).

Por fim, um agradecimento muito especial à Isabel pelo apoio e amor incondicional em todos estes anos. Por estares sempre presente, tanto nos bons momentos como naquelas alturas em que tudo parecia (ou eu achava que) correr mal. Sem ti, tudo seria mais dificil e sem graça.

Resumo

A emissão de luz por parte de um organismo vivo é um dos fenómenos da natureza mais bonitos e fascinantes. Este processo foi chamado de bioluminescência e resulta geralmente de uma reação de oxidação de um substrato, luciferina, catalisado por uma enzima, luciferase. O sistema bioluminescente mais conhecido e estudado é aquele dos pirilampos. Este sistema consiste uma reação de dois passos: numa primeira fase, a luciferase catalisa uma adenilação entre a luciferina e a adenosina-5'-trifosfato (ATP), na presença de Mg^{2+}, dando origem ao luciferil-adenilado; no segundo passo reacional, o adenilado é oxidado na presença de oxigénio molecular, o que resulta na formação de um intermediário com um conteúdo altamente energético, a dioxetanona do pirilampo. É a decomposição deste intermediário que leva à formação do emissor de luz, oxiluciferina, já num estado excitado.

Devido a propriedades muito desejáveis (alto rendimento, dependência por ATP, simplicidade e alta sensibilidade analítica), a reação bioluminescente do pirilampo tem ganho muitas aplicações nas áreas de medicina, bioanálise e farmacêutica. Mais especificamente, tem sido usada para a deteção de analitos como ATP, como gene repórter e em bioimagem, entre outros. No entanto, este sistema bioluminescente apresenta alguns constrangimentos que impedem o seu uso em novas aplicações, ou um uso mais eficaz em aplicações já existentes.

A alta K_m do ATP e a formação de produtos inibitórios, que criam um perfil de luz emitida de tipo *flash*, limitam a sensibilidade analítica desta reação. Para além disso, a luz emitida tem um comprimento máximo na zona do verde no espectro visível, quando os fotodetectores usados em ensaios *in vitro* são mais sensíveis na zona do azul. Os ensaios *in vivo* também estão associados a limitações, pois os tecidos e células absorbem fortemente na zona do verde, pelo que seria mais benéfico a luz emitida numa reação bioluminescente ter um máximo na zona do vermelho.

Vários grupos têm tentado ultrapassar estes problemas ao modificar tanto a luciferina com a própria luciferase. No entanto, estas tentativas estão geralmente associadas a uma baixa significativa da intensidade da luz emitida. Esta diminuição estará relacionada com um destes fatores: o rendimento da formação da oxiluciferina, o rendimento do passo de chemiexcitação e o rendimento da fluorescência da oxiluciferina. A dificuldade está em saber qual destes parâmetros é responsável pela

diminuição da intensidade de luz, e como se pode inverter este fenómeno, já que grande parte do mecanismo da reação bioluminescente está longe de estar clarificada.

Neste trabalho foram usadas várias técnicas teóricas e experimentais para explicar vários aspetos da reação bioluminescente: a formação de compostos inibitórios e a razão para o seu poder inibitório (Capítulo 2); o mecanismo de reação que leva à formação da dioxetanona do pirilampo (Capítulo 3); a determinação do mecanismo de decomposição das dioxetanonas, e o estudo de como estas moléculas permitem a formação de estados excitados (Capítulo 4); a clarificação do mecanismo da bioluminescência multicor (Capítulo 5); as propriedades da oxiluciferina enquanto fotoácido e as implicações destes processos na reação bioluminescente (Capítulo 6). O objetivo deste trabalho de investigação é que as conclusões aqui obtidas possam ser usadas pela comunidade científica interessada para desenvolver sistemas luciferase-oxiluciferina mais adequados para aplicações *in vivo* e *in vitro.*

Foi estudada teoricamente a ligação de três importantes adenilados à luciferase do pirilampo, revelando assim os principais aminoácidos responsáveis por esta ligação. Deste modo foi possível apresentar mais dados relativos ao mecanismo responsável pelo perfil de *flash* da bioluminescência. Foi também excluída a possibilidade de formação da desidroluciferina e de um isómero da luciferina a partir do substrato da reação bioluminescente, o que elimina estes compostos como possíveis inibidores da reação de emissão de luz.

Foi também estudada, de forma comparativa, o possível papel de um carbanião ou de um radical na formação da importante dioxetanona do pirilampo. Os nossos resultados teóricos favoreceram a presença de um radical, já que este permite explicar a interação do oxigénio molecular com um composto singleto para dar origem a um produto singleto. Este mecanismo também permite explicar a formação do inibidor desidroluciferil-adenilado. Estes resultados foram corroborados pela descoberta do envolvimento de um intermediário radicalar na reação quimioluminescente entre a luciferina e o anião superóxido.

O estudo de várias dioxetanonas mostrou que estas moléculas se decompõem através de um mecanismo concertado, e que a quimioexcitação se deve maioritariamente a fenómenos de *intersystem crossing* entre estados fundamentais/excitados singletos e estados tripletos, para além de transições entre estados singletos. Estes resultados levaram à elaboração da teoria "*Interstate Crossing Induced Chemiexcitation"* (ICIC), que nos permite explicar a formação de estados excitados a partir da decomposição de dioxetanonas.

Estudos computacionais da ligação da oxiluciferina a duas conformações da luciferase permitiram determinar que o comprimento máximo de emissão da reação bioluminescente é controlado pelo campo electroestático, formado pelas interações intermoleculares entre a oxiluciferina e o centro ativo da enzima. Mais especificamente, a cor da emissão é determinada por interações electroestáticas repulsivas com a adenosina-5'-monofosfato, pontes de hidrogénio com moléculas de água e interações π-π com uma fenilalanina. A análise a vários análogos da oxiluciferina permitiu determinar que um maior comprimento de emissão e uma maior intensidade de fluorescência se deve a efeitos de conjugação π-π e a uma maior sobreposição entre orbitais HOMO e LUMO, especialmente na região conectiva entre as duas porções que constituem as moléculas emissoras de luz.

Finalmente, o ciclo fotoprotolítico da oxiluciferina, luciferina e desidroluciferina em solução aquosa foram estudados e caracterizados. Isto permitiu-nos identificar estas moléculas como fotoácidos, determinar caminhos de desativação de fluorescência, e observar o envolvimento de complexos supramoleculares. Mais importante, permitiu-nos prever o envolvimento da espécie oxiluciferina-enolato na reação bioluminescente, e propô-la como um dos possíveis emissores de luz.

Palavras-chave:

Bioluminescência; Quimioluminescência; Fluorescência; Luciferase do Pirilampo; Luciferina; Oxiluciferina; Dioxetanonas; Métodos Teóricos; Fotoácidos; Perfil de Flash; Inibição Enzimática; Mecanismos de Reação;

Abstract

Light emission from a living organism is one of the most pretty and fascinating natural phenomenon observed. This process is called bioluminescence and it originates from an oxidation of a substrate, luciferin, in a reaction catalyzed by an enzyme, luciferase. The most well-known and studied bioluminescent system is that of fireflies. This process consists on a two-step reaction: in the first step, luciferase catalyzes an adenylation reaction between luciferin and adenosine-5'-triphosphate (ATP), in the presence of Mg^{2+}, which results in the formation of luciferyl-adenylate; in the second step, the adenylate is oxidized in the presence of molecular oxygen, which produces an high-energy intermediate, firefly dioxetanone. It is the decomposition reaction of this latter compound that gives origin to the light emitter, oxyluciferin, already in a singlet excited state.

Due to very desirable properties (high quantum yield, ATP-dependence, ease to use and high analytic sensibility), the firefly bioluminescent reaction has gained a great number of applications in the pharmaceutical, bioanalytical and biomedical fields. More specifically, it has been used in the detection of several analytes (as ATP), as a gene reporter, and in bioimaging, among others. However, this bioluminescent system presents some problems that prevent its use in new applications or an increase in its efficiency in existent ones.

The high K_m of ATP and the formation of inhibitory products, which are responsible for a flash profile of emitted light, decrease the analytical sensibility of this reaction. Moreover, the emitted light presents a wavelength maximum in the green region of the visible spectrum, while the photodetectors used in *in vitro* assays have more sensibility in the blue region. *In vivo* applications are also associated with restrictions, as cells and tissues absorb more strongly on the green region of the visible spectrum, and such, it would be more beneficial if the light emitted in the bioluminescent reaction present a wavelength maximum in the red region.

Several groups have tried to overcome these problems by modifying both luciferin and luciferase. However, these attempts are generally associated with a significant decrease of the intensity of emitted light. This decrease is related with one of these three factors: the yield of oxyluciferin formation, the chemiexcitation step, and the fluorescence quantum yield of oxyluciferin. The difficulty is in understand which one of these three parameters is responsible for the decrease in the intensity of light, and how

we can invert this phenomenon, as a large part of the firefly bioluminescence reaction mechanism is far from clarified.

In this work were used several theoretical and experimental techniques in order to explain different features of the firefly bioluminescent reaction: the formation of inhibitory compounds and the reason behind their inhibition power (Chapter 2); the reaction mechanism that is responsible for the formation of firefly dioxetanone (Chapter 3); the determination of the reaction of dioxetanone decomposition, and the clarification of how these molecules allow the formation of excited states (Chapter 4); the characterization of the multicolor bioluminescence tuning mechanism (Chapter 5); the properties of oxyluciferin as a photoacid, and the implication of this feature in the bioluminescent reaction (Chapter 6). The goal of this research work is that the conclusions here obtained can be used by the scientific community to develop luciferase-oxyluciferin systems more appropriated for *in vivo* and *in vitro* applications.

It was studied theoretically the binding of three important adenylates to firefly luciferase, revealing in that way the amino-acid residues responsible for that binding. In that way was possible to present more data related to the mechanism responsible for the flash profile of bioluminescence. It was also excluded the possibility of the formation of dehydroluciferin and a luciferin isomer from the bioluminescent substrate, which eliminates these compounds as possible inhibitors of the light emitting reaction.

It was also comparatively studied the potential role of a carbanion and a radical in the formation of firefly dioxetanone. Our theoretical results favor the presence of a radical, as it allows the interaction of molecular oxygen with a singlet compound in order to give origin to a singlet product. This mechanism also allows the formation of the inhibitor dehydroluciferyl-adenylate. These results were corroborated by the discovery of the involvement of a radical intermediate in the chemiluminescent reaction between luciferin and superoxide anion.

The study of several dioxetanones showed that these molecules decompose via a concerted mechanism, and that chemiexcitation is due to intersystem crossing processes between ground/excited singlet and triplet states, besides transitions between singlet states. These results lead to the proposal of the Interstate Crossing Induced Chemiexcitation (ICIC) theory, which allows us to explain the formation of excited states from dioxetanone decomposition.

Computational studies of the binding of oxyluciferin to two conformations of luciferase allowed the determination that the bioluminescent wavelength maximum is controlled by the electrostatic field, formed by intermolecular interactions between

oxyluciferin and the enzymatic active site. More specifically, the color of light emitted is determined by repulsive electrostatic interactions with adenosine-5'-monophosphate, hydrogen bonds with water molecules, and π-π stacking interactions with a phenylalanine residue. The analysis of several oxyluciferin analogues related increased emission wavelength and fluorescence intensity to π-π conjugation effects and to a higher HOMO-LUMO overlap, especially in the connective region between the two moieties of oxyluciferin.

Finally, the photoprotolytic cycle of oxyluciferin, luciferin and dehydroluciferin in aqueous solution were studied and characterized. This allowed us to identify these molecules as photoacids, determine possible deactivation pathways, and observe the involvement of supramolecular π-π complexes. More importantly, it allowed us to predict the involvement of enolate oxyluciferin in the firefly bioluminescent reaction, and propose it as one of the possible light emitters.

Keywords:

Bioluminescence; Chemiluminescence; Fluorescence; Firefly Luciferase; Luciferin; Oxyluciferin; Dioxetanones; Theoretical Methods; Photoacids; Flash Profile; Enzymatic Inhibition; Reaction Mechanisms;

Publications and Presentations of the Author Containing Work Related with this Thesis

The work here reported was presented in scientific meetings, and was published in peer-reviewed journals.

A. Papers

1. L. Pinto da Silva, J.C.G. Esteves da Silva, TD-DFT/Molecular Mechanics Study of the Photinus pyralis Bioluminescence Study, Journal of Physical Chemistry B **2012**, *116*, 2008-13.
2. L. Pinto da Silva, J.C.G. Esteves da Silva, Firefly Chemiluminescence and Bioluminescence: Efficient Generation of Excited States, *ChemPhysChem* **2012**, *13*, 2257-62.
3. L. Pinto da Silva, J.C.G. Esteves da Silva, Theoretical analysis of the color tuning mechanism of oxyluciferin and 5-hydroxyoxyluciferin, *Computational and Theoretical Chemistry* **2012**, *988*, 56-62.
4. Y. Erez, I. Presiado, R. Gepshtein, L. Pinto da Silva, J.C.G. Esteves da Silva, Comparative Study of the Photoprotolytic Reactions of D-Luciferin and Oxyluciferin, *Journal of Physical Chemistry A* **2012**, *116*, 7452-61.
5. L. Pinto da Silva, J. Vieira, J.C.G. Esteves da Silva, Comparative theoretical study of the binding of luciferyl-adenylate and dehydroluciferyl-adenylate to firefly luciferase, *Chemical Physics Letters* **2012**, *543*, 137-41.
6. J. Vieira, L. Pinto da Silva and J.C.G. Esteves da Silva, Advances in the knowledge of light emission by firefly luciferin and oxyluciferin, *Journal of Photochemistry and Photobiology B: Biology* **2012**, *117C*, 33-39.
7. L. Pinto da Silva, J.C.G. Esteves da Silva, Density functional theory study of 1,2-dioxetanone decomposition in condensed phase, *Journal of Computational Chemistry* **2012**, *33*, 2118-23.
8. L. Pinto da Silva, J.C.G. Esteves da Silva, Response to “comment on density functional theory study of 1,2-dioxetanone decomposition in condensed phase”, *Journal of Computational Chemistry* **2012**, *33*, 2127-30.
9. I. Presiado, Y. Erez, R. Simkovitch, S. Shomer, R. Gepshtein, L. Pinto da Silva, J.C.G. Esteves da Silva, D. Huppert, Excited-State Proton Transfer of Firefly Dehydroluciferin, *Journal of Physical Chemistry A* **2012**, *116*, 10770-9.
10. L. Pinto da Silva, A.J.M. Santos, J.C.G. Esteves da Silva, Efficient Firefly Chemi/Bioluminescence: Evidence for Chemiexcitation Resulting from the Decomposition of a Neutral Firefly Dioxetanone Molecule, *Journal of Physical Chemistry A* **2012**, *117*, 94-100.

11. L. Pinto da Silva, J.C.G. Esteves da Silva, Evidence of the absence of a biradical intermediate in the decomposition of 1,2-dioxetanones, *Science Letters Journal* **2012**, *1*:29.

12. L. Pinto da Silva, J.C.G. Esteves da Silva, Interstate Crossing-Induced Chemiexcitation as the Reason for the Chemiluminescence of Dioxetanones, *ChemPhysChem* **2013**, *14*, 1071-1079.

13. L. Pinto da Silva, J.C.G. Esteves da Silva, Chemiluminescence of 1,2-Dioxetanone Studied by a Closed-Shell DFT Approach, *International Journal of Quantum Chemistry* **2013**, *113*, 1709-1716.

14. L. Pinto da Silva, J.C.G. Esteves da Silva, Mechanistic Study of the Unimolecular Decomposition of 1,2-Dioxetanedione, *Journal of Physical Organic Chemistry* **2013**, *26*, 659-663.

15. L. Pinto da Silva, J.C.G. Esteves da Silva, Theoretical Study of the Correlation between Superoxide Anion Consumption and Firefly Luciferin Chemiluminescence, *Chemical Physics Letters* **2013**, *577*, 127-130.

16. L. Pinto da Silva, R. Simkovitch, D. Huppert, J.C.G. Esteves da Silva, Oxyluciferin Photoacidity: The Missing Element for Solving the Keto-Enol Mystery?, *ChemPhysChem* **2013**, *14*, 3441-3446.

17. L. Pinto da Silva, R. Simkovitch, D. Huppert, J.C.G. Esteves da Silva, Theoretical Study of the Efficient Fluorescence Quenching Process of the Firefly Luciferin, *Journal of Photochemistry and Photobiology A: Chemistry* **2013**, *266*, 47-54.

18. L. Pinto da Silva, R. Simkovitch, D. Huppert, J.C.G. Esteves da Silva, Theoretical Photodynamic Study of the Photoprotolytic Cycle of Firefly Oxyluciferin, *ChemPhysChem* **2013**, *14*, 2711-2716.

19. L. Pinto da Silva, J.C.G. Esteves da Silva, Theoretical fingerprinting of the photophysical properties of four firefly bioluminophores, *Photochemical and Photobiological Sciences* **2013**, *12*, 2028-2035.

20. L. Pinto da Silva, J.C.G. Esteves da Silva, Theoretical evaluation of the role of carbanion and radical molecules on the formation of firefly dioxetanone, *Journal of Spectroscopy and Dynamics* **2014**, *4*:17.

21. L. Pinto da Silva, J.C.G. Esteves da Silva, Dioxetanones' Peroxide Bond as a Charge-Shifted Bond: Implications in the Chemiluminescence Process, *Structural Chemistry* **2014**, *25*, 1075-1081.

22. L. Pinto da Silva, J.C.G. Esteves da Silva, Theoretical Study of the Superoxide Anion Assisted Firefly Oxyluciferin Formation, *Chemical Physics Letter* **2013**, *590*, 180-182.

23. L. Pinto da Silva, J.C.G. Esteves da Silva, Study of Firefly Luciferin Oxidation and Isomerism as Possible Inhibition Pathways for Firefly Bioluminescence, *Chemical Physics Letters* **2014**, *592*, 188-191.

24. L. Pinto da Silva, M.S. Miranda, J.C.G. Esteves da Silva, Theoretical Study of the Effect of Resonance on pi-pi Stacked Firefly Oxyluciferin Dimers, *Journal of Photochemistry and Photobiology A: Chemistry* **2014**, *278*, 9-13.

25. L. Pinto da Silva, J.C.G. Esteves da Silva, Quantum/Molecular Mechanics Study of Firefly Bioluminescence on Luciferase Oxidative Conformation, *Chemical Physics Letters* **2014**, *608*, 45-49.
26. L. Pinto da Silva, J.C.G. Esteves da Silva, Chemiexcitation Induced Proton Transfer: Enolate Oxyluciferin as Firefly Bioluminophore, *Journal of Physical Chemistry B* **2015**, *119*, 2140-2148.
27. L. Pinto da Silva, J.C.G. Esteves da Silva, A theoretical analysis of the potential role of pi-pi stacking interactions in the photoprotolytic cycle of firefly luciferin, *ChemPhysChem* **2014**, *15*, 3761-3767.
28. L. Pinto da Silva, J.C.G. Esteves da Silva, Theoretical study of the nontraditional enol-based photoacidity of firefly oxyluciferin, *ChemPhysChem* **2015**, *16*, 455-464.

B. Invited Oral Presentations

1. L. Pinto da Silva (2015), Theoretical Insight into the Intermolecular CIEEL Mechanism, International Workshop on Bioluminescence, Beijing, China.
2. L. Pinto da Silva (2012), TD-DFT/MM Studies of the Firefly Bioluminescence Phenomenon, 2nd International Conference on Computation for Science and Technology, Nidge, Turkey.

C. Oral Presentations

1. L. Pinto da Silva (2014), Oxyluciferin strong photoacidity in firefly bioluminescence, 248th American Chemical Society National Meeting, San Francisco, CA, USA.
2. L. Pinto da Silva (2014), The Photoacidity of Oxyluciferin: Excited State Processes Behind Firefly Bioluminescence, 18th International Symposium on Bioluminescence and Chemiluminescence (ISBC 2014), Uppsala, Sweden.
3. L. Pinto da Silva (2012), Computational investigations of the Photinus pyralis luciferase-oxyluciferin system, 17th International Symposium on Bioluminescence and Chemiluminescence (ISBC 2012), Guelph, Canada.

D. Posters

1. L. Pinto da Silva, J.C.G. Esteves da Silva (2014), Firefly Color Tuning Mechanism: A TD-DFT/MM Characterization, 248th, American Chemical Society National Meeting, San Francisco, CA, USA.
2. L. Pinto da Silva, J.C.G. Esteves da Silva (2014), The Characterization of the Nontraditional Enol-Based Photoacidity of Firefly Oxyluciferin, 248th, American Chemical Society National Meeting, San Francisco, CA, USA.
3. L. Pinto da Silva, J.C.G. Esteves da Silva (2013), The Firefly Dioxetanone Mechanisms, XXIII Encontro Nacional da SPQ, Aveiro, Portugal.

4. L. Pinto da Silva, J.C.G. Esteves da Silva (2013), Chemiluminescence of Dioxetanones as the Result of Interstate Crossing-Induced Chemiexcitation, 11º Encontro Nacional de Química-Física, Porto, Portugal.

Structure of the Thesis

This Thesis is divided into three major sections, the introduction, the presentation and discussion of the results obtained in the study of firefly bioluminescence, and a conclusion plus future perspective section. Each section is composed of chapters, corresponding to papers already published in specialized peer-review international journals.

The introduction section presents one chapter (Chapter one) in which bioluminescence and chemiluminescence concepts are described. More specifically are presented the available data regarding the reaction mechanism of firefly bioluminescence, its flash profile of emitted light and the properties of the light emitter, oxyluciferin. There are also described selected examples of applications. This section ends with a brief description of the main objectives of the project that led to the Thesis.

The second section encompasses five chapters corresponding to the study of inhibitors potentially responsible for the bioluminescent flash profile (Chapter 2), the mechanism of firefly dioxetanone formation (Chapter 3), the decomposition reaction of dioxetanones and subsequent chemiexcitation (Chapter 4), the multicolor tuning mechanism of firefly bioluminescence (Chapter 5), and the characterization of firefly oxyluciferin as a photoacid (Chapter 6).

The fourth and last section presents the main conclusion of the work performed, as well as perspective of future research.

Table of Contents

List of Figures

List of Abbreviations

AMP	Adenosine-5'-Monophosphate
ATP	Adenosine-5'-Triphosphate
CoA	Coenzyme A
DFT	Density functional theory
D-LH_2	Firefly D-luciferin
ESPT	Excited state proton transfer
HOMO	Highest occupied molecular orbital
kDa	Kilodalton
L	Firefly dehydroluciferin
L-AMP	Dehydroluciferyl-adenylate
L-CoA	Dehydroluciferyl-Coenzyme A
LH_2-AMP	D-luciferyl-adenylate
L-LH_2	Firefly L-luciferin
L-LH_2-AMP	L-luciferyl-adenylate
L-LH_2-CoA	L-luciferyl-Coenzyme A
LUMO	Lowest unoccupied molecular orbital
nm	Nanometer
$OxyLH_2$	Firefly oxyluciferin
PP_i	Pyrophosphate
TD-DFT	Time dependent density functional theory

Chapter 1 – Introduction

The purpose of this chapter is to present the fundamental aspects of firefly bioluminescence, which is the main subject of this Ph.D. thesis.

1.1. Introduction to Bioluminescence

The term luminescence was used for the first time in the year 1888 by the german Eilhardt Wiedemann, and it was used to identify all light phenomena that are not the result of a temperature increase.[1,2] Luminescence can be classified using as criteria the energetic source responsible for the formation of the electronic state. So, for example, photoluminescence occur when light emission is originated by the absorption of electronic radiation and bioluminescence when a biochemical reaction is responsible for light production by living organisms.[3,4] Chemiluminescence is related to bioluminescence, in which light arises from a chemical reaction. For the purpose of this thesis, both chemi- and bioluminescence assume a role of particular interest.

Bioluminescence can be found in a variety of living organisms, as fungi, insects, bacteria and fishes.[5] The role of bioluminescence in these different organisms is wide-ranging and includes prey attraction, sexual communication, aposematic signaling and camouflage/protection.[6-8]

Among these different systems the biochemistry, color and method of display of light can be very different.[9] There is, however, one common thread tying together all these different systems: all bioluminescent processes are luciferase-catalyzed reactions of molecular oxygen with luciferins. However, the term luciferin and luciferase are only generic, referring to the substrate and enzyme in a bioluminescent reaction, irrespective of their structure. For example, in bacteria a luciferase is a heterodimer of 40 and 35 kDa that catalyze the oxidation of $FMNH_2$-luciferin, while in dinoflagellates a luciferase of 137 kDa oxidizes a tetrapyrrolic luciferin.

In more recent years, bioluminescent systems have gained several bioanalytical, biomedical and pharmaceutical applications, among others.[10-12] The most studied bioluminescent system is that of North-American firefly, *Photinus pyralis.* Other species include *Luciola cruciata, Luciola lateralis*, *Luciola mingrélica*, *Phritxotrix hirtus*, *Lampyris noctiluca* and *Lampyris turkestanicus*.[9,13] The most important characteristics of these systems, which justify their use in the development of novel applications, are: high quantum yield (~40-60%);[14,15] a dependence for adenosine-5´-triphosphate (ATP);

being a near-instantaneous reaction; the fact of not being needed an excitation source allows for a very low “background noise”.

1.2. Firefly Luciferase

The cloning and sequencing of several luciferases of various firefly and beetle species revealed that these enzymes are closely related to a large family of nonbioluminescent enzymes, which catalyze reactions of ATP with carboxylate substrates to form acyl-adenylates.[16,17] Firefly luciferase is then a 62 kDa protein that catalyzes the oxidation of firefly luciferin (D-LH_2, Fig. 1A), in the presence of ATP and molecular oxygen. The reaction proceeds through the formation of an adenyl intermediate (LH_2-AMP, Fig. 1B), leading to the formation of the light emitter oxyluciferin ($OxyLH_2$, Fig. 1C), and subsequent emission of visible light[18,19]:

D-LH_2 + ATP-Mg^{2+} ↔ LH_2-AMP + PPi-Mg^{2+} (1)

D-LH_2-AMP + O_2 → $OxyLH_2$ + AMP + CO_2 + *hv* (2)

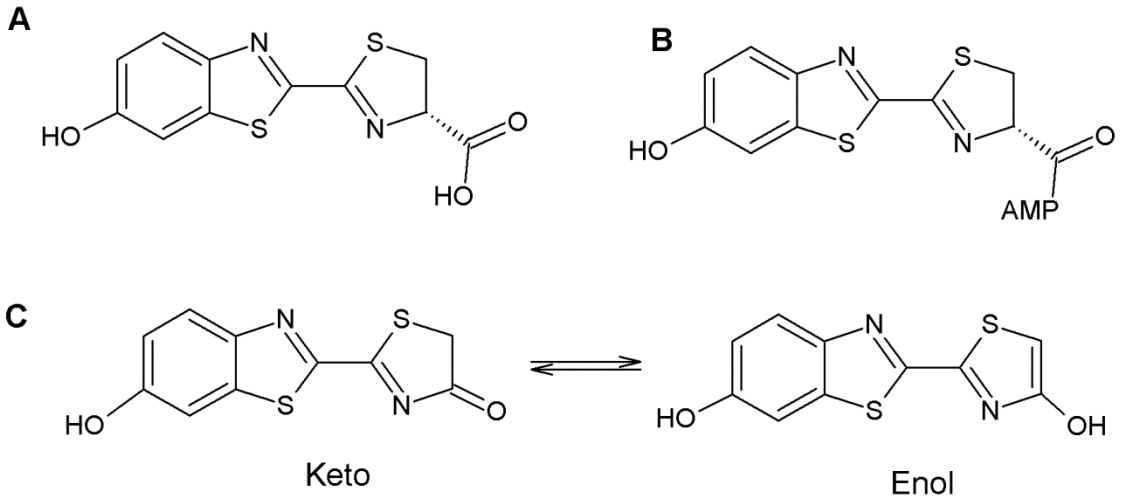

Figure 1 - Schematic representation of D-LH_2 (A), LH_2-AMP (B) and $OxyLH_2$ (C).

The luciferase crystal structure revealed an unique molecular architecture, which consists of a large N-terminal domain (residues 1-436) and a small C-terminal domain (residues 440-550), with the active site of this enzyme enclosing amino-acid residues on the surface of both domains (Fig. 2).[20] The major part of the amino-acid residues important to the bioluminescent activity is located in the N-terminal portion and only one in the C-terminal domain.[21]

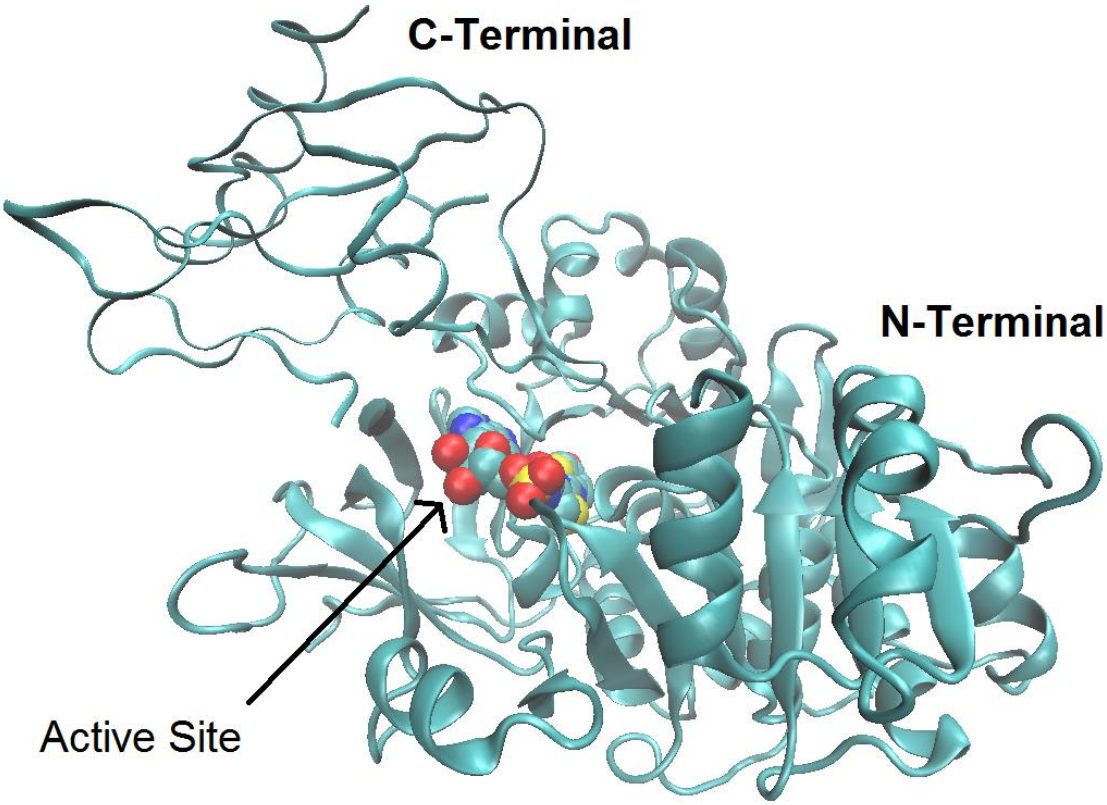

Figure 2 – Representation of firefly luciferase (from the *Photinus pyralis* species), when binding a LH_2-AMP analog.

1.3. Firefly Luciferin and Oxyluciferin, and their Light Emitting Properties

Article 1

Advances in the knowledge of light emission by firefly luciferin and oxyluciferin
João Vieira, Luís Pinto da Silva and Joaquim C.G. Esteves da Silva
J. Photochem. Photobiol. B: Biology **2012**, *117*, 809-817.

The bibliographic research was performed by Luís Pinto da Silva, who also supervised João Vieira in the writing of this review paper.

Journal of Photochemistry and Photobiology B: Biology 117 (2012) 33–39

Contents lists available at SciVerse ScienceDirect

Journal of Photochemistry and Photobiology B: Biology

journal homepage: www.elsevier.com/locate/jphotobiol

Short Review

Advances in the knowledge of light emission by firefly luciferin and oxyluciferin

João Vieira, Luís Pinto da Silva, Joaquim C.G. Esteves da Silva *

Centro de Investigação em Química, Departamento de Química e Bioquímica, Faculdade de Ciências da Universidade do Porto, R. Campo Alegre 687, 4169-007 Porto, Portugal

ARTICLE INFO

Article history:
Received 19 April 2012
Received in revised form 20 August 2012
Accepted 27 August 2012
Available online 5 September 2012

Keywords:
Bioluminescence
Luciferase
Fluorescence
Oxyluciferin
Luciferin
Firefly

ABSTRACT

Firefly luciferase is the most important and studied bioluminescence system. Due to very interesting characteristics, this system has gained numerous biomedical, pharmaceutical and bioanalytical applications, among others. In order to improve the use of this system, various researchers have tried to understand experimentally the colour of bioluminescence, and to create ways of tuning the colour emitted. The objective of this manuscript is to review the experimental studies of firefly luciferin and oxyluciferin, and related analogues, fluorescence and bioluminescence.

Contents

1. Introduction

Bioluminescence is considered to be a light emission phenomenon, which originates from an enzyme-catalysed chemical reaction. The most studied bioluminescence system is that of the fireflies. Firefly luciferase catalyses a two-step reaction: firefly luciferin (D-LH_2, Scheme 1) reacts with adenosine-5′-triphosphate (ATP), subsequently generating luciferyl-adenylate (LH_2-AMP); The latter molecule will then be oxidised, in the presence of molecular oxygen, which results in the formation of oxyluciferin ($OxyLH_2$), CO_2 and adenosine-5′-monophosphate (AMP) [1–4].

$OxyLH_2$ is usually thought to exist in solution as one of six possible species, due to a complex chemical equilibrium (Scheme 2). However, it is known that in the bioluminescence reaction, this molecule is formed in its anionic keto-form (Keto-(-1), Scheme 2) [5–7]. Keto-(-1) is formed in the excited state, due to the formation and subsequent decomposition of firefly dioxetanone [8,9]. The bioluminophore will then decay to the ground state, with emission of green light [4,10–12]. The colour of bioluminescence was demonstrated to be modulated by intermolecular interactions (mostly electrostatic, π–π stacking and hydrogen-bonding) and the polarity of the microenvironment [5,7,13–20].

* Corresponding author. Tel.: +351 226082869; fax: +351 226082959.
E-mail addresses: jdanav@gmail.com (J. Vieira), luist311@hotmail.com (L. Pinto da Silva), jcsilva@fc.up.pt (J.C.G. Esteves da Silva).

1011-1344/$ - see front matter © 2012 Elsevier B.V. All rights reserved.
http://dx.doi.org/10.1016/j.jphotobiol.2012.08.017

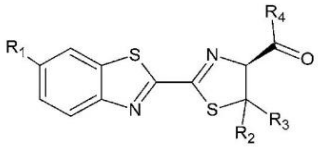

R_1 = OH, R_2 = R_3 = H, R_4 = OH: LH_2
R_1 = OH, R_2 = R_3 = H, R_4 = AMP: LH_2-AMP
R_1 = OH, R_2 = CH_3, R_3 = H, R_4 = OH: MLH_2
R_1 = OH, R_2 = R_3 = CH_3, R_4 = OH: $DMLH_2$
R_1 = CH_3O, R_2 = R_3 = H, R_4 = OH: $MeOLH_2$

Scheme 1. D-LH_2 and analogues.

Table 2
Emission spectra of D-LH_2.

Compound	Solvent (E_T (kcal mol^{-1}))	λ_{em} (nm)	Refs.
($^-$O)-LH_2	Ethanol[a] (0.654)	532	[33]
	Methanol (0.762)	530	[34]
	Ethanol (0.654)	530	[34]
	Ethanol[b] (0.654)	450	[33]
(HO)-LH_2	Ethanol[a] (0.654)	444	[33]
	Acetonitrile (0.460)	430	[35]
	Methanol (0.762)	425	[34]
	Ethanol (0.654)	425	[34]
	Ethanol[b] (0.654)	404	[33]
	p-Dioxane[a] (0.164)	399	[33]

[a] Measured at room temperature.
[b] Measured at 77 K.

Due to very interesting characteristics, the firefly bioluminescence system has been gaining numerous biomedical, pharmaceutical, bioanalytical and bioimaging applications, among others [21–26]. The modulation of the colour of bioluminescence would be of extreme importance for a better use of this system. Red-emitting luciferase-Keto-(-1) complexes could be used in *in vivo* medical imaging, as red light is absorbed very poorly by mammalian tissues in comparison with the natural colour of the emitted light. Furthermore, it was hypothesised that the control of the colour of bioluminescence could be the basis for using luciferase as a single dual reporter gene, a bioindicator of cellular stress, and a probe for intracellular changes of pH [3].

The objective of this manuscript is to review the experimental findings regarding the fluorescence and bioluminescence of LH_2 and $OxyLH_2$, and related analogues, in several conditions of polarity, pH and in different luciferase enzymes. With this review, we intend to summarise the knowledge obtained so far, regarding the effect of structural and environmental effects on the colour of light emitted by these molecules.

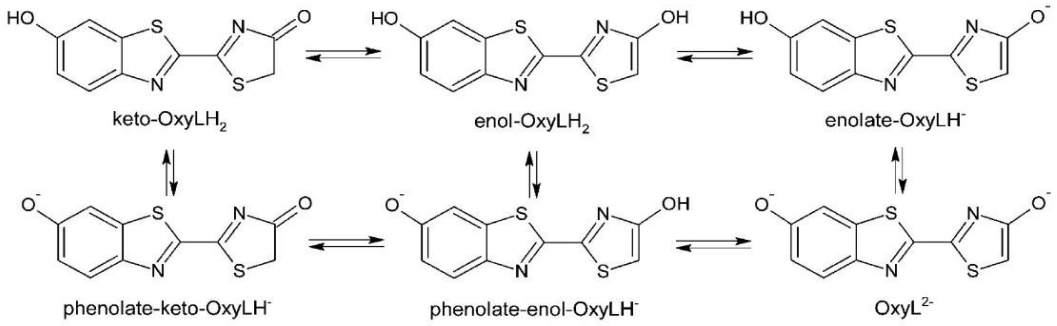

Scheme 2. Possible forms of $OxyLH_2$ in solution.

Table 1
Absorption and emission spectra of D-LH_2 and analogues.

Compound	Solvent (E_T (kcal mol^{-1}))	pH	λ_{abs} (nm)	λ_{em} (nm) (quantum yield)	Refs.
(HO)-LH_2	Tris–acetate buffer[a]	7.7	330	530 (~0.90)	[30]
	Water (1.000)	5.0	328	542 (0.25)	[27]
	Neutral aqueous solution	<pK_a	330	440	[35]
	Ethanol > 99%, acetate buffer	5.0	331	435 (0.03)	[27]
+$HNRO^-$	HCl 20–220 mM	Acidic	-	590	[36]
($^-$O)-L	Water (1.000)	11	396	560 (0.62)	[27]
	Ethanol 90%, carbonate buffer	11	348	560 (0.26)	[27]
(HO)-LH_2-AMP	Water (1.000)	5.0	336	551 (0.11)	[27]
(HO)-L	Ethanol 98%, acetate buffer	4.5	–	550 (0.62)	[27]
	Water (1.000)	4.5	–	435 (0.20)	[27]
($^-$O)-LH_2	Water (1.000)	11	384	542 (0.62)	[27]
	Neutral aqueous solution	<pK_a	–	530	[35]
AL	Tris–acetate buffer[a]	7.7	350	520	[30]
(HO)-L-AMP	Ethylene glycol 95%, acetate buffer	4.5	–	457 (0.25)	[27]
	Water (1.000)	4.5	354	(0.01)	[27]
Gly–AL	Tris–acetate buffer[a]	7.7	327	450	[30]
$MeOLH_2$	Water (1.000)	5.23	323	441 (0.03[b])	[27]
	Water (1.000)	11.1	323	441 (0.03[b])	[27]
	Ethanol 99%, acetate buffer	5.2	325	420 (0.01[b])	[27]
($^-$O)-L-AMP	Water (1.000)	11	407	(0.01)	[27]

[a] 1 mM EDTA, 0.2 M NaCl.
[b] Approximate value owing to extreme photosensitivity.

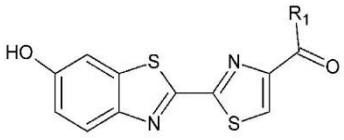

R_1 = OH: L
R_1 = AMP: L-AMP

Scheme 3. L and adenylate.

2. Fluorescence

2.1. D-LH_2 and analogues

The data referring to the absorption and emission of D-LH_2 and analogues are presented in Tables 1 and 2. The structures of these molecules are schematically represented in Schemes 1 and 3.

It has been documented that a redshift in the emission wavelength of D-LH_2 occurs by increasing the temperature or lowering the pH [27–32]. A dependence on solvent polarity has also been proposed, as luciferin fluorescence at neutral pH is known to be blue in solvents which prevent proton transfer and/or of medium polarity, such as DMSO, methanol, ice or acetone, and yellow–green in water [27].

An early study by Jung et al. [33], in which the light emitted by the phenolate form ($^-$O)-LH_2 (Scheme 1) in ethanol shifted from 450 nm at 77 K to 532 nm at room temperature, backs up the correlation between temperature and fluorescence. In the same study, a similar shift was observed for the neutral (HO)-LH_2 form (Scheme 1).

On the other hand, Morton et al. [27] demonstrated that for the analogue 6′-methoxyLH_2 (MeOLH_2, Scheme 1), while the emission spectrum suggested sensitivity to solvent polarity, there was no observable variation in colour at different pH values. The authors noted, however, that the reported values were approximated due to the extreme photosensitivity of the compound, and therefore not entirely reliable.

Three separate experiments [33–35] produced concordant results regarding the difference in emission wavelength between the neutral and the phenolate forms of LH_2. In different mediums, the phenolate form emitted closer to red than the neutral form. This deviation seems to carry over to some luciferin analogues, namely dehydroLH_2 (L, Scheme 3) and its adenylated form (L-AMP, Scheme 3) [27]. In both cases, either the absorption or emis-

Table 3
Absorption and emission spectra of amino analogues of D-LH_2 [37].

Solvent (E_T (kcal mol^{-1}))[a]	λ_{abs} (nm)				λ_{em} (nm)			
	AL	QAL	NAL	CAL	AL	QAL	NAL	CAL
NaPi	349	353	322	399	523	500	465	458
Methanol (0.762)	363	363	327	414	492	479	440	461
Acetonitrile (0.460)	362	364	333	401	478	460	425	462
DMSO (0.444)	377	380	342	415	487	468	437	472
Dimethylformamide (0.386)	363	372	329	408	479	464	425	468
Dichloromethane (0.309)	357	361	332	393	463	438	410	461
Chloroform (0.259)	357	359	329	393	466	439	412	457
THF (0.207)	367	372	334	403	461	438	417	462
Benzene (0.111)	356	358	327	396	437	423	400	469

[a] Measurements at pH 7.4 in NaPi and pH 7.7 in remaining solvents.

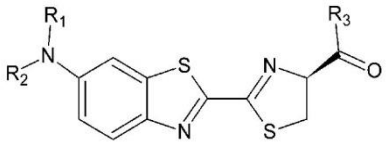

R_1 = R_2 = H, R_3 = OH: AL
R_1 = R_2 = H, R_3 = AMP: AL-AMP
R_1 = Gly, R_2 = H, R_3 = OH: Gly-AL
R_1 = CH_3, R_2 = H, R_3 = OH: MAL
R_1 = R_2 = CH_3, R_3 = OH: DMAL

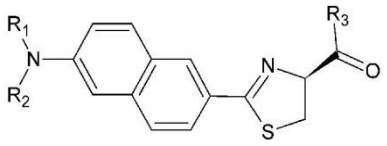

R_1 = R_2 = H, R_3 = OH: QAL
R_1 = R_2 = H, R_3 = AMP: QAL-AMP
R_1 = CH_3, R_2 = H, R_3 = OH: MQAL
R_1 = R_2 = CH_3, R_3 = OH: DMQAL

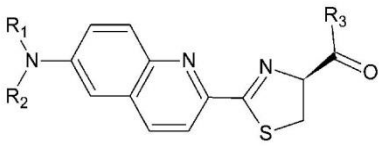

R_1 = R_2 = H, R_3 = OH: NAL
R_1 = R_2 = H, R_3 = AMP: NAL-AMP
R_1 = CH_3, R_2 = H, R_3 = OH: MNAL
R_1 = R_2 = CH_3, R_3 = OH: DMNAL

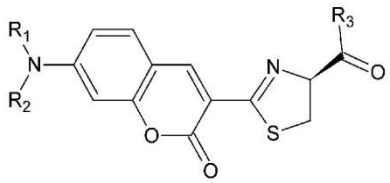

R_1 = R_2 = H, R_3 = OH: CAL
R_1 = R_2 = H, R_3 = AMP: CAL-AMP
R_1 = CH_3, R_2 = H, R_3 = OH: MCAL
R_1 = R_2 = CH_3, R_3 = OH: DMCAL

Scheme 4. Amino analogues of D-LH_2.

Table 4
Absorption and emission spectra of $OxyLH_2$.

Solvent (E_T (kcal mol^{-1}))	λ_{abs} (nm)	λ_{em} (nm) (quantum yield)	Refs.
Water (1.000)	409	553 (0.470)	[38]
DMSO, excess PhOK	475	570	[28]
Chloroform (0.259)	376	471 (0.308)	[38]
Dichloromethane (0.309)	369	465 (0.231)	[38]
Acetonitrile (0.460)	369	457 (0.305)	[38]
Methanol (0.762)	372	457 (0.345)	[38]
DMSO (0.444)	377	448 (0.511)	[38]
Acetone (0.355)	367	436 (0.277)	[38]

sion spectra of the phenolate form peaked at longer wavelengths than its protonated counterpart.

In a series of studies by Erez et al. [34–36], an emission peak at approximately 590 nm in acidic aqueous solution was attributed to the zwitterion form of D-LH_2 ($^+$HNRO$^-$), which predominated over the phenolate and neutral forms' emission bands at 220 mM HCl [36].

Adenylation of LH_2 produced a redshift in both the absorption and emission spectra in water [27]. Although L-AMP also displayed a peak in absorption closer to red, no conclusion could be drawn in regards to its emission on account of the low quantum yield of the experiment.

2.2. Amino analogues of D-LH_2

The data referring to the absorption and emission of aminoLH$_2$ (AL) and analogues are presented in Table 3, while their structures are schematically represented in Scheme 4.

A study by Nagano et al. [37] showed that the fluorescence spectrum of coumarylAL (CAL), an analogue of LH_2 bearing an amino group, is practically independent of solvent polarity, whereas in general those of AL, naphtylAL (NAL) and quinolylAL (QAL) shift to red in more polar solvents, even though there is no discernible pattern when solvents of medium polarity are taken into account. CAL also differs from the other amino analogues in that it displays fluorescence at lower wavelengths than D-LH_2.

An emission peak at 450 nm in buffer was reported for glycine-D-AL (Gly–AL) [30]. The authors proposed that the lower ionisation level of the glycine group could be responsible for the low fluores-

Table 5
Absorption and emission spectra of $OxyLH_2$ analogues.

Compound	Solvent (E_T (kcal mol^{-1}))	λ_{abs} (nm)	λ_{em} (nm) (quantum yield)	Refs.
($^-$O)-DMOxyLH$_2$	Tris–acetate buffer[a]	485	639	[40]
	DMSO (0.444)	–	630 (0.53)	[32]
	Methanol (0.762)	–	630 (0.08)	[32]
	2-Propanol (0.546)	–	624 (0.29)	[32]
	Acetonitrile (0.460)	–	624 (0.26)	[32]
	Chloroform (0.259)	–	588 (0.75)	[32]
	Benzene (0.111)	–	541 (0.82)	[32]
	p-Xylene (0.074)	–	541 (0.46)	[32]
DMOxyLH$_2$	Water (1.000)	486	640[c] (0.04)	[32]
	p-Xylene (0.074)	366	~420 (0.001)	[32]
	Benzene (0.111)	366	~420 (0.001)	[32]
	DMSO, excess PhOK	580	633 (0.62)	[28]
	Methanol (0.762)	388	526 (0.19)	[32]
	DMSO (0.444)	579	522 (0.07)	[32]
	2-Propanol (0.546)	526	504 (0.11)	[32]
	Acetonitrile (0.460)	372	479 (0.03)	[32]
	Chloroform (0.259)	370	454 (0.001)	[32]
MOxyLH$_2$ dianion	Tris–acetate buffer[a]	440	550	[40]
DHOxyLH$_2$	Water (1.000)	361	541 (0.156)	[39]
	DMSO (0.444)	367	451 (0.185)	[39]
	Dimethylformamide (0.386)	365	449 (0.212)	[39]
	1-Butanol (0.586)	363	441 (0.42)	[39]
	Ethanol (0.654)	362	440 (0.242)	[39]
	Methanol (0.762)	361	440 (0.073)	[39]
	2-Propanol (0.546)	361	439 (0.262)	[39]
	CCl_4 (0.052)	367	439 (0.676)	[39]
	Hexane (0.009)	360	439 (0.283)	[39]
	Toluene (0.099)	366	439 (0.711)	[39]
	Benzene (0.111)	366	438 (0.767)	[39]
	1,2-Dichloroethane (0.327)	359	436 (0.610)	[39]
	m-Xylene	367	435 (0.601)	[39]
	Acetone (0.355)	358	434 (0.51)	[39]
	Acetonitrile (0.460)	355	434 (0.883)	[39]
	Dichloromethane (0.309)	348	434 (0.40)	[39]
	Chloroform (0.259)	356	433 (0.279)	[39]
	Ethyl acetate (0.228)	359	432 (0.544)	[39]
MDMOxyLH$_2$	p-Xylene (0.074)	368	Weak	[32]
	Water (1.000)	~380[b]	535	[32]
	Methanol (0.762)	378	505 (0.12)	[32]
	DMSO (0.444)	380	499 (0.008)	[32]
	2-Propanol (0.546)	380	487 (0.02)	[32]
	Acetonitrile (0.460)	373	478 (0.02)	[32]
	Chloroform (0.259)	380	454 (0.002)	[32]
	Benzene (0.111)	371	440 (0.001)	[32]

[a] 2 mM EDTA, 10 mM $MgSO_4$, 1 mM dithiothreitol.
[b] Not determined accurately due to decomposition of the substrate.
[c] Fluorescence attributed to the phenolate ion.

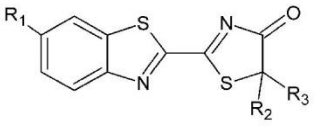

R_1 = H, R_2 = R_3 = H: DHOxyLH_2
R_1 = OH, R_2 = H, R_3 = CH3: MOxyLH_2
R_1 = OH, R_2 = R_3 = CH_3: DMOxyLH_2
R_1 = CH_3O, R_2 = R_3 = CH_3: MDMOxyLH_2

Scheme 5. OxyLH_2 analogues.

cence peak, tying the result to earlier experiments by another group on MeOLH_2 and analogues.

2.3. OxyLH_2

The data referring to the absorption and emission of OxyLH_2 are presented in Table 4, while their structures are schematically represented in Scheme 2.

As with D-LH_2 and some of its analogues, the phenolate ion of OxyLH_2 emits closer to red than its protonated form [32,38]. Spectroscopic studies with an ample range of solvents showed that there is no linearity between solvent polarity and emission wavelength, possibly due to the presence of several forms of OxyLH_2 in solution [32,38].

In an article regarding the spectral–structural effect of the equilibria between these forms, Naumov and Kochunnoonny stated that if only the enol-enolate-keto equilibrium is taken into account, greater solvent polarity does not necessarily translate into a greater redshift in luminescence [39].

2.4. OxyLH_2 analogues

The data referring to the absorption and emission of OxyLH_2 analogues are presented in Table 5, while their structures are schematically represented in Scheme 5.

Substitution of both hydrogen atoms in the thiazolone moiety for methyl groups shifted the emission peak towards greater wavelengths, with the phenolate form emitting closer to red than the neutral form. Further substitution of the hydroxyl in position 6′ for a methoxy group caused a small blueshift [32] for 6′-methoxy-5,5-dimethylOxyLH_2 (MDMOxyLH_2), parallel to the effect observed for MeOLH_2 [27]. This analogue showed decomposition in water, presumably due to hydrolysis of the thiazolone ring.

MDMOxyLH_2 and 5,5-dimethylOxyLH_2 (DMOxyLH_2) absorbed at around the same wavelengths in solvents of different polarity and showed considerable diversity in emission maxima. Additionally, both compounds presented very low quantum yields in less polar solvents. By comparing their emission spectra with that of bioluminescence, the authors ruled out the neutral form of OxyLH_2 as the light-emitting species [32].

Ugarova proposed that while 5-methylOxyLH_2 (MOxyLH_2), like OxyLH_2, can exist in six forms, DMOxyLH_2 can only be found in its phenolate and 6′-OH forms, as the steric hindrances caused by the two methyl groups obstruct any significant changes in the adjacent C–O double bond [40].

DehydroxyOxyLH_2 (DHOxyLH_2) emitted at 541 nm in water and produced mostly violet light (432–451 nm) in several solvents of lower polarity. The authors attributed these results to the role of the hydroxyl anion in lowering the energy of the excited state at physiological pH, which would partially account for a redshift of the emitted light; in the absence of this group, and as a result of inefficient charge transfer, DHOxyLH_2 can only emit orange light [39].

Table 6
Bioluminescence of D-LH_2, OxyLH_2 and analogues.

Compound	Enzyme	Bioluminescence (nm)	Refs.
D-LH_2	Luc	560	[30]
AL	Luc	596	[37]
CAL	Luc	500	[37]
D-AL	Luc	578	[30]
DMAL	Luc	615	[37]
DMCAL	Luc	526	[37]
DMNAL	Luc	564	[37]
DMQAL	Luc	601	[37]
Enolate-OxyLH_2	Luc	556	[40]
Enol-OxyLH_2	Luc	587	[40]
Gly–AL	Luc	570	[30]
Keto-OxyLH_2	Luc	618	[40]
MAL	Luc	615	[37]
MCAL	Luc	515	[37]
MNAL	Luc	560	[37]
MQAL	Luc	588	[37]
NAL	Luc	559	[37]
QAL	Luc	570	[37]
MOxyLH_2 dianion	Luc	450	[37]
AL	CBRLuc	582	[37]
CAL	CBRLuc	499	[37]
NAL	CBRLuc	547	[37]
QAL	CBRLuc	548	[37]
D-DMLH_2-AMP	PplGR	624	[41]
	Ppy	560	[41]
D-DMLH_2	Ppy, Luc, PplGR	No emission	[41]

3. Bioluminescence

3.1. Bioluminescence emission by OxyLH_2 analogues

The data referring to bioluminescence emission by OxyLH_2 analogues is presented in Table 6.

No bioluminescence was observed for 5,5-dimethylLH_2 (DMLH_2). It was suggested that the addition of the two methyl groups interferes with the orientation of the carboxylate ion, ultimately preventing the adenylation of the compound due to steric hindrances. Spectroscopic studies of its adenylated form (DMLH_2-AMP) show that these hindrances may also have a negative influence in the oxidation step of the reaction [41]. Analysis of the Ppy- and PplGR-catalysed reactions involving D-DMLH_2-AMP, of which DMOxyLH_2 was the resulting compound, led the authors to conclude that red and green bioluminescence could be attributed to the keto form of this product [41].

Methylation of NAL was shown to cause a minor variation in its bioluminescence spectrum. Methyl- and dimethyl-forms of AL, QAL and CAL absorbed and emitted light at greater wavelengths [37].

3.2. Bioluminescence emission by point mutated luciferase enzymes

The data referring to bioluminescence emission by point mutated luciferase enzymes is presented in Table 7.

Point mutations of residues His245, Arg215, Thr343 or Arg337 were shown to change the emission peak of *Photinus pyralis* luciferase towards the red region. The authors noted that there was no correlation between polarizability and emission wavelength for His245 mutants, and that the consequent spectral changes can possible be explained by a combination of effects of the protein microenvironment as a whole rather than by particular properties of residues that were introduced, pointing out that native muta-

Table 7
Bioluminescence of wild-type and mutated luciferases [12].

Enzyme (inset: mutation)	Bioluminescence (nm)
Luciola mingrelica	570
Ser286Lys	608
Ser286Gln	609
Ser286Tyr	613
Ser286Leu	619
His433Tyr	606
Luciola cruciata	562
Ser286Asn	607
Gly326Ser	609
His433Tyr	612
Pro452Ser	595
Photinus pyralis	562
Native	558
His245Phe	595
His245Ala	604
His245Arg	579
His245Gln	606
His245Asn	613
His245Asp	617
Thr343Ser	560
Thr343Ala	617
Arg218Lys	572
Arg218Gln	608
Arg218Ala	611
Arg337Lys	595
Arg337Gln	594
Hotaria parvula	568
His433Tyr	610
Phrixothrix viviani	549
Arg215Ser	589

tions of residues distant from the active site also produced redshift [12].

Mutations of Ser286 for amino acids which increased the orientation polarizability in that position were responsible for redshifts in *Luciola cruciata* and *Luciola mingrelica* luciferases [12]. Substitution of the hystidine residue in position 433 for a tyrosine caused a redshift in both enzymes [12] and produced the same result in that of *Hotaria parvula* [40].

4. Conclusion

The effect of variations in pH and temperature on the emitted light has been confirmed in several instances and is uncontroversial in respect to D-LH_2. It is known that either a decrease in pH or an increase in temperature leads to a redshift in its fluorescence wavelength. Additionally, consistent evidence pointing to a difference between the emission spectra of the neutral ligands and those of their respective phenolate ions, with the latter forms tending to emit light closer to red, further support the role of pH in colour modulation.

It has been established, however, that these factors alone would not control the light-emitting process in its entirety. As other studies with analogues of D-LH_2 and OxyLH_2 indicated that they were affected differently by pH and temperature changes, it became clear that other aspects of the system had to be taken into account. Spectroscopic studies of LH_2-related compounds in various mediums were carried out in an effort to correlate emission wavelength and solvent polarity, and despite the lack of linearity between the two, it has been proven that in general more polar solvents (i.e. water and methanol) cause a redshift compared to mediums of very low polarity.

For their prospective applications as substrates in bioluminescence assays, analogues of D-LH_2 and OxyLH_2 were analysed in regards to their spectroscopic properties under enzyme-catalysed reaction with various luciferases (most notably Luc and Ppy), and while these studies were not focused or conclusive in the search for correlations between light emission and external factors (either environmental or compound-related), they may also benefit from any significant discoveries on this subject, advancing the enhancement of the Luc system in its current medical and analytical uses.

There has also been an attempt to understand the individual role of certain residues in the active site of firefly luciferase and in what capacity a modification in those positions would affect the bioluminescence reaction. Synthetic and natural mutants of luciferases effectively produced a wider range of colours than the respective wild types, and a redshifting effect was attributed to the insertion of positive residues in the active site. Nevertheless, there are no definitive answers concerning a specific position that stands out from the others, and it has been noted that the modification of residues further away from the active site is not inconsequential, which adds to the difficulty of narrowing down the search for key regions in the enzyme. Such results emphasise the current assumption that the research on the overall mechanism of colour modulation must not take the possible factors into account separately, but rather encompass all the variables that are known to influence the outcome of the light-emitting process and eventually uncover any connections between them.

Acknowledgments

Financial support from Fundação para a Ciência e Tecnologia (FCT, Lisbon) (Programa Operacional Temático Factores de Competitividade (COMPETE) e comparticipado pelo Fundo Comunitário Europeu (FEDER) (Project PTDC/QUI/71366/2006) is acknowledged. A Ph.D. Grant to Luís Pinto da Silva (SFRH\76612\2011), attributed by FCT, is also acknowledged.

References

[1] S.M. Marques, J.C. Esteves da Silva, Firefly bioluminescence. a mechanistic approach of luciferase catalyzed reactions, IUBMB Life 61 (1) (2009) 6–17.
[2] J.M. Leitão, J.C. Esteves da Silva, Firefly luciferase inhibition, J. Photochem. Photobiol. B. 101 (1) (2010) 1–8.
[3] V.R. Viviani, F.G. Arnoldi, A.J. Neto, T.L. Oehlmeyer, E.J. Bechara, Y. Ohmiya, The structural origin and biological function of pH-sensitivity in firefly luciferases, Photochem. Photobiol. Sci. 7 (2) (2008) 159–169.
[4] L.P. da Silva, J.C. Esteves da Silva, Computational studies of the luciferase light-emitting product: oxyluciferin, J. Chem. Theory Comput. 7 (4) (2011) 809–817.
[5] L.P. da Silva, J.C. Esteves da Silva, Computational investigation of the effect of pH on the color of firefly bioluminescence by DFT, ChemPhysChem 12 (5) (2011) 951–960.
[6] S.F. Chen, Y.J. Liu, I. Navizet, N. Ferre, W.H. Fang, R. Lind, Systematic theoretical investigation on the light emitter of firefly, J. Chem. Theory Comput. 7 (3) (2011) 798–803.
[7] C.I. Song, Y.M. Rhee, Dynamics on the electronically excited state surface of the bioluminescent firefly luciferase-oxyluciferin system, J. Am. Chem. Soc. 133 (31) (2011) 12040–12049.
[8] M. Matsumoto, Advanced chemistry of dioxetane-based chemiluminescent substrates originating from bioluminescence, J. Photochem. Photobiol. C. 5 (1) (2004) 27–53.
[9] L. Pinto da Silva, J.C.G. Esteves da Silva, Firefly chemiluminescence and bioluminescence. Efficient generation of excited states, ChemPhysChem 13 (9) (2012) 2257–2262.
[10] J.Y. Hasegawa, K.J. Fujimoto, H. Nakatsuji, Color tuning in photofunctional proteins, ChemPhysChem 12 (17) (2011) 3106–3115.
[11] S. Hosseinkhani, Molecular enigma of multicolor bioluminescence of firefly luciferase, Cell Mol. Life Sci. 68 (7) (2011) 1167–1182.
[12] N.N. Ugarova, L.Y. Brovko, Protein structure and bioluminescent spectra for firefly bioluminescence, Luminescence 17 (5) (2002) 321–330.
[13] L.P. da Silva, J.C. Esteves da Silva, Theoretical modulation of the color of light emitted by firefly oxyluciferin, J. Comput. Chem. 32 (12) (2011) 2654–2663.
[14] L.P. da Silva, J.C. Esteves da Silva, Study on the effects of intermolecular interactions on firefly multicolor bioluminescence, ChemPhysChem 12 (16) (2011) 3002–3008.

[15] L.P. da Silva, J.C. Esteves da Silva, TD-DFT/molecular mechanics study of the Photinus pyralis bioluminescence system, J. Phys. Chem. B. 116 (6) (2012) 2008–2013.
[16] L.P. da Silva, J.C. Esteves da Silva, Theoretical analysis of the color tuning mechanism of oxyluciferin and 5-hydroxyoxyluciferin, Comput. Theor. Chem. 988 (2012) 56–62.
[17] A. Tagami, N. Ishibashi, D. Kato, N. Taguchi, Y. Mochizuki, H. Watanabe, M. Ito, S. Tanaka, Ab initio quantum-chemical study on emission spectra of bioluminescent luciferases by fragment molecular orbital method, Chem. Phys. Lett. 472 (1–3) (2009) 118–123.
[18] N. Nakatani, J.Y. Hasegawa, H. Nakatsuji, Red light in chemiluminescence and yellow–green light in bioluminescence. Color-tuning mechanism of firefly, *Photinus pyralis*, studied by the symmetry-adapted cluster-configuration interaction method, J. Am. Chem. Soc. 129 (28) (2007) 8756–8765.
[19] B.R. Branchini, T.L. Southworth, M.H. Murtiashaw, R.A. Magyar, S.A. Gonzalez, M.C. Ruggiero, J.G. Stroh, An alternative mechanism of bioluminescence color determination in firefly luciferase, Biochemistry 43 (23) (2004) 7255–7262.
[20] C.G. Min, A.M. Ren, J.F. Guo, Z.W. Li, L.Y. Zou, J.D. Goddard, J.K. Feng, A time-dependent density functional theory investigation on the origin of red chemiluminescence, ChemPhysChem 11 (1) (2010) 251–259.
[21] A. Roda, M. Guardigli, Analytical chemiluminescence and bioluminescence. Latest achievements and new horizons, Anal. Bioanal. Chem. 402 (1) (2012) 69–76.
[22] L. Mezzanotte, I. Que, E. Kaijzel, B.R. Branchini, A. Roda, C. Löwik, Sensitive dual color in vivo bioluminescence imaging using a new red codon optimized firefly luciferase and a green click beetle luciferase, PLoS ONE 6 (4) (2011) e1. 9277.
[23] B.R. Branchini, E. Michelini, L. Cenenini, A. Roda, A portable bioluminescence engineered cell-based biosensor for on-site applications, Biosens. Bioelectron. 26 (8) (2011) 3647–3653.
[24] S.M. Marques, F. Peralta, J.C. Esteves da Silva, Optimized chromatographic and bioluminescent methods for inorganic pyrophosphate based on its conversion to ATP by firefly luciferase, Talanta 77 (4) (2009) 1497–1503.
[25] S.M. Marques, J.C. Esteves da Silva, An optimized luciferase bioluminescent assay for coenzyme A, Anal. Bioanal. Chem. 391 (6) (2008) 2161–2168.
[26] E. Michelini, L. Cenenini, L. Mezzanotte, A. Roda, Luminescent probes and visualization of bioluminescence, Methods Mol. Biol. 574 (2009) 1–13.
[27] R.A. Morton, T.A. Hopkins, H.H. Seliger, Spectroscopic properties of firefly luciferin and related compounds; an approach to product emission, Biochemistry 8 (4) (1969) 1598–1607.
[28] E.H. White, M.G. Steinmetz, J.D. Miano, P.D. Wildes, R. Morland, Chemi- and bioluminescence of firefly luciferin, J. Am. Chem. Soc. 102 (9) (1980) 3199–3208.
[29] V.R. Viviani, The origin, diversity, and structure function relationships of insect luciferases, Cell. Mol. Life Sci. 59 (2002) 1833–1850.
[30] R. Shinde, J. Perkins, C.H. Contag, Luciferin derivatives for enhanced in vitro and in vivo bioluminescence assays, Biochemistry 45 (37) (2006) 11103–11112.
[31] V.R. Viviani, F.G.C. Arnoldi, A.J.S. Neto, T.L. Oehlmeyer, E.J.H. Bechara, Y. Ohmiya, The structural origin and biological function of pH-sensitivity in firefly luciferases, Photochem. Photobiol. Sci. 7 (2008) 159–169.
[32] T. Hirano, Y. Hasumi, K. Ohtsuka, S. Maki, H. Niwa, M. Yamaji, D. Hashizume, Spectroscopic studies of the light-color modulation mechanism of firefly (beetle) bioluminescence, J. Am. Chem. Soc. 131 (2009) 2385–2396.
[33] J. Jung, C. Chin, P. Song, Electronic excited states of D-(-)-luciferin and related chromophores, J. Am. Chem. Soc. 98 (13) (1976) 3949–3954.
[34] I. Presiado, Y. Erez, D. Huppert, Excited-state intermolecular proton transfer of the firefly's chromophore D-luciferin. 2. Water–methanol mixtures, J. Phys. Chem. A. 114 (35) (2010) 9471–9479.
[35] Y. Erez, D. Huppert, Excited-state intermolecular proton transfer of the firefly's chromophore D-luciferin, J. Phys. Chem. A. 114 (31) (2010) 8075–8082.
[36] Y. Erez, I. Presiado, R. Gepshtein, D. Huppert, Excited-state intermolecular proton transfer of firefly luciferin IV. Temperature and pH dependence, J. Phys. Chem. A. 115 (9) (2011) 1617–1626.
[37] H. Takakura, K. Sasakura, T. Ueno, Y. Urano, T. Terai, K. Hahaoka, T. Tsuboi, T. Nagano, Development of luciferin analogues bearing an amino group and their application as BRET donors, Chem. – An Asial J. 5 (2010) 2053–2061.
[38] P. Naumov, Y. Ozawa, K. Ohkubo, S. Fukuzumi, Structure and spectroscopy of oxyluciferin, the light emitter of the firefly bioluminescence, J. Am. Chem. Soc. 131 (32) (2009) 11590–11605.
[39] P. Naumov, M. Kochunnoonny, Spectral–structural effects of the keto–enol–enolate and phenol–phenolate equilibria of oxyluciferin, J. Am. Chem. Soc. 132 (33) (2010) 11566–11579.
[40] N.N. Ugarova, Interaction of firefly luciferase with substrates and their analogs: a study using fluorescence spectroscopy methods, Photochem. Photobiol. Sci. 7 (2008) 218–227.
[41] B.R. Branchini, M.H. Murtiashaw, R.A. Magyar, N.C. Portier, M.C. Ruggiero, J.G. Stroh, Yellow–green and red firefly bioluminescence from 5,5-dimethyloxyluciferin, J. Am. Chem. Soc. 124 (10) (2002) 2112–2113.

1.4. Firefly Bioluminescent Reaction

Firefly bioluminescence is a complex phenomenon, which is based on a two-step enzymatic reaction catalyzed by luciferase (Fig. 3). The first step is an adenylation involving the carboxylic group at the thiazolone moiety of D-LH_2 and the phosphate groups of ATP, in the presence of Mg^{2+}.[22] In the second step LH_2-AMP is oxidized in the presence of molecular oxygen, giving origin to $OxyLH_2$ and the release of adenoside-5'-monophosphate (AMP) and carbon dioxide (CO_2). $OxyLH_2$ is formed in a singlet excited state, subsequently decaying to the ground state with emission of green-red light (530-640 nm), depending on the firefly species.[5,13]

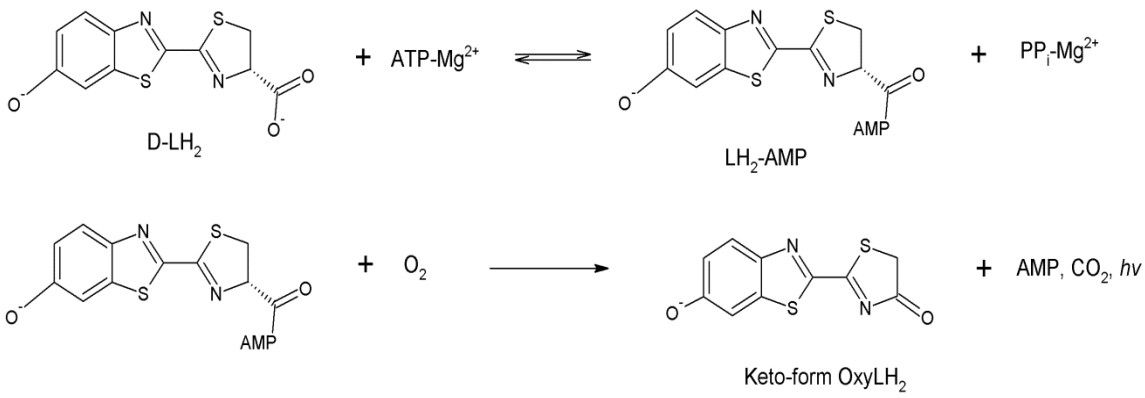

Figure 3 – Overall reaction mechanism of firefly bioluminescence.

It is generally accepted that the phenolic group of D-LH_2 is deprotonated in the bioluminescent reaction, and it is its anionic species that is converted into $OxyLH_2$. The adenylation reaction is depicted as a S_N2 nucleophilic displacement (Fig. 4), where the oxygen attack of the electrophilic phosphorus at the α-phosphoryl group of ATP displaces inorganic pyrophosphate (PP_i), and transfers the adenylate moiety to the carboxylic group of the substrate.[22]

In the second step luciferase acts as an oxygenase, oxidizing LH_2-AMP and generating a dioxetanone intermediate (Fig. 5).[22-24] To oxidize this adenylate, luciferase is thought to abstract the C_4 proton producing a carbanion.[12,22,24] This proton abstraction is assisted by the adenylation of D-LH_2, as the AMP moiety increases the acidity of the C_4 proton.[12,22,24] Subsequently, the carbanion is the target of a nucleophilic attack from molecular oxygen, which leads to the formation of a linear hydroperoxide.[22,25] The next step is a intramolecular nucleophilic attack of the hydroperoxide group, supported by the release of AMP.

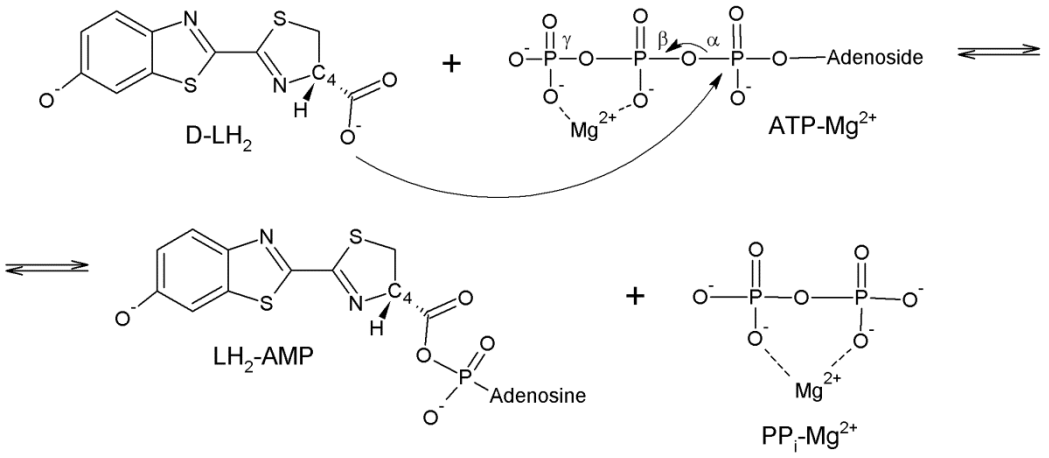

Figure 4 – Formation of LH_2-AMP from the adenylation reaction between D-LH_2 and ATP-Mg^{2+}.

This last partial reaction leads to the formation of the dioxetanone intermediate, generally referred as firefly dioxetanone.[22,25] It is the decomposition of this high-energy compound that allows the formation of excited state $OxyLH_2$.[22,25]

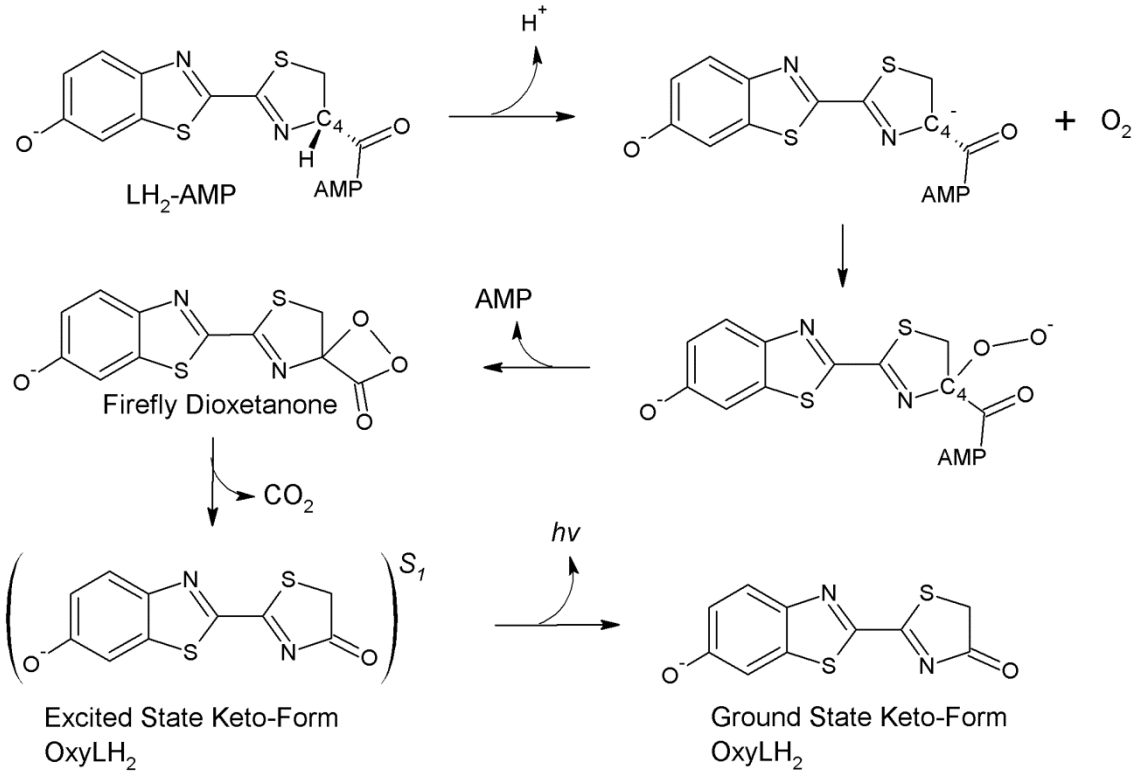

Figure 5 – Formation and decomposition of firefly dioxetanone, with subsequent light emission from $OxyLH_2$.

While this carbanion-based mechanism has been proposed and generally accepted by more than forty years, it is indeed problematic that the dioxetanone intermediate is stated to be formed from unactivated triplet oxygen in a spin forbidden process. In order to overcome this problem, two new mechanisms were recently proposed: a radical mechanism based on molecular oxygen abstraction of a C_4 H atom (Fig. 6A), and a single electron-transfer (SET) mechanism involving superoxide anion formation (Fig. 6B).[26,27] Nevertheless, these mechanisms are still very hypothetical in nature.

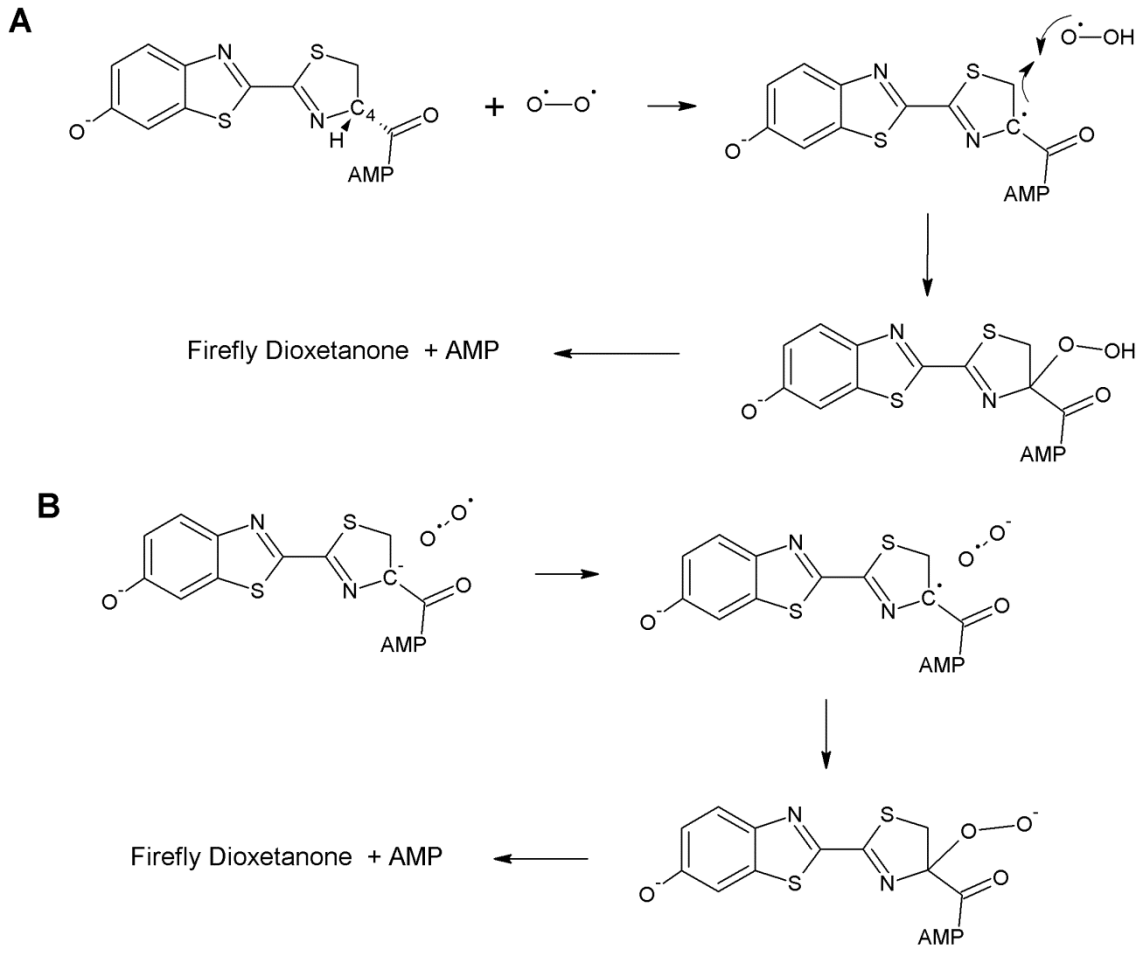

Figure 6 – Schematic representation of the radical (A) and single electron transfer (B) oxidation mechanisms for firefly dioxetanone formation.

It is important to note that these reaction mechanisms were obtained in an indirect way through experimental studies, and still it is not well known the role of luciferase in which reaction step. It is also not clear which the protonation state is of D-LH_2, LH_2-

AMP, $OxyLH_2$ and firefly dioxetanone inside luciferase, although the fact that they are generally regarded as anionic.

1.5. Formation of Excited State $OxyLH_2$ due to the Decomposition of Firefly Dioxetanone

Article 2

Firefly Chemiluminescence and Bioluminescence: Efficient Generation of Excited States

Luís Pinto da Silva and Joaquim C.G. Esteves da Silva

ChemPhysChem **2012**, *13*, 2257-2252.

The bibliographic research and the writing of the paper were performed by Luís Pinto da Silva, under supervision of Professor Joaquim Esteves da Silva.

CHEMPHYSCHEM MINIREVIEWS

DOI: 10.1002/cphc.201200195

Firefly Chemiluminescence and Bioluminescence: Efficient Generation of Excited States

Luís Pinto da Silva and Joaquim C. G. Esteves da Silva*[a]

Firefly luciferase catalyzes a light-emitting reaction in which an excited-state product is formed. Both experimental and theoretical methodologies are used to study this system, and the reactions catalyzed by luciferase are relatively well characterized. However, the mechanism by which an excited-state product is formed is still unknown. This Minireview deals with the current understanding of firefly bioluminescence and chemiluminescence. Thermal decomposition of simple 1,2-dioxetanes is also discussed, due to their role in formation of the excited-state bioluminophore.

1. Introduction

Chemiluminescence is the emission of light that results from a chemical reaction in which excited-state products are formed.[1] This phenomenon is thought to arise from a crossing point between the ground-state and excited-state potential energy surfaces (PES) on the reaction coordinate (Scheme 1).[1,2] The efficiency of chemiluminescence is described in terms of quantum yield, which is controlled by the efficiency of the chemical reaction, the efficiency of crossing from the ground to the excited state, and the efficiency of fluorescence of the excited-state product.[1] Most of the known chemiluminescence substrates have a peroxide bond (O—O).[1,2] The basic scaffold of the most important family of chemiluminescence substrates is represented by 1,2-dioxetane (see Scheme 5, below).

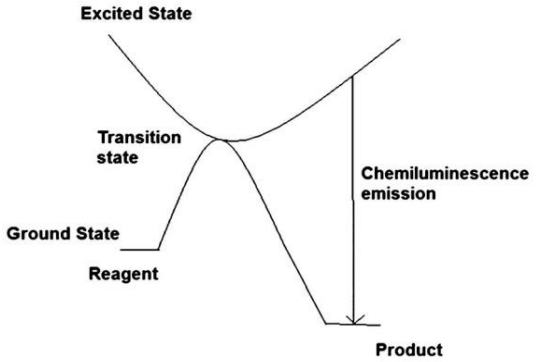

Scheme 1. Schematic of the chemiluminescence mechanism.

When chemiluminescence occurs in living organisms by an enzyme-catalyzed reaction, it is called bioluminescence.[1] This enzyme is generally termed luciferase, despite its showing different structures and amino-acid contents for different bioluminescent organisms.[3] This phenomenon can be found in bacteria, dinoflagellates, fungi, crustaceans, worms, insects, and fishes.[3,4] The better-characterized system is that of the North American firefly *Photinus pyralis*. Firefly luciferase (Luc) catalyzes a two-step reaction: firefly luciferin (LH_2, Scheme 2) reacts with adenosine-5′-triphosphate (ATP) to generate an adenylyl intermediate (LH_2-AMP, Scheme 2); in the second step, LH_2-AMP is oxidized in the presence of atmospheric oxygen, releasing CO_2, firefly oxyluciferin ($OxyLH_2$) and adenosine-5′-monophosphate (AMP).[5–8]

Studies aimed at characterization of the bioluminescence reaction allowed the development of several Luc-based techniques. These rely on various intrinsic and advantageous characteristics of this system: specificity, sensitivity, high quantum yield (45–61%),[9] speed of reaction, and possibility of color modulation. Nowadays, Luc has gained numerous biomedical, pharmaceutical, and bioanalytical applications. More specifically, it is used in analytical determination of ATP, microbial detection, biosensing, bioimaging, and as a gene reporter.[10–16]

Many good reviews have been written on the color-tuning mechanism,[17–20] Luc-catalyzed reactions,[4,5,7,8,21] firefly inhibition,[6] and general chemiluminescence of several chemiluminescence substrates.[1,2,22–26] Hence, we focus on the experimental and theoretical findings regarding the mysterious generation of excited-state $OxyLH_2$. The chemistry of 1,2-dioxetanes is also addressed, due to its relevance to firefly bioluminescence and chemiluminescence.

2. Firefly Light Emission

2.1. Bioluminescence Reaction Mechanism

The firefly bioluminescence reaction is an S_N2 nucleophilic displacement which involves the carboxyl group of LH_2 and the

[a] *Dr. L. Pinto da Silva, Prof. Dr. J. C. G. Esteves da Silva*
Centro de Investigação em Química (CIQ-UP)
Departamento de Química e Bioquímica
Faculdade de Ciências da Universidade do Porto
Rua do Campo Alegre 687
4169-007 Porto (Portugal)
E-mail: jcsilva@fc.up.pt

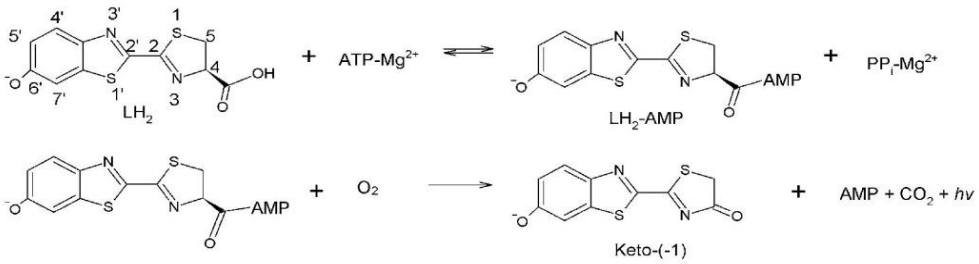

Scheme 2. Bioluminescence reaction mechanism.

phosphate groups of ATP.[27–29] After the adenylation step, LH_2-AMP loses a proton from the C4 atom, creating a carbanion. This occurs because ATP increases the acidity of C4.[30] Subsequently, the carbanion undergoes nucleophilic attack by atmospheric oxygen, and a linear hydroperoxide is formed.[31] The next step of the reaction is an intramolecular nucleophilic attack of the hydroperoxy group, favored by AMP release. This step forms a high-energy intermediate, namely, firefly dioxetanone (Scheme 3), which is a member of the 1,2-dioxetane family of chemiluminescence substrates.[32] This step is the key to firefly bioluminescence, as decomposition of this intermediate leads to formation of singlet excited-state $OxyLH_2$, which then decays to the ground state with emission of light.[1,2,33–35] The involvement in bioluminescence of a dioxetanone intermediate was supported by double-labeling experiments with ^{18}O and $H_2{}^{16}O$,[36] which demonstrated that a major portion of the CO_2 produced contained one atom of ^{18}O, and thus suggested that one oxygen atom in CO_2 arises from the atmospheric oxygen that oxidized LH_2 and not from the solvent.

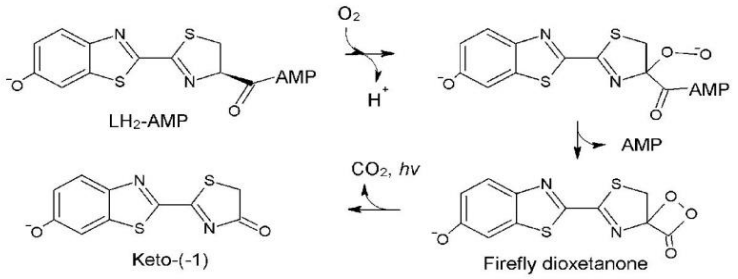

Scheme 3. Formation and decomposition of firefly dioxetanone.

For a correct description of the bioluminescence phenomenon, exact identification of the bioluminophore is essential. However, only rather recently was the anionic keto form of $OxyLH_2$ (Keto-(−1), Scheme 2) identified as the sole light emitter. This conclusion was validated by analysis of the dissociation and tautomeric constants of $OxyLH_2$ as a function of pH,[37] by studying the direct excited-state product of firefly dioxetanone,[38] and by investigating the possibility of keto-enol tautomerism in *Luciola cruciata* Luc (LcLuc) active site.[39] However, these studies are theoretical, and no conclusive experimental evidence was presented so far that validates this conclusion. The bioluminophore decays to the ground state with emission of light (≈562 nm at basic pH).[17–20] Luc is a pH-sensitive enzyme, and at acid pH the emission wavelength is shifted to the red region of the visible spectrum (≈620 nm).[17–20] Both experimental and theoretical studies have indicated that this multicolor bioluminescence is caused by changes in the conformation of the active site.[4,38–49] These changes increase the polarity of the active site with decreasing pH and affect the electrostatic, π–π stacking, and hydrogen-bonding interactions formed between the bioluminophore and active-site molecules.

It is known that methylation of the benzothiazole oxygen atom greatly decreases the efficiency of bioluminescence, which indicates a role of intramolecular charge-transfer involving the phenolate anion in the formation of Keto-(−1).[50] Currently, there are two mechanisms that try to rationalize the role of charge transfer in dioxetanone decomposition: chemically initiated electron-exchange luminescence (CIEEL)[51–54] and charge transfer induced luminescence (CTIL).[55] In the CIEEL mechanism a radical ion pair is formed by electron transfer from the electron-donating fragment to the dioxetanone moiety. Subsequently, a back electron transfer annihilates the radical ion pair, yielding singlet excited state Keto-(−1). In the CTIL mechanism, a charge-transfer diradical species is generated by breaking of the dioxetanone O–O bond. Formation of the diradical species is immediately followed by subsequent dioxetanone C–C bond breaking with simultaneous back charge transfer, which is responsible for accessing the singlet excited state. However, both the CTIL/CIEEL mechanisms and firefly dioxetanone structure were not characterized by direct experimental evidence, and remain only a possible way for the efficient generation of singlet excited-state Keto-(−1).

2.2. Firefly Chemiluminescence

Besides bioluminescence, $OxyLH_2$ also exhibits chemiluminescence. This latter phenomenon gained attention from biolu-

minescence researchers due to difficulties in isolating/identifying the bioluminophore by using radioactive and spectroscopic techniques. Hopkins et al. studied the chemiluminescence of LH_2-AMP and 5,5-dimethyl-luciferin-adenylate ($DMLH_2$-AMP) in DMSO and in basic aqueous solution.[56] For both compounds, red chemiluminescence was observed in different solvents (≈629 nm in DMSO and ≈649 nm in water). The different emission wavelengths suggested a redshift with increasing polarity of the microenvironment.[56] Furthermore, it was found that the fluorescence of spent chemiluminescence reaction mixtures in DMSO was identical to the chemiluminescence of LH_2-AMP and $DMLH_2$-AMP. These authors have also noticed a similarity between firefly chemiluminescence and the chemiluminescence of lophine derivatives and of acridinium carboxylic acids.[57,58] This finding thus associated firefly chemiluminescence with dioxetanone decomposition. Further evidence for this association was also highlighted in this work: the chemiluminescence of LH_2 proceeded more slowly when this molecule was labeled at C4 with deuterium; $DMLH_2$ (Scheme 4) must be bonded to a conjugate base of a strong acid for efficient chemiluminescence; 6′-methyl-LH_2 ($MOLH_2$, Scheme 4) is ineffective in both chemi- and bioluminescence.

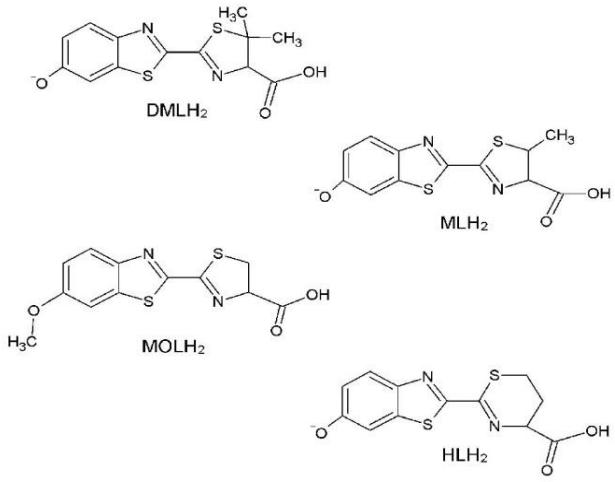

Scheme 4. LH_2 analogues.

The firefly chemiluminescence reaction mechanism was further studied by McCapra et al.[59] Previous work by these researchers allowed them to suggest that firefly chemiluminescence occurs through formation of a reactive four-membered peroxide intermediate.[60,61] They supported the findings of Hopkins et al.[56] by studying the chemiluminescence of a phenyl ester derivative of $DMLH_2$ in DMSO.[59] This compound showed bright red chemiluminescence, the emission spectrum of which was identical to fluorescence spectrum of the supposed chemiluminophore, 5,5-dimethyl-oxyluciferin (DMOxy-LH_2).[59] McCapra also presented an explanation of why an excited-state product is formed by ring opening. He postulated that if the decomposition is concerted, conservation of orbital symmetry in the formation of the products necessarily results in the excitation of one of the fragments.[62]

So far, experimentalists had only observed red chemiluminescence. However, in 1969, White et al. reported base concentration dependent shifts in the chemiluminescence emission.[63,64] The phenyl esters of LH_2 and 5-methyl-LH_2 (MLH_2, Scheme 4) show red chemiluminescence in DMSO (≈631 nm), and red and yellow-green chemiluminescence when more base was added to the reaction mixture. An even larger amount of base lead exclusively to yellow-green emission (≈556 nm). This base-dependent emission lead these authors to suggest that red chemi-/bioluminescence was emitted by Keto-(−1) and that yellow-green emission was caused by Enol-(−2).[63,64] This assignment was supported by the fact that $DMLH_2$ and homoLH_2 (HLH_2, Scheme 4), which are non-enolizable compounds, showed base-independent red chemiluminescence.[63,64]

The findings of these authors thus indicated that light emission should be accompanied by CO_2 liberation. This aspect of firefly chemiluminescence was supported by Plant et al., who studied the decarboxylation of carboxyl-labeled ^{14}C-LH_2. They have found that after the chemiluminescence reaction, 80% of the ^{14}C in the carboxyl group of LH_2 appeared as CO_2.[65] These results were supported by another work regarding decarboxylation of carboxyl-labeled ^{14}C-LH_2.[66] This topic was further explored by White et al.,[67] who studied the chemiluminescence (in DMSO) of an ethoxyvinyl ester analogue of $DMLH_2$, by adding oxygen enriched in ^{18}O to the reaction mixture. Their measurements revealed degrees of ^{18}O incorporation in the chemiluminophore and in CO_2 of 94 and 66%, respectively, which is consistent with the dioxetanone mechanism. Further work of White et al. demonstrated degrees of ^{18}O incorporation in CO_2 produced from LH_2 esters of 57–83%.[68]

Some theoretical studies have been performed on firefly dioxetanone, in order to explain the chemiluminescence of $OxyLH_2$. Wada and Sakai employed a semi-empirical methodology to study the in vacuo decomposition of $OxyLH_2$.[69] They found that firefly dioxetanone may be a unstable transition state, and not an intermediate; that the activation energy on the ground state PES is 37.5 kcal mol^{-1}; and that the singlet excited-state PES approaches the ground state PES in a concave manner, whereby dioxetanone decomposes into Keto-(−1). Thus, they provided an explanation for the formation of singlet excited states. However, the activation barrier present in this work is too high in energy to allow efficient chemiluminescence. Another in vacuo study of firefly dioxetanone demonstrated that the decomposition reaction reaches a transition state by O–O bond breaking.[70] Charge analysis demonstrated that 0.19 e was transferred from the phenoxide to the dioxetanone moiety, and thus indicated a role for charge transfer. When the C–C bond of the dioxetanone moiety is sufficiently elongated, a conical intersection is found between the singlet ground and excited states.

Min et al. employed a density functional approach in the only condensed-phase theoretical study on firefly dioxetanone decomposition in the literature.[71] These authors did not explore the interaction between the singlet ground- and excited-

state PESs, but demonstrated that the activation barrier of the ground-state reaction is only 8.4 kcal mol^{-1} (in diethylamine), which is more realistic than the value presented by Wada and Sakai.[69]

These results, along with those presented in Section 2.1., have demonstrated that a dioxetanone intermediate is indeed responsible for formation of $OxyLH_2$ in the excited state. Furthermore, these results demonstrate that $OxyLH_2$ is formed in the singlet excited state Keto-(−1), and charge transfer is expected to play a role in these phenomena, in the form of the CIEEL or CTIL mechanism. Thus, for a better understanding of the complex firefly chemi-/bioluminescence, it is necessary to clarify the reaction mechanism of dioxetanone formation and decomposition.

3. Thermal Decomposition of 1,2-Dioxetanes

3.1. Decomposition Reaction of 1,2-Dioxetanes

1,2-Dioxetanes received much attention from the research community, due to the suggestion that they are involved in bright chemiluminescence and bioluminescence. The first synthesis of an 1,2-dioxetane (3,3,4-trimethyl-1,2-dioxetane), by Kopecky and Mumford, facilitated the study of these compounds.[72]

This type of chemical system is essential in the chemiluminescence process, as it provides a route for a ground-state chemical reaction to produce excited-state products by thermal decomposition. Therefore, to be efficient chemiluminescence substrates, they must meet an energetic criterion that allows formation of a chemiluminophore by thermal decomposition.[2] This criterion is effectively met by 1,2-dioxetanes: heats of reaction of typical 1,2-dioxetanes are about 69–90 kcal mol^{-1}, while the activation energies range between 20 and 30 kcal mol^{-1}.[26,73] This situation is facilitated by the fact that 1,2-dioxetanes have O–O and C–O bonds, and not S–S/N–N and C–S/C–N bonds. O–O bonds are weaker than S–S/N–N bonds, while C–O bonds are stronger than C–S/C–N bonds. The resulting shortfall in enthalpy would be fatal to excited-state formation in non-oxygen compounds.[1]

Both experiment and theory have established that the decomposition of 1,2-dioxetanes has a merged mechanism.[2,19,74–77] The first phase of the reaction is characterized by O–O bond breaking and some C–C bond stretching. This leads to a biradical species with a broken O–O bond prior to decomposition (by C–C bond breaking). This biradical species has a very short lifetime (< 10 ps), direct experimental characterization of which is difficult.[1] Moreover, experimental and computational studies have determined that ground-state O–O bond breaking of 1,2-dioxetanes is the rate-determining step of chemiluminescence.[78–80]

3.2. Chemiexcitation Mechanisms

The participation of 1,2-dioxetanes in bright light emission was originally proposed to explain the chemiluminescence of lophine, firefly luciferin, and acridinium esters, which produced mainly singlet excited-state products.[1,2] However, it was discovered that simple 1,2-dioxetanes produced mainly triplet excited-state products (with a small amount of singlet excited-state products).[2,74] Therefore, the observed light is very weak. The ratio between triplets and singlets do vary, depending on the structure of 1,2-dioxetanes, but triplet excited-state products were always found to be produced in higher quantities.[74] Due to various experimental problems (difficulties in synthesis, low thermal and catalytic stabilities),[81,82] the formation of excited-state products remained a mystery. To overcome these obstacles, several groups employed different computational methodologies in the study of 1,2-dioxetanes chemiluminescence.[75,76,79,82–84]

Lindh and co-workers employed a state-of-the-art complete active site second-order perturbation theory (CASPT2)/complete active space self-consistent field (CASSCF) approach in an in vacuo study on 1,2-dioxetane,[75] 1,2-dioxetanone,[76] and three different thiazole-modified dioxetanones (Scheme 5).[84]

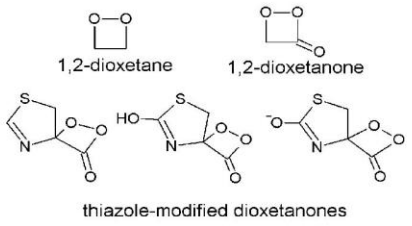

Scheme 5. 1,2-Dioxetane, 1,2-dioxetanone, and thiazole-modified dioxetanones.

Their computational results showed that the decomposition of 1,2-dioxetane reaches a transition state by O–O bond breaking, which is induced by an O-C-C-O torsional motion.[75] The first singlet and triplet excited states were found to be degenerate or near-degenerate with the singlet ground state, near the transition-state region of the PES. The key factor of this mechanism is an entropic trap, which prevents 1,2-dioxetane from quickly decaying to the ground state and allows formation of excited-state products. This means that the molecule is prevented from decaying rapidly toward the ground-state reaction path by entropic effects. Instead, the molecule is forced to spend some time on an almost flat region of the PES, where the singlet ground state is degenerate/near-degenerate with the singlet and triplet excited states. This trapping allows some molecules to cross to the singlet or triplet excited states. Eventually, excited-state formaldehyde decays to the ground state with emission of light.[75] 1,2-Dioxetanone decomposition is characterized by a different reaction mechanism.[76] A biradical transition state is reached by O–O elongation, while the molecule remains planar. After the transition state is reached, C–C bond stretching leads to 1,2-dioxetanone dissociation. Around the biradical intermediate, the ground state reaches an intersystem crossing with the triplet state and a conical intersection with the singlet excited state. These two excited states cross again with the ground state, near a second transition

state, which corresponds to C–C bond breaking. Excited-state formaldehyde is formed, which will subsequently decay to the ground state with emission of light.[76] In the reaction mechanism of the two neutral thiazole-modified dioxetanones, decomposition proceeds with two transition states and one excited-state intermediate.[84] No conical intersection was found between the singlet ground and excited states, but they were found to be sufficiently close in energy to afford formation of excited-state products.

These studies have developed reaction mechanisms that explain the formation of excited-state products by ground-state ring opening. However, the activation energy for the fragmentation step was found to be too high for it to occur in living organisms. This high energy of activation can be explained by the fact that all these 1,2-dioxetanes are neutral molecules, which in both the CIEEL and CTIL mechanisms are inefficient chemiluminescence substrates. In support of this, Lindh and co-workers found that the activation energy for the deprotonated hydroxyl-thiazole-modified dioxetanone is 8 kcal mol^{-1} lower than that in the decomposition of protonated hydroxythiazole-modified dioxetanone.[84] More evidence was provided by Isobe et al.,[55] who demonstrated, by theoretical means, that deprotonation of a phenol-substituted dioxetanone decreases the activation barrier from 19.4 to 3.8 kcal mol^{-1}. These theoretical data are in line with the experimental evidence obtained for the chemiluminescence of bicyclic dioxetanones,[85] and for the bioluminescence of $MOLH_2$.[50] $MOLH_2$ is known to be an inefficient bioluminescence substrate, due to methylation of the benzothiazole oxygen atom, while deprotonation of the phenolic oxygen atom of bicyclic dioxetanones leads to chemiluminescence.

Isobe et al. studied computationally the differences between the CIEEL and CTIL mechanisms.[55] They found that the CTIL mechanism is favored in vacuo, while the CIEEL mechanism is favored in solution. Furthermore, they demonstrated that the chemiluminescence of deprotonated *meta*-phenol-substituted dioxetanone proceeds through the CTIL mechanism. For the deprotonated *para*-phenol-substituted dioxetanone the CIEEL mechanism is favored. Also, their results suggest that the CTIL process may be favored in bioluminescence, due to the fact that this mechanism suppresses some harmful side reactions (e.g. intersystem crossing with the triplet state), contrary to CIEEL.

4. Conclusion

We have reviewed the studies that have tried to characterize firefly chemiluminescence and bioluminescence. Although no direct experimental evidence was found, sufficient data support the involvement of a high-energy dioxetanone intermediate in bright light emission. However, there are some aspects that still require further research.

Both chemiluminescence and bioluminescence reactions produce Keto-(−1) as a singlet excited state. However, decomposition of simple 1,2-dioxetanes yields mainly triplet excited-state products. The mechanism by which triplet products are formed is now rationalized, and some theoretical studies have presented some answers for in vacuo formation of singlet Keto-(−1). However, no satisfactory explanation was given for the absence of triplet excited-state Keto-(−1).

Both theoretical and experimental studies have proven that a charge-transfer mechanism is involved in firefly chemiluminescence and bioluminescence. The CIEEL and CTIL mechanisms were developed in order to explain the role of charge transfer in the formation of excited-state products. However, so far there is not sufficient evidence to exclude any of the mechanisms. The work of Isobe et al. indicated that the CTIL process may be present in firefly light emission, as it avoids harmful side reactions. However, the evidence that the CIEEL mechanism is favored in solution sheds some doubt on this question. Moreover, the possible effects of charged species (AMP and arginine and lysine residues) near firefly dioxetanone in the enzyme active site on both the CIEEL and CTIL mechanisms have not been considered.

Most of the studies so far have considered that Keto-(−1) has the same structure in fluorescence and in chemiluminescence/bioluminescence. However, a rather recent study has demonstrated that 2-acetamido-3-methylpyrazine shows geometrical and electronic differences between fluorescence and chemiluminescence.[86] Thus, it is essential to discover whether Keto-(−1) shows the same differences between the two light-emitting phenomena.

In conclusion, the remaining unanswered questions in firefly chemiluminescence and bioluminescence are why predominantly singlet excited-state products are formed and which charge-transfer mechanism is involved in this process. To clarify these topics, computational methodologies should be fundamental. These techniques could bypass the experimental difficulties associated with the study of this phenomenon, while providing detailed information (down to the atomic level). A theoretical approach could then finally allow the interaction of the dioxetanone intermediate with Luc to be studied.

Acknowledgements

Financial support from Fundação para a Ciência e Tecnologia (FCT, Lisbon) (Programa Operacional Temático Factores de Competitividade (COMPETE) e comparticipado pelo Fundo Comunitário Europeu FEDER) (Project PTDC/QUI/71366/2006) is acknowledged. A Ph.D. grant to L.P.S. (SFRH\BD\76612\2011), attributed by FCT, is also acknowledged.

Keywords: oxygen heterocycles · bioluminescence · chemiluminescence · reaction mechanisms · oxyluciferin

[1] F. McCapra, *Methods Enzymol.* **2000**, *305*, 3.
[2] M. Matsumoto, *J. Photochem. Photobiol. C* **2004**, *5*, 27.
[3] V. R. Viviani, *Cell. Mol. Life Sci.* **2002**, *59*, 1833.
[4] V. R. Viviani, F. G. C. Arnoldi, A. J. S. Neto, T. L. Oehlmeyer, E. J. H. Bechara, Y. Ohmiya, *Photochem. Photobiol. Sci.* **2008**, *7*, 159.
[5] S. M. Marques, J. C. G. Esteves da Silva, *IUBMB Life* **2009**, *61*, 6.
[6] J. M. M. Leitão, J. C. G. Esteves da Silva, *J. Photochem. Photobiol. B* **2010**, *101*, 1.
[7] H. Fraga, *Photochem. Photobiol. Sci.* **2008**, *7*, 146.
[8] S. Inouye, *Cell. Mol. Life Sci.* **2010**, *67*, 387.

[9] K. Niwa, Y. Ichino, S. Kumata, Y. Nakajima, Y. Hirashi, D. Kato, V. R. Viviani, Y. Ohmiya, *Photochem. Photobiol. Sci.* **2010**, *86*, 1046.
[10] T. C. Doyle, S. M. Burns, C. H. Contag, *Cell. Microbiol.* **2004**, *6*, 303.
[11] A. Roda, P. Pasini, M. Mirasoli, E. Michelini, M. Guardigli, *Trends Biotechnol.* **2004**, *22*, 295.
[12] K. E. Luker, G. D. Luker, *Antiviral Res.* **2008**, *78*, 179.
[13] F. Fan, K. V. Wood, *Assay Drug Dev. Technol.* **2007**, *5*, 127.
[14] B. R. Branchini, T. R. Southworth, N. F. Khattak, E. Michelini, A. Roda, *Anal. Biochem.* **2005**, *345*, 140.
[15] P. Billard, M. S. DuBow, *Clin. Biochem.* **1998**, *31*, 1.
[16] A. Roda, M. Guardigli, *Anal. Bioanal. Chem.* **2012**, *402*, 69.
[17] L. Pinto da Silva, J. C. G. Esteves da Silva, *J. Chem. Theory Comput.* **2011**, *7*, 809.
[18] S. Hosseinkhani, *Cell. Mol. Life Sci.* **2011**, *68*, 1167.
[19] I. Navizet, Y. J. Liu, N. Ferre, D. Roca-Sanjuan, R. Lindh, *ChemPhysChem* **2011**, *12*, 3064.
[20] J. Y. Hasegawa, K. J. Fujimoto, H. Nakatsuji, *ChemPhysChem* **2011**, *12*, 3106.
[21] H. Fraga, R. Fontes, *Biochem. Biophys. Acta* **2011**, *1810*, 1195.
[22] E. H. White, D. F. Roswell, *Chemi- and Bioluminescence* (Ed.: J. R. Burr), Marcel Dekker, New York, **1985**, p. 215.
[23] A. G. Mohan, *Chemi- and Bioluminescence* (Ed.: J. R. Burr), Marcel Dekker, New York, **1985**, p. 245.
[24] F. McCapra, K. D. Perring, *Chemi- and Bioluminescence* (Ed.: J. R. Burr), Marcel Dekker, New York, **1985**, p. 249.
[25] T. Wilson, *Singlet O_2, Vol. 2* (Ed.: A. A. Frimer), CRC, **1985**, Boca Raton, Florida, p. 37.
[26] W. Adam, *The Chemistry of Peroxide* (Ed.: S. Patai), Wiley, New York, **1986**, p. 829.
[27] A. Dukhovich, A. Sillero, M. A. G. Sillero, *FEBS Lett.* **1996**, *395*, 188.
[28] W. C. Rhodes, W. D. McElroy, *J. Biol. Chem.* **1958**, *233*, 1528.
[29] H. Fraga, J. C. G. Esteves da Silva, R. Fontes, *ChemBioChem* **2004**, *5*, 110.
[30] H. H. Seliger, W. D. McElroy, *Science* **1962**, *138*, 683.
[31] M. DeLuca, W. D. McElroy, *Biochemistry* **1974**, *13*, 921.
[32] T. Wilson, J. W. Hastings, *Annu. Rev. Cell Dev. Biol.* **1998**, *14*, 197.
[33] N. Suzuki, M. Sato, K. Nishikawa, T. Goto, *Tetrahedron Lett.* **1969**, *10*, 4683.
[34] N. Suzuki, T. Goto, *Tetrahedron* **1972**, *28*, 4075.
[35] J. C. G. Esteves da Silva, J. M. C. S. Magalhães, R. Fontes, *Tetrahedron Lett.* **2001**, *42*, 8173.
[36] O. Shimomura, T. Goto, F. H. Johnson, *Proc. Natl. Acad. Sci. USA* **1977**, *74*, 2799.
[37] L. Pinto da Silva, J. C. G. Esteves da Silva, *ChemPhysChem* **2011**, *12*, 951.
[38] S. F. Chen, Y. J. Liu, I. Navizet, N. Ferré, W. H. Fang, R. Lindh, *J. Chem. Theory Comput.* **2011**, *7*, 798.
[39] C. I. Song, Y. M. Rhee, *J. Am. Chem. Soc.* **2011**, *133*, 12040.
[40] L. Pinto da Silva, J. C. G. Esteves da Silva, *ChemPhysChem* **2011**, *12*, 3002.
[41] L. Pinto da Silva, J. C. G. Esteves da Silva, *J. Phys. Chem. B* **2012**, *116*, 2008.
[42] T. Nakatsu, S. Ichiyama, J. Hiratake, A. Saldanha, N. Kobashi, K. Sakata, H. Kato, *Nature* **2006**, *440*, 372.
[43] P. Naumov, Y. Ozawa, K. Ohkubo, S. Fukuzumi, *J. Am. Chem. Soc.* **2009**, *131*, 11590.
[44] A. Tagami, N. Ishibashi, D. Kato, N. Taguchi, Y. Mochizuki, H. Watanabe, M. Ito, S. Tanaka, *Chem. Phys. Lett.* **2009**, *472*, 118.
[45] L. Pinto da Silva, J. C. G. Esteves da Silva, *J. Comput. Chem.* **2011**, *32*, 2654.
[46] N. Nakatani, J. Y. Hasegawa, H. Nakatsuji, *J. Am. Chem. Soc.* **2007**, *129*, 8756.
[47] B. F. Milne, M. A. Marques, F. Nogueira, *Phys. Chem. Chem. Phys.* **2010**, *12*, 14285.
[48] C. G. Min, A. M. Ren, J. F. Guo, L. Y. Zou, J. D. Goddard, C. C. Sun, *ChemPhysChem* **2010**, *11*, 2199.
[49] F. McCapra, *Pure Appl. Chem.* **1970**, *24*, 611.
[50] J. Y. Koo, S. P. Schmidt, G. B. Schuster, *Proc. Natl. Acad. Sci. USA* **1978**, *75*, 30.
[51] L. H. Catalani, T. Wilson, *J. Am. Chem. Soc.* **1989**, *111*, 2633.
[52] F. McCapra, *J. Photochem. Photobiol. A* **1990**, *51*, 21.
[53] T. Wilson, *Photochem. Photobiol.* **1995**, *62*, 601.
[54] H. Isobe, Y. Takano, M. Okumura, S. Kuramitsu, K. Yamaguchi, *J. Am. Chem. Soc.* **2005**, *127*, 8667.
[55] T. A. Hopkins, H. H. Seliger, E. H. White, M. W. Cass, *J. Am. Chem. Soc.* **1967**, *89*, 7148.
[56] E. H. White, M. J. C. Harding, *J. Am. Chem. Soc.* **1964**, *86*, 5686.
[57] F. McCapra, D. G. Richardson, *Tetrahedron Lett.* **1964**, *5*, 3167.
[58] F. McCapra, Y. C. Chang, V. P. Francois, *Chem. Commun.* **1968**, 22.
[59] F. McCapra, Y. C. Chang, *Chem. Commun.* **1966**, 522.
[60] F. McCapra, Y. C. Chang, *Chem. Commun.* **1967**, 1011.
[61] F. McCapra, *Chem. Commun.* **1968**, 155.
[62] E. H. White, E. Rapaport, T. Hopkins, H. H. Seliger, *J. Am. Chem. Soc.* **1969**, *91*, 2178.
[63] E. H. White, E. Rapaport, H. H. Seliger, T. Hopkins, *Bioorg. Chem.* **1971**, *1*, 92.
[64] P. J. Plant, E. H. White, W. D. McElroy, *Biochem. Biophys. Res. Commun.* **1968**, *31*, 98.
[65] J. Wannlund, M. DeLuca, K. Stempel, P. D. Boyer, *Biochem. Biophys. Res. Commun.* **1978**, *81*, 987.
[66] E. H. White, J. D. Miano, M. Umbreit, *J. Am. Chem. Soc.* **1975**, *97*, 198.
[67] E. H. White, M. G. Steinmetz, J. D. Miano, P. D. Wildes, R. Morland, *J. Am. Chem. Soc.* **1980**, *102*, 3199.
[68] N. Wada, H. Sakai, *J. Biol. Phys.* **2005**, *31*, 403.
[69] L. W. Chung, S. Hayashi, M. Lundberg, T. Nakatsu, H. Kato, K. Morokuma, *J. Am. Chem. Soc.* **2008**, *130*, 12880.
[70] C. G. Min, A. M. Ren, X. N. Li, J. F. Guo, L. Y. zou, Y. Sun, J. D. Goddard, C. C. Sun, *Chem. Phys. Lett.* **2011**, *506*, 269.
[71] K. R. Kopecky, C. Mumford, *Can. J. Chem.* **1969**, *47*, 709.
[72] W. H. Richardson, H. E. O'Neal, *J. Am. Chem. Soc.* **1972**, *94*, 8665.
[73] W. Adam, W. J. Baader, *J. Am. Chem. Soc.* **1985**, *107*, 410.
[74] N. J. Turro, P. Lechtken, *J. Am. Chem. Soc.* **1973**, *95*, 264.
[75] L. De Vico, Y. J. Liu, J. W. Krogh, R. Lindh, *J. Phys. Chem. A* **2007**, *111*, 8013.
[76] F. Liu, Y. J. Liu, L. De Vico, R. Lindh, *J. Am. Chem. Soc.* **2009**, *131*, 6181.
[77] T. Wilson, A. P. Schaap, *J. Am. Chem. Soc.* **1971**, *93*, 4126.
[78] H. C. Steinmetzer, A. Yekta, N. J. Turro, *J. Am. Chem. Soc.* **1974**, *96*, 282.
[79] C. Tanaka, J. Tanaka, *J. Phys. Chem. A* **2000**, *104*, 2078.
[80] W. Adam, J. C. Liu, *J. Am. Chem. Soc.* **1972**, *94*, 2894.
[81] W. Adam, G. A. Simpson, F. Yany, *J. Phys. Chem.* **1974**, *78*, 2559.
[82] S. Wilsey, F. Bernardi, M. Olivucci, M. A. Robb, S. Murphy, W. Adam, *J. Phys. Chem. A* **1999**, *103*, 1669.
[83] E. L. Bastos, W. J. Baader, *ARKIVOC* **2007**, *8*, 257.
[84] F. Liu, Y. Liu, L. De Vico, R. Lindh, *Chem. Phys. Lett.* **2009**, *484*, 69.
[85] M. Tanimura, N. Watanabe, H. K. Ijuin, M. Matsumoto, *J. Org. Chem.* **2011**, *76*, 902.
[86] D. Roca-Sanjuán, M. G. Delcey, I. Navizet, N. Ferré, Y. J. Liu, R. Lindh, *J. Chem. Theory Comput.* **2011**, *7*, 4060.

Received: March 6, 2012
Published online on April 24, 2012

1.6. The Flash Profile of Firefly Bioluminescence

The *in vitro* emission of light follows, under well defined condition, a flash pattern with a rise in the intensity of light that decays to low levels in a few seconds.[28,29] This light profile is attributed to the formation of inhibitory products during the course of the bioluminescent reaction, in lateral or "dark" pathways also catalyzed by luciferase.[28-31]

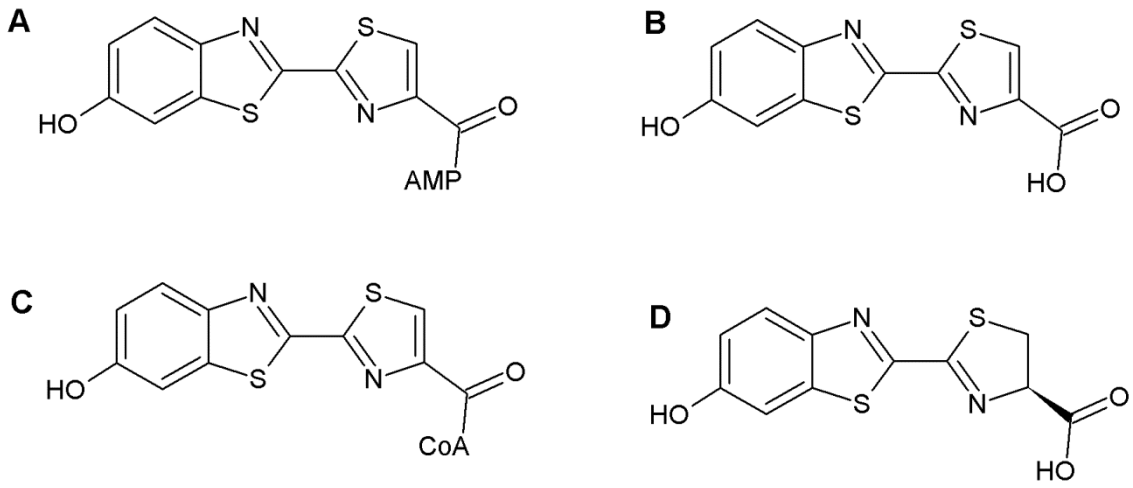

Figure 7 – Representation of the most important inhibitors of firefly bioluminescence: L-AMP (A), L (B), L-CoA (C) and L-LH_2 (D).

OxyLH_2 is by itself a known competitive inhibitor of D-LH_2 (K_i = 0.50 ± 0.03 □M).[30] However, experimental findings indicates that the true responsible for the flash profile of firefly bioluminescence is dehydroluciferyl-adenylate (L-AMP, Fig. 7A), an oxidation product of LH_2-AMP. L-AMP acts as a tight-binding competitive inhibitor of D-LH_2 (K_i = 3.8 ± 0.7 nM), and its formation is also catalyzed by luciferase.[30] The formation reaction of L-AMP also involves the production of hydrogen peroxide.[32] Such metabolite could impair biological functions if its concentrations is different from cellular demand. However, as luciferase produced in the firefly light organs are directed into peroxisomes, the production of hydrogen peroxide will be innocuous as the consequence of high catalase concentrations present there.

L-AMP is capable of reacting with PP_i-Mg^{2+}, released in the light-production pathway, forming dehydroluciferin (L, Fig. 7B) and AMP. L is a tight-binding uncompetitive inhibitor towards D-LH_2 (αK_i = 4.90 ± 0.09 nM).[31]

Coenzyme A (CoA) it is not involved in the classic bioluminescent reaction, but it has been added to commercial luciferase kits due to its stimulating effects on light emission.[22,29,31] This happens because CoA can react with L-AMP, thus leading to the

formation of dehydroluciferyl-coenzyme A (L-CoA, Fig. 7C) in a luciferase catalyzed reaction. L-CoA is also an inhibitor towards D-LH_2 (K_i = 0.88 ± 0.03 μM) but it is much less potent than L-AMP, which accounts for the stimulating effect of CoA.[31]

Another possible inhibitor of the bioluminescent reaction is the L enantiomer of D-LH_2 (Fig. 7D).[31] This compound is also a inhibitor of D-LH_2 (K_i = 0.68 ± 0.14 μM and αK_i = 0.34 ± 0.16 μM), and it can be adenylated by luciferase into L-LH_2-AMP, which is thought as not being able to produce light in the bioluminescent reaction.[31]

1.7. Evolution of Firefly Luciferase

In 1967 McElroy and co-workers noted certain similarities between the reactions catalyzed by luciferase and those catalyzed by acyl-CoA synthetases:[33]

Fatty-acid + ATP-Mg^{2+} → acyl-AMP + PP_i-Mg^{2+} (3)

Acyl-AMP + CoA → acyl-CoA + AMP (4)

Twenty years later, by studying rat long-chain acyl-CoA synthetase, Suzuki *et al.* supported McElroy observations.[16] This group reported that luciferase has a striking resemblance with the acyl-CoA synthetases, having a degree of sequence identity of 35.8%. These results showed that luciferase is definitively related with long-chain acyl-CoA synthetases.[16] Based on these findings, firefly luciferase was considered part of the acyl-adenylate/thioester-forming enzyme superfamily, which includes also numerous acyl-CoA ligases (eg. Acetate-CoA ligase, fatty-acid-CoA ligase and coumarate-CoA ligase).[34]Another evidence of this relationship was the discovery that fatty-acids are competitive inhibitors towards D-LH_2 in the bioluminescent reaction.[28] Following this discovery, Oba *et al.* predicted and demonstrated that the catalytic ability of luciferase to synthesize long-chain fatty acyl-CoA from various long-chain fatty-acid, in the presence of ATP-Mg^{2+} and CoA.[35]

In addition to long-chain fatty acyl-CoA synthetic ability, luciferase has also CoA ligase activity for LH_2 and L.[22,31] In a matter of fact, it was reported that luciferase exhibits different activities depending on which LH_2 enantiomer acts as a substrate. This means that luciferase strictly recognize the stereogenic center at C_4 of LH_2, having CoA ligase activity for the L-isomer (yielding L-LH_2-CoA) or catalyzing the oxidation of D-LH_2 (leading to light production).[36]

In conclusion, the bi-functional nature of luciferase supports the idea that this enzyme was initially a fatty-acid-CoA ligase. Later on, LH_2 emerged and competed with

fatty acids as a substrate for the same enzyme, resulting in the formation of LH_2-AMP that reacted with molecular oxygen and leading to the emission of light.

1.8. Color Tuning Mechanism of Firefly Bioluminescence

As was already stated, the luciferase-$OxyLH_2$ system can emit in a vast range of the visible spectrum, depending on the firefly species to which the luciferase enzyme belongs.[5,22,25] An increase in the emission wavelength maximum can be obtained with higher temperatures, addition of metal cations and enzyme denaturation.[37,38] The luciferase-$OxyLH_2$ complexes of certain firefly species are also sensitive to pH changes, emitting green light at basic pH (pH~7-8), while at acidic pH (pH~5-6) emit red light.[37,38] Several groups have been trying to understand the color tuning mechanism of the pH-sensitive bioluminescent reaction, both by experimental and theoretical approachs.[37,38]

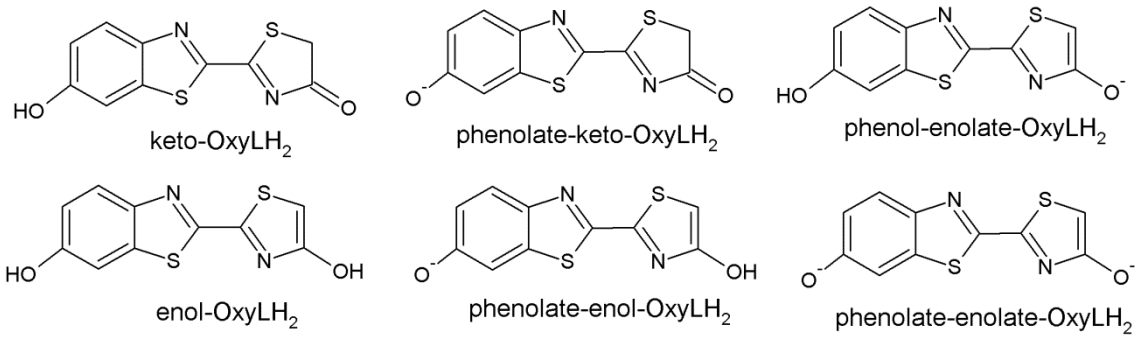

Figure 8 – Possible chemical forms of $OxyLH_2$ in solution.

The first proposed hypothesis that tried to explain the multicolor bioluminescence, was that the high color range of light emitted could be explained by keto-enol equilibrium of $OxyLH_2$ (Fig. 8).[39] However, later studies with an $OxyLH_2$ analog constrained to its keto species have demonstrated that the enolic species are not needed to obtain emission wavelength maxima in the green and red regions of the visible spectra.[40] These findings were supported by three different and independent theoretical studies, which have indicated that the anionic keto species of $OxyLH_2$ is the sole bioluminescent emitter.[41-43]

Given this, several researchers have tried to develop an explanation as to how a single species could emit in a so different wavelength range (530-640 nm). One of the most important studies in this field was that of Nakatsu *et al.*[20] This group obtained the

tridimensional structure of the luciferase enzyme of the *Luciola cruciata* firefly species, complexed with several ligands. These authors have come up with the hypothesis that a "closed" conformation of luciferase active site, associated to a more rigid and hydrophobic medium, would be responsible for the emission of green light at basic pH. A more "open" conformation, corresponding to a less rigid and more polar active site, would then be responsible for red light emission at acidic pH. Thus, it would be the degree of polarity and rigidity of the active site to control the emission wavelength maximum of firefly bioluminescence.[20] However, several groups have demonstrated that the rigidity degree of the luciferase active site cannot be associated to the color tuning mechanism, and that the microenvironment polarity cannot explain by itself color shifts in firefly bioluminescence.[20,37,38,41,44-48] However, it was indeed demonstrated theoretically that these two conformations can be correlated with the emission of the luciferase-$OxyLH_2$ complex at acidic and basic pH.[48]

More recently, our group has been demonstrating by computational methods that the light emitted by $OxyLH_2$ can be modulated by intermolecular interactions that this bioluminophore can form with other molecules.[41,49,50] Our computational study of the *Luciola cruciata* luciferase-$OxyLH_2$ complex, on both active site conformations, have demonstrated that the increase in emission wavelength associated with pH decrease is related with different intermolecular interactions, formed between the light emitter and active site molecules.[49,50] More specifically, there is a decrease in the interaction strength between $OxyLH_2$ and AMP, while it can be observed an increased interaction with a phenylalanine residue.[50] Another important factor is a rupture in a hydrogen bond between a water molecule and the $OxyLH_2$ benzothiazole oxygen, while another hydrogen bond is formed between a water molecule and the light emitter thiazolone oxygen.[50]

1.9. Firefly Oxyluciferin and Related Compounds as Photoacids

Article 3

Oxyluciferin Photoacidity: The Missing Element for Solving the Keto-Enol Mystery?
Luís Pinto da Silva, Ron Simkovitch, Dan Huppert and Joaquim C.G. Esteves da Silva
ChemPhysChem **2013**, *14*, 3441-3446.

The bibliographic research and the writing of the paper were performed by Luís Pinto da Silva, under supervision and collaboration with Ron Simkovitch, and Professors Dan Huppert and Joaquim Esteves da Silva.

CHEMPHYSCHEM
MINIREVIEWS

ChemPubSoc Europe

DOI: 10.1002/cphc.201300402

Oxyluciferin Photoacidity: The Missing Element for Solving the Keto–Enol Mystery?

Luís Pinto da Silva,[a] Ron Simkovitch,[b] Dan Huppert,[b] and Joaquim C. G. Esteves da Silva*[a]

The oxyluciferin family of fluorophores has been receiving much attention from the research community and several systematic studies have been performed in order to gain more insight regarding their photophysical properties and photoprotolytic cycles. In this minireview, we summarize the knowledge obtained so far and define several possible lines for future research. More importantly, we analyze the impact of the discoveries on the firefly bioluminescence phenomenon made so far and explain how they re-open again the discussion regarding the identity (keto or enol species) of the bioluminophore.

1. Introduction

D-luciferin is one of the substrates of the bioluminescence reaction, which is catalyzed by firefly luciferase[1–5] in a two-step reaction (Schemes 1): D-luciferin reacts with adenosine-5′-triphosphate-Mg^{2+} (ATP-Mg^{2+}), which results in the formation of D-luciferyl-adenylate. In the presence of O_2, the adenylyl intermediate is oxidized the subsequent step and gives rise to oxyluciferin, CO_2 and adenosine-5′-monophosphate (AMP).[6–8] The formed oxyluciferin is in a singlet excited state, which decays to the ground state with emission of visible light. Computational studies have stated that the light emitting form of oxyluciferin is the anionic keto species, but no experimental study has ever supported these results in a definitive manner.[8–11]

The interesting features of this phenomenon (e.g. ATP-dependence, high quantum yield, low background noise, and high speed of the reaction among others) have triggered the development of numerous applications in pharmaceutical, biomedical, and bioanalytical areas.[12–15] The luciferase–oxyluciferin system has been used in the rapid-trace determination of ATP, in bioimaging, and as a reporter gene among other applications.

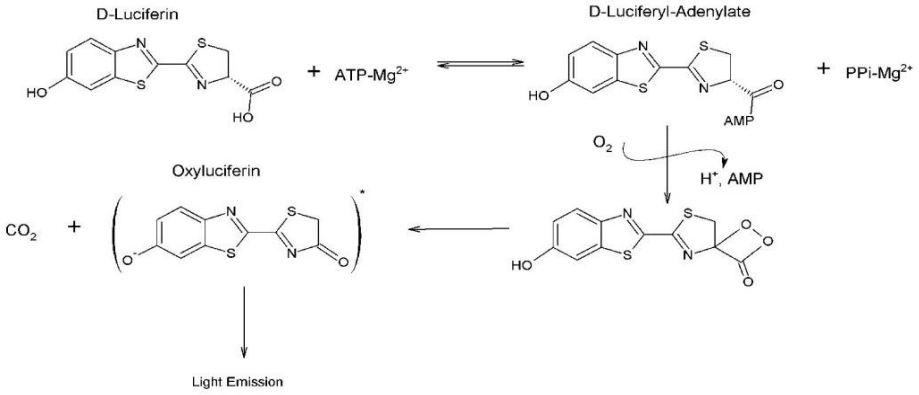

Scheme 1. The bioluminescence reaction.

The photophysics and photochemistry of D-luciferin were extensively studied in the 1970s and 1980s but much less in the following decades.[16] The photophysics and photochemistry of the light emitter oxyluciferin is much less studied due to its known instability. As a matter of fact, only some years ago the crystal structure of this molecule has been determined for the first time.[17]

More recently, the photophysics and photochemistry of D-luciferin, oxyluciferin, and various derivatives (Scheme 2) have been extensively studied due to the discovery that these molecules act as strong photoacids and can undergo excited-state proton transfer (ESPT) with the solvent.[18–25] A typical photoacid is a weak acid in the ground state with a pK_a in the range of 5–10. The steady-state emission of the acidic form of a photoacid should have two emission bands, of which one is attributed to the acidic form and the other to the basic form. If an ESPT process takes place, the time-resolved emission of the protonated form should decay rapidly in water, whereas the basic form's emission signal should be increasing, indicating

[a] Dr. L. Pinto da Silva, Prof. Dr. J. C. G. Esteves da Silva
Centro de Investigação em Química
Departamento de Química e Bioquímica
Faculdade de Ciências da Universidade do Porto
R. Campo Alegre 687, 4169-007 Porto (Portugal)
Fax: (+351) 220 402 659
E-mail: jcsilva@fc.up.pt

[b] Dr. R. Simkovitch, Prof. Dr. D. Huppert
Raymond and Beverly Sackler Facult y of Exact Sciences
School of Chemistry, Tel Aviv University
Tel Aviv 69978 (Israel)

CHEMPHYSCHEM
MINIREVIEWS
www.chemphyschem.org

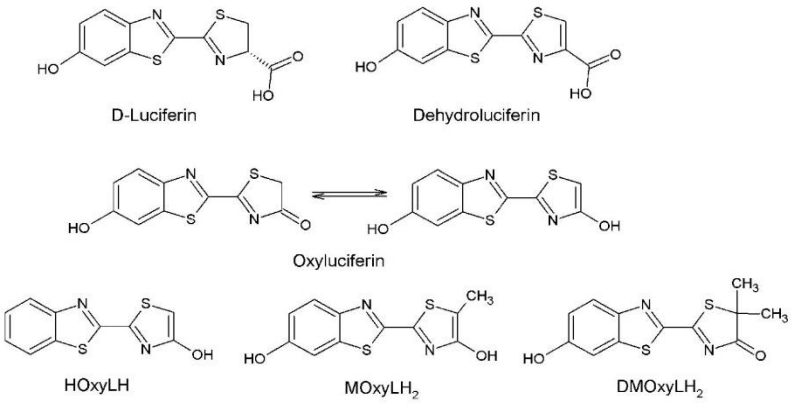

Scheme 2. Firefly oxyluciferin and derivatives.

the formation of a deprotonated species. As is seen in the subsequent sections of this perspective, D-luciferin, oxyluciferin, and various derivatives present the typical features of a photoacid.[18–25]

In recent years, the firefly bioluminescence phenomenon has been documented in detail. Thus, given the myriad of information already published, readers interested in more detailed information regarding the general background of this system are advised to look up refs. [1–5, 16, 26–28]. In this minireview, we focus on the photoacidity of oxyluciferin and derivatives and their implication in firefly bioluminescence, which is a topic that lacks a critical review.

2. Photoprotolytic Cycle of D-Luciferin

In aqueous solution, if D-luciferin is photoexcited at $pH < pK_a$ (≈8), the absorption spectrum presents a band at ~330 nm.[18] This band corresponds to the protonated hydroxyl-benzothiazole species of D-luciferin (here designated as NROH). If the pH is higher than the pK_a, the absorption spectrum presents a band at ~390 nm, which corresponds to the deprotonated hydroxyl-benzothiazole species (here designated as NRO^-).[18]

If D-luciferin is photoexcited at $pH < pK_a$, the emission spectrum consists of two bands, of which one band belongs to NROH (at ~440 nm) and the other to NRO^- (at ~530 nm). The intensity of the NRO^- band is much higher than that of the NROH one.[18] The excited-state NRO^- is formed by deprotonation of the NROH species, due to an ESPT process with the solvent.[18] The ESPT process was found to be fast in water with a constant of $\approx 3.0 \times 10^{10}\ s^{-1}$. The photoprotolytic cycle of the NROH species of D-luciferin is represented in Scheme 3.

A unique feature of the photoprotolytic cycle of D-luciferin is the large quenching of the fluorescence of the NRO^- species.[18–22] Time-resolved measurements indicate that this quenching is due to an irreversible proton geminate recombination process with the fluorophore.[18] It was proposed that a solvent bridge composed of protic solvent molecules connects the hydroxyl-benzothiazole group (proton donor group) and one of the nitrogens of D-luciferin (potential photobase), thereby acting as efficient proton transporter.[18] This process would account for the effective fluorescence quenching process.

A systematic study of the photoprotolytic cycle of D-luciferin in water–methanol mixtures demonstrated that in the concentration range of $0 < \chi_{MeOH} < 0.8$ the ESPT process rate decreases exponentially with the increase in methanol concentration.[19] At higher methanol concentrations, there is an even faster decrease in the ESPT process rate. In neat methanol, the

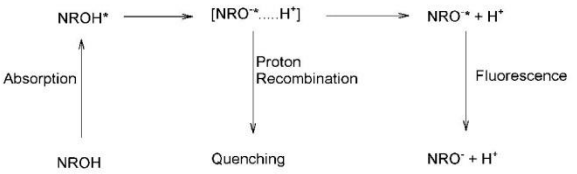

Scheme 3. Photoprotolytic cycle of the NROH D-luciferin species.

ESPT rate was calculated to be equal or inferior to $2 \times 10^8\ s^{-1}$.

Different spectroscopic techniques were also used to study the ESPT process between D-luciferin and various mild bases.[20,21] The chromophore molecules and the bases form an ion pair prior to photoexcitation. The measurements showed nonexponential and complex fluorescence signals, and three different time components were found.[20,21] The fastest decay component was suggested to arise from a direct proton transfer from the hydroxyl-benzothiazole group of D-luciferin to the mild bases. The second decay component was attributed to a proton transfer in a contact pair bridged by one water molecule. Finally, the longest decay component was thought to be due to both the ESPT to the solvent and a diffusion-assisted proton-transfer process between D-luciferin and the base, which were positioned remotely from each other prior to photoexcitation.

As the acid concentration increases in an aqueous solution, the intensity of the ~330 nm band decreases, and a band appears at ~390 nm[2]. At an acid (HCl) concentration equal to or higher than 20 mM, a new emission band is formed at ~590 nm.[22] At a HCl concentration of 220 mM, the intensity of this new band is the highest of all three D-luciferin light-emitting species.[22] The redshift associated with an increase in acid concentration was attributed to the protonation of one of the nitrogen atoms of D-luciferin. Thus, the ~390 nm band was assigned to the ^+HNROH species, while the ~590 nm band was assigned to the excited-state zwitterion $^+HNRO^-$ species.[22] The experimental deduction that the protonation of a nitrogen heteroatom is responsible for the redshift in the absorption

CHEMPHYSCHEM
MINIREVIEWS
www.chemphyschem.org

spectrum was corroborated by two theoretical computational studies.[29,30]

It was also found that the emission intensity of the NRO^- species decreases with increasing acid concentration, while that of the NROH species remains mostly unchanged.[22] The decrease in the intensity of the NRO^- band was attributed to the reaction with excess protons, which leads to quenching. The excited-state ^+HNROH species was also thought to be involved in an ESPT process with the solvent, involving the hydroxyl-benzothiazole group in order to form the zwitterion fluorophore.[22] This species is also involved in a recombination process with the geminate and excess protons that leads to a quenching of the fluorescence.[22] The photoprotolytic cycle of the zwitterion $^+HNRO^-$ species is represented in Scheme 4.

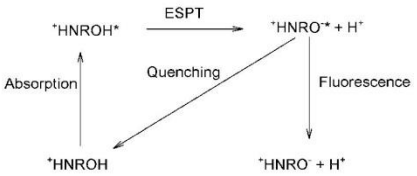

Scheme 4. Photoprotolytic cycle of the zwitterion $^+HNRO^-$ D-luciferin species.

It was also found that the fluorescence intensity of NRO^- is approximately five times higher, when D-luciferin is photoexcited as NRO^- and not as NROH.[19] The reason for this is that if D-luciferin is photoexcited as NROH, the intensity of the emission is decreased due to both the nonradiative process of the excited-state NROH and the irreversible recombination process with a proton, as discussed above.

3. Photoprotolytic Cycle of Dehydroluciferin

Dehydroluciferin (Scheme 2) is an oxidized analogue of D-luciferin, and can be formed in a luciferase-catalyzed lateral reaction.[31–33] Dehydroluciferin is also an inhibitor of the firefly bioluminescence reaction by effectively preventing the binding of D-luciferin to luciferase.[33]

Dehydroluciferin presents an absorption band at ~350 nm in acidic aqueous solutions (pH~6).[23] The emission spectrum consists of a weak band at ~446 nm, corresponding to the NROH species of dehydroluciferin, and a stronger band at ~550 nm, which corresponds to NRO^-. Dehydroluciferin, similar to D-luciferin, is a photoacid and the NRO^- light-emitting species is formed due to an ESPT process between NROH and solvent molecules.[23] The ESPT rate of dehydroluciferin is $1.1\times10^{10}\ s^{-1}$, which is three times smaller than that presented for D-luciferin.[18,23] The excited-state pK_a of dehydroluciferin was calculated to be ~0.7.[23] The NRO^- species of dehydroluciferin is also involved in an irreversible proton geminate recombination process, which leads to fluorescence quenching.[23]

In neat methanol, the emission spectrum of dehydroluciferin consists of the NROH band only, as the efficiency of the ESPT process is very low.[23] By increasing the water content to 10%, the emission spectrum is now composed of two emission bands. The weak one corresponds to the NROH species, while the stronger band corresponds to the NRO^- species.[23]

Even in the presence of low concentrations of HCl, the intensity of the bands of both NROH and NRO^- is strongly reduced, with the intensity of the NRO^- band being affected the most.[23] This effective fluorescence quenching was explained by ground-state protonation of one of the nitrogen atoms of dehydroluciferin.[23]

4. Photoprotolytic Cycle of Oxyluciferin

Oxyluciferin (Scheme 2) is thought to exist in one of six chemical forms when in solution, owing to a complex chemical equilibrium (possible deprotonation of the two hydroxyl groups, and neutral/anionic keto–enol tautomerism).[6,16,17] In the interior of the luciferase active site, oxyluciferin is thought to exist as the anionic keto species, while in the solid state it exists as the neutral enol species.[9–11,17]

Due to the well-known instability of this compound, little is known about its structural and photophysical properties. Nevertheless, it was found that in an aqueous solution its absorption spectrum has a band at ~380 nm at acidic/neutral pH, and a band at ~420 nm at basic pH.[6,16,17,24] The emission spectrum was found to be characterized by a peak at ~550 nm at acidic/neutral pH and a peak at ~540 nm at basic pH.[24]

In organic solvents, the absorption spectra of oxyluciferin is characterized by a single band, with a maximum between 369–377 nm.[17] The emission spectra were found to be characterized by a single band in the blue region of the visible spectrum (maximum between 436-471 nm).[17] In some organic solvents (methanol and acetonitrile), a broad band or a shoulder, emitting in the green region of the visible spectrum, was found.[17]

Regarding the ground-state protolytic cycle of oxyluciferin, the experimental studies performed so far indicate that this molecule has a pK_a of ~7, and it is deprotonation which is responsible for the redshift in the aqueous solution absorption spectrum associated with increasing pH.[24] Organic solvents appear to inhibit such deprotonation.[17]

In terms of the photoprotolytic cycle in aqueous solutions, it was found that if oxyluciferin is photoexcited in its neutral form (acidic/neutral pH) it undergoes an ESPT process with the solvent, which generates an excited-state anionic fluorophore.[24] The ESPT rate coefficient of oxyluciferin in water was found to be $2.2\times10^{10}\ s^{-1}$, which is lower than the one found for D-luciferin ($3.2\times10^{10}\ s^{-1}$), but higher than that found for dehydroluciferin ($1.1\times10^{10}\ s^{-1}$).[18,23,24] This anionic fluorophore emits at ~550 nm, as discussed above.[17,24] If oxyluciferin is photoexcited from its deprotonated form, an anionic fluorophore is formed without the need of an ESPT process with the solvent. This anionic fluorophore also emits in the green region, but at different wavelengths (~540 nm). The different time-resolved emission spectra of oxyluciferin at acidic/neutral and basic pH values indicate that these two different wavelengths maxima (~550 and ~540 nm) correspond to two different emitters.[24]

CHEMPHYSCHEM
MINIREVIEWS
www.chemphyschem.org

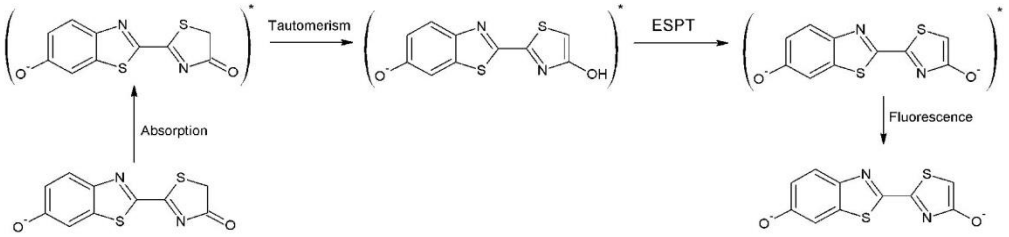

Scheme 5. Photoinduced base-catalyzed enolization of firefly oxyluciferin.

A recent computational study found that in water oxyluciferin forms π–π-stacked complexes both in the ground and in the excited state at basic and acidic/neutral pH values.[34] However, the deprotonation at pK_a ~7 leads to changes in the conformations of these complexes, which explains the higher emission wavelength at acidic/neutral pH values compared to that at basic pH.[24,34]

In the fluorescence spectra of oxyluciferin a fast quenching process was also seen, which was attributed to an irreversible geminate recombination of the proton lost during the ESPT process with one of its nitrogen heteroatoms. This reaction is probably efficient because it is assisted by a water bridge forming a proton wire between the hydroxyl group and one of the nitrogen heteroatoms.[24]

Steady-state and time-resolved emission spectra revealed that oxyluciferin is apparently incapable of transferring a proton to organic solvents, which explains its emission in the blue region of the visible spectrum in those solvents.[17,24]

Studies regarding D-luciferin and dehydroluciferin led researchers to think that the ESPT process between oxyluciferin and solvent molecules, would include the hydroxyl-benzothiazole group.[16,18–24] However, a comparative time-resolved photophysical study of oxyluciferin, HOxyLH (an oxyluciferin derivative lacking one of the two proton-generating hydroxyl groups, Scheme 2), and $MOxyLH_2$ (an oxyluciferin derivative supplemented with a methyl group, Scheme 2) indicated that this is not the case.[25] This was verified by a strong reddish emission from the anionic HOxyLH form, which can only undergo an ESPT process between its hydroxyl-thiazole group and the solvent.[25] Moreover, it was found that HOxyLH is a stronger photoacid than both oxyluciferin and $MOxyLH_2$. This provided reliable evidence that at acidic/neutral pH it is the neutral enol ground state that it is more stable. This finding also indicated that it is the enol functional group that is involved in the ESPT process.[25] These results were supported by the work of White et al.[35] They studied two O-methylated derivatives of oxyluciferin. The methylation of the hydroxyl-benzothiazole group resulted in an emission from the anionic species (emission in the green region), while methylation of the hydroxyl-thiazole group resulted in an emission from a neutral molecule (emission in the blue region).[35] Finally, it should be noted that the photoacidity of an enol group in a five-membered ring is considered to be rather exceptional.[36] Nevertheless, computational studies performed by our own group had already predicted that the enol group is more acidic/photoacidic than the phenol group, when oxyluciferin is in its enol form.[9]

The study of HOxyLH in a mixture of toluene and 1,8-diazabicyclo [5.4.0]-undec-7-ene (DBU) revealed another unexpected phenomenon.[25] In this mixture and in the ground state, HOxyLH exists in an equilibrium between its enolate and keto forms.[25] Time-resolved emission data revealed that the keto form emits at ~590 nm with a lifetime of 2.4 ns, whereas the enolate ion emits at ~605 nm with a lifetime of 7.9 ns. However, the most important finding was the observation of a slow photoinduced base-catalyzed enolization (Scheme 5).[25] According to the authors, this phenomenon includes keto–enol tautomerism and subsequent ESPT from the enol group to DBU. Due to the ultrafast deprotonation of the enol group, the limiting step is believed to be the keto–enol-tautomerism reaction with a characteristic time of 2.4 ns.[25] The authors suggested that the enolization of the keto species should be considered in the bioluminescence reaction, due to the presence of a basic residue (AMP) approaching the keto/enol group of oxyluciferin.

5. Outlook

The study of the photophysical properties and the photoprotolytic cycle of compounds belonging to the firefly oxyluciferin family revealed many interesting, complex and unexpected photoinduced phenomena: Efficient fluorescence quenching, ESPT processes with the solvent, strong photoacidity of the enol group, and a slow photoinduced base-catalyzed tautomerism reaction.[18–25] However, these discoveries have only opened new exciting lines of future research.

One of the possible new lines is the complete definition of the photoprotolytic cycle of oxyluciferin in aqueous solution. So far, experimental studies have indicated that the green emitter at acidic/neutral pH is the enolate anion, while at basic pH green light is emitted by an unknown fluorophore. Recent theoretical studies determined that the enolate anion is the only emitter at different pH values, and that the wavelength shift is caused by changes in the conformation of π–π-stacking complexes.

There is an intrinsic interest in studying this type of compounds due to the role of oxyluciferin in firefly bioluminescence.[1–11] Thus, the elucidation of the mechanism behind the efficient fluorescence quenching is of the utmost importance,

CHEMPHYSCHEM
MINIREVIEWS
www.chemphyschem.org

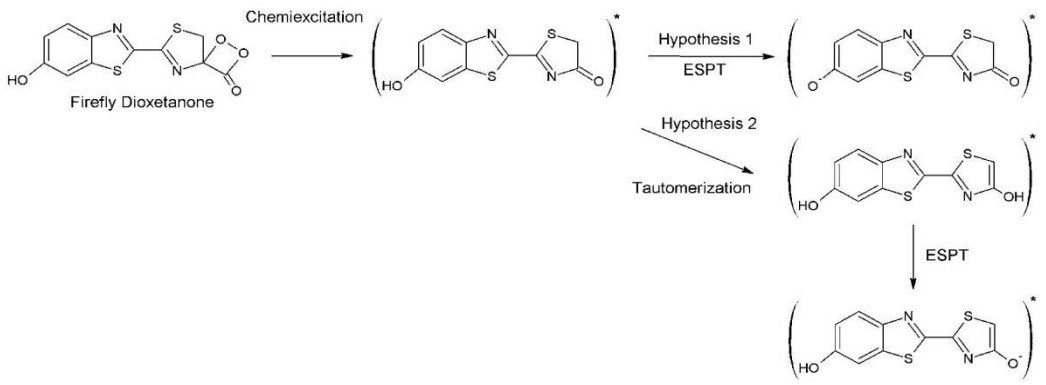

Scheme 6. Hypotheses for the two possible formation pathways yielding the excited-state anionic bioluminophore from a neutral firefly dioxetanone.

as it can also be occurring inside the active site of the protein, thereby decreasing bioluminescence efficiency.

Even more important is the study of the strong photoacidity of the enol group and the slow photoinduced base-catalyzed tautomerism reaction.[25] The discussion regarding the identity of the bioluminophore is an old one and lately it has been considered as solved, since the anionic keto species has been appointed as the bioluminescence emitter. Both experimental and theoretical studies have agreed at this point.[9–11,37] Experimentally, Branchini et al. have obtained green and red bioluminescence with a keto-restrained oxyluciferin derivative ($DMOxyLH_2$, Scheme 2), diminishing the importance of the enol species, which was in line with the cited computational works.[9–11,37] More importantly, Song and Rhee have computationally studied the keto–enol-tautomerism reaction inside the luciferase active site and have found that this reaction is not favorable.[11] However, recent experimental studies made by Branchini and co-workers have indicated that computational studies made inside the luciferase active site have not been using the correct luciferase conformation.[38] It is still not clear if the structures proposed by Branchini and co-workers are more correct than those presented by Nakatsu et al. (the computational studies are based on the latter ones).[38,39] However, the results obtained by Branchini and co-workers certainly cast some doubt in the conclusions of Song and Rhee, which, combined with the discoveries made by Naumov and co-workers, once again open the doors for the possibility of the bioluminophore being an enol species.

It should be noted that a recent theoretical/experimental work has demonstrated that firefly dioxetanone (the precursor of firefly oxyluciferin in the bioluminescence reaction) must be a neutral molecule under the conditions associated with the firefly bioluminescence reaction.[40] Therefore, this study, along with another theoretical work, indicates that oxyluciferin is chemiexcited in its neutral keto form.[8,40] However, as the bioluminescence wavelength is only compatible with an anionic species, the neutral oxyluciferin must donate a proton.[17] In conclusion, two hypotheses must be considered (Scheme 6). The first one is that the neutral keto form donates a proton via ESPT, forming an anionic keto species. The second one is that the neutral keto form tautomerizes into the neutral enol form, which donates a proton via ESPT, thus forming the enolate anion.

Also, no experimental time-resolved data exists for $DMOxyLH_2$, which does not allow us to estimate the effect of the double methylation on the photoacidity of the hydroxyl-benzothiazole group. Thus, if this substitution increases the photoacidity of the hydroxyl-benzothiazole group, the bioluminescence could be explained without excluding the hypothesis of natural bioluminescence being originated from an enol species.[37]

These unanswered questions indicated that future studies should include experimental characterization of the time-resolved fluorescence of $DMOxyLH_2$ and computational studies of the excited-state keto–enol-tautomerism reaction inside the active site of the correct conformation of firefly luciferase. Computational methodologies appear to be the only ones capable of giving reliable and detailed atomistic information on this complex reaction. Computational methodologies could also be of great importance in defining the mechanism behind the efficient fluorescence quenching.

Acknowledgements

Financial support from Fundação para Ciência e Tecnologia (FCT, Lisbon) (Programa Operacional Temático Factores de Competitividade (COMPETE) e comparticipado pelo Fundo Comunitário Europeu (FEDER) (Project PTDC/QUI/71366/2006) is acknowledged. A Ph.D. Grant to L.P.d.S. is also acknowledged. This work was also supported by grants from the Israel Science Foundation and from the James-Franck German–Israeli Program in Laser-Matter Interaction.

Keywords: bioluminescence · oxyluciferin · photoacids · proton transfer · tautomerism

[1] L. Pinto da Silva, J. C. G. Esteves da Silva, *J. Chem. Theory Comput.* **2011**, *7*, 809–817.
[2] J. Y. Hasegawa, K. J. Fujimoto, H. Nakatsuji, *ChemPhysChem* **2011**, *12*, 3106–3115.

[3] L. Pinto da Silva, J. C. G. Esteves da Silva, *ChemPhysChem* **2012**, *13*, 2257 – 2262.
[4] S. M. Marques, J. C. G. Esteves da Silva, *IUBMB Life* **2009**, *61*, 6 – 17.
[5] J. M. Leitão, J. C. G. Esteves da Silva, *J. Photochem. Photobiol. B* **2010**, *101*, 1 – 8.
[6] J. C. G. Esteves da Silva, J. M. C. S. Magalhães, R. Fontes, *Tetrahedron Lett.* **2001**, *42*, 8173 – 8176.
[7] B. R. Branchini, J. C. Rosenberg, D. M. Fontaine, T. L. Southworth, C. E. Behney, L. Uzasci, *J. Am. Chem. Soc.* **2011**, *133*, 11088 – 11091.
[8] S. F. Chen, Y. J. Liu, I. Navizet, N. Ferré, W. H. Fang, R. Lindh, *J. Chem. Theory Comput.* **2011**, *7*, 798 – 803.
[9] L. Pinto da Silva, J. C. G. Esteves da Silva, *ChemPhysChem* **2011**, *12*, 951 – 960.
[10] C. I. Song, Y. M. Rhee, *J. Am. Chem. Soc.* **2011**, *133*, 12040 – 12049.
[11] I. Navizet, Y. J. Liu, N. Ferré, H. Y. Xiao, W. N. Fang, R. Lindh, *J. Am. Chem. Soc.* **2010**, *132*, 706 – 712.
[12] A. Roda, M. Guardigli, *Anal. Bioanal. Chem.* **2012**, *402*, 69 – 76.
[13] R. Fazzina, L. Lombardini, L. Mezzanotte, A. Roda, P. Hrelia, A. Pession, R. Tonelli, *Int. J. Oncol.* **2012**, *41*, 621 – 628.
[14] A. Roda, L. Cevenini, E. Michelini, B. R. Branchini, *Biosens. Bioelectron.* **2011**, *26*, 3647 – 3653.
[15] S. M. Marques, F. Peralta, J. C. G. Esteves da Silva, *Talanta* **2009**, *77*, 1497 – 1503.
[16] J. Vieira, L. Pinto da Silva, J. C. G. Esteves da Silva, *J. Photochem. Photobiol. B* **2012**, *117*, 33 – 39.
[17] P. Naumov, K. Ohkubo, S. Fukuzumi, *J. Am. Chem. Soc.* **2009**, *131*, 11590 – 11605.
[18] Y. Erez, D. Huppert, *J. Phys. Chem. A* **2010**, *114*, 8075 – 8082.
[19] I. Presiado, Y. Erez, D. Huppert, *J. Phys. Chem. A* **2010**, *114*, 9471 – 9479.
[20] I. Presiado, Y. Erez, D. Huppert, *J. Phys. Chem. A* **2010**, *114*, 13337 – 13346.
[21] I. Presiado, R. Gepshtein, Y. Erez, D. Huppert, *J. Phys. Chem. A* **2011**, *115*, 7591 – 7601.
[22] Y. Erez, I. Presiado, R. Gepshtein, D. Huppert, *J. Phys. Chem. A* **2011**, *115*, 1617 – 1626.
[23] I. Presiado, Y. Erez, R. Simkovitch, S. Shomer, R. Gepshtein, L. Pinto da Silva, J. C. G. Esteves da Silva, D. Huppert, *J. Phys. Chem. A* **2012**, *116*, 10770 – 10779.
[24] Y. Erez, I. Presiado, R. Gepshtein, L. Pinto da Silva, J. C. G. Esteves da Silva, D. Huppert, *J. Phys. Chem. A* **2012**, *116*, 7452 – 7461.
[25] K. M. Solntsev, S. P. Laptenok, P. Naumov, *J. Am. Chem. Soc.* **2012**, *134*, 16452 – 16455.
[26] I. Navizet, Y. J. Liu, N. Ferré, D. Roca-Sanjuán, R. Lindh, *ChemPhysChem* **2011**, *12*, 3064 – 3076.
[27] S. Inouye, *Cell. Mol. Life Sci.* **2010**, *67*, 387 – 404.
[28] S. Hosseinkhani, *Cell. Mol. Life Sci.* **2011**, *68*, 1167 – 1182.
[29] M. Hiyama, H. Akiyama, K. Yamada, N. Koga, *Photochem. Photobiol.* **2012**, *88*, 889 – 898.
[30] M. Hiyama, H. Akiyama, K. Yamada, N. Koga, *Photochem. Photobiol.* **2013**, *89*, 571 – 578.
[31] H. Fraga, D. Fernandes, R. Fontes, J. C. G. Esteves da Silva, *FEBS J.* **2005**, *272*, 5206 – 5216.
[32] H. Fraga, D. Fernandes, J. Novotny, R. Fontes, J. C. G. Esteves da Silva, *ChemBioChem* **2006**, *7*, 929 – 935.
[33] L. Pinto da Silva, J. C. G. Esteves da Silva, *Photochem. Photobiol. Sci.* **2011**, *10*, 1039 – 1045.
[34] L. Pinto da Silva, R. Simkovitch, D. Huppert, J. C. G. Esteves da Silva, *ChemPhysChem* **2013**, DOI: 10.1002/cphc.201300330.
[35] E. H. White, D. F. Roswell, *Photochem. Photobiol.* **1991**, *53*, 131 – 136.
[36] *The Chemistry of Enols* (Ed. Z. Rappoport), Wiley, New York, **1990**.
[37] B. R. Branchini, M. H. Murtiashaw, R. A. Magyar, N. C. Portier, M. C. Ruggiero, J. G. Stroh, *J. Am. Chem. Soc.* **2002**, *124*, 2112 – 2113.
[38] J. A. Sundlov, D. M. Fontaine, T. L. Southworth, B. R. Branchini, A. M. Gulick, *Biochemistry* **2012**, *51*, 6493 – 6495.
[39] T. Nakatsu, S. Ichiyama, J. Hiratake, A. Saldanha, N. Kobashi, K. Sakata, H. Kato, *Nature* **2006**, *440*, 372 – 376.
[40] L. Pinto da Silva, A. J. M. Santos, J. C. G. Esteves da Silva, *J. Phys. Chem. A* **2013**, *117*, 94 – 100.

Received: April 23, 2013
Revised: June 21, 2013
Published online on July 10, 2013

1.10. Applications of the Luciferase-OxyLH_2 Bioluminescent System

Progress in molecular biology has made available new bioanalytical tools that take advantage of the great detectability and the simple analytical format of bioluminescence. In general there are two broad areas of interest: the use of luciferase in analytical assays of metabolites and molecular biology studies.

The luciferase-OxyLH_2 system is widely used in the detection and quantification of ATP, as the light intensity is proportional to the ATP concentration present in the sample that is to be analyzed. Besides ATP, the firefly bioluminescence reaction is also used to quantify CoA, PP_i and AMP.[51-54]

Luciferase can also be used as a reporter gene. The luciferase gene can be introduced into the desired organism by means of an expression vector, and inside the cell is translated into functional luciferase protein. An extract is made and the addition of its substrates leads to light production, which can be recorder in a luminometer. This strategy is used to identify regulatory sequences and in drug screening.[55,56]

Another application for firefly bioluminescence is that of bioimaging, which is the most widely used method to measure transgene experession *in vivo*.[10-12] In such approach, light production can be measured *in vivo* in a living organism. This application has attracted great interest as it can be used in so diverse and important fields as that of oncology, infection progression and protein expression.[10-12]

The technology of bioluminescence resonance energy transfer has been developed as a mean of detecting protein-protein interactions, and conformational changes of biomolecules in a nanometer scale.[10]

Finally, mutagenesis studies on luciferase enabled the production of proteins with novel and improved properties, as new light color emission, increased catalytic efficiency and higher luminescence intensity.[11,57,58]

1.11. Unsolved Problems

Despite the importance gained by firefly bioluminescence in recent years, there are still aspects associated with it that prevent its use in new applications, and in increasing the efficiency of existent ones.

The high K_m of ATP and the formation of inhibitory compounds responsible for the flash profile impair the analytic detection of the light emitted by the luciferase-OxyLH_2 system.

One of the most studied features of this bioluminescent system is it multicolor light emission. This is due to the fact that the yellow-green light typically emitted by this system is not the most appropriated for its *in vivo* and *in vitro* applications. The photodetectors used in *in vitro* assays are more sensitive in the blue region of the visible spectrum. In *in vivo* applications it would be more effective if the wavelength maximum of emitted light was in the red region of the visible spectrum, as yellow-green light is more easily absorbed by tissues than red light. Moreover, hemoglobin absorbs more in the yellow-green region than in the red one.

Several groups have been trying to modify both the enzyme and D-LH_2 in order to obtain emission wavelengths in the red region of the visible spectrum. However, even if this red shift is achieved, the intensity of emitted light is always lower than that obtained by unmodified luciferase-OxyLH_2 system.[59-61] Moreover, not all attempts to red shift firefly bioluminescence are successful.[59-61] This lack of success is explain by a lack of knowledge regarding the firefly color tuning mechanism.

The decrease in the intensity of emitted light of mutated luciferase-OxyLH_2 systems is also related with three factors: decrease in the yield of the luciferase-catalyzed ground state reaction; efficiency decrease in the chemiexcitation step; decrease of the fluorescence quantum yield of the light emitter. However, it is quite difficult to correlate each one of the factors with a decrease of emitted light given that the reaction mechanism regarding OxyLH_2 formation is far from clarified. Moreover, there are very few data regarding the chemiexcitation step, and the involvement of luciferase active site in it. Finally, there is still no comprehensive comparison between the fluorescence maxima/intensity of unmodified and mutated OxyLH_2, both in solvent and luciferase active. Without such information, one cannot obtain structure-function relationships that allow the rational development of new and improved firefly bioluminophores.

1.12. The Contribute of this Ph.D. Thesis

This Ph.D. Thesis has the goal of allowing the development of new solutions for the problems that prevent a more effective and productive use of firefly bioluminescence, by employing a combination of theoretical and experimental methods. To achieve that goal, it were planned a series of small and interconnected research projects, which allowed the clarification of several unresolved features of the luciferase catalyzed reactions.

It was theoretically studied the binding of LH_2-AMP and two adenylates known to be inhibitors of the bioluminescence reaction. In that way was possible to present more

data related to the mechanism responsible for the flash profile of bioluminescence. It was also excluded the possibility of the formation of L and L-LH_2 from D-LH_2, which eliminates these compounds as possible inhibitors of the light emitting reaction.

It was also studied the potential role of a carbanion and a radical in the formation of firefly dioxetanone. Our theoretical results favor the presence of a radical, as it allows the interaction of molecular oxygen with singlet LH_2-AMP in order to produce singlet $OxyLH_2$, as well as allowing the formation of L-AMP. These results were corroborated by the discovery of the involvement of a radical intermediate in the chemiluminescent reaction between D-LH_2 and superoxide anion.

The study of several dioxetanones revealed a concerted mechanism for their decomposition reactions, and that chemiexcitation is due to intersystem crossing processes between ground/excited singlet and triplet states, besides transitions between singlet states. These results lead to the proposal of the Interstate Crossing Induced Chemiexcitation (ICIC) theory, which allows us to explain the formation of excited states from dioxetanone decomposition.

Computational studies of the binding of $OxyLH_2$ to two conformations of luciferase allowed the determination that the bioluminescent wavelength maximum is controlled by the electrostatic field, formed by intermolecular interactions between the bioluminophore and the enzymatic active site. More specifically, the color of light emitted is determined by repulsive electrostatic interactions with AMP, hydrogen bonds with water molecules, and π-π stacking interactions with a phenylalanine residue. The analysis of several $OxyLH_2$ analogues related increased emission wavelength and fluorescence intensity to π-π conjugation effects and to a higher HOMO-LUMO overlap, especially in the connective region between the two moieties of oxyluciferin.

Finally, the photoprotolytic cycle of $OxyLH_2$, D-LH_2 and L in aqueous solution were studied and characterized. This allowed us to identify these molecules as photoacids, determine possible deactivation pathways, and observe the involvement of supramolecular π-π complexes. More importantly, it allowed us to predict the involvement of enolate $OxyLH_2$ in the firefly bioluminescent reaction, and propose it as one of the possible light emitters.

Chapter 2 – Study of the Flash Profile of Firefly Bioluminescence

2.1. Comparative Study of the Binding Mode to Luciferase of LH_2-AMP and Related Adenylates

Article 4

Comparative theoretical study of the binding of luciferyl-adenylate and dehydroluciferyl-adenylate to firefly luciferase

Luís Pinto da Silva, João Vieira and Joaquim C.G. Esteves da Silva

Chem. Phys. Lett. **2012**, *543*, 137-141.

The theoretical calculations were performed by Luís Pinto da Silva and João Vieira, while the paper was written by Luís Pinto da Silva under supervision of Professor Esteves da Silva.

Chemical Physics Letters 543 (2012) 137–141

Contents lists available at SciVerse ScienceDirect

Chemical Physics Letters

journal homepage: www.elsevier.com/locate/cplett

Comparative theoretical study of the binding of luciferyl-adenylate and dehydroluciferyl-adenylate to firefly luciferase

Luís Pinto da Silva, João Vieira, Joaquim C.G. Esteves da Silva *

Centro de Investigação em Química (CIQ-UP), Departamento de Química e Bioquímica, Universidade do Porto, R. Campo Alegre 687, 4169-007 Porto, Portugal

ARTICLE INFO

Article history:
Received 19 April 2012
In final form 19 June 2012
Available online 26 June 2012

ABSTRACT

This is the first report of a study employing a computational approach to study the binding of (D/L)-luciferyl-adenlyates and dehydroluciferyl-adenylate to firefly luciferase. A semi-empirical/molecular mechanics methodology was used to study the interaction between these ligands and active site molecules. All adenylates are complexed with the enzyme, mostly due to electrostatic interactions with cationic residues. Dehydroluciferyl-adenylate is expected to be a competitive inhibitor of luciferyl-adenylate, as their binding mechanism and affinity to luciferase are very similar. Both luciferyl-adenylates adopt the L-orientation in the active site of luciferase.

1. Introduction

An enzyme-catalyzed light emitting reaction is known as bioluminescence. This phenomenon can be found in various types of living organisms, such as dinoflagellates, fungi, crustacean, insects and fishes [1–5].

The most studied bioluminescence system is that of fireflies [1–5]. Firefly luciferase catalyzes a two-step reaction: in the first step, firefly D-luciferin (D-LH_2) reacts with adenosine-5'-triphosphate–Mg^{2+} (ATP–Mg^{2+}), thereby generating an adenylyl intermediate (D-LH_2-AMP, Figure 1); in the second step, D-LH_2-AMP reacts with molecular oxygen, which results in the formation of anionic keto-form oxyluciferin, CO_2 and adenosine-5'-monophosphate (AMP) [6–12].

Due to very interesting characteristics, the bioluminescence phenomenon has received attention from the research community and has gained numerous analytical, biomedical and pharmaceutical applications [13–17]. However, the *in vitro* emission of light follows a flash pattern, which prevents a more efficient use of this system [2,18–22]. This pattern is characterized by a rise in the intensity of emission that decays to low levels in a few seconds, even in the presence of available substrate [2,18–22].

The typical flash profile is explained by the formation of inhibitory products, during the course of the reaction. The most potent inhibitor known to date is dehydroluciferyl-adenylate (L-AMP, Figure 1) [2,18–22]. L-AMP was discovered to be a tight-binding competitive inhibitor of D-LH_2 ($K_i = 0.0038 \pm 0.0007$ μM), and is considered to be the major responsible for the flash profile [18]. L-AMP is thought to be formed due to a dark reaction between D-LH_2-AMP and molecular oxygen. This reaction results in the formation of L-AMP and hydrogen peroxide [22]. Due to the high structural similarity between L-AMP and D-LH_2-AMP, it is expected that the former compound can have an inhibitory effect on the latter. Thus, the characterization of the possible inhibition exerted by L-AMP on D-LH_2-AMP binding to the enzyme could be of enormous importance in the clarification of the flash profile mechanism. Another important inhibitor is L-LH_2-AMP (Figure 1) [1,20]. L-LH_2 is known to be an important inhibitor of D-LH_2 ($K_i = 0.68 \pm 0.14$ μM and $\alpha K_i = 0.34 \pm 0.16$ μM) [20]. Moreover, it is known that luciferase can catalyze the formation of L-LH_2-AMP, from L-LH_2 and ATP-Mg^{2+} [1]. Therefore, studying the possible inhibition of D-LH_2-AMP-derived reactions, by L-LH_2-AMP could provide valuable information. However, the high instability of (D/L)-LH_2-AMP and the difficulties associated with their chemical synthesis make the experimental study of this topic very difficult.

The purpose of this article is to use for the first time a computational approach in the study of luciferase flash profile. This approach will allow us to study the possible inhibition exerted by L-AMP and L-LH_2-AMP with regard to D-LH_2-AMP, without the difficulties associated with experimental studies. Furthermore, this approach will allow us to obtain information, down to the atomistic level, of the interaction between these ligands and luciferase. To this end, a molecular mechanics approach was used to obtain complexes between (D/L)-LH_2-AMP and L-AMP with *Luciola cruciata* luciferase [23]. PM3 Semi-empirical calculations were used to determine the energetic contribution of several active site molecules to the binding of (D/L)-LH_2-AMP and L-AMP [24].

2. Theoretical methods

The PBD structure 2D1S (*Luciola cruciata* luciferase complexed with a high-energy adenylate analog) was used as starting structure

* Corresponding author.
E-mail address: jcsilva@fc.up.pt (J.C.G. Esteves da Silva).

0009-2614/$ - see front matter © 2012 Elsevier B.V. All rights reserved.
http://dx.doi.org/10.1016/j.cplett.2012.06.038

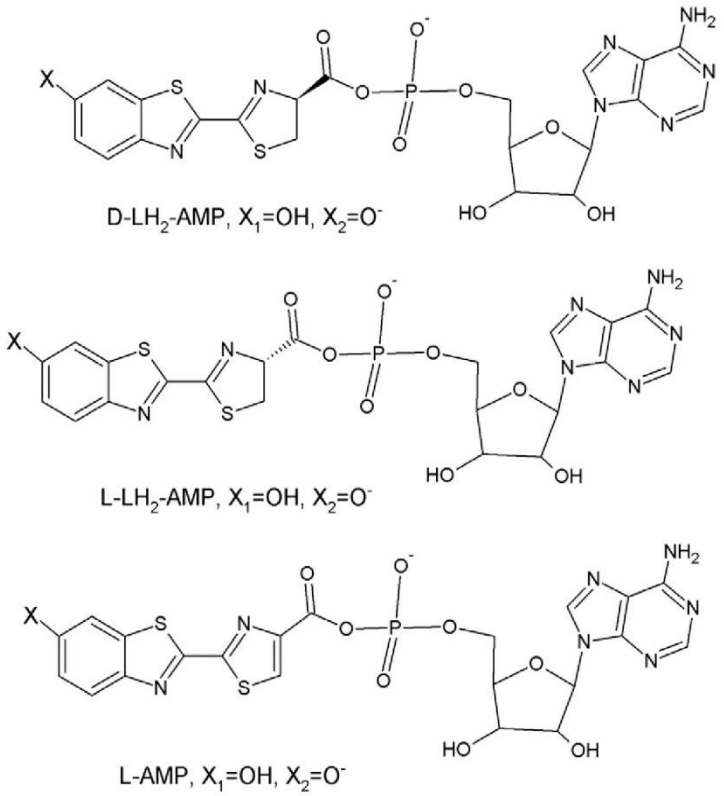

Figure 1. Schematic representation of the structures of (D/L)-LH_2-AMP and L-AMP. The major differences are the orientation of the thiazole carboxylic group, and the presence/absence of a double bond in the thiazole moiety.

[23]. The hydrogen atoms, the missing atoms, and TIP3P water molecules up to 12 Å were added by the LEAP module of the AMBER 11 suite of programs [25]. The ff03 force field was used for intramolecular interactions [26]. The geometries of (D/L)-LH_2-AMP and L-AMP were obtained with the semi-empirical PM6 method, due to the very high number of atoms present in the molecules [27]. These geometry optimizations were made with the MOPAC2009 software package [28]. As the protonation state of the benzothiazole –OH group is still not clearly defined, we have considered both the protonated and deprotonated states (Figure 1). The PM6-obtained geometries were used in the parameterization of the ligands with the ANTECHAMBER module of AMBER and the general AMBER force field [29]. These molecules were docked to the active site with the use of the software AUTODOCK 4.2 [30]. The genetic algorithm was used as a search engine. The molecular docking was performed with the water molecules present in the original PDB file.

One phase of 30000 steps of energy minimizations was performed for each enzyme–ligand complex, by using the Not (just) Another Molecular Dynamics program (NAMD) molecule dynamic code with AMBER potential functions, parameters, and the file formats [31]. In this process, the Particle Mesh Ewald method was used to include the long-range interactions [32]. All the minimizations steps were performed in a NVT ensemble, with a temperature of 298.15 K.

In the end of the molecular mechanics simulations, L-AMP, (D/L)-LH_2-AMP and two selections of active site molecules were withdrawn from the enzyme–ligand complexes. Two selections were made due to the high number of atoms involved. The first selection consisted on: Arg339, Gln340, Gly341, Thr345, Ala350, Asp424, Lys531, Wat1, Wat2 and Wat3. The second selection consisted on: Ser200, Ser201, Arg220, Phe249, His247, Thr253 and Gly318. These active site molecules were chosen due to their presence in previous firefly bioluminescence studies [11,12,23].

The energies of association of the ligands with luciferase were estimated through single point energy calculations with the semi-empirical method PM3 [24]. To assess the energy of association for each ligand (ΔE_{ass}), three calculations were performed (Eq. (1)): PM3 single point energy calculations on the model composed by the ligand and all the chosen active site molecules ($E_{complex}$); PM3 single point energy calculations on a model including only the chosen active site molecules ($E_{active\ site}$); PM3 single point calculations on the ligand (E_{ligand}). After the calculation of ΔE_{ass} for each ligand, the energetic contribution to the ΔE_{ass} of each active site molecule was evaluated. For an active site molecule *X*, its contribution was estimated by removing it from the respective model and by calculation of the corresponding energy of association as already described. By comparing the ΔE_{ass} obtained for the model in the absence of that molecule, with the results obtained with all the active site molecules present, it is possible to get a quantitative picture of the contribution of each molecule to the associating energy of the ligands ($\Delta\Delta E_{ass}$, Eq. (2)). The removal of the molecules that contribute favorably to the interaction of the ligands with the active site will lead to less stable complexes and consequently to more positive $\Delta\Delta E_{ass}$. The PM3 method was used due to the very high number of atoms present in these models, and due to its use in previous studies where interaction/binding energies were calculated [33–36]. The single point energy calculations were performed with the GAUSSIAN 03 program package [37].

$$\Delta E_{ass} = E_{complex} - (E_{enzyme} + E_{ligand}) \quad (1)$$

$$\Delta\Delta E_{ass}(\text{Molecule}X) = \Delta E_{ass}(\text{Without Mol}X) - \Delta E_{ass}(\text{With All Mol}) \quad (2)$$

3. Results and discussion

Our calculations indicate that the benzothiazole oxygen of these adenylates is indeed protonated. After the molecular mechanics simulation, the luciferin/dehydroluciferin moieties of the fully deprotonated ligands adopt a *cis* conformation, despite their docking and parameterization conformation being *trans* (Figure 2). The ligands with a protonated benzothiazole –OH group adopted a *trans* conformation, as indicated in the literature [22]. Thus, we have only subsequently studied (D/L)-LH_2-AMP and L-AMP with protonated benzothiazole –OH group. The protonation state now attributed to this functional group is in line with the recent work of Huppert and co-workers [38,39].

Another interesting and unexpected result was the state of isomerisation of (D/L)-LH_2-AMP. While protonated L-LH_2-AMP adopted still an L-orientation, after the molecular mechanics simulation protonated D-LH_2-AMP also adopted an L-orientation (Figure 3). The finding that both LH_2-AMP presented a L-orientation in the active site could be a defiant notion, as it was stated that L-LH_2 was involved in the formation of luciferyl-coenzyme A (LH_2-CoA) and D-LH_2 in the bioluminescence reaction [40]. The reason for the absence of bioluminescence, when L-LH_2 is used as a luciferase substrate, was thought to be the orientation of the C_4 proton (see Figure 3 in Ref. [1]), which is contrary to that presented by D-LH_2 [1]. However, in 1996 Lembert demonstrated that L-LH_2 could produce light with decreased efficiency when comparing with D-LH_2 [41]. Thus, this finding demonstrated that the orientation of the C_4 proton of L-LH_2 only diminishes its efficiency as a bioluminescence substrate. However, this notion is difficult to conjugate with the possibility that the C_4 proton of these molecules have an opposite orientation during all the bioluminescence reaction. Thus, our results indicate that during the bioluminescence reaction the LH_2-AMP molecules adopt the same isomerisation state (L-orientation), which indicates that both ligands can produce light. As the two LH_2-AMP molecules present somewhat different conformations in the active site (Figure 3), we hypothesize that the one adopted by the former D-LH_2-AMP is more favorable for the bioluminescence reaction than the one presented by the other LH_2-AMP molecule. However, further study would be needed to elucidate this point.

In Table 1 are presented the energetic contributions of the active site molecules of the first selection to the binding of protonated (D/L)-LH_2-AMP and L-AMP. The complexes formed between the three adenylates and the active site molecules of the first selection are represented in Figure 4. It can be seen that some active site

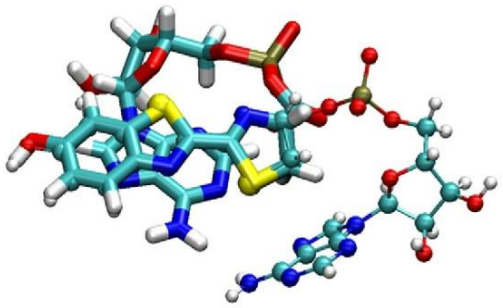

Figure 3. Comparison between the protonated conformations of L-LH_2-AMP (CPK representation) and D-LH_2-AMP (licorice representation), after the molecular mechanics simulation.

Table 1
Energetic contributions of active site molecules (first selection) to the binding of (D/L)-LH_2-AMP and L-AMP.

	D-LH_2-AMP	L-LH_2-AMP	L-AMP
Arg339	16	18	22
Gln340	2	1	2
Gly341	−2	−5	−1
Thr345	−4	−1	−0
Ala350	−1	1	0
Asp424	−43	−53	−32
Lys531	64	83	49
Wat1	−1	−1	1
Wat2	2	1	−1
Wat3	−1	1	0

molecules (Gln340, Ala350 and Wat1-3) give very low energetic contributions to the binding of all ligands. Also, there are some molecules that give a very low contribution to one of the ligands and a higher one to other adenylate (Gly341 and Thr345). Nevertheless, we can say that the majority of the active site molecules of the first selection appear to be irrelevant in the binding of L-AMP and (D/L)-LH_2-AMP. The exceptions are the ionic amino-acid residues (Arg339, Lys531 and Asp424). Cationic Arg339 (16–22 kcal/mol) and Lys531 (49–83) appear to be very important favorable contributors, while anionic Asp424 (−32 to −53 kcal/mol) is a significant negative contributor. These contributions can be explained by the single negative charge of the ligands. The contribution of Arg339 is very similar for all adenylates, while the contribution of Lys531 is higher for (D/L)-LH_2-AMP. However, this higher contribution appears to be counteracted by the higher negative contribution of Asp424 to the binding of (D/L)-LH_2-AMP.

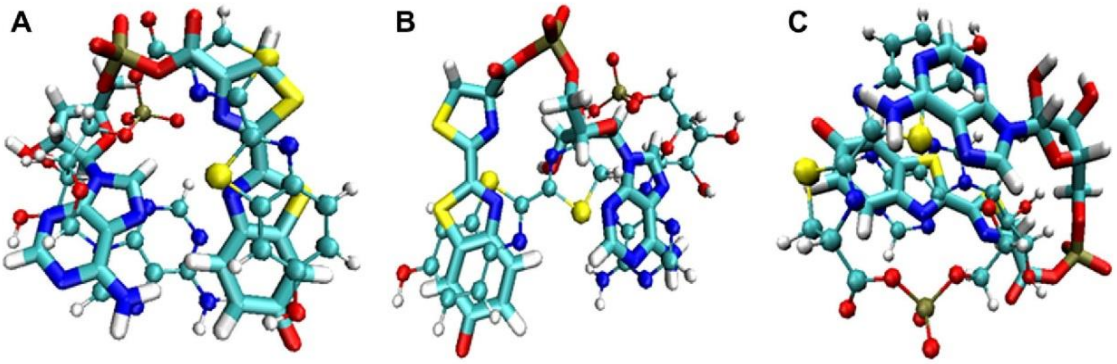

Figure 2. Comparison between the conformation of deprotonated/protonated L-AMP (A), L-LH_2-AMP (B) and D-LH_2-AMP (C), after the molecular mechanics simulation.

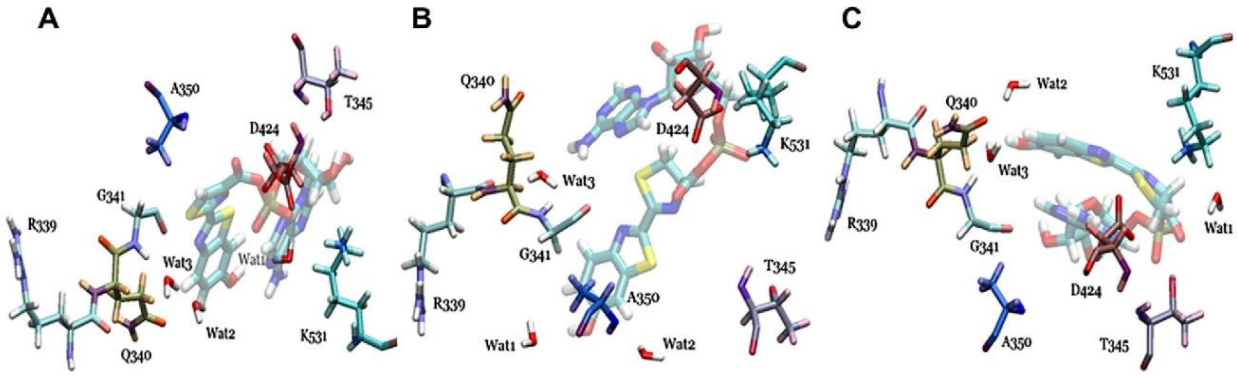

Figure 4. Complexes formed between active site molecules of the first selection, and L-AMP (A), L-LH_2-AMP (B) and D-LH_2-AMP (C), after the molecular mechanics simulation.

Table 2
Energetic contributions of active site molecules (second selection) to the binding of (D/L)-LH_2-AMP and L-AMP.

	D-LH_2-AMP	L-LH_2-AMP	L-AMP
Ser200	8	2	−1
Ser201	−7	−6	−4
Arg220	23	22	30
Phe249	5	−1	−3
His247	12	3	−3
Thr253	1	1	2
Gly318	−6	−8	1

In Table 2 are presented the energetic contribution of the active site molecules of the second selection to the binding of (D/L)-LH_2-AMP and L-AMP. The complexes formed between the three adenylates and the active site molecules of the second selection are represented in Figure 5. Generally, the active site molecules present in this selection have more relevant energetic contributions than the molecules present in the first selection. However, their contribution is still low. The general exception is Arg220 (22–30 kcal/mol). However, it should be noted that Ser200 (8 kcal/mol), Phe249 (5 kcal/mol) and His247 (12 kcal/mol) present relevant positive contributions to D-LH_2-AMP, while presenting negligible contributions to the other ligands. Gly318 presents a relevant negative contribution to the binding of (D/L)-LH_2-AMP.

Summarizing the findings presented in this manuscript, our results indicated that the binding of D-LH_2-AMP to luciferase is mainly caused by electrostatic interactions between the ligand and cationic residues (Arg220, Arg339 and Lys531), present in the active site. L-AMP and L-LH_2-AMP are expected to behave as competitive inhibitors of D-LH_2-AMP, due to their very similar binding mode. As in the case of the latter, the former ligands bind to luciferase mainly by electrostatic interactions. Furthermore, our results indicate that (D/L)-LH_2-AMP have similar affinity to the enzyme as L-AMP. Thus, it appears that this latter molecule is a weaker inhibitor of D-LH_2-AMP than it is for D-LH_2. This is consistent with experiment, as an L-AMP analog proven to be a stronger inhibitor of luciferin ($K_i = 34 \pm 5$ nM) and ATP–Mg^{2+} ($K_i = 41 \pm 3$ nM), than for D-LH_2-AMP ($K_i = 340 \pm 50$ nM) [42]. In our opinion, this finding is important to understand the flash-profile of firefly bioluminescence [1]. The data regarding this phenomenon indicate that a compound must be formed during the bioluminescence reaction, which can act as a very powerful inhibitor of molecules involved in the formation of oxyluciferin [1]. L-AMP is indeed a powerful inhibitor of D-LH_2 [18]. However, it was not clear which was the inhibitory power of L-AMP in regard to D-LH_2-AMP. The present study indicates that L-AMP is not as potent as inhibitor of D-LH_2-AMP as of D-LH_2, due to the similar binding affinity of these two adenylates to the luciferase enzyme. Therefore, it appears that L-AMP has a key role in the flash-profile mainly by inhibiting the binding of D-LH_2, and not of D-LH_2-AMP.

4. Conclusion

The binding of (D/L)-LH_2-AMP and L-AMP to *Luciola cruciata* luciferase was studied by means of a semi-empirical/molecular mechanics approach. This study was performed with the objective of elucidating the binding of adenylates to this enzyme, and to

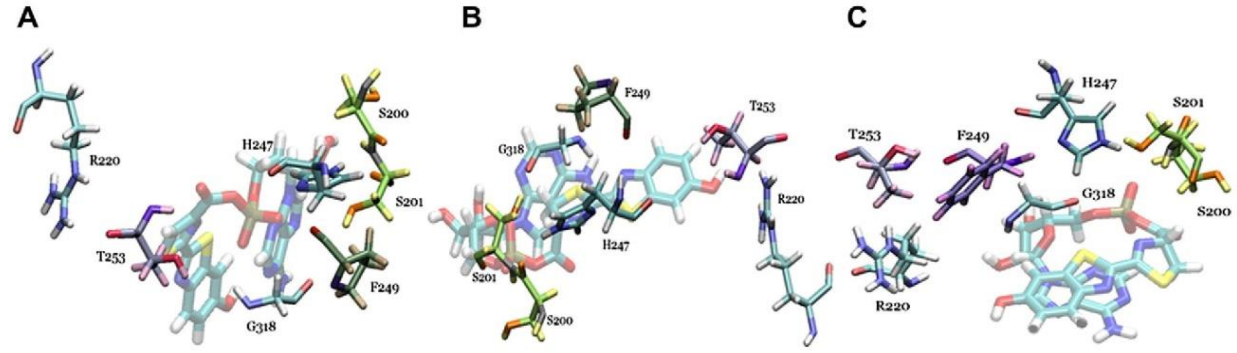

Figure 5. Complexes formed between active site molecules of the second selection, and L-AMP (A), L-LH_2-AMP (B) and D-LH_2-AMP (C), after the molecular mechanics simulation.

analyze the possible inhibitory effect of L-AMP/L-LH_2-AMP in regard to D-LH_2-AMP.

We have found that the binding of these molecules is governed mainly by electrostatic interactions with ionic amino-acids present in the active site, which is due to the single anionic charge of the adenylates. Arg220, Arg339 and Lys531 contribute favorably to the binding, while Asp424 is a very important unfavorable contributor.

We have also found that L-AMP and L-LH_2-AMP may act as competitive inhibitors of D-LH_2-AMP, due to their similar binding mode and similar affinity to luciferase. This indicates that L-AMP has a key role in the flash-profile, more by inhibiting the binding of D-LH_2 than by inhibiting the binding of D-LH_2-AMP.

Asp424, Gly318, Ser201 and Thr345 appear to be good mutagenesis targets, in order to increase the affinity of D-LH_2-AMP without equally increasing the affinity of L-AMP. Gly318, Ser201 and Thr345 present relevant negative contributions to the binding of D-LH_2-AMP, but are irrelevant contributors to the binding of L-AMP. Asp424 is a relevant negative contributor to the binding of both adenylates, but its contribution is higher to the binding of D-LH_2-AMP.

Acknowledgment

Financial support from Fundação para a Ciência e Tecnologia (FCT, Lisbon) (Programa Operacional Temático Factores de Competitividade (COMPETE) e comparticipado pelo Fundo Comunitário Europeu FEDER) (Project PTDC/QUI/71366/2006) is acknowledged. A Ph.D. Grant to Luís Pinto da Silva (SFRH\kBD\76612\2011), attributed by FCT, is also acknowledged.

Appendix A. Supplementary data

Supplementary data associated with this article can be found, in the online version, at http://dx.doi.org/10.1016/j.cplett.2012.06.038.

References

[1] S.M. Marques, J.C.G. Esteves da Silva, IUBMB Life 61 (2009) 6.
[2] J.M. Leitão, J.C.G. Esteves da Silva, J. Photochem. Photobiol. 01 (2010) 1.
[3] L. Pinto da Silva, J.C.G. Esteves da Silva, J. Chem. Theory Comput. 7 (2012) 809.
[4] V.R. Viviani, F.G.C. Arnoldi, A.J.S. Neto, T.L. Oehlmeyer, E.J.H. Bechara, Y. Ohmiya, Photochem. Photobiol. Sci. 7 (2008) 159.
[5] N.N. Ugarova, L.Y. Brovko, Luminescence 17 (2002) 321.
[6] L. Pinto da Silva, J.C.G. Esteves da Silva, ChemPhysChem 12 (2011) 951.
[7] L. Pinto da Silva, J.C.G. Esteves da Silva, J. Comput. Chem. 32 (2011) 2654.
[8] C.I. Song, Y.M. Rhee, J. Am. Chem. Soc. 133 (2011) 12040.
[9] J.C.G. Esteves da Silva, J.M.C.S. Magalhães, R. Fontes, Tetrahedron Lett. 42 (2001) 8173.
[10] B.R. Branchini, M.H. Murtiashaw, R.A. Magyar, N.C. Portier, M.C. Ruggiero, J.G. Stroh, J. Am. Chem. Soc. 124 (2002) 2112.
[11] L. Pinto da Silva, J.C.G. Esteves da Silva, ChemPhysChem 12 (2011) 3002.
[12] L. Pinto da Silva, J.C.G. Esteves da Silva, J. Phys. Chem. B 116 (2012) 2008.
[13] S.M. Marques, J.C.G. Esteves da Silva, Anal. Bioanal. Chem. 391 (2008) 2161.
[14] S.M. Marques, F. Peralta, J.C.G. Esteves da Silva, Talanta 77 (2009) 1497.
[15] B.R. Branchini, T.R. Southworth, N.F. Khattak, E. Michelini, A. Roda, Anal. Biochem. 345 (2005) 140.
[16] A. Roda, P. Pasini, M. Mirasoli, E. Michelini, M. Guardigli, Trends Biotechnol. 22 (2004) 295.
[17] A. Roda, M. Guardigli, Anal. Bioanal. Chem. 402 (2012) 69.
[18] C. Ribeiro, J.C.G. Esteves da Silva, Photochem. Photobiol. Sci. 7 (2008) 1085.
[19] H. Fraga, D. Fernandes, R. Fontes, J.C.G. Esteves da Silva, FEBS J. 272 (2005) 5206.
[20] L. Pinto da Silva, J.C.G. Esteves da Silva, Photochem. Photobiol. Sci. 10 (2011) 1039.
[21] R. Fontes, D. Fernandes, F. Peralta, H. Fraga, I. Maio, J.C.G. Esteves da Silva, FEBS J. 275 (2008) 1500.
[22] H. Fraga, D. Fernandes, J. Novotny, R. Fontes, J.C.G. Esteves da Silva, ChemBioChem 7 (2006) 929.
[23] T. Nakatsu, S. Ichiyama, J. Hiratake, A. Saldanha, N. Kobashi, K. Sakata, H. Kato, Nature 440 (2006) 372.
[24] J.J.P. Stewart, J. Comput. Chem. 10 (1989) 221.
[25] D.A. Case et al., J. Comput. Chem. 26 (2005) 1668.
[26] Y. Duan et al., J. Comput. Chem. 24 (2003) 1999.
[27] J.J.P. Stewart, J. Mol. Modeling 13 (2007) 1173.
[28] MOPAC2009, James J.P. Stewart, Stewart Computational Chemistry, Colorado Springs, CO, USA, http://OpenMOPAC.net (2008).
[29] J.M. Wang, R.M. Wolf, J.W. Caldwell, P.A. Kollman, D.A. Case, J. Comput. Chem. 25 (2004) 1157.
[30] G.M. Morris, R. Huey, W. Lindstrom, M.F. Sanner, R.K. Belew, D.S. Goddsell, J. Comput. Chem. 30 (2009) 2785.
[31] J.C. Philips et al., J. Comput. Chem. 26 (2005) 1781.
[32] U. Essmann, L. Perera, M.L. Berkowitz, T. Darden, H. Lee, L.G. Pedersen, J. Chem. Phys. 103 (1995) 8577.
[33] K.D. Dubey, R.P. Ojha, J. Biol. Phys. 37 (2011) 69.
[34] V.M. Anisimov, C.N. Cavasotto, J. Comput. Chem. 32 (2011) 2254.
[35] N. Nunthaboot, F. Tanaka, S. Kokpol, H. Chosrwjan, S. Taniguchi, N. Mataga, J. Phys. Chem. B 112 (2008) 15837.
[36] Y.Z. Xiong, P.Y. Chen, J. Mol. Model. 14 (2008) 1083.
[37] Gaussian 03 (Revision C.02), M.J. Frisch, Gaussian, Inc., Wallingford, CT, 2004.
[38] Y. Erez, D. Huppert, J. Phys. Chem. A 114 (2010) 8075.
[39] I. Presiado, Y. Erez, D. Huppert, J. Phys. Chem. A 114 (2010) 9471.
[40] M. Nakamura et al., Biochem. Biophys. Res. Commun. 331 (2005) 471.
[41] N. Lembert, Biochem. J. 317 (1996) 273.
[42] B.R. Branchini, M.H. Murtiashaw, J.N. Carmody, E.E. Mygatt, T.L. Southworth, Bioorg. Med. Chem. Lett. 15 (2005) 3860.

2.2. Evalution of the Potential Role of the Oxidation and Isomerism Reactions of D-LH_2

Article 5

Study of firefly luciferin oxidation and isomerism as possible inhibition pathways for firefly bioluminescence

Luís Pinto da Silva, and Joaquim C.G. Esteves da Silva

Chem. Phys. Lett. **2014**, *592*, 188-191.

The theoretical calculations and the writing of the paper were performed by Luís Pinto da Silva, under supervision of Professor Esteves da Silva.

Chemical Physics Letters 592 (2014) 188–191

Contents lists available at ScienceDirect

Chemical Physics Letters

journal homepage: www.elsevier.com/locate/cplett

Study of firefly luciferin oxidation and isomerism as possible inhibition pathways for firefly bioluminescence

Luís Pinto da Silva, Joaquim C.G. Esteves da Silva *

Centro de Investigação em Química, Departamento de Química e Bioquímica, Faculdade de Ciências da Universidade do Porto, R. Campo Alegre 687, 4169-007 Porto, Portugal

ARTICLE INFO

Article history:
Received 18 November 2013
In final form 17 December 2013
Available online 24 December 2013

ABSTRACT

Firefly bioluminescence presents a light emitting profile with a form of a flash, due to the firefly luciferase-catalyzed formation of inhibitory products. These impair the binding of the substrate luciferin to the active site of the enzyme. However, this luciferase catalyzed pathways may not be the only ones responsible for the flash profile. The oxidation and isomerisation of the substrate luciferin lead to the formation of compounds that are also known inhibitors of firefly bioluminescence. So, the objective of this Letter was to analyze if these reactions could be capable of interfering with the bioluminescence reaction.

1. Introduction

Firefly bioluminescence is an astonishing and interesting light-emitting phenomenon, in which an enzyme (firefly luciferase) catalyzes the conversion of a ground state substrate into an excited state product (luciferin → oxyluciferin) [1–4]. Oxyluciferin then decays to the ground state with emission of visible light (~530–640 nm) [1–4].

The high quantum yield of firefly bioluminescence (~40–60%) has attracted many researchers, due to high potential of this light-emitting system to be used in biomedical, bioanalytical and pharmaceutical fields, among others [5]. Firefly bioluminescence has been used in rapid trace determination of ATP, in bio imaging and as gene reporter, among other applications [6–8].

The *in vitro* bioluminescence follows, even at high substrate concentration, a flash pattern (Figure 1) [9,10]. The emission of light starts almost instantaneously in a flash-like manner that decays quickly to a low basal level. This characteristic of light emission is attributed to the accumulation of inhibitory products. The light emission product, oxyluciferin, is a known competitive inhibitor of the reaction substrate, luciferin [9]. This indicates that the firefly bioluminescence reaction is self-inhibitory. However, the main inhibitor is thought to be dehydroluciferyl-adenylate [9,10]. This molecule is also produced by luciferase in dark reaction, lateral to the bioluminescence one. Dehydroluciferyl-adenylate is a tight-binding competitive inhibitor of luciferin, with an inhibition constant in the order of the nanomolars [9–10].

Due to its broad range of applications, it is crucial to have a deep knowledge of the inhibitors of bioluminescence and their inhibition parameters. These compounds may have a non-negligible effect on this reaction and lead to erroneous results in luciferase-catalyzed applications. Thus, more compounds were studied in order to see their inhibition profile regarding firefly luciferin.

It was found that dehydroluciferin, an oxidation product of luciferin, and the L-isomer of the luciferin subtract are also compounds with high inhibitory strength [10]. Nevertheless, these compounds do not receive much attention when researchers are dealing with firefly bioluminescence, as they are not produce in a luciferase-catalyzed way.

It should be noted that it is thought that the substrate luciferin may suffer oxidation and/or racemization in water, the solvent used in *in vitro* bioluminescence applications. So, it is possible that the substrate luciferin can be converted into an inhibitory compound (by either oxidation or isomerisation) outside of the luciferase active site. This would increase the concentration of inhibitors in the bioluminescence reaction mixture, while decreasing the concentration of substrate. Moreover, the inhibitors formed in the reaction mixture would be competing with the remaining luciferin for binding to luciferase active site. Thus, even the non-catalyzed formation of dehydroluciferin and the L-isomer of the luciferin subtract may favor the flash profile.

Given this, the objective of this research work is the theoretical analysis of the luciferin oxidation and isomerisation reactions in water, in order to see if these reactions are favorable enough to impair the *in vitro* bioluminescence applications.

2. Theoretical methodology

The geometries of reactants, products and transition states were obtained with optimization calculations at the PBE0/6-311G(d,p) level of theory [11]. Vibrational analysis at the same level of theory were performed in order to verify if obtained geometries were stationary or transition states. Intrinsic reaction coordinates (IRC) cal-

* Corresponding author. Fax: +351 226082959.
E-mail address: jcsilva@fc.up.pt (J.C.G. Esteves da Silva).

0009-2614/$ - see front matter © 2013 Elsevier B.V. All rights reserved.
http://dx.doi.org/10.1016/j.cplett.2013.12.047

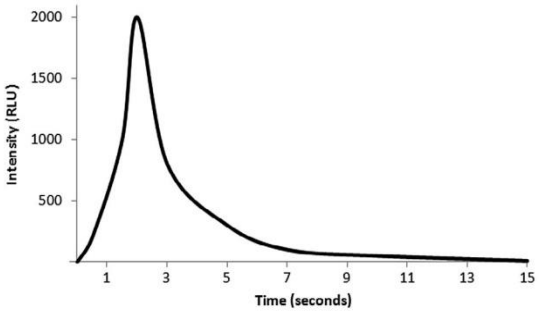

Figure 1. Representation of the typical flash profile of emitted light in firefly bioluminescence reaction.

culations, at the PBE0/6-311G(d,p) level of theory, were made in order to connect the transition states to the reactants and products [12].

A restricted (R) approach was used for closed-shell molecules, while an unrestricted one (U) was used for open-shell molecules. The stability of the wavefunction was verified, and optimized when needed, by using the stable = opt and guess = mix keywords.

We have used the PBE0 functional because it has been shown to consistently provide satisfactory results for several structural and thermodynamic properties [13–15].

All calculations were performed in implicit solvent by using the polarized continuum model (PCM), with parameters set for water [16]. All calculations were performed with the GAUSSIAN 09 electronic structure software package [17].

3. Results and discussion

3.1. Luciferin → dehydroluciferin conversion by oxidation reactions

Luciferin and dehydroluciferin are quite similar compounds, with only one difference. While the carboxylic-thiazole moiety of luciferin (Figure 2) has three hydrogen atoms and two double bonds, dehydroluciferin has one hydrogen atom and three double bonds in the same moiety. This small difference may explain the very strong inhibition constant of dehydroluciferin in regard to luciferin (~4.90 nM) [10].

In the present Letter, we present a reaction mechanism in which luciferin is converted into dehydroluciferin in result of molecular oxygen oxidation (Figure 3). We have considered that

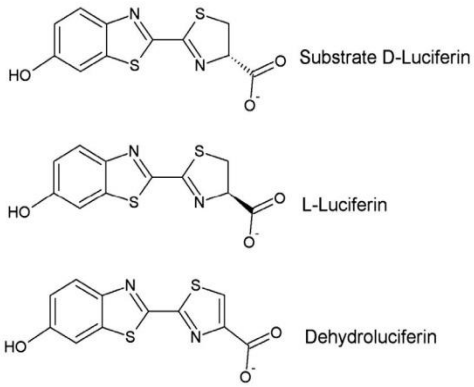

Figure 2. Schematic representation of substrate D-luciferin, L-luciferin and dehydroluciferin. The hydroxyl group is deprotonated in order to simulate a pH of ~7–7.5 [1–4].

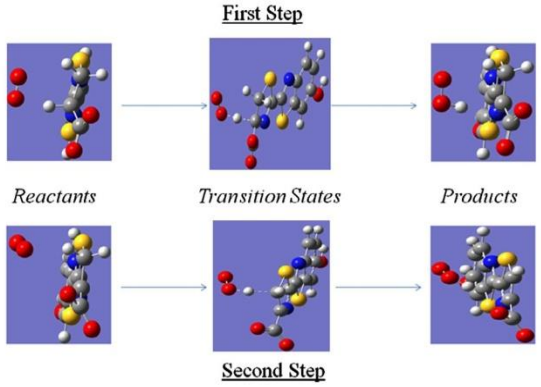

Figure 3. Important structures of the two-step oxidation reaction mechanism of firefly luciferin.

the proton of the C_4 atom (Figure 3) is the first one to be abstracted, because all the information regarding luciferin chemistry indicates that this is the most reactive proton of the ones involved in this reaction [18,19]. This mechanism is composed of two steps, each one consisting on the abstraction of one hydrogen atom by molecular oxygen (·O—O·). In each step, the oxygen molecule is converted into a hydroperoxyl radical (HO_2·), while anionic luciferin is firstly converted into a luciferyl radical and then into dehydroluciferin.

We can see by the energy profile of the reaction (Figure 4) that it is not expected that luciferin → dehydroluciferin conversion has any effect on the profile of bioluminescence emission. The energy barrier of the first step of the oxidation step is significantly high (17.9 kcal/mol), which indicates that this step is not feasible. Moreover, this step is apparently endothermic as the products are 10.1 kcal/mol higher in energy than the reactants (Figure 4). Therefore, it is not expected that the oxidative reaction occurs, as the abstraction of the first proton is not feasible without any type of catalysis.

In the case of the second step, this part of the reaction appears to be more favorable (Figure 4). The energy barrier is not very high (6.5 kcal/mol), and the products are lower in energy than the reactants by 1.5 kcal/mol. However, these values are not enough to overcome the very unfavorable ones found on step one.

In Table 1 are present the atomic Mulliken charges of the benzothiazole and carboxylic-thiazole moieties, of the reactants and products of each step of the oxidation reaction. With these data, we think that we can explain why the products of the first step are higher in energy than the reactants, while in the second step we verify the opposite.

First, we will consider the first step. We can see that the benzothiazole moiety of the reactant has a neutral charge, while the carboxylic-thiazole has a charge of nearly −1. This indicate that the polarization in this molecule is great, which we think that indicates stabilization by polarization. Given the neutral charge of one moiety and the high negative charge of the other, we think that there is little effect exerted by electrostatic forces. However, we see that some delocalization of charge occurs between the two moieties during the first step. In the product luciferin molecule, the benzothiazole moiety has now some negative charge, which decreased the negative charge of the carboxylic-thiazole moiety. Thus, it would expect that in comparison with the reactant, the luciferin product would be destabilized due to decrease in polarization interaction energy and some unfavorable electrostatic charges (as now both moieties are negative).

This line of thinking is supported by the atomic charge distribution in the moieties of the luciferin reactant and product of the second step (Table 1). We can see that both moieties of the reactant

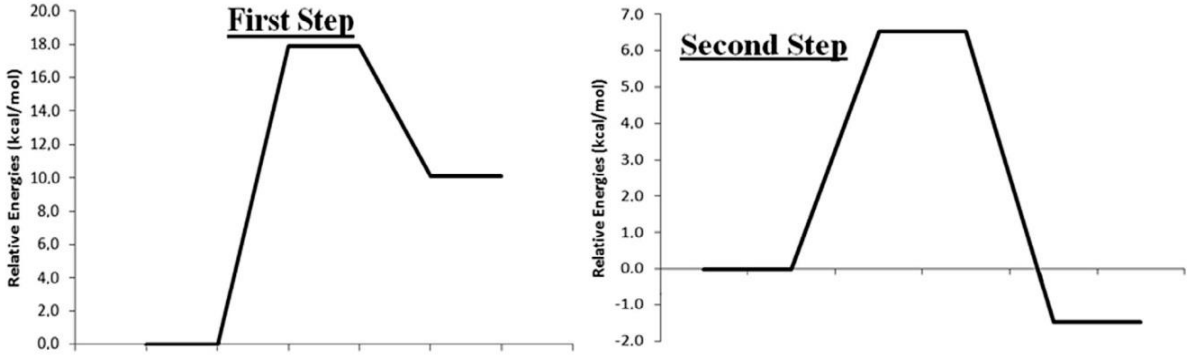

Figure 4. Representation of the energies of substrate, transition states, products and intermediates of the oxidation reaction of firefly luciferin.

Table 1
Atomic Mulliken charges of the benzothiazole and carboxylic-thiazole moieties of the two-step oxidation reaction reactants and products, at the PBE0/6-311G(d,p) level of theory in implicit water.

	Benzothiazole moiety	Carboxylic-thiazole moiety
First-step reactant	0.00	−0.99
First-step product	−0.05	−0.96
Second-step reactant	−0.10	−0.91
Second-step product	−0.01	−0.95

are negative, and that the negative charge difference is more significant than verified in the first step. So, it is expected that the polarization stabilization energy is decreased, while the repulsive electrostatic interactions are higher. Due to the second abstraction of the proton that constitutes the second step, the negative charge delocalization is lower in the final luciferin product. The negative charge of the benzothiazole moiety is nearly zero, while the negative charge of the carboxylic-thiazole moiety increased. Thus, the fact that in the second step the luciferin product is more stable than the luciferin reactant can be explained by increased polarization stabilization and decreased repulsive electrostatic interactions between the moieties.

3.2. Isomerisation of firefly luciferin

Firefly luciferin is a chiral molecule, and can be found in two different species (L- and D-isomers, Figure 2). It is known that luciferase uses the D-isomer as the bioluminescence substrate, while the L-isomers is an inhibitor of luciferase light-emitting reaction [10,18,19]. Therefore, if some of the D-luciferin added to the bioluminescence reaction mixture could be converted to the D-isomer, the concentration of substrate would decrease while the concentration of inhibitor would increase.

We have found a two-step reaction mechanism in which the D ⇄ L isomerisation is water assisted (Figure 5). In the first step, the proton of C_4 atom is abstracted by a water molecule, which will transfer it to the deprotonated oxygen atom of the carboxylic moiety. In the second step, the carboxylic atom will transfer the proton to a water molecule, which will return the proton to C_4 atom in a new isomerisation state.

As in the case of luciferin → dehydroluciferin oxidation, the D ⇄ L isomerisation appears to not be very feasible. As can be seen in the energetic profile of this reaction (Figure 6), the energy barrier of the first step is very high (22.3 kcal/mol). Moreover, the product of this step is higher in energy than the reactant by 11.5 kcal/mol. The second step appears to be more favorable, as the energy barrier is lower than in second step. Moreover, the product is lower in energy than the reactant (by 11.5 kcal/mol). Nevertheless, the complete energy profile is far from indicating a

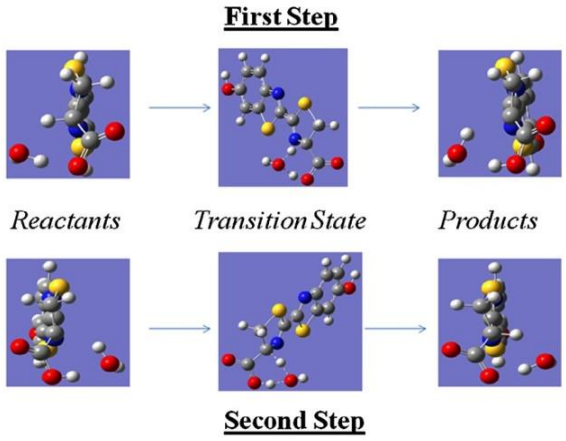

Figure 5. Important structures of the two-step isomerisation reaction mechanism of firefly luciferin.

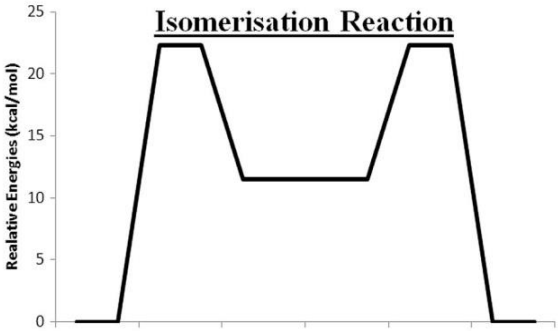

Figure 6. Representation of the energies of substrate, transition states, products and intermediates of the isomerisation reaction of firefly luciferin.

favorable reaction, especially as the initial reactants and final products have exactly the same energy. Our data shows that D ⇄ L isomerisation should not occur in aqueous solution, thereby not affecting the light-emitting profile of the bioluminescence reaction. Thus, if the D-luciferin sample used is pure, no inhibitory effect should be expected from the L-isomer.

4. Conclusions

Firefly bioluminescence presents a flash profile of emitted light. This profile is attributed to the production of inhibitory products.

This notion was supported by the finding that two products of luciferase-catalyze reactions (oxyluciferin and dehydroluciferyl-adenylate) strongly inhibit the binding of the reaction substrate (Luciferin).

Due to these data, it was expected that the flash profile was caused mainly by production of inhibitors by luciferase itself. However, it is known that exist more inhibitors of the binding of luciferin to the enzyme. Two of them (dehydroluciferin and L-luciferin) are so similar to the substrate luciferin that the hypothesis existed that this compound could be converted in inhibitors in aqueous solution, without the aid of luciferase catalytic functions. Thus, the objective of this Letter was to see if the formation of dehydroluciferin and L-luciferin from D-luciferin, in water, could be feasible enough to be responsible for some part of the flash profile.

Our results have indicated that both the oxidative and isomerisation reactions are not feasible in aqueous solutions. We have found a two-step reaction mechanism for both, in which either molecular oxygen or water molecules were involved. These reactions mechanisms presented very high activation barriers for the first step, and we have also found that the products of the first step were always higher in energy than the initial reactant. Therefore, despite the second step of both reactions being more favorable, these reactions are not expected to occur in water and affect the firefly bioluminescence reaction.

Acknowledgments

Financial support from Fundação para a Ciência e Tecnologia (FCT, Lisbon) (Programa Operacional Temático Factores de Competitividade (COMPETE) e comparticipado pelo Fundo Comunitário Europeu (FEDER) (Project PTDC/QUI/71 366/2006) is acknowledged. A Ph.D. Grant to Luís Pinto da Silva (SFRH/BD/76 612/2011), attributed by FCT, is also acknowledged.

Appendix A. Supplementary data

Supplementary data associated with this article can be found, in the online version, at http://dx.doi.org/10.1016/j.cplett.2013.12.047.

References

[1] L. Pinto da Silva, J.C.G. Esteves da Silva, ChemPhysChem 13 (2012) 2257.
[2] L. Pinto da Silva, R. Simkovitch, D. Huppert, J.C.G. Esteves da Silva, ChemPhysChem 14 (2013) 3441.
[3] S. Hosseinkhani, Cell. Mol. Life Sci. 68 (2010) 1167.
[4] L. Pinto da Silva, J.C.G. Esteves da Silva, J. Chem. Theory Comput. 7 (2011) 809.
[5] K. Niwa et al., Photochem. Photobiol. 86 (2010) 1046.
[6] R. Alam, J. Zylstra, D.M. Fontaine, B.R. Branchini, M.M. Maye, Nanoscale 5 (2013) 5303.
[7] A. Roda, L. Cevenini, E. Michelini, B.R. Branchini, Biosens. Bioelectron. 26 (2011) 3647.
[8] A. Roda, M. Guardigli, Anal. Bioanal. Chem. 402 (2012) 69.
[9] J.M. Leitão, J.C.G. Esteves da Silva, J. Photochem. Photobiol. B 101 (2010) 1.
[10] L. Pinto da Silva, J.C.G. Esteves da Silva, Photochem. Photobiol. Sci. 10 (2011) 1039.
[11] C. Adamo, V. Barone, J. Chem. Phys. 110 (1999) 6158.
[12] H.P. Hratchian, H.B. Schlegel, J. Chem. Theory Comput. 1 (2005) 61–69.
[13] L. Pinto da Silva, J.C.G. Esteves da Silva, ChemPhysChem 12 (2011) 951.
[14] G.A.A. Saracino, R. Improta, V. Barone, Chem. Phys. Lett. 373 (2003) 411.
[15] D. Jacquemim, E.A. Perpète, C. Ciofini, C. Adamo, Acc. Chem. Res. 42 (2009) 326.
[16] J. Tomasi, B. Mennucci, R. Cammi, Chem. Rev. 105 (2005) 2999.
[17] M.J. Frisch et al., GAUSSIAN 09, Revision A.02, Gaussian Inc, Wallingford, CT, 2009.
[18] S. Inouye, Cell. Mol. Life Sci. 67 (2010) 387.
[19] S.M. Marques, J.C.G. Esteves da Silva, IUBMB Life 61 (2009) 6.

Chapter 3 – Study of the Formation Mechanism of Firefly Dioxetanone

3.1. Evaluation of the Potential Role of a Carbanion or a Radical Intermediate in the Formation of Firefly Dioxetanone

Article 6

Theoretical evaluation of the role of carbanion and radical molecules on the formation of firefly dioxetanone
Luís Pinto da Silva and Joaquim C.G. Esteves da Silva
J. Spectrosc. Dyn. **2014**, *4*:*17*.

The theoretical calculations and the writing of the paper were performed by Luís Pinto da Silva, under supervision of Professor Esteves da Silva.

Journal of Spectroscopy and Dynamics J. Spectrosc. Dyn. x, x: x

Theoretical evaluation of the role of carbanion and radical molecules on the formation of firefly dioxetanone

Luís Pinto da Silva, Joaquim C.G. Esteves da Silva*

Centro de Investigação em Química, Departamento de Química e Bioquímica, Faculdade de Ciências da Universidade do Porto, R. Campo Alegre 687, 4169-007 Porto, Portugal

*Author for correspondence: Joaquim C.G. Esteves da Silva, email: jcsilva@fc.up.pt
Received 13 Aug 2013; Accepted 2 Sep 2013; Available Online 2 Sep 2013

Abstract

A theoretical approach was used in order to evaluate the possible role of carbanion and radical molecules on the formation of firefly dioxetanone, from luciferyl-adenylate. Implicit solvent models were used in order to simulate the hydrophobicity of the enzymatic active site. Our calculations do not support the carbanion-based mechanism, as no factors were found that would promote the expected interaction of the luciferyl carbanion with triplet oxygen. On the contrary, our theoretical calculations do support the radical-based mechanism. This mechanism has the advantage of providing an explanation for the formation of dehydroluciferyl-adenylate, and for the interaction of a triplet molecule with a singlet one with formation of a singlet product.

Keywords: Firefly dioxetanone; Firefly bioluminescence; Oxyluciferin; Luciferin oxidation; Carbanion; Free radicals

1. Introduction

Firefly bioluminescence is one of the most well-known and studied light-emitting systems [1-5]. In this system, the enzyme firefly luciferase catalyzes the formation of the light emitter firefly oxyluciferin, from the reaction between firefly luciferin and adenosine-5'-triphosphate-Mg^{2+} (ATP-Mg^{2+}) (Figure 1) [1-5]. Due to very important and interesting characteristics, the firefly bioluminescence system has been gaining practical applications in the pharmaceutical, biomedical and bioanalytical areas, among others [6-8].

Oxyluciferin is formed directly in a singlet excited state due to the formation and subsequent decomposition of firefly dioxetanone (Figures 2, 3), during the bioluminescence reaction [4,5]. It is thought that in the vicinities of the ground state transition state of this decomposition reaction, there is a path for singlet chemiexcitation. Numerous theories have been proposed in order to explain this phenomenon: Chemically Initiated Electron-Exchange Luminescence (CIEEL), Charge Transfer Induced Luminescence (CTIL), Gradually Reversed Charge Transfer Initiated Luminescence (GRCTIL) and Interstate Crossing-Induced Chemiexcitation (ICIC) mechanisms [9-12].

It is commonly said that the firefly bioluminescence reaction consists of two general steps: first, firefly luciferin and ATP-Mg^{2+} react with each other, giving origin to the intermediate luciferyl-adenylate; subsequently, this latter intermediate is oxidized in the presence of molecular oxygen, which leads to the formation of oxyluciferin [1-5]. This second step is crucial for the formation of excited state products. Prior to oxyluciferin formation, the oxidation of luciferyl-adenylate results in the formation of firefly dioxetanone. The reason for the subsequent chemiexcited formation of oxyluciferin is the decomposition of this latter molecule [4,5].

Two mechanisms have been proposed in order to explain the formation of firefly dioxetanone from luciferyl-adenylate. The oldest mechanism postulates that luciferyl-adenylate loses a proton from a carbon atom, creating a carbanion (Figure 2) [1]. Subsequently, the carbanion

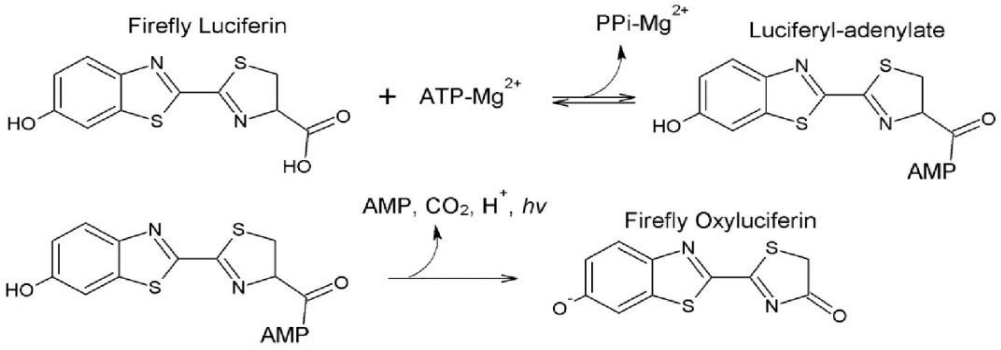

Figure 1. Schematic representation of the firefly bioluminescence reaction.

Journal of Spectroscopy and Dynamics J. Spectrosc. Dyn. x, x: x

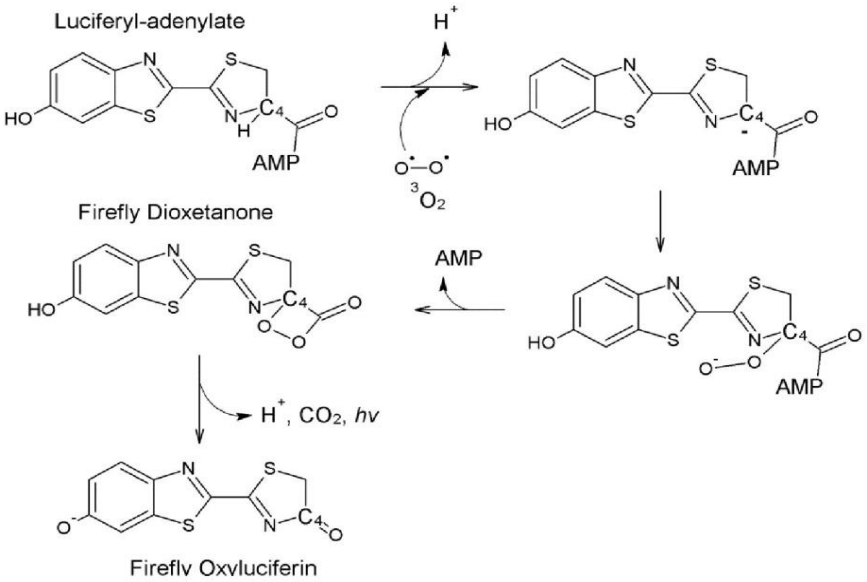

Figure 2. Schematic representation of the carbanion-based mechanism for the formation of firefly dioxetanone.

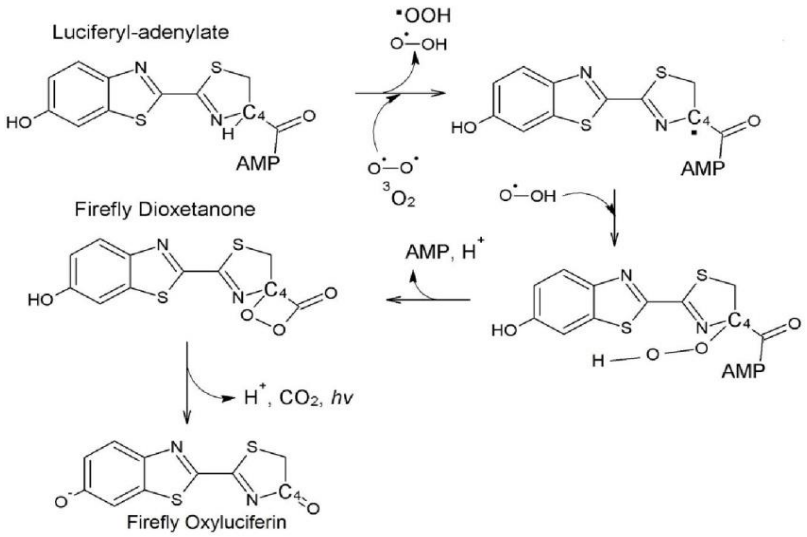

Figure 3. Schematic representation of the radical-based mechanism for the formation of firefly dioxetanone.

undergoes a nucleophilic attack of the molecular oxygen, forming a linear peroxide. The newly formed hydroperoxy group is involved in an intramolecular nucleophilic attack, forming firefly dioxetanone (Figure 2) [1].

Rather recently, Branchini and co-workers have proposed an alternative mechanism for the formation of firefly dioxetanone (Figure 3) [13]. In this reaction mechanism, it is the molecular oxygen that abstracts the proton of the carbon atom of luciferyl-adenylate, leading to the formation of two radical molecules. Recombination of these radicals will then result in the formation of firefly dioxetanone. One of the benefits of this new reaction mechanism is that it would better explain why a triplet molecule (molecular oxygen) is capable of reacting with a singlet molecule (luciferyl-adenylate) and form a singlet product (firefly dioxetanone). Moreover, this reaction mechanism can supposedly account for the formation of dehydroluciferyl-adenylate from luciferyl-adenylate and molecular oxygen, which is formed in a dark lateral luciferase-catalyzed reaction, alongside with hydrogen peroxide [14,15]. Nevertheless, this new mechanism is only a hypothesized one and without any experimental or computational support.

Journal of Spectroscopy and Dynamics J. Spectrosc. Dyn. x, x: x

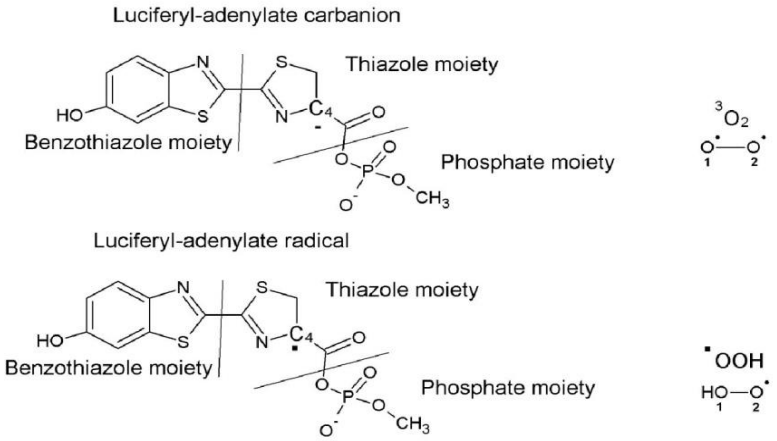

Figure 4. Schematic representation of the molecules studied in this work. As already said in the main text, the adenylate region was decreased to a methylated-phosphate moiety.

Table 1. ESP and Mulliken atomic charges of the atoms of $^3O_2$ and $^\bullet$OOH, as well as their spin densities.

	$^3O_2$		$^\bullet$OOH	
	O_1	O_2	O_1	O_2
ESP	0.000	0.000	-0.254	-0.164
Mulliken	0.000	0.000	-0.045	-0.168
Spin density	1.000	1.000	0.269	0.741

Table 2. Mulliken and ESP atomic charges of the different moieties and C_4 atom of luciferyl-adenylate carbanion.

	Mulliken	ESP
Benzothiazole	-0.402	-0.381
Thiazole	-0.533	-0.399
Phosphate	-1.065	-1.220
C_4	-0.082	-0.184

The objective of this work is then the theoretical evaluation of the role of both carbanion and radical molecules on the formation of firefly dioxetanone, in order to understand which the more probable mechanism is: the carbanion- or radical-based one.

2. Computational Methods

Optimization, frequency and single point energies were calculated at the CAM-B3LYP/cc-pVDZ level of theory [16]. This functional was chosen because besides behaving well for organic molecules, it also provides good estimates for possible charge transfer and Rydberg states [17]. The solvent was modeled in the calculations by employing the conductor-like polarized continuum (CPCM) model with a dielectric constant of 4 [18]. This empirical value of 4 was chosen because it gives good agreement with experimental results regarding protein active sites, by accounting for the average effect of the protein and buried water molecules [19-21].

The studied species were molecular oxygen ($^3O_2$), hydroperoxyl radical ($^\bullet$OOH), and the carbanion and radical species of luciferyl-adenylate (Figure 4). The adenylate portion of the adenylyl intermediates was reduced to a methylated phosphate group, in order to facilitate the calculations. The benzothiazole oxygen of the luciferyl portion is protonated because recent studies have indicated that this group cannot be deprotonated during the bioluminescence reaction [22].

All the calculations were performed with the Gaussian 09 software package [23].

3. Results and Discussion

In Tables 1 and 2 are presented the ESP and Mulliken atomic charges of $^3O_2$ and luciferyl-adenylate carbanion, as well as the atomic Mulliken spin densities of the former molecule. The atomic charges (both ESP and Mulliken) of the two oxygen atoms of $^3O_2$ are zero, which is consistent with the neutral charge of this molecule. The atomic Mulliken spin densities of $^3O_2$ indicate that each oxygen atom possesses a sole electron with a spin-up orientation, consistent with the triplet multiplicity of this molecule.

As shown in the Table 2, we can see that the negative charge originated by the deprotonated oxygen of the phosphate moiety of luciferyl-adenylate carbanion, is confined in that moiety. On the contrary, the negative charge originated by the deprotonation of the C_4 atom of the thiazole moiety is distributed along the entire luciferyl moiety. We can also see that the C_4 atom has an electronegative charge, in both schemes of atomic partial charges.

The data here presented appears to support some aspects of the carbanion-based mechanism for the formation of firefly dioxetanone. $^3O_2$ presents two atoms that do not have an octet of electrons, thereby being an electrophile species. The double negative charge of the luciferyl-adenylate carbanion indicates that this molecule does indeed have free pair of electrons to donate, thereby acting as a nucleophile. However, we cannot see any factors that justify the specific bonding between C_4 and $^3O_2$, after the nucleophilic attack of $^3O_2$ by the luciferyl-adenylate carbanion. Electrophiles are attacked by the most electron-populated part of one nucleophile. However, C_4 presents low negative atomic

Journal of Spectroscopy and Dynamics J. Spectrosc. Dyn. x, x: x

Table 3. Mulliken and ESP atomic charges, and spin densities of the different moieties and C_4 atom of luciferyl-adenylate radical.

	Mulliken	ESP	Spin densities
Benzothiazole	-0.097	-0.041	0.148
Thiazole	0.003	0.179	0.845
Phosphate	-0.951	-1.138	0.007
C_4	0.011	0.022	0.440

charges (Table 2). Moreover, our calculations indicate that the thiazole moiety of the luciferyl-adenylate carbanion is not the most electron-populated region of this molecule. The phosphate moiety has basically the double of negative charge than the thiazole moiety. The latter moiety presents a negative charge slightly higher than the benzothiazole moiety. So, the electrophilic $^3O_2$ should not be particularly attracted by the thiazole portion of the carbanion. Finally, the N-C_4 bond (Figure 4) has a bond length of 1.32 Å, which suggest that this is a double bond. As C_4 is also bonded to other two carbons, by single bonds, this double bond indicates that C_4 has already eight electrons in its valence shells. This octet configuration of C_4 indicates that this is not a reactive atom, and therefore not likely to bond to one of the oxygen atoms of $^3O_2$, as postulated by the carbanion-based mechanism (Figure 2) [1].

In Tables 1 and 3 are presented the ESP and Mulliken atomic charges of $^{\bullet}$OOH and luciferyl-adenylate radical, as well as the atomic Mulliken spin densities of the two molecules. The calculated atomic charges indicate that both oxygen atoms of $^{\bullet}$OOH are negative. However, the ESP scheme indicates that the negative charge of O_1 is higher than O_2, while the Mulliken scheme predicts the opposite. The calculated atomic densities indicate that O_2 is atom with higher spin-density, thus being the oxygen that will supposedly bind to luciferyl-adenylate radical.

As shown in the Table 3, we can see that the negative charge of the phosphate group is contained in the moiety of the luciferyl-adenylate radical. As for the luciferyl region, the benzothiazole moiety is slightly negative, while the thiazole one is positive (more with the ESP scheme than with the Mulliken one). As for the spin density, it mainly resides in the thiazole moiety, being basically inexistent in the phosphate group and slightly positive in the benzothiazole moiety. The C_4 atom presents a high and positive atomic spin density.

The results presented so far indeed support some features of the radical-based mechanism of firefly dioxetanone mechanism [13]. While the oxygen atom of $^{\bullet}$OOH that will supposedly bind to luciferyl-adenylate has negative charge, the thiazole moiety in general and C_4 in particular have positive charges, which will favor an electrostatic attraction between $^{\bullet}$OOH and luciferyl-adenylate radical in order to form firefly dioxetanone. Moreover, C_4 has the higher atomic spin density of all atoms of luciferyl-adenylate radical, which indicates that it is in this atom that the probability of finding the sole electron is higher. Thus, our calculations indeed support the radical-based mechanism, as it can be seen a specificity that will allow an efficient C_4-O_2 bond forming.

Summarizing the results presented so far, while some data indeed support some features of these mechanisms, our calculations do not fully support the carbanion-based mechanisms. It should be noted that any direct evidence does not exist to support this mechanism, as there is only direct evidence for the formation of luciferyl-adenylate and indirect evidence of the formation of firefly dioxetanone [1,4,5]. Therefore, it should not be a shock to the readers that this mechanism is not supported by theoretical evidence, although its newly found inadequacy may lead to a paradigm shift in the study of the mechanism of firefly dioxetanone formation. As for the radical-based mechanism, no features were found that could contradict this recent proposal.

4. Conclusions

In this work, we have studied both the carbanion- and radical-based mechanisms for the formation of firefly dioxetanone. To this end, we have used a density functional theory based approach, with implicit solvent models that were used to simulate the very hydrophobic environment of an enzymatic active site.

In the carbanion-based mechanism, luciferyl-adenylate loses a proton, thereby becoming a carbanion. Subsequently, it would attack nucleophilically the electrophile $^3O_2$. However, we have found that there is no factor that specifically causes an interaction of the thiazole moiety of luciferyl-adenylate carbanion with $^3O_2$. This moiety is not the most electron-populated region of the adenylate and the C_4 atom, which would supposedly bind to $^3O_2$, has already an octet configuration in the carbanion form.

In the radical-based mechanism, $^3O_2$ would abstract the proton of the C_4 atom of the adenylate, thus generating $^{\bullet}$OOH and luciferyl-adenylate radical. A latter recombination of these two radicals would trigger the formation of firefly dioxetanone. Our calculations indeed support the binding of C_4 (from luciferyl-adenylate radical) to O_2 (from $^{\bullet}$OOH), thus leading to the recombination of the radicals. Moreover, this mechanism has the advantages of better explaining why a triplet molecule binds to a singlet intermediate, thus forming a singlet product, and also provides some explanation for the formation of dehydroluciferyl-adenylate.

Acknowledgments

Financial support from Fundação para a Ciência e Tecnologia (FCT, Lisbon) (Programa Operacional Temático Factores de Competitividade (COMPETE) e comparticipado pelo Fundo Comunitário Europeu (FEDER) (Project PTDC/QUI/71366/2006) is acknowledged. A Ph. D. grant to Luís Pinto da Silva (SFRH/BD/76612/2011), attributed by FCT, is also acknowledged.

Supporting Information

Cartesian coordinates of the structures of $^3O_2$, $^{\bullet}$OOH, and the carbanion and radical species of luciferyl-adenylate.

References

1. S. M. Marques, and J. C. G. Esteves da Silva, IUBMB Life 61 (2009) 6.
2. S. Inouye, Cell. Mol. Life Sci. 67 (2010) 387.
3. L. Pinto da Silva, and J. C. G. Esteves da Silva, J. Chem. Theory Comput. 7 (2011) 809.
4. L. Pinto da Silva, and J. C. G. Esteves da Silva, ChemPhysChem 13 (2012) 2257.
5. I. Navizet, Y. J. Liu, N. Ferré, D. Roca-Sanjuán, and R. Lindh, Chemphyschem 12 (2011) 3064.

6. A. Roda, and M. Guardigli, Anal. Bioanal. Chem. 402 (2012) 69.
7. A. Roda, L. Cevenini, E. Michelini, and B. R. Branchini, Biosens. Bioelectron. 26 (2011) 3647.
8. R. Alam, D. M. Fontaine, B. R. Branchini, and M. M. Maye, Nano Lett. 12 (2012) 3251.
9. J. A. Koo, S. P. Schmidt, and G. B. Schuster, PNAS 75 (1978) 30.
10. H. Isobe, Y. Takano, M. Okumura, S. Kuramitsu, and K. Yamaguchi, J. Am. Chem. Soc. 127 (2005) 8667.
11. L. Yue, Y. J. Liu, and W. H. Fang, J. Am. Chem. Soc. 134 (2012) 11632.
12. L. Pinto da Silva, and J. C. G. Esteves da Silva, ChemPhysChem 14 (2013) 1071.
13. J. A. Sundlov, D. M. Fontaine, T. L. Southworth, B. R. Branchini, and A. M. Gulick, Biochemistry-us 51 (2012) 6493.
14. L. Pinto da Silva, and J. C. G. Esteves da Silva, Photoch. Photobio. Sci. 10 (2011) 1039.
15. C. Ribeiro, ando J. C. G. Esteves da Silva, Photoch. Photobio. Sci. 7 (2008) 1085.
16. T. Yanai, D. P. Tew, and N. C. Handy, Chem. Phys. Lett. 393 (2004) 51.
17. C. Adamo, and D. Jacquemin, Chem. Soc. Rev. 42 (2013) 845.
18. M. Cossi, N. Rega, G. Scalmani, and V. Barone, J. Comput. Chem. 24 (2003) 669.
19. L. Pinto da Silva, and J. C. G. Esteves da Silva, ChemPhysChem 12 (2011) 3002.
20. L. Pinto da Silva, and J. C. G. Esteves da Silva, J. Phys. Chem. B 116 (2012) 2008.
21. L. Pinto da Silva, and J. C. G. Esteves da Silva, ChemPhysChem 12 (2011) 951.
22. L. Pinto da Silva, and J. C. G. Esteves da Silva, J. Phys. Chem. A 117 (2013) 94.
23. M. J. Frisch et al., Gaussian 09 (Revision A.02), Gaussian Inc., Wallingford CT (2009).

Cite this article as:

Luís Pinto da Silva *et al.*: **Theoretical evaluation of the role of carbanion and radical molecules on the formation of firefly dioxetanone.** *J. Spectrosc. Dyn.* x, **x:** x

3.2. Characterization of the Reaction Mechanism of the Chemiluminescent Reaction between D-LH_2 and Superoxide Anion

Article 7

Theoretical study of the correlation between superoxide anion consumption and firefly luciferin chemiluminescence
Luís Pinto da Silva and Joaquim C.G. Esteves da Silva
Chem. Phys. Lett. **2013**, *577*, 127-130.

The theoretical calculations and the writing of the paper were performed by Luís Pinto da Silva, under supervision of Professor Esteves da Silva.

Chemical Physics Letters 577 (2013) 127–130

Contents lists available at SciVerse ScienceDirect

Chemical Physics Letters

journal homepage: www.elsevier.com/locate/cplett

Theoretical study of the correlation between superoxide anion consumption and firefly luciferin chemiluminescence

Luís Pinto da Silva, Joaquim C.G. Esteves da Silva *

Centro de Investigação em Química, Departamento de Química E Bioquímica, Faculdade de Ciências da Universidade do Porto, R. Campo Alegre 687, 4169-007 Porto, Portugal

ARTICLE INFO

Article history:
Received 12 April 2013
In final form 23 May 2013
Available online 31 May 2013

ABSTRACT

This is the first theoretical study of the relationship between superoxide anion and firefly chemiluminescence, in DMSO. Electron transfer reactions between luciferin dianionic/carbanionic/radical species and superoxide were studied in order see if an alternative explanation existed for the consumption of the latter species, without correlating it with a role on luciferin chemiluminescence. Despite the finding that luciferin may indeed inhibit the formation of the superoxide anion, no theoretical evidence was found that showed that this molecule is consumed in a non-chemiluminescence reaction. Therefore, it is concluded that the superoxide anion is indeed related to the firefly luciferin chemiluminescence.

1. Introduction

Firefly bioluminescence is a firefly luciferase-catalyzed light emitting reaction [1–3]. This enzyme catalyzes a two step reaction: first, firefly luciferin reacts with adenosine-5′-triphosphate, leading to the formation of an adenylyl intermediate; this latter molecule will be oxidized in the presence of molecular oxygen, giving origin to firefly oxyluciferin [1–3]. Oxyluciferin is the light emitter and it is formed already in a singlet excited state, thereby decaying to the ground state with emission of visible light [4–6]. This chemiexcitation is the result of the formation and subsequent decomposition of firefly dioxetanone [4–6]. Several theories have been present along the years, in order to explain this dioxetanone-dependent oxyluciferin chemiexcitation [7–10]. Due to very interesting characteristics, this bioluminescence system has been gaining numerous practical applications, in the pharmaceutical, biomedical and bioanalytical fields, among others [11–15].

Besides bioluminescence, firefly luciferin also exhibits chemiluminescence due to oxyluciferin formation via dioxetanone formation and decomposition (Scheme 1) [5,6]. Therefore, luciferin chemiluminescence became a good (and easier to study) model for firefly bioluminescence. It is generally thought that the C_4 atom of luciferin is deprotonated in order to create a carbanion, thus allowing for a nucleophilic attack on molecular oxygen [1,5,6]. This attack leads to the formation of linear peroxide. The next step of the reaction is thought to be an intramolecular nucleophilic attack of the hydroperoxy group, thus forming firefly dioxetanone [1,5,6]. Nevertheless, no direct evidence for this mechanism exists in order to support it.

Rather recently, Branchini and co-workers have proposed an alternative mechanism reaction for the formation of firefly dioxetanone, based on radical formation and recombination [16]. According to these authors, molecular oxygen abstracts the proton of C_4 atom, leading to the formation of two radical molecules. Recombination of these radicals will then form firefly dioxetanone. Nevertheless, this is also a hypothesized mechanism with no direct experimental/computational support.

In 1989, Wada and co-workers have proposed that the superoxide anion ($\cdot O_2^-$) plays an important role in the primary step of luciferin chemiluminescence [17,18]. These authors have demonstrated that $\cdot O_2^-$ is generated and is stably present in dimethyl sulphoxide (DMSO), and that is consumed on mixing with solutions containing luciferin, which produce light [17–19]. However, the correlation between $\cdot O_2^-$ consumption and chemiluminescence emission was not clearly defined. Nevertheless, the elucidation of this topic gains a renewed interest due to the proposal of Branchini and co-workers, that radical molecules are involved in the formation of firefly dioxetanone [16–18]. Thus, the objective of this work is to theoretically analyze the correlation between $\cdot O_2^-$ consumption and chemiluminescence emission, in order to fully understand the role of $\cdot O_2^-$ in the chemiluminescence of luciferin.

2. Computational methods

Geometry optimization calculations were made *in vacuo* at the M06-2X/cc-pVDZ level of theory (unless stated otherwise) [20]. Frequency calculations were performed at the same level of theory, in order to ensure that the obtained structures were minimums in their potential energy surfaces. The energies of the structures were obtained in implicit solvent, at the M06-2X/aug-cc-pVDZ level of theory. The conductor-like polarized continuum model (CPCM) was used to simulate the implicit solvent, with parameters set

* Corresponding author. Fax: +351 226082959.
E-mail address: jcsilva@fc.up.pt (J.C.G. Esteves da Silva).

0009-2614/$ - see front matter © 2013 Elsevier B.V. All rights reserved.
http://dx.doi.org/10.1016/j.cplett.2013.05.054

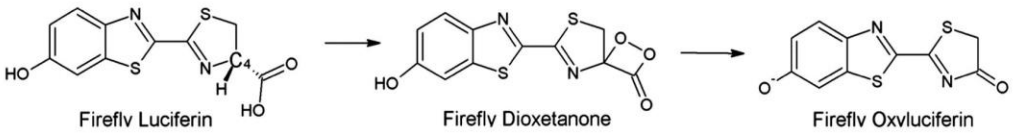

Scheme 1. Schematic representation of the firefly chemiluminescence reaction.

for DMSO [21]. A restricted (R) approach was used for closed-shell molecules, while an unrestricted (U) approach was used for open-shell molecules. The M06-2X density functional was used due to its excellent results in calculations regarding thermochemistry, kinetics and noncovalent interactions [22]. As M06-2X is known to yield some grid integration problems, we have specified the use of an ultrafine integration grid in all calculations, in order to avoid such problems.

All calculations were performed with the GAUSSIAN 09 program package [23].

3. Results and discussion

Despite verifying that $^{\cdot}O_2^-$ is consumed in a solution containing *tert*-BuOK and luciferin in DMSO, and that reaction can emit chemiluminescence, Wada and co-workers did not demonstrate a direct correlation between $^{\cdot}O_2^-$ consumption and chemiluminescence emission [18]. No experiment was made in order to see which was the effect of $^{\cdot}O_2^-$ consumption in the emission of light (enhancement or inhibition), or even if the superoxide anion was needed for the chemiluminescence reaction take place. Thus, while $^{\cdot}O_2^-$ is indeed consumed, this phenomenon may not be correlated with luciferin chemiluminescence. Moreover, their experiments only showed that the amount of $^{\cdot}O_2^-$ in the solution containing luciferin was lower than the amount found in a solution not containing luciferin. Therefore, it is not even clear if $^{\cdot}O_2^-$ was consumed or if its formation was inhibited. So, before attributing this consumption to role in the chemiluminescence reaction, we must ensure that the decrease in $^{\cdot}O_2^-$ concentration is not due to any another causes.

Wada and co-workers have found that $^{\cdot}O_2^-$ is formed in DMSO, due to an electron transfer from *tert*-BuO$^-$ to $_3O_2$ (Scheme 2.1) [18,19]. So, a possible reason for the low amount of $^{\cdot}O_2^-$ in the solution containing luciferin may be the inhibition of this electron transfer. *tert*-BuO$^-$ is a strong base and so it can accept protons. Firefly luciferin has two functional groups that can act as proton donors for *tert*-BuO$^-$, the carboxylic and the hydroxyl groups (Scheme 1). Thus, the low amount of $^{\cdot}O_2^-$ in the presence of luciferin may be explained by the inhibition of the electron transfer from *tert*-BuO$^-$ to the superoxide anion, due to the neutralization of the base via proton-donning from luciferin. Indeed, we can see in Scheme 2 that the deprotonation of neutral and anionic luciferin, by proton transfer to *tert*-BuO$^-$, are very favorable reactions (ΔE_{theor} of −20.5 and −13.5 kcal/mol, respectively). So it is possible that luciferin diminishes the quantity of *tert*-BuO$^-$ available for superoxide formation [18,19]. Moreover, this indicates that luciferin, in the presence of *tert*-BuOK, is present as a dianion in DMSO solution.

Nevertheless, in the study made by Wada and co-workers, the concentration of *tert*-BuOK used was higher than that of luciferin (8.6×10^{-3} M *versus* 9.6×10^{-4} M) [18]. So, even if all luciferin molecules are deprotonated, the concentration *tert*-BuOK used may still be enough to form $^{\cdot}O_2^-$. Another hypothesis for the low concentration of $^{\cdot}O_2^-$ in solutions containing luciferin, without the former molecule being involved in the firefly chemiluminescence reaction, is that if luciferin can act as an antioxidant in DMSO and transform $^{\cdot}O_2^-$ into $^1O_2$. In order to analyze this hypothesis we have calculated the in DMSO-energies of dianionic luciferin species and respective radical, and of $^{\cdot}O_2^-$ and $^1O_2$. The ΔE_{theor} of this reaction were calculated at the M06-2X-aug-cc-pVDZ, in implicit DMSO, and the results are presented in Scheme 3. In this case, the geometries were calculated by employing the CPCM model, with parameters set for DMSO, as in the *in vacuo* geometry of luciferin radical its CO_2^- group detached from the remaining molecule. The computed ΔE_{theor} showed us that our working hypothesis did not hold, as the obtained value was too high and positive. Therefore, the so called consumption of $^{\cdot}O_2^-$ cannot be explained by $^{\cdot}O_2^- \rightarrow {}^1O_2$ reaction, due to an electron transfer from luciferin dianion.

Our next hypothesis was that firefly luciferin may act as free radical scavenger for *tert*-BuO$^{\cdot}$, by electron transfer to this radical. This step would generate a luciferin radical, which may be annihilated by electron transfer from $^{\cdot}O_2^-$, thus re-forming luciferin anionic species and $^3O_2$. This would explain the consumption of $^{\cdot}O_2^-$, alongside with the protonation of *tert*-BuO$^-$, without the superoxide anion being directly involved in the chemiluminescence reaction. These reactions are depicted in Scheme 4, alongside

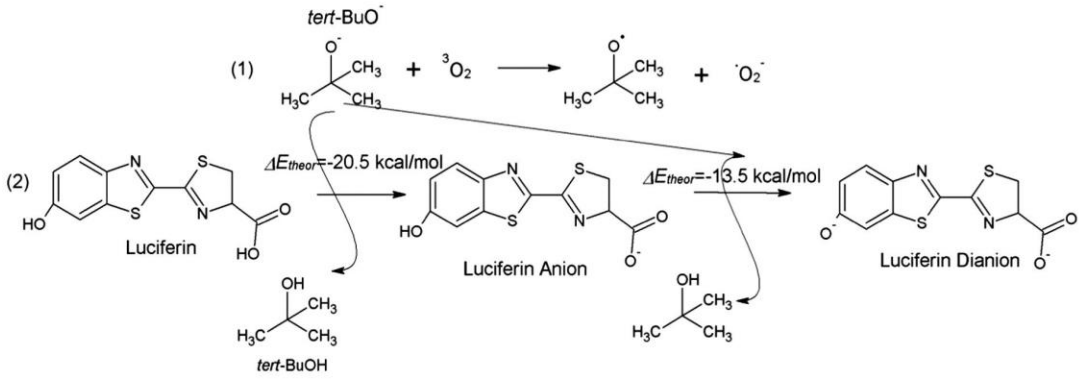

Scheme 2. (1) Schematic representation formation of $^{\cdot}O_2^-$ in DMSO, as proposed by Wada and co-workers [18,19]. (2) Deprotonation reaction of luciferin, in implicit DMSO, with *tert*-BuO$^-$ as a proton acceptor. The ΔE_{theor} values were calculated at the CPCM-M06-2X/aug-cc-pVDZ level of theory.

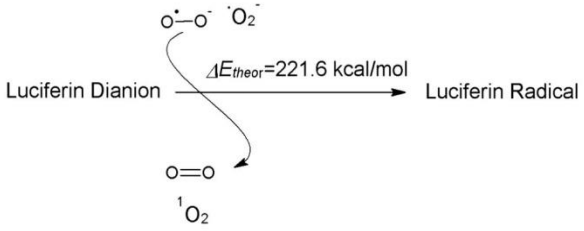

Scheme 3. $^{\cdot}O_2^-\rightarrow{}^1O_2$ reaction, with the involvement of an electron transfer from luciferin dianion. The ΔE_{theor} values were calculated at the CPCM-M06-2X/aug-cc-pVDZ level of theory.

with the computed ΔE_{theor}. In this case, the geometries were also calculated by employing the CPCM model, with parameters set for DMSO. It can be seen that the radical annihilation reaction between $^{\cdot}O_2^-$ and luciferin radical, in order to re-form $^3O_2$ and luciferin radical, would be very favorable (with a ΔE_{theor} of −30.3 kcal/mol). However, the computed ΔE_{theor} for luciferin dianion + *tert*-BuO$^{\cdot}$ indicates that an electron transfer do not take place (ΔE_{theor} of 7.5 kcal/mol), and so, no luciferin radical is formed than can react with $^{\cdot}O_2^-$.

Given that the re-formation of $^3O_2$ from $^{\cdot}O_2^-$, with the involvement of the luciferin molecule (Scheme 4), is a favorable reaction we have devised a new working hypothesis. It may be possible that luciferin dianion is transformed in a radical by receiving an electron from superoxide, which would re-form $^3O_2$. Luciferin dianion may then be re-formed by electron transfer to *tert*-BuO$^{\cdot}$. The proposed reaction and the obtained ΔE_{theor} are presented in Scheme 5. However, our calculations have demonstrated that the electron transfer from $^{\cdot}O_2^-$ to luciferin dianion is not feasible (ΔE_{theor} of 28.6 kcal/mol), contrary to the electron transfer from luciferin radical to *tert*-BuO$^{\cdot}$ (ΔE_{theor} of −50.3 kcal/mol).

All the calculations made so far support the hypothesis defended by Wada and co-workers, that $^{\cdot}O_2^-$ has a key role in the luciferin chemiluminescence reaction, and we have been unable to give an alternative explanation for the consumption of superoxide in the presence of luciferin [17,18]. Nevertheless, we still can imagine two possible explanations for the consumption of $^{\cdot}O_2^-$. As said in the Section 1, in order to occur the binding of $^3O_2$ to luciferin in order to firefly dioxetanone be formed, the proton of the C_4 atom of luciferin must be detached from luciferin to form a carbanion or a luciferin radical [1,5,6,16]. If a carbanion if formed, it may transfer an electron to $^{\cdot}O_2^-$, thus forming a luciferin C_4-deprotonated dianionic radical and $^1O_2$ (Scheme 6.1). If instead a luciferin radical is formed, it may receive an electron from $^{\cdot}O_2^-$, thus forming a luciferin C_4-deprotonated carbanion and $^3O_2$ (Scheme 6.2). The computed ΔE_{theor} are presented in Scheme 6. Both ΔE_{theor} indicate that $^{\cdot}O_2^-$ cannot be consumed due to formation of $^1O_2$ or $^3O_2$, with the involvement of luciferin C_4-deprotonated carbanion/radical. Thus, this indicates that the consumption of $^{\cdot}O_2^-$, in a DMSO solution of firefly luciferin, might indeed be related to the firefly chemiluminescence reaction [17,18].

4. Conclusion

Firefly chemi/bioluminescence results from the formation of firefly dioxetanone, which decomposition produces excited state oxyluciferin. Despite the importance of the formation reaction of dioxetanone, little is known about this feature of firefly light emission. Two potential mechanisms, carbanion and radical based, have been proposed but with few evidence that could support either of these proposals.

Wada and co-workers have stated that $^{\cdot}O_2^-$ is consumed during the firefly chemiluminescence reaction, which indicated that this radical has a role in this light-emitting reaction. However, no direct evidence was shown that could correlate this consumption with a role in the chemiluminescence reaction. Thus, the objective of this paper was to analyze theoretically other alternative paths that could explain the $^{\cdot}O_2^-$ consumption, before correlating this process to a role in firefly luciferin chemiluminescence.

We have used density functional theory, based on the M06-2X functional, in implicit DMSO. We have found that luciferin molecules can protonate *tert*-BuO$^-$, which is involved in the formation

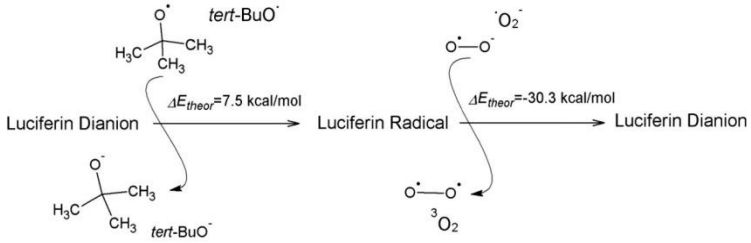

Scheme 4. *tert*-BuO$^{\cdot}\rightarrow$*tert*-BuO$^-$ and $^{\cdot}O_2^-\rightarrow{}^3O_2$ reactions, with the involvement of luciferin dianion. The ΔE_{theor} values were calculated at the CPCM-M06-2X/aug-cc-pVDZ level of theory.

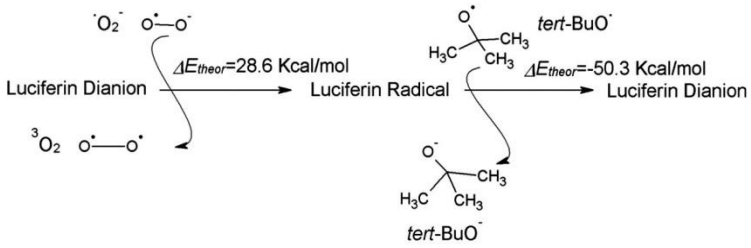

Scheme 5. $^{\cdot}O_2^-\rightarrow{}^3O_2$ and *tert*-BuO$^{\cdot}\rightarrow$*tert*-BuO$^-$ reactions, with the involvement of luciferin dianion. The ΔE_{theor} values were calculated at the CPCM-M06-2X/aug-cc-pVDZ level of theory.

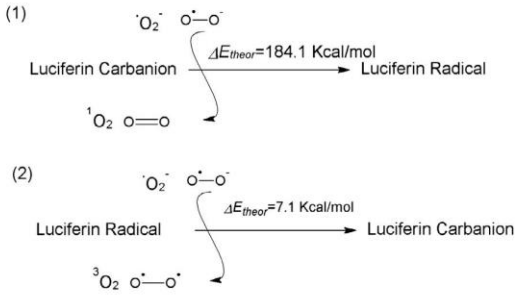

Scheme 6. (1) $^{\cdot}O_2^- \rightarrow {}^1O_2$ reaction, with the involvement of luciferin C_4-deprotonated carbanion. (2) $^{\cdot}O_2^- \rightarrow {}^3O_2$ reaction, with the involvement of luciferin C_4-deprotonated radical. The ΔE_{theor} values were calculated at the CPCM-M06-2X/aug-cc-pVDZ level of theory.

of $^{\cdot}O_2^-$ in DMSO, therefore inhibiting the superoxide forming reaction. However, given the much higher concentration of *tert*-BuO^-, than that of luciferin in Wada and co-workers experimental setup, this finding is not enough to explain the consumption of $^{\cdot}O_2^-$. Several electron transfer reactions between luciferin anionic, carbanionic and radical species and $^{\cdot}O_2^-$ were studied, but none of those could provide an alternative explanation for the superoxide consumption. Therefore, our calculations support the conclusions obtained by Wade and co-workers, in which $^{\cdot}O_2^-$ is somewhat involved in luciferin chemiluminescence. Given this, the next step in the study of firefly chemiluminescence should be to find the role of $^{\cdot}O_2^-$ in this light-emitting reaction.

Acknowledgment

Financial support from Fundação para a Ciência e Tecnologia (FCT, Lisbon) (Programa Operacional Temático Factores de Competitividade (COMPETE) e comparticipado pelo Fundo Comunitário Europeu FEDER) (Project PTDC/QUI/71 366/2006) is acknowledged. A Ph.D. Grant to Luís Pinto da Silva (SFRH/BD/76 612/2011), attributed by FCT, is also acknowledged.

Appendix A. Supplementary data

Cartesian coordinates of important structures studied in this work. Supplementary data associated with this article can be found, in the online version, at http://dx.doi.org/10.1016/j.cplett.2013.05.054.

References

[1] S.M. Marques, J.C.G. Esteves da Silva, IUBMB Life 61 (2009) 6.
[2] L. Pinto da Silva, J.C.G. Esteves da Silva, J. Chem. Theory Comput. 7 (2012) 809.
[3] V.R. Viviani, F.G.C. Arnoldi, A.J.S. Neto, T.L. Oehlmeyer, E.J.H. Bechara, Y. Ohmiya, Photochem. Photobiol. Sci. 7 (2008) 159.
[4] J. Vieira, L. Pinto da Silva, J.C.G. Esteves da Silva, J. Photochem. Photobiol. B 117 (2012) 33.
[5] L. Pinto da Silva, J.C.G. Esteves da Silva, ChemPhysChem 13 (2012) 2257.
[6] I. Navizet, Y.J. Liu, N. Ferré, D. Roca-Sanjuán, R. Lindh, ChemPhysChem 12 (2011) 3064.
[7] J.A. Koo, S.P. Schmidt, G.B. Schuster, Proc. Natl. Acad. Sci. USA 75 (1978) 30.
[8] H. Isobe, Y. Takano, M. Okumura, S. Kuramitsu, K. Yamaguchi, J. Am. Chem. Soc. 127 (2005) 8667.
[9] L. Yue, Y.J. Liu, W.H. Fang, J. Am. Chem. Soc. 134 (2012) 11632.
[10] L. Pinto da Silva, J.C.G. Esteves da Silva, ChemPhysChem 14 (2013) 1071.
[11] S.M. Marques, J.C.G. Esteves da Silva, Anal. Bioanal. Chem. 391 (2008) 2161.
[12] S.M. Marques, F. Peralta, J.C.G. Esteves da Silva, Talanta 77 (2009) 1497.
[13] B.R. Branchini, T.R. Southworth, N.F. Khattak, E. Michelini, A. Roda, Anal. Biochem. 345 (2005) 140.
[14] A. Roda, P. Pasini, M. Mirasoli, E. Michelini, M. Guardigli, Trends Biotechnol. 22 (2004) 295.
[15] A. Roda, M. Guardigli, Anal. Bioanal. Chem. 402 (2012) 69.
[16] J.A. Sundlov, D.M. Fontaine, T.L. Southworth, B.R. Branchini, A.M. Gulick, Biochemistry 51 (2012) 6493.
[17] N. Wada, R. Shibata, M. Shibazaki, N. Suzuki, Photochem. Photobiol. 49 (1989) 513.
[18] N. Wada, K. Mitsuta, M. Kohno, N. Suzuki, J. Phys. Soc. Jpn. 58 (1989) 3501.
[19] N. Wada, K. Mitsuta, J. Phys. Soc. Jpn. 62 (1993) 1816.
[20] Y. Zhao, D.G. Truhlar, Theor. Chem. Acc. 120 (2008) 215.
[21] M. Cossi, N. Rega, G. Scalmani, V. Barone, J. Comput. Chem. 24 (2003) 669.
[22] Y. Zhao, D.G. Truhlar, Acc. Chem. Res. 41 (2008) 157.
[23] M.J. Frisch et al., Gaussian 09, Revision A.02, Gaussian, Inc., Wallingford, CT, 2009.

Article 8

Theoretical study of the superoxide anion assisted firefly oxyluciferin formation
Luís Pinto da Silva and Joaquim C.G. Esteves da Silva
Chem. Phys. Lett. **2013**, *590*, 180-182.

The theoretical calculations and the writing of the paper were performed by Luís Pinto da Silva, under supervision of Professor Esteves da Silva.

Chemical Physics Letters 590 (2013) 180–182

Contents lists available at ScienceDirect

Chemical Physics Letters

journal homepage: www.elsevier.com/locate/cplett

Theoretical study of the superoxide anion assisted firefly oxyluciferin formation

Luís Pinto da Silva, Joaquim C.G. Esteves da Silva *

Centro de Investigação em Química, Departamento de Química e Bioquímica, Faculdade de Ciências da Universidade do Porto, R. Campo Alegre 687, 4169-007 Porto, Portugal

ARTICLE INFO

Article history:
Received 23 September 2013
In final form 14 October 2013
Available online 19 October 2013

ABSTRACT

This a theoretical Letter based on density functional theory, on the role of superoxide anion in firefly chemiluminescence in DMSO. We have found that this anion can attack luciferin radical molecules, thus forming a luciferin-like trianion. This latter molecule transfers an oxygen atom, which results in the formation of oxyluciferyl radical dianion and carbon dioxide molecules. Oxyluciferin is finally formed after an electron transfer from oxyluciferyl radical dianion to *tert*-BuO· radical molecules. Thus, we have found evidence that firefly oxyluciferin can be formed in a energetically favorable superoxide anion-assisted reaction, without the need for the formation of firefly dioxetanone.

1. Introduction

Firefly luciferase catalyzes a light emitting reaction, which is termed bioluminescence [1–3]. This enzyme catalyzes a two step reaction: first, firefly luciferin reacts with adenosine-5′-triphosphate, leading to the formation of an adenylyl intermediate; the second step consists in the oxidation of the adenylyl intermediate in the presence of O_2, giving origin to firefly oxyluciferin [1–3]. Oxyluciferin is formed already in a singlet excited state, thus decaying to the ground state with emission of visible light [4–6]. This is the result of the formation and subsequent decomposition of firefly dioxetanone, which leads to the chemiexcitation of the light emitter oxyluciferin [4–6]. Several theories have been present along the years, in order to explain this dioxetanone-dependent oxyluciferin chemiexcitation [7–10]. Due to very interesting characteristics, this bioluminescence system has been gaining numerous practical applications, in the pharmaceutical, biomedical and bioanalytical fields, among others [11–15].

More recently, Branchini et al. have proposed a mechanism reaction for the formation of firefly dioxetanone [16]. According to these authors, the mechanism is based on radical formation and recombination. Molecular oxygen abstracts the proton of C_4 atom, leading to the formation of two radical molecules (Scheme 1). Recombination of these radicals will then form firefly dioxetanone. Nevertheless, this is also a hypothesized mechanism with no direct experimental/computational support.

Besides bioluminescence, chemiluminescence is also possible due to oxyluciferin formation via dioxetanone formation and decomposition [5,6]. Therefore, luciferin chemiluminescence became a good (and easier to study) model for firefly bioluminescence. Some authors have proposed that the superoxide anion ($\cdot O_2^-$) plays an important role in the primary step of firefly dioxetanone-based chemiluminescence [17,18]. These authors have demonstrated that $\cdot O_2^-$ is generated and is stably present in dimethyl sulphoxide (DMSO), and that is consumed on mixing with solutions containing luciferin, which produce light [17–19]. However, the correlation between $\cdot O_2^-$ consumption and chemiluminescence emission was not clearly defined.

We have analyzed various electron transfer reactions between several luciferin and $\cdot O_2^-$, in order to find alternative pathways for the consumption of this radical anion, but none of those could provide an alternative explanation for the superoxide consumption [20]. Thus, our calculations support the conclusions obtained by Wada et al., in which $\cdot O_2^-$ is a necessary compound in luciferin chemiluminescence.

Given this information, the next objective of the present study is to find the role of $\cdot O_2^-$ in the firefly chemiluminescence reaction in DMSO. In order to do so, we have studied the energetic profile of several reactions that we think that will lead to oxyluciferin formation.

2. Computational methods

Geometry optimization calculations were made *in vacuo* at the M06-2X/cc-pVDZ level of theory [21]. Frequency calculations were performed at the same level of theory, in order to ensure that the obtained structures were minimums in their potential energy surfaces. The energies of the structures were obtained in implicit solvent with a basis set augmented with diffuse functions, at the M06-2X/aug-cc-pVDZ level of theory. The conductor-like polarized continuum model (CPCM) was used to simulate the implicit solvent, with parameters set for DMSO [22]. A restricted (R) approach was used for closed-shell molecules, while an unrestricted (U)

* Corresponding author. Fax: +351 226082959.
E-mail address: jcsilva@fc.up.pt (J.C.G. Esteves da Silva).

0009-2614/$ - see front matter © 2013 Elsevier B.V. All rights reserved.
http://dx.doi.org/10.1016/j.cplett.2013.10.036

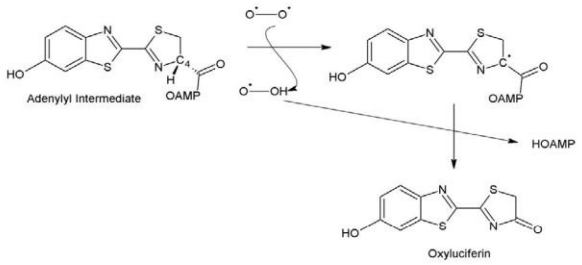

Scheme 1. Schematic representation of the radical based firefly oxyluciferin formation.

approach was used for open-shell molecules. The M06-2X density functional was used due to its excellent results in calculations regarding thermochemistry, kinetics and noncovalent interactions [23]. We have specified the use of an ultrafine integration grid in all calculations, as the used density functional is known to yield some grid integration problems.

All calculations were performed with the GAUSSIAN 09 program package [24].

3. Results and discussion

In order to firefly be formed, the proton of the C_4 atom must be abstracted in order to the superoxide anion can bind to luciferin (Scheme 2) [17–19]. Given the 'Radical Theory' proposed by Branchini et al. for firefly bioluminescence, and the presence of free radicals in *tert*-BuO^--containing DMSO, we think that the proton must be abstracted in a way that generates a luciferin radical [16–19]. Our recent calculations have showed that, in *tert*-BuO^--containing DMSO, luciferin is in its dianionic form (Scheme 2) [20].

Wada et al. have found that $\cdot O_2^-$ is formed in DMSO, due to an electron transfer from *tert*-BuO^- to $^3O_2$ [18,19]. So, besides $\cdot O_2^-$, a *tert*-$BuO^\cdot$ radical is also formed in this reaction. We think that *tert*-$BuO^\cdot$ is a good acceptor of the $H^\cdot$ radical provided by luciferin, as it would annihilate the *tert*-$BuO^\cdot$ unstable species while forming a more stable *tert*-BuOH (Scheme 2). Our calculations have demonstrated that this is a favorable reaction as the ΔE_{theor} of the reaction is of −19.9 kcal/mol. Another hypothesis for the C_4 proton acceptor would be $\cdot O_2^-$ (Scheme 2). This molecule could abstract the proton, while forming a O_2H^- species and explaining the consumption of $\cdot O_2^-$ [17–19]. However, the ΔE_{theor} of the reaction indicates that this is not a favorable one (7.8 kcal/mol).

Following this line of thinking, the next step in firefly dioxetanone formation should be the binding of $\cdot O_2^-$ or $^3O_2$ to the luciferyl radical (Scheme 3). This step is expected to generate a luciferin-like trianion or radical, depending on the attacking species (Scheme 3) [17–19]. The obtained ΔE_{theor} (−25.7 and −14.1 kcal/mol, Scheme 3) indicate that both reaction routes are feasible. Nevertheless, the formation of a luciferin-like trianion due to $\cdot O_2^-$ is expected to be the most favorable reaction path.

First, we will consider a reaction path in which is $^3O_2$, and not $\cdot O_2^-$, to attack the luciferin radical (Scheme 4). The next step of the luciferin-like radical formation will be the release of an oxygen atom. The dioxetanone moiety has only three oxygen atoms, while the luciferin-like radical has four oxygen atoms in that region of the molecule (Scheme 4). A possible reaction route would be the abstraction of an oxygen radical atom from the luciferin-like radical, by *tert*-$BuO^\cdot$ (Scheme 4). This step would generate a *tert*-BuO_2^- anion, and the firefly dioxetanone molecule. However, the calculated ΔE_{theor} (78.3 kcal/mol) indicates that firefly dioxetanone cannot be formed in this way. This result is not strange, as previous results have indicated that it is $\cdot O_2^-$, and not $^3O_2$, to be consumed in the firefly chemiluminescence reaction.

Given the previous results, we expect that the chemiluminescence reaction would proceed from the luciferin-like trianion (Scheme 4). As in the case of the luciferin-like radical (Scheme 4), one oxygen atom will have to be abstracted by an accepting molecule. The *tert*-$BuO^\cdot$ is still a good candidate for abstracting the oxygen atom, thereby forming *tert*-BuO_2^- anion (Scheme 4). It should be noted that the abstraction of the oxygen atom from the luciferin-like trianion, leads the resulting luciferyl molecule with an extra electron. Therefore, instead of the formation of firefly dioxetanone, it is more likely that the oxygen abstraction step generations an oxyluciferyl radical dianion and carbon dioxide (Scheme 4). The computed ΔE_{theor} supports our reaction mechanism, by presenting a significantly favorable value (−32.7 kcal/mol).

The conversion of oxyluciferyl radical dianion into oxyluciferin anion will be dependent in the electron transfer from the former molecule to an electron-accepting molecule (Scheme 5). Once again, *tert*-$BuO^\cdot$ appears to be a good candidate as an electron transfer reaction will lead to the formation of more stable *tert*-BuO^-. The calculated ΔE_{theor} for this reaction indicates that this is a favorable reaction (−29.1 kcal/mol). Thus, we have found a possible reaction route that leads to the conversion of firefly luciferin into firefly oxyluciferin, in a $\cdot O_2^-$ assisted reaction.

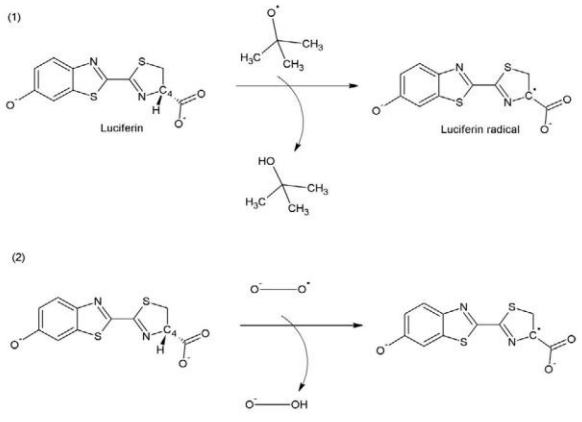

Scheme 2. Schematic representation of the C_4 proton abstraction from luciferin by *tert*-$BuO^\cdot$ (1) and $\cdot O_2^-$ (2). The corresponding ΔE_{theor} were −19.9 and 7.8 kcal/mol, respectively.

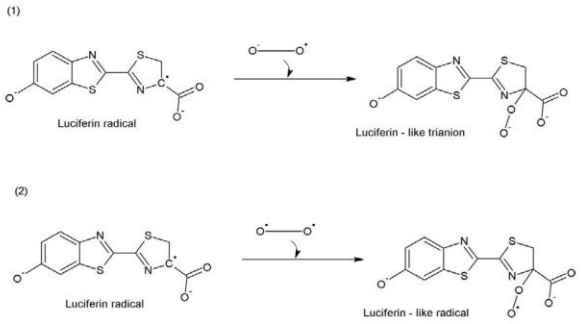

Scheme 3. Schematic representation of the luciferin radical attack by $\cdot O_2^-$ (1) and $^3O_2$ (2). The corresponding ΔE_{theor} were −25.7 and −14.1 kcal/mol, respectively.

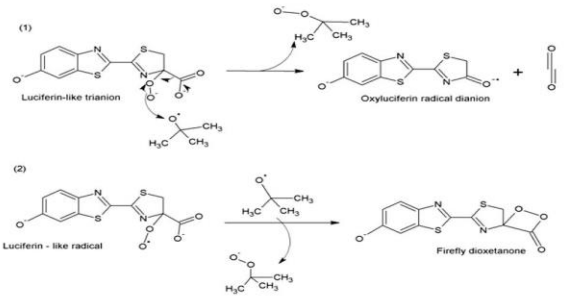

Scheme 4. Schematic representation of the oxygen atom donation to *tert*-BuO·, forming an oxyluciferyl radical dianion (1) and firefly dioxetanone (2). The corresponding ΔE_{theor} were −32.7 and 78.3 kcal/mol, respectively.

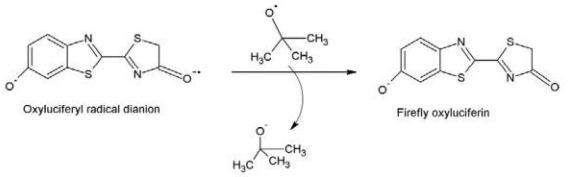

Scheme 5. Schematic representation of the electron transfer from oxyluciferyl radical dianion to *tert*-BuO·, forming firefly oxyluciferin. The corresponding ΔE_{theor} was −29.1 kcal/mol, respectively.

4. Conclusion

Firefly luciferin can produce chemiluminescence in solution, due to the excited state production of firefly oxyluciferin (the light emitter). Some researchers have demonstrated that $\cdot O_2^-$ has a role on firefly luciferin chemiluminescence reaction in DMSO, when *tert*-BuO^- is added to the reaction mixture.

We have used the M06-2X density functional, in implicit DMSO, in order to better understand the role of $\cdot O_2^-$ in firefly luciferin chemiluminescence. We have found that *tert*-BuO· molecules can abstract the C_4 proton of luciferin, thus allowing the attack of luciferin radical by $\cdot O_2^-$. This step leads to the formation of a key intermediate, a luciferin-like trianion.

The most interesting features of this $\cdot O_2^-$-assisted oxyluciferin production reside in the subsequent steps. Luciferin-like trianion can transfer an oxygen atom, in a energy favorable step, to *tert*-BuO· radical molecules. This transfer leads not to the formation of firefly dioxetanone, but to the production of oxyluciferyl radical dianion and carbon dioxide molecules, besides *tert*-BuO_2^- anion. Oxyluciferin is then formed by donation of the extra electron present in the oxyluciferyl radical dianion to *tert*-BuO· radical.

Given these results, we have found a reaction route in which oxyluciferin is produced with the consumption of $\cdot O_2^-$, as described in the literature, but without the need for the formation of a firefly dioxetanone molecule. Thus, in this Letter we show evidence that firefly dioxetanone is not always needed for firefly luciferin chemiluminescence.

Acknowledgments

Financial support from Fundação para a Ciência e Tecnologia (FCT, Lisbon) (Programa Operacional Temático Factores de Competitividade (COMPETE) e comparticipado pelo Fundo Comunitário Europeu FEDER) (Project PTDC/QUI/71366/2006) is acknowledged. A Ph.D. Grant to Luís Pinto da Silva (SFRH/BD/76612/2011), attributed by FCT, is also acknowledged.

Appendix A. Supplementary data

Supplementary data (Cartesian coordinates of important structures studied in this work) associated with can be found, in the online version, at http://dx.doi.org/10.1016/j.cplett.2013.10.036.

References

[1] S.M. Marques, J.C.G. Esteves da Silva, IUBMB Life 61 (2009) 6.
[2] L. Pinto da Silva, J.C.G. Esteves da Silva, J. Chem. Theory Comput. 7 (2012) 809.
[3] V.R. Viviani, F.G.C. Arnoldi, A.J.S. Neto, T.L. Oehlmeyer, E.J.H. Bechara, Y. Ohmiya, Photochem. Photobiol. Sci. 7 (2008) 159.
[4] J. Vieira, L. Pinto da Silva, J.C.G. Esteves da Silva, J. Photochem. Photobiol. B 117 (2012) 33.
[5] L. Pinto da Silva, J.C.G. Esteves da Silva, ChemPhysChem 13 (2012) 2257.
[6] I. Navizet, Y.J. Liu, N. Ferré, D. Roca-Sanjuán, R. Lindh, ChemPhysChem 12 (2011) 3064.
[7] J.A. Koo, S.P. Schmidt, G.B. Schuster, Proc. Natl. Acad. Sci. USA 75 (1978) 30.
[8] H. Isobe, Y. Takano, M. Okumura, S. Kuramitsu, K. Yamaguchi, J. Am. Chem. Soc. 127 (2005) 8667.
[9] L. Yue, Y.J. Liu, W.H. Fang, J. Am. Chem. Soc. 134 (2012) 11632.
[10] L. Pinto da Silva, J.C.G. Esteves da Silva, ChemPhysChem 14 (2013) 1071.
[11] S.M. Marques, J.C.G. Esteves da Silva, Anal. Bioanal. Chem. 391 (2008) 2161.
[12] S.M. Marques, F. Peralta, J.C.G. Esteves da Silva, Talanta 77 (2009) 1497.
[13] B.R. Branchini, T.R. Southworth, N.F. Khattak, E. Michelini, A. Roda, Anal. Biochem. 345 (2005) 140.
[14] A. Roda, P. Pasini, M. Mirasoli, E. Michelini, M. Guardigli, Trends Biotechnol. 22 (2004) 295.
[15] A. Roda, M. Guardigli, Anal. Bioanal. Chem. 402 (2012) 69.
[16] J.A. Sundlov, D.M. Fontaine, T.L. Southworth, B.R. Branchini, A.M. Gulick, Biochemistry 51 (2012) 6493.
[17] N. Wada, R. Shibata, M. Shibazaki, N. Suzuki, Photochem. Photobiol. 49 (1989) 513.
[18] N. Wada, K. Mitsuta, M. Kohno, N. Suzuki, J. Phys. Soc. Jpn. 58 (1989) 3501.
[19] N. Wada, K. Mitsuta, J. Phys. Soc. Jpn. 62 (1993) 1816.
[20] L. Pinto da Silva, J.C.G. Esteves da Silva, Chem. Phys. Lett. 577 (2013) 127.
[21] Y. Zhao, D.G. Truhlar, Theor. Chem. Acc. 120 (2008) 215.
[22] M. Cossi, N. Rega, G. Scalmani, V. Barone, J. Comput. Chem. 24 (2003) 669.
[23] Y. Zhao, D.G. Truhlar, Acc. Chem. Res. 41 (2008) 157.
[24] M.J. Frisch et al., GAUSSIAN 09, Revision A.02, Gaussian, Inc., Wallingford, CT, 2009.

Chapter 4 – Characterization of the Decomposition Reaction of Dioxetanone Molecules and the Subsequent Chemiexcitation Step

4.1. Characterization of the Decomposition Reaction of Simple 1,2-Dioxetanone

Article 9

Density functional theory of 1,2-dioxetanone decomposition in condensed phase
Luís Pinto da Silva and Joaquim C.G. Esteves da Silva
J. Comput. Chem. **2012**, *33*, 2118-2123.

The theoretical calculations and the writing of the paper were performed by Luís Pinto da Silva, under supervision of Professor Esteves da Silva.

FULL PAPER WWW.C-CHEM.ORG Journal of COMPUTATIONAL CHEMISTRY

Density Functional Theory Study of 1,2-Dioxetanone Decomposition in Condensed Phase

Luís Pinto da Silva[a] and Joaquim C.G. Esteves da Silva*[a]

The decomposition of 1,2-dioxetanone into a CO_2 molecule and into an excited state formaldehyde molecule was studied in condensed phase, using a density functional theory approach. Singlet and triplet ground and excited states were all included in the calculations. The calculations revealed a novel mechanism for the chemiluminescence of this compound. The triplet excitation can be explained by two intersystem crossings (ISCs) with the ground state, while the singlet excitation can be accounted by an ISC with the triplet state. The experimentally verified small excitation yield can then be explained by the presence of an energy barrier present in the potential energy surface of the triplet excited state, which will govern both triplet and singlet excitation. It was also found that the triplet ground state interacts with both the triplet excited and singlet ground states. A MPWB1K/mPWKCIS approach provided results in agreement with the existent literature. © 2012 Wiley Periodicals, Inc.

DOI: 10.1002/jcc.22997

Introduction

Chemiluminescence is the emission of energy with limited emission of heat, as the result of a chemical reaction. In all the reactions of this type, a peroxide or hydroperoxide compound undergoes a thermal decomposition (Fig. 1). The decomposition reaction produces two carbonyl compounds, one of which is electronically excited.[1,2] When chemiluminescence occurs in a living organism, it is termed as bioluminescence.[3] This latter light-emitting phenomenon occurs in marine vertebrates and invertebrates, as well as terrestrial animals and microorganisms.[3] The studied bioluminescence system is that of firefly *Photinus pyralis* luciferase. This enzyme catalyzes a two-step reaction: first, firefly luciferin reacts with ATP, thus generating an adenylyl intermediate; in the second step, this intermediate is oxidized into a high energy dioxetanone (Firefly dioxetanone, Fig. 1). Subsequently, firefly dioxetanone decomposes into excited state oxyluciferin, which decays to the ground state with emission of light.[4,5] Nowadays, chemiluminescence and bioluminescence have many biomedical, bioanalytical, and pharmaceutical applications, among others.[6–8]

Despite the attention given to this topic by researchers, there are still details of the thermal decomposition of the peroxide or hydroperoxide compounds that remain unclear. This is due to both experimental (low thermal and catalytic stabilities, etc.)[9,10] and computational (possible inability of single-reference methods in the study of these systems)[11,12] difficulties. However, it is generally accepted that the peroxide and hydroperoxide compounds start decomposing in the ground state mainly by O—O bond elongation, and by some C—C stretching. By this reaction path a transition state, where the O—O bond is broken, is reached prior to C—C breaking and subsequent peroxide or hydroperoxide decomposition.[11–16] Near this transition state, the reaction reaches a point of degeneracy or near-degeneracy between the ground and excited states.[11–16] This point of the potential energy surface (PES) is responsible for the population of the excited state and subsequent emission of light. The ground state decomposition, by O—O bond elongation, appears to be the rate-determining step for the production of the excited state chemiluminophore.[17,18]

Simple 1,2-dioxetanone (Fig. 1) is one of the smallest molecules capable of chemiluminescence. It decomposes into a CO_2 molecule and into an excited state formaldehyde molecule, which will decay to the ground state by emitting light.[11] Both singlet and triplet excited states can be responsible for the production of the photon of light. However, the ratio of triplet to singlet is very high, so that the observed light is very weak.[1,9,10,19,20] Furthermore, even the triplet excitation yield was found to be small for the most simple 1,2-dioxetane and 1,2-dioxetanone.[1,9,10,19,20] This type of molecules have been receiving attention of the research community because they represent a simple model of the dioxetanone-like molecules present in the diverse bioluminescence systems.

Several authors have tried to clarify the chemiluminescence phenomenon, with computational methodologies, by studying the decomposition reaction of 1,2-dioxetanes and 1,2-dioxetanones.[11–16,21–23] However, and despite the good contribution to the literature, there are some aspects of these studies that call for more investigation of this topic. Studies using a state of the art complete active space second-order perturbation

L. P. da Silva, J. C. G. Esteves da Silva
Departamento de Química e Bioquímica, Centro de Investigação em Química (CIQ-UP), Faculdade de Ciências da Universidade do Porto, Campo Alegre 687, 4169-007 Porto, Portugal
E-mail: jcsilva@fc.up.pt

Contract/grant sponsor: Fundação para a Ciência e Tecnologia (FCT, Lisbon) (Programa Operacional Temático Factores de Competitividade (COMPETE) e comparticipado pelo Fundo Comunitário Europeu FEDER); Contract/grant number: PTDC/QUI/71366/2006; Contract/grant sponsor: Fundação para a Ciência e Tecnologia (FCT); Contract/grant number: SFRH\BD\76612\2011 (L.P.d.S)

Journal of COMPUTATIONAL CHEMISTRY WWW.C-CHEM.ORG FULL PAPER

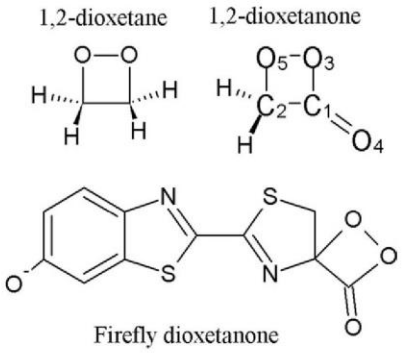

Figure 1. Schematic representation of some chemiluminescence compounds.

theory (CASPT2)[24]/complete active space self-consistent field (CASSCF)[25] approach provided valuable information about the *in vacuo* chemiluminescence reaction, especially regarding the zone of degeneracy or near-degeneracy between the ground and excited states.[11–14] However, the inclusion of implicit and/or explicit solvent models in the calculations, which could be crucial in the chemiluminescence mechanism, could lead to high times of calculations due to the already high computational cost of CASPT2/CASSCF. Moreover, the high computational cost of these methods difficult even the *in vacuo* study of firefly dioxetanone, due to the expected size of the active space and the corresponding CI-expansion. Therefore, a new strategy with similar reliability and lower computational cost is needed.

Another theoretical approach is using popular density functional theory (DFT) methods. One of the main reasons for the popularity of these methods is the inclusion of electron correlation, without being too computationally demanding. This characteristic enables calculations on models of over 100 atoms and inclusion of solvent models in the calculations, within a realistic timeframe. Some authors have used this characteristic to include implicit solvation models in their studies of 1,2-dioxetane and 1,2-dioxetanones.[15,21] However, both *in vacuo* and in condensed phase DFT studies used density functionals without providing convincing proof of their reliability in the computation of chemiluminescence system analyzed in their work. Because of the current variety of DFT functionals, it is difficult to be aware of which functional is best for the system or property of interest. Furthermore, these authors used basis sets of low level of theory [6-31+G(d)], which are below of the required accuracy needed to study these complex reactions.[15,21,22]

Thus, the objective of the present work is to study the chemiluminescence of 1,2-dioxetanone in implicit solvent (benzene, dichloromethane, and dimethyl sulfoxide (DMSO)), using a DFT approach. With this study, we intend to improve the level of knowledge regarding the chemiluminescence of this type of molecules, and to focus on some aspects not explored by other theoretical studies. In regard with other DFT-based works, we have performed a DFT benchmarking study for the calculation of the activation barrier of 1,2-dioxetanone decomposition. To this end, we have compared the results obtained *in vacuo* with 17 density functionals with the result obtained with a Multistate-CASPT2 (MS-CASPT2)[24]//State-average-CASSCF (SA-CASSCF)[25]/ANO-RCC-VDZP state of the art approach. The top ranked functional was then used in subsequent implicit solvation calculations. Also, basis sets of higher level of theory were used (cc-pVDZ and aug-cc-pVDZ). In regard to *in vacuo* studies which used state of the art computational methods, we included implicit solvation in our calculations to provide results more comparable with experiment. Furthermore, with this study, we intend to develop a strategy with similar accuracy to these state of the art methods but with lower computational cost.

Computational Methods

Ground state geometry optimizations and frequency calculations were performed at the mPWKCIS/cc-pVDZ level of theory,[26–28] while single point calculations were performed at the DFT/aug-cc-pVDZ level of theory. Intrinsic reaction coordinate (IRC) calculations, at the mPWKCIS/cc-pVDZ level of theory, were conducted to connect the ground state transition state to the reactant and products.[29] Both the IRC and geometry optimization calculations were performed *in vacuo*. It should be noted that the IRC calculation was performed by calculating the force constants in all SCF cycles. The downward IRC calculation toward the products was interrupted when the two molecule were clearly separated, a procedure adopted from Ref. [12].

Seventeen density functionals were used in the DFT benchmarking study (Supporting Information Table S1), including generalized gradient approximation (GGA), hybrid GGA (H-GGA), meta GGA (M-GGA), and hybrid-meta GGA (HM-GGA). To analyze the performance of these functionals in the calculation of the activation energy of 1,2-dioxetanone decomposition, *in vacuo* frequency calculations (at the DFT/aug-cc-pVDZ level of theory) were performed for both the reactant and transition state founded prior to the IRC calculation. From these calculations, both the single point and zero-point correction energies were taken to calculate the activation energy. The obtained values were then compared with an *in vacuo* activation energy of 26.0 kcal/mol, calculated for 1,2-dioxetanone at the MS-CASPT2//SA-CASSCF/ANO-RCC-VDZP level of theory.[11]

The energies of the ground state IRC-obtained structures were re-evaluated by single point calculations with the top ranked functional and the aug-cc-pVDZ basis set, with implicit solvent effects. To obtain the energy levels of the triplet (T_1) and singlet (S_1) excited states, we have performed time dependent (TD)[30,31] DFT/aug-cc-pVDZ vertical excitations calculations, with solvent effects and with the top ranked functional in the benchmarking study. The energy levels of the triplet ground state (T_0) were obtained by DFT/aug-cc-pVDZ single point calculations, with solvent effects and with the top ranked functional in the benchmarking study. This approach was adopted from Ref. [15]. Open-shell triplet and singlets molecules were treated using unrestricted (U) DFT, while closed-shell molecules were treated with restricted (R) DFT.

Solvent effects were considered by using the conductor-like polarized continuum model.[32] The implicit solvents chosen were benzene, dichloromethane, and DMSO. All calculations were performed with the Gaussian 03 program package.[33]

Results and Discussion

DFT benchmarking study

The purpose of this benchmarking study is to evaluate the performance of DFT functionals in the correct calculation of the activation barrier for 1,2-dioxetanone decomposition. Supporting Information Table S2 shows the calculated activation barrier for the various tested functionals and the mean absolute error (MAE), which is the ranking criterion. The reference value is 26.0 kcal/mol.[11] The top five best density functional are MPWB1K (HM-GGA),[34] MPW1K (H-GGA),[35] MPW1B95 (HM-GGA),[34] PBE1PBE (H-GGA),[36] and PBE1KCIS (HM-GGA).[37] However, it can be seen that the activation energies calculated by the latter density functionals already differ significantly from the reference values (3.8–6.2 kcal/mol). Nevertheless the top two ranked functional presented low MAE, especially MPWB1K, which provided excellent agreement with the reference value (MAE of 0.6 kcal/mol). Thus, this indicate that MPWB1K can be used safely in the study of the decomposition of 1,2-dioxetanone, as the results calculated with this method are very similar to those obtained with a state of the art methodology. Also, it can be seen that there is a relationship between better accuracy and increase in the level of theory used, as the best five functionals are mostly HM-GGA functionals and the worst five are mostly GGA methods. Finally, it should be noted that the popular B3LYP functional,[38,39] also used in this field of research,[15,22] presented an activation energy significantly different from the reference value (MAE of 7.0 kcal/mol).

Singlet ground state decomposition of 1,2-dioxetanone

The nature of the stationary point of the singlet ground state PES was verified by frequency analysis. This structure was then used as a starting point for the IRC calculation. Subsequently, the energies of the structures obtained with this approach were re-evaluated with MPWB1K/aug-cc-pVDZ single point calculations, with solvent effects. The IRC paths for the three solvent are represented in Figures 2a–2c. In Figure 2d are represented the variations of the O_5—O_3, C_2—C_1, C_2—O_5, and C_1—O_3 bond lengths. The O_5—C_2—C—O_3 dihedral variation was not presented as no significant difference was found in the IRC path. In Supporting Information Figure S1 are presented the full singlet ground state PES (from the reactant to the products), along with the triplet ground and excited states, and with the singlet excited states.

The reaction proceeds from the reactant to the transition structure, through a high activation barrier in all solvents: 28.0 kcal/mol for benzene, 27.7 kcal/mol for dichloromethane, and 27.6 kcal/mol for DMSO. These values were calculated at the MPWB1K/aug-cc-pVDZ level of theory with zero-point correction energies. Zero-point corrections were obtained with both

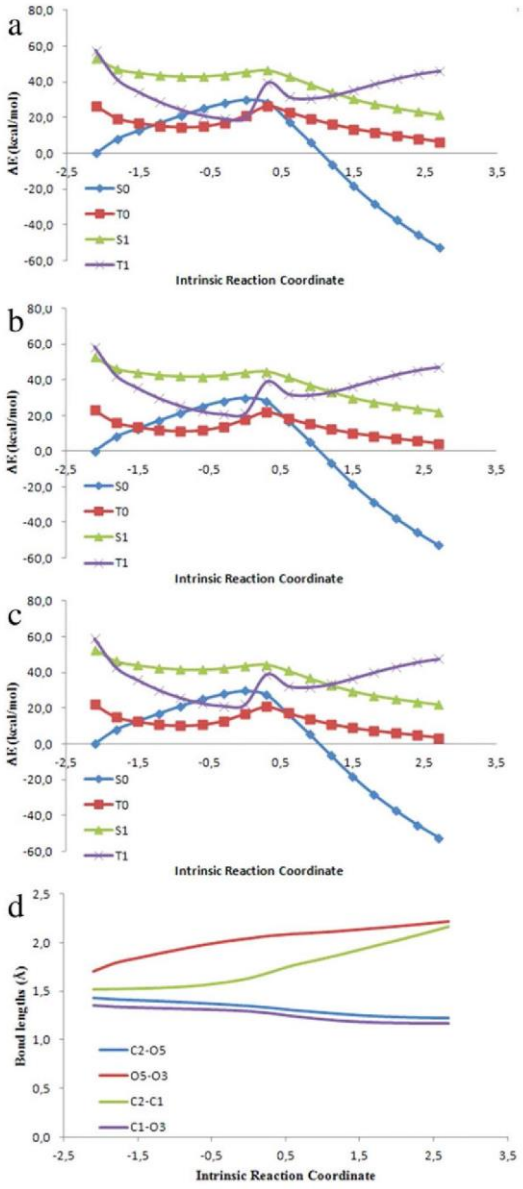

Figure 2. Energy profiles of the IRC path determined for 1,2-dioxetanone decomposition, in benzene a), dichloromethane b), and DMSO c). Bond length variations recorded during the IRC calculation d).

the aug-cc-pVDZ and the implicit solvent model. There is a negligible decrease of the activation barrier with increasing value of the dielectric constant of the medium. Furthermore, the values are in line with those obtained in another theoretical study of 1,2-dioxetanone.[11] As in line with the existent literature, it can be seen that the reaction proceeds to the transition state mainly by O_5—O_3 bond elongation and by some C_2—C_1 bond stretching.[11–16]

The transition state is characterized by a broken O_5—O_3 bond, and by a slightly elongated C_2—C_1 bond and by slightly shorter C_2—O_5 and C_1—O_3 bonds. From this point, the reaction

Journal of COMPUTATIONAL CHEMISTRY WWW.C-CHEM.ORG FULL PAPER

proceeds exothermally toward the reactants without a visible energy barrier. This phase of the reaction proceeds by an accentuated elongation of the C_2—C_1 bond, and by a minor O_5—O_3 elongation, and by a slightly decrease of the C_2—O_5 and C_1—O_3 bonds. These results are all in line with other theoretical studies of 1,2-dioxetane and 1,2-dioxetanone,[11–16] further supporting the use of the present DFT approach in this field of research.

Interaction between the ground and excited states during 1,2-dioxetanone decomposition

Figures 2a–2c presents the ground state (S_0) IRC path, along with the $T_{0/1}$ and S_1 PES as a function of the reaction coordinates, for all three solvents considered for this study.

The interaction between S_0 and T_1 PES have some similarities when compared with another theoretical study of unmodified 1,2-dioxetanone.[11] As in the study of Liu et al.,[11] we have found two intersystem crossing (ISC) between S_0 and T_1 PES. Furthermore, also as in the study of Liu et al.,[11] the points of the T_1-PES, between the two ISC, are below the points of the S_0-PES. However, major differences are seen in the interaction of the S_0 and S_1 PES. Contrary to the work of Liu et al.,[11] no conical intersection (CI) between the S_0 and S_1 were found. There is no point of the S_0 and S_1 PES, in all three solvents, in which the two states are closer than 14.0 kcal/mol. These values are expected to be too high to allow efficient nonadiabatic coupling (NAC). Therefore, there is no point in the singlets- PES that could allow the formation of products in the S_1 state, in contradiction with the experiment.[1,9,10,19,20] However, there is a ISC between the S_1 and T_1 PES that can be the reason for the formation of products in the S_1-PES. Another difference, regarding the results obtained by other authors,[11] is the existence of a significant energy barrier in the T_1-PES, between the two ISC with the S_0 PES, for all solvents: 19.3 kcal/mol for benzene, 18.2 kcal/mol for dichloromethane and 17.7 kcal/mol for DMSO. These values were calculated at the TD-MPWB1K/aug-cc-pVDZ level of theory with no zero-point correction energies.

We have also analyzed the role of the T_0-PES in the decomposition of 1,2-dioxetanone. There are two ISC between the S_0- and T_0-PES. The first ISC can be responsible for lowering the efficiency of generation of excited state products. In the second ISC, it is possible that there is a crossing of the T_0- to S_0-PES. More importantly is the interaction between the T_0- and T_1-PES. Between the ISCs defined above, there is a CI (in benzene) and possibility of NAC (in dichloromethane and DMSO) between the two triplets states defined in this study. This is an important mechanism responsible for lowering the formation of excited state products. Furthermore, the existence of a zone of the PES where the triplets ground and excited states are closer in energy explain the presence of ISCs between the S_0- and T_1-PES.

The rationalization of the chemiluminescence mechanism here presented should be made by comparison with the results of Liu et al.,[11] due to the fact that their study focused on the same molecule, and major differences were found between the two studies. The experimental evidence obtained so far regarding small 1,2-dioxetanes and 1,2-dioxetanones, indicates that the chemiexcitation step should be very inefficient and the chemiluminophore should be formed mainly in the triplet excited state.[1,9,10,19,20] For dimethyldioxetanone, a very similar analogue of 1,2-dioxetanone, it was verified that its thermolysis generates excited singlet and triplet with an efficiency of 0.05–0.10 and 1.5%, respectively.[1,10] Furthermore, for 1,2-dioxetanone the efficiency of excited state products should be lower than that, as the degree of methylation increases the efficiency of triplet and singlet excitation.[40] This can be seen, as we compare the efficiency of dimethyldioxetanone and tetramethyldioxetane (yields of singlet and triplet excitation were measured to be of 0.2 and 30%).[41] Moreover, it should be noted that for tetramethyldioxetane, the yield of singlet formation is still rather low. Therefore, a correct mechanism for 1,2-dioxetanone decomposition and excited state formaldehyde formation, should be particularly inefficient and the reason for the predominance of triplet products should be clear. However, the results of Liu et al.[11] are not in line with the expected for the chemiluminescence of 1,2-dioxetanone. They have found two CI between S_0- and S_1-PES, the possibility of NAC between these two states, and two ISC between S_0- and T_1-PES (nearly in the same zone of the two CI). Thus, the major questions regarding the decomposition of this molecule are not completely elucidated by these findings: why the product are formed in these states with such low efficiency and why is the T_1 so much efficiently populated than the S_1?[1,9,10,19,20] Why are both T_1 and S_1 populated with such low efficiency if there are so much points of crossing with the S_0-PES? Why is S_1 formaldehyde formed with so much less efficiency than T_1 formaldehyde, if besides having two CI between S_1- and S_0-PES, there is also a zone where NAC effects may take place? Even considering that after the two CI/ISC the T_1-PES is lower in energy than the S_1-PES, the energetic difference do not appear to be so large as to cause such differences in the efficiency of the formation of T_1 and S_1 formaldehyde.

It should be noted that an *in vacuo* CASPT2/CASSCF study of three thiazole-modified dioxetanones have not found any CI between S_1- and S_0-PES.[13] In this work, the role of electron-donating groups and charge-transfer processes in the decomposition of 1,2-dioxetanone was studied. These additions to the decomposition mechanism are expected to significantly enhance chemiluminescence, as indicated by experimental evidence.[42,43] Thus, the chemiexcitation mechanism of thiazole-modified dioxetanones should be more efficient than the one presented by simple 1,2-dioxetanone. However, when we compare both computational studies, it is indicated that the chemiexcitation of 1,2-dioxetane if more efficient, contrary to experimental evidence. A similar mechanism was proposed for a phenol-substituted dioxetanone, which was intended to serve as a model for firefly dioxetanone and AMPPD.[15] No CI was found between the S_1- and S_0-PES, and singlet excited state formation was explained by NAC effects. Also, an *in vacuo* study of firefly dioxetanone only found one CI between S_1- and S_0-PES.[14] Therefore, according to the reaction proposed by Liu et al.,[11] the chemiexcitation step of an inefficient

chemiluminescence substrate (expected singlet yield lower than 0.05–0.10 %) is much more efficient than the chemiexcitation step of a more efficient chemiluminescence substrate (singlet yield of 33–53% for an oxyluciferin analogue),[44] an hypothesis that we think that cannot be correct. Some authors consider that this mechanism is in question,[11] as the lone pairs on oxygen of the dioxetanone moiety were excluded from the active site. However, to our knowledge, no study has ever demonstrated that the mechanism proposed by Chung et al.[14] is wrong. To the contrary, their proposed mechanism is similar to that proposed for thiazole- and phenol-modified dioxetanones,[13,15] which can be used as small models of firefly dioxetanone.

We think that our study can provide a mechanism more in line with the current knowledge of dioxetanone chemiluminescence. The formation of excited state formaldehyde can be explained by the presence of two ISC, between S_0- and T_1-PES, near the S_0 transition state. The expected very small triplet excitation yield can then be explained by the presence of an energy barrier in the T_1- PES, right after the second ISC, and by CI/NAC between the T_0- and T_1-PES. The presence of an energy barrier in the T_1-PES was also reported for 1,2-dioxetane.[16,22] Therefore, due to this barrier the reaction will proceed more favorably in the S_0-PES than the T_1-PES. The much smaller S_1 yield, in comparison with the T_1 yield, is due to the fact that there is no point of crossing between the S_0- and S_1-PES. Formaldehyde is only formed in the S_1 state due an ISC between S_1- and T_1-PES, after the transition state found in the T_1-PES. Therefore, the production of S_1 formaldehyde will be dependent of the T_1 excitation. Also, it was experimentally determined that the difference between the chemiluminescence-intensity activation energy (E_{chl}) of dimethyldioxetanone, is 3–4 kcal/mol higher than its activation energy (E_a).[1] Effectively, the difference between the energy of the point of S_1-PES that intersects with the T_1 surface, and the energy of S_0 transition state is: 3.9 (benzene), 3.4 (dichloromethane), and 3.3 kcal/mol (DMSO).

Conclusion

The mechanism of decomposition of solvated 1,2-dioxetanone, a model of firefly dioxetanone, was studied with a DFT approach. Besides the S_0-PES, The S_1, T_0, and T_1 states were studied by using TD-DFT methodologies.

The first part of this study focused on finding a DFT approach that could be used in the correct reproduction of the activation barrier present in the *in vacuo* S_0-PES. This part of the present work was performed with the objective of developing an approach to study this system, which have similar accuracy than state of the art methodologies but lower computational cost. We have found that mPWKCIS/cc-pVDZ geometry optimization followed by MPWB1K/aug-cc-pVDZ frequency analysis, provided results which are in excellent agreement with the reference value.

A novel reaction mechanism for the chemiluminescence of 1,2-dioxetanone was presented. In the vicinity of the transition state present in the S_0-PES, there are two ISC between S_0 and T_1 that can account for the triplet excitation verified in this reaction. The presence of an energy barrier in the T_1-PES, after the two ISC, can then explain the small triplet excitation yield. There are also two ISC between S_0 and T_0. More important, between the two ISCs present between the S_0- and $T_{0/1}$-PES, exist a CI (in benzene) and possibility of NAC (in dichloromethane and DMSO) between the ground and excited triplets state, which can further account for the small triplet excitation yield. The even smaller singlet excitation can then be explained by the fact that there is no point of crossing between the S_0- and S_1-PES. The singlet excitation can only be explained by the presence of an ISC between the T_1- and S_1-PES, after the two ISC between the S_0- and T_1-PES. Therefore, singlet excitation is dependent of triplet excitation, which could account for the higher yield of the formation of T_1 products. The increase of excited triplets and singlets generation with the degree of methylation can then possibly be explained by decrease of the energy barrier in the T_1-PES, by decrease of the interaction between the triplet ground and excited states, and by increase of the interaction between the singlet ground and excited states.

Keywords: chemiluminescence · DFT benchmarking · 1,2-dioxetanone · condensed phase · excited states

How to cite this article: L. P. da Silva and J. C. G. Esteves da Silva, *J. Comput. Chem.* **2012,** *33,* 2118–2123. DOI: 10.1002/jcc.22997

Additional Supporting Information may be found in the online version of this article.

[1] S. P. Schmidt, G. B. Schuster, *J. Am. Chem. Soc.* **1978**, *100,* 5559.
[2] S. P. Schmidt, G. B. Schuster, *J. Am. Chem. Soc.* **1978**, *100,* 1966.
[3] J. H. Kastle, F. A. McDermott, *Am. J. Physiol.* **1910**, *27,* 122.
[4] L. Pinto da Silva, J. C. G. Esteves da Silva, *J. Chem. Theory Comput.* **2011**, *7,* 809.
[5] S. M. Marques, J. C. G. Esteves da Silva, *IUBMB Life* **2009**, *61,* 6.
[6] K. E. Luker, G. D. Luker, *Antivir. Res.* **2008**, *78,* 179.
[7] F. Fan, K. V. Wood, *Assay Drug Dev. Technol.* **2007**, *5,* 127.
[8] A. Roda, M. Guardigli, *Anal. Bioanal. Chem.* **2012**, *402,* 69.
[9] W. Adam, J. C. Liu, *J. Am. Chem. Soc.* **1972**, *94,* 2894.
[10] W. Adam, G. A. Simpson, F. Yany, *J. Phys. Chem.* **1974**, *78,* 2559.
[11] F. Liu, Y. Liu, L. De Vico, R. Lindh, *J. Am. Chem. Soc.* **2009**, *131,* 6181.
[12] L. De Vico, Y. J. Liu, J. W. Krogh, R. Lindh, *J. Phys. Chem. A* **2007**, *111,* 8013.
[13] F. Liu, Y. Liu, L. De Vico, R. Lindh, *Chem. Phys. Lett.* **2009**, *484,* 69.
[14] L. W. Chung, S. Hayashi, M. Lundberg, T. Nakatsu, H. Kato, K. Morokuma, *J. Am. Chem. Soc.* **2008**, *130,* 12880.
[15] H. Isobe, Y. Tanako, M. Okumura, S. Kuramistu, K. Yamaguchi, *J. Am. Chem. Soc.* **2005**, *127,* 8667.
[16] S. Wilsey, F. Bernardi, M. Olivucci, M. A. Robb, S. Murphy, W. Adam, *J. Phys. Chem. A.* **1999**, *103,* 1669.
[17] T. Wilson, A. P. Schaap, *J. Am. Chem. Soc.* **1971**, *93,* 4126.
[18] H. C. Steinmetzer, A. Yekta, N. J. Turro, *J. Am. Chem. Soc.* **1974**, *96,* 282.
[19] G. B. Schuster, S. P. Schmidt, *J. Am. Chem. Soc.* **1980**, *102,* 306.
[20] N. J. Turro, M. F. Chow, *J. Am. Chem. Soc.* **1980**, *102,* 5058.
[21] C. G. Min, A. M. Ren, X. N. Li, J. F. Zon, Y. Sung, J. D. Goddard, C. C. Sun, *Chem. Phys. Lett.* **2011**, *506,* 269.
[22] C. Tanaka, J. Tanaka, *J. Phys. Chem. A* **2000**, *104,* 2078.
[23] D. Roca-Sanjuán, M. G. Delcey, I. Navizet, N. Ferre, Y. J. Liu, R. Lindh, *J. Chem. Theory Comput.* **2011**, *7,* 4060.
[24] J. Finley, P. A. Malmqvist, B. O. Roos, L. Serrano-Andrés, *Chem. Phys. Lett.* **1998**, *288,* 299.

[25] B. O. Roos, *Ab initio* Methods in Quantum Chemistry II; Wiley: New York, **1987**; p 399.
[26] J. B. Krieger, J. Q. Chen, G. J. Iafrate, A. Savin, In Electron Correlations and Materials Properties; A. Gonis, N. Kioussis, M. Ciftan, Eds.; Plenum: New York, **1999**.
[27] J. P. Perdew, In Eletronic Structure of Solids '91; P. Zieche, H. Eschrig, Eds.; Akademie Verlag: Berlin, **1991**.
[28] C. Adamo, V. Barone, *J. Chem. Phys.* **1998**, *108,* 664.
[29] C. Gonzalez, H. B. Schlegel, *J. Phys. Chem.* **1990**, *94,* 5523.
[30] E. K. U. Gross, W. Kohn, *Adv. Quantum Chem.* **1990**, *21,* 255.
[31] M. E. Casida, Recent Advances in Density Functional Methods; World Scientific: Singapore, **1995**.
[32] V. Barone, M. Cossi, *J. Phys. Chem A* **1998**, *102,* 1995.
[33] M. J. Frisch, G. W. Trucks, H. B. Schlegel, G. E. Scuseria, M. A. Robb, J. R. Cheeseman, J. A. Montgomery, Jr., T. Vreven, K. N. Kudin, J. C. Burant, J. M. Millam, S. S. Iyengar, J. Tomasi, V. Barone, B. Mennucci, M. Cossi, G. Scalmani, N. Rega, G. A. Petersson, H. Nakatsuji, M. Hada, M. Ehara, K. Toyota, R. Fukuda, J. Hasegawa, M. Ishida, T. Nakajima, Y. Honda, O. Kitao, H. Nakai, M. Klene, X. Li, J. E. Knox, H. P. Hratchian, J. B. Cross, C. Adamo, J. Jaramillo, R. Gomperts, R. E. Stratmann, O. Yazyev, A. J. Austin, R. Cammi, C. Pomelli, J. W. Ochterski, P. Y. Ayala, K. Morokuma, G. A. Voth, P. Salvador, J. J. Dannenberg, V. G. Zakrzewski, S. Dapprich, A. D. Daniels, M. C. Strain, O. Farkas, D. K. Malick, A. D. Rabuck, K. Raghavachari, J. B. Foresman, J. V. Ortiz, Q. Cui, A. G. Baboul, S. Clifford, J. Cioslowski, B. B. Stefanov, G. Liu, A. Liashenko, P. Piskorz, I. Komaromi, R. L. Martin, D. J. Fox, T. Keith, M. A. Al-Laham, C. Y. Peng, A. Nanayakkara, M. Challacombe, P. M. W. Gill, B. Johnson, W. Chen, M. W. Wong, C. Gonzalez, J. A. Pople, Gaussian 03 (Revision C.02); Gaussian: Wallingford, CT, **2004**.
[34] Y. Zhao, D. G. Truhlar, *J. Phys. Chem. A* **2004**, *108,* 6908.
[35] B. J. Lynch, P. L. Fast, M. Harris, D. G. Truhlar, *J. Phys. Chem. A* **2000**, *104,* 4811.
[36] C. Adamo, V. Barone, *J. Chem. Phys.* **1999**, *110,* 6158.
[37] Y. Zhao, D. G. Truhlar, *J. Chem. Theory Comput.* **2005**, *1,* 415.
[38] A. D. Becke, *J. Chem. Phys.* **1993**, *93,* 5648.
[39] C. T. Lee, W. T. Yang, R. G. Parr, *Phys. Rev. B: Condens. Matter Mater. Phys.* **1988**, *37,* 785.
[40] W. Adam, W. J. Baader, *J. Am. Chem. Soc.* **1985**, *107,* 410.
[41] T. Wilson, D. E. Golan, M. S. Harris, A. L. Baumstark, *J. Am. Chem. Soc.* **1976**, *98,* 1086.
[42] K. A. Zaklika, A. L. Thayer, A. P. Schaap, *J. Am. Chem. Soc.* **1978**, *100,* 4916.
[43] N. Watanabe, T. Mizuno, M. Matsumoto, *Tetrahedron* **2005**, *61,* 9569.
[44] E. M. White, M. G. Steinmetz, J. D. Miano, P. D. Wildes, R. Morland, *J. Am. Chem. Soc.* **1980**, *102,* 3199.

Received: 13 January 2012
Revised: 27 March 2012
Accepted: 28 March 2012
Published online on 20 April 2012

Article 10

Response to “Comment on density functional theory study of 1,2-dioxetanone decomposition in condensed phase”

Luís Pinto da Silva and Joaquim C.G. Esteves da Silva

J. Comput. Chem. **2012**, *33*, 2127-2130.

The theoretical calculations and the writing of the paper were performed by Luís Pinto da Silva, under supervision of Professor Esteves da Silva.

Journal of COMPUTATIONAL CHEMISTRY WWW.C-CHEM.ORG LETTER TO THE EDITOR

Response to "Comment on Density Functional Theory Study of 1,2-Dioxetanone Decomposition in Condensed Phase"

Luís Pinto da Silva and Joaquim C.G. Esteves da Silva*

Roca-Sanjuan et al. commented on our paper "Density Functional Theory Study of 1,2-Dioxetanone Decomposition in Condensed Phase", by criticizing the use of a closed-shell approach and the differences encountered regarding other previous studies. However, our suggested reaction mechanism was in line with experimental findings, contrary to other computational studies. Moreover, we have presented data to support our use of a closed-shell approach. © 2012 Wiley Periodicals, Inc.

DOI: 10.1002/jcc.23039

Chemiluminescence is the emission of energy with limited emission of heat, as the result of a chemical reaction. When this reaction occurs in a living organism, by an enzyme-catalyzed reaction, it is termed bioluminescence. The most well-known chemi/bioluminescence phenomenon is that of firefly oxyluciferin.[1–3] This molecule can be formed in a singlet excited state by formation and subsequent decomposition of firefly dioxetanone. This latter molecule is related to unmodified 1,2-dioxetanone, which is also a chemiluminescence substrate (Fig. 1).[4,5] The chemiluminescence mechanisms of these molecules are far from rationalized and have attracted much attention from the research community.[6–15]

Experimental data on the 1,2-dioxetanones indicate that both singlet and triplet excited state products are produced, with a large preference for triplet excited state products.[16–21] Moreover, the chemiexcitation mechanism should be particularly inefficient. The decomposition of 1,2-dimethyldioxetanone results in the production of excited state singlet and triplet products with an yield of 0.05–0.10 and 1.5%, respectively.[16,18] Furthermore, for 1,2-dioxetanone the efficiency of excited states production should be lower than that, as the degree of methylation increases the efficiency of triplet and singlet excitation.[21] Thus, a correct mechanism for the chemiluminescence mechanism of 1,2-dioxetanone should be particularly inefficient and the reason for triplet predominance should be clear.

Recently, we have used a density functional theory (DFT) approach to better explain the chemiluminescence of 1,2-dioxetanone and to increase the existent knowledge regarding this topic.[6] Our involvement on this topic of research is due to our interest in the elucidation, by using both computational and experimental means, of the firefly bioluminescence phenomenon.[1–4,22–30] Our calculations revealed a novel mechanism for the chemiluminescence of this compound. The triplet excitation is explained by two intersystem crossings (ISC) with the singlet ground state, while the singlet excitation can only be accounted by an ISC with the triplet excited state. The experimentally observed small excitation yield can then be explained by the presence of an energy barrier in the potential energy surface of the triplet excited state, which will govern both triplet and singlet excitation. The triplet predominance is explained by the fact that the singlet excitation is dependent of an ISC with the triplet excited state, whereas this latter state is populated directly by two ISC with the singlet ground state. Thus, ours calculations revealed a mechanism that was in line with experimental findings and provided an explanation for the three key aspects of 1,2-dioxetanone decomposition: a path for triplet and singlet excitation; a reason for the triplet predominance; and a reason for the inefficiency of the chemiexcitation mechanism.

Our objective was, by using the theoretical means available to us, to provide a chemiexcitation mechanism for 1,2-dioxetanone that would be in line with previous experimental findings. To this end, we studied 1,2-dioxetanone in implicit solvents (dichloromethane, dimethyl sulfoxide (DMSO), and benzene), and not *in vacuo*, to work with a model closer to experimental conditions.

In response to the online publication of our manuscript, Roca-Sanjuán et al.[31] have written a joint commentary where they state some of their concerns regarding our work. One of their concerns is that our DFT-obtained results are in disagreement with the ones obtained in other studies of 1,2-dioxetanone, which were presented as independent and complementary.[8,10,11] First, it should be noted that these studies are not entirely independent, despite being made by different

L. Pinto da Silva, J.C.G. Esteves da Silva
Departamento de Química e Bioquímica, Centro de Investigação em Química (CIQ-UP), Faculdade de Ciências da Universidade do Porto, Campo Alegre 687, 4169-007 Porto, Portugal
E-mail: jcsilva@fc.up.pt

Contract/grant sponsor: Fundação para a Ciência e Tecnologia (FCT, Lisbon) (Programa Operacional Temático Factores de Competitividade (COMPETE) e comparticipado pelo Fundo Comunitário Europeu FEDER); Contract/grant number: PTDC/QUI/71366/2006; Contract/grant sponsor: FCT (Luís Pinto da Silva); Contract/grant number: SFRH\BD\76612\2011.

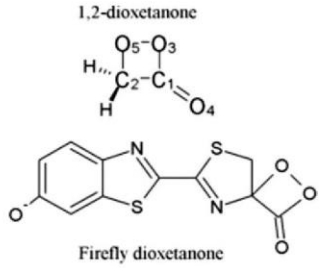

Figure 1. Schematic representation of firefly dioxetanone and 1,2-dioxetanone.

authors.[8,10,11] By reading the work of Mazziotti and coworker, it is clear that the authors already taken for granted the results and reasoning presented by Lindh and coworkers, the ANO-RCC-VDZP was used in all studies, and Mazziotti and coworker have even used the CASSCF pathway calculated by Lindh and coworkers.[8,10,11] Therefore, the fact that these studies have presented similar results is much more a consequence of the way Mazziotti and coworker have approach their study, than evidence that the chemiluminescence mechanism of 1,2-dioxetanone is indeed the one presented by these authors. Moreover, the methodologies used by these authors are not being able to explain this complicated phenomenon.

In 2009, Lindh and coworkers have tried to explain the chemiluminescence mechanism of unmodified 1,2-dioxetanone, by using multiconfigurational methods (CASPT2/CASSCF).[8] Lindh and coworkers proposed that singlet excited state products were produced due to two conical intersections with the singlet ground state, and possibility of nonadiabatic coupling between the singlet ground and excited states during a significant part of the potential energy surface.[8] Triplet excited state products were produced due to two ISC between the singlet ground state and the triplet excited state.[8] The results regarding singlet ground and excited states were supported by the findings of Mazziotti and coworker, who have used different multiconfigurational methods (two-electron reduced-density matrix).[10,11] Despite providing a reason for the formation of excited state products, these findings did not explain two key aspects of the chemiluminescence of 1,2-dioxetanone: the triplet predominance and the inefficiency of excited state production. The mechanism of triplet and singlet excited state formation is very similar, which is in disagreement with experimental findings, as it did not explain the triplet predominance. Furthermore, the proposed chemiexcitation is much more efficient than expected.

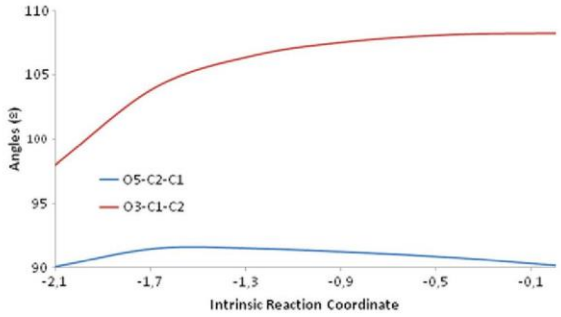

Figure 2. Angle variations recorded during the O_5—O_3 bond elongation, from the reactant to the transition state.

It should be noted that Lindh and coworkers used the same multiconfigurational methods to study the chemiluminescence mechanism of anionic thiazole-substituted dioxetanone (a model of firefly dioxetanone).[9] Also, it was verified that the formation of singlet excited state products, by firefly dioxetanone decomposition, is much higher than that presented by simple 1,2-dioxetanone (singlet yield of 33–53% for an oxyluciferin analogue).[32] However, the mechanism proposed by these authors for anionic thiazole-substituted dioxetanone is much less efficient than the one presented for 1,2-dioxetanone: singlet excited state products can only be formed by nonadiabatic coupling between the singlet ground and excited states (at the transition structure, these two states are separated by $\sim$ 5 kcal/mol).[9] Even the chemiluminescence mechanism of 1,2-dioxetane (singlet yield expected to be lower than 0.20%), proposed by the same authors with the same multiconfigurational methods, was calculated to be more efficient than the one calculated for anionic thiazole–dioxetanone.[7,21,33] Moreover, another multiconfigurational study, performed by Lundberg and coworkers, indicated that in firefly dioxetanone decomposition reaction, the singlet excited state potential energy surface is only populated by one conical intersection with the singlet ground state.[12] Thus, these results indicate that multiconfigurational methods are having difficulties to correctly describe the chemiluminescence mechanism of these molecules, as they are presenting much more efficient mechanisms for inefficient substrates (1,2-dioxetanone and 1,2-dioxetane) than for much more efficient substrates (anionic thiazole–dioxetanone and firefly dioxetanone).

Taking this information into consideration, the fact that our proposed reaction mechanism is different from the one presented by previous studies should not be used to discredit this new hypothesis.[6,8,10,11] Therefore, the articles cited by the commentators should not be used as a standard reference to evaluate new reaction mechanisms presented by other researchers.[8,10,11] Given the lack of results that accurately described the chemiluminescence of 1,2-dioxetanone, the presentation of new mechanisms was already expected, and their presentation should be highly desired by researchers that are truly interested in the advance of the scientific knowledge regarding this phenomenon. Indeed, our study was done in order to try to fill this gap in the existent literature.[6]

Another concern is a large energy difference between triplet and singlet states.[31] However, our work is not the first report of a large energy difference between the triplet and singlet states, in dioxetanone decomposition reactions.[13] Moreover, there are points on our Intrinsic reaction coordinate (IRC) paths where the singlet and triplet excited states are close in energy, as well are the singlet and triplet ground states (which can be exemplified by the ISC between the states) (Table 1).[6]

Table 1. Relative energies (ΔE, in kcal/mol) of singlet/triplet excited and ground states (S_0, T_0, S_1, and T_1, in kcal/mol) near three reported ISC in benzene.

ISC	ΔE
ISC-(S_0/T_0)-1	17.1/15.1
ISC-(S_0/T_0)-2	28.2/26.2
ISC-(S_1/T_1)	34.0/32.3

Journal of COMPUTATIONAL CHEMISTRY WWW.C-CHEM.ORG LETTER TO THE EDITOR

Table 2. ESP charge for the singlet ground transition state, in benzene and DMSO, calculated at the MPWB1K/aug-cc-pVDZ level of theory[6].

Closed-shell				Open-shell			
Formaldehyde fragment	Carbon dioxide fragment	O_5	O_3	Formaldehyde fragment	Carbon dioxide fragment	O_5	O_3
Benzene							
0.159	−0.161	−0.154	−0.356	0.078	−0.078	−0.239	−0.141
DMSO							
0.204	−0.205	−0.157	−0.403	0.094	−0.093	−0.258	−0.147

This structure was considered to be both open- and closed-shell.

Finally, the commentators indicated that exist some differences between their DFT singlet calculations and the one present in our manuscript.[6,31] They have found an open-shell singlet ground state lower in energy than our closed-shell singlet solution. First, it should be noted that our calculations were obtained with a stable closed-shell singlet ground state wavefunction. Second, the potential energy surfaces obtained with our approach describe better the experimental findings described in the literature. Thus, in our opinion, the IRC described by us should be taken into account when one would try to explain the chemiluminescence mechanism of 1,2-dioxetanone.

It is suggested that during the decomposition of dioxetanes/dioxetanones, there is the formation of a biradical intermediate.[7,8] To explain this biradical mechanism, these decomposition reactions were even compared with the ring-opening reaction of cyclobutane, in which a biradical intermediate was proven to be involved.[34] However, it should be noted that this molecule is indeed symmetric, which would favor a biradical mechanism, contrary to 1,2-dioxetanone. This molecule is not symmetric, the oxygen on the carbon dioxide fragment is expected to be more electronegative than the oxygen on the formaldehyde moiety (which is expected to be stabilized by solvents of increasing polarity). Moreover, the O_5—O_3 bond breaking occurred mainly by O_3 separation, in relationship to O_5, and not by mutual O_5—O_3 elongation. This can be seen in Figure 2, where is depicted the changes in O_5—C_2—C_1 and O_3—C_1—C_2 angles. All of this indicates that the ground state transition state may not be a true biradical molecule.

To clarify this situation, we calculated the electrostatic potential (ESP) charges of 1,2-dioxetanone (in benzene and DMSO) of the singlet ground state transition structure, by considering it both an open- and closed-shell molecule.[6] This was done by single point calculations at the MPWB1K/aug-cc-pVDZ level of theory, and by using the conductor-like polarized continuum model.[35,36] These calculations were performed with the Gaussian 03 program package.[37] The objective of these calculations is to see if the atomic charge is evenly distributed in the $O_{5/3}$ atoms, thereby indicating the presence of a pure biradical intermediate, or not.

Table 3. ESP charge for the open- and closed-shell singlet ground states, and triplet ground state, in benzene, calculated at the MPWB1K/aug-cc-pVDZ level of theory.

States	O_5	O_3
Triplet state	−0.037	−0.331
Open-shell singlet	−0.182	−0.167
Closed-Shell singlet	−0.170	−0.224

This structure corresponds to the intrinsic reaction coordinate of −1.2.[6]

The results are presented in Table 2. Our results indicate that the transition state is not a true biradical species as the negative charge is separated distinctly between O_5 and O_3. Moreover, it can be seen that in open-shell singlet structure the negative charge is higher in O_5 than in O_3. In the closed-shell singlet structure, the charge distribution between $O_{5/3}$ is the opposite. Also, the increase in the polarity of the microenvironment leads to an increased charge separation between $O_{5/3}$, thereby decreasing the biradical character of the transition state. This is in line with studies that have indicated that preferential formation of triplet states is in conflict with the biradical mechanism and that solvent effects seem to rule out the viability of the biradical mechanism.[21,38] Thus, this could explain the difference to the results presented by Lindh, Mazziotti and coworkers, who have suggested the involvement of a biradical intermediate.[8,10,11] Moreover, the fact that only the closed-shell singlet ground state calculations predicted a reaction mechanism more in line with experiment indicates that our line of reasoning was correct. Also, the expected charge difference between the formaldehyde and carbon dioxide fragments was better defined by the closed-shell singlet ground state structure, with the latter moiety being more electronegative. This is especially expected as all calculations demonstrated that the charge density initially involved in the O_3—O_5 bond was not evenly distributed, after the breaking of the bond. Therefore, it appears that a closed-shell approach deals better with the singlet ground state, than an open-shell approach.

This conclusion is further supported by the analysis of the ESP charge of the triplet ground state of 1,2-dioxetanone, at the point of the first ISC with the singlet ground state (Intrinsic reaction coordinates of −1.2).[6] These calculations were performed in benzene, as described above. The results are presented in Table 3. The ESP charges were also calculated for open- and closed-shell singlet ground states, at the same coordinate. The calculations demonstrated that O_3 is more electronegative than O_5, in the triplet and closed-shell singlet ground states. This suggests higher electron density in O_3.

Table 4. ESP charge for the open- and closed-shell singlet ground states, in benzene, calculated at the MPWB1K/aug-cc-pVDZ level of theory.

States	O_5	O_3
Open-shell singlet	−0.292	−0.399
Closed-shell singlet	−0.292	−0.399

This structure corresponds to the intrinsic reaction coordinate of 1.2.[6]

It should be noted that only some points in the

singlet ground state potential energy surface present energetic differences, when we compare our calculations with those presented by Roca-Sanjuán et al.[6,31] For example, at intrinsic reaction coordinate of 1.2, the energy of the singlet state is the same, despite being open- or closed-shell. We have then calculated the ESP charges of open- and closed-shell singlet ground state, at that coordinate, in benzene. The results are presented in Table 4. It can be seen that the charge of O_5 and O_3 is the same.

Combining all results, we think that closed-shell approach should be considered in the singlet ground state because it correctly describes the charge density of 1,2-dioxetanone in all points of the reaction. An open-shell approach probably fails because it describes a wrong charge density for 1,2-dioxetanone in some points of the reaction.

In conclusion, our computational study was performed with the objective of presenting a possible new perspective to the study of the chemiluminescence of 1,2-dioxetanone. The presented reaction mechanism was in line with previous experimental findings, and provided explanations to aspects not elucidated by other computational studies. Reasons were given to the differences encountered between this mechanism and previous theoretical investigations. Thus, we think that our work presented a valid interpretation of the available experimental data, and that should be taken into consideration by researchers interested in this complicated and exciting phenomenon.

Keywords: chemiluminescence · DFT benchmarking · 1,2-dioxetanone · condense phase · intersystem crossings

How to cite this article: L. Pinto da Silva, J. C. G. Esteves da Silva, *J. Comput. Chem.* **2012,** *33,* 2127–2130. DOI: 10.1002/jcc.23039

[1] L. Pinto da Silva, J. C. G. Esteves da Silva, *J. Chem. Theory Comput.* **2011**, *7,* 809.
[2] S. M. Marques, J. C. G. Esteves da Silva, *IUBMB Life* **2009**, *61,* 6.
[3] J. M. Leitão, J. C. G. Esteves da Silva, *J. Photochem. Photobiol. B* **2010**, *101,* 1.
[4] L. Pinto da Silva, J. C. G. Esteves da Silva, *ChemPhysChem* **2012**, *000,* 00. DOI: 10.1002/cphc.201200195.
[5] M. Matsumoto, *J. Photochem. Photobiol. C* **2004**, *5,* 27.
[6] L. Pinto da Silva, J. C. G. Esteves da Silva, *J. Comput. Chem.* **2012**, *000,* 00. DOI: 10.1002/jcc.22997.
[7] L. De Vico, Y. J. Liu, J. W. Krogh, R. Lindh, *J. Phys. Chem. A* **2007**, *111,* 8013.
[8] F. Liu, Y. Liu, L. De Vico, R. Lindh, *J. Am. Chem. Soc.* **2009**, *131,* 6181.
[9] F. Liu, Y. Liu, L. De Vico, R. Lindh, *Chem. Phys. Lett.* **2009**, *484,* 69.
[10] L. Greenman, D. A. Mazziotti, *J. Chem. Phys.* **2010**, *133,* 164110.
[11] L. Greenman, D. A. Mazziotti, *J. Chem. Phys.* **2011**, *134,* 174110.
[12] L. W. Chung, S. Hayashi, M. Lundberg, T. Nakatsu, H. Kato, K. Morokuma, *J. Am. Chem. Soc.* **2008**, *130,* 12880.
[13] H. Isobe, Y. Tanako, M. Okumura, S. Kuramistu, K. Yamaguchi, *J. Am. Chem. Soc.* **2005**, *127,* 12880.
[14] C. G. Min, A. M. Ren, X. N. Li, J. F. Zon, Y. Sung, J. D. Goddard, C. C. Sun, *Chem. Phys. Lett.* **2011**, *506,* 269.
[15] C. Tanaka, J. Tanaka, *J. Phys. Chem. A* **2000**, *104,* 2078.
[16] S. P. Schmidt, G. B. Schuster, *J. Am. Chem. Soc.* **1978**, *100,* 5559.
[17] W. Adam, J. C. Liu, *J. Am. Chem. Soc.* **1972**, *94,* 2894.
[18] W. Adam, G. A. Simpson, F. Yany, *J. Phys. Chem.* **1974**, *78,* 2559.
[19] G. B. Schuster, S. P. Schmidt, *J. Am. Chem. Soc.* **1980**, *102,* 306.
[20] N. J. Turro, M. F. Chow, *J. Am. Chem. Soc.* **1980**, *102,* 5058.
[21] W. Adam, W. J. Baader, *J. Am. Chem. Soc.* **1985**, *107,* 410.
[22] L. Pinto da Silva, J. C. G. Esteves da Silva, *ChemPhysChem* **2011**, *12,* 3002.
[23] L. Pinto da Silva, J. C. G. Esteves da Silva, *ChemPhysChem* **2011**, *12,* 951.
[24] L. Pinto da Silva, J. C. G. Esteves da Silva, *J. Phys. Chem. B* **2012**, *116,* 2008.
[25] L. Pinto da Silva, J. C. G. Esteves da Silva, *J. Comput. Chem.* **2011**, *32,* 2654.
[26] L. Pinto da Silva, J. C. G. Esteves da Silva, *Comput. Theory Chem.* **2012**, *988,* 56.
[27] R. Fontes, D. Fernandes, F. Peralta, H. Fraga, I. Maio, J. C. G. Esteves da Silva, *FEBS J.* **2008**, *275,* 1500.
[28] H. Fraga, D. Fernandes, J. Novotny, R. Fontes, J. C. G. Esteves da Silva, *ChemBioChem* **2006**, *7,* 929.
[29] H. Fraga, R. Fontes, J. C. G. Esteves da Silva, *Angew. Chem. Int. Ed. Engl.* **2005**, *44,* 3427.
[30] L. Pinto da Silva, J. C. G. Esteves da Silva, *Photochem. Photobiol. Sci.* **2011**, *10,* 1039.
[31] D. Roca-Sanjuán, M. Lundberg, D. A. Mazziotti, R. Lindh, *J. Comput. Chem.* **2012**, *000,* 00.
[32] E. M. White, M. G. Steinmetz, J. D. Miano, P. D. Wildes, R. Morland, *J. Am. Chem. Soc.* **1980**, *102,* 3199.
[33] T. Wilson, D. E. Golan, M. S. Harris, A. L. Baumstark, *J. Am. Chem. Soc.* **1976**, *98,* 1086.
[34] J. C. Polanyi, A. H. Zewail, *Acc. Chem. Res.* **1995**, *28,* 119.
[35] Y. Zhao, D. G. Truhlar, *J. Phys. Chem. A* **2004**, *108,* 6908.
[36] V. Barone, M. Cossi, *J. Phys. Chem. A* **1998**, *102,* 1995.
[37] M. J. Frisch, G. W. Trucks, H. B. Schlegel, G. E. Scuseria, M. A. Robb, J. R. Cheeseman, J. A. Montgomery, Jr., T. Vreven, K. N. Kudin, J. C. Burant, J. M. Millam, S. S. Iyengar, J. Tomasi, V. Barone, B. Mennucci, M. Cossi, G. Scalmani, N. Rega, G. A. Petersson, H. Nakatsuji, M. Hada, M. Ehara, K. Toyota, R. Fukuda, J. Hasegawa, M. Ishida, T. Nakajima, Y. Honda, O. Kitao, H. Nakai, M. Klene, X. Li, J. E. Knox, H. P. Hratchian, J. B. Cross, C. Adamo, J. Jaramillo, R. Gomperts, R. E. Stratmann, O. Yazyev, A. J. Austin, R. Cammi, C. Pomelli, J. W. Ochterski, P. Y. Ayala, K. Morokuma, G. A. Voth, P. Salvador, J. J. Dannenberg, V. G. Zakrzewski, S. Dapprich, A. D. Daniels, M. C. Strain, O. Farkas, D. K. Malick, A. D. Rabuck, K. Raghavachari, J. B. Foresman, J. V. Ortiz, Q. Cui, A. G. Baboul, S. Clifford, J. Cioslowski, B. B. Stefanov, G. Liu, A. Liashenko, P. Piskorz, I. Komaromi, R. L. Martin, D. J. Fox, T. Keith, M. A. Al-Laham, C. Y. Peng, A. Nanayakkara, M. Challacombe, P. M. W. Gill, B. Johnson, W. Chen, M. W. Wong, C. Gonzalez, and J. A. Pople, Gaussian 03 (Revision C.02); Gaussian, Inc.: Wallingford, CT, **2004**.
[38] N. J. Turro, P. Lechtken, *J. Am. Chem. Soc.* **1973**, *95,* 264.

Received: 17 May 2012
Accepted: 20 May 2012
Published online on 7 June 2012

Article 11

Chemiluminescence of 1,2-dioxetanone studied by a closed-shell DFT approach
Luís Pinto da Silva and Joaquim C.G. Esteves da Silva
Int. J. Quantum Chem. **2013**, *113*, 1709-1716.

The theoretical calculations and the writing of the paper were performed by Luís Pinto da Silva, under supervision of Professor Esteves da Silva.

International Journal of QUANTUM CHEMISTRY WWW.Q-CHEM.ORG FULL PAPER

Chemiluminescence of 1,2-Dioxetanone Studied by a Closed-Shell DFT Approach

Luís Pinto da Silva and Joaquim C.G. Esteves da Silva*

The chemiluminescence of simple 1,2-dioxetanone has already been studied by both multiconfigurational and density functional theory calculations. The former approach revealed a step-wise biradical mechanism for its decomposition, whereas the latter revealed a concerted mechanism. The first approach was not in line with both computational and experimental findings, whereas the second mechanism was. Due to these apparent mechanistic contradictions and some concerns regarding our concerted mechanism, and the use of a closed-shell approach and different methods for geometry and single-point calculations, we have revisited the chemiluminescence of this molecule. Once again the concerted mechanism was found to be prevailing, and a closed-shell approach was able to rationalize the chemiluminescence of 1,2-dioxetanone. It was once again noted that an open-shell and a step-wise biradical mechanism cannot explain the chemiluminescence of this molecule. © 2013 Wiley Periodicals, Inc.

DOI: 10.1002/qua.24389

Introduction

Chemiluminescence is the emission of light that results from a chemical reaction, with limited emission of heat, due to the production of excited state products.[1,2] The formation of the products already in an excited state is thought to be due to a crossing point between the ground and excited states potential energy surfaces (PES). One of the most important chemiluminescence substrates is firefly dioxetanone

C1

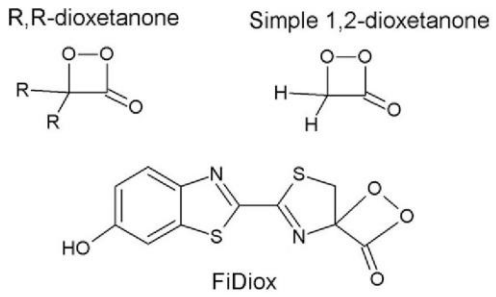

Chart 1. R,R-dioxetanone, simple 1,2-dioxetanone and FiDiox.

(FiDiox, Chart 1), in which decomposition is responsible for the formation of the light emitter responsible for the bioluminescence of the fireflies.[1–4] As firefly bioluminescence has been gaining numerous practical applications due to very advantageous characteristics, this phenomenon has been the target of numerous computational studies to get a better comprehension of this enzyme-catalyzed chemiluminescence reaction.[5–7]

FiDiox is part of the family of R,R-dioxetanones (Chart 1).[1,2] Simple 1,2-dioxetanone is the simplest chemiluminescence substrate of this family of molecules, and has been used as a model for the chemiluminescence of FiDiox.[8–13] Experimental data on R,R-dioxetanones indicate that both singlet and triplet excited states are produced in their decomposition, in a large triplet to singlet ratio.[14–16] The decomposition of a dimethylated analog of simple 1,2-dioxetanone resulted in the production of singlet and triplet excited state products, with an efficiency of 0.05–0.10 and 1.50%, respectively.[14,15] For simple 1,2-dioxetanone, this efficiency should be even lower, as the degree of methylation increase these efficiencies, which indicates that this molecule basically does not emit chemiluminescence.[14–16] Therefore, a correct mechanism for the chemiluminescence of simple 1,2-dioxetanone should explain its inefficiency and the reason for the triplet excited state predominance.

An unanswered topic of the chemiluminescence of this type of molecules is the mechanism of their thermal decomposition. A step-wise biradical mechanism was postulated by Richardson and O'Neal[17] (Scheme 1). Other authors have proposed a concerted mechanism, in which no biradical intermediate was found (Scheme 1).[18,19] Further experimental studies have indicated that the preferential formation of triplet states is in conflict with the biradical mechanism and that solvent effects rule out the viability of the biradical mechanism.[16,20] Moreover, these authors have proposed a reaction mechanism which involved simultaneous O—O and C—C bond elongation.[16,20]

S1

Some researchers have tried to investigate the chemiluminescence of simple 1,2-dioxetanone by using different multiconfigurational methods.[8–11] These authors have proposed a step-wise biradical mechanism for the reaction path (Scheme

L. Pinto da Silva, J. C. G. Esteves da Silva
Departamento de Química e Bioquímica, Centro de Investigação em Química, Faculdade de Ciências da Universidade do Porto, Campo Alegre 687, 4169-007 Porto, Portugal
E-mail: jcsilva@fc.up.pt

Contract grant sponsor: Fundação para a Ciência e Tecnologia (FCT, Lisbon) [Programa Operacional Temático Factores de Competitividade (COMPETE) e comparticipado pelo Fundo Comunitário Europeu FEDER] (Project PTDC/QUI/71366/2006).
Contract grant sponsor: FCT (L. P. da S.); Contract grant number: SFRH/BD/76612/2011.

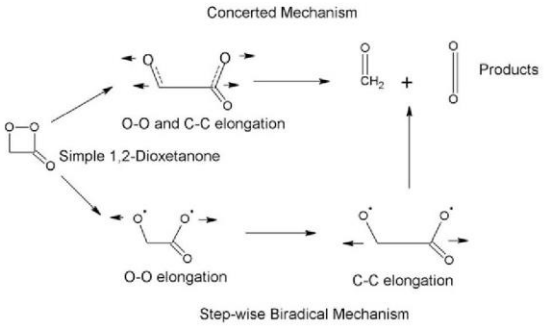

Scheme 1. The concerted and step-wise biradical decomposition mechanisms, proposed for simple 1,2-dioxetanone.

1). Moreover, they have proposed that the singlet chemiexcitation is caused by two conical intersections between the singlet ground and excited state PES, and possibility of nonadiabatic crossing between these intersections. The triplet excitation was proposed to be caused by two intersystem crossings between the singlet ground and the triplet excited states PES.[8–10] However, there are various problems with the proposed reaction mechanism. The proposed reaction mechanism does not explain the high triplet to singlet ratio, as the path for the chemiexcitation is very similar.[8–11,14–16] Moreover, the paths for triplet and singlet chemiexcitation are far more efficient than expected.[8–11] It should be noted that the path for singlet chemiexcitation, for simple 1,2-dioxetanone, is more efficient than the mechanisms computationally calculated for FiDiox and two FiDiox analogs, even when multiconfigurational methods were used.[8–11,21–24] Moreover, the most consensual thermal decomposition mechanism (a more concerted mechanism), in the experimentalist community, is one where both O—O and C—C bond elongations occur simultaneous, which was not the case of the mechanism calculated by these authors.[8–11,16–20] Therefore, these works were not in line with other experimental and computational studies.

Given the incapacity of the previous computational works in describing the chemiluminescence of simple 1,2-dioxetanone, we have tried to contribute to the existent literature by using a closed-shell density functional theory (DFT) approach.[12] Our calculations revealed a concerted mechanism for simple 1,2-dioxetanone (Scheme 1), in which no biradical intermediate was found, as postulated by experimentalist chemiluminescence researchers.[12,13,16,18–20] Also, the triplet predominance was explained by the fact that there were two points of crossing between the singlet ground and triplet excited states PES, whereas the first singlet state could only be chemiexcited due to crossing with the triplet excited state PES.[12] The low efficiency of chemiluminescence was attributed to an energy barrier in the triplet excited state PES and deexcitation due to crossings between the triplet excited and ground state PES.[12] Our reaction mechanism was more in line with the experimental findings than previous computational studies as we provided an explanation for: triplet and singlet chemiexcitation, the triplet predominance, and the inefficiency of the chemiluminescence mechanism.[12,14–16,20] Moreover, our reaction mechanism did not involved a biradical intermediate, which is in line with the aforementioned experimental findings.[16,20] Also, we have showed that while other researchers predicted a symmetrical O—O bond cleavage, our calculations predicted a nonsymmetrical bond elongation (which was caused by an increase of one of the O—C—C angles).[8–13] This difference may explain the different mechanisms calculated by different groups. However, we which to note that simple 1,2-dioxetanone is not so isoelectronic as other molecules which decomposition leads to a symmetrical bond cleavage and biradical formation (as cyclobutane).[13] So, we think that a nonsymmetrical bond cleavage is more plausible for simple 1,2-dioxetanone.

In another DFT-based study, we have studied the peroxide bond breaking step of the thermal decomposition of a methylated analog of the simple 1,2-dioxetanone.[25] Both closed- and open-shell calculations were made. We also compared this bond breaking step with the ring-opening reaction of cyclobutane, in which a biradical intermediate was experimentally demonstrated to be formed.[25] The calculations regarding this 1,2-dioxetanone derivative, along with the comparison with the formation of the tetramethylene biradical, allowed us to state that no biradical intermediate was formed in the decomposition reaction of the methylated 1,2-dioxetanone derivative.

More recently, the chemiluminescence of simple 1,2-dioxetanone was revisited.[26] The authors have stated that some features of our reaction mechanism were computational artifacts, due to the use of two different computational methods for geometry optimizations and single-point energy calculations. Moreover, it was stated that an open-shell approach predicted a step-wise biradical mechanism, which was consistent with previous calculations. These findings allow the authors to state that a closed-shell approach cannot be used in R,R-dioxetanone thermolysis, and that the step-wise biradical mechanism was found to be prevailing.[26] First, we once again note that the step-wise biradical mechanism failed to explain the chemiluminescence of simple 1,2-dioxetanone, and it is not in line with calculations made for FiDiox and analogs, nor with the thermal decomposition mechanisms presented by experimental chemiluminescence researchers.[8,13–25] Therefore, this reaction mechanism is not able to rationalize the chemiluminescence of 1,2-dioxetanone, and the fact that a DFT open-shell approach found a similar mechanism is only a signal of failure of this approach.

Nevertheless, in this study, we revisit the chemiluminescence of simple 1,2-dioxetanone, to see the impact of potential computational artifacts in our reaction mechanism and to validate the use of a DFT closed-shell approach. Therefore, we have calculated the decomposition reaction of simple 1,2-dioxetanone with three DFT functionals with different Hartree–Fock (HF) exchange, and two different basis sets (cc-pVDZ and aug-cc-pVDZ). Geometry optimizations and single-point energy calculations were made with the same functional and basis set.

Methodology

Ground state geometry optimizations, frequency, and intrinsic reaction coordinate (IRC) calculations were performed with three different DFT functionals and two basis sets (cc-pVDZ and

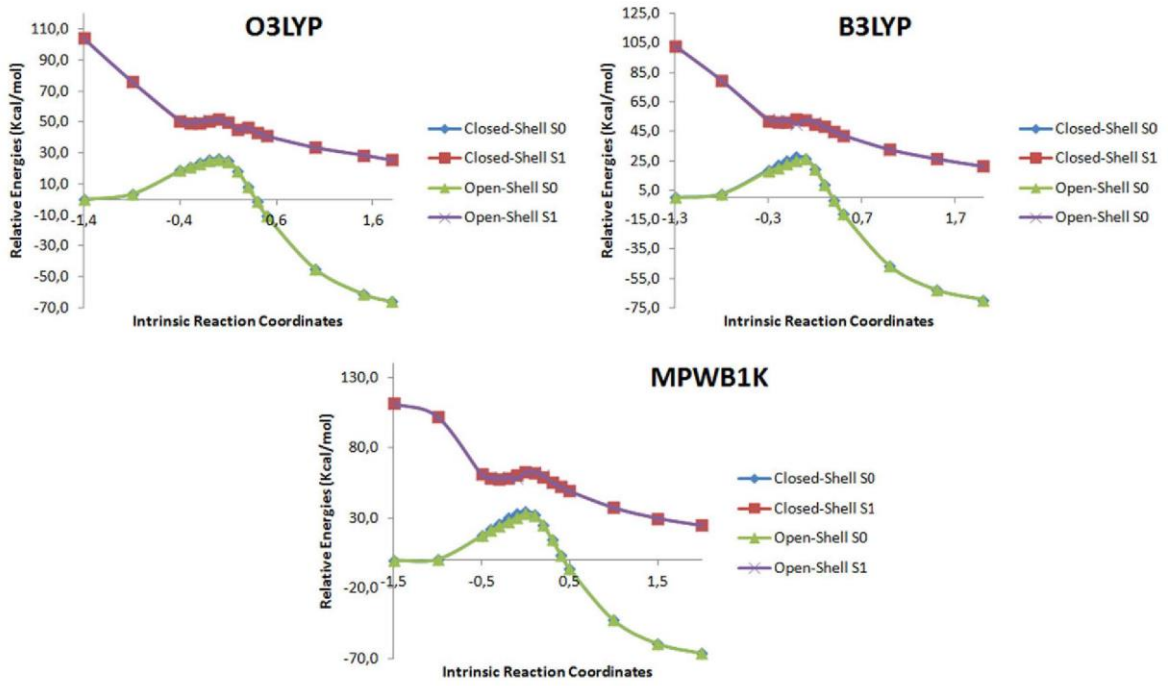

Figure 1. IRC paths for stables closed- and open-shell $S_{0/1}$, obtained with the aug-cc-pVDZ basis set. [Color figure can be viewed in the online issue, which is available at wileyonlinelibrary.com.]

aug-cc-pVDZ).[27] The energy of a given IRC path were recalculated with the same DFT functional and basis set. Both IRC and geometry calculations were performed *in vacuo*. The singlet (S_0) and triplet (T_0) ground state energies were calculated at the DFT/(cc-pVDZ or aug-cc-pVDZ) level of theory, whereas the singlet (S_1) and triplet (T_1) excited states (forgotten in the study made by Yue et al.) were calculated at the time-dependent (TD) DFT/(cc-pVDZ or aug-cc-pVDZ) level of theory.[26,28]

The DFT functionals used in this study were O3LYP (HF exchange of 11.61%), B3LYP (HF exchange of 20%), and MPWB1K (HF exchange of 44%).[29–33] We think that a HF exchange range of 11.61–44% is more reliable than the one used by Yue et al. (20–100%), as our initial study only used DFT functionals with a HF exchange range of 0–44%.[11,26]

Geometry and IRC calculations were made by using a closed-shell approach. The S_0 and S_1 energies were reevaluated by using both a closed- and open-shell approach. The wavefunctions of the closed-shell $S_{0/1}$ energies were spin-restricted stables, whereas that of the open-shell $S_{0/1}$ energies were spin-unrestricted stables. The T_0 and T_1 energies were calculated by using only an open-shell approach. These energies were obtained by single point calculations at the structures of the S_0 IRC path.

All the present calculations were performed with the Gaussian 09 program package.[34]

Results and Discussion

In Figures 1 and, Supporting Information, S1 are depicted the IRC paths for stables closed- and open-shell $S_{0/1}$ PES. It can be seen that there are little difference in the energy of the PES, irrespective of the amount of HF exchange present in the DFT functional used. Moreover, as can be seen in Supporting Information, Tables S1–S6, the lower energies of open-shell S_0 can be more due to spin contamination than to real higher stability. In an open-shell calculation, the wavefunction is no longer an eigenfunction of S^2, and so some errors may be introduced in the calculations. This occurs because although the wavefunction may appear to be of the desired spin state, it may have a bit of some other spin states mixed in. Thus, spin contamination may cause the increase or decrease of the total computed energy. However, these changes are only artifacts of an incorrect wavefunction. As can be seen in Supporting Information, Tables S1–S6, the spin contamination in the open-shell S_0 calculations is large as the S^2 value (especially, before spin annihilation) is always larger than 0.0000 (which is the expected S^2 value for a singlet state). The IRC present in those tables are the one which energies are different, depending on what approach we used (closed- or open-shell). Thus, the fact that there are only differences between open- and closed-shell results, where these differences may result from spin-contamination derived errors in the open-shell approach, indicates that we can consider the closed-shell $S_{0/1}$ energies as reliable.

Also, it is stated in the literature that a S^2 value near 1 indicates the existence of a biradical.[26] However, as can be seen in Supporting Information, Tables S1–S6, the value of S^2 never reaches the value of 1 for open-shell S_0, which indicates the absence of a biradical intermediate.

In Figures 2 and, Supporting Information, S2 are represented the variations of the O_5—O_3, C_2—C_1, O_5—C_2, and O_3—C_1 bond lengths. Figures 3 and, Supporting Information, S3 represent

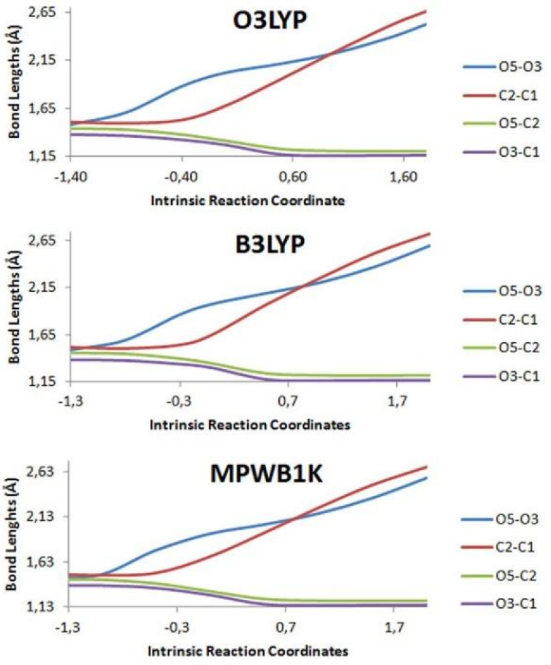

Figure 2. Variations of the O_5—O_3, C_2—C_1, O_5—C_2, and O_3—C_1 bond lengths, with the aug-cc-pVDZ basis set. [Color figure can be viewed in the online issue, which is available at wileyonlinelibrary.com.]

the variations of the O_5—C_2—C_1 and O_3—C_1—C_2 angles. Figures 2 and, Supporting Information, S2 indicate that the decomposition reaction of simple 1,2-dioxetanone is a concerted one, irrespective of the HF exchange of the DFT functional and the basis set. It should be noted that Lindh and coworkers have also attributed a concerted decomposition mechanism for a FiDiox analog, with the use of multiconfigurational methods.[24] The reaction proceeds from the reactant to the transition state both by O_5—O_3 (more predominant) and C_2—C_1 (less predominant) bond breaking. From the transition state to the products, the reaction proceeds without a visible barrier, and still by O_5—O_3 and C_2—C_1 elongation.

Figures 3 and, Supporting Information, S3 demonstrate that the O_5—O_3 bond breaking (especially until the transition state) is not a symmetrical event. The breaking of this bond corresponds more to changes in the coordinate of the O_3 atom (as demonstrated by the higher variation of the O_3—C_1—C_2 angle), than to mutual $O_{5/3}$ separation. This is in line with what is to be expected from this kind of reaction as O_5 and O_3 belong to two different moieties, and so are not so chemical equivalents to allow a symmetrical bond cleavage. From the contrary, the original work of Lindh and coworkers calculated a reaction path in which the O_5—O_3 bond cleavage was symmetrical, which could explain the presence of a biradical intermediate contrary to the experimental findings.[8,16,20]

Figures 4 and, Supporting Information, S4 represent the variation of the natural bond orbital (NBO) charges of the formaldehyde (CH_2O) and carbon dioxide (CO_2) moieties of simple 1,2-dioxetanone, during the course of the reaction. It can be seen that there is a small charge transfer between the two moieties, until near the transition state. At this region, there is a large increase in the positive charge of the CH_2O moiety, and a large increase in the negative charge in the CO_2 moiety, followed by a back charge transfer phenomenon.

In Figures 5 and, Supporting Information, S5 are represented the atomic NBO charges of O_5, O_3, and O_4, during the course of the reaction. In a step-wise biradical mechanism as depicted in Scheme 1, it would be expected that the negative charge of O_5 and O_3 would decrease similarly, due to O_5—O_3 bond breaking and subsequent end of electron sharing. However, as we can see in Figures 5 and, Supporting Information, S5, the atomic NBO charges of O_5 and O_3 vary independently. The negative charge of O_5 decreases until a zone of the PES near the transition state, from which there is a large increase in its negative charge. For the contrary, there is a large and independent increase in the negative charge of O_3, until a zone of the PES near the transition state, from which there is a decrease in its negative charge. From the figures, it can be seen that the increase in the negative charge of O_3 is triggered not by O_5 but by O_4. The behavior of the charge of this atom is basically the opposite of that of O_3. Thus, the results presented so far indicates that initially O_5—O_3 bond breaking occurs due to charge transfer between O_3 and O_4, which increases the negative charge of the former atom,

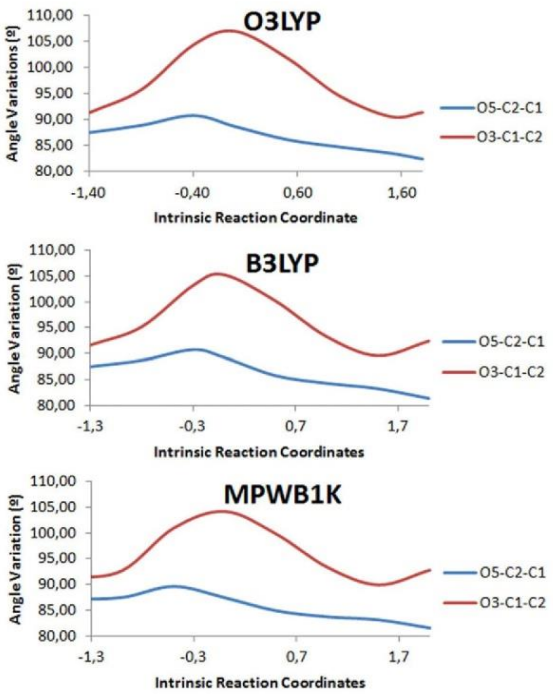

Figure 3. Variations of the O_5—C_2—C_1 and O_3—C_1—C_2 angles, with the aug-cc-pVDZ basis set. [Color figure can be viewed in the online issue, which is available at wileyonlinelibrary.com.]

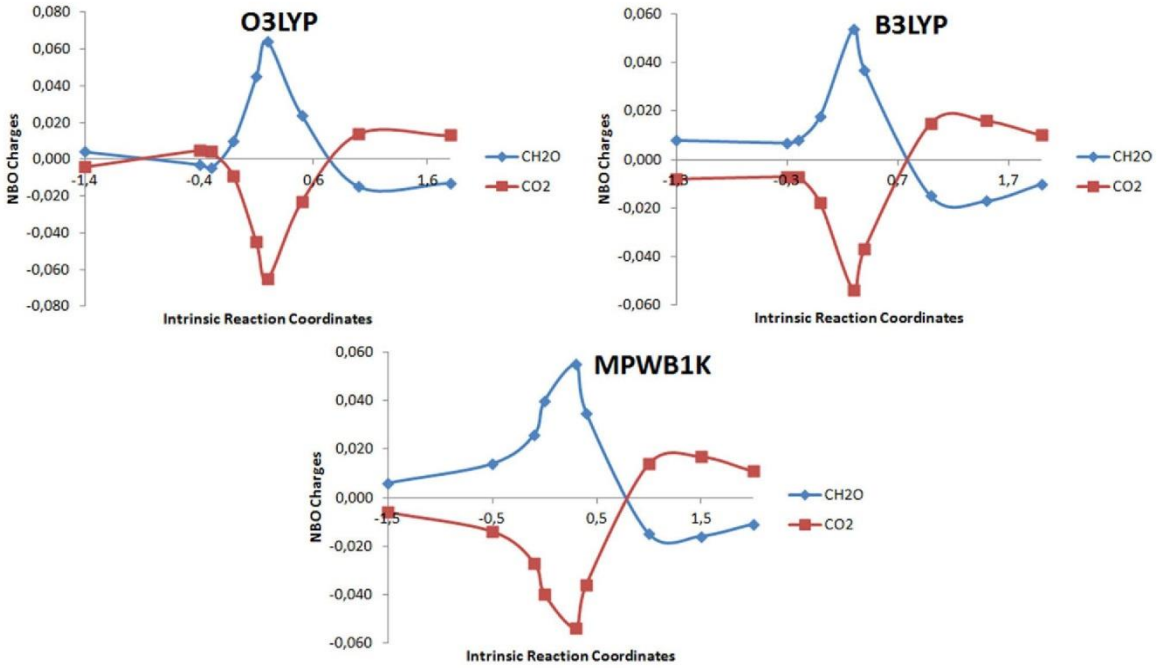

Figure 4. Closed-shell NBO charges of the CH_2O and CO_2 moieties during the decomposition reaction, with the aug-cc-pVDZ basis set. [Color figure can be viewed in the online issue, which is available at wileyonlinelibrary.com.]

thereby increasing the repulsion between O_3 and O_5. The higher the negative charge of O_3 the higher the repulsion between O_3 and O_5, which causes a higher O_3—C_1—C_2 angle variation.

Figure 6 represents the stable closed-shell S_0 IRC path, along with the $T_{0/1}$ and S_1 PES as a function of the reaction coordinates, for the three DFT functionals and the cc-pVDZ basis set.

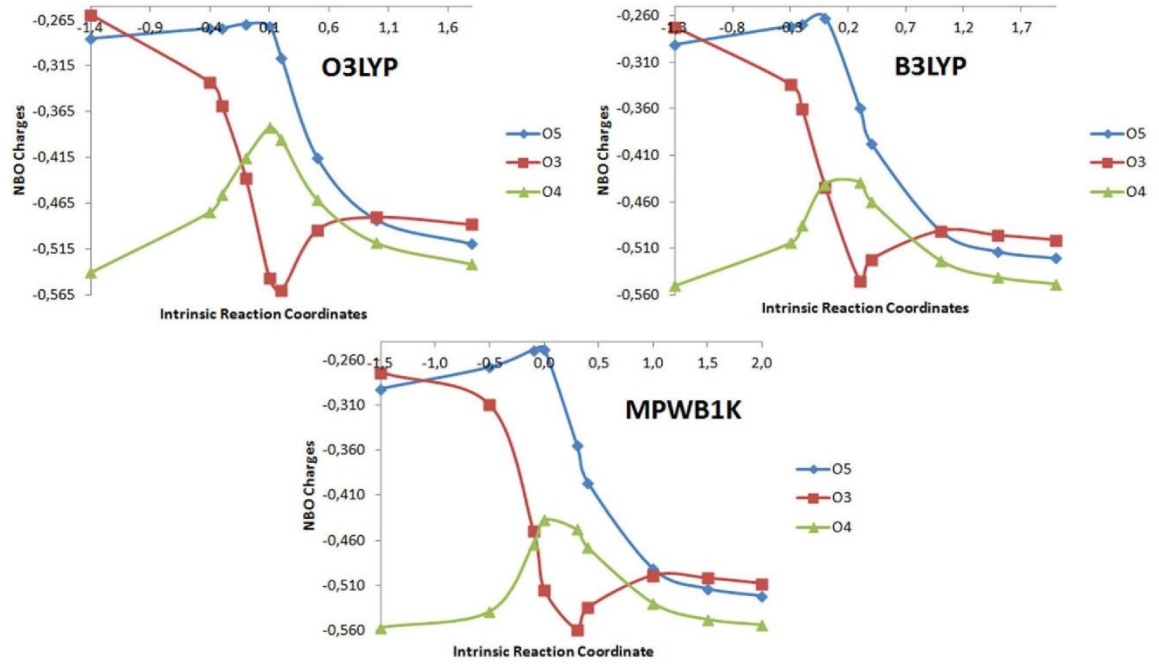

Figure 5. Closed-shell NBO charges of O_5, O_3, and O_4 during the decomposition reaction, with the aug-cc-pVDZ basis set. [Color figure can be viewed in the online issue, which is available at wileyonlinelibrary.com.]

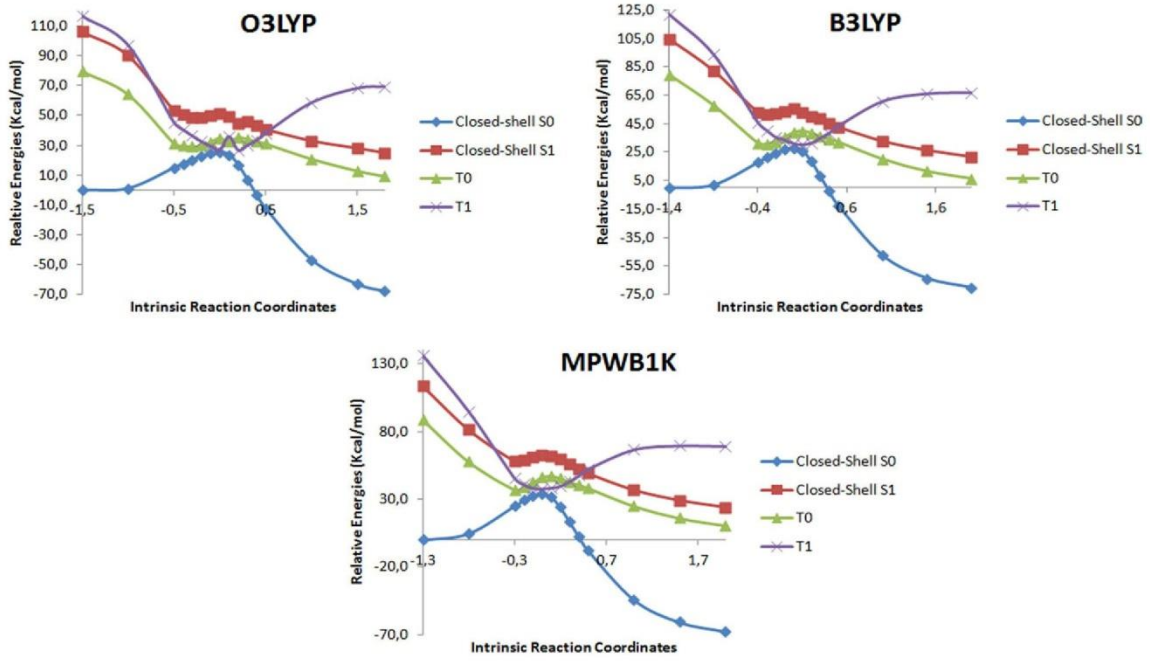

Figure 6. Stable closed-shell S_0 IRC path, along with the $T_{0/1}$ and S_1 PES as a function of the reaction coordinates, with the cc-pVDZ basis set. [Color figure can be viewed in the online issue, which is available at wileyonlinelibrary.com.]

Table 1 indicates the activation energies for the S_0 decomposition reaction, with zero-point corrections.

As in our previous study, no direct point of crossing between S_0 and S_1 PES was found.[12] Also, irrespective of the DFT functional used, there was always found a point of crossing between T_1 and S_1 PES, after the S_0 transition state, which could account for the singlet chemiexcitations.[12]

Nevertheless, these results indeed indicate that some features of our reaction mechanism presented previously were computational artifacts, obtained by the use of different methods for geometry optimizations and single-point energy calculations. An energy barrier in the T_1 PES was only found with calculations at the TD O3LYP/cc-pVDZ level of theory. Moreover, there was not found any direct point of crossing between S_0 and both T_0 and T_1 PES, contrary to what we have observed before.[12] It should be noted that the higher the HF exchange of the DFT functional used the higher the $T_{0/1}/S_0$ difference. However, the results obtained here still allow us to rationalize the inefficient chemiluminescence of simple 1,2-dioxetanone.[14–16] Despite there were not found any direct points of crossing between the S_0 and T_1 PES, the lowest T_1/S_0 energy differences are not so great to completely forbid an inefficient transition: 1.5 kcal/mol for O3LYP, 3.0 kcal/mol for B3LYP, and 3.9 kcal/mol for MPWB1K. These T_1/S_0 energies differences, along with T_1 deexcitation due to interaction with T_0, can explain the inefficient triplet chemiexcitation. The fact that S_1 can only be chemiexcited due to a point of crossing with T_1, can explain the inefficient singlet chemiexcitation and the high triplet to singlet ratio.[14–16] Therefore, the results with this basis set indicate that, although some of the features of our proposed reaction mechanism could be indeed computational artifacts, the "skeleton" of the mechanism is still able to rationalize the experimental results.[12,14–16]

Table 1. Activation barriers (in kcal/mol) of the closed-shell S_0 IRC path, calculated at the DFT/basis set level of theory, with zero-point corrections.

	cc-pVDZ	Aug-cc-pVDZ
O3LYP	23.0	24.1
B3LYP	25.8	25.4
MPWB1K	31.2	32.2

Figure 7 represents the stable closed-shell S_0 IRC path, along with the $T_{0/1}$ and S_1 PES as a function of the reaction coordinates, for the three DFT functionals and the aug-cc-pVDZ basis set. Table 1 indicates the activation energies for the S_0 decomposition reaction, with zero-point corrections.

The addition of the diffuse functions to the calculations has altered some features of the decomposition mechanisms presented here. First, and contrary to the case when diffuse functions are not present, the T_1/S_0 energies differences decrease with increasing HF exchange of the DFT functional. Also, in no case, there was found any energy barrier in the T_1 PES. This indicate that this energy barrier is indeed a computational artifact and it is not involved in the chemiluminescence of simple 1,2-dioxetanone.[12] To the contrary, no point of crossing between S_0 and S_1 was found, whereas a T_1/S_1 crossing was always present,

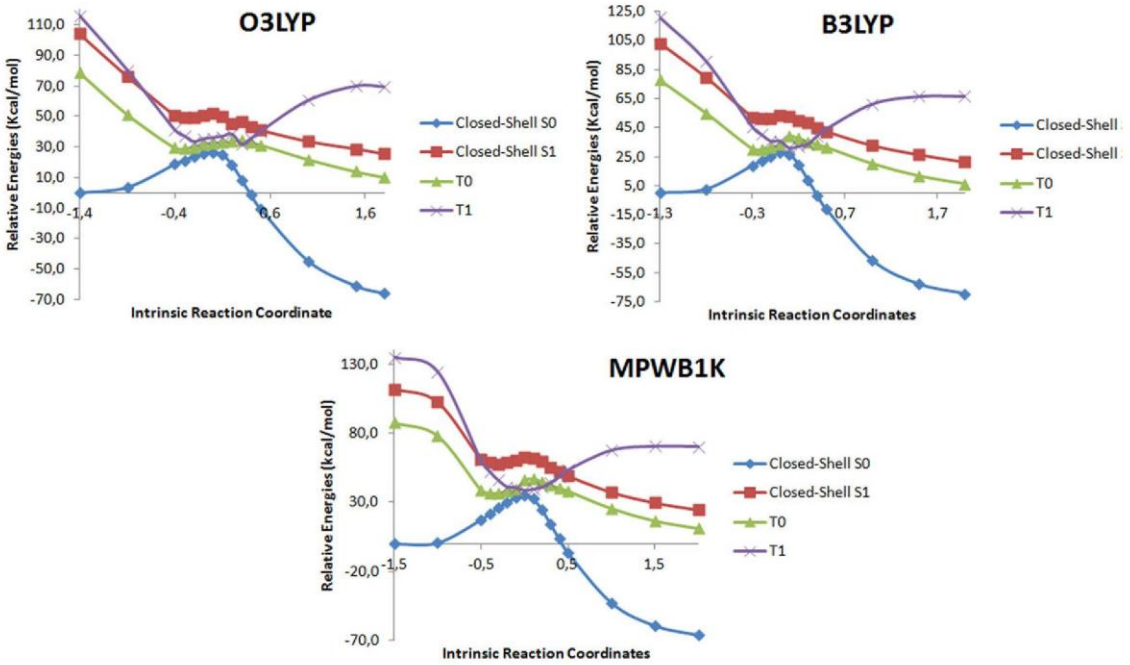

Figure 7. Stable closed-shell S_0 IRC path, along with the $T_{0/1}$ and S_1 PES as a function of the reaction coordinates, with the aug-cc-pVDZ basis set. [Color figure can be viewed in the online issue, which is available at wileyonlinelibrary.com.]

which indicates that a T_1/S_1 crossing is indeed the reason for singlet chemiexcitation and the high triplet to singlet ratio.[12]

As for the case of triplet chemiexcitation, there are some different possibilities according to the different DFT methods used. In the case of O3LYP/aug-cc-pVDZ, it appears to not be possible to chemiexcite T_1 directly from S_0, as the lowest energy difference between the states is of 9.2 kcal/mol. However, it may be possible to occur a S_0–>T_0 transition (lowest energy difference of 5.8 kcal/mol), which will allow the chemiexcitation of T_1 by T_0–>T_1 transition (at reaction coordinate of 0.3, T_1 is 2.7 kcal/mol lower in energy than T_0). This is an inefficient mechanism of triplet chemiexcitation, which could explain the experimental findings.[14–16]

In the case of B3LYP/aug-cc-pVDZ, it is possible that T_1 may be chemiexcited directly from S_0, as these states differ in energy 4.3 kcal/mol at reaction coordinate of 0.1. The relatively high T_1/S_0 energy difference and the interaction between T_1 and T_0 PES can explain the inefficient triplet chemiexcitation.[14–16] The case of MPWB1K/aug-cc-pVDZ is similar to that of B3LYP/aug-cc-pVDZ, with the lowest energy difference between T_1 and S_0 being of 3.8 kcal/mol.

It should be noted that the explanation for the triplet chemiexcitation is basically the same for the cases of B3LYP/aug-cc-pVDZ, MPWB1K/aug-cc-pVDZ, B3LYP/cc-pVDZ, MPWB1K/cc-pVDZ, and O3LYP/cc-pVDZ. A different explanation was only provided for O3LYP/aug-cc-pVDZ. This indicates that the HF exchange value of O3LYP, when coupled with diffuse functions, may be too low to properly describe the triplet chemiexcitation.

We have not calculated the S_0 IRC path with an open-shell approach, as the previous study of Lindh and coworkers already demonstrated that these type of calculations result in a reaction mechanism not in line with experimental findings and computational studies regarding other dioxetanone molecules (step-wise biradical mechanism).[14–16,20–26] Moreover, the reactions barriers (10.1–17.5 kcal/mol) calculated for this mechanism are not in line with the typical experimental range attributed to these molecules (20–30 kcal/mol).[1,2,26] For the contrary, the activation barriers calculated with a closed-shell approach, presented in Table 1, are in line the this typical experimental range.[1,2]

Conclusions

In this study, we have revisited the chemiluminescence of simple 1,2-dioxetanone, with a DFT approach. The same DFT functional and basis set were used for geometry, frequency, single-point energies, and IRC calculations. Three DFT functionals with different HF exchange were used (O3LYP, B3LYP, and MPWB1K), along with the cc-pVDZ and aug-cc-pVDZ basis sets. Besides the S_0 IRC path, the S_1 and $T_{0/1}$ reaction paths were calculated by DFT and TD DFT single-point energies calculations.

The initial S_0 IRC path was calculated with a closed-shell approach, while the S_0 and S_1 energies were reevaluated with a closed- and open-shell approach. No particular energy differences were seen between the two approaches, which support our use of a closed-shell approach.

Analysis of the S_0 IRC path once again revealed a concerted mechanism for the decomposition of simple 1,2-dioxetanone. However, some features of our previous reported chemiluminescence mechanism for this molecule were indeed found to

be computational artifacts, which occurred due to use of different methods of geometry optimizations and single-point energy calculations. Nevertheless, the present calculations indicated that our closed-shell approach still can describe qualitatively the practically inexistent chemiluminescence of simple 1,2-dioxetanones. Energy differences between T_1 and S_0, besides deexcitation due to interactions between T_1 and T_0, explain the triplet chemiexcitation inefficiency. The fact that S_1 is much higher than S_0 in energy during all the reaction, and that the former state can only be chemiexcited due to T_1/S_1 interaction, explains the inefficient singlet chemiexcitation and the high triplet to singlet ratio.

Further refinement of the chemiluminescence mechanism proposed for simple 1,2-dioxetanone should include interaction with explicit solvent molecules and the study of the dynamics of the decomposition reaction and transition between states. Moreover, the systematic study of other simple dioxetanones should be able to reveal more features of the chemiluminescence mechanism of this type of molecules.

Keywords: chemiluminescence · 1,2-dioxetanone · closed-shell approach · density functional theory · thermal decomposition

How to cite this article: L. Pinto da Silva, J. C. G. Esteves da Silva, *Int. J. Quantum Chem.* **2013,** *113*, 1709–1716. DOI: 10.1002/qua.24389

Additional Supporting Information may be found in the online version of this article.

[1] L. Pinto da Silva, J. C. G. Esteves da Silva, *ChemPhysChem* **2012**, *13,* 2257.
[2] M. Matsumoto, *J. Photochem. Photobiol. C* **2004**, *5,* 27.
[3] S. M. Marques, J. C. G. Esteves da Silva, *IUBMB Life* **2009**, *61,* 6.
[4] J. Vieira, L. Pinto da Silva, J. C. G.Esteves da Silva, *J. Photochem. Photobiol. B* **2012**, *117,* 33.
[5] A. Roda, M. Guardigli, *Anal. Bioanal. Chem.* **2012**, *402,* 69.
[6] L. Pinto da Silva, J. C. G. Esteves da Silva, *J. Chem. Theory Comput.* **2011**, *7,* 809.
[7] J. Y. Hasegawa, K. J. Fujimoto, H. Nakatsuji, *ChemPhysChem* **2011**, *12,* 3106.
[8] F. Liu, Y. Liu, L. De Vico, R. Lindh, *J. Am. Chem. Soc.* **2009**, *131,* 6181.
[9] L. Greenman, D. A. Mazziotti, *J. Chem. Phys.* **2010**, *133,* 164110.
[10] L. Greenman, D. A. Mazziotti, *J. Chem. Phys.* **2011**, *134,* 174110.
[11] D. Roca-Sanjuán, M. Lundberg, D. A. Mazziotti, R. Lindh, *J. Comput. Chem.* **2012**, *33,* 2124.
[12] Pinto da Silva, L.; Esteves da Silva, J.C.G. *J. Comput. Chem.* **2012**, *33,* 2118.
[13] L. Pinto da Silva, J. C. G. Esteves da Silva, *J. Comput. Chem.* **2012**, *33,* 2127.
[14] S. P. Schmidt, G. B. Schuster, *J. Am. Chem. Soc.* **1978**, *100,* 5559.
[15] W. Adam, G. A. Simpson, F. Yany, *J. Phys. Chem.* **1974**, *78,* 2559.
[16] W. Adam, W. J. Baader, *J. Am. Chem. Soc.* **1985**, *107,* 410.
[17] W. H. Richardson, H. E. O'Neal, *J. Am. Chem. Soc.* **1972**, *94,* 8665.
[18] F. McCapra, *Pure Appl. Chem.* **1970**, *24,* 611.
[19] D. R. Kearns, *Chem. Rev.* **1971**, *71,* 395.
[20] N. J. Turro, P. Lechtken, *J. Am. Chem. Soc.* **1973**, *95,* 264.
[21] L. Yue, Y. J. Liu, W. H. Fang, *J. Am. Chem. Soc.* **2012**, *134,* 11632.
[22] L. W. Chung, S. Hayashi, M. Lundberg, T. Nakatsu, H. Kato, K. Morokuma, *J. Am. Chem. Soc.* **2008**, *130,* 12880.
[23] H. Isobe, Y. Takano, M. Okumura, S. Kuramitsu, K. Yamaguchi, *J. Am. Chem. Soc.* **2005**, *127,* 8667.
[24] F. Liu, Y. Liu, L. De Vico, R. Lindh, *Chem. Phys. Lett.* **2009**, *484,* 69.
[25] L. Pinto da Silva, J. C. G. Esteves da Silva, *ScienceJet* **2012**, *1,* 29.
[26] L. Yue, D. Roca-Sanjuán, R. Lindh, N. Ferré, Y. J. Liu, *J. Chem. Theory Comput.* **2012**, *8,* 4359.
[27] C. Gonzalez, H. B. Schlegel, *J. Phys. Chem.* **1990**, *94,* 5523.
[28] E. K. U. Gross, W. Kohn, *Adv. Quantum Chem.* **1990**, *21,* 255.
[29] C. Lee, W. Yang, R. G. Parr, *Phys. Rev. B: Condens. Matter* **1988**, *37,* 785.
[30] N. C. Handy, A. J. Cohen, *Mol. Phys.* **2001**, *99,* 403.
[31] A. D. Becke, *J. Chem. Phys.* **1993**, *98,* 5648.
[32] W. M. Hoe, A. J. Cohen, N. C. Handy, *Chem. Phys. Lett.* **2001**, *341,* 319.
[33] Y. Zhao, D. G. Truhlar, *J. Phys. Chem. A* **2004**, *108,* 6908.
[34] M. J. Frisch, G. W. Trucks, H. B. Schlegel, G. E. Scuseria, M. A. Robb, J. R. Cheeseman, G. Scalmani, V. Barone, B. Mennucci, G. A. Petersson, H. Nakatsuji, M. Caricato, X. Li, H. P. Hratchian, A. F. Izmaylov, J. Bloino, G. Zheng, J. L. Sonnenberg, M. Hada, M. Ehara, K. Toyota, R. Fukuda, J. Hasegawa, M. Ishida, T. Nakajima, Y. Honda, O. Kitao, H. Nakai, T. Vreven, J. A. Montgomery, Jr., J. E. Peralta, F. Ogliaro, M. Bearpark, J. J. Heyd, E. Brothers, K. N. Kudin, V. N. Staroverov, R. Kobayashi, J. Normand, K. Raghavachari, A. Rendell, J. C. Burant, S. S. Iyengar, J. Tomasi, M. Cossi, N. Rega, J. M. Millam, M. Klene, J. E. Knox, J. B. Cross, V. Bakken, C. Adamo, J. Jaramillo, R. Gomperts, R. E. Stratmann, O. Yazyev, A. J. Austin, R. Cammi, C. Pomelli, J. W. Ochterski, R. L. Martin, K. Morokuma, V. G. Zakrzewski, G. A. Voth, P. Salvador, J. J. Dannenberg, S. Dapprich, A. D. Daniels, O. Farkas, J. B. Foresman, J. V. Ortiz, J. Cioslowski, D. J. Fox, Gaussian 09, Revision A.02, Gaussian, Inc.: Wallingford, CT, **2009**.

Received: 6 November 2012
Revised: 14 December 2012
Accepted: 17 December 2012
Published online on 8 January 2013

4.2. Characterization of the Decomposition Reaction of Dimethyl-1,2-Dioxetanone

Article 12

Interstate crossing-induced chemiexcitation as the reason for the chemiluminescence of dioxetanones

Luís Pinto da Silva and Joaquim C.G. Esteves da Silva

ChemPhysChem **2013**, *14*, 1071-1079.

The theoretical calculations and the writing of the paper were performed by Luís Pinto da Silva, under supervision of Professor Esteves da Silva.

CHEMPHYSCHEM ARTICLES

ChemPubSoc Europe

DOI: 10.1002/cphc.201200872

Interstate Crossing-Induced Chemiexcitation as the Reason for the Chemiluminescence of Dioxetanones

Luís Pinto da Silva and Joaquim C. G. Esteves da Silva*[a]

The decomposition reaction of dimethyl-1,2-dioxetanone in dichloromethane was studied by using a DFT approach. The low efficiency of triplet and singlet excited-state formation was rationalised. A charge-transfer process was demonstrated to be involved in the chemiluminescence process. Present and previous results allow us to define an interstate crossing-induced chemiexcitation (ICIC) mechanism for the chemiluminescence of dioxetanones. Charge transfer is needed to reach a transition state, in the vicinity of which direct population of excited states is possible. The chemiexcitation process is then governed by singlet/triplet intersystem crossings. Structural modifications then modify the rate of these crossings and the singlet ground and excited-state interaction, thereby modulating the efficiency of this process and the spin of the resulting products.

1. Introduction

Chemiluminescence is the emission of light as a result of a chemical reaction. When this reaction is catalysed by an enzyme, this phenomenon is termed bioluminescence. The most studied bioluminescence system is that of firefly luciferase.[1–4] This enzyme catalyses a two step reaction: firstly, the formation of an adenylate intermediate throughout the reaction of firefly luciferin and ATP–Mg^{2+} (ATP = adenosine triphosphate); the second step involves the oxidation of the intermediate, with subsequent formation of oxyluciferin.[1,4] Oxyluciferin is formed in an excited state and decays to the ground state with emission of visible light.[5–12] The firefly bioluminescence system has gained numerous analytical, biomedical and pharmaceutical applications, among others.[13–20]

Excited-state oxyluciferin is thought to be a consequence of the formation of firefly dioxetanone (Scheme 1).[4,21] The strongly exergonic decomposition of firefly dioxetanone leads to the formation of singlet excited-state oxyluciferin and ground-state carbon dioxide. Firefly dioxetanone is of the family of 1,2-dioxetanone (Scheme 1), which is one of the most simple compounds capable of chemiluminescence.[4,21,22] The decomposition of both simple 1,2-dioxetanone and firefly dioxetanone has a similar mechanism, in general terms.[4,21–30] A transition state is reached by O–O bond breaking, from which the decomposition reaction proceeds by C–C bond breaking.

Nevertheless, the chemiexcitation mechanism of both compounds has different features. While the decomposition of firefly dioxetanone generates mainly singlet excited-state products

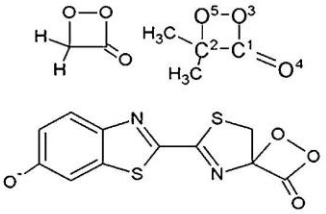

Scheme 1. Schematic representation of simple 1,2-dioxetanone, dimethyl-1,2-dioxetanone and firefly dioxetanone.

with high efficiency, simple 1,2-dioxetanone generates mainly triplet excited products with very low efficiency.[21–30] For example, the decomposition of a firefly dioxetanone analogue leads to the formation of singlet excited-state products, with a yield of 33–53%.[23] For 1,2-dioxetanone, the formation of singlet excited-state products with a yield lower than 0.05–0.10% is expected.[22,27]

The reason for these discrepancies is still unclear. In the case of firefly dioxetanone, two different multi-configurational studies indicate that singlet excited states are produced due to conical intersections (CIs) between the singlet ground and excited potential energy surfaces (PESs). Yue et al.[24] refer to two CIs, while only one CI was found in the study performed by Chung et al.[21] In the case of simple 1,2-dioxetanone, there is still controversy with regard to its decomposition and chemiexcitation mechanism. By using the complete active-space second-order perturbation theory (CASPT2) multi-configurational method, Liu et al. indicated that singlet excited-state products could be formed due to two CIs between singlet ground and excited PESs, and to the possibility of non-adiabatic crossing (NAC) between these PESs.[28] The results obtained herein were supported by studies performed by other researchers, with another multi-configurational method: two-

[a] Dr. L. Pinto da Silva, Prof. Dr. J. C. G. Esteves da Silva
Centro de Investigação em Química (CIQ-UP)
Departamento de Química e Bioquímica
Universidade do Porto, Campo Alegre 687
4169-007 Porto (Portugal)
E-mail: jcsilva@fc.up.pt

Supporting information for this article is available on the WWW under http://dx.doi.org/10.1002/cphc.201200872.

CHEMPHYSCHEM
ARTICLES
www.chemphyschem.org

electron reduced-density matrix (2RDM).[29,30] However, by reading the work of Mazziotti and Greenman,[29,30] it is clear that they took for granted the results and reasoning presented by Liu et al.:[28] the same basis set was used in all studies, and Mazziotti and Greenman even used the complete active-space self-consistent field (CASSCF) pathway calculated by Liu et al. Therefore, the similarity between the results obtained is more likely to be due to the way that Mazziotti and Greenman conducted their studies, as opposed to evidence that the chemiluminescence reaction of simple dioxetanone is that presented by these authors.

More importantly, it can be seen that Liu et al. and Mazziotti and Greenman predicted a singlet chemiexcitation mechanism for 1,2-dioxetanone that was more efficient that those predicted for firefly dioxetanone, despite the fact that all studies used multi-configurational methods and that it is experimentally known that the chemiexcitation mechanism of firefly dioxetanone should be much more efficient than that presented by simple 1,2-dioxetanone (≈33–53% vs less than 0.05–0.10%, respectively).[21–24,27–30] In our opinion, the presence of two CIs between the first singlet ground and excited states of 1,2-dioxetanone, besides non-adiabatic crossing between them, is a singlet chemiexcitation mechanism that is too efficient to provide the expected yield of less than 0.05–0.10% of singlet excited-state products. Moreover, experiments tell us that the decomposition of 1,2-dioxetanone should provide a high triplet-to-singlet ratio of excited-state products.[22,27] However, calculations by Liu et al. indicated that triplet excitation was possible by two intersystem crossings (ISCs) between the singlet ground and triplet excited state PESs, which appears to be a less efficient mechanism than the mechanism presented by the same authors for singlet excitation, when it should, in fact, be the opposite.[28] In addition, the possibility of the formation of triplet excited-state products by two ISCs appear also to be a mechanism that is more efficient than that required for the formation of less than 1.5% of triplet excited-state products.[22,27,28] Therefore, it appears that the calculations performed by Liu et al. and Mazziotti and Greenman failed to correctly describe the chemiluminescence of simple 1,2-dioxetanone.[22,27–30]

Given these facts, we have tried a new computational approach to better understand the chemiluminescence of simple 1,2-dioxetanone by performing calculations with DFT methods.[26] Our calculations revealed novel chemiluminescence for this compound that is more in line with experimental data. Triplet excitation can be explained by two ISCs with singlet ground-state PESs, while singlet excitation is only possible due to ISC with the triplet first excited state. The very low chemiluminescence efficiency of this compound can then be explained by the presence of an energy barrier in the PES of the triplet excited state, which govern both triplet and singlet excitation. Therefore, our calculations, besides presenting a mechanism that is less efficient than that presented by firefly dioxetanone, provided an explanation for the three key aspects of 1,2-dioxetanone decomposition: a path for the formation of excited-state products, a reason for the triplet predominance and a reason for the inefficiency of the chemiexcitation mechanism. Thus, we think that we have provided a valid and useful rationalisation of the chemiluminescence mechanism of simple 1,2-dioxetanone, contrary to other previous works.

This is the first report of a computational study of the decomposition of dimethyl-1,2-dioxetanone (Scheme 1) in the condensed phase (dichloromethane). With this study we intend to further clarify the chemiluminescence of this type of molecule, and to further understand the differences observed between the chemiexcitation mechanisms of simple and firefly dioxetanones. Moreover, we also intend to see the consistency of our DFT approach in the study of the chemiluminescence mechanism of these compounds by studying a more complex chemiluminescence substrate than 1,2-dioxetanone. Moreover, there are direct experimental data regarding dimethyl-1,2-dioxetanone, which is not the case for simple 1,2-dioxetanone because it has never been synthesised and will help the evaluation of the results obtained. Dimethyl-1,2-dioxetanone is known to be an ineffective chemiluminescence substrate, in its unimolecular decomposition reaction (singlet yield of 0.05–0.10% and triplet yield of 1.5%).[22] However, this molecule is expected to be a more effective substrate than 1,2-dioxetanone.[22,27] Thus, the calculations should lead to an ineffective chemiexcitation mechanism, but with features that explain the differences encountered between dimethyl-1,2-dioxetanone and 1,2-dioxetanone.

2. Results and Discussion

2.1. Singlet Ground-State Decomposition of Dimethyl-1,2-Dioxetanone

The nature of the transition state of the S_0 PES was verified by frequency analysis. This structure was then used as a starting point for an intrinsic reaction coordinate (IRC) calculation. The IRC path of dimethyl-1,2-dioxetanone decomposition, in dichloromethane, is presented in Figure 1. Figure 2A gives representations of the variations of the bond lengths of O5–O3, C2–C1, C2–O5 and C1–O3, while Figure 2B gives representations of the variations of O5–C2–C1 and O3–C1–C2 angles.

From the reactant to the transition state, the reaction proceeds mostly by O5–O3 bond elongation and by some C2–C1 bond stretching. After the transition state, the reaction proceeds toward the products without any visible energy barrier. This phase is characterised by C2–C1 bond breaking and some O5–O3 bond elongation. The bond lengths of C2–O5 and C1–O3 decrease steadily during the decomposition reaction. It is interesting to note that O5–O3 bond breaking occurs mainly by increasing the O3–C1–C2 angle. This was also seen in the case of simple 1,2-dioxetanone.[26,31] This indicates that O_5–O_3 bond breaking is not a very symmetrical process, contrary to that proposed by Lindh and co-workers for simple 1,2-dioxetanone.[28] In this work, the O3–C1–C2 and O5–C2–C1 angles increased similarly during O5–O3 bond cleavage. However, we think that, in the case of both simple 1,2-dioxetanone and dimethyl-1,2-dioxetanone, their two corresponding moieties are chemically too different to afford symmetrical O5–O3 bond breaking.

CHEMPHYSCHEM
ARTICLES
www.chemphyschem.org

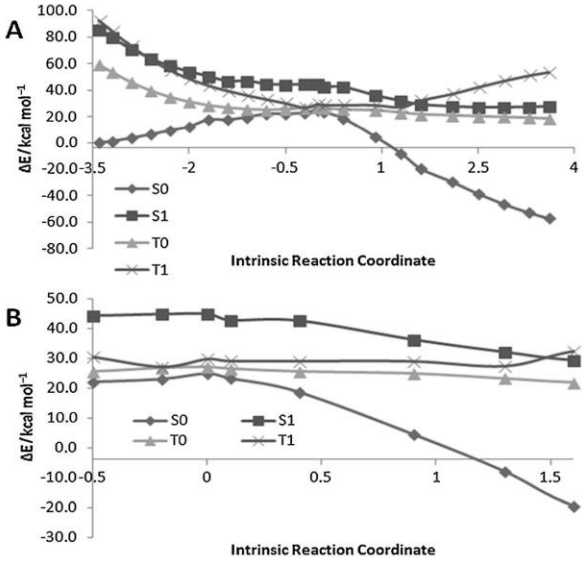

Figure 1. A) Full energy profile of the IRC path determined for dimethyl-1,2-dioxetanone. B) Energy profile of the IRC path determined for dimethyl-1,2-dioxetanone between the reaction coordinate of −0.5 and 1.6.

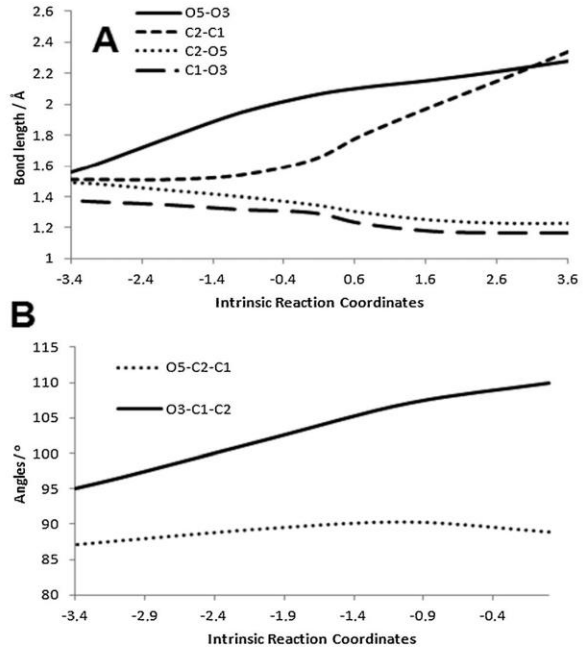

Figure 2. Bond lengths (A) and angle variations (B) recorded during the IRC calculations.

The activation energy of this reaction is, with zero-point corrections, 22.6 kcal mol^{-1}. We think that this value is in line with the experimental values obtained for this molecule (mean absolute errors of 0.3, 1.8 and 2.8 kcal mol^{-1}).[22,32,33] Although some mean absolute errors presented are not within the range of chemical accuracy (within 1 kcal mol^{-1}), we think that the impossibility of including the reaction/solvent dynamics and the complete explicit solvation shell of the target molecule in modern computational studies of chemical reactions indicates that achieving chemical accuracy is more due to a coincidence than to the accuracy of the method employed.

Figure 3 shows the atomic Mulliken charges of the acetone and carbon dioxide moieties, and their corresponding atoms. Atomic Mulliken charge analysis was used because it was also used in previous studies of firefly dioxetanone.[21,24,25] By analysing Figure 3 A, it can be seen that, in this reaction, there are three different phases of charge transfer: firstly, there is transfer of negative charge from the carbon dioxide to the acetone moiety; subsequently, there is a short phase where there is back charge transfer from the acetone to the carbon dioxide moiety; finally, the negative charge is once again transferred from the carbon dioxide to the acetone moiety.

By analysing Figure 3 A–E, it can be seen that the first phase of negative charge transfer is triggered by transfer from O4 and C1 to the other atoms of dimethyl-1,2-dioxetanone. In turn, the second phase is triggered by negative charge transfer from O5, the two methyl groups and O4 to the other atoms of this dioxetanone. Finally, in the third phase (in which the carbon dioxide moiety becomes more positive than acetone) is triggered by negative charge transfer from O3, O4 and C2 to the other atoms involved in this reaction.

We think that this approximation of the charges of O5 and O3 is important in the decomposition reaction, since the increase of the negative charge of both atoms will cause increasing repulsion between them, thereby causing breaking of the bond. A similar mechanism can possibly be seen in C2–C1 bond breaking because, after the transition state, the positive charge of C1 decreases, while the negative charge of C2 decreases. Finally, the approximation between the negative charges of O3 and O4 may be necessary for the carbon dioxide fragment to become linear.

2.2. Interaction between the Singlet and Triplet PESs

Figure 1 presents the restricted (R) $S_{0/1}$ and unrestricted (U) $T_{0/1}$ IRC paths as a function of the reaction coordinates in dichloromethane. Figure S1 in the Supporting Information shows the R and U $S_{0/1}$ IRC paths, which are very similar to each other.

The interaction between S_0 and T_1 PESs present some similarities and differences to that found for our study of simple 1,2-dioxetanone.[26] Near the S_0 transition state, S_0 and T_1 are close in energy (between 2.5 and 5.5 kcal mol^{-1}), but do not cross directly. However, given the low energy difference between these two states and possible errors associated with this method, we think that, in this region, T_1 can be populated by $S_0 \rightarrow T_1$ crossing (especially at the reaction coordinate of −0.2, where the difference is only 2.5 kcal mol^{-1}). Another interesting feature of the T_1 PES is the absence of an energy barrier, contrary to the case of simple 1,2-dioxetanone.[26]

CHEMPHYSCHEM
ARTICLES
www.chemphyschem.org

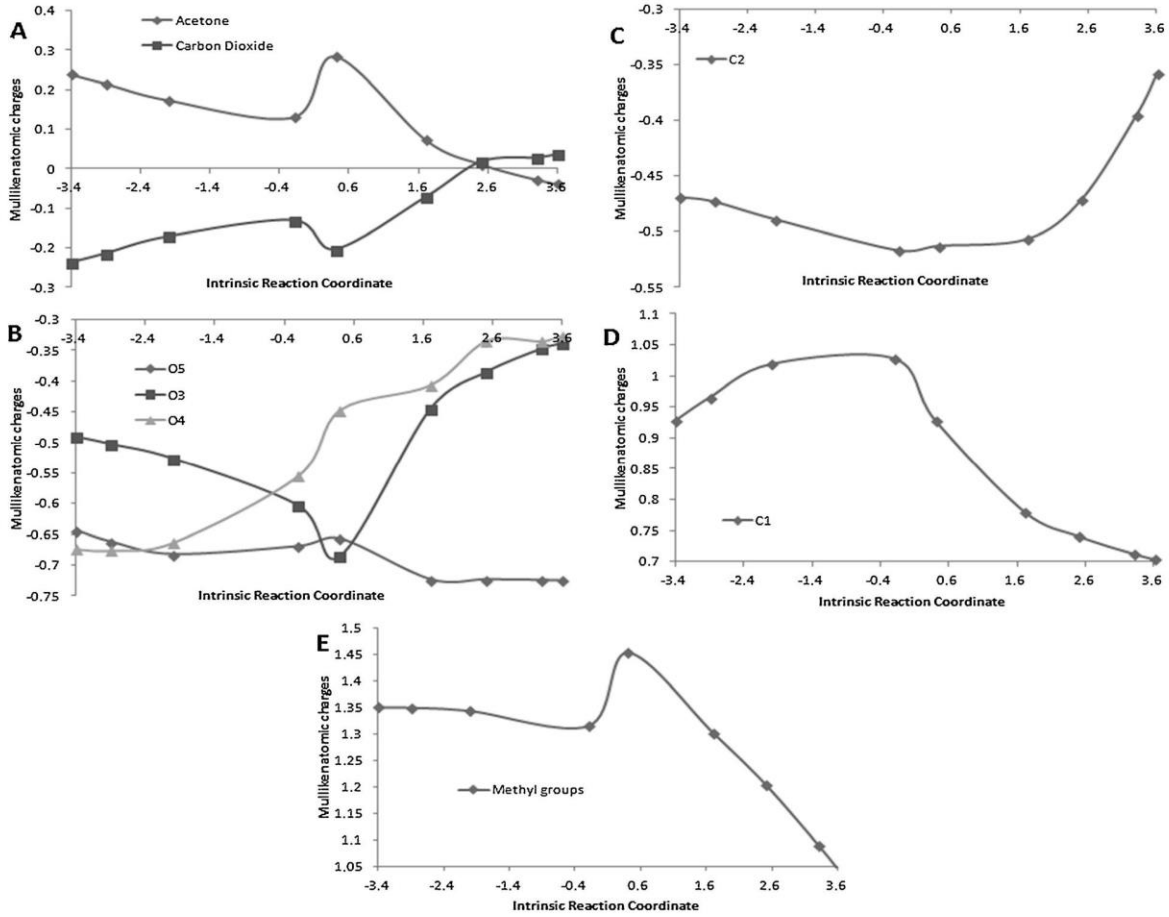

Figure 3. Atomic Mulliken charges of acetone and carbon dioxide moieties (A), O3–5 (B), C2 (C), C1 (D) and the two methyl groups (E).

Thus, T_1 can be populated near the S_0 transition state in two possible ways. Firstly, it can be populated by $S_0 \rightarrow T_1$ crossing, at the reaction coordinate of −0.2, due to the low energy difference between the states (2.5 kcal mol^{-1}). The second way is by $T_0 \rightarrow T_1$ NAC, at reaction coordinates of −0.5 to 1.3 (energy gap of 0.4–4.2 kcal mol^{-1}). In this region of the PES, T_0 is involved in an entropic trap with S_0, which can allow the population of former state.[34,35] The presence of an entropic trap is indicated by the fact that these states differ so little in energy for a significant part of the reaction. This means that the molecule is prevented from decaying rapidly toward the ground-state reaction path by entropic effects. Instead, the molecule is forced to spend some time in this almost flat region of the PES, where S_0 is almost degenerate with T_0. This trapping allows some molecules to cross to T_0. Being populated, T_0 can then be involved in the population of T_1.

Despite being populated, triplet chemiexcitation was experimentally proven to be very inefficient, although still much more effective than singlet excitation.[22] This can be explained by three aspects of the proposed reaction mechanism. Firstly, no direct $S_0 \rightarrow T_1$ crossing point was found, only points of the reaction in which these states were very close in energy. Secondly, at the reaction coordinate of −0.2 (in which the S_0/T_1 energy difference is lower) there is also an intersection between T_0 and T_1. This indicates that, at this reaction coordinate, S_0 molecules may cross to one chemiluminescence state (T_1) and to one non-chemiluminescence state (T_0) state, besides continuing in the S_0 PES. Finally, the region of the PES in which T_0/T_1 crossing can occur can also be a region in which T_1 molecules can decay to T_0, thereby lowering the formation yield of T_1 products.

Theoretical studies of the chemiluminescence of tetramethyldioxetane, which is a chemiluminescence substrate for which unimolecular decomposition produces 20% of triplet excited-state products, have led to an explanation for the efficiency of triplet production.[4] After the interaction between the first triplet excited state and the singlet ground state, the energy of T_1 increases (which can also be seen for dimethyl-1,2-dioxetanone; Figure 1 from reaction coordinate 1.3 onwards). The degree of energy increase will then control the

CHEMPHYSCHEM
ARTICLES
www.chemphyschem.org

triplet chemiexcitation efficiency. Therefore, we expect that the degree of energy increase for tetramethyldioxetane is much lower than that for dimethyl-1,2-dioxetanone.

As already stated, triplet chemiexcitation is expected to be more efficient for dimethyl-1,2-dioxetanone than for 1,2-dioxetanone. This can be explained by the presence of a high energy barrier in the T_1 PES of 1,2-dioxetanone, near the transition state, which is not present in the case of dimethyl-1,2-dioxetanone.[26]

Despite the very low singlet yield observed for dimethyl-1,2-dioxetanone, the formation of singlet excited states was verified experimentally.[22] Nevertheless, no crossing point between S_0 and S_1 was seen, as in the case of simple 1,2-dioxetanone.[26] This is in line with the low singlet excited state yield of this type of molecules.[22,27] Thus, the S_1 state must be populated by other mechanism than $S_0 \rightarrow S_1$ crossing. The calculated IRC paths demonstrated that S_1 and T_1 cross at one point of their corresponding paths (Figure 1). This finding indicates that some molecules present in the T_1 PES may cross to the S_1 IRC path, which would result in the experimentally verified singlet chemiexcitation.[22] The finding that the S_1 state may be populated in another way than from $S_0 \rightarrow S_1$ crossing is in line with experimental results.[22] It was experimentally determined that the difference between the chemiluminescence-intensity activation energy of dimethyl-1,2-dioxetanone, in dichloromethane, was (4.0 ± 0.4) kcal mol^{-1} higher than the activation energy.[22] This is in line with our results because the difference between the energy of the point of the S_1 PES that intersects with the T_1 surface and the ground-state transition state is 4.6 kcal mol^{-1}. Another experimental study reported did not find any difference between the activation energy and the activation energy of the chemiexcitation pathway.[32] However, the fact that our calculations on dimethyl-1,2-dioxetanone and simple 1,2-dioxetanone corroborates the work of Schmidt and Schuster indicates that a difference between the two activation energies previously referred to is likely to be found.[22,26,31]

2.3. Discussion of the Dimethyl-1,2-Dioxetanone Decomposition Reaction

Our results have demonstrated that triplet excited-state products may be formed by crossing with S_0 near the S_0 transition state. The low yield of triplet formation is explained by an intersection between T_0 and T_1, in addition to the possibility of NAC in a significant part of the PES. The even lower singlet excited-state yield is explained by the fact that S_1 may only be populated by crossing with T_1. No interaction point was found between S_0 and S_1. These various features of dimethyl-1,2-dioxetanone explain the inefficient ability of this molecule to form excited-state products.[22] The higher efficiency of dimethyl-1,2-dioxetanone, in comparison with simple 1,2-dioxetanone, is explained by the absence of a high energy barrier in the T_1 PES near the transition state.[22,26,27]

These results are in line with the experimental data for dimethyl-1,2-dioxetanone, which is a very good indicator of the accuracy of our calculations.[22,27] Moreover, the fact that this newly proposed mechanism is similar to that proposed for simple 1,2-dioxetanone, but still explains the higher efficiency presented by dimethyl-1,2-dioxetanone, is a further indicator of the accuracy and consistency of our calculations.[22,26,27] A third good indicator is that this new mechanism appears to be less efficient than those proposed for firefly dioxetanone, as it should be.[21–24] Thus, in our opinion, this indicates that the chemiluminescence mechanism proposed by us for simple 1,2-dioxetanone is closer to reality than those presented by Liu et al. and Mazziotti and Greenman.[26,28–30] As already mentioned in the Introduction, the results of these studies are neither consistent with experimental data nor with the proposed mechanisms for firefly dioxetanone.[21,24] It may occur to the reader the mechanisms proposed by us for firefly dioxetanone, in addition to our mechanisms for dimethyl-1,2-dioxetanone and simple 1,2-dioxetanone, contain errors and that the studies performed by Liu et al. and Mazziotti and Greenman are the ones that are correct. However, it should be noted that Liu et al. used the same multi-configurational methods to study the chemiluminescence mechanism of anionic thiazole-substituted dioxetanone, which is a model for firefly dioxetanone.[36] Thus, this molecule should present a more efficient mechanism than simple 1,2-dioxetanone. However, the calculations performed by this research group indicated that singlet chemiexcitation could only occur by NAC between S_0 and S_1 (at the transition structure, these two states are separated by $\approx$5 kcal mol^{-1}). This is a much less efficient mechanism than that proposed by the same group, with the same methods, for 1,2-dioxetanone when it should, in fact, be the opposite.[28,36] Therefore, the studies on chemiluminescence performed by Liu et al. even present inconsistencies when we compare calculations performed by them in different molecules and in different papers.

In conclusion, we think all the facts and statements presented herein demonstrate that we have provided accurate and consistent qualitative chemiluminescence mechanisms for dimethyl-1,2-dioxetanone and simple 1,2-dioxetanone.[26] Moreover, the differences between our results and those of Liu et al. and Mazziotti and Greenman should not devalue our studies because the calculations performed by those authors were not in agreement with experimental data and with the computational results obtained by them and other researchers.

2.4. Proposal of the Interstate Crossing-Induced Chemiexcitation Mechanism

Koo and Schuster have proposed chemically induced electron-exchange luminescence (CIEEL) to explain the efficient generation of singlet excited states by some organic peroxides.[37,38] In this mechanism there is electron transfer from an electron-rich moiety to the peroxide with the formation of a radical ion pair. The radical ion pair can either diffuse to free radical ions, or suffer C–C bond cleavage followed by back electron transfer from the newly formed carbonyl radical anion to the radical cation (Scheme 2). This hypothesis leads to the formation of singlet excited states with high efficiency due to charge annihilation. If the electron-rich moiety is part of the organic peroxide, the mechanism is termed intramolecular CIEEL. If the elec-

CHEMPHYSCHEM
ARTICLES
www.chemphyschem.org

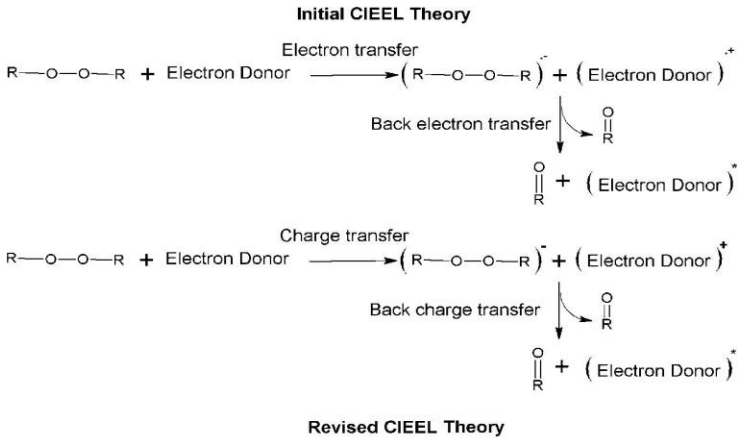

Scheme 2. Schematic representation of the initial and revised CIEEL theories.

tron-rich moiety is part of a molecule present in solution, that is, not the organic peroxide, then this mechanism is called intermolecular CIEEL. Examples of molecules that can undergo intramolecular CIEEL can be found in references [39] and [40], while diphenoyl peroxides and dimethyldioxetanone were presented as prime examples of intermolecular CIEEL.[41–44]

However, the re-examination of the chemiluminescence of diphenoyl peroxide and dimethyldioxetanone, and the study of polyacenes endoperoxides and two more complex 1,2-dioxetanones, revealed that these molecules presented rather low chemiluminescence quantum yields for intermolecular CIEEL decay.[44,45] Therefore, the basis on which this theory was elaborated was demonstrated to be incorrect in the case of intermolecular CIEEL. In conclusion, the available experimental data indicates that intermolecular CIEEL is a baseless theory because the presence of a catalytic activator on the chemiluminescence reactions of a variety of prime examples of this mechanism only resulted in inefficient chemiluminescence, contrary to what intermolecular CIEEL stated. Thus, until today, only one system (the peroxyoxalate reaction system) based on intermolecular CIEEL presented high singlet chemiexcitation efficiencies.[45]

Thus, different authors have proposed revised CIEEL mechanisms (Scheme 2) to explain some efficient CIEEL reactions (the majority of which are intramolecular CIEEL reactions), in which neither full electron transfer nor the formation of a radical ion pair are involved.[24,25,44,46,47] In these revised mechanisms, the presence of electron-donating substituents is responsible for charge-transfer development during the chemical reaction, leading to the formation of a charge-transfer transition state. The excited singlet state is then formed directly at an efficient rate. These revised mechanisms are similar to the initial CIEEL, but they are based more on subtle charge and back charge transfers than full electron transfer. Nevertheless, these theories are all based on the assumption that efficient singlet excitation is dependent on these charge transfers, possible only due to the presence of an electron-donating substituent, while inefficient singlet excitation occurs due to the absence of these charge transfers.

In our opinion, the present results (along with previous ones) indicate that these charge-transfer-based mechanisms are not able to explain the chemiluminescence of organic peroxides. Firstly, as seen above, despite being presented to explain efficient generation of singlet excited states, CIEEL failed to explain this phenomenon entirely and gave birth to revised theories. Secondly, and contrary to expectations, our results indicate that charge-transfer development can be seen in the decomposition of dimethyl-1,2-dioxetanone, despite this reaction being involved in the inefficient generation of triplet excited states. Moreover, dimethyl-1,2-dioxetanone does not have an electron-rich substituent. Our results indicate that charge transfer develops during the course of the reaction because both charge and back charge transfers can be seen between the acetone and carbon dioxide moieties, leading to a charge-transfer transition state. In the vicinities of this transition state, S_0 is almost degenerate with T_0 and T_1, which can explain the inefficient formation of excited triplet molecules, as already discussed. This is a very similar mechanism to those proposed in the revised CIEEL theories.[24,25,44,46,47] In our opinion, this is evidence which indicates that these revised CIEEL mechanisms also fail to explain efficient singlet chemiexcitation because a supposedly key reason for this efficiency (charge-transfer development) can also be seen in inefficient chemiluminescence reactions where triplet states are the predominant excited-state products. The presence/absence of an electron-donating substituent could justify the inefficiency/efficiency of singlet excitation. However, as already discussed, the presence of electron-donating group as catalytic activators in intermolecular CIEEL reactions do not enable the efficient production of singlet excited states.[44,47] Moreover, there are also intramolecular CIEEL reactions in which electron-rich moieties are present that have low singlet chemiexcitation efficiency and high triplet-to-singlet ratios.[4] Therefore, it appears that the presence/absence of an electron-donating group cannot by itself explain the efficiency/inefficiency of chemiluminescence reactions. Taking all this evidence into consideration, we think that a new theory is needed that can take into account the evident complexity of the chemiluminescence of various 1,2-dioxetanone substrates.

Diverse computational studies (regarding the unimolecular decomposition of dioxetane/dioxetanone molecules) have demonstrated that, in the vicinity of the transition state, S_0 is generally degenerate/near degenerate with T_1, even in cases in which experience indicates the efficient production of singlet excited states.[24–26,28,37–49] Therefore, we think that charge trans-

fer is necessary for the reaction to reach the region of transition state, in which direct population of T_1 is achieved by ISC. We think that this population of T_1 is of crucial importance in the chemiluminescence of dioxetanones. It was demonstrated for different 1,2-dioxetanones that $T_1 \rightarrow S_1$ ISC generally occurs.[24–26] In addition to this ISC, direct $S_0 \rightarrow S_1$ crossing was also found for cases in which singlet excited states were expected to be formed with high efficiency.[21,24,25]

Thus, we now propose the interstate crossing-induced chemiexcitation (ICIC) mechanism for the chemiluminescence of different dioxetanones (Figure 4). The computed and literature-derived data presented herein leads us to believe that inter- and intramolecular charge transfer is needed to reach a ground transition state of the decomposition reaction. In the vicinity of the transition state, $S_0 \rightarrow T_1$ ISC is common (as demonstrated by the computational works presented so far), thereby directly generating excited-state products.[24–26,28,37–49] The rate of this ISC would then be modulated by structural modifications of the chemiluminescence substrate. This is already seen for the unimolecular decomposition of 1,2-dioxetanes, in which the degree of methylation has a direct influence on chemiexcitation efficiencies.[27] The $T_1 \rightarrow S_1$ ISC can then populate S_1, depending on the rate of this ISC. This type of crossing is also commonly seen in computational studies of dioxetanes and dioxetanones.[24–26,28,37–49] Some structural modifications may even allow direct $S_0 \rightarrow S_1$ crossing, as already stated.[21,24,25]

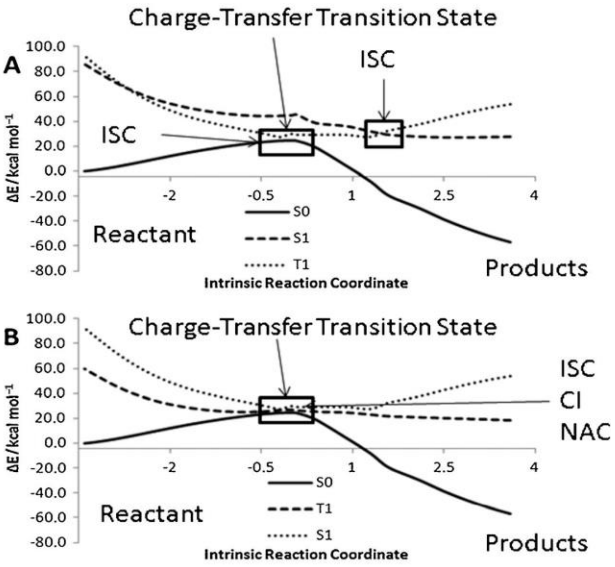

Figure 4. Representation of the ICIC mechanism for dioxetanones. A) ICIC mechanism for chemiluminescence reactions in which triplet excited-state products are favoured: There is the formation of an S_0 charge-transfer transition state, in the vicinity of which ISC with T_1 is possible. S_1 chemiexcitation is only possible by ISC with T_1 in a more advanced zone of the IRC path. The efficiency of chemiluminescence is modulated by the ISC rates. B) ICIC mechanism for chemiluminescence reactions in which singlet excited-state products are favoured: S_1 chemiexcitation is not only dependent on ISC with T_1, but there is also the possibility of NAC and CI with S_0. S_0 molecules can still cross to T_1 due to ISC. The efficiency of chemiluminescence is modulated by the ISC, CI and NAC rates. Structural modifications of the chemiluminescence substrates are expected to modulate the rate and the presence/absence of these ISCs, CIs and NACs.

We feel that this proposed mechanism is in line with known experimental and theoretical data. The role of charge transfer is rationalised, which is in agreement with the fact that charge transfer is seen for both effective and ineffective chemiluminescence processes.[40,47] The importance ascribed by us to singlet–triplet ISCs is also in accordance with both experimental and computational claims that ISC may be possible for different peroxides.[25,26,31,43,44] Our claim that some structural modifications allow for direct $S_0 \rightarrow S_1$ crossing, while in other chemiluminescence substrates S_1 is only populated due to $T_1 \rightarrow S_1$ crossing, is expected to explain the difference in the spin of the predominant products verified in various chemiluminescence reactions.[3,4,21,23,26–28,31,44] Finally, our claim that structural modifications affect the ISC rate is expected to explain the increase in the triplet and singlet excited yield, which was verified for dioxetanes with increasing degrees of methylation.[27]

Evidently, more experimental and computational work is needed to further define this new mechanism. However, we believe that herein we have provided sufficient information to demonstrate that a new chemiexcitation theory is needed and that the ICIC mechanism has the potential to be the one to explain the complex chemiluminescence of 1,2-dioxetanones.

3. Conclusions

The mechanism of decomposition of dimethyl-1,2-dioxetanone was studied with a TD-DFT/DFT approach in dichloromethane. Both the singlet and triplet ground and excited states (S_0, S_1, T_0 and T_1) were included in the calculations.

The triplet chemiexcitation yield may be explained by $S_0 \rightarrow T_1$ and $T_0 \rightarrow T_1$ crossing, whereas the singlet excited-state yield can only be explained by crossing with T_1. The low triplet excited-state yield can be explained by crossing between T_0 and T_1. The activation barrier was well reproduced, as well as the energy difference between the S_0 transition state and the point of the reaction in which S_1 is populated. Charge-transfer processes appear to be very important for the ground-state decomposition of dimethyl-1,2-dioxetanone. Three different phases of charge transfer were found.

Our results and literature data inspired us to propose the ICIC mechanism to rationalise the chemiexcitation mechanism of dioxetanones and to explain the difference found in the triplet/singlet ratio of various chemiluminescence products. Different computational studies have demonstrated that, despite different spins of the predominant chemiluminescence products, in the decomposition of these molecules there is always S_0/T_1 and T_1/S_1 ISC. Therefore, there must be some features in the different chemiluminescence mechanisms that determine the spin of the resulting excited-state products. We think that different structural modifications of various chemiluminescence substrates affect the S_0/T_1 and T_1/S_1 ISC rates, thereby modulating the spin of the resulting chemiluminophores. Charge-transfer processes cannot explain the efficiency

CHEMPHYSCHEM
ARTICLES
www.chemphyschem.org

of chemiluminescence and the spin of the predominant excited-state products. However, these processes appear to be required to reach the S_0 transition state, in the vicinity of which direct population of excited states is possible.

Future studies in this topic should include performing dynamics to better understand the interstate crossings efficiencies. Additionally, computational studies of these simple dioxetanones coupled with electron-donating or -withdrawing groups should be performed to see the effect of these groups on the charge-transfer processes and interstate crossings.

Computational Details

Ground-state geometry optimisations and frequency calculations were performed at the mPWKCIS/aug-cc-pVDZ level of theory.[50,51] An IRC calculation, at the mPWKCIS/aug-cc-pVDZ level of theory, was conducted to connect the S_0 transition state to the reactants and products.[52] Both IRC and geometry optimisations were performed in vacuo. It should be noted that the IRC calculation was performed by calculating the force constant in all SCF cycles. The downward IRC calculation toward the products was interrupted when the two molecules were clearly separated. This procedure was adopted from reference [26].

The energies of the ground-state IRC-obtained structures were re-evaluated by single-point calculations with O3LYP and the aug-cc-pVDZ basis set, with implicit solvent.[53–56] To obtain the energy levels of T_1 and S_1, we performed time-dependent (TD) O3LYP/aug-cc-pVDZ.[56] The energies of T_0 were calculated by O3LYP/aug-cc-pVDZ single-point calculations. This procedure was adopted from reference [26]. We chose the mPWKCIS functional for the geometry optimisations because we think that it provided good results in our study of simple 1,2-dioxetanone, and O3LYP for the other calculations because it provided results in good agreement with experimental data. Using one computational method for the geometry optimisations and another for single-point calculations is a standard procedure in computational studies of chemiluminescence.[21,24–26,28–30,57–59] Moreover, these two functionals present very low Hartree–Fock (HF) exchange (0.0% for mPWKCIS and 11.6% for O3LYP), which is in line with the paper by Liu et al.[57] DFT methods with large HF exchange are not good choices for the study of the decomposition of 1,2-dioxetanones.[57] Open-shell states were treated by using U DFT, while closed-shell states were treated with R DFT.[25,26,55] The Stable=opt keyword was used for all ground-state single-point calculations. When these calculations were at the R DFT level of theory, the reoptimisation of the wavefunction was real, spin-restricted. These newly optimised wavefunctions were used as initial guesses for TD-DFT calculations. No particular S_0 energetic difference between the intrinsic reaction coordinates, as calculated by both U and R DFT, was seen. Comparison between the full energy profile of the S_0 IRC path determined for dimethyl-1,2-dioxetanone, at both U and R DFT levels of theory, can be found in Figure S1 in the Supporting Information. Moreover, as seen in Figure S1 in the Supporting Information, both restricted and unrestricted S_1 energies are very similar. Given the similarity between the U/R $S_{0/1}$ results, only the R $S_{0/1}$ results were presented herein, to better compare with the results that obtained previously for simple 1,2-dioxetanone.[26]

Dichloromethane was included in the calculations by using the conductor-like polarised continuum model (CPCM).[60] All calculations were performed with the Gaussian 03 program package.[61]

Acknowledgements

Financial support from the Fundação para a Ciência e a Tecnologia (FCT, Lisbon), the Programa Operacional Temático Factores de Competitividade (COMPETE) and the Fundo Comunitário Europeu (FEDER) (project PTDC/QUI/71366/2006) is acknowledged. A Ph.D. grant to L.P.d.S. (SFRH/BD/76612/2011), also given by FCT, is also acknowledged.

Keywords: charge transfer · density functional theory · dioxetanones · interstate crossing-induced chemiexcitation · luminescence

[1] S. M. Marques, J. C. G. Esteves da Silva, *IUBMB Life* **2009**, *61*, 6–17.
[2] L. Pinto da Silva, J. C. G. Esteves da Silva, *J. Chem. Theory Comput.* **2011**, *7*, 809–817.
[3] L. Pinto da Silva, J. C. G. Esteves da Silva, *ChemPhysChem* **2012**, *13*, 2257–2262.
[4] M. Matsumoto, *J. Photochem. Photobiol. C* **2004**, *5*, 27–53.
[5] L. Pinto da Silva, J. C. G. Esteves da Silva, *J. Comput. Chem.* **2011**, *32*, 2654–2663.
[6] L. Pinto da Silva, J. C. G. Esteves da Silva, *ChemPhysChem* **2011**, *12*, 3002–3008.
[7] L. Pinto da Silva, J. C. G. Esteves da Silva, *J. Phys. Chem. B* **2012**, *116*, 2008–2013.
[8] L. Pinto da Silva, J. C. G. Esteves da Silva, *ChemPhysChem* **2011**, *12*, 951–960.
[9] J. Vieira, L. Pinto da Silva, J. C. G. Esteves da Silva, *J. Photochem. Photobiol. B* **2012**, *117*, 33–39.
[10] S. Hosseinkhani, *Cell. Mol. Life Sci.* **2011**, *68*, 1167–1182.
[11] S. Inouye, *Cell. Mol. Life Sci.* **2010**, *67*, 387–404.
[12] B. R. Branchini, T. L. Southworth, M. H. Murtiashaw, R. A. Magyar, S. A. Gonzalez, M. C. Ruggiero, J. G. Stroh, *Biochemistry* **2004**, *43*, 7255–7262.
[13] S. M. Marques, J. C. G. Esteves da Silva, *Anal. Bioanal. Chem.* **2008**, *391*, 2161–2168.
[14] S. M. Marques, F. Peralta, J. C. G. Esteves da Silva, *Talanta* **2009**, *77*, 1497–1503.
[15] B. R. Branchini, J. C. Rosenberg, D. M. Ablamsky, K. P. Taylor, T. L. Southworth, S. J. Linder, *Anal. Biochem.* **2011**, *414*, 239.
[16] A. Roda, M. Guardigli, *Anal. Bioanal. Chem.* **2012**, *402*, 69–76.
[17] L. Mezzanotte, I. Que, E. Kaijzel, B. Branchini, A. Roda, C. Löwik, *PloS One* **2011**, *6*, e19277.
[18] A. Roda, L. Mezzanotte, R. Aldini, E. Michelini, L. Cevenini, *Neurogastroenterol. Motil.* **2010**, *22*, 1117.
[19] A. N. Kudryavtsev, V. V. Krasitskaya, A. I. Petunin, A. Y. Burakov, L. A. Frank, *Anal. Chem.* **2012**, *84*, 3119–3124.
[20] J. T. Au, L. Gonzalez, C. H. Chen, I. Serganova, Y. Fong, *Ann. Surg. Oncol.* **2012**, *19*, 3116–3122.
[21] L. W. Chung, S. Hayashi, M. Lundberg, T. Nakatsu, H. Kato, K. Morokuma, *J. Am. Chem. Soc.* **2008**, *130*, 12880–12881.
[22] S. P. Schmidt, G. B. Schuster, *J. Am. Chem. Soc.* **1978**, *100*, 5559–5561.
[23] E. H. White, M. G. Steinmetz, J. D. Miano, P. D. Wildes, R. Morland, *J. Am. Chem. Soc.* **1980**, *102*, 3199–3208.
[24] L. Yue, Y. J. Liu, W. H. Fang, *J. Am. Chem. Soc.* **2012**, *134*, 11632–11369.
[25] H. Isobe, Y. Tanaka, M. Okumura, S. Kuramitsu, K. Yamaguchi, *J. Am. Chem. Soc.* **2005**, *127*, 8667–8679.
[26] L. Pinto da Silva, J. C. G. Esteves da Silva, *J. Comput. Chem.* **2012**, *33*, 2118–2123.
[27] W. Adam, W. J. Baader, *J. Am. Chem. Soc.* **1985**, *107*, 410–416.
[28] F. Liu, Y. J. Liu, L. De Vico, R. Lindh, *J. Am. Chem. Soc.* **2009**, *131*, 6181–6188.
[29] L. Greenman, D. A. Mazziotti, *J. Chem. Phys.* **2010**, *133*, 164110–164118.
[30] L. Greenman, D. A. Mazziotti, *J. Chem. Phys.* **2011**, *134*, 174110–174118.
[31] L. Pinto da Silva, J. C. G. Esteves da Silva, *J. Comput. Chem.* **2012**, *33*, 2127–2130.
[32] N. J. Turro, M. F. Chow, *J. Am. Chem. Soc.* **1980**, *102*, 5058–5064.
[33] W. Adam, O. Cueto, *J. Am. Chem. Soc.* **1979**, *101*, 6511–6515.

[34] N. W. Moriarty, R. Lindh, G. Karlstrom, *Chem. Phys. Lett.* **1998**, *289*, 442 – 450.
[35] S. de Feyter, E. W. G. Diau, A. A. Scala, A. H. Zewail, *Chem. Phys. Lett.* **1999**, *303*, 249 – 260.
[36] F. Liu, Y. Liu, L. De Vico, R. Lindh, *Chem. Phys. Lett.* **2009**, *484*, 69 – 75.
[37] J. Y. Koo, G. B. Schuster, *J. Am. Chem. Soc.* **1977**, *99*, 6107 – 6109.
[38] J. Y. Koo, G. B. Schuster, *J. Am. Chem. Soc.* **1978**, *100*, 4496 – 4503.
[39] A. L. P. Nery, D. Weiß, L. H. Catalani, W. J. Baader, *Tetrahedron* **2000**, *56*, 5317 – 5327.
[40] L. F. M. L. Ciscato, F. H. Bartoloni, D. Weiss, R. Beckert, W. J. Baader, *J. Org. Chem.* **2010**, *75*, 6574 – 6580.
[41] J. Y. Koo, G. B. Schuster, *J. Am. Chem. Soc.* **1977**, *99*, 5403 – 5408.
[42] S. P. Schmidt, G. B. Schuster, *J. Am. Chem. Soc.* **1980**, *102*, 306 – 314.
[43] B. G. Dixon, G. B. Schuster, *J. Am. Chem. Soc.* **1981**, *103*, 3068 – 3077.
[44] L. H. Catalani, T. Wilson, *J. Am. Chem. Soc.* **1989**, *111*, 2633 – 2639.
[45] M. A. de Oliveira, F. H. Bartoloni, F. A. Augusto, L. F. M. L. Ciscato, E. L. Bastos, W. J. Baader, *J. Org. Chem.* **2012**, *77*, 10537 – 10544.
[46] T. Wilson, *Photochem. Photobiol.* **1995**, *62*, 601 – 606.
[47] F. McCapra, *J. Photochem. Photobiol. A* **1990**, *51*, 21 – 28.
[48] N. J. Turro, P. Lechtken, *J. Am. Chem. Soc.* **1973**, *95*, 264 – 266.
[49] S. Wilsey, F. Bernardi, M. Olivucci, M. A. Robb, S. Murphy, W. Adam, *J. Phys. Chem. A* **1999**, *103*, 1669 – 1677.
[50] J. B. Krieger, J. Q. Chen, G. J. Iafrate, A. Savin, *Electron Correl. Mater. Prop.* **1999**, 463 – 477.
[51] C. Adamo, V. Barone, *J. Chem. Phys.* **1998**, *108*, 664 – 675.
[52] C. Gonzalez, H. B. Schlegel, *J. Phys. Chem.* **1990**, *94*, 5523 – 5527.
[53] C. T. Lee, W. T. Yang, R. G. Parr, *Phys. Rev. B* **1988**, *37*, 785 – 789.
[54] N. C. Handy, A. J. Cohen, *Mol. Phys.* **2001**, *99*, 403 – 412.
[55] W. M. Hoe, A. J. Cohen, N. C. Handy, *Chem. Phys. Lett.* **2001**, *341*, 319 – 328.
[56] E. K. U. Gross, W. Kohn, *Adv. Quantum Chem.* **1990**, *21*, 255 – 291.
[57] L. Yue, E. Roca-Sanjuán, R. Lindh, N. Ferré, Y. J Liu, *J. Chem. Theory Comput.* **2012**, *8*, 4359 – 4363.
[58] C. Tanaka, J. Tanaka, *J. Phys. Chem. A* **2000**, *104*, 2078 – 2090.
[59] L. De Vico, Y. J. Liu, J. W. Krogh, R. Lindh, *J. Phys. Chem. A* **2007**, *111*, 8013 – 8019.
[60] V. Barone, M. Cossi, *J. Phys. Chem. A* **1998**, *102*, 1995 – 2001.
[61] Gaussian 03 (Revision C.02), M. J. Frisch, G. W. Trucks, H. B. Schlegel, G. E. Scuseria, M. A. Robb, J. R. Cheeseman, J. A. Montgomery, Jr., T. Vreven, K. N. Kudin, J. C. Burant, J. M. Millam, S. S. Iyengar, J. Tomasi, V. Barone, B. Mennucci, M. Cossi, G. Scalmani, N. Rega, G. A. Petersson, H. Nakatsuji, M. Hada, M. Ehara, K. Toyota, R. Fukuda, J. Hasegawa, M. Ishida, T. Nakajima, Y. Honda, O. Kitao, H. Nakai, M. Klene, X. Li, J. E. Knox, H. P. Hratchian, J. B. Cross, C. Adamo, J. Jaramillo, R. Gomperts, R. E. Stratmann, O. Yazyev, A. J. Austin, R. Cammi, C. Pomelli, J. W. Ochterski, P. Y. Ayala, K. Morokuma, G. A. Voth, P. Salvador, J. J. Dannenberg, V. G. Zakrzewski, S. Dapprich, A. D. Daniels, M. C. Strain, O. Farkas, D. K. Malick, A. D. Rabuck, K. Raghavachari, J. B. Foresman, J. V. Ortiz, Q. Cui, A. G. Baboul, S. Clifford, J. Cioslowski, B. B. Stefanov, G. Liu, A. Liashenko, P. Piskorz, I. Komaromi, R. L. Martin, D. J. Fox, T. Keith, M. A. Al-Laham, C. Y. Peng, A. Nanayakkara, M. Challacombe, P. M. W. Gill, B. Johnson, W. Chen, M. W. Wong, C. Gonzalez, J. A. Pople, Gaussian, Inc., Wallingford, CT, **2004**.

Received: October 19, 2012
Revised: December 13, 2012
Published online on February 5, 2013

4.3. Characterization of the Decomposition Reaction of Dioxetanedione

Article 13

Mechanistic study of the unimolecular decomposition of 1,2-dioxetanedione
Luís Pinto da Silva and Joaquim C.G. Esteves da Silva
J. Phys. Org. Chem. **2013**, *26*, 659-663.

The theoretical calculations and the writing of the paper were performed by Luís Pinto da Silva, under supervision of Professor Esteves da Silva.

Research Article

Journal of Physical Organic Chemistry

Received: 5 February 2013, Revised: 2 April 2013, Accepted: 17 May 2013, Published online in Wiley Online Library: 23 June 2013

(wileyonlinelibrary.com) DOI: 10.1002/poc.3149

Mechanistic study of the unimolecular decomposition of 1,2-dioxetanedione

Luís Pinto da Silva[a] and Joaquim C. G. Esteves da Silva[a]*

The unimolecular decomposition of 1,2-dioxetanedione, the high-energy intermediate of the chemiluminescence peroxyoxalate reaction, was studied by theoretical means for the first time. Our calculations have provided results in line with the experimental data regarding this compound. 1,2-Dioxetanedione decomposes due to a step-wise biradical mechanism. In the biradical region of the decomposition path, there is a path for singlet chemiexcitation. Interactions between the singlet ground and excited states with triplet states can explain the weak unimolecular chemiluminescence of 1,2-dioxetanedione. Copyright © 2013 John Wiley & Sons, Ltd.
Supporting information may be found in the online version of this paper.

Keywords: 1,2-dioxetanedione; chemiluminescence; CIEEL; ICIC; interstate crossing; peroxyoxalate system; step-wise biradical; unimolecular decomposition

INTRODUCTION

Firefly bioluminescence is the emission of light, in the fireflies, due to a luciferase catalyzed reaction.[1–5] This reaction is composed of two different steps: the first is an adenylation step, in which firefly luciferin is converted into luciferyl-adenylate due to the reaction with adenosine-5′-triphosphate; the second step is an oxidation, in which luciferyl-adenylate is converted into excited state oxyluciferin by reaction with molecular oxygen.[6–8] This system has been gaining numerous practical applications in the pharmaceutical, biomedical and bioanalytical areas, among others, due to very interesting characteristics.[9,10]

Excited state oxyluciferin is thought to be formed due to the formation and subsequent decomposition of firefly dioxetanone (Fig. 1).[6] Schuster and co-workers have proposed a chemically initiated electron exchange luminescence (CIEEL) mechanism, first to explain the efficient chemiluminescence of diphenoyl peroxide and dimethyl-1,2-dioxetanone (activated by perylene), and latter to explain the efficient firefly bioluminescence.[11–16] The initiating step of this mechanism is an electron transfer from an easily oxidizable electron-rich moiety to an acceptor energy-rich moiety (denominated as the high-energy intermediate, HEI). Due to this transfer, the electron acceptor decomposes via bond cleavage to form a radical ion pair with the electron donor. The radical ion pair can then transfer an electron backwards in order to generate excited state products. If the electron-rich moiety is part of the molecule on which the HEI is found, we use the term intramolecular CIEEL (the case of firefly bioluminescence), but if the electron-rich moiety (now called the activator, ACT) is not part of the same molecule as the HEI, the term intermolecular is used (the case of diphenoyl peroxide and dimethyl-1,2-dioxetanone, where the ACT was perylene).[6,11–17]

However, revaluation of the intermolecular CIEEL-based chemiluminescence of diphenoyl peroxide and dimethyl-1,2-dioxetanone revealed that the efficiency of this process is much lower than expected.[18,19] The analysis of an ACT-activated chemiluminescence of two novel 1,2-dioxetanones also revealed an inefficient intermolecular CIEEL-based chemiluminescence efficiency.[19] Thus, this findings indicates that CIEEL mechanism must be reassessed, as the study of model compounds of this theory presented inefficient chemiluminescence contrary to the postulated by Schuster and co-workers. In this case, it is fair to say that the application of the CIEEL theory to the explanation of the efficient firefly bioluminescence should be questioned.

The only known intermolecular CIEEL-based efficient chemiluminescence is that of the peroxyoxalate reaction (Fig. 2).[20] In this reaction, it is thought that 1,2-dioxetanedione is formed as the HEI. Subsequently, this molecule forms a supramolecular charge transfer complex with an ACT. Electron and back electron transfers between the ACT and the HEI will provoke a bond cleavage step and chemiexcite the ACT to a singlet excited state, which then decays to the ground state with emission of light.[20–23] 1,2-Dioxetanedione was also found to emit weak chemiluminescence, in a unimolecular decomposition reaction in the absence of an ACT.[20,23]

Given this, it appears to be very important to study the ACT-catalyzed chemiluminescence of 1,2-dioxetanedione, in order to fully understand the features of a efficient intermolecular CIEEL-based chemiluminescence. Besides giving insights of an efficient chemiluminescence reaction, this type of study can also give some information regarding the application of the CIEEL theory to the efficient firefly bioluminescence.

However, as 1,2-dioxetanedione presents an intrinsic and non-catalyzed chemiluminescence, it is of most importance to characterize the unimolecular decomposition of this HEI, in order to better understand its ACT-catalyzed chemiluminescence. Thus, the objective of this study is the characterization

* *Correspondence to: J. C. G. Esteves da Silva, Centro de Investigação em Química, Departamento de Química e Bioquímica, Faculdade de Ciências da Universidade do Porto, R. Campo Alegre 687, 4169-007 Porto, Portugal. E-mail: jcsilva@fc.up.pt*

a *L. Pinto da Silva, J. C. G. Esteves da Silva*
Centro de Investigação em Química, Departamento de Química e Bioquímica, Faculdade de Ciências da Universidade do Porto, R. Campo Alegre 687, 4169-007 Porto, Portugal

Journal of Physical Organic Chemistry

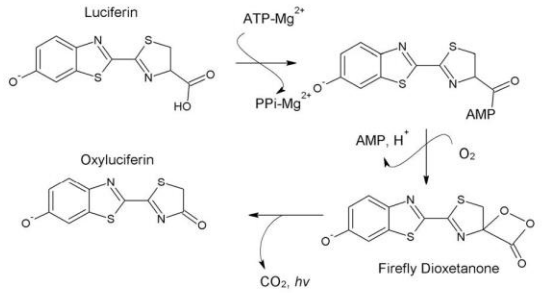

Figure 1. Schematic representation of firefly bioluminescence reaction

of the unimolecular decomposition of 1,2-dioxetanedione, by using a computational approach. To our knowledge, this is the first direct characterization at the atomistic level of this important reaction.

COMPUTATIONAL METHODS

Ground-state geometry optimizations, frequency and single point calculations were performed at the UCAM-B3LYP/6-31G(d,p) level of theory with the guess = mix keyword.[24] Intrinsic reaction coordinates (IRC) calculations, at the CAM-B3LYP/6-31G(d,p) level of theory, were made in order to connect the ground-state transition state to the reactants and products.[25] Both the geometry, IRC and single point calculations were performed *in vacuo*. The forward path (transition state to the products) was obtained with an IRC calculation (at the unrestricted (U) CAM-B3LYP/6-31G(d,p) with the guess = mix keyword). The reverse path (transition state to the reactant) could not be obtained with the guess = mix keyword, and was only obtained at the UCAM-B3LYP/6-31G(d,p) level of theory. After the IRC calculations, the stability of the wavefunction of the singlet ground-state (S_0) IRC path was optimized, by using the stable = opt and guess = mix keywords, at the UCAM-B3LYP/6-31G(d,p) level of theory. The reactant was considered to be a closed shell molecule, so the stability of its wavefunction was tested at the RCAM-B3LYP/6-31G(d,p) level of theory.

The S_0 structures obtained with the IRC calculations were used to calculate the energies of the S_1 and $T_{0/1}$ states. The energies of the S_1 and T_1 states were obtained at the time-dependent UCAM-B3LYP/6-31G(d,p) level of theory, while the energies of the T_0 state was obtained with UCAM-B3LYP/6-31G(d,p).[26] The wavefunction of the T_0 states was also optimized by using the stable = opt and guess = mix keywords, at the UCAM-B3LYP/6-31G(d,p) level of theory. These stability and single point calculations were also made *in vacuo*.

The use of the CAM-B3LYP density functional is recommended in order to obtain accurate estimates for possible charge transfer and

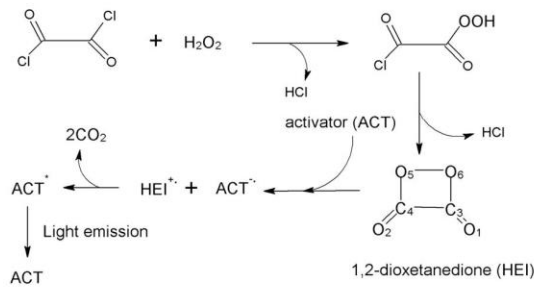

Figure 2. Elementary peroxyoxalate chemiluminescence reaction. O_2–C_4–O_5 corresponds to carbon dioxide moiety 1 (CO_2-1), while O_1–C_3–O_6 corresponds to carbon dioxide moiety 2 (CO_2-2)

Rydberg states.[27] Moreover, this functional was already used with success in other studies of chemiluminescence reactions.[28–30] The same functional and basis set were used in both geometry optimization, frequency, single point and IRC calculations in order for our results to not get contaminated by computational artifacts.[31]

All calculations were obtained with the Gaussian 09 program package.[32]

RESULTS AND DISCUSSION

Interactions between $S_0/S_1/T_0/T_1$

In Fig. 3.a is represented the S_0 reaction path for the decomposition of 1,2-dioxetanedione, along the $S_1/T_0/T_1$. In Fig. 3.b are presented these reaction paths, between the coordinates −1.1 and 0.8. The theoretical activation free energy ΔG_{theo} (with thermal corrections) is of 19.7 kcal/mol, which is in line with the experimental value of 18.2 ± 0.6 kcal/mol.[21]

Contrary to the case of simple 1,2-dioxetanone, there is a direct path for singlet chemiexcitation (which can account for the weak chemiluminescence of this molecule).[23,33,34] There is a point of the reaction in which the S_0 and S_1 states differ only by 4.6 kcal/mol. This value can possibly afford some non-adiabatic $S_0 \rightarrow S_1$ transitions.

It can also be seen for Fig. 3, that the S_0 and T_0 are basically degenerate in the biradical region of the reaction path. This near-degeneracy in a so large portion of the reaction path indicates the presence of an entropic trap.[6,35,36] This means that 1,2-dioxetanedione is forced to spend some time on this almost flat region of the reaction path, where S_0 is near-degenerate with T_0 which allows for some S_0/T_0 transitions. The

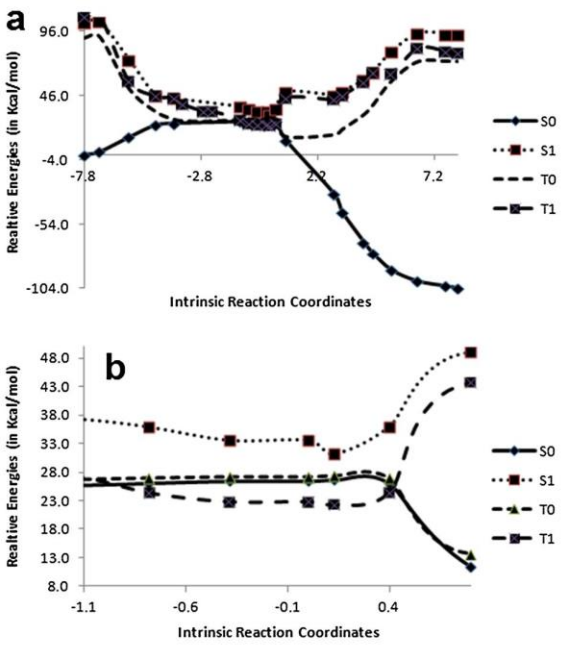

Figure 3. Stable energy profile of the IRC path determined for the unimolecular decomposition of 1,2-dioxetanedioxe, calculated at the TD-CAM-B3LYP/6-31G(d,p) and CAM-B3LYP/6-31G(d,p) level of theory (a). IRC reaction path between coordinates −1.1 and 0.8 (b), in which exist degeneracy/near-degeneracy between the states. The intrinsic reaction coordinates are in amu$^{-0.5}$Bohr

transition of some S_0 molecules to a non-chemiluminescence state may help to explain the weak non-catalyzed chemiluminescence of 1,2-dioxetanedione.

Another interesting feature of the unimolecular decomposition of 1,2-dioxetanedione is that the T_1 state is lower in energy than the T_0 and S_0 states (between reaction coordinates of −0.8 and 0.4). Moreover, between reaction coordinates of 2.9 and 4.5, T_1 is near-degenerate with S_1, similarly to what is seen for simple 1,2-dioxetanone.[33,34]

The interaction of T_1 with the other three states may be fundamental to explain the weak non-catalyzed chemiluminescence of the HEI of the peroxyoxalate reaction.[20] According to the Intersate Crossing-Induced Chemiexcitation (ICIC) mechanism, chemiexcitation is achieved by crossing between states near the transition state of the decomposition reaction.[37] More importantly, triplet chemiexcitation is caused by $S_0 \rightarrow T_1$ crossing, while singlet excitation is caused mainly by $T_1 \rightarrow S_1$ crossing. In some cases, singlet excitation can also occur due to direct $S_0 \rightarrow T_1$ crossing. The case of the weak non-catalyzed decomposition/chemiluminescence of 1,2-dioxetanedione fits in the ICIC mechanism, due to the interaction of T_1 with other states. The interaction between T_1 and S_0 suggests the possibility of $S_0 \rightarrow T_1$ intersystem crossing, leading to triplet chemiexcitation. T_1 is also near-degenerate with S_1 which suggest the possibility of $T_1 \rightarrow S_1$ intersystem crossing, thus leading to singlet chemiexcitation. Singlet chemiexcitation may also be explained by some non-adiabatic $S_0 \rightarrow S_1$ transitions. Adiabatic and non-adiabatic transitions between T_1 and T_0 may lead to non-radiative decay of the triplet excited state, which will lead to a decreased efficiency of the triplet and singlet chemiexcitations. The increase in energy of the excited states, after the transition state, can also control the efficiency of the chemiluminescence process.[17] The fact that the excited states increase in energy, in regard to singlet ground state, further supports the weak non-catalyzed chemiluminescence of 1,2-dioxetanedione.

Finally, Fig. 4 presents the Mulliken spin densities of the two carbon dioxide moieties during the 1,2-dioxetanedione decomposition. The deviation from zero after the coordinate of −5.9 corresponds to the O–O bond breaking and the distribution of each one of its two electrons by the two carbon dioxide moieties. This supports the formation of a biradical intermediate. Furthermore, the values of spin density tend to zero as the products are being formed (coordinate 2.1 onwards). It can also be seen that during the decomposition of 1,2-dioxetanedione, the spin densities of the two carbon dioxide moieties go from negative/positive to positive/negative values, and once again to negative/positive. Figure 4 also shows that these spin densities changes are mainly caused by O_5 and O_6. This indicates that the spin-orientation of the sole electrons present in each moiety is changing during the decomposition reaction. It is not clear if these changes affect the chemiexcitation mechanism, but it is possible that they do. If the spin-orientation of the sole electrons of the singlet biradical matches the spin-orientation of the electrons of the triplet states, it may favour a singlet to triplet intersystem crossing. On the contrary, if the spin-orientation doesn't match, it may impair a possible singlet to triplet intersystem crossing.

S_0 decomposition of 1,2-dioxetanedione

In Fig. 3.a is represented the S_0 reaction path for the decomposition of 1,2-dioxetanedione. In Fig. S1 are presented the bond

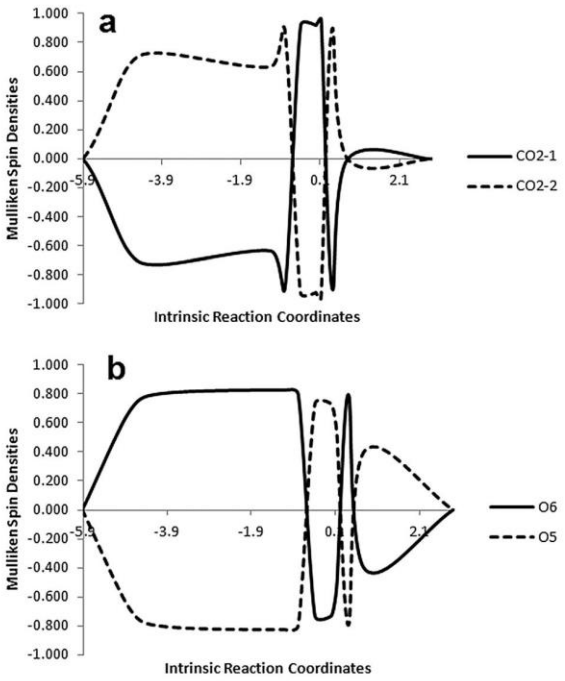

Figure 4. Mulliken spin densities variation during the IRC path

lengths variation, as a function of the reaction coordinates, of O_6–O_5, C_4–C_3, O_5–C_4, O_2–C_4, O_6–C_3 and O_1–C_3. In Fig. S2 are presented the angles variation, as a function of the reaction coordinates, of O_6–C_3–C_4, O_5–C_4–C_3, O_5–C_4–O_2 and O_6–C_2–C_1.

By analysis of Fig. S1, it can be seen that the unimolecular decomposition of 1,2-dioxetanedione occurs due to a stepwise mechanism. Until the transition state is reached, there is only O_5–O_6 bond elongation, which continues after this transition state. However, there is no C_4–C_3 bond elongation until the transition state is reached. The lengths of O_5–C_4 and O_6–C_3 bonds are the same during all the reaction. The same is seen for O_2–C_4 and O_1–C_3 bonds. However, before the transition state, the lengths of the O_5–C_4 and O_6–C_3 bonds are higher than the lengths of O_2–C_4 and O_1–C_3. After the transition state, the lengths of these four bonds are the same (Fig. S2). This is expected as the decomposition of 1,2-dioxetanedione results in the formation of two identical molecules: two carbon dioxide molecules. As the C–O bonds of carbon dioxide are expected to be identical, the length of the four C–O bonds of 1,2-dioxetanedione must be the same after decomposition in order to form two identical carbon dioxide molecules.

The analysis of the value of S^2 before spin annihilation (Fig. S3) reveals the existence of a biradical intermediate due to $S^2 \approx 1$ in a portion of the reaction coordinate.[31] The finding of a biradical intermediate is in line with experimental findings.[22]

Figure 5 demonstrates that O_6 and O_5 have the same atomic Mulliken charges, which is also seen for O_2 and O_1, and C_4 and C_3. Moreover, this figure indicates that there is some charge difference between $O_{6/5}$ and $O_{2/1}$ before the transition state, some charge transfer in the vicinities of the transition state, and finally these atoms possess the same atomic Mulliken charges after the transition state. There is no charge transfer between the two CO_2 moieties that form 1,2-dioxetanedione.

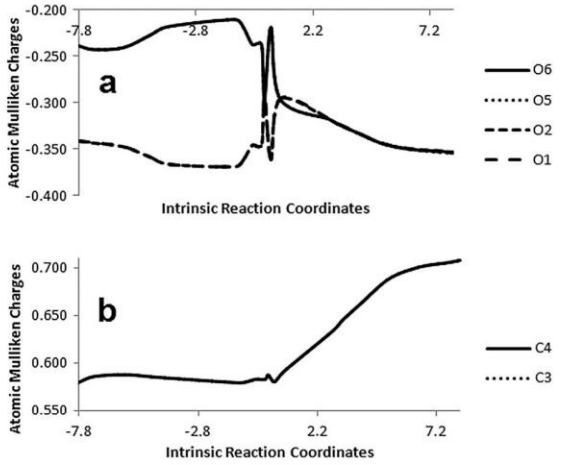

Figure 5. Atomic Mulliken charges variation during the IRC path. The $O_{5/6}$, $O_{1/2}$ and $C_{3/4}$ lines are superimposed

CONCLUSIONS

Nowadays, the only confirmed intermolecular CIEEL-based efficient chemiluminescence system is that of the peroxyoxalate reaction. Therefore, in order to understand the chemiluminescence of organic peroxides and the CIEEL mechanism, it is crucial that the scientific community study the peroxyoxalate system light emission. 1,2-dioxetanedione is thought to be the HEI of the peroxyoxalate reaction. Moreover, the unimolecular decomposition of this HEI leads to weak chemiluminescence. In order to better understand the chemiluminescence of the peroxyoxalate system, we have performed the first theoretical study of the unimolecular decomposition of 1,2-dioxetanedione.

Our calculations have revealed that the unimolecular decomposition reaction of 1,2-dioxetanedione occurs due to a step-wise biradical mechanism. We have found that the reaction is initiated by –O–O– bond breaking, until a transition state is reached in the potential energy surface of the singlet ground state. Each one of the two electrons that constitute this bond is distributed by the two carbon dioxide moieties of 1,2-dioxetanedione. After the transition state, the reaction proceeds toward the products without any more energy barriers due to –C–C– bond breaking.

Further calculations have revealed degeneracy/near-degeneracy between $S_{0/1}/T_{0/1}$ states, in the biradical region of the reaction path, in such a way that the weak chemiluminescence of this molecule could be rationalized. These calculations revealed a chemiexcitation mechanism in line with the ICIC theory. Triplet excitation is achieved by $S_0 \rightarrow T_1$ crossing, while singlet excitation is achieved by $T_1 \rightarrow S_1$ crossing and non-adiabatic $S_0 \rightarrow S_1$ transitions. Interaction between T_1/S_0 and T_0 may lead to population of a non-chemiluminescence state, thereby decreasing triplet and singlet chemiexcitation.

SUPPORTING INFORMATION

Cartesian coordinates of the reactant, transition state and final products of the IRC path calculated here. Bond lengths and angles, and S^2 values.

Acknowledgements

Financial support from Fundação para a Ciência e Tecnologia (FCT, Lisbon) (Programa Operacional Temático Factores de Competitividade (COMPETE) e comparticipado pelo Fundo Comunitário Europeu (FEDER) (Project PTDC/QUI/71366/2006)) is acknowledged. A Ph.D. Grant to L. Pinto da Silva, also by FCT, is also acknowledged.

REFERENCES

[1] J. Vieira, L. Pinto da Silva, J. C. G. Esteves da Silva, *J. Photochem. Photobiol. B* **2012**, *117*, 33.
[2] J. M. Leitão, J. C. G. Esteves da Silva, *J. Photochem. Photobiol. B* **2010**, *101*, 1.
[3] L. Pinto da Silva, J. C. G. Esteves da Silva, *J. Chem. Theory Comput.* **2011**, *7*, 809.
[4] S. Hosseinkhani, *Cell. Mol. Life Sci.* **2011**, *68*, 1167.
[5] J. Y. Hasegawa, K. J. Fujimoto, H. Nakatsuji, *Chemphyschem* **2011**, *12*, 3106.
[6] L. Pinto da Silva, J. C. G. Esteves da Silva, *Chem. Phys. Chem.* **2012**, *13*, 2257.
[7] S. M. Marques, J. C. G. Esteves da Silva, *IUBMB Life* **2009**, *61*, 6.
[8] V. R. Viviani, F. G. Arnoldi, A. J. Neto, T. L. Oehlmeyer, E. J. Bechara, Y. Ohmiya, *Photochem. Photobiol. Sci.* **2008**, *7*, 159.
[9] A. Roda, M. Guardigli, *Anal. Bioanal. Chem.* **2012**, *402*, 69.
[10] A. Roda, P. Pasini, M. Mirasoli, E. Michelini, M. Guardigli, *Trends Biotechnol.* **2004**, *22*, 295.
[11] G. B. Schuster, S. P. Schmidt, *Adv. Phys. Org. Chem.* **1982**, *18*, 187.
[12] S. P. Schmidt, G. B. Schuster, *J. Am. Chem. Soc.* **1980**, *102*, 306.
[13] J.-Y. Koo, G. B. Schuster, *J. Am. Chem. Soc.* **1978**, *100*, 4496.
[14] G. B. Schuster, *Acc. Chem. Res.* **1979**, *12*, 366.
[15] J.-Y. Koo, G. B. Schuster, *J. Am. Chem. Soc.* **1977**, *99*, 5403.
[16] J.-Y. Koo, S. P. Schmidt, G. B. Schuster, *Proc. Natl. Acad. Sci. U.S.A.* **1978**, *75*, 30.
[17] M. Matsumoto, *J. Photochem. Photobiol. C* **2004**, *5*, 27.
[18] L. H. Catalani, T. Wilson, *J. Am. Chem. Soc.* **1989**, *111*, 2633.
[19] M. Almeida de Oliveira, F. H. Bartoloni, F. A. Augusto, L. F. M. L. Ciscatto, E. L. Bastos, W. J. Baader, *J. Org. Chem.* **2012**, *77*, 10537.
[20] L. F. M. L. Ciscato, F. A. Augusto, D. Weiss, F. H. Bartoloni, S. Albrecht, H. Brandl, T. Zimmermann, W. J. Baader, *Arkivoc* **2012**, *iii*, 391.
[21] L. F. M. L. Ciscato, F. H. Bartoloni, E. L. Bastos, W. J. Baader, *J. Org. Chem.* **2009**, *74*, 8974.
[22] R. Bos, S. A. Tonkin, G. R. Hanson, C. M. Hindson, K. F. Lim, N. W. Barnett, *J. Am. Chem. Soc.* **2009**, *131*, 2770.
[23] B. Mann, M. L. Grayeski, *Anal. Chem.* **1990**, *62*, 1532.
[24] T. Yanai, D. Tew, N. Handy, *Chem. Phys. Lett.* **2004**, *393*, 51.
[25] H. P. Hratchian, H. B. Schlegel, *J. Chem. Theory Comput.* **2005**, *1*, 61.
[26] G. Scalmani, M. J. Frisch, B. Mennucci, J. Tomasi, R. Cammi, V. Barone, *J. Chem. Phys.* **2006**, *124*, 1.
[27] C. Adamo, D. Jacquemin, *Chem. Soc. Rev.* **2013**. DOI: 10.1039/C2CS35394F.
[28] L. Yue, Y. J. Liu, W. H. Fang, *J. Am. Chem. Soc.* **2012**, *134*, 11632.
[29] I. Navizet, D. Roca-Sanjuán, L. Yue, Y. J. Liu, N. Ferré, R. Lindh, *Photochem. Photobiol.* **2013**, *89*, 319.
[30] S. F. Chen, I. Navizet, D. Roca-Sanjuán, R. Lindh, Y. J. Liu, N. Ferré, *J. Chem. Theory Comput.* **2012**, *8*, 2796.
[31] L. Yue, D. Roca-Sanjuán, R. Lindh, N. Ferré, Y. J. Liu, *J. Chem. Theory Comput.* **2012**, *8*, 4359.
[32] M. J. Frisch, G. W. Trucks, H. B. Schlegel, G. E. Scuseria, M. A. Robb, J. R. Cheeseman, G. Scalmani, V. Barone, B. Mennucci, G. A. Petersson, H. Nakatsuji, M. Caricato, X. Li, H. P. Hratchian, A. F. Izmaylov, J. Bloino, G. Zheng, J. L. Sonnenberg, M. Hada, M. Ehara, K. Toyota, R. Fukuda, J. Hasegawa, M. Ishida, T. Nakajima, Y. Honda, O. Kitao, H. Nakai, T. Vreven, J. A. Montgomery, Jr., J. E. Peralta, F. Ogliaro, M. Bearpark, J. J. Heyd, E. Brothers, K. N. Kudin, V. N. Staroverov, R. Kobayashi, J. Normand, K. Raghavachari, A. Rendell, J. C. Burant, S. S. Iyengar, J. Tomasi, M. Cossi, N. Rega, J. M. Millam, M. Klene, J. E. Knox, J. B. Cross, V. Bakken, C. Adamo, J. Jaramillo, R. Gomperts, R. E. Stratmann, O. Yazyev, A. J. Austin, R. Cammi, C. Pomelli, J. W. Ochterski, R. L. Martin, K. Morokuma, V. G. Zakrzewski, G. A. Voth, P. Salvador, J. J. Dannenberg, S. Dapprich, A. D. Daniels, O. Farkas, J. B. Foresman, J. V. Ortiz, J. Cioslowski, D. J. Fox, *Gaussian 09, Revision A.02*, Gaussian, Inc.: Wallingford CT, **2009**.

[33] L. Pinto da Silva, J. C. G. Esteves da Silva, *J. Comput. Chem.* **2012**, *33*, 2118.
[34] L. Pinto da Silva, J. C. G. Esteves da Silva, *J. Comput. Chem.* **2012**, *33*, 2127.
[35] N. W. Moriarty, R. Lindh, G. Karlstrom, *Chem. Phys. Lett.* **1998**, *289*, 442.
[36] S. De Feyter, E. W. G. Diau, A. A. Scala, A. H. Zewail, *Chem. Phys. Lett.* **1999**, *303*, 249.
[37] L. Pinto da Silva, J. C. G. Esteves da Silva, *Chem. Phys. Chem* **2013**. DOI: 10.1002/cphc.201200872

4.4. Evaluation of the Possibility of the Presence of a Biradical Intermediate in Dioxetanone Decomposition

Article 14

Evidence of the absence of a biradical intermediate in the decomposition of 1,2-dioxetanones

Luís Pinto da Silva and Joaquim C.G. Esteves da Silva

Science Letters Journal **2012**, *1:29*.

The theoretical calculations and the writing of the paper were performed by Luís Pinto da Silva, under supervision of Professor Esteves da Silva.

ScienceJet

ScienceJet 2012, 1: 29

Evidence of the absence of a biradical intermediate in the decomposition of 1,2-dioxetanones

Luís Pinto da Silva, Joaquim C.G. Esteves da Silva*

Centro de Investigação em Química (CIQ-UP), Departamento de Química e Bioquímica, Faculdade de Ciências da Universidade do Porto, Campo Alegre 687, 4169-007 Porto, Portugal

**Author for correspondence: Joaquim C.G. Esteves da Silva, email: jcsilva@fc.up.pt*
Received 12 Sep 2012; Accepted 8 Oct 2012; Available Online 8 Oct 2012

Abstract

The peroxide bond breaking step of the decomposition reaction of dimethyl-1,2-dioxetanone was studied by using a density functional theory approach, in implicit dichloromethane. The calculations performed in this work revealed an interesting feature, the absence of a biradical intermediate, contrary to the expectations of some authors. However, this is in line with our previous study of the chemiluminescence of simple 1,2-dioxetanone and some experimental studies. The evidence for the absence of a biradical intermediate in the decomposition reaction of these molecules can also help to clarify the recent controversy regarding the chemiluminescence of simple 1,2-dioxetanone.

Keywords: Chemiluminescence; Bioluminescence; 1,2-dioxetanones; Biradical intermediate; Charge transfer; Dimethyl-1,2-dioxetanone

1. Introduction

Chemiluminescence is the emission of energy (in the form of visible light) with limited emission of heat, as the result of a chemical reaction [1,2]. When this reaction occurs within a living organism, due to a enzyme-catalyzed reaction, it is termed bioluminescence [3,4]. Both chemi- and bioluminescence have been attracting the attention of the research community, due to their successful application in the biomedical, pharmaceutical and bioanalytical areas [5-7].

The most important chemiluminescence and bioluminescence phenomena are that of the firefly: firefly dioxetanone decomposes in a highly exergonic reaction, and the light emitter oxyluciferin is formed in a singlet excited state with high efficiency (Figure 1) [1,8]. Oxyluciferin then decays to the ground state with the emission of visible light.

Firefly dioxetanone is of the family of simple 1,2-dioxetanone (Figure 2), one the most simple substrates of a chemiluminescence reaction [1,2]. It is thought that the compounds of this family of chemiluminescence substrates decompose by the same general mechanism: first, a transition state is reached by O-O bond breaking; after this transition state, the reaction proceeds toward the products by C-C bond breaking. Despite this similarity, while the decomposition of firefly dioxetanone originates the efficient production of singlet excited state products, the decomposition of more simple dioxetanones (as 1,2-dioxetanone and dimethyl-1,2-dioxetanone, Figure 2) originates the inefficient production of triplet excited states in a high triplet to singlet ratio [1,2,9,10].

It is suggested that in the decomposition of 1,2-dioxetanones and similar molecules, the singlet ground state is indeed a biradical intermediate [11,12]. In order to explain this biradical mechanism, these decomposition reactions were even compared with the ring-opening of cyclobutane, in which a biradical intermediate was proven to be involved [13]. According to these works, the biradical intermediate would arise from the evenly distribution between O_5 and O_3 of the two electrons present in the O_5-O_3 bond. However, our previous study of simple 1,2-dioxetanone indicated that the formation of a biradical intermediate did not occur in the case of that molecule [14,15]. This result is in line with experimental studies that have indicated that preferential formation of triplet states is in conflict with the biradical mechanism and that solvent effects seem to rule out the viability of the biradical mechanism [10,16].

The elucidation of the presence or absence of a biradical intermediate in the decomposition reaction of these molecules is now a prerequisite for the complete understanding of the chemiluminescence of 1,2-dioxetanones. Moreover, it can help to sort out the controversy behind the decomposition and chemiexcitation mechanisms of simple 1,2-dioxetanone, for which different authors have presented different results [11,14,15]. To this end, we have tried to find evidence that could demonstrate the presence or absence of the

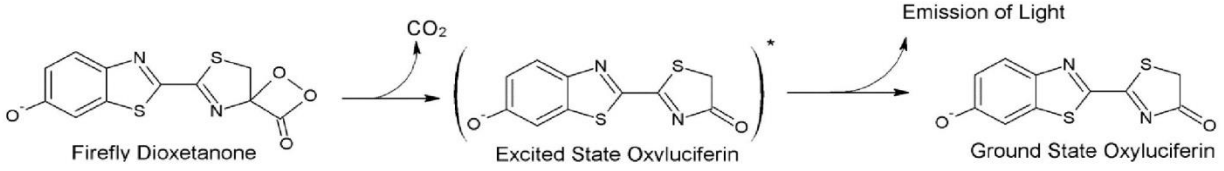

Figure 1. Schematic representation of the firefly dioxetanone decomposition, and light emission from excited state oxyluciferin.

ScienceJet ScienceJet 2012, 1: 29

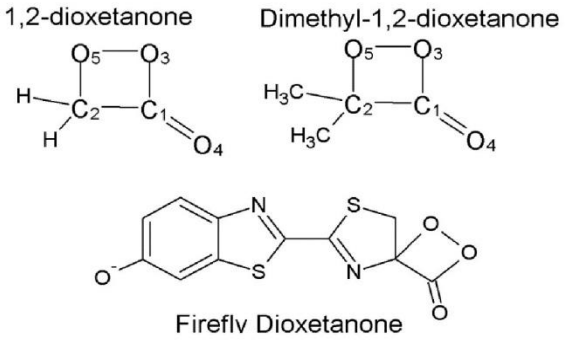

Figure 2. Schematic representation of the firefly dioxetanone, simple 1,2-dioxetanone and dimethyl-1,2-dioxetanone.

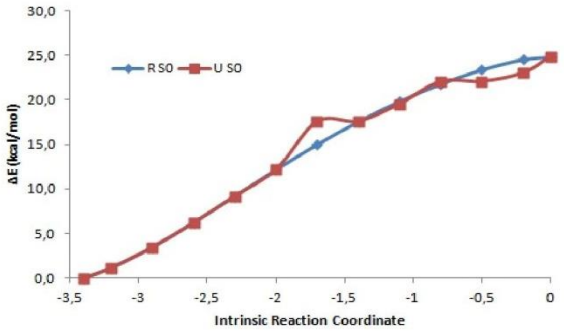

Figure 3. Representation the energy profile of IRC path determined for dimethyl-1,2-dioxetanone O_5-O_3 bond breaking step.

biradical intermediate in the decomposition reaction of dimethyl-1,2-dioxetanone. This study was performed with a computational methodology, and implicit solvent models were used to simulate dichloromethane.

2. Experimental Details

The ground state (S_0) transition state geometry was optimized at the mPWKCIS/aug-cc-pVDZ level of theory [17]. Frequency calculations were performed at the same level of theory, in order to confirm that the obtained structure was indeed a transition state. *in vacuo* Intrinsic Reaction Coordinate (IRC) calculations were conducted to connect the S_0 transition state to the dimethyl-1,2-dioxetanone reactant [18]. The force constants were calculated in all SCF cycles.

The S_0 energies of the IRC-obtained structures were re-evaluated by single point calculations with the O3LYP functional and the aug-cc-pVDZ basis set, with implicit solvent [19]. The S_0 energies were calculated at both the restricted (R) and unrestricted (U) level of theory. The Stable=opt keyword was used for all single point calculations. When these calculations were at the RO3LYP/aug-cc-pVDZ level of theory, the reoptimization of the wavefunction was real, spin restricted. Implicit solvent effects were included in the single point calculations by using the conductor-like polarized continuum model (CPCM), with parameters set for dichloromethane [20].

All calculations were performed with the Gaussian03 program package [21].

3. Results and Discussion

The IRC path between dimethyl-1,2-dioxetanone and the S_0 transition state of its decomposition reaction is presented in Figure 3. Similar IRC path energies were seen for both U and R S_0. Given the similarity between the U and R results, we will focus more on the R S_0 results in order to better compare with results that we have already obtained for simple 1,2-dioxetanone [14,15]. The activation energy of this reaction is 22.6 kcal/mol, with zero-point corrections, which is in line with the experimental value of 20.8±0.1 kcal/mol [9]. The transition state is reached by O_5-O_3 bond elongation, as already expected [1,2].

In Table 1 are presented the atomic Mulliken charges of both O_5 and O_3, at some points of the R IRC path. It can be seen that their negative charge is similar at the S_0 transition state (coordinate 0.0). However, it can be seen that this increase is not similar in both atoms, contrary to what is to be expected in the formation of a biradical intermediate. While the increase of the negative charge of O_3 is much accentuated, the increase of O_5 is not. Moreover, as the charge of O_5 doesn't change so much in this phase of the decomposition reaction, it can be seen that the steady increase of the negative charge of O_3 is not caused by the evenly distribution of the electrons present in the O_5-O_3, but by charge transfer from other atoms. In Table 1 are also presented the atomic Mulliken charges of both acetone and carbon dioxide moieties, at some points of the R IRC path. It can be seen that there are charge transfers between the moieties, which can explain the increase in the negative charge on both O_5 and O_3. Thus, our results indicate that instead of the formation of a biradical intermediate, there is a continuous reorganization of the charge density of the moieties during this phase of the decomposition reaction.

For best assessing the nonexistence of the biradical intermediate, we have studied the ring-opening reaction of cyclobutane [13]. This reaction can proceed with the formation of a biradical intermediate, tetramethylene, before

Table 1. Atomic Mulliken Charges of O_5, O_3 and the acetone and carbon dioxide moieties, during the O_5-O_3 bond breaking step of the R S_0 IRC path.

Coordinates	O_5	O_3	Acetone	Carbon Dioxide
-3.4	-0.644	-0.490	0.238	-0.237
-2.3	-0.677	-0.517	0.184	-0.186
-2.0	-0.682	-0.526	0.173	-0.171
-1.4	-0.691	-0.549	0.146	-0.146
0.8	-0.694	-0.578	0.135	-0.135
-0.2	-0.688	-0.614	0.141	-0.141
0.0	-0.683	-0.627	0.146	-0.147

Simplex Academic Publishers
www.simplex-academic-publishers.com

ScienceJet ScienceJet 2012, 1: 29

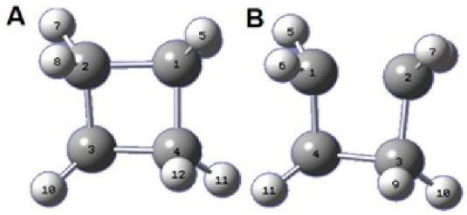

Figure 4. Structures of cyclobutane (A) and tetramethylene biradical intermediate (B).

Table 2. Bond lengths of C_1-C_2 bond, and atomic Mulliken charges of C_1 and C_2 atoms, during the formation of the tetramethylene biradical intermediate.

In vacuo		
Bond length	**C_1**	**C_2**
1.56	0.760	0.760
1.58	0.764	0.764
1.60	0.768	0.768
1.62	0.771	0.771
1.64	0.774	0.774
dichloromethane		
Bond length	**C_1**	**C_2**
1.56	0.771	0.771
1.58	0.774	0.774
1.60	0.778	0.778
1.62	0.781	0.781
1.64	0.784	0.784

reaching a transition state. The formation of the tetramethylene biradical was already demonstrated experimentally [13]. We have then obtained the S_0 geometry of cyclobutane (Figure 4), at the mPWKCIS/cc-pVDZ level of theory, in the gas phase. Subsequently, we have scanned the elongation of the C_1-C_2 bond, until the formation of the tetramethylene biradical (Figure 4). The Mulliken atomic charges of these two atoms were calculated at the UO3LYP/aug-cc-pVDZ level of theory, both *in vacuo* and in dichloromethane. These results are presented in Table 2. These results further support the nonexistence of a biradical intermediate in the decomposition of simple 1,2-dioxetanone and of dimethyl-1,2-dioxetanone [14,15]. The atomic charges of C_1 and C_2 are the same in all situations. Moreover, it can be seen an equal increase of the positive charge of both atoms with increasing C_1-C_2 bond length, due to the evenly distribution of the two electrons that have formed that bond. None of this was seen in the case of the two dioxetanones already referred, which indicates that no biradical is formed in the chemiluminescence of these molecules.

Further proof for the absence of a biradical intermediate can be found in Table 3. This Table presents the atomic Mulliken charges of the O_5 and O_3 atoms of dimethyl-1,2-dioxetanone, at some points of the U S_0 IRC path. As in the case of the R S_0 calculations, there is not an evenly distribution charge transfer between these two atoms, but there is an unbalanced increase in the negative charge of both atoms.

The results present so far in this paper, combined with our previous calculations for simple 1,2-dioxetanone, indicate that there is no evidence for the formation of a biradical intermediate in the decomposition reaction of this

Table 3. Atomic Mulliken charges of O_5 and C_3 atoms, during the O_5-O_3 of the bond breaking step of the U S_0 IRC path.

Intrinsic Reaction Coordinate	**O_5**	**O_3**
-3,4	-0,644	-0,490
-2,6	-0,662	-0,502
-1,7	-0,687	-0,537
-1,1	-0,690	-0,551
-0,2	-0,669	-0,603

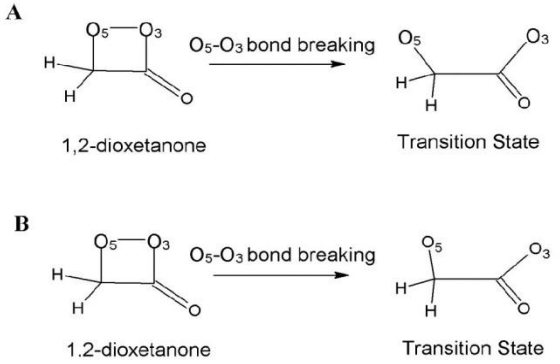

Figure 5. Schematic representation of the reagent and transition state of the decomposition reaction of simple 1,2-dioxetanone, as described by Lindh and co-workers (A) and by us (B) [11,14,15].

type of molecules [14,15]. This is in line with experimental studies that have indicated that preferential formation of triplet states is in conflict with the biradical mechanism and that solvent effects seem to rule out the viability of the biradical mechanism [10,16]. Moreover, O_5 and O_3 are chemically unequivalent atoms, and so are the moieties they belong to, and so an evenly distribution of the electrons present in the O_5-O_3 bond was difficult to occur.

The fact that our calculations for the decomposition reaction of 1,2-dioxetanone and dimethyl-1,2-dioxetanone indicated that there is no biradical intermediate, contrary to the calculations made by Lindh and co-workers, may explain the different mechanisms obtained for the chemiexcitation mechanism of simple 1,2-dioxetanone [11,14,15]. Therefore, to better sort out this controversy, it needs an explanation to why our calculations didn't find a biradical intermediate, while that of Lindh and co-workers did. An explanation may be the different geometries obtained by the different studies. In our calculations of simple 1,2-dioxetanone, we have found that the O_5-O_3 bond cleavage occurs mainly by the increase of the O_3-C_1-C_2 angle, and not by a symmetrical cleavage of the bond [14,15]. Contrary to these results, the calculations of Lindh and co-workers indicated that the O_5-O_3 bond breaking occurs by a similar increase of the O_3-C_1-C_2 and O_5-C_2-C_1 angles [11]. This leads to a more symmetrical bond cleavage and transition state. This can be more clearly seen in Figure 5. In Figure 6, it can be seen that our calculations of dimethyl-1,2-dioxetanone also indicate that the O_5-O_3 bond is mainly breaking by increasing the O_3-C_1-C_2 angle, leading to a not so symmetrical bond cleavage.

We think that our decomposition reaction mechanism is the more correct for two main reasons [13,14,22]. In the

ScienceJet ScienceJet 2012, 1: 29

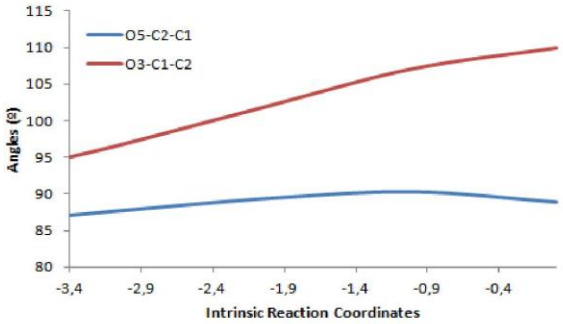

Figure 6. Angle variations recorded during the IRC calculation of the O_5-O_3 bond breaking step of dimethyl-1,2-dioxetanone.

case of both simple 1,2-dioxetanone and dimethyl-1,2-dioxetanone, their two corresponding moieties are too chemically unequivalent to allow a so symmetrical O_5-O_3 bond cleavage as that proposed by Lindh and co-workers [11]. More importantly, our calculations of simple 1,2-dioxetanone and dimethyl-1,2-dioxetanone have been able to be in line with experimental evidence by rationalizing the triplet and singlet inefficient chemiexcitation and the high triplet to singlet ratio [9,10,13,14,22]. The work of Lindh and co-workers was not able to rationalize these important features of simple 1,2-dioxetanone decomposition, and moreover, their results were not in line with other computational studies of other dioxetanone molecules [9,10,11,14,23-26].

4. Conclusions

The O_5-O_3 bond breaking step of the decomposition reaction of dimethyl-1,2-dioxetanone was studied with an O3LYP/mPWKCIS approach, in implicit dichloromethane. Both the R and U S_0 states were included in the calculations. The ring-opening reaction of cyclobutane was also studied by a similar methodology.

The objective of this work was to search for evidence of the presence or absence of a biradical intermediate in the decomposition reaction of simple 1,2-dioxetanone and dimethyl-1,2-dioxetanone, in order to better clarify the complex chemiluminescence of dioxetanones. Present and previous calculations, along with the comparison to the formation of the tetramethylene biradical, allow us to state that no biradical intermediate is formed during these decomposition reactions.

The fact that we have found no biradical intermediate, contrary to the work of other authors, may explain the recent controversy regarding the decomposition and chemiexcitation mechanism of simple 1,2-dioxetanone. The fact that we have presented mechanisms in line with experimental data and other computational studies regarding other dioxetanones, contrary to the work of these authors, is a point in favor of the accuracy of our conclusions. Moreover, the fact that these authors have computed a very symmetrical bond cleavage for two unequivalent atoms, while we have computed a non-symmetrical bond cleavage, explains why they haven't found evidence for the absence of a biradical intermediate, while we have.

Acknowledgments

Financial support from Fundação para a Ciência e a Tecnologia (FCT, Lisbon), Programa Operacional Temático Factores de Competitividade (COMPETE) e comparticipado pelo Fundo Comunitário Europeu (FEDER) (Project PTDC/QUI/71366/2006) is acknowledged. A Ph.D. Grant to Luís Pinto da Silva (SFRH\BD\76612\2011), also attributed by FCT, is also acknowledged.

References

1. L. Pinto da Silva, J. C. G. Esteves da Silva, ChemPhysChem 13 (2012) 2257.
2. M. Matsumoto, J. Photochem. Photobiol. C 5 (2004) 27.
3. L. Pinto da Silva, J. C. G. Esteves da Silva, J. Chem. Theory Comput. 7 (2011) 809.
4. J. Vieira, L. Pinto da Silva, J. C. G. Esteves da Silva, J. Photochem. Photobiol. B 117 (2012) 33.
5. A. Roda, Guardigli, Anal. Bioanal. Chem. 402 (2012) 69.
6. B. R. Branchini, J. C. Rosenber, D. M. Ablamsky, K. P. Taylor, T. L. Southworth, S. J. Linder, Anal. Biochem. 414 (2011) 239.
7. S. M. Marques, F. Peralta, J. C. G. Esteves da Silva, Talanta 77 (2009) 1497.
8. L. Pinto da Silva, J. C. G. Esteves da Silva, ChemPhysChem 12 (2011) 951.
9. S. P. Schmidt, G. B. Schuster, J. Am. Chem. Soc. 100 (1978) 5559.
10. W. Adam, W. J. Baader, J. Am. Chem. Soc. 107 (1985) 410.
11. F. Liu, Y. Liu, L. De Vico, R. Lindh, J. Am. Chem. Soc. 131 (2009) 6181.
12. L. De Vico, Y. J. Liu, J. W. Krogh, R. Lindh, J. Phys. Chem. A 111 (2007) 8013.
13. J. C. Polanyi, A. H. Zewail, Acc. Chem. Res. 28 (1995) 119.
14. L. Pinto da Silva, J. C. G. Esteves da Silva, J. Comput. Chem. 33 (2012) 2118.
15. L. Pinto da Silva, J. C. G. Esteves da Silva, J. Comput. Chem. 33 (2012) 2127.
16. N. J. Turro, P. Lechtken, J. Am. Chem. Soc. 95 (1973) 264.
17. C. Adamo, V. Barone, J. Chem. Phys. 108 (1998) 664.
18. C. Gonzalez, H. B. Schlegel, J. Phys. Chem. 94 (1990) 5523.
19. N. C. Handy, A. J. Cohen, Mol. Phys. 99 (2001) 403.
20. V. Barone, M. Cossi, J. Phys. Chem. A 102 (1998) 1995.
21. Gaussian 03 (Revision C. 02), M. J. Frisch, G. W. Trucks, H. B. Schlegel, G. E. Scuseria, M. A. Robb, J. R. Cheeseman, J. A. Montgomery, Jr., T. Vreven, K. N. Kudin, J. C. Burant, J. M. Millam, S. S. Iyengar, J. Tomasi, V. Barone, B. Mennucci, M. Cossi, G. Scalmani, N. Rega, G. A. Petersson, H. Nakatsuji, M. Hada, M. Ehara, K. Toyota, R. Fukuda, J. Hasegawa, M. Ishida, T. Nakajima, Y. Honda, O. Kitao, H. Nakai, M. Klene, X. Li, J. E. Knox, H. P. Hratchian, J. B. Cross, C. Adamo, J. Jaramillo, R. Gomperts, R. E. Stratmann, O. Yazyev, A. J. Austin, R. Cammi, C. Pomelli, J. W. Ochterski, P. Y. Ayala, K. Morokuma, G. A. Voth, P. Salvador, J. J. Dannenberg, V. G. Zakrzewski, S. Dapprich, A. D. Daniels, M. C. Strain, O. Farkas, D. K. Malick, A. D. Rabuck, K. Raghavachari, J. B. Foresman, J. V. Ortiz, Q. Cui, A. G. Baboul, S. Clifford, J. Cioslowski, B. B. Stefanov, G. Liu, A. Liashenko, P. Piskorz, I. Komaromi, R. L. Martin, D. J. Fox, T. Keith, M. A. Al-Laham, C. Y. Peng, A. Nanayakkara, M. Challacombe, P. M. W. Gill, B. Johnson, W. Chen, M. W. Wong, C. Gonzalez, and J. A. Pople, Gaussian, Inc., Wallingford, CT (2004).
22. L. Pinto da Silva, J. C. G. Esteves da Silva, Submitted (2012).
23. F. Liu, Y. Liu, L. De Vico, R. Lindh, Chem. Phys. Lett. 484 (2009) 69.

Simplex Academic Publishers
www.simplex-academic-publishers.com

24. H. Isobe, Y. Takano, M. Okumura, S. Kuramitsu, K. Yamaguchi, J. Am. Chem. Soc. 127 (2005) 8667.
25. L. Yue, Y. J. Liu, W. H. Fang, J. Am. Chem. Soc. 134 (2012) 11632.
26. L. W. Chung, S. Hayashi, M. Lundberg, T. Nakatsu, H. Kato, K. Morokuma, J. Am. Chem. Soc. 130 (2008) 12880.

Cite this article as:

Luís Pinto da Silva *et al.*: **Evidence of the absence of a biradical intermediate in the decomposition of 1,2-dioxetanones.** ScienceJet 2012, **1**: 29

Article 15

Dioxetanones' peroxide bond as a charge-shifted bond: implications in the chemiluminescence process

Luís Pinto da Silva and Joaquim C.G. Esteves da Silva

Struct. Chem. **2014**, *25*, 1075-1081.

The theoretical calculations and the writing of the paper were performed by Luís Pinto da Silva, under supervision of Professor Esteves da Silva.

Struct Chem (2014) 25:1075–1081
DOI 10.1007/s11224-013-0383-1

ORIGINAL RESEARCH

Dioxetanones' peroxide bond as a charge-shifted bond: implications in the chemiluminescence process

Luís Pinto da Silva · Joaquim C. G. Esteves da Silva

Received: 24 October 2013 / Accepted: 4 December 2013 / Published online: 15 December 2013

Abstract Six dioxetanone molecules, ranging in complexity from simple dioxetanone to firefly dioxetanone, were studied by performing M06/6-311G(d,p) calculations. The quantum theory of atoms in molecules and the electron localization function was applied to analyze the peroxide and carbon–carbon bonds of the dioxetanone ring. Both approaches demonstrated that the peroxide bond is not covalent, but charge-shifted. This means that for this bond the covalent "electron sharing" is relatively unimportant, and it is the stabilizing resonance energy that causes the bonding. For the contrary, the carbon–carbon bond is covalent. These discoveries indicate that no biradical species should be formed in the dioxetanone decomposition, and that the most probable rate-determining step should be the carbon–carbon cleavage.

Keywords Firefly dioxetanone · Charge-shifted bonds · Chemiluminescence · Peroxide bond · Electron localization function · Quantum theory of atoms in molecules

Introduction

Bioluminescence is a remarkable natural phenomenon, in which light is emitted in an enzyme-catalyzed chemical reaction [1–3]. When no enzyme is present, this light emitting chemical process is termed chemiluminescence [1–3]. The most important bioluminescence system is that of the fireflies, due to their very high quantum yields (~40–60 %) [4, 5]. Given the obtained efficiency, among other properties, this system has been gained numeral practical applications over the years [6–8].

Firefly chemi and bioluminescence are emitted by excited state oxyluciferin, the product of the chemical reaction [9, 10]. Oxyluciferin is thought to be formed directly into an excited state by decomposition of firefly dioxetanone (Fig. 1) [11–13]. The latter molecule is able to produce electronically excited states by decomposition as the four-membered peroxide ring involves high strain energy. Typical dioxetanones present heats of reaction that vary around ~70–90 kcal/mol, while the activation energies range between 20 and 30 kcal/mol [11–13]. Thus, the process of dioxetanone decomposition is expected to provide sufficient energy for the chemiexcitation of one of the resulting products. Several theories have been proposed in order to explain the chemiexcitation step: chemically initiated electron exchange luminescence (CIEEL), charge transfer induced luminescence (CTIL), gradually reversible charge transfer initiated luminescence (GRCTIL), and interstate crossing induced chemiexcitation (ICIC) [14–17].

Mechanistically, there are two proposed decomposition routes for dioxetanone. Richardson and O'Neal [18] postulated a stepwise biradical mechanism (Fig. 2). In this mechanism, the homolytic cleavage of the peroxide bond is both the first and the rate-determining step of the reaction. The homolysis of the peroxide bond generates the biradical. The second and final step is cleavage of the carbon–carbon bond. Other authors have proposed a concerted mechanism, in which no biradical is found (Fig. 2) [19, 20]. The bond cleavage of the peroxide and carbon–carbon bonds is simultaneous/near-simultaneous.

Electronic supplementary material The online version of this article (doi:10.1007/s11224-013-0383-1) contains supplementary material, which is available to authorized users.

L. Pinto da Silva · J. C. G. Esteves da Silva (✉)
Centro de Investigação em Química, Departamento de Química e Bioquímica, Faculdade de Ciências da Universidade do Porto, R. Campo Alegre 687, 4169-007 Porto, Portugal
e-mail: jcsilva@fc.up.pt

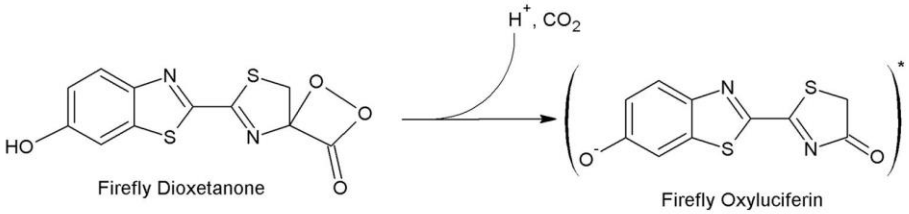

Fig. 1 Conversion of firefly dioxetanone into excited state firefly oxyluciferin

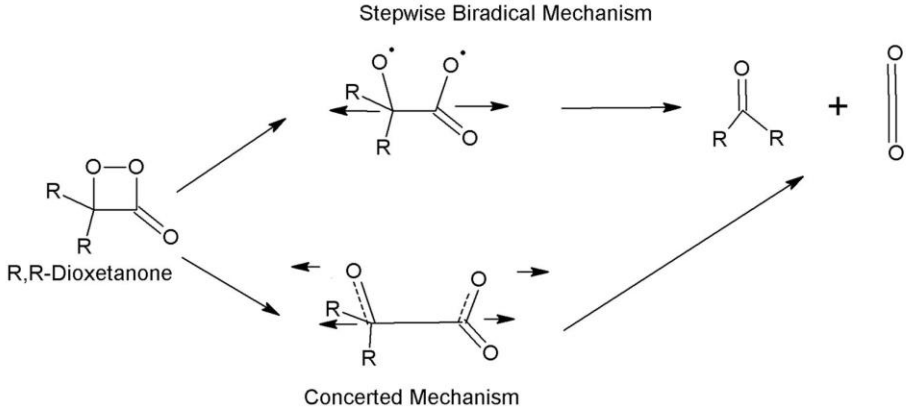

Fig. 2 Representation of the stepwise biradical and concerted reaction mechanisms for dioxetanone decomposition

Some experimental studies have indicated that the preferential formation of triplet excited states (in simple dioxetanones) is in conflict with the biradical mechanism and that solvent effects rule out the viability of this mechanism [21, 22]. In the field of theoretical chemistry, this matter has been a topic of controversy with different studies and with different methods targeting different dioxetanone molecules having presented both types of decomposition mechanisms [16, 17, 23–27].

Thus, given all the data provided so far, we think that the key to elucidating the topic of the decomposition mechanism of dioxetanone is to study the peroxide bond. An detailed analysis of this bond may allows us to determine if an homolytic cleavage is really an option and if this bond is strong enough to its breaking being the rate-determining step. In order to succeed in such an analysis, we have studied the peroxide and the carbon–carbon bonds in different dioxetanone molecules with a theoretical approach. This approach is the only one able to give precise and electronically detailed information. The dioxetanones range between simple dioxetanone and neutral/anionic firefly dioxetanone, in terms of structural complexity (Fig. 3). The studied molecules are simple 1,2-dioxetanone (Diox1), thiazole–dioxetanone (Diox2), thiazole–thiazole–dioxetanone (Diox3), benzothiazole–thiazole–dioxetanone (Diox4), neutral firefly dioxetanone (Diox5), and anionic firefly dioxetanone (Diox6).

Computational methodology

The geometries of the six dioxetanone molecules present in Fig. 3 were optimized at the M06/6-311G(d,p) level of theory [28]. Frequency analysis was made, at the same level of theory, in order to ensure that the obtained structures were minima in their potential energy surface. This functional was chosen due to good results in a combination of main-group thermochemistry, kinetics, and noncovalent interactions [28].

All calculations were performed in implicit dichloromethane, by using the conductor-polarized continuum model (CPCM) [29]. This particular solvent was chosen because it is already used in experimental chemiluminescence studies, and its dielectric constant (8.93) is similar to what is expected to be the dielectric constant of an enzymatic active site ($\sim$4) [30, 31].

All geometry, frequency, and single point energy calculations were made with the Gaussian 09 software package [32].

Results and discussion

Contrary to most of the theoretical studies performed in this subject, we will not try to model the decomposition reaction of the six dioxetanones here presented. There is a

Struct Chem (2014) 25:1075–1081

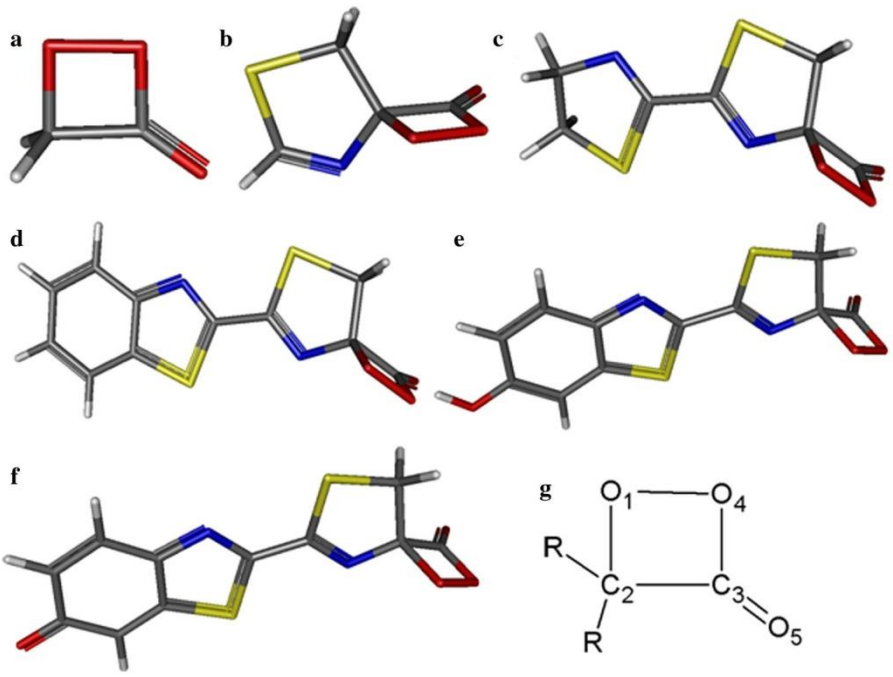

Fig. 3 **a–f** Representation of Diox1–6, respectively; **g** dioxetanones atom labeling

great controversy in the literature regarding the appropriated approach for dioxetanone decomposition modeling: closed- or open-shell approach [16, 17, 23–27]. It is known that a closed-shell approach leads to the calculation of a concerted mechanism, without any biradical, while the use of an open-shell approach leads to the prediction of the stepwise biradical mechanism [16, 17, 23–27]. So far, no consensus was reached regarding this topic. Nonetheless, it is generally accepted that the dioxetanone substrate itself is a closed-shell molecule [16, 17, 23–27]. Thus, we have chosen to only study the dioxetanone substrates closed-shell structures, in order to avoid the closed-/open-shell controversy.

In Table 1 are presented the O_1–O_4 and C_2–C_3 bond lengths for all dioxetanones. In geometrical terms, both bonds appear to be covalent, as their length is in line with is expected for these types of bonds. However, the analysis of the atomic charges of these four atoms shed some doubt regarding the absolute and relative strength of these bonds. A Voronoi deformation density (VDD) population analysis was performed by using the Multiwfn code with the CPCM-M06/6-311G(d,p) wavefunctions [33]. The results are presented in Table 2.

Both oxygen atoms present in the peroxide bond have negative charge, which indicates that there are repulsive electrostatic interactions between them. The situation is similar for the C_2–C_3 bond, as both carbon atoms have positive charge. However, the peroxide bond is expected to be more affected by these repulsive interactions, as the charge difference between the two oxygen atoms range only between 0.026 and 0.041. In the case of the C_2–C_3 bond, the charge difference between atoms range between 0.116 and 0.219. This higher charge separation indicates that the repulsive effects may be more attenuated by polarization effects. However, this would indicate that the C_2–C_3 bond is stronger than the O_1–O_4 bond. This is not in

Table 1 O_1–O_4 and C_2–C_3 bond lengths (in Å) for all dioxetanones

	O_1–O_4	C_2–C_3
Diox1	1.46	1.50
Diox2	1.46	1.52
Diox3	1.46	1.52
Diox4	1.46	1.52
Diox5	1.46	1.52
Diox6	1.46	1.52

Table 2 Results of the VDD population analysis, at the CPCM-M06/6-311G(d,p) level of theory, for all dioxetanones

	O_1	C_2	C_3	O_4
Diox1	−0.094	0.025	0.243	−0.068
Diox2	−0.100	0.113	0.233	−0.063
Diox3	−0.094	0.112	0.235	−0.060
Diox4	−0.098	0.108	0.235	−0.061
Diox5	−0.099	0.112	0.230	−0.063
Diox6	−0.116	0.111	0.227	−0.074

line with the literature, which states that the rate-determining step is O_1–O_4 bond cleavage [16, 17, 23–27]. But, if C_2–C_3 is stronger than the peroxide bond, the rate-determining step should be the cleavage of the carbon–carbon bond.

There are various tools based on theoretical chemistry that can be used in the analysis of inter- and intramolecular interactions. In this study we used the quantum theory of atoms in molecules (QTAIM) and the topology of the electron localization function (ELF), in order to clarify the present topic of research [34, 35].

The QTAIM methodology identifies the coordinates of a particular type of saddle-point in the electron density distribution, which is known as a bond critical point (BCP). Two of the electronic properties at the BCP are generally used to characterize the bonding nature in this region: the value of electron density distribution ($\rho(r)$) and the Laplacian $\nabla^2\rho(r)$. Negative values of $\nabla^2\rho(r)$, combined with high values of $\rho(r)$, are associated with covalent character in the bonding region. Positive values of $\nabla^2\rho(r)$ indicate excess kinetic energy density over potential energy density, which is signal of either ionic or charge-shift character [36, 37]. Ionic bonds, which experience exchange repulsions, are associated with contractions of electrons toward an atom and a low value of $\rho(r)$ at the BCP regions. For the contrary, charge-shifted bonds retain high values for $\rho(r)$ [36, 37]. In this type of bond, the covalent "electron sharing" is relatively unimportant, and it is the large stabilizing resonance energy, originated between charge-shifted or ionic valence-bond forms, that causes the binding [36–38].

In Tables 3 and 4 are presented the $\nabla^2\rho(r)$ and $\rho(r)$ values for the O_1–O_4 and C_2–C_3 BCPs (respectively) found in the six dioxetanones. It can be seen that $\nabla^2\rho(r)$ for all O_1–O_4 BCPs is positive, while the values for this electronic parameter are negative for all the C_2–C_3 BCPs (Tables 3 and 4). This means that the peroxide bond character is either ionic or charge-shifted, while C_2–C_3 is a covalent bond. The values of $\rho(r)$, present in Tables 3 and 4, indicate that O_1–O_4 is a charge-shifted bond. The $\rho(r)$ values for the peroxide bond are relatively high, and range between 0.274 and 0.277. Moreover, the values found for O_1–O_4 are higher than the ones found for C_2–C_3 (0.264–0.269), which is a covalent bond. It should be noted that a positive value for $\nabla^2\rho(r)$ indicates the presence of charge-depletion zone associated with the BCP, a phenomenon common to most weak interactions [39].

In Tables 3 and 4 are also presented the values obtained for the ellipticity (ε) and for the ratio $-(G(r_b)/V(r_b))$. $G(r_b)$ refers to the Lagrangian kinetic energy, while the value $V(r_b)$ is a measure of the potential energy density. ε provides a measure of π and σ bond character: values higher than 0.1 indicate pi character, while values equal or lower than 0.1 demonstrate sigma bond character [40]. Analysis of Tables 3 and 4 indicates that both O_1–O_4 and C_2–C_3 have sigma bond character. However, we can also see that the ε values for the peroxide bond are near the limit that indicates pi bond character. For the C_2–C_3 bond this is only true of Diox1, while in the other dioxetanone molecules, the ε clearly indicates sigma bond character.

Table 3 $\nabla^2\rho(r)$, $\rho(r)$, ε, and $-G(r_b)/V(r_b))$ values for the O_1–O_4 BCP, for all dioxetanones

	$\nabla^2\rho(r)$	$\rho(r)$	ε	$-(G(r_b)/V(r_b))$
Diox1	0.0516	0.277	0.097	0.52
Diox2	0.0579	0.275	0.090	0.52
Diox3	0.0577	0.275	0.090	0.52
Diox4	0.0581	0.275	0.090	0.52
Diox5	0.0586	0.275	0.089	0.52
Diox6	0.0632	0.274	0.088	0.52

Table 4 $\nabla^2\rho(r)$, $\rho(r)$, ε, and $-G(r_b)/V(r_b))$ values for the C_2–C_3 BCP, for all dioxetanones

	$\nabla^2\rho(r)$	$\rho(r)$	ε	$-(G(r_b)/V(r_b))$
Diox1	−0.6887	0.269	0.087	0.22
Diox2	−0.6693	0.265	0.047	0.21
Diox3	−0.6659	0.265	0.046	0.21
Diox4	−0.6651	0.264	0.047	0.21
Diox5	−0.6664	0.265	0.047	0.21
Diox6	−0.6702	0.265	0.052	0.21

The $-(G(r_b)/V(r_b))$ ratio is an important measure for the nature of the bonds [41]. For values above 1, the bond is noncovalent. Between 0.5 and 1, this ratio indicates that the bond is partially covalent [41]. For the peroxide bond, the $-(G(r_b)/V(r_b))$ ratio has always the value of 0.52 (Table 3). This indicates the O_1–O_4 is only a partially covalent bond, which is in line with its charge-shifted character. For theC_2–C_3 bond, the values for these parameters are lower even than the range indicating partially covalent character, supporting the notion that this is a fully covalent bond.

The finding that the peroxide bond in dioxetanone is not covalent is in line with previous studies [42, 43]. Bil and Latajka have studied peroxide bonds in HOO radical and HOOH molecules by means of topological methods. The data obtained by them indicated that these were not typical covalent bonds, having being classified as "covalent depleted."

In quantum chemistry, ELF measures the extent of spatial localization of the reference electron, thus providing a method for mapping the electron pair probability in multielectronic systems. Silvi and Savin [35] have generalized this approach for density functional theory.

Figure 4 shows the visual representation of the ELF for the six dioxetanones, obtained with the Gabedit program [44]. Visual representation of the ELF for the six dioxetanones, obtained with the Multiwfn program, is presented in Figure S1 of the Supporting Information. The ELF results obtained with these two different programs are very similar in regard to each other.

Analysis of Fig. 4 confirms the covalent character of the C_2–C_3 bond, as indicated by the presence of a lobe indicating electron pair sharing between the carbon atoms. As for the peroxide bond, visualization of the ELF further supports the idea that this is not a covalent bond, as no lobe indicating electron pair sharing is found between oxygen atoms. In fact, the visualization of the ELF for the six dioxetanones supports the data presented above, which indicates that O_1–O_4 is a charge-shifted bond. In this type of bonds, the electron density is depleted form the internuclear region, and the ELF does not show the shared two-electron basin that is associated with electron sharing covalent bonds [38]. This occurs as in a charge-shifted bond, the attraction of electrons to the bond center is diminished, while the attraction to the electrons to the atomic centers is increased. This is well in line with what is seen in the visualization of the ELF, showed in Fig. 4.

In Fig. 5 are presented the ELF attractors present in and near the dioxetanone ring, localized by using the Multiwfn code. In Diox molecules one to four, it was found two valence-type ELF attractors in the O_1–O_4 bond axis. In the firefly dioxetanone molecules (Diox5 and Diox6, Fig. 5), only one valence-type ELF attractor was found in the peroxide bond axis. In the case of C_2–C_3 bond, only one valence-type ELF attractor was found in all dioxetanones. In Table 5 are presented the average population number of the above-referred valence-type ELF attractors. These results support the notion that the peroxide bond is not covalent, contrary to the C_2–C_3 bond. The valence-type attractor of the carbon–carbon bond present an average population of 2.20 electrons in all dioxetanone molecules. This a strong evidence for the presence of an electron pair in the C_2–C_3 bonding region. For the contrary, the average population number of the valence-type ELF attractors of the peroxide bond does not support a covalent bond character, further highlighting the charge-shifted character. The number of electrons in each attractor indicates that there is some electron density in the peroxide bonding region, but far from values associated with an electron pair.

The results here obtained have important and very interesting implications in firefly chemi/bioluminescence, in particular, and in dioxetanone chemiluminescence, in general. As already referred, the dioxetanone decomposition is thought to occur via one of two possible mechanisms: stepwise biradical or concerted (Fig. 2) [16–27]. Moreover, until now, there is little unequivocal evidence to support one mechanism over the other. However, the fact that O_1–O_4 is a charge-shifted bond, and not a covalent one, may tip the scales against the stepwise biradical mechanism.

The biradical, in the stepwise biradical mechanism, is thought to be formed due the homolytic cleavage of the

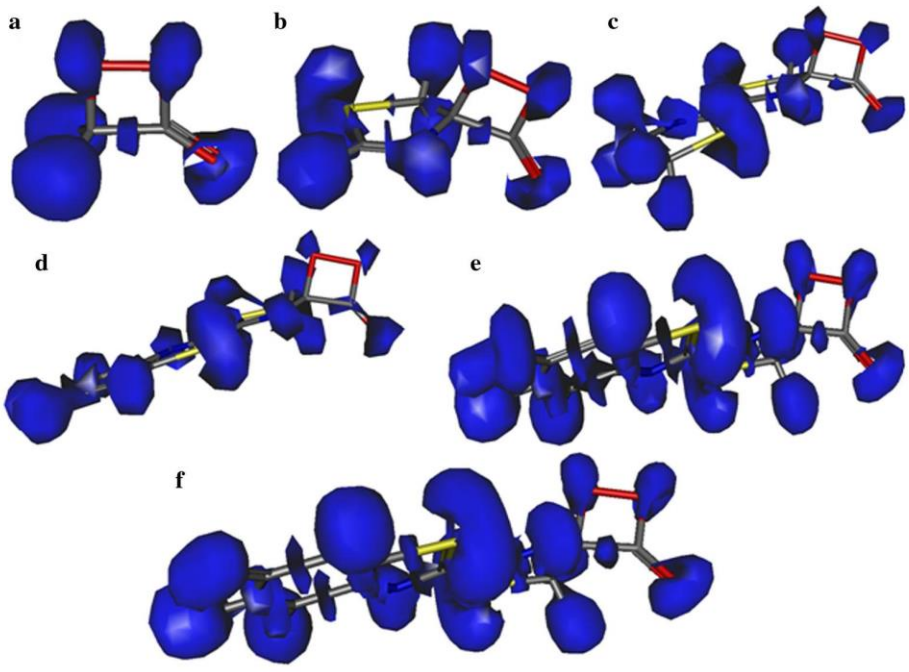

Fig. 4 Representation of the ELF for the six dioxetanone molecules; **a**–**f** Diox1–6, respectively. The value of ELF used for the presentation of the isosurfaces was of 0.8

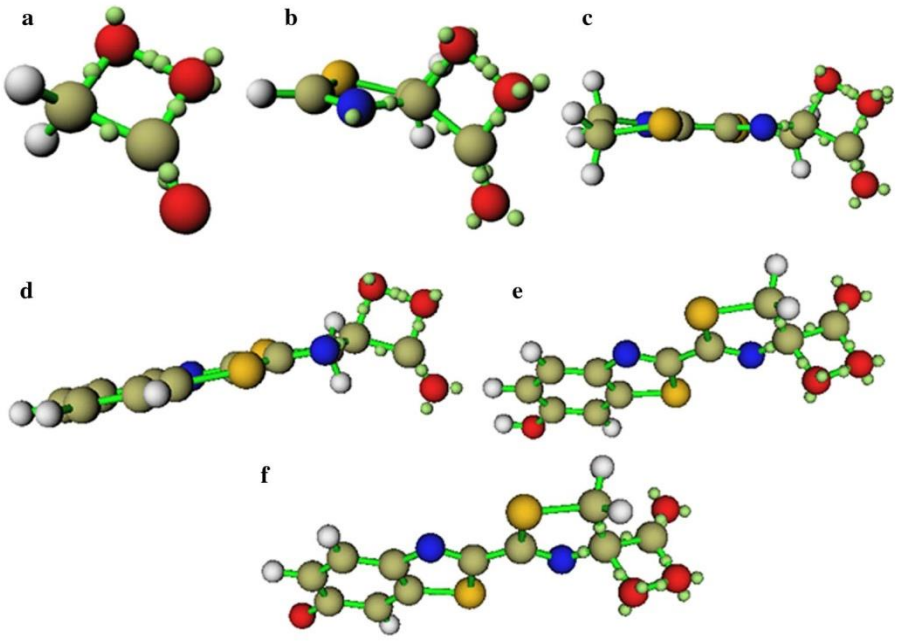

Fig. 5 Representation of ELF attractors in and near the dioxetanone ring; **a–f** Diox1–6

Table 5 Average population number (in electrons) of the valence-type ELF attractors present in the O_1–O_4 and C_2–C_3 bond axis, for all dioxetanones

	O_1–O_4		C_2–C_3
Diox1	0.21	0.38	2.05
Diox2	0.22	0.36	2.23
Diox3	0.22	0.36	2.23
Diox4	0.36	0.22	2.23
Diox5	0.57		2.23
Diox6	0.58		2.24

peroxide bond. In this process, also known as homolysis, the two originally shared electrons in a cleaved covalent bond are divided equally between the products. However, we have found that the peroxide is a charge-shifted and not a covalent bond. Moreover, by ELF analysis we have found that the attraction of electrons to the peroxide bond center is diminished before dioxetanone decomposition. So, no equal electron distribution should occur after peroxide bond destruction, as there is not a typical electron pair shared between the oxygen atoms. Therefore, our theoretical calculations indicate that no biradical species should be found in dioxetanone decomposition. This means that while a stepwise mechanism is still possible, a stepwise biradical is expected to not be able to occur.

Another implication on the chemiluminescence process of dioxetanones is the identity of the rate-determining step of the decomposition process. Until now, it is generally accepted that this step is the peroxide bond cleavage [16–27]. However, our calculations indicate that this bond is of the charge-shifted type, and the positive value for the $\nabla^2\rho(r)$ of this bond indicates that O_1–O_4 is a weak interaction [39]. For the contrary, C_2–C_3 is a covalent bond, and so, should be much stronger than the O_1–O_4 bond. Given that the decomposition reaction of dioxetanone is composed of two bond cleavages (O_1–O_4 and C_2–C_3), is somewhat strange that the rate-determining step refers to the cleavage of the weaker bond. Moreover, the rate-determining step is associated with an activation energy of ~20–30 kcal/mol [11]. Thus, in our opinion is that the most likely rate-determining step should be the covalent C_2–C_3 bond cleavage, irrespectively of if the decomposition mechanism is stepwise or concerted.

Conclusion

The closed-shell structure of six dioxetanone molecules, ranging in complexity from simple dioxetanone to firefly dioxetanone, was studied by using a variety of theoretical approaches. QTAIM and ELF analysis allowed us to discover that the peroxide bond is not covalent, but has charge-shifted character. This finding has serious implications in the chemiluminescence of these molecules. The properties of this type of bond prevents its homolytic cleavage which was a process thought to be fundamental for the formation of a biradical intermediate species. Therefore, a stepwise biradical mechanism appears to not be possible for dioxetanone decomposition.

It was also seen that other bond that is cleaved in dioxetanone decomposition, C_2–C_3 bond, is of covalent nature. Therefore, this bond should stronger than the charge-shifted peroxide bond. Given this, our opinion is that the rate-determining step should be C_2–C_3 bond cleavage and not peroxide bond breaking, irrespective of the decomposition reaction mechanism.

Supporting information

Cartesian coordinates of the six dioxetanones, and ELF graphics computed with Multiwfn code.

Acknowledgments Financial support from Fundação para a Ciência e Tecnologia (FCT, Lisbon) (Programa Operacional Temático Factores de Competitividade (COMPETE) e comparticipado pelo Fundo Comunitário Europeu (FEDER) (Project PTDC/QUI/71366/2006) is acknowledged. A Ph.D. grant to Luís Pinto da Silva (SFRH/76612/2011), attributed by FCT, is also acknowledged.

References

1. Marques SM, Esteves da Silva JCG (2009) IUBMB Life 61:6
2. Inouye S (2010) Cell Mol Life Sci 67:387
3. Hosseinkhani S (2011) Cell Mol Life Sci 68:1167
4. Niwa K, Ichino Y, Kumata S, Nakajima Y, Hiraishi Y, Kato D, Viviani VR, Ohmiya Y (2010) Photochem Photobiol 86:1046
5. Ando Y, Niwa K, Yamada N, Enomoto T, Irie T, Kubota H, Ohmiya Y, Akiyama H (2008) Nat Photonics 2:44
6. Roda A, Guardigli M (2012) Anal Bioanal Chem 402:69
7. Alam R, Zylstra J, Fontaine DM, Branchini BR, Maye MM (2013) Nanoscale 5:5303
8. Li J, Chen L, Du L, Li M (2013) Chem Soc Rev 42:662
9. Vieira J, Pinto da Silva L, Esteves da Silva JCG (2012) J Photochem Photobiol B 117:33
10. Pinto da Silva L, Esteves da Silva JCG (2011) J Chem Theory Comput 7:809
11. Matsumoto M (2004) J Photochem Photobiol C 5:27
12. Pinto da Silva L, Esteves da Silva JCG (2012) ChemPhysChem 13:2257
13. Navizet I, Liu YJ, Ferré N, Roca-Sanjuán D, Lindh R (2011) ChemPhysChem 12:3064
14. Schuster GB (1979) Acc Chem Res 12:366
15. Isobe H, Takano Y, Okumura M, Kuramitsu S, Yamaguchi K (2005) J Am Chem Soc 127:8667
16. Yue L, Liu YJ, Fang WH (2012) J Am Chem Soc 134:11632
17. Pinto da Silva L, Esteves da Silva JCG (2013) ChemPhysChem 14:1071
18. Richardson WH, O'Neal HE (1972) J Am Chem Soc 94:8665
19. McCapra F (1970) Pure Appl Chem 24:611
20. Kearns DR (1971) Chem Rev 71:395
21. Adam W, Baader WJ (1985) J Am Chem Soc 107:410
22. Turro NJ, Lechtken P (1973) J Am Chem Soc 95:264
23. Yue L, Roca-Sanjuán D, Lindh R, Ferré N, Liu YJ (2012) J Chem Theory Comput 8:4359
24. Liu F, Liu YJ, De Vico L, Lindh R (2009) J Am Chem Soc 131:6181
25. Pinto da Silva L, Esteves da Silva JCG (2012) J Comput Chem 33:2118
26. Pinto da Silva L, Esteves da Silva JCG (2012) J Comput Chem 33:2127
27. Pinto da Silva L, Esteves da Silva JCG (2013) Int J Quantum Chem 113:1709
28. Zhao Y, Truhlar DG (2008) Theor Chem Acc 120:215
29. Cossi M, Rega N, Scalmani G, Barone V (2003) J Comput Chem 24:669
30. Schmidt SP, Schuster GB (1978) J Am Chem Soc 100:5559
31. Pinto da Silva L, Esteves da Silva JCG (2011) ChemPhysChem 12:951
32. Frisch MJ, Trucks GW, Schlegel HB, Scuseria GE, Robb MA, Cheeseman JR, Scalmani G, Barone V, Mennucci B, Petersson GA, Nakatsuji H, Caricato M, Li X, Hratchian HP, Izmaylov AF, Bloino J, Zheng G, Sonnenberg JL, Hada M, Ehara M, Toyota K, Fukuda R, Hasegawa J, Ishida M, Nakajima T, Honda Y, Kitao O, Nakai H, Vreven T, Montgomery JA Jr, Peralta JE, Ogliaro F, Bearpark M, Heyd JJ, Brothers E, Kudin KN, Staroverov VN, Kobayashi R, Normand J, Raghavachari K, Rendell A, Burant JC, Iyengar SS, Tomasi J, Cossi M, Rega N, Millam JM, Klene M, Knox JE, Cross JB, Bakken V, Adamo C, Jaramillo J, Gomperts R, Stratmann RE, Yazyev O, Austin AJ, Cammi R, Pomelli C, Ochterski JW, Martin RL, Morokuma K, Zakrzewski VG, Voth GA, Salvador P, Dannenberg JJ, Dapprich S, Daniels AD, Farkas O, Foresman JB, Ortiz JV, Cioslowski J, Fox DJ (2009) Gaussian 09, revision A.02. Gaussian, Inc., Wallingford
33. Lu T, Chen F (2012) J Comput Chem 33:580
34. Bader RFW (1985) Acc Chem Res 18:9
35. Silvi B, Savin A (1994) Nature 371:683
36. Shaik S, Danovich D, Wu W, Hiberty PC (2009) Nat Chem 1:443
37. Rzepa HS (2011) J Chem Theory Comput 7:97
38. Jenkins S, Kirk SR, Guevara-García A, Ayers PW, Echegaray E, Toro-Labbe A (2011) Chem Phys Lett 510:18
39. Vidal I, Melchor S, Dobado JÁ (2008) J Phys Chem B 112:3414
40. Mitra S, Chandra AK, Gashnga PM, Jenkins S, Kirk SR (2012) J Mol Model 18:4225
41. Nasiri M, Shakourian-Fard M, Fattahi A (2012) J Phys Org Chem 25:803
42. Bil A, Latajka Z (2004) Chem Phys 303:43
43. Bil A, Latajka Z (2005) Chem Phys Lett 406:366
44. Allouche AR (2011) J Comput Chem 32:174

Chapter 5 – Study of the Color Tuning Mechanism of the Bioluminescent Luciferase-OxyLH_2 System

5.1. Analysis of OxyLH_2 Light Emission inside *Photinus pyralis* Luciferase

Article 16

TD-DFT/Molecular Mechanics Study of the *Photinus pyralis* Bioluminescence System
Luís Pinto da Silva and Joaquim C.G. Esteves da Silva
J. Phys. Chem. B **2012**, *116*, 2008-2013.

The theoretical calculations and the writing of the paper were performed by Luís Pinto da Silva, under supervision of Professor Esteves da Silva.

THE JOURNAL OF PHYSICAL CHEMISTRY B
Article
pubs.acs.org/JPCB

TD-DFT/Molecular Mechanics Study of the *Photinus pyralis* Bioluminescence System

Luís Pinto da Silva and Joaquim C. G. Esteves da Silva*

Centro de Investigação em Química (CIQ-UP), Departamento de Química e Bioquímica, Universidade do Porto, Porto, Portugal

Supporting Information

ABSTRACT: This is the first report of a computational study of the bioluminescence of ligand-bound *Photinus pyralis* luciferase. A time-dependent PBE0/molecular mechanics approach was used to study the interaction between excited-state oxyluciferin (Keto-(−1)) and neighboring active site molecules. The results of these calculations demonstrated that the most important intermolecular interactions are: blue-shifting ionic interactions, red-shifting $\pi-\pi$ stacking, and red/blue shifting hydrogen bonding. Subsequent molecular dynamics simulations further supported these conclusions.

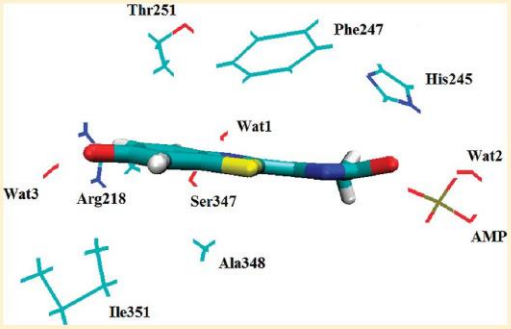

INTRODUCTION

Bioluminescence is a light-emitting phenomenon that occurs in living organisms, in which an excited-state molecule is produced in a luciferase-catalyzed reaction.[1] The most studied bioluminescence system is that of the North American firefly, *Photinus pyralis*.[1] Firefly luciferase (Luc, EC 1.13.12.7) catalyzes a two-step reaction: first, it catalyzes the formation of an adenylyl intermediate, from firefly luciferin (LH_2) and adenosine-5′-triphosphate (ATP); in the second step, that intermediate is oxidized, in the presence of molecular oxygen, into oxyluciferin ($OxyLH_2$).[1] This molecule has a great importance in this system, as besides being the light emitter, it appears to be one of the major responsible for the flash profile of the emitted light.[1−5] In more recent years, the bioluminescence phenomenon has received attention from the research community and has gained numerous biomedical, pharmaceutical, and bioanalytical applications. More specifically, it is involved in the analytical determination of ATP, in microbial detection, biosensing, and bioimaging, and is used as a gene reporter.[6−10]

One of the most studied and elusive aspects of firefly bioluminescence is its multicolor emission.[11] Luc is a pH-sensitive enzyme, and at basic pH (pH ≈ 7.5) the emission has a peak at 562 nm. At acid pH (pH ≈ 5−6), the emission shifts to the red region of the visible spectrum, with a maximum at 620 nm.[11] The understanding of this feature could be used to improve the efficiency of Luc-based applications. Lower energy emitting Luc could be used in the in vivo medical imaging, as red light is absorbed very poorly in comparison with natural emitted light. Viviani et al. also hypothesized that the control of the multicolor emission could be applied in the use of Luc as a single dual reporter gene, as a bioindicator of cellular stress, and as a probe for intracellular changes of pH.[12] Numerous authors have tried to explain this natural phenomenon. The indication and analysis of all of the experimental and theoretical contributions for this topic can be found in these four recent reviews.[11,13−15]

For a correct description of the bioluminescence phenomenon, an exact identification of the luminophore is needed. The identification of Keto-(−1) (Figure 1) as the light emitter was only achieved rather recently, by analysis of the dissociation and tautomeric constants of $OxyLH_2$ as a function of pH, by the study of the direct excited-state product of firefly dioxetanone, and by the study of the possibility of keto−enol tautomerism in *Luciola cruciata* Luc (LcLuc) active site.[16−18] However, it should be stressed that all of these studies are theoretical, and until now no experimental study has conclusively defined Keto-(−1) as the sole light emitter.

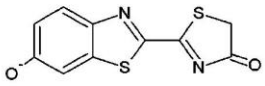

Figure 1. Schematic representation of Keto-(−1).

One of the most fundamental studies in this field of research was the determination of the crystal structure of LcLuc.[19] This experimental work indicated that LcLuc is capable of assuming different conformations during the various stages of the bioluminescence reaction. Thus, the complex of LcLuc with an adenylyl intermediate analogue presented a more hydrophobic and closed active site, while in the case of the enzyme-

Received: December 13, 2011
Revised: January 14, 2012
Published: January 14, 2012

dx.doi.org/10.1021/jp2120059 | J. Phys. Chem. B 2012, 116, 2008−2013

$OxyLH_2$-adenosine-5′-monophosphate (AMP) complex a more open and polar active site was found. Because of the fact that a red-emitting LcLuc mutant only presents the second conformation, it was hypothesized by the authors that the more closed conformation could be responsible for green emission, and the more open one for red emission.[19]

In some previous Time-Dependent Density Functional Theory (TD-DFT)-based studies, some authors have tried to analyze the effect of various small molecules and of polarity in the multicolor emission of $OxyLH_2$.[16,20−24] These calculations demonstrated that the color of light by Keto-(−1) can be modulated by the type of intermolecular interactions that the luminophore may form with other molecules. Furthermore, the polarity of the microenvironment has also an effect in the emission maxima. On the basis of these findings, we have studied the effect on intermolecular interactions and polarity in the multicolor bioluminescence. To this end, we have docked excited-state Keto-(−1) to both conformations of LcLuc and have analyzed the different effects exerted by active site molecules on emission.[24,25] We have then stated that a red-shift can be achieved by modification of the hydrogen-bond network, and changes in the electrostatic and $\pi-\pi$ stacking interactions between Keto-(−1) and AMP and Phe249, respectively. These conclusions are in line with both theoretical and experimental works from other researchers.[26−30] More recently, Song and Rhee developed some new force field parameters for both the ground and the excited states of Keto-(−1).[16,31] Also, they have demonstrated the importance of taking into account the environmental dynamics in the study of the multicolor bioluminescence. Moreover, they have stated that the most important factor, in the color tuning mechanism, is the electrostatic interactions between the luminophore and neighboring molecules. Thus, this conclusion devalues the importance of other types of intermolecular interactions and contradicts the results of other authors.

The purpose of this Article is to study, for the first time, the bioluminescence phenomenon in the more closed and hydrophobic active site of *Photinus pyralis* Luc (PDB ID: 3IES).[32] It should be noted that, while Nakatani et al. also have tried to study theoretically the bioluminescence of *Photinus pyralis* Luc, they have used a structure derived from unbound Luc and a working model.[30] Therefore, their structure may have significant differences regarding the crystal structure of bound Luc, here computationally studied for the first time. To this end, we have docked excited-state Keto-(−1) to the active site of Luc in the closed conformation, by means of protein−ligand docking. The Luc−emitter complex was minimized by using molecular mechanics (MM). Subsequently, the emitters and some chosen active site molecules were withdrawn from the resulting structure. Theoretical calculations on these models demonstrated the effect of these static active site molecules in the emission of Keto-(−1). Finally, molecular dynamics (MD) simulations were performed to study the effect of environmental dynamics in the bioluminescence phenomenon. Thus, our approach will enable the expansion of the bioluminescence research to ligand-bounded crystal structures other than LcLuc, and the study of the luminophore−active site interactions as a function of time.

The results achieved in this Article demonstrated that the intermolecular interactions that are fundamental to the color tuning mechanism are ionic interactions, $\pi-\pi$ stacking, and hydrogen bonding. These results are in line with previous experimental and theoretical bioluminescence studies.[18,25−28,30,33] Also, it was demonstrated that the inclusion of dynamic features affects quantitatively (but not qualitatively) the emission wavelength of Keto-(−1) and Keto-(−1)−X complexes. The present and some previous results validate the hypothesis that there are intermolecular interactions that modulate the color of bioluminescence, as they have a similar effect on the emission of Keto-(−1) in different firefly species.[25]

■ COMPUTATIONAL METHODS

The PDB structure 3IES was used as starting structure, in the study of the bioluminescence of Keto-(−1). The hydrogens atoms, the missing atoms, and TIP3P water molecules up to 12 Å were added by the LEAP module of the AMBER 11 suite of programs.[34] The ff03 force field was used for intramolecular interactions.[35] The ground-state geometries of AMP and Keto-(−1) were calculated at the HF/6-31G(d) level of theory.[36] The configuration interaction singles (CIS) functional, with the 6-31G(d) basis set, was used to calculate the first singlet (S_1) excited-state geometry of Keto-(−1).[37] The CIS method was chosen as Nakatani et al. demonstrated that it is comparable to methods of higher levels of theory.[30] The ground-state structure of AMP and the excited-state geometries of Keto-(−1) were used in their parametrization with the ANTECHAMBER module of AMBER and the general AMBER force field.[38] These two molecules were docked to the active site by use of the software AUTODOCK 4.2.[39] The genetic algorithm was used as a search engine.

One phase of energy minimization (30 000 steps) was performed, using the Not (just) Another Molecular Dynamics program (NAMD) molecular dynamic code with AMBER potential functions, parameters, and the file formats.[40] All of the minimizations steps were performed in a NVT ensemble, with a temperature of 298.15 K. In this process, the Particle Mesh Ewald method was used to include the long-range interactions.[41] In the end of the energy minimizations, Keto-(−1) was withdrawn from the resulting structures along with Arg218, His245, Phe247, Thr251, Ser347, Ala348, Ile351, AMP, and three water molecules. Because of the high number of atoms involved, only the interacting side chains of the amino acids and the phosphate group of AMP were considered in the calculations, as can be seen in Figure 1 of the Supporting Information. These molecules were chosen on the basis of previous computational studies on LcLuc, to detect possible differences and similarities between the color tuning mechanism of the two enzymes.[18,19,22,25,26,30] All of the active site molecules were within 6 Å from Keto-(−1).

MD simulations were performed with NAMD, on the MM-minimized system composed by Luc, AMP, Keto-(−1), and water molecules up to 12 Å. These coordinates were used in a MD simulation of 500 ps, at 298.15 K. Nonbonded interactions were considered with 14 Å cutoffs. The integration step size was 2 fs, and all bonds involving hydrogen and heavy atoms were constrained.

The emission wavelengths of Keto-(−1) and respective complexes with active site molecules were computed at the time-dependent (TD) PBE0/6-31+G(d) level of theory, with solvent effects.[42−44] Despite some critics to the use of TD-DFT in bioluminescence research due to errors regarding charge transfer (CT) states, the work of Li et al. showed us that CT is small on planar $OxyLH_2$, thus devaluing this flaw of TD-DFT methods.[45−47] The complexes that resulted from both the MM and MD simulations were used in the TD-DFT calculations

dx.doi.org/10.1021/jp2120059 | J. Phys. Chem. B 2012, 116, 2008−2013

without further optimization. To simulate the polarity of the active site of Luc, the conductor-like polarized continuum model (CPCM) was used to treat the effects due to bulk solvent.[48] The dielectric constant of 4 was used to simulate the hydrophobic environment of the active site. All HF/CIS/TD-DFT calculations were performed with the Gaussian 03 program package.[49]

RESULTS AND DISCUSSION

Analysis of the Static Interaction between Keto-(−1) and Active Site Molecules. In Table 1 are indicated the wavelength maxima of excited-state Keto-(−1), when interacting with each one of the active site molecules and without directly interacting with that molecule. In Figure 2 are represented Keto-(−1) and surrounding active site molecules. When in comparison with the active site of LcLuc, the major difference is that Keto-(−1) is interacting with three water molecules (with the benzothiazole/thiazolone oxygen and the benzothiazole nitrogen) at the same time.

Table 1. Calculated Emission Wavelength (λ_{max}, in nm) of Keto-(−1) and Keto-(−1)−X Complexes[a]

	λ_{max}	$\Delta\lambda_{max}$
Keto-(−1)	528	
Keto-(−1)−Arg218	521	7
Keto-(−1)−His245	531	−3
Keto-(−1)−Phe247	531	−3
Keto-(−1)−Thr251	528	0
Keto-(−1)−Ser347	529	−1
Keto-(−1)−Ala348	528	0
Keto-(−1)−Ile351	531	−3
Keto-(−1)−AMP	501	27
Keto-(−1)−Wat1	538	−10
Keto-(−1)−Wat2	537	−9
Keto-(−1)−Wat3	516	12

[a]In the third column are indicated the difference between the emission wavelength of Keto-(−1) and Keto-(−1)−X ($\Delta\lambda_{max}$, in nm). Positive values correspond to blue-shifting contributions, while negative values refer to red-shifting ones.

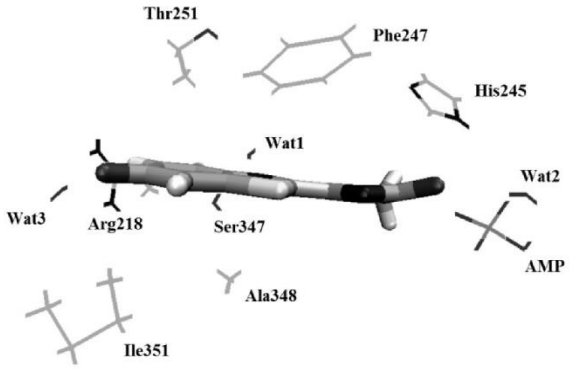

Figure 2. Representation of the complex between Keto-(−1) and active site molecules.

As was already expected due to our previous studies, Table 1 results demonstrate that ionic interactions blue-shift the emission.[16,21,22] Positively charged Arg218 and negatively charged AMP both decrease the emission of Keto-(−1), with different extents. The calculated blue-shifting contribution of AMP differs by 20 nm from the contribution of Arg218.

Our analysis also reveals that the polarization of the benzothiazole moiety, made here by Ser347, has a small red-shifting contribution as in the case of LcLuc.[25] The polar Thr251 has no effect in the emission, also as in the case of LcLuc.[25] Ala348 also does not modulate the color of light emitted by the emitter. The also hydrophobic molecule Ile351 red-shifts the emission of Keto-(−1). Phe247 presents opposite contribution in Luc than its corresponding phenylalanine residue in LcLuc closed conformation, by red-shifting the emission of Keto-(−1).[25] His245, as Phe247, is a red-shifting molecule.

Analysis of Table 1 also demonstrated the importance of the hydrogen-bond network in the tuning of the emission of Keto-(−1), as all three water molecules gave importance contributions to the wavelength maxima. Wat3 interacts with the benzothiazole oxygen, thereby decreasing its emission wavelength by 12 nm.[19−21] Wat1 and Wat2 interact with the thiazole and the thiazolone moieties, respectively, which leads to increased emission wavelengths.[16,20−22,25]

In conclusion, we can state that the most important blue-shifting interactions are ionic interactions (AMP and Arg218) and hydrogen bonding with the benzothiazole oxygen (Wat3). The most important red-shifting interactions are π-interactions (Phe247) and hydrogen bonding with the thiazole/thiazolone moieties (Wat1 and Wat2). The effect of hydrophobic interactions (Ile351 and Ala348) and polarization of the benzothiazole microenvironment (Thr251 and Ser347) appears to be less important, as indicated in previous studies.[16,20,25] Also, we can state that our decision of modeling the active site molecules, as represented in Figure 1 of the Supporting Information, does not affect this study as the values found here are similar to those calculated in the case of LcLuc with full active site molecules.[25]

MD Simulation Regarding Excited-State Keto-(−1)−Luc Complex. In Table 2 are represented the emission wavelengths of sole Keto-(−1) and Keto-(−1) complexed with one active site at 125, 250, 375, and 500 ps of the MD simulation. In Table 3 are represented the red- or blue-shifting contribution of the active site molecules to the emission of Keto-(−1), in the form of the difference between the emission

Table 2. Calculated Emission Wavelength (λ_{max}, in nm) of Keto-(−1) and Keto-(−1)−X Complexes, at 125, 250, 375, and 500 ps (ps) of MD Simulation

	λ_{max}			
	125 ps	250 ps	375 ps	500 ps
Keto-(−1)	518	538	545	561
Keto-(−1)−Arg218	514	535	541	556
Keto-(−1)−His245	526	541	548	565
Keto-(−1)−Phe247	522	543	556	566
Keto-(−1)−Thr251	519	538	545	561
Keto-(−1)−Ser347	520	539	546	563
Keto-(−1)−Ala348	518	538	545	561
Keto-(−1)−Ile351	521	539	546	564
Keto-(−1)−AMP	495	511	522	538
Keto-(−1)−Wat1	528	546	555	573
Keto-(−1)−Wat2	524	545	545	577
Keto-(−1)−Wat3	507	525	534	544

dx.doi.org/10.1021/jp2120059 | J. Phys. Chem. B 2012, 116, 2008−2013

Table 3. Calculated Difference between the Emission Maxima of Keto-(−1) ($\Delta\lambda_{max}$, in nm) and Keto-(−1)−X Complexes, at 125, 250, 375, and 500 ps (ps) of MD Simulation[a]

	$\Delta\lambda_{max}$			
	125 ps	250 ps	375 ps	500 ps
Keto-(−1)−Arg218	4	3	4	5
Keto-(−1)−His245	−8	−3	−3	−4
Keto-(−1)−Phe247	−4	−5	−11	−5
Keto-(−1)−Thr251	−1	0	0	0
Keto-(−1)−Ser347	−2	−1	−1	−2
Keto-(−1)−Ala348	0	0	0	0
Keto-(−1)−Ile351	−3	−1	−1	−3
Keto-(−1)−AMP	23	27	23	24
Keto-(−1)−Wat1	−10	−8	−10	−12
Keto-(−1)−Wat2	−6	−7	0	−16
Keto-(−1)−Wat3	11	13	11	17

[a]Positive values correspond to blue-shifting contributions, while negative values refer to red-shifting ones.

wavelength of Keto-(−1) and the emission maxima of Keto-(−1)−X complexes. It should be stated that, while Wat1 and Wat3 are hydrogen-bonded to Keto-(−1) during the period of the simulation, the bond between Wat2 and Keto-(−1) is broken in some points of the simulation. This breaking thereby explains the contribution of 0 nm of Wat2, at 375 ps of the MD simulation.

As was already noticed by Song and Rhee, the inclusion of a dynamic component in the calculations has an effect on the bioluminescence of Keto-(−1).[18] As can be seen by comparing Tables 1 and 2, the emission maxima computed at different periods of the MD simulation are all blue- or red-shifted as compared to the maxima calculated for the MM energy minimizations. However, the trends regarding the effect of intermolecular interaction in the emission remain the same.

Ala348 and Thr251 still have a zero contribution in the emission of Keto-(−1). Arg218 and AMP still behave as blue-shifting molecules. However, AMP blue-shifts the emission by 23−27 nm, while Arg218 only has a small contribution to the emission of Keto-(−1). This large effect indicates that AMP is one of the most important molecules in the color tuning mechanism, as stated in previous studies.[18,25,27]

Both Ile351 and Ser347 have small red-shifting contributions to the emission. These data further support previous results, which indicate that the polarization of the benzothiazole moiety, and hydrophobic interactions with that same moiety, red-shift the emission.[20,25,26]

As was already indicated both by theory and by experiment, $\pi-\pi$ stacking interaction is a key factor in the color tuning mechanism. Phe247 is one of the most important red-shifting molecules, with contributions as high as 11 nm. This importance is also seen in LcLuc.[25] His245 is also of some importance, with red-shifting contributions as high as 8 nm.

The hydrogen-bond network appears also to be of great importance in the color tuning mechanism. Wat3 is an important blue-shifting molecule, with a steady contribution of 11−17 nm. Wat1 and Wat2 are also molecules that are fundamental for the multicolor bioluminescence, by increasing the emission wavelength of Keto-(−1) . Wat1 appears to be the more important of the two water molecules, by presenting higher red-shifting contributions. Furthermore, this molecule is hydrogen bonded to Keto-(−1) during the 500 ps of the simulation, while Wat2 has no interaction with the light emitter in some points (as exemplified at 375 ps of simulation). These results further support some previous studies, which demonstrated that some types of intermolecular interactions (as hydrogen bonding) have opposite effects, if made with the benzenic or with the thiazole/thiazolone moieties.[20,25]

Thus, the results here presented support our working hypothesis, which states that the multicolor bioluminescence is achieved by modulation of the color of light by intermolecular interactions.[16,20,25] Furthermore, this study allows us to clearly define the most important type of the intermolecular interactions: ionic, $\pi-\pi$ stacking, and hydrogen bonding. The conclusions of this Article gain more strength, as they support the conclusions achieved for other firefly species (*Luciola cruciata*).[25] Therefore, this indicates that we have defined a mechanism for the multicolor bioluminescence that can be found in different species of firefly, with similar results, as seen experimentally.[12] Also, the importance of performing dynamic simulations in the study of the multicolor bioluminescence (as stated by Song and Rhee)[18] was corroborated.

To try to understand the effect of intermolecular interactions in color modulation, we have calculated the energy of the excited state of Keto-(−1) complexed with Phe247, AMP, or Wat1. All three complexes suffer from a red-shift, with increasing time in the MD simulation. Therefore, it was expected that the excited state would be more stabilized during the course of the calculations. However, as can be seen in Table 4, there is no stabilization of the excited state with increasing

Table 4. Energy Levels (in hartrees) of the Ground and Excited States of Keto-(−1)−Phe247, Keto-(−1)−AMP, and Keto-(−1)−Wat1, at 125, 250, 375, and 500 ps (ps) of the MD Simulation

	Keto-(−1)−Phe247			
	125 ps	250 ps	375 ps	500 ps
excited state	−1671.391	−1671.391	−1671.390	−1671.377
ground state	−1671.478	−1671.475	−1671.472	−1671.458
	Keto-(−1)−AMP			
	125 ps	250 ps	375 ps	500 ps
excited state	−2082.087	−2082.079	−2082.090	−2082.073
ground state	−2082.179	−2082.168	−2082.178	−2082.158
	Keto-(−1)−Wat1			
	125 ps	250 ps	375 ps	500 ps
excited state	−1515.783	−1515.775	−1515.779	−1515.765
ground state	−1515.870	−1515.859	−1515.861	−1515.845

emission wavelength. Thus, as emission wavelength depends also on the ground state, we have computed the energy level of this state for all three complexes. Similarly to the excited state, there is no destabilization of the ground state with decreasing emission energies. However, an approximation of the energy level between both states can be seen for all complexes, indicating that intermolecular interactions modulate the color of emission, not by stabilizing/destabilizing one of the states but by affecting both the excited and the ground states.

A final note should be made regarding the study of Roca-Sanjuán et al., published after we performed the calculations here presented.[50] The authors state that the more appropriate strategy for modeling correctly the bioluminescence state is to use a peroxo intermediate as the starting structure, while it is

dx.doi.org/10.1021/jp2120059 | J. Phys. Chem. B 2012, 116, 2008−2013

common to start by the ground-state optimized structure of the reaction product (as performed here). However, other authors who also did not describe their modeling of Keto-(−1) as starting with the peroxo intermediate achieved results that agree very well with experiment.[18,26] Therefore, the impact of the recommendation of Roca-Sanjuán et al., in the bioluminescence research, needs further assessing.[50]

CONCLUSIONS

We have employed various computational methodologies to study the color tuning mechanism behind the multicolor bioluminescence. By using for the first time the crystal structure of the closed conformation of *Photinus pyralis* Luc, we have studied the interaction of Keto-(−1) with active site molecules.

Our calculations demonstrated that the most important types of intermolecular interactions are: blue-shifting ionic interactions (with AMP), red-shifting $\pi-\pi$ stacking (with Phe247), and red-/blue-shifting hydrogen bonding (with Wat1/2/3). Amino acids Arg218 and His245 present smaller but also important blue- and red-shifting contributions, respectively, while Ser347, Ile351, Thr251, and Ala348 appear to be irrelevant in the color tuning mechanism. Thus, these molecules may be good targets to amino acids mutations, with the objective of modulating the emission wavelength.

We have also performed molecular dynamics simulations with the Luc−emitter complex. Analysis of the results supported the conclusions derived from the study of the static Luc−Keto-(−1) complex. Furthermore, this study (along with our previous studies) demonstrated that the key role of intermolecular interactions can be seen in different firefly species, as in the presence or absence of dynamic features.

Analysis of the energy levels of both the ground and the excited states of three different Keto-(−1)−X complexes revealed the mechanism in which intermolecular interactions tune the color of emission. There is no stabilization/destabilization of a single state, but rather a stabilization/destabilization of both states. Thus, red- or blue-shifts are achieved by approximating or spacing between the energy levels of the ground and excited states, respectively.

ASSOCIATED CONTENT

Supporting Information

Schematic representation of the active site molecules studied in this Article, and Cartesian coordinates of the excited-state geometry of Keto-(−1) used for its parametrization and of the MM-resulting complex between Keto-(−1) and the modified active site molecules. This material is available free of charge via the Internet at http://pubs.acs.org.

AUTHOR INFORMATION

Corresponding Author

*Tel.: (+351) 220-402-569. Fax: (+351) 220-402-659. E-mail: jcsilva@fc.up.pt.

Notes

The authors declare no competing financial interest.

ACKNOWLEDGMENTS

Financial support from Fundação para a Ciência e Tecnologia (FCT, Lisbon) (Programa Operacional Temático Factores de Competitividade (COMPETE) e comparticipado pelo Fundo Comunitário Europeu FEDER) (Project PTDC/QUI/71366/2006) is acknowledged. A Ph.D. grant to L.P.d.S. (SFRH\BD\76612\2011), attributed by FCT, is also acknowledged.

REFERENCES

(1) Marques, S. M.; Esteves da Silva, J. C. G. *IUBMB Life* **2009**, *61*, 6−17.
(2) Esteves da Silva, J. C. G.; Magalhães, J. M. C. S.; Fontes, R. *Tetrahedron Lett.* **2001**, *42*, 8173−8176.
(3) Ribeiro, C.; Esteves da Silva, J. C. G. *Photochem. Photobiol. Sci.* **2008**, 1085−1090.
(4) Leitão, J. M.; Esteves da Silva, J. C. G. *J. Photochem. Photobiol.* **2010**, *101*, 1−8.
(5) Pinto da Silva, L.; Esteves da Silva, J. C. G. *Photochem. Photobiol. Sci.* **2011**, *10*, 1039−1045.
(6) Roda, A.; Pasini, P.; Mirasoli, M.; Michelini, E.; Guardigli, M. *Trends Biotechnol.* **2004**, *22*, 295−303.
(7) Luker, K. E.; Luker, G. D. *Antiviral Res.* **2008**, *78*, 179−187.
(8) Fan, F.; Wood, K. V. *Assay Drug Dev. Technol.* **2007**, *5*, 127−136.
(9) Branchini, B. R.; Southworth, T. R.; Khattak, N. F.; Michelini, E.; Roda, A. *Anal. Biochem.* **2005**, *345*, 140−148.
(10) Doyle, T. C.; Burns, S. M.; Contag, C. H. *Cell Microbiol.* **2004**, *6*, 303−317.
(11) Pinto da Silva, L.; Esteves da Silva, J. C. G. *J. Chem. Theory Comput.* **2011**, *7*, 809−817.
(12) Viviani, V. R.; Arnoldi, F. G. C.; Neto, A. J. S.; Oehlmeyer, T. L.; Bechara, E. J. H.; Ohmiya, Y. *Photochem. Photobiol. Sci.* **2008**, *7*, 159−169.
(13) Hosseinkhani, S. *Cell. Mol. Life Sci.* **2011**, *68*, 1167−1182.
(14) Hasegawa, J. Y.; Fujimoto, K. J.; Nakatsuji, H. *ChemPhysChem* **2011**, *12*, 3106−3115.
(15) Navizet, I.; Liu, Y. J.; Ferré, N.; Roca-Sanjuá, D.; Lindh, R. *ChemPhysChem* **2011**, *12*, 3064−3076.
(16) Pinto da Silva, L.; Esteves da Silva, J. C. G. *ChemPhysChem* **2011**, *12*, 951−960.
(17) Chen, S.-F.; Liu, Y.-J.; Navizet, I.; Ferré, N.; Fang, W.-H.; Lindh, R. *J. Chem. Theory Comput.* **2011**, *7*, 798−803.
(18) Song, C.-I.; Rhee, Y. M. *J. Am. Chem. Soc.* **2011**, *133*, 12040−12049.
(19) Nakatsu, T.; Ichiyama, Y.; Hiratake, J.; Saldanha, A.; Kobashi, N.; Sakata, K.; Kato, H. *Nature* **2006**, *440*, 372−376.
(20) Pinto da Silva, L.; Esteves da Silva, J. C. G. *J. Comput. Chem.* **2011**, *32*, 2654−2663.
(21) Min, C. G.; Ren, A. M.; Guo, J. F.; Li, Z. W.; Zou, L. Y.; Goddard, J. D.; Feng, J. K. *ChemPhysChem* **2010**, *11*, 251−259.
(22) Min, C. G.; Ren, A. M.; Guo, J. F.; Zou, L. Y.; Goddard, J. D.; Sun, C. C. *ChemPhysChem* **2011**, *11*, 2199−2204.
(23) Liu, Y. J.; De Vico, L.; Lindh, R. *J. Photochem. Photobiol., A* **2008**, *194*, 261−267.
(24) Chen, S. F.; Yue, L.; Liu, Y. J.; Lindh, R. *Int. J. Quantum Chem.* **2011**, *111*, 3371.
(25) Pinto da Silva, L.; Esteves da Silva, J. C. G. *ChemPhysChem* **2011**, *12*, 3002−3008.
(26) Navizet, I.; Liu, Y. J.; Ferré, N.; Fang, W. H.; Lindh, R. *J. Am. Chem. Soc.* **2010**, *132*, 706−712.
(27) Milne, B. F.; Marques, M. A.; Nogueira, F. *Phys. Chem. Chem. Phys.* **2010**, *12*, 14285−14293.
(28) Naumov, P.; Ozawa, Y.; Ohkubo, K.; Fukuzumi, S. *J. Am. Chem. Soc.* **2009**, *131*, 11590−11605.
(29) Cai, D.; Marques, M. A.; Nogueira, F. *J. Phys. Chem. B* **2011**, *115*, 329.
(30) Nakatani, N.; Hasegawa, J.-Y.; Nakatsuji, H. *J. Am. Chem. Soc.* **2007**, *129*, 8756−8765.
(31) Song, C. I.; Rhee, Y. M. *Int. J. Quantum Chem.* **2011**, *111*, 4091−4105.
(32) Auld, D. S.; Lovell, S.; Thorne, N.; Lea, W. A.; Maloney, D. J.; Shen, M.; Rai, G.; Battaile, K. P.; Thomas, C. J.; Simeonov, A.; et al. *Proc. Natl. Acad. Sci. U.S.A.* **2010**, *107*, 4878−4883.
(33) Naumov, P.; Kochunnoonny, M. *J. Am. Chem. Soc.* **2010**, *132*, 11566−11579.

(34) Case, D. A.; Cheatham, T. E.; Darden, T.; Gohlke, H.; Luo, R.; Merz, K. M.; Onufriev, A.; Simmelring, C.; Wang, B.; Wodds, R. *J. Comput. Chem.* **2005**, *26*, 1668−1688.
(35) Duan, Y.; Wu, C.; Chowdhury, S.; Lee, M. C.; Xiong, G. M.; Zhang, W.; Yang, R.; Cieplak, P.; Luo, R.; Lee, T.; et al. *J. Comput. Chem.* **2003**, *24*, 1999−2012.
(36) Cramer, C. J. *Essentials of Computational Chemistry*; Wiley: New York, 2002; p 153.
(37) Foresman, J. B.; Head-Gordon, M.; Pople, J. A.; Frisch, M. J. *J. Phys. Chem.* **1992**, *96*, 135−149.
(38) Wang, J. M.; Wolf, R. M.; Caldwell, J. W.; Kollman, P. A.; Case, D. A. *J. Comput. Chem.* **2004**, *25*, 1157−1174.
(39) Morris, G. M.; Huey, R.; Lindstrom, W.; Sanner, M. F.; Belew, R. K.; Goddsell, D. S.; Olsen, A. J. *J. Comput. Chem.* **2009**, *30*, 2785−2791.
(40) Philips, J. C.; Braun, R.; Wang, W.; Gumbart, J.; Tajkhorshid, E.; Villa, E.; Chipot, C.; Skell, R. D.; Kale, L.; Schulten, K. *J. Comput. Chem.* **2005**, *26*, 1781−1802.
(41) Essmann, U.; Perera, L.; Berkowitz, M. L.; Darden, T.; Lee, H.; Pedersen, L. G. *J. Chem. Phys.* **1995**, *103*, 8577−8593.
(42) Gross, E. K. U.; Kohn, W. *Adv. Quantum Chem.* **1990**, *21*, 255−291.
(43) Casida, M. E. *Recent Advances in Density Functional Methods*; World Scientific: Singapore, 1995.
(44) Adamo, C.; Barone, V. *J. Chem. Phys.* **1999**, *110*, 6158−6170.
(45) Yang, T.; Goddard, J. D. *J. Phys. Chem. A* **2007**, *111*, 4489−4497.
(46) Fujimoto, K.; Hayashi, S.; Hasegawa, J.-Y.; Nakatsuji, H. *J. Chem. Theory Comput.* **2007**, *3*, 605−618.
(47) Li, Z.-W.; Ren, A.-M.; Guo, J.-F.; Yang, T.; Goddard, J. D.; Feng, J.-K. *J. Phys Chem. A* **2008**, 9796−9800.
(48) Barone, V.; Cossi, M. *J. Phys. Chem. A* **1998**, *102*, 1995−2001.
(49) Frisch, M. J.; Trucks, G. W.; Schlegel, H. B.; Scuseria, G. E.; Robb, M. A.; Cheeseman, J. R.; Montgomery, J. A., Jr.; Vreven, T.; Kudin, K. N.; Burant, J. C.; et al. *Gaussian 03*, revision C.02; Gaussian, Inc.: Wallingford, CT, 2004.
(50) Roca-Sanjuán, D.; Delcey, M.; Navizet, I.; Ferré, N.; Liu, Y. J.; Lindh, R. *J. Chem. Theory Comput.* **2011**, *7*, 4060−4069.

Article 17

Quantum/molecular mechanics study of firefly bioluminescence on luciferase oxidative conformation

Luís Pinto da Silva and Joaquim C.G. Esteves da Silva

Chem. Phys. Lett. **2014**, *608*, 45-49.

The theoretical calculations and the writing of the paper were performed by Luís Pinto da Silva, under supervision of Professor Esteves da Silva.

Chemical Physics Letters 608 (2014) 45–49

Contents lists available at ScienceDirect

Chemical Physics Letters

journal homepage: www.elsevier.com/locate/cplett

Quantum/molecular mechanics study of firefly bioluminescence on luciferase oxidative conformation

Luís Pinto da Silva, Joaquim C.G. Esteves da Silva *

Centro de Investigação em Química (CIQ-UP), Departamento de Química e Bioquímica, Faculdade de Ciências da Universidade do Porto, R. Campo Alegre 687, 4169-007 Porto, Portugal

ARTICLE INFO

Article history:
Received 6 May 2014
In final form 21 May 2014
Available online 27 May 2014

ABSTRACT

This is the first report of a computational study of the color tuning mechanism of firefly bioluminescence, using the oxidative conformation of luciferase. The results of these calculations demonstrated that the electrostatic field generated by luciferase is fundamental both for the emission shift and efficiency. Further calculations indicated that a shift in emission is achieved by modulating the energy, at different degrees, of the emissive and ground states. These differences in energy modulation will then lead to changes in the energy gap between the states.

1. Introduction

Firefly bioluminescence is generated in a two-step reaction: luciferase catalyzes the adenylation reaction of firefly luciferin, in the presence of ATP-Mg^{2+}, leading to the formation of an adenylyl intermediate; in the second step, this adenylate is oxidized and from this result the products of the firefly bioluminescence reaction (Figure 1) [1–3]. These are oxyluciferin, adenosine-5′-monophosphate (AMP) and carbon dioxide. Oxyluciferin is the light emitter, and is produced in a singlet excited state [4,5].

Oxyluciferin emits in the yellow–green region (~2.14–2.34 eV) [1–5]. However, addition of metal cations or decrease of the pH lead to an emission shift to the red region of the visible spectrum (~2.00 eV) [1–5]. This multicolor bioluminescence has been the target of extensive research, as the understanding of this feature may be used to improve the efficiency of applications based on the firefly luciferase system, and even allow the creation of new applications [6].

Several hypotheses have been proposed in order to try to explain the multicolor bioluminescence [7–11]. Nevertheless, these theories were discarded as they were unable to explain the multicolor bioluminescence [5,12–14]. By reviewing the literature, one can see that a consensus was reached, in which the color of light emitted by oxyluciferin is modulated by intermolecular interactions with active site molecules. Thus, the multicolor bioluminescence is caused by subtle changes in the conformation of the active site, which result from changes in intermolecular interactions network formed by oxyluciferin and active site molecules [10,15–22].

Oxyluciferin can exist as one of six possible species, due to complex keto–enol equilibria. Branchini and co-workers found that a keto-constrained oxyluciferin analog was able to emit yellow–green and red bioluminescence, thus indicating that the bioluminophore was a keto species [23]. Further evidence supporting the role of anionic keto was obtained by analysis of the dissociation and tautomeric constants of oxyluciferin, by the study of the direct excited product of firefly dioxetanone, and by the study of the possibility of keto–enol tautomerism in the active site of luciferase (Figure 1) [22,24,25].

More recently, Gulick and co-workers uncovered crystallographic structures of firefly luciferase that revolutionized our view of the role of the enzyme in firefly bioluminescence reaction [26]. It was thought that the conformation of firefly luciferase remained the same during this reaction, despite some subtle changes in the active site [10]. However, this work by Gulick et al. demonstrated that the C-terminal domain of luciferase undergoes a ~140° rotation in order to adopt a different conformation of each of the two steps of the bioluminescence reaction [26]. This indicates that the conclusions derived from studies dealing with the interaction of excited state oxyluciferin with luciferase active site are now unsupported [10,15–22]. These studies were performed by using the adenylation step conformation, which was previously thought to be the only conformation employed by luciferase, and not the oxidation step enzymatic structure in which light emission is expected to take place.

Given all of these data, the present study has a main aim: theoretically study for the first time the effect of luciferase in the oxidative step conformation on the excited state of anionic keto

* Corresponding author. Fax: +351 226082959.
E-mail address: jcsilva@fc.up.pt (J.C.G. Esteves da Silva).

http://dx.doi.org/10.1016/j.cplett.2014.05.061
0009-2614/

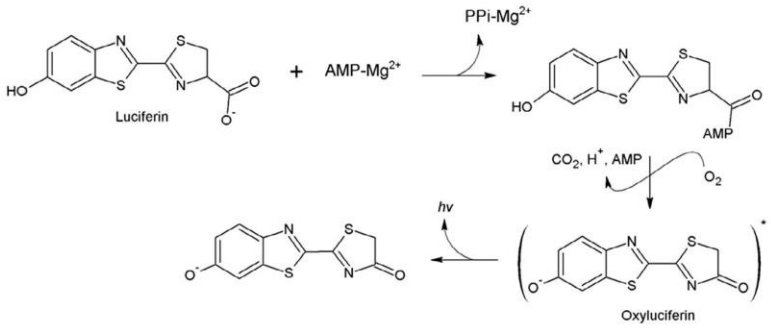

Figure 1. Schematic representation of firefly bioluminescence reaction.

oxyluciferin. To this end, we have employed a quantum mechanics/molecular mechanics (QM/MM) methodology, given its ability to provide detailed and down-to-atomistic level information. With the present Letter, we expect to provide valuable information regarding the multicolor bioluminescence mechanism.

2. Theoretical methodology

The PDB structure 4G37 (firefly luciferase in the second catalytic conformation, complexed with an adenylyl intermediate) was used as a starting structure. Hydrogen atoms were added by the Molprobity server [27]. Subsequently, the adenylyl intermediate and twenty active site residues were withdrawn from the PDB file: Arg218, His245, Gly246, Phe247, Thr251, Leu286, Ala313, Ser314, Gly315, Gly316, Arg337, Gln338, Gly339, Gly341, Leu342, Thr343, Thr346, Ser347, Ala348 and Lys443. The GaussView 5.0.8 software was then used to convert the adenylyl intermediate into oxyluciferin and AMP.

The emissive geometry of oxyluciferin, complexed with active site molecules, was obtained by using the ONIOM method [28]. Oxyluciferin was included in the Higher layer, while the remaining active site molecules were included in the Low layer. The excited state geometry of the luminophore was obtained at the time-dependent (TD) *w*B97XD/6-311G(d,p) level of theory [29,30]. The active site molecules were treated with the UFF force field with an electrostatic embedding scheme [31]. The excited state geometry of bare oxyluciferin was obtained at the TD *w*B97XD/6-311G(d,p) level of theory. All geometry calculations were performed *in vacuo*.

More accurate energies were obtained by performing single point calculations at the TD *w*B97XD/6-311+G(d,p)/UFF and TD *w*B97XD/6-311+G(d,p) level of theory, in the presence or absence of active site molecules respectively. TD *w*B97XD/6-311+G(d,p)/UFF calculations were performed in implicit solvent, by using the conductor-like polarizable continuum model (CPCM) [32]. We have done the implicit solvated calculations in dibutyl ether ($\varepsilon = 3.05$), as its dielectric constant is in line with values that are expected to account for the average effect of the protein and buried water molecules [33–35].

We have used the *w*B97XD functional due to good results in local $n \rightarrow \pi^*$ and $\pi \rightarrow \pi^*$, charge transfer and Rydberg excited states [36].

All calculations were done with the Gaussian 09 program package [37].

3. Results and discussion

The emissive geometry of anionic keto oxyluciferin, inside luciferase active site, was obtained by using the two-layer ONIOM method [28]. Excited state oxyluciferin was included in the High layer, while the Low layer was composed by active site residues and AMP. Both layers are presented in Figure 2.

Based on previous computational studies of photo-proteins, we have considered that luciferase may affect the color of light emitted by oxyluciferin by electrostatic effects and structural modifications of the bioluminophore [38,39]. Thus, we have defined the vertical emission of oxyluciferin inside luciferase (E_{em}^{luc}) as: $E_{em}^{luc} = E_{em}^{bare} + \Delta ES + \Delta STRUCT$. E_{em}^{bare} represents the *in vacuo* emission energy of a bare oxyluciferin molecule, optimized *in vacuo* in the absence of any other molecules. ΔES is the electrostatic effect by luciferase on the emission energy. This parameter was obtained by performing two single point calculations: one was an ONIOM calculation on excited state oxyluciferin complexed with active site molecules, in implicit solvent; the other was an *in vacuo* single point calculation on the ONIOM-derived excited state geometry of oxyluciferin, but without the active site molecules. So, the geometry of oxyluciferin used in both calculations was the same. However in the first calculation, oxyluciferin is subjected to electrostatic effects induced by intermolecular interactions with active site molecules and by the bulk protein, while these electrostatic effects are absent in the second calculation. Thus, the difference between these two calculations allowed us to obtain ΔES. $\Delta STRUCT$ was also obtained as a result of the difference between two single point calculations. Both were *in vacuo* emission energy calculations of bare oxyluciferin. However, one calculation was made at a geometry obtained

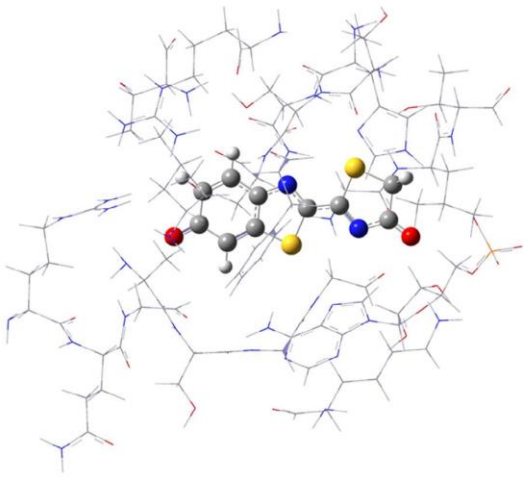

Figure 2. Representation of the complex between anionic keto oxyluciferin and active site molecules.

Table 1
Emission energies (in eV) and oscillator strengths of bare and luciferase complexed oxyluciferin, at TD *w*B97XD/6-311G+(d,p) and TD *w*B97XD/6-311G+(d,p)/UFF level of theory.

E_{em}^{luc}	E_{em}^{bare}	ΔES	$\Delta STRUCT$
2.398	2.542	−0.139	−0.005
f_{em}^{luc}	f_{em}^{bare}	ΔES	$\Delta STRUCT$
0.9265	0.7167	0.2177	−0.0079

in an ONIOM calculation involving active site molecules, while the other was obtained in the absence of any other compounds except for oxyluciferin. Similarly, we have defined the oscillator strength as $f_{em}^{luc} = f_{em}^{bare} + \Delta ES + \Delta STRUCT$. These results can be found in Table 1.

The obtained E_{em}^{luc} value (2.398 eV) is in line with the experimental one of ~2.206 eV, attributed to the typical bioluminescence of the *Photinus pyralis* species [1–5]. This small difference between theoretical and experimental results, within the error associated with density functionals, supports the reliability of our calculations [40–42].

Previous theoretical studies have indicated that the emission energy of oxyluciferin is sensitive to changes in the structure of the luminophore [43]. Given the very small contribution of $\Delta STRUCT$ to E_{em}^{luc}, we can say that luciferase has little effect in the geometry of firefly oxyluciferin. This small contribution of $\Delta STRUCT$ is also seen for f_{ex}^{luc}.

More significant is the electrostatic effect induced by luciferase. This effect can be explained in terms of internal and external Stark effects. The former effect arises from a protein cavity field that is associated with charged/polar active site. The latter effect is associated with external fields as applied electric fields or electrostatic fields from polar solvent molecules and bulk protein [44]. Following this line of thinking, Nogueira and co-workers demonstrated that the color shift of firefly bioluminophore can be described as a unified Stark effect [44]. The unified Stark effect in this Letter was achieved by introducing active site molecules (internal effect) and implicit solvation (external effect) into the calculations.

The emission energy of oxyluciferin is significantly red-shifted when subjected to the electrostatic field produced by luciferase. This is in line with previous studies that have emphasized the role of the enzyme in the color tuning mechanism, specially by electrostatic interactions [10,15–22,43,44]. This high sensitivity to the electrostatic field of luciferase makes it easy to understand the high range of possible firefly bioluminescence maximum, associated with pH changes, metal cations, changes of firefly species and amino acid mutations (~2.00–2.34 eV). The two later causes of multicolor bioluminescence are able to change the positioning/amino acid content of residues present in luciferase, which will lead to changes in the direction and/or magnitude of the electrostatic field of the enzyme. Metal cations should be attracted to luciferase in an electrostatic manner, due to its negative charge [45]. This electrostatic interaction is bound to affect the electrostatic field generated by luciferase, and so, affect the ΔES and consequently E_{em}^{luc}. Changes in pH can affect the emission by changing the concentration of water ions, and so, the electrostatic field generated by luciferase [44]. pH changes are also associated with conformational changes regarding luciferase, thus affecting the unified Stark field [10].

The electrostatic effect is also very important in the case of the oscillator strength. The analysis of Table 1 shows us that ΔES increase significantly f_{em}^{luc}, thus demonstrating that luciferase is able to increase the probability of oxyluciferin excited → ground state radiative decay. One should note that the quantum yield of a chemi/bioluminescence reaction is controlled by the efficiency of the ground state reaction, the efficiency of chemiexcitation and the efficiency of fluorescence of the emissive product [12,14]. Moreover, it is considered that bioluminescence reactions have higher quantum yields than chemiluminescence ones [1–5,12,14]. Our calculations indicate, that in the case of firefly bioluminescence, this higher quantum yield arise from a significant increase in the oscillator strength of the bioluminophore due to the electrostatic field generated by the enzyme.

Recent theoretical studies have suggested that the color of light emitted by oxyluciferin is modulated by changing, to different degrees, the energy of the excited and ground states [25,43]. As the energy of the states changes differently, the energy gap between them will become different, thus leading to new emission wavelengths. In order to further study this topic, we have calculated the energy of the excited and ground states of oxyluciferin in three different calculations: a single point calculation ONIOM calculation on oxyluciferin complexed with active site molecules, in implicit solvent (denoted Oxy_{ONIOM}); *in vacuo* single point calculation on bare oxyluciferin, at a geometry obtained in an ONIOM calculation on oxyluciferin complexed with active site molecules (denoted $Oxy_{in\ vacuo}$); and *in vacuo* single point calculation on bare oxyluciferin, at a geometry of bare oxyluciferin (denoted Oxy_{bare}). The emission energies of each oxyluciferin and the energy levels of the excited and ground states, which resulted from these three calculations, are presented in Table 2.

Oxy_{bare} and $Oxy_{in\ vacuo}$ present nearly identical emission energies. This results from the fact that both excited and ground states of $Oxy_{in\ vacuo}$ are stabilized by the same amount (~0.001 hartrees), in regard to Oxy_{bare}. As both states are stabilized by the same amount, there is no change in the energy gap between the excited and ground states of $Oxy_{in\ vacuo}$, thus resulting in the same emission energy as Oxy_{bare}. This was expected, given the results previously presented in this Letter. The only difference between $Oxy_{in\ vacuo}$ and Oxy_{bare} should be the geometry, as the former luminophore was optimized in the presence of luciferase active site molecules while the later was optimized in the absence of any molecules. However, as we have seen, luciferase induces only almost negligible effects on the geometry of oxyluciferin. For the contrary, Oxy_{ONIOM} is significantly red-shifted (0.14 eV) in comparison with both $Oxy_{in\ vacuo}$ and Oxy_{bare}. This occurs as Oxy_{ONIOM} is subjected to the electrostatic field induced by luciferase. In the case of Oxy_{ONIOM}, both the ground and excited states are significantly stabilized when compared with the cases of $Oxy_{in\ vacuo}$ and Oxy_{bare}. However, the excited state is more stabilized than the ground state (−0.049 *versus* ~−0.043 hartrees). This difference induces a decrease in the excited-ground states energy gap of ~−0.005 hartrees, which is converted to −0.139 eV (the difference between the emission of Oxy_{ONIOM} and $Oxy_{in\ vacuo}/Oxy_{bare}$). Thus, our calculations support the hypothesis that shifts in the emission are not achieved by stabilizing/destabilizing either the excited or ground state, but by affecting both states [20,35].

In Table 3 are the atomic Mulliken charges of the benzothiazole and thiazolone moieties of Oxy_{ONIOM}, $Oxy_{in\ vacuo}$ and Oxy_{bare}, in the ground and excited states. In all cases it can be seen that the ground state is more polar than the excited emissive one. Despite the negative charge being higher in the benzothiazole moiety, there is only a small difference between the charges of the moieties in the excited state. For the contrary, in the ground state the majority of the negative charge is placed in the benzothiazole moiety.

Table 2
Energies of both ground and excited states (in hartrees) of Oxy_{ONIOM}, $Oxy_{in\ vacuo}$ and Oxy_{bare}. The emission energies (in eV) are presented within parentheses.

	Oxy_{bare} (2.54)	$Oxy_{in\ vacuo}$ (2.54)	Oxy_{ONIOM} (2.40)
Ground state	−1440.442	−1440.441	−1440.485
Excited state	−1440.348	−1440.347	−1440.396

Table 3
Atomic Mulliken charges of the benzothiazole and thiazolone moieties, at both ground and excited states, of Oxy_{ONIOM}, $Oxy_{in\ vacuo}$ and Oxy_{bare}.

	Benzothiazole	Thiazolone
Oxy_{bare}		
Ground state	−0.673	−0.327
Excited state	−0.552	−0.446
$Oxy_{in\ vacuo}$		
Ground state	−0.674	−0.327
Excited state	−0.552	−0.448
Oxy_{ONIOM}		
Ground state	−0.709	−0.289
Excited state	−0.520	−0.479

The atomic charges of the two moieties are near identical when comparing $Oxy_{in\ vacuo}$ and Oxy_{bare}, which is expected given the similarity between their emission energies. Following this trend, the atomic charges of the benzothiazole and thiazolone moieties of Oxy_{ONIOM} are different than the ones presented by $Oxy_{in\ vacuo}$ and Oxy_{bare}. The ground state of Oxy_{ONIOM} is more polar than the same state of $Oxy_{in\ vacuo}$ and Oxy_{bare}, while the charge difference between the moieties in the excited state is even lower in Oxy_{ONIOM}. Navizet and co-workers have demonstrated that excited → ground state radiative decay of oxyluciferin leads to charge transfer from the thiazolone moiety to the benzothiazole ring [15]. Given this, they have postulated that destabilization of the charge on the benzothiazole moiety will stabilize the excited state relative to the ground state, thus decreasing the transition energy. This finding is supported by our calculations. We have seen that Oxy_{ONIOM} is the most red-shifted oxyluciferin, with regard to $Oxy_{in\ vacuo}$ and Oxy_{bare}, and that this is the molecule with lower negative charge in the benzothiazole moiety at the excited state. However, it should be noted that the charge distribution also changed in the ground state. At this state, the negative charge in the benzothiazole moiety of Oxy_{ONIOM} was the highest among Oxy_{ONIOM}, $Oxy_{in\ vacuo}$ and Oxy_{bare}. Moreover, we know that both states of Oxy_{ONIOM} were stabilized, and not only either the excited or the ground state.

Given these results, we think that the postulate made by Navizet and co-workers is incomplete [15]. While excited state charge transfer may stabilize/destabilize the excited state, the present and previous studies indicate that charge transfer also occur in the ground state, thereby also stabilizing/destabilizing this state [20,35]. As we have seen, the question regarding the color tuning mechanism should not be if a state is stabilized/destabilized, but the difference in the stabilization/destabilization between the emissive and ground states [20,35].

In the case of Oxy_{ONIOM} we have seen that charge transfer is more pronounced in the ground state, despite the fact that the most stabilized state was the excited state. Thus further studies are needed in order to verify if more factors are in play, other than charge transfer, or if the excited state is more sensible to charge transfer than the ground state. This possible higher sensitivity would explain why a lower charge transfer in the excited state is more stabilizing, than a higher charge transfer in the ground state.

4. Conclusions

We have employed a quantum mechanics/molecular mechanics (QM/MM) approach to study the color tuning mechanism of firefly bioluminescence. In order to achieve this goal we have used for the first time the crystal structure of firefly luciferase at the oxidative step conformation, the one from which light is emitted.

Our calculations demonstrated that firefly oxyluciferin is significantly affected by the electrostatic field generated by the enzyme. The emission energy is significantly affected by this, as well as the oscillator strength. Moreover, we have found that luciferase is able to increase the quantum yield of the bioluminescence reaction by increasing the oscillator strength of the bioluminophore. For the contrary, luciferase has an almost negligible effect on the structure of oxyluciferin.

Further calculations have supported previous findings that have stated that a shift in the emission is not achieved by stabilizing/destabilizing a given state, but by stabilizing/destabilizing the emissive and ground states. It is the different degree of stabilization/destabilization between the emissive and ground states that will determine the energy gap between these states, and consequently the emission energy.

Charge transfer processes were found to be involved in the color tuning mechanism as they have modulated the energy of both ground and excited states. However, we have seen that charge transfer is more pronounced in the ground state, despite the fact that the most stabilized state was the excited state. Thus, the question that remains is that if other factors are in play or if the excited state is more sensitive to charge transfer processes than the ground state.

Acknowledgments

Financial support from Fundação para a Ciência e Tecnologia (FCT, Lisbon) (Programa Operacional Temático Factores de Competitividade (COMPETE) e comparticipado pelo Fundo Comunitário Europeu (FEDER) (Project PTDC/QUI/71366/2006)) is acknowledged. A Ph.D. Grant to Luís Pinto da Silva (SFRG/BD/76612/2011), also attributed by FCT, is acknowledged.

Appendix A. Supplementary data

Supplementary data associated with this article can be found, in the online version, at http://dx.doi.org/10.1016/j.cplett.2014.05.061.

References

[1] S.M. Marques, J.C.G. Esteves da Silva, IUBMB Life 61 (2009) 6.
[2] S. Inouye, Cell. Mol. Life Sci. 67 (2010) 387.
[3] L. Pinto da Silva, J.C.G. Esteves da Silva, ChemPhysChem 13 (2012) 2257.
[4] J. Vieira, L. Pinto da Silva, J.C.G. Esteves da Silva, J. Photochem. Photobiol. B 117 (2012) 33.
[5] S. Hosseinkhani, Cell. Mol. Life Sci. 68 (2011) 1167.
[6] V.R. Viviani, F.G. Arnoldi, A.J. Neto, T.L. Oehlmeyer, E.J. Bechara, Y. Ohmiya, Photochem. Photobiol. Sci. 7 (2008) 159.
[7] E.H. White, E. Rapaport, H.H. Seliger, T.A. Hopkins, Bioorg. Chem. 1 (1971) 92.
[8] F. McCapra, D.J. Gilfoyle, D.W. Young, N.J. Church, P. Spencer, in: A.K. Campbell, L.J. Kricka, P.E. Stanley (Eds.), Bioluminescence and Chemiluminescence: Fundamental and Applied Aspects, Wiley, New York, 1994.
[9] B.R. Branchini, T.L. Southworth, M.H. Murtiashow, R.A. Magyar, S.A. Gonzalez, M.C. Ruggiero, J.G. Stroh, Biochemistry 43 (2004) 7255.
[10] T. Nakatsu, Y. Ichiyama, J. Hiratake, A. Saldanha, N. Kobashi, K. Sakata, H. Kato, Nature 440 (2006) 372.
[11] T. Hirano, Y. Hasumi, K. Ohtsuka, S. Maki, H. Niwa, M. Yamaji, D. Hashizume, J. Am. Chem. Soc. 131 (2009) 2385.
[12] I. Navizet, Y.J. Liu, N. Ferré, D. Roca-Sanjuán, R. Lindh, ChemPhysChem 12 (2011) 3064.
[13] J.Y. Hasegawa, K.J. Fujimoto, H. Nakatsuji, ChemPhysChem 12 (2011) 3106.
[14] L. Pinto da Silva, J.C.G. Esteves da Silva, J. Chem. Theory 7 (809) (2011) 809.
[15] I. Navizet, Y.J. Liu, N. Ferré, H.Y. Xiao, W.H. Fang, R. Lindh, J. Am. Chem. Soc. 132 (2010) 706.
[16] C.G. Min, A.M. Ren, J.F. Guo, L.Y. Zou, J.D. Goddard, C.C. Sun, ChemPhysChem 11 (2010) 2199.
[17] B.F. Milne, M.A. Marques, F. Nogueira, Phys. Chem. Chem. Phys. 12 (2010) 14285.
[18] D. Cai, M.A. Marques, F. Nogueira, J. Phys. Chem. B 115 (2011) 329.
[19] L. Pinto da Silva, J.C.G. Esteves da Silva, ChemPhysChem 12 (2011) 3002.
[20] L. Pinto da Silva, J.C.G. Esteves da Silva, J. Phys. Chem. B 116 (2012) 2008.
[21] Y.M. Rhee, H.W. Kim, J. Phys. Chem. B 117 (2013) 7260.
[22] C.I. Song, Y.M. Rhee, J. Am. Chem. Soc. 133 (2011) 12040.
[23] B.R. Branchini, M.H. Murtiashaw, R.A. Magyar, N.C. Portier, M.C. Ruggiero, J.G. Stroh, J. Am. Chem. Soc. 124 (2002) 2112.
[24] L. Pinto da Silva, ChemPhysChem 12 (2011) 951.

[25] S.F. Chen, Y.J. Liu, I. Navizet, N. Ferré, W.H. Fang, R. Lindh, J. Chem. Theory Comput. 7 (2011) 798.
[26] J.A. Sundlov, D.M. Fontaine, T.L. Southworth, B.R. Branchini, A.M. Gulick, Biochemistry 51 (2012) 6493.
[27] I.W. Davis et al., Nucleic Acids Res. 35 (2007) 375.
[28] S. Dapprich, I. Komáromi, K.S. Byun, K. Morokuma, M.J. Frisch, J. Mol. Struct. (Theochem) 462 (1999) 1.
[29] J.D. Chai, M. Head-Gordon, Phys. Chem. Chem. Phys. 10 (2008) 6615.
[30] R. Bauernschmitt, R. Ahlrichs, Chem. Phys. Lett. 256 (1996) 454.
[31] A.K. Rappé, C.J. Casewit, K.S. Colwell, W.A. Goddard III, W.M. Skiff, J. Am. Chem. Soc. 114 (1992) 10024–10035.
[32] V. Barone, M. Cossi, J. Phys. Chem. A 102 (1998) 1995.
[33] P.E.M. Siegbahn, L. Eriksson, F. Himo, M. Pavlov, J. Phys. Chem. B 102 (1998) 10622.
[34] P.J. Siegbahn, J. Am. Chem. Soc. 120 (1998) 8417.
[35] P.A. Fernandes, M.J. Ramos, J. Am. Chem. Soc. 125 (2003) 6311.
[36] C. Adamo, D. Jacquemin, Chem. Soc. Rev. 42 (2013) 845.
[37] M.J. Frisch et al., Gaussian 09, Revision A.02, Gaussian Inc., Wallingford, CT, 2009.
[38] K. Fukimoto, J.Y. Hasegawa, H. Nakatsuji, Chem. Phys. Lett. 462 (2008) 318.
[39] K. Fujimoto, J.Y. Hasegawa, S. Hayashi, H. Nakatsuji, Chem. Phys. Lett. 432 (2006) 252.
[40] L. Pinto da Silva, J.C.G. Esteves da Silva, Int. J. Quantum Chem. 113 (2013) 45.
[41] M.R. Silva-Junior, M. Schreiber, S.P. Sauer, W. Thiel, J. Chem. Phys. 14 (2008) 104103.
[42] D. Jacquemin, E.A. Perpète, I. Ciofini, C. Adamo, Theor. Chem. Acc. 128 (2011) 127.
[43] L. Pinto da Silva, J.C.G. Esteves da Silva, Theor. Chem. 988 (2012) 56.
[44] D. Cai, M.A.L. Marques, F. Nogueira, J. Phys. Chem. B 117 (2013) 13725.
[45] L. Pinto da Silva, J.C.G. Esteves da Silva, J. Comput. Chem. 32 (2011) 2654.

5.2. Study of $OxyLH_2$ Excited State Properties in Water and in Gas Phase

Article 18

Theoretical analysis of the color tuning mechanism of oxyluciferin and 5-hydroxyoxyluciferin

Luís Pinto da Silva and Joaquim C.G. Esteves da Silva

Comput. Theor. Chem. **2012**, *988*, 56-62.

The theoretical calculations and the writing of the paper were performed by Luís Pinto da Silva, under supervision of Professor Esteves da Silva.

Computational and Theoretical Chemistry 988 (2012) 56–62

Contents lists available at SciVerse ScienceDirect

Computational and Theoretical Chemistry

journal homepage: www.elsevier.com/locate/comptc

Theoretical analysis of the color tuning mechanism of oxyluciferin and 5-hydroxyoxyluciferin

Luís Pinto da Silva, Joaquim C.G. Esteves da Silva *

Centro de Investigação em Química (CIQ-UP), Departamento de Química e Bioquímica, Universidade do Porto, Campo Alegre 687, 4169-007 Porto, Portugal

ARTICLE INFO

Article history:
Received 12 December 2011
Received in revised form 22 February 2012
Accepted 22 February 2012
Available online 3 March 2012

Keywords:
Bioluminescence
Oxyluciferin
Color tuning
Intermolecular interactions
Fluorescence
Oxyluciferin analogues

ABSTRACT

Firefly luciferase exhibits a multicolor bioluminescence, which is caused by the modulation of the emission of oxyluciferin by intermolecular interactions. One of the objectives of the present paper was analyze the possible effect of the charge density of the emitter in the color tuning. Theoretical calculations on oxyluciferin, and its respective moieties, demonstrated that no correlation between charge density and light emission can be found once solvent effects are considered. Further computational calculations demonstrate that intermolecular interactions modulate the emission by affecting the geometry of oxyluciferin, which controls the energy gap between the excited and ground state. Direct intermolecular interactions and polarity also affect the color of emission of oxyluciferin, by the same mechanism. Also, the effect of charge density modulation of Keto-(−1). A novel emitter, 5-hydroxyoxyluciferin, was considered and demonstrated to be more red-shifted that oxyluciferin.

1. Introduction

Bioluminescence is a phenomenon that occurs in living organisms in which an excited state substance is produced in an enzyme-catalyzed chemical reaction [1]. This product decays to the ground level, by emitting light. Bioluminescence is widespread in nature and has roles in sexual communication, appealing to prey and disguising. The most studied bioluminescence system is that of the North-American firefly, *Photinus pyralis* [1]. This type of insect uses an enzyme, firefly luciferase (Luc, EC 1.13.12.7), to catalyze the formation of the light emitter oxyluciferin ($OxyLH_2$) [1]. This formation occurs in a two-step reaction: in the first step, Luc catalyzes the reaction between firefly luciferin (LH_2) and adenosine-5′-triphosphate (ATP), which results in the formation of an adenylyl intermediate; in the second step, this intermediate is oxidized into $OxyLH_2$. This latter molecule is very important in this system, as besides being the light emitter, it appears to be one of the substances responsible for the flash-profile of light emitted [2–5]. The flash-profile is a term used to define the *in vitro* pattern of light emission. The *in vitro* emission of light follows, under well-defined conditions a flash pattern, with a rise in the intensity of emission that decays to low levels in a few seconds. This profile is attributed to the formation of inhibitory products, one of which is $OxyLH_2$ (competitive inhibitor of LH_2) [2–5]. In recent years, the existent bioluminescence systems have gained numerous biomedical, bioanalytical and pharmaceutical applications, among others. More specifically, it is involved in the analytical determination of adenosine-5′-triphosphate (ATP), in microbial detection, biosensing, bioimaging and is used as a gene reporter [1,6–10].

One of the more interesting and relevant characteristic of the firefly bioluminescence is its multicolor variation [1,11]. Luc is a pH-sensitive enzyme, which affects the color of the emitted light. At basic pH (pH ~7.5), $OxyLH_2$ emission has a peak at 562 nm. At acid pH (~5–6), the emission shifts to the red region of the visible spectrum (maximum at 620 nm) [11]. The understating of this feature could be of incredible importance in bioluminescence research. Lower energy emitting Luc could be used in *in vivo* medical imaging, as red light is absorbed very poorly in comparison with natural emitted light. Viviani et al. also hypothesized that the control of the multicolor bioluminescence could be used in the development of Luc as a single dual reporter gene, as a bioindicator of cellular stress and as a probe for intracellular changes of pH [12].

Numerous authors have tried to explain the color tuning mechanism. These researchers considered keto-enol tautomerism [13], rotation of the C–C bond between the benzothiazole and thiazolone rings [14], control of the resonance form of $OxyLH_2$ [15], interaction of the light emitter with a protonated basic moiety present in Luc active site [16], and the polarity and rigidity of the active site [17]. More information, regarding these and other studies, could be encountered in these four very recent reviews [11,18–20]. For the accurate study of the firefly bioluminescence is required the identification of the bioluminophore. However, the identification of Keto-(−1) as the light emitter (Fig. 1) was only achieved recently

* Corresponding author. Tel.: +351 220 402 569; fax: +351 220 402 659.
E-mail address: jcsilva@fc.up.pt (J.C.G. Esteves da Silva).

2210-271X/$ - see front matter © 2012 Elsevier B.V. All rights reserved.
doi:10.1016/j.comptc.2012.02.029

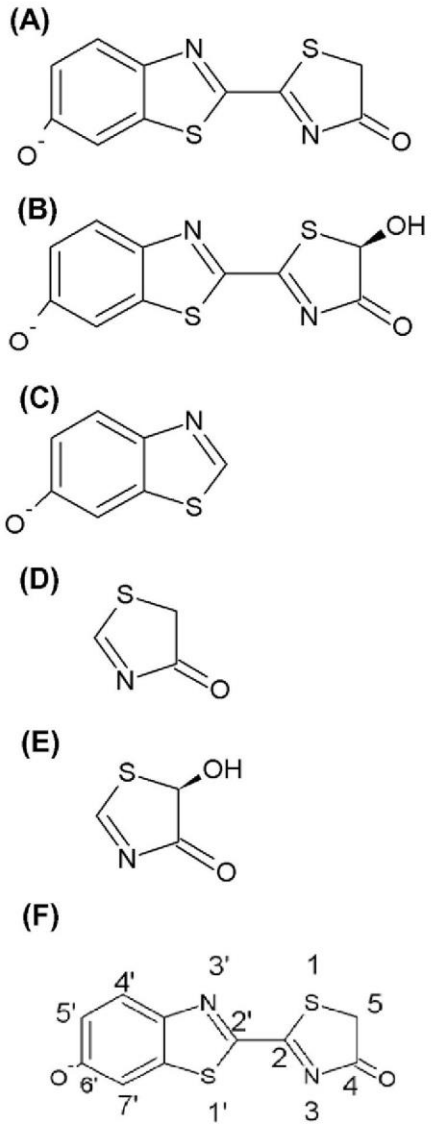

Fig. 1. Chemical structure of Keto-(−1) (A), HOxyLH2 (B), Keto-(−1) and HOxyLH2 benzothiazole moieties (C), Keto-(−1) (D) and HOxyLH2 (E) thiazolone moieties (F) indicates the numbering of the atoms of Keto-(−1).

by three different computational approaches: analysis of the dissociation and tautomeric constants of $OxyLH_2$ as a function of pH [21]; study of the direct excited-state product of firefly dioxetanone [22]; study of the possibility of keto-enol tautomerism in *Luciola cruciata* Luc (LcLuc) active site [23].

Theoretical calculations on Keto-(−1) complexed with small molecules revealed that intermolecular interactions have a very significant effect in the color tuning mechanism, by originating different emission wavelengths for the same luminophore [21,24–26]. The key importance of intermolecular interactions was further demonstrated by computational studies of the light emission of Keto-(−1) in both Luc and LcLuc active sites [23,27–31]. Overall, it is thought that the most important intermolecular interactions are electrostatic, hydrogen-bonding and π–π stacking. Furthermore, the color of bioluminescence is also modulated by the polarity of the microenvironment [16,17,24–27,30,32]. Therefore, the effect of active site molecules in the emission maxima of Keto-(−1) is fairly clarified. However, in order to rationally tune the color of bioluminescence we need to understand why intermolecular interactions have this effect on the excited state of the luminophore. Several groups have proposed that shifts in the emission are controlled by modulation of the charge density of the emitter, but no conclusive proof of this has been presented so far [15,23,27,28,30].

The objective of the computational study is the further clarification of the color tuning mechanism. To this end we have studied the first excited state of Keto-(−1) and of its benzothiazole and thiazolone moieties, separately (Fig. 1), both *in vacuo* and in solution (explicit and explicit/implicit water). Within this work, we intend to study the delocalization of charge within the moieties of the emitter and its effect on light emission. Also if intermolecular interactions modulate the color of emission by modifying the charge density of the emitter, it is reasonable to assume that the same effect can be achieved by altering the chemical structure of $OxyLH_2$. Therefore, to prove this assumption we have studied (*in vacuo*, and in explicit and explicit/implicit water) the photophysical properties of the first excited state of a novel emitter, 5-hydroxyOxyLH$_2$ ($HOxyLH_2$) and its separate moieties (Fig. 1). With these calculations, we could compare the properties of these molecules that caused their different wavelength maxima. However, our calculations demonstrated that charge density modulation cannot explain the color tuning mechanism. Further calculations on the ground and excited state of Keto-(−1) and $HOxyLH_2$, revealed that intermolecular interactions modulate the emission by modifying the geometry of the emitter and by direct interaction. These two factors can then red-shift the emission by decreasing the energy gap between the emitting excited state and the ground state. The polarity of the microenvironment modulates the color of emission by the same mechanism.

2. Computational methods

The initial structures of Keto-(−1) and $HOxyLH_2$ were constructed with the software Avogadro [33]. An initial guess was obtained by using Avogadro geometry optimization function, and subsequent ground state optimizations were performed by using the Density Functional Theory (DFT) functional O3LYP [34–36] and the 6-31+G(d,p) basis set, with no solvent effects. The excited state geometries were obtained by using configuration interaction with single excitations (CIS) [37] and the 6-31G(d) basis set. The first excited state refers to a fluorescence state (π–π^* excitation). We have used the CIS method for excited state geometry optimizations as other authors have stated that it can be compared with methods of higher levels of theory [28]. The separated moieties were obtained by substitution of the other moiety with a hydrogen atom, with the software Avogadro. This approach was adopted by the fact that our objective was to study the effect of charge transfer in the color tuning mechanism. So, with this approach there are not changes in geometry between a sole moiety and its corresponding moiety in the full emitter, which could influence the emission of the studied molecules. The emission energies of the emitters were computed at the time-dependent (TD) [38,39] O3LYP/6-31+G(d,p) level of theory, with no solvent effects. Despite some critics to the use of TD-DFT in the study of the multicolor bioluminescence, due to errors regarding charge transfer (CT) states [40,41] the work of another authors demonstrated that CT is small on planar $OxyLH_2$, devaluing this flaw of TD-DFT [42]. Moreover this functional provided good results for dehydroluciferin, an $OxyLH_2$ analogue [43].

To study the effect of intermolecular interactions in the emission of Keto-(−1), $HOxyLH_2$ and respective moieties, molecular mechanics methods were used. TIP3P water molecules were added

up to 12 Å by the LEAP module of the AMBER 11 suite of programs [44]. The excited state CIS/6-31G(d) geometries of the emitters were used in their parameterization with the ANTECHAMBER module of AMBER and the general AMBER force field [45]. One phase of energy minimizations (30,000 steps) was performed, by using the Not (just) Another Molecular Dynamics program (NAMD) molecular dynamic code with AMBER potential functions, parameters and file formats [46]. In this process, the Particle Mesh Ewals method was used to include the long-range interactions [47]. All the minimization steps were performed in a NVT ensemble, with a temperature of 298.15 K. In the end of the minimizations, the studied molecules and the water molecules up to 3 Å were withdrawn from the six final structures. These models were then subjected to emission energies calculation, at the TD-O3LYP/6-31+G(d) level of theory. The basis set used in these calculations was reduced, due to the high number of atoms involved. Some calculations were performed with implicit solvation, by using the conductor-like polarized continuum model (CPCM) [48]. The dielectric constant used was that of water. All DFT/TD-DFT/CIS calculations were carried out with the Gaussian 03 program package [49].

3. Results and discussion

The emission wavelength and the oscillator strength of Keto-(−1), $HOxyLH_2$ and respective moieties are indicated in Table 1. In Table 2 are indicated the atomic Mulliken charge of the benzothiazole and the thiazolone moieties of the emitters. Analysis of Table 1 shows that *in vacuo* Keto-(−1) and $HOxyLH_2$ are green emitters. The benzothiazole moieties of Keto-(−1) and $HOxyLH_2$ are violet emitters, while theirs thiazolone moieties emit outside of the visible spectrum.

Analysis of Tables 1 and 2 indicates that charge density modulation may explain the multicolor light emission. In the case of Keto-(−1) and its benzothiazole moiety, there is effectively a decrease of the negative charge in this moiety with increasing emission wavelength (405–504 nm). There is also an increase in the negative charge of the thiazolone moiety of Keto-(−1) with increasing wavelength maxima (287–504 nm). It should be noted that the negative charge of the sole benzothiazole moiety is much higher than in Keto-(−1). The inverse is true for the sole thiazolone moiety, which negative charge is lower than in Keto-(−1). This indicate that, when in conjunction by forming Keto-(−1), there is a delocalization of the negative charge from the benzothiazole to the thiazolone moiety. This delocalization may then be responsible for the higher wavelength maximum observed for the bioluminescence emitter, $OxyLH_2$. In the case of $HOxyLH_2$, a higher negative charge is also seen in its sole benzothiazole moiety (386 nm) than in its full form (510 nm). For the thiazolone moiety, an increase in the negative charge is accompanied by an increase in the emission wavelength (245–510 nm).

Table 1
Emission wavelength (λ_{em}, in nm) and oscillator strength (f) of Keto-(−1), $HOxyLH_2$ and their respective moieties.

	TD-O3LYP/6-31+G(d,p)	
	λ_{em}	F
Keto-(−1)	504	0.5442
Keto-(−1) benzothiazole moiety	405	0.0469
Keto-(−1) thiazolone moiety	287	0.0836
$HOxyLH_2$	510	0.5452
$HOxyLH_2$ benzothiazole moiety	386	0.2290
$HOxyLH_2$ thiazolone moiety	245	0.0510

Table 2
Atomic Mulliken charges of Keto-(−1), $HOxyLH_2$ and their respective moieties.

	TD-O3LYP/6-31+G(d,p)	
	Benzothiazole moiety	Thiazolone moiety
Keto-(−1)	−0.691	−0.311
Keto-(−1) benzothiazole moiety	−1.139	
Keto-(−1) thiazolone moiety	−0.199	
$HOxyLH_2$	−0.679	−0.322
$HOxyLH_2$ benzothiazole moiety	−1.139	
$HOxyLH_2$ thiazolone moiety	−0.205	

Having studied these six emitters *in vacuo*, we have passed to the study of the effect exerted by intermolecular interactions in the emission of these molecules. This type of study can be used to try to extrapolate the possible behavior of these emitters in the active site of Luc, and to further confirm the mechanism by which the intermolecular interactions affect the emission of $OxyLH_2$ and analogs. We have chosen to perform this subsequent study in explicit and implicit water, as the choice of a more homogeneous microenvironment is expected to simplify the effect exerted by intermolecular interactions in the excited state properties of the emitters. Thereby allowing focusing in the internal modifications of Keto-(−1) and analogs, which affect the color of light emitted. Furthermore, it should be noted that recent works are highlighting the importance of studying this type of system by modeling correctly both implicit and explicit solvation, due to their color tuning capability [21,24,27,50].

In Table 3 are presented the emission wavelength and oscillator strengths of Keto-(−1), $HOxyLH_2$ and respective moieties, in explicit water and in explicit/implicit water. These models were obtained by performing molecular mechanics based calculations using NAMD, as indicated in the Computational methods section. The geometries of the emitters, which resulted from the molecular mechanics calculations, were also used in *in vacuo* calculations of the wavelength maxima. Analysis of these results further supports our working hypothesis. The emission maxima of the emitters, when solvated with explicit and/or implicit water, suffer from significant shifts when in comparison with the *in vacuo* emission energies (Table 3). Keto-(−1) is still a green emitter, but suffers from a red-shift of 9–14 nm. The emission of the benzothiazole moiety of Keto-(−1) is also affected, with a blue-shift of 18–32 nm, falling outside of the visible spectrum. For the contrary, the thiazolone moiety is red-shifted (5–58 nm). $HOxyLH_2$ suffers from a significant red-shift. When explicit and explicit/implicit solvation is considered, a red-shift of 20–30 nm is verified. Thus, the present results further state that intermolecular interactions can affect the color of the emission, which is also modulated by the polarity of the microenvironment. We also wish to note the good correlation between the emission maxima of Keto-(−1) in explicit and explicit/implicit water with known experimental results [32].

Having analyzed the emission wavelength of Keto-(−1) and analogs in solution, we have studied their atomic Mulliken charge in order to verify if the mechanism of charge density modulation still applies in these calculations. These results are presented in Table 4.

By comparing the atomic charges, we see that the blue-shifted sole benzothiazole moiety of Keto-(−1) has always a higher negative charge than the benzothiazole moiety of the red-shifted full Keto-(−1). However, the negative charge of the benzothiazole moiety of full Keto-(−1) increases with increasing wavelength maximum, when we compare *in vacuo* Keto-(−1) and the emitter in explicit water. In the comparison between explicit and explicit/implicit models, the negative charge of the benzothiazole of full Keto-(−1) decreases with increasing emission wavelength. For the contrary, in the case of the sole benzothiazole moiety, its negative charge decreases with decreasing emission wavelength. This indi-

Table 3
Emission wavelength (λ_{em}, in nm) and oscillator strength (f) of Keto-(−1), HOxyLH$_2$ and their respective moieties, at the TD-O3LYP/6-31+G(d) level of theory.

	In vacuo		Explicit water		Explicit/implicit water	
	λ_{em}	f	λ_{em}	f	λ_{em}	f
Keto-(−1)	541	0.4865	554	0.2784	563	0.5412
Keto-(−1) benzothiazole moiety	412	0.1507	394	0.1049	362	0.2230
Keto-(−1) thiazolone moiety	216	0.0995	274	0.0677	279	0.1208
HOxyLH$_2$	540	0.4566	560	0.2975	590	0.4692
HOxyLH$_2$ benzothiazole moiety	413	0.1548	391	0.1563	376	0.1934
HOxyLH$_2$ thiazolone moiety	290	0.0632	401	0.0052	325	0.0154

Table 4
Atomic Mulliken charges of Keto-(−1), HOxyLH$_2$ and their respective moieties, at the TD-O3LYP/6-31+G(d) level of theory.

	In vacuo		Explicit water		Explicit/implicit water	
Keto-(−1)	−0.790	−0.209	−1.301	−0.229	−1.275	−0.146
Keto-(−1) benzothiazole moiety	−1.191		−1.732		−1.674	
Keto-(−1) thiazolone moiety	−0.253		−0.375		−0.378	
HOxyLH$_2$	−0.620	−0.380	−0.915	−0.992	−0.814	−0.961
HOxyLH$_2$ benzothiazole moiety	−1.191		−1.827		−1.793	
HOxyLH$_2$ thiazolone moiety	−0.259		−0.482		−0.425	

cates that for the benzothiazole moiety of Keto-(−1), no visible trend can be observed regarding the control of the color of light emitted by charge density modulation. For the thiazolone moiety of Keto-(−1), the situation is similar. The negative charge of the thiazolone moiety of red-shifted full Keto-(−1) is always smaller than the negative charge of its blue-shifted sole thiazolone moiety. When we compare the emission of *in vacuo* and in explicit solvent of full Keto-(−1), it can be seen that the negative charge of the thiazolone moiety increases with increasing emission wavelength. For the contrary, for the comparison between explicit and explicit/implicit solvent, the negative charge of the thiazolone moiety decreases with increasing wavelength maximum. For the sole thiazolone moiety of Keto-(−1), the negative charge increases with increasing emission wavelength. In conclusion, the present results indicate that there is no correlation between the charge density of Keto-(−1) and its emission wavelength. Therefore, and contrary to our expectations, the modulation of charge density is not involved in the color tuning mechanism of Keto-(−1).

Analysis of Table 4 indicates that charge density modulation may also not be involved in the color tuning mechanism of HOxyLH$_2$. The negative charge of its blue-shifted sole benzothiazole moiety is always higher than the negative charge of the benzothiazole of the red-shifted full HOxyLH$_2$. For the sole benzothiazole moiety of HOxyLH$_2$, there is an increase in the negative charge with decreasing wavelength maximum, when we compare the *in vacuo* and the explicit solvation results. In the comparison between the explicit and explicit/implicit solvation results, the negative charge of the sole benzothiazole moiety decreases with decreasing emission wavelength. The behavior of the benzothiazole moiety of full HOxyLH$_2$ is identical to that of its sole benzothiazole moiety. For the thiazolone moiety of HOxyLH$_2$, its negative charge is always higher in the full form of the emitter than in the sole moiety. For both the full form and the sole thiazolone moiety of HOxyLH$_2$, its negative charge is higher when only explicit solvation is used, despite the higher emission wavelength being calculated in other solvation conditions.

The results presented so far in this paper further demonstrate that intermolecular interactions can effectively modulate the emission wavelength of OxyLH$_2$ and analogs. However intermolecular interactions do not tune the color of emission by modulating the charge density of the emitter. Thus other factors are responsible for the modulation, by intermolecular interactions, of the color of light emitted by Keto-(−1) and analogs. Comparison between the emission wavelength presented in Tables 1 and 3, demonstrates that there is a more significant shift in the emission between the *in vacuo* results of the two tables, than between the comparison between the *in vacuo* and explicit solvent results of Table 3. It should be pointed out that the gas phase emission wavelength of Keto-(−1) (504 nm) and HOxyLH$_2$ (511 nm), at the TD-O3LYP/6-31+G(d), are very similar to the ones calculated at the TD-O3LYP/6-31+G(d,p) level of theory (Table 1). This indicates that the most important effect exerted by intermolecular interactions is the modulation of the excited state geometry of the emitter, thereby modulating the energy level of the excited state. If intermolecular interactions could decrease the energy of the excited state, in the comparison with the gas phase, it could explain the red-shift of the emission. To test this hypothesis we have calculated the *in vacuo* (from the geometries represented in Fig. 1) and solvated bond lengths of Keto-(−1) and HOxyLH$_2$. The bond lengths are represented in Fig. 2. Also, as the thiazolone moieties of the emitters present some distortion when in comparison with the *in vacuo* structures, the angles of the thiazolone moieties are presented in Table 5.

Analysis of both Fig. 2 and Table 5, it can be seen that intermolecular interactions effectively induce changes in the geometry of the emitters. In solution, the thiazolone moiety of both Keto-(−1) and HOxyLH$_2$ suffers from clear distortion. Moreover, despite not being drastic, it can be seen that the interaction with water molecules caused changes in the bond lengths of the emitters. In Keto-(−1), this change is more clearly seen in the benzothiazole moiety. For the contrary, in the case of HOxyLH$_2$, the thiazolone moiety appears to be the one more affected by intermolecular interactions. Thus, this indicates that intermolecular interactions modulate slightly the excited state geometry of the emitter, which is in line with the clear but not drastic shift in the emission wavelength. To analyze this new hypothesis, we have calculated the stability of Keto-(−1) and HOxyLH$_2$ different geometries. With this objective, we have calculated the energies of those geometries both at the excited and ground state, which are presented in Table 6. For a better comparison, the energies of the solvated geometries of the emitters were calculated without any explicit or implicit solvation. By analysis of this Table, it can be seen that gas phase and solvated geometries, of both molecules, have different energies in both the ground and excited state. In the case of Keto-(−1), the solvated geometry is 0.038 hartrees less stable (in the ground state) than the gas phase geometry. In the excited state, the solvated geometry

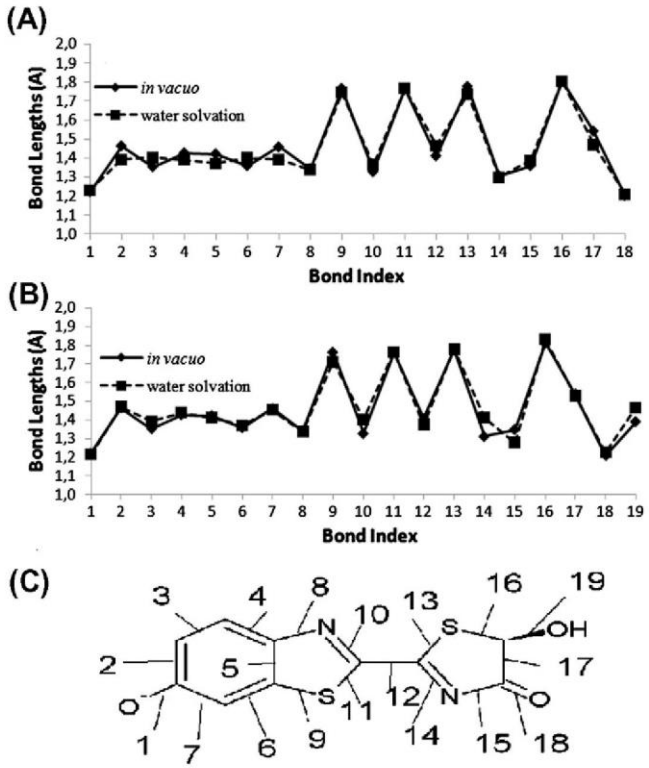

Fig. 2. Bond lengths of the excited state of Keto-(−1) (A), and HOxyLH2 (B). (C) identify the bond numbers used in the above graphics.

Table 5
Angles (in degrees) of the thiazolone moiety of excited state Keto-(−1) and $HOxyLH_2$, both in the gas phase and in water.

Angles	Keto-(−1)		$HOxyLH_2$	
	Gas phase	Water	Gas phase	Water
$C_{2'}-C_2-S_1$	119.07	122.89	119.43	124.26
$C_{2'}-C_2-N_3$	123.58	121.21	123.03	121.41
$C_2-S_1-C_5$	88.87	87.58	88.62	90.76
$N_3-C_4-C_5$	113.66	109.51	114.66	120.58
C_5-C_4-O	120.07	123.16	117.69	124.57
C_4-C_5-OH			110.56	117.83

Table 6
Energies (in hartrees) of the ground and excited state Keto-(−1) and $HOxyLH_2$, at the TD-O3LYP/6-31+G(d) and O3LYP/6-31+G(d) level of theory.

	Keto-(−1)		$HOxyLH_2$	
	Gas phase geometry	Solvated geometry	Gas phase geometry	Solvated geometry
Ground state	−1440.278	−1440.240	−1515.459	−1515.406
Excited state	−1440.188	−1440.155	−1515.370	−1515.322

is 0.033 hartrees less stable than the gas phase geometry. In the case of $HOxyLH_2$, the solvated geometry is 0.053 hartrees less stable (in the ground state) than the gas phase geometry. In the excited state, the solvated geometry is 0.048 hartrees less stable than the gas phase geometry. Thus, these results indicate that modulation of the geometry can affect the energy of both ground and excited states. Moreover, the different destabilization of the ground and excited state energies of Keto-(−1), by solvent-dependent geometry modification, caused a 0.006 hartrees decrease in the energy gap between the two states. This decrease corresponds to a 37 nm red-shift, which is the shift verified between the emission of the gas phase (504, Table 1) and the solvated geometry (541, Table 3) of Keto-(−1). The destabilization of the ground and excited states of $HOxyLH_2$ caused a 0.005 hartrees decrease in the energy gap between the two states, which corresponds to a 30 nm red-shift. Indeed, this was the red-shift verified between the emission of the gas phase (510, Table 1) and the solvated geometry (540, Table 3) of $HOxyLH_2$. Therefore, with these results we can state that changes in the geometry of the emitter affect the energy of both the ground and excited states, but with different extents. These differences in the stabilization/destabilization of both states will modify the energy gap between the ground and excited state, thereby originating shifts in the emission.

Having determined the effect exerted by the modulation of the geometry of the emitter in the emission, we have tried to understand the effect exerted by direct intermolecular interactions between the emitter and other molecules, and by polarity of the microenvironment. The presented study indicated that these factors can red- or -blue-shift the emission by modulating the energy gap between the ground and excited state, of the studied emitter. To test this hypothesis, we have calculated the energy, of both the excited and ground state, of Keto-(−1) and $HOxyLH_2$ in explicit and explicit/implicit water. The same geometries were also used in *in vacuo* calculations. The results, calculated at the TD-O3LYP/6-31+G(d) level of theory, are presented in Table 7.

These results further demonstrate the effect exerted by direct intermolecular interactions and polarity. For Keto-(−1), we can see that direct intermolecular interactions diminishes the energy gap between the ground and excited, explaining the 13 nm red-shift (541–554 nm, Table 3). When an implicit solvation is introduced in the calculations, a further decrease in the energy gap be-

Table 7
Energies (in hartrees) of the ground and excited state Keto-(−1) and $HOxyLH_2$, at the TD-O3LYP/6-31+G(d) and O3LYP/6-31+G(d) level of theory.

	Keto-(−1)		$HOxyLH_2$	
	Ground state	Excited state	Ground state	Excited state
In vacuo	−1440.240	−1440.155	−1515.406	−1515.322
Explicit water	−2357.026	−2356.944	−2814.185	−2814.104
Explicit/implicit water	−2357.193	−2357.113	−2814.390	−2814.313

tween the ground and excited state is observed. This decrease is also in line with the 22 nm red-shift (541–563 nm, Table 3). Intermolecular interactions and polarity modulate the emission of $HOxyLH_2$ in a similar way.

In conclusion, our results indicate that the emission maxima of $OxyLH_2$ and analogues are modulated by three different factors: direct intermolecular interactions; modulation of their geometry, also controlled by intermolecular interactions; polarity of the microenvironment. Furthermore, all of these factors appear to control the color of emission by affecting both the energy of the ground and of the excited state. This allows us to define a mechanism for the different wavelength maxima verified for the various firefly luciferases (538–623 nm) [12]. All of these enzymes present, with various extents, active sites with different amino-acids constitutions. This will lead to different types and/or strength of intermolecular interactions that the active site molecules can perform with the universal firefly bioluminophore (Keto-(−1)). These differences will then affect the emission by modulating differently the geometry of Keto-(−1), and by direct intermolecular interaction (also depending of the constitution of the active site). Also, the different constitution of the active site will affect its polarity, leading to more tuning of the color of bioluminescence. Therefore, if the differences in types/strength of intermolecular interactions and polarity are small between the active sites of different luciferases, the differences between the emission maxima will also be small. This can be seen in the small differences between the green maxima presented by various luciferases (538–570 nm) [12]. If the differences between the active sites are more significant, the difference between the wavelength maxima will also be more relevant. This can be seen in the difference between the emission of LcLuc at basic (561 nm) and at acid pH (609 nm), which is thought to be caused by different conformations of the active site [17,27].

4. Conclusion

In this paper we have studied the role of intermolecular interactions and polarity in the light emission of Keto-(−1) and a novel emitter, $HOxyLH_2$. This study was performed calculating the first excited state of the emitters, and their separate moieties, at the CIS and TD-DFT level of theory. Further calculations were performed in explicit and explicit/implicit water, by means of molecular mechanics energy minimizations and TD-DFT calculations.

The results obtained in this paper allow us to define the color tuning mechanism of Keto-(−1), both in solution and in Luc active site (by extrapolation). Our results demonstrate that intermolecular interactions can affect the geometry of the emitter, thus modulating the energy difference between the emitting excited and ground, which can originate different emission wavelengths. Besides affecting the geometry of the emitter, direct intermolecular interactions between Keto-(−1) and other molecules can further affect the energy difference between the ground and excited state. The polarity of the microenvironment can also modulate the emission, by modulating the energy gap between the emitting excited and ground states. Therefore different solvents and different active site conformations/constitutions, originate different intermolecular interactions networks between the emitter and other neighboring molecules, leading to different energy gaps and subsequently different emission wavelengths. This mechanism can then explain the different emission wavelength of Keto-(−1) in different solvents, in different Luc species and at different pH (due to its effect in pH-sensitive Luc).

A novel emitter was also considered, by hydroxylation of the C_5 carbon of Keto-(−1). $HOxyLH_2$ could be of use in *in vivo* Luc-based applications, due to its higher emission wavelength.

Acknowledgments

Financial support from Fundação para a Ciência e a Tecnologia (FCT, Lisbon), Programa Operacional Temático Factores de Competitividade (COMPETE) e comparticipado pelo Fundo Comunitário Europeu (FEDER) (Project PTDC/QUI/71366/2006) is acknowledged. A PhD Grant to Luís Pinto da Silva (SFRH/BD/76612/2011) from Fundação para a Ciência e Tecnologia (FCT, Lisbon) is acknowledged.

References

[1] S.M. Marques, J.C.G. Esteves da Silva, Firefly bioluminescence: a mechanistic approach of luciferase catalyzed reactions, IUBMB Life 61 (2009) 6–17.
[2] J.C.G. Esteves da Silva, J.M.C.S. Magalhães, R. Fontes, Identification of enzyme produced firefly oxyluciferin by reverse phase HPLC, Tetrahedron Lett. 42 (2001) 8173–8176.
[3] C. Ribeiro, J.C.G. Esteves da Silva, Kinetics of inhibition of firefly luciferase and oxyluciferin and dehydroluciferyl-adenylate, Photochem. Photobiol. Sci. (2008) 1085–1090.
[4] J.M. Leitão, J.C.G. Esteves da Silva, Firefly luciferase inhibition, J. Photochem. Photobiol. 101 (2010) 1–8.
[5] L. Pinto da Silva, J.C.G. Esteves da Silva, Kinetics of inhibition of firefly luciferase by dehydroluciferyl-coenzyme A, dehydroluciferin and l-luciferin, Photochem. Photobiol. Sci. 10 (2011) 1039–1045.
[6] A. Roda, P. Pasini, M. Mirasoli, E. Michelini, M. Guardigli, Biotechnological applications of bioluminescence and chemiluminescence, Trends. Biotechnol. 22 (2004) 295–303.
[7] K.E. Luker, G.D. Luker, Applications of bioluminescence imaging to antiviral research and therapy: multiple luciferases enzymes and quantitation, Antiviral Res. 78 (2008) 179–187.
[8] F. Fan, K.V. Wood, Bioluminescent assays for high-throughput screening, Assay Drug Dev. Technol. 5 (2007) 127–136.
[9] B.R. Branchini, T.R. Southworth, N.F. Khattak, E. Michelini, A. Roda, Red- and green-emitting firefly luciferase mutants for bioluminescent reporter applications, Anal. Biochem. 345 (2005) 140–148.
[10] T.C. Doyle, S.M. Burns, C.H. Contag, In vivo bioluminescence imaging for integrated studies of infection, Cell Microbiol. 6 (2004) 303–317.
[11] L. Pinto da Silva, J.C.G. Esteves da Silva, Computational studies of the luciferase light-emitting product: oxyluciferin, J. Chem. Theory Comput. 7 (2011) 809–817.
[12] V.R. Viviani, F.G.C. Arnoldi, A.J.S. Neto, T.L. Oehlmeyer, E.J.H. Bechara, Y. Ohmiya, The structural origin and biological function of pH-sensitivity in firefly luciferases, Photochem. Photobiol. Sci. 7 (2008) 159–169.
[13] E.H. White, E. Rapaport, H.H. Seliger, T.A. Hopkins, The chemi- and bioluminescence of firefly luciferin: An efficient chemical production of electronically excited states, Bioorg. Chem. 1 (1971) 92–122.
[14] F. McCapra, D.J. Gilfoyle, D.W. Young, N.J. Church, P. Spencer, Bioluminescence and Chemiluminescence. Fundamental and Applied Aspects, Wiley, New York, 1971.
[15] B.R. Branchini, T.L. Southworth, M.H. Murtiashow, R.A. Magyar, S.A. Gonzalez, M.C. Ruggiero, J.G. Stroh, An alternative mechanism of bioluminescence color determination in firefly luciferase, Biochemistry 43 (2004) 7255–7262.
[16] T. Hirano, Y. Hasumi, K. Ohtsuka, S. Maki, H. Niwa, M. Yamaji, D. Hashizume, Spectroscopic studies of the light-color modulation mechanism of firefly (beetle) bioluminescence, J. Am. Chem. Soc. 131 (2009) 2385–2396.
[17] T. Nakatsu, Y. Ichiyama, J. Hiratake, A. Saldanha, N. Kobashi, K. Sakata, H. Kato, Structural basis for the spectral difference in luciferase bioluminescence, Nature 440 (2006) 372–376.
[18] S. Hosseinkhani, Molecular enigma of multicolor bioluminescence of firefly luciferase, Cell Mol. Life Sci. 68 (2011) 1167–1182.
[19] I. Navizet, Y.J. Liu, N. Ferré, D. Roca-Sanjuán, R. Lindh, The chemistry of bioluminescence. an analysis of chemical functionalities, Chem. Phys. Chem. 12 (2011) 3064–3076.
[20] J.Y. Hasegawa, K.J. Fujimoto, H. Nakatsuji, Color tuning in photofunctional proteins, Chem. Phys. Chem. 12 (2011) 3106–3115.

[21] L. Pinto da Silva, J.C.G. Esteves da Silva, Computational investigation of the effect of pH on the color of firefly bioluminescence by DFT, Chem. Phys. Chem. 12 (2011) 951–960.
[22] S.F. Chen, Y.J. Liu, I. Navizet, N. Ferré, W.H. Fang, R. Lindh, Systematic theoretical investigation on the light emitter of firefly, J. Chem. Theory Comput. 7 (2011) 798–803.
[23] C.I. Song, Y.M. Rhee, Dynamics on the electronically excited state surface of the bioluminescent firefly luciferase-oxyluciferin system, J. Am. Chem. Soc. 133 (2011) 12040–12049.
[24] L. Pinto da Silva, J.C.G. Esteves da Silva, Theoretical modulation of the color of light emitted by firefly oxyluciferin, J. Comput. Chem. 32 (2011) 2654–2663.
[25] C.G. Min, A.M. Ren, J.F. Guo, Z.W. Li, L.Y. Zou, J.D. Goddard, J.K. Feng, A time-dependent density functional theory investigation on the origin of red chemiluminescence, Chem. Phys. Chem. 18 (2010) 251–259.
[26] Y.J. Liu, L. De Vico, R. Lindh, Ab initio investigation on the chemical origin of the firefly bioluminescence, J. Photochem. Photobiol. A 194 (2008) 261–267.
[27] L. Pinto da Silva, J.C.G. Esteves da Silva, Study of the effects exerted by intermolecular interactions on the firefly multicolor bioluminescence, Chem. Phys. Chem. 12 (2011) 3002–3008.
[28] N. Nakatani, J.Y. Hasegawa, H. Nakatsuji, Red light in chemiluminescence and yellow-green light in bioluminescence. Color-tuning mechanism of firefly; photinus pyralis: studied by the symmetry-adapted cluster-configuration interaction method, J. Am. Chem. Soc. 129 (2007) 8756–8765.
[29] C.G. Min, A.M. Ren, J.F. Guo, L.Y. Zou, J.D. Goddard, C.C. Sun, Theoretical investigation on the origin of yellow-green firefly bioluminescence by time-dependent density functional theory, Chem. Phys. Chem. 11 (2010) 2199–2204.
[30] I. Navizet, Y.J. Liu, N. Ferré, H.Y. Xiao, W.H. Fang, R. Lindh, Color-tuning mechanism of firefly investigated by multi-configurational perturbation method, J. Am. Chem. Soc. 132 (2010) 706–712.
[31] B.F. Milne, M.A. Marques, F. Nogueira, Fragment molecular orbital investigation of the role of AMP protonation in firefly luciferase pH-sensitivity, Phys. Chem. Chem. Phys. 12 (2010) 14285–14293.
[32] P. Naumov, Y. Ozawa, K. Ohkubo, S. Fukuzumi, Structure and spectroscopy of oxyluciferin, the light emitter of the firefly bioluminescence, J. Am. Chem. Soc. 131 (2009) 11590–11605.
[33] Avogadro: An open-source molecular builder and visualization tool. Version 1.0.0. <http://avogadro.openmolecules.net/> (accessed 10.02.11).
[34] C.T. Lee, W.T. Yang, R.G. Parr, Development of the colle-salvetti correlation-energy formula into a functional of the electron-density, Phys. Rev. B: Condens. Matter Mater. Phys. 37 (1998) 785–789.
[35] N.C. Handy, A.J. Cohen, Left-right correlation energy, Mol. Phys. 99 (2001) 403–412.
[36] W.N. Hoe, A.J. Cohen, N.C. Handy, Assessment of a new local exchange functional OPTZ, Chem. Phys. Lett. 341 (2001) 319–328.
[37] J.B. Foresman, M. Head-Gordon, J.A. Pople, M.J. Frisch, Towards a systematic molecular-orbital theory for excited-states, J. Phys. Chem. 96 (1992) 135–149.
[38] E.K.U. Gross, W. Kohn, Time-dependent density-functional theory, Adv. Quantum Chem. 21 (1990) 255–291.
[39] M.E. Casida, Recent Advances in Density Functional Methods, World Scientific, Singapore, 1995.
[40] T. Yang, J.D. Goddard, Predictions of the geometries and fluorescence emission energies of oxyluciferins, J. Phys. Chem. A 111 (2007) 4489–4497.
[41] K. Fujimoto, S. Hayashi, J.Y. Hasegawa, H. Nakatsuji, Theoretical studies on the color-tuning mechanism in retinal proteins, J. Chem. Theory Comput. 3 (2007) 605–618.
[42] Z.W. Li, A.M. Ren, J.F. Guo, T. Yang, J.D. Goddard, J.K. Feng, Color-tuning mechanism in firefly luminescence: theoretical studies on fluorescence of oxyluciferin in aqueous solution using time dependent density functional theory, J. Phys. Chem. A (2008) 9796–9800.
[43] L. Pinto da Silva, J.C.G. Esteves da Silva, Analysis of the performance of DFT functionals in the study of light emission by oxyluciferin analogues, Int. J. Quantum Chem. (2012), doi:10.1002/qua.24014.
[44] D.A. Case, T.E. Cheatham, T. Darden, H. Gohlke, R. Luo, K.M. Merz, A. Onufriev, C. Simmelring, B. Wang, R. Wodds, The amber biomolecular simulation programs, J. Comput. Chem. 26 (2005) 1668–1688.
[45] J.M. Wang, R.M. Wolf, J.W. Caldwell, P.A. Kollman, D.A. Case, Development and testing of a general amber force field, J. Comput. Chem. 25 (2004) 1157–1174.
[46] J.C. Philips, R. Braun, W. Wang, J. Gumbart, E. Tajkhorshid, E. Villa, C. Chipot, R.D. Skell, L. Kale, K. Schulten, Scalable molecular dynamics with NAMD, J. Comput. Chem. 26 (2005) 1781–1802.
[47] U. Essmann, L. Perera, M.L. Berkowitz, T. Darden, H. Lee, L.G. Pedersen, A smooth particle Mesh Ewald method, J. Chem. Phys. 103 (1995) 8577–8593.
[48] V. Barone, M. Cossi, Quantum calculation of molecular energies and energy gradients in solution by a conductor solvent model, J. Phys. Chem. A 102 (1998) 1995–2001.
[49] Gaussian 03 (Revision C.02), M.J. Frisch, G.W. Trucks, H.B. Schlegel, G.E. Scuseria, M.A. Robb, J.R. Cheeseman, J.A. Montgomery Jr., T. Vreven, K.N. Kudin, J.C. Burant, J.M. Millam, S.S. Iyengar, J. Tomasi, V. Barone, B. Mennucci, M. Cossi, G. Scalmani, N. Rega, G.A. Petersson, H. Nakatsuji, M. Hada, M. Ehara, K. Toyota, R. Fukuda, J. Hasegawa, M. Ishida, T. Nakajima, Y. Honda, O. Kitao, H. Nakai, M. Klene, X. Li, J.E. Knox, H.P. Hratchian, J.B. Cross, C. Adamo, J. Jaramillo, R. Gomperts, R.E. Stratmann, O. Yazyev, A.J. Austin, R. Cammi, C. Pomelli, J.W. Ochterski, P.Y. Ayala, K. Morokuma, G.A. Voth, P. Salvador, J.J. Dannenberg, V.G. Zakrzewski, S. Dapprich, A.D. Daniels, M.C. Strain, O. Farkas, D.K. Malick, A.D. Rabuck, K. Raghavachari, J.B. Foresman, J.V. Ortiz, Q. Cui, A.G. Baboul, S. Clifford, J. Cioslowski, B.B. Stefanov, G. Liu, A. Liashenko, P. Piskorz, I. Komaromi, R.L. Martin, D.J. Fox, T. Keith, M.A. Al-Laham, C.Y. Peng, A. Nanayakkara, M. Challacombe, P.M.W. Gill, B. Johnson, W. Chen, M.W. Wong, C. Gonzalez, J.A. Pople, Gaussian, Inc., Wallingford, CT, 2004.
[50] M. Anselmi, S. Marocchi, M. Aschi, A. Amadei, Theoretical modeling of the spectroscopic absorption properties of luciferin and oxyluciferin: a critical comparison with recent exerimental studies, Chemical Physics (2011), doi:10.1016/j.chemphys.2011.11.021.

Article 19

Theoretical fingerprinting of the photophysical properties of four firefly bioluminophores
Luís Pinto da Silva and Joaquim C.G. Esteves da Silva
Photochem. Photobiol. Sci. **2013**, *12*, 2028-2035.

The theoretical calculations and the writing of the paper were performed by Luís Pinto da Silva, under supervision of Professor Esteves da Silva.

Photochemical & Photobiological Sciences

RSC Publishing

PAPER

View Article Online
View Journal | View Issue

Cite this: *Photochem. Photobiol. Sci.*, 2013, **12**, 2028

Theoretical fingerprinting of the photophysical properties of four firefly bioluminophores†

Luís Pinto da Silva and Joaquim C. G. Esteves da Silva*

Received 1st July 2013,
Accepted 29th August 2013

DOI: 10.1039/c3pp50203a

www.rsc.org/pps

The photophysical properties of four bare firefly bioluminophores were studied *in vacuo* by means of a density functional theory approach. The objective of this work was to fingerprint the excited-state properties of these molecules without perturbations of the microenvironment (either solution or enzyme active site). It is known that intermolecular interactions formed between the light-emitter and active site molecules govern the bioluminescence multicolor tuning mechanism. However, it is difficult to disentangle the numerous active site-oxyluciferin interactions and understand the effect exerted by each one of these interactions on the color of light emitted. Thus, the study of these isolated bioluminophores allows us to obtain their intrinsic photophysics properties, which can serve as a reference in studies aiming to understand the role of perturbations from the microenvironment.

Introduction

Firefly bioluminescence is a chemical reaction catalyzed by firefly luciferase that results in the emission of visible light (λ_{max} of 530–640 nm).[1–4] In this reaction, firefly luciferin is converted into firefly dioxetanone (FiDiox), due to adenylation and oxidation reactions.[4–6] Subsequently, the unstable FiDiox decomposes into excited state firefly oxyluciferin, a light emitter.[7–10]

The high quantum yield determined for the bioluminescence reaction (~40–60%) makes this type of reaction more efficient than non-natural chemiluminescence reactions.[11,12] This efficient system has found numerous practical applications in the pharmaceutical, biomedical and bioanalytical areas, among others.[13–17]

The typical bioluminescence spectrum of this system has a peak in the yellow-green region of the visible spectrum (at basic pH).[1–4] However, in some firefly species, the bioluminescence emission presents a pH-sensitivity, and the emission is shifted to the red region.[1–4] Understanding this peculiar aspect could be of enormous importance in firefly research. Red-emitting firefly bioluminescence systems could be used in *in vivo* medical imaging, as red light is absorbed very poorly in comparison with natural emitted light. It was also proposed that the control of the multicolor bioluminescence could be the basis for using this system as a single dual reporter gene, a bioindicator of cellular stress, and a probe for intracellular changes of pH.[2] Moreover, the control of the emission maximum could increase the potential for application of firefly bioluminescence in secondary energy-transfer processes.[18–21]

Various experimental and theoretical studies have been performed in order to better understand this phenomenon. For a more detailed analysis of all these studies, the readers are suggested to read these recent review papers.[1–6] Both experimental and theoretical studies indicate that the color of the emitted bioluminescence is modulated by intermolecular interactions between excited state oxyluciferin and other active site molecules.[22–30] However, it is far from clear why and in what way these interactions modulate the color of light emitted by the bioluminophore. Nevertheless, the elucidation of this topic is of the utmost importance if one wants to rationally develop modified luciferase–oxyluciferin complexes, with more appropriate emission properties.

One strategy that may be able to overcome these difficulties is the study of the photophysical properties of the bare light emitter in the absence of active site and solvent molecules.[31] By knowing the intrinsic photophysical properties of a sole bioluminophore molecule, we can better understand the effect of intermolecular interactions on the bio-emissive state of firefly oxyluciferin.

To this end, we have studied the absorption properties of firefly oxyluciferin and three non-natural analogues. While bioluminescence corresponds to the emission of light, the study of the absorption process can provide a unique insight into the excited state properties of these molecules. It should be

Centro de Investigação em Química (CIQ-UP), Departamento de Química e Bioquímica, Faculdade de Ciências da Universidade do Porto, R. Campo Alegre 687, 4169-007 Porto, Portugal. E-mail: jcsilva@fc.up.pt; Fax: +351 22 6082959; Tel: +351 22 6082869

†Electronic supplementary information (ESI) available: Cartesian coordinates of firefly oxyluciferin, $BtOxyLH_2$, $AminoSeOxyLH_2$ and $CALOxyLH_2$. See DOI: 10.1039/c3pp50203a

noted that the absorption spectrum often reflects the main excited state features, with a difference of a red-shift that occurs after excited state relaxation, and that this approach was already used both experimentally and theoretically.[29–33] Moreover, Navizet *et al.* have demonstrated that the emissive state in firefly chemi/bioluminescence and fluorescence is the same (either *in vacuo* or within the protein), which supports the use of bare oxyluciferin as a model for the study of firefly bioluminophore excited state properties.[34]

A theoretical approach was used as it can provide accurate and detailed (down to the atomistic level) information of important electronically excited states. Moreover, by using this approach we can really attribute all the obtained results to a single molecule of the studied chemical species. Density functional theory (DFT) and time dependent-DFT (TD-DFT) were the methods of choice, as they are the most widely used tools to model optical spectra of organic molecules *in vacuo*, in solution or in more complex environments. It should also be noted that this is the first work to study theoretically the photophysical properties of Bt and AminoSe, non-natural oxyluciferin analogues.

Theoretical methods

All the calculations were carried out using the Gaussian 09 program package.[35] The ground state (S_0) geometries of the studied molecules were determined at the PBE0/cc-pVDZ level of theory.[36] Subsequent vibrational frequency calculations, at the same level of theory, were made in order to ensure that the obtained geometries were indeed minimal in their S_0 potential energy surface. The PBE0 functional was chosen due to its good performance in the geometry optimizations of organic molecules, as demonstrated by its use in TD-DFT benchmarking studies as the method of choice for obtaining geometrical parameters.[37–39]

Within the vertical approximation, the properties of the electronically singlet excited states (S_x) were calculated with TD-DFT single point calculations on the S_0 geometries. The chosen DFT functional was M06-HF,[40] while the basis set was augmented with diffuse functions (aug-cc-pVDZ). This density functional was used due to the good performance for valence, Rydberg and charge transfer excited states.[41]

All calculations were made *in vacuo*.

Besides firefly oxyluciferin, $BtOxyLH_2$ (which has a benzothiophene ring system instead of a benzothiazole),[42] $AminoSeOxyLH_2$ (which has an amino group instead of a hydroxyl one, and the sulphur heteroatom of the thiazolone replaced by a selenium atom),[43] and coumarylaminooxyluciferin ($CALOxyLH_2$) were also studied.[18] These species are represented in Fig. 1. All these species were considered to be ketonic species (anionic when possible), as the majority of theoretical and experimental studies have agreed that the firefly light emitter is the anionic keto-form oxyluciferin.[24,25,44–48] Nevertheless, it should be mentioned that there are still authors who think that the enolic species might have some role in firefly bioluminescence.[24,25,44–48]

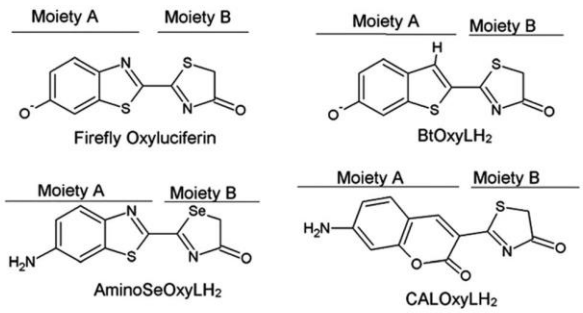

Fig. 1 Schematic representation of the four bioluminophores here studied, divided into two moieties (A and B).

The Gabedit program was used to obtain absorption spectra from the TD-DFT calculations for each bioluminophore.[49] The spectra were obtained using a Lorentzian lineshape. This program was also used to visualize the molecular orbitals of the bioluminophores.

Results and discussion

Photophysical properties of firefly oxyluciferin

In Table 1 are presented the absorption maxima (λ_{abs}, in nm), absorption energies (E_{abs}, in eV) and oscillator strengths (f) of the first six singlet excited states calculated at TD-M06-2HF/aug-cc-pVDZ level of theory for firefly oxyluciferin.

It can be seen that the most important excited state is S_1, because it is the only non-dark state, as it presents a very high f. The theoretical absorption spectrum (Fig. 2a) of this molecule *in vacuo* consists of only one band, which arises only from a $S_0 \rightarrow S_1$ transition. This transition consists of HOMO $\rightarrow$ LUMO(+2) and HOMO $\rightarrow$ LUMO(+3) excitations (58.8% and 35.6%, respectively). The λ_{abs} of this $S_0 \rightarrow S_1$ transition (462 nm) is in line with the results obtained with the equation-of-motion coupled cluster theory including single and double excitations (EOM-CCSD), with both the Def2-SVPD and Def2-TZVPPD basis sets (478 and 477 nm, respectively).[31]

In Table 2 are presented the Natural Bond Orbital (NBO) atomic charges of the two moieties of firefly oxyluciferin. At S_0, most of the negative charge of this anion is placed on moiety A.

Table 1 Absorption maxima (λ_{abs}, in nm), absorption energies (E_{abs}, in eV) and oscillator strengths (f) of the first six singlet excited states calculated at TD-M06-2HF/aug-cc-pVDZ level of theory for firefly oxyluciferin

S_x	λ_{abs}	E_{abs}	f
S_1	462	2.68	0.9515
S_2	350	3.54	0.0001
S_3	325	3.82	0.0000
S_4	322	3.85	0.0001
S_5	311	3.99	0.0015
S_6	308	4.02	0.0030

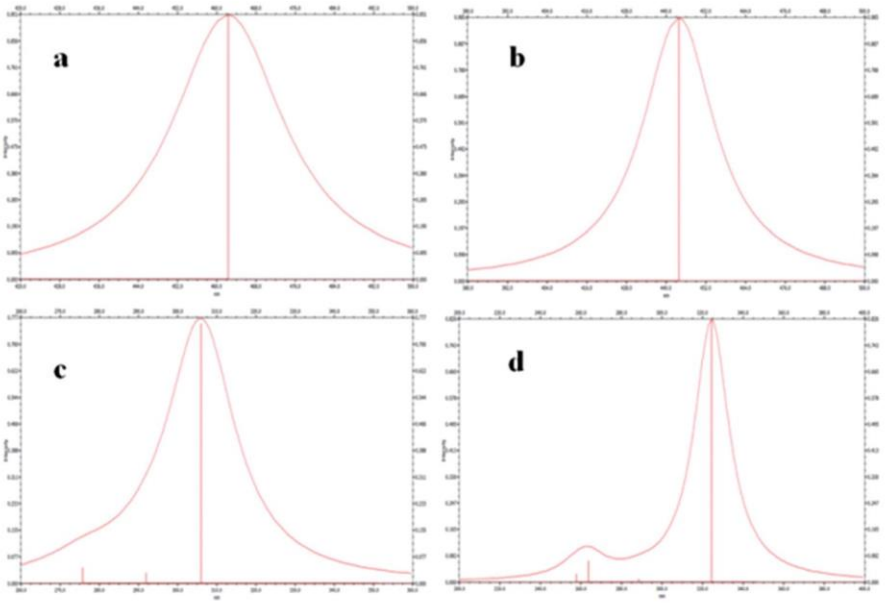

Fig. 2 Theoretical absorption spectra of firefly oxyluciferin (a), $BtOxyLH_2$ (b), $AminoSeOxyLH_2$ (c), and $CALOxyLH_2$ (d).

Table 2 Atomic NBO charges for S_0 and S_x (S_1 or S_2) of the four bioluminophores

	S_0		S_x	
	Moiety A	Moiety B	Moiety A	Moiety B
Oxyluciferin	−0.714	−0.287	−0.553	−0.450
$BtOxyLH_2$	−0.661	−0.337	−0.531	−0.472
$AminoSeOxyLH_2$	0.057	−0.058	0.315	−0.315
$CALOxyLH_2$	0.053	−0.052	0.187	−0.187

However, the $S_0 \rightarrow S_1$ transition leads to a charge transfer between the two moieties. The negative charge of the moiety A decreases by about 0.161, while the negative charge of the moiety B increases by about 0.163. So, at S_1 the two moieties present similar values of NBO atomic charges, which indicate that the negative charge becomes more delocalized in the bioluminophore at the electronically excited state. This is consistent with the fact that firefly oxyluciferin is more polar at S_0 than at S_1 (7.13 and 4.36 Debyes, respectively). This decrease in the polarization of the molecule is the result of a great decrease in the dipolar moment in the *x*-orientation, while the dipole moments in both *y*- and *z*-orientations remain the same (Table 3).

In Fig. 3 is presented firefly oxyluciferin with the HOMO, LUMO(+2) and LUMO(+3) orbitals. It can be seen that the HOMO orbitals are mainly localized on moiety A, which is consistent with the atomic NBO charges analysis. The LUMO(+2) and LUMO(+3) orbitals are not similar between the two moieties, and these orbitals are more localized on moiety B.

All the data gathered so far indicate that the excitation of firefly luciferin, due to a $S_0 \rightarrow S_1$ transition, leads to an orbital and charge delocalization from moiety A to moiety B. This delocalization towards the entire molecule leads to a diminished polarization in S_1, in comparison with S_0.

Photophysical properties of $BtOxyLH_2$

In Table 4 are presented the absorption maxima (λ_{abs}, in nm), absorption energies (E_{abs}, in eV) and oscillator strengths (f) of the first six singlet excited states calculated at TD-M06-2HF/aug-cc-pVDZ level of theory for $BtOxyLH_2$.

Table 3 Dipolar moments of the four bioluminophores at S_0 and S_x

	States	Dipolar moment	*x*-Orientation	*y*-Orientation	*z*-Orientation
Oxyluciferin	S_0	7.13	5.67	4.31	0.00
	S_1	4.36	1.73	4.01	0.00
$BtOxyLH_2$	S_0	8.50	5.61	6.39	0.00
	S_1	6.25	2.62	5.68	0.00
$AminoSeOxyLH_2$	S_0	6.09	5.46	−2.54	0.91
	S_2	13.89	13.50	−3.16	0.86
$CALOxyLH_2$	S_0	11.12	−8.57	−7.03	0.96
	S_2	14.90	−13.30	−6.65	1.00

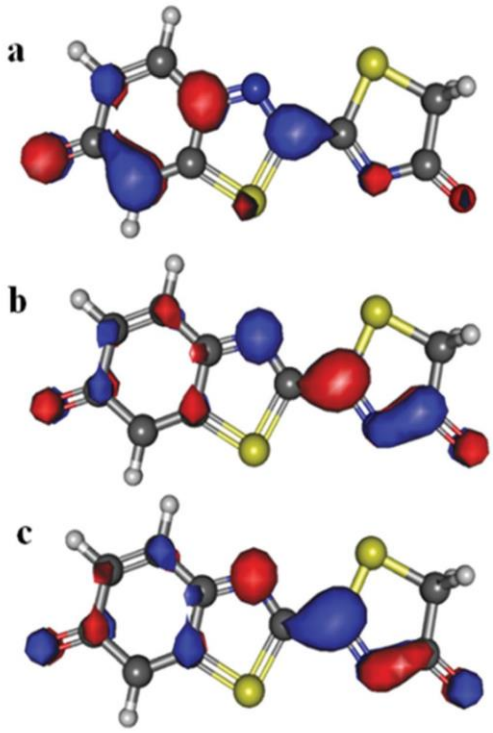

Fig. 3 Molecular orbitals of firefly oxyluciferin: HOMO (a), LUMO(+2) (b) and LUMO(+3) (c).

Table 4 Absorption maxima (λ_{abs}, in nm), absorption energies (E_{abs}, in eV) and oscillator strengths (f) of the first six singlet excited states calculated at TD-M06-2HF/aug-cc-pVDZ level of theory for $BtOxyLH_2$

S_x	λ_{abs}	E_{abs}	f
S_1	444	2.79	0.9856
S_2	364	3.41	0.0001
S_3	327	3.80	0.0002
S_4	321	3.87	0.0012
S_5	319	3.89	0.0002
S_6	300	4.13	0.0012

In this molecule, the most important excitation transition is also $S_0 \rightarrow S_1$, as all other transitions lead to dark states. This transition consists of a HOMO → LUMO(+4) excitation (93.6%). As in the case of firefly luciferin, the absorption spectrum (Fig. 2b) of $BtOxyLH_2$ consists only of one band that arises from the $S_0 \rightarrow S_1$ transition. Still in comparison with firefly oxyluciferin, we can see that the band of $BtOxyLH_2$ is blue-shifted 18 nm in regard to the *in vacuo* absorption peak of the natural firefly bioluminophore. No direct experimental absorption data are available for $BtOxyLH_2$. However, it is known that this molecule presents a bioluminescence maximum ~36–39 nm lower than that presented by firefly oxyluciferin.[42] This difference is in line with the theoretical λ_{abs} differences between these two molecules here calculated.

In Table 2 are presented the NBO atomic charges of the moieties A and B of $BtOxyLH_2$. As in the case of firefly oxyluciferin, the negative charge of this anion resides mostly on moiety A. However, the difference in negative charge between moieties A and B is lower than in the case of firefly oxyluciferin. Upon $S_0 \rightarrow S_1$ transition, there was a negative charge transfer from moiety A to moiety B, and so, the negative charge is almost evenly distributed between the moieties. This almost even distribution in S_1 leads to a decrease of 2.25 Debyes in the dipolar moment of $BtOxyLH_2$, in regard to S_0 (Table 3). Once again, this decrease is mainly associated with a decrease in the dipolar moment in the *x*-orientation.

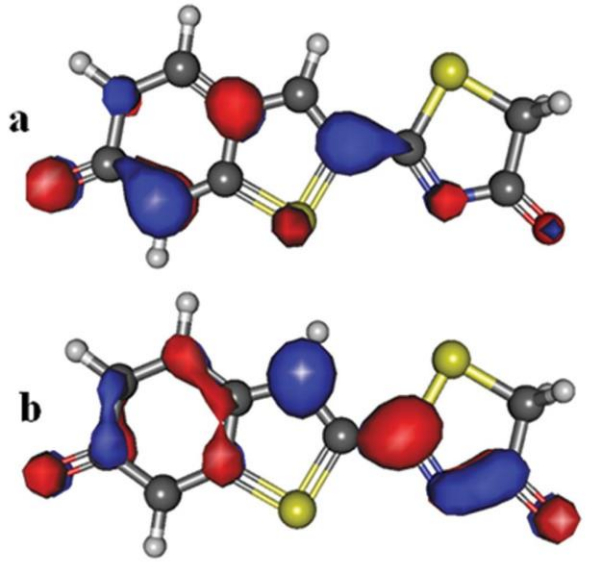

Fig. 4 Molecular orbitals of $BtOxyLH_2$: HOMO (a) and LUMO(+4) (b).

In Fig. 4 is presented $BtOxyLH_2$ with the HOMO and LUMO(+4) orbitals. From this figure, we can see that with the $S_0 \rightarrow S_1$ transition there is an orbital delocalization in this molecule. This is in line with charge and dipolar moment variations associated with $S_0 \rightarrow S_1$ transition.

Photophysical properties of $AminoSeOxyLH_2$

In Table 5 are presented the absorption maxima (λ_{abs}, in nm), absorption energies (E_{abs}, in eV) and oscillator strengths (f) of the first six singlet excited states calculated at TD-M06-2HF/aug-cc-pVDZ level of theory for $AminoSeOxyLH_2$.

Contrary to firefly oxyluciferin and $BtOxyLH_2$, the bright absorption state of $AminoSeOxyLH_2$ results from a $S_0 \rightarrow S_2$ transition. This transition is composed of HOMO(−5) → LUMO (3.4%), HOMO(−1) → LUMO (2.5%) and HOMO → LUMO (84.8%) excitations. The *in vacuo* spectrum (Fig. 2c) of this molecule presents only one band. The peak of this band (306 nm) is significantly blue-shifted in comparison with firefly oxyluciferin and $BtOxyLH_2$. While firefly oxyluciferin presents λ_{abs} in the blue region and $BtOxyLH_2$ λ_{abs} in the violet region, $AminoSeOxyLH_2$ presents λ_{abs} in the ultraviolet region (Tables 1, 3 and 5). The theoretical λ_{abs} for the $S_0 \rightarrow S_2$ transition of $AminoSeOxyLH_2$ is in line with the local maximum,

Table 5 Absorption maxima (λ_{abs}, in nm), absorption energies (E_{abs}, in eV) and oscillator strengths (f) of the first six singlet excited states calculated at TD-M06-2HF/aug-cc-pVDZ level of theory for AminoSeOxyLH$_2$

S_x	λ_{abs}	E_{abs}	f
S_1	351	3.53	0.0002
S_2	306	4.05	0.7615
S_3	300	4.14	0.0001
S_4	292	4.25	0.0312
S_5	280	4.43	0.0000
S_6	276	4.50	0.0471

of an absorbance spectrum in 50 mM Tris-HCl buffer (pH 7.5), of 350 nm.[43]

Given that this bioluminophore is a neutral molecule, the absolute NBO charges of its two moieties and the charge differences between the moieties are rather small at S_0 (Table 2). However, it should be noted that the charges of the two moieties have opposite signals, which creates a dipolar moment of 6.09 Debyes (Table 3). Upon excitation, at S_2 the charge difference between the moieties increases significantly, with the charges of the moieties still presenting opposite signals (Table 2). This originates a large dipolar moment (13.89 Debyes, Table 3), which is 7.80 Debyes higher than the S_0 dipolar moment. Once again, this large difference between the S_0 and excited states dipolar moments can be attributed to changes in the dipolar moment in the x-orientation (Table 3).

In Fig. 5 is presented AminoSeOxyLH$_2$ with the HOMO, HOMO(−1), HOMO(−5) and LUMO orbitals. From this Figure, it can be seen that both the HOMO(−1) and HOMO(−5) orbitals are delocalized along the two moieties of this bioluminophore. In contrast, the HOMO orbitals reside mostly in the moiety A. It should be noted that even in the case of HOMO (−5) and HOMO(−1) there is a stronger presence of these orbitals in the moiety A. In the case of LUMO, a delocalization of the orbitals can be seen. However, these orbitals now reside mostly in the two thiazole moieties of AminoSeOxyLH$_2$. So, and contrary to the case of firefly oxyluciferin and BtOxyLH$_2$, the excitation process does not really cause a delocalization of the molecular orbitals. Instead, it causes a shift of orbital localization, from moiety A to the thiazole–thiazole moiety.

Photophysical properties of CALOxyLH$_2$

In Table 6 are presented the absorption maxima (λ_{abs}, in nm), absorption energies (E_{abs}, in eV) and oscillator strengths (f) of the first six singlet excited states calculated at TD-M06-2HF/aug-cc-pVDZ level of theory for CALOxyLH$_2$.

As in the case of AminoSeOxyLH$_2$, the most important $S_0 \rightarrow S_x$ transition is $S_0 \rightarrow S_2$. This transition corresponds to a HOMO $\rightarrow$ LUMO excitation (88.4%). The λ_{abs} associated with this transition (325 nm) is red-shifted in regard to AminoSeOxyLH$_2$, but it is still significantly blue-shifted in regard to firefly oxyluciferin and BtOxyLH$_2$. According to the work of Naumov and co-workers, this sequence of λ_{abs} can be attributed to presence of a single negative charge in firefly oxyluciferin and BtOxyLH$_2$, and its absence in AminoSeOxyLH$_2$ and CALOxyLH$_2$.[46] The absorption spectrum of CALOxyLH$_2$ is presented in Fig. 2d. Besides a band associated with the important $S_0 \rightarrow S_2$ transition, a smaller band associated with $S_0 \rightarrow S_5$ and $S_0 \rightarrow S_6$ transitions can also be seen.

The obtained dipolar moment shows us that CALOxyLH$_2$ is a very polar molecule at S_0, with a dipolar moment of 11.12 Debyes (Table 3). Upon $S_0 \rightarrow S_2$ transition, CALOxyLH$_2$ becomes even more polarized with a dipolar moment of 14.90 Debyes (Table 3). However, this increase in the dipolar

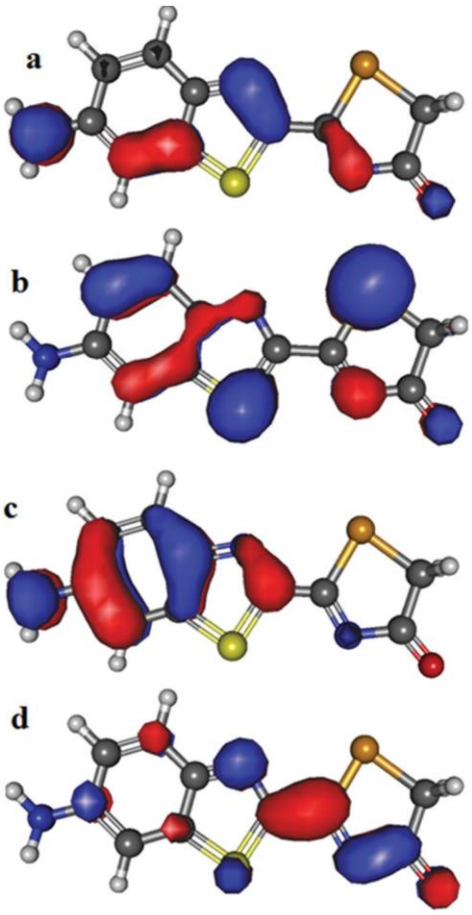

Fig. 5 Molecular orbitals of AminoSeOxyLH$_2$: HOMO(−5) (a), HOMO(−1) (b), HOMO (c) and LUMO (d).

Table 6 Absorption maxima (λ_{abs}, in nm), absorption energies (E_{abs}, in eV) and oscillator strengths (f) of the first six singlet excited states calculated at TD-M06-2HF/aug-cc-pVDZ level of theory for CALOxyLH$_2$

S_x	λ_{abs}	E_{abs}	f
S_1	347	3.57	0.0004
S_2	325	3.82	0.8227
S_3	289	4.30	0.0108
S_4	277	4.47	0.0002
S_5	264	4.70	0.0684
S_6	258	4.81	0.0263

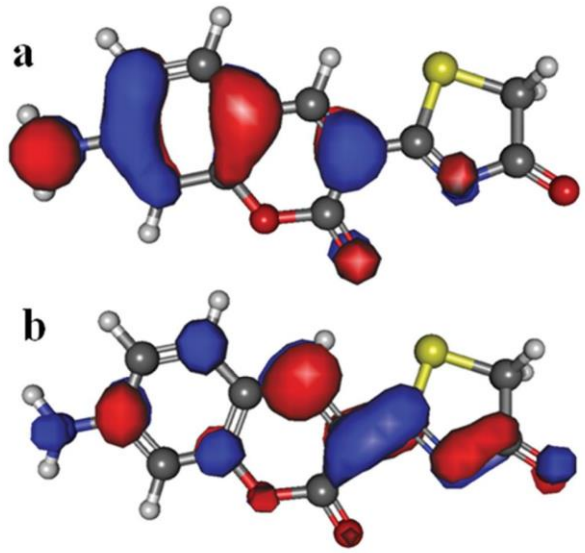

Fig. 6 Molecular orbitals of $CALOxyLH_2$: HOMO (a) and LUMO (b).

moment upon $S_0 \rightarrow S_2$ transition is less marked than in the case of $AminoSeOxyLH_2$ (increases in the order of 3.78 Debyes *versus* increases in the order of 7.80 Debyes). Nevertheless, these data indicate that $CALOxyLH_2$ is the most polar molecule both in the ground and excited states.

The NBO charge variation associated with $S_0 \rightarrow S_2$ transition of $CALOxyLH_2$ is similar to that presented by $AminoSeOxyLH_2$, but dissimilar to that presented by firefly oxyluciferin and $BtOxyLH_2$ (Table 2).

In Fig. 6 is presented $CALOxyLH_2$ with the HOMO and LUMO orbitals. It can be seen that the HOMO → LUMO excitation is associated with a small orbital delocalization.

Comparison between the photophysical properties of the four bare firefly bioluminophores

Our calculations demonstrate that anionic bioluminophores present higher wavelength maxima than neutral bioluminophores. Moreover, while the excitation of these anions corresponds to $S_0 \rightarrow S_1$ transitions, the excitation of neutral species corresponds to $S_0 \rightarrow S_2$ transitions.

Upon excitation, the negative atomic charges of the anionic bioluminophores become delocalized along the two moieties of the studied molecules, which decrease their dipolar moment. Hence, anionic bioluminophores are more polarized in S_0 than in S_1. In contrast, for the neutral bioluminophores there is an increase in the charge difference between the two moieties upon excitation. The excitation process creates two poles of significant opposite charge, each one residing on one moiety, thus increasing the polarization of the neutral bioluminophores in the excited state.

The analysis of the molecular orbitals of the four bare bioluminophores demonstrated that upon excitation, there is delocalization of the orbitals along the entire structure of the studied molecules. However, this delocalization is more easily seen for the anionic bioluminophores (firefly oxyluciferin and $BtOxyLH_2$).

Another interesting feature seen in the molecular orbital analysis is that HOMO(x) orbitals can be seen placed on the C–C bond that connects the two moieties of the bioluminophores of the anionic bioluminophores (Fig. 1). In contrast, no HOMO(x) orbitals are seen on this bond for the neutral light emitters ($AminoSeOxyLH_2$ and $CALOxyLH_2$). Nevertheless, there are always LUMO(x) orbitals on this C–C bond for all molecules. Cai *et al.* have suggested that this region may be most crucial in determining the efficiency of oxyluciferin excited state transitions.[33] It was also suggested that higher HOMO(x)/LUMO(x) orbital overlapping results in greater transition probability.[33] Our results support these conclusions as firefly oxyluciferin and $BtOxyLH_2$ present higher f than $AminoSeOxyLH_2$ and $CALOxyLH_2$.

Orbital overlapping may also be a helpful concept for understanding color shifts in light absorption/emission processes. The neutral species present a higher C–C bond length (~1.45–1.46 Å), while the anionic species present a lower length (~1.40–1.41 Å). This and the remaining data presented here point to the formation of π–π conjugation between moieties A and B of the anionic bioluminophores and to σ–π hyperconjugation between the moieties of the two neutral oxyluciferin analogues. Given that orbital overlap is rather weak in the C–C bond of $AminoSeOxyLH_2$ and $CALOxyLH_2$, in comparison with the π–π conjugation in firefly oxyluciferin and $BtOxyLH_2$ would stabilize this bond. Thus, the HOMO(x)/LUMO(x) gap would decrease, thus increasing the λ_{abs}, as a result of π–π conjugation between the moieties A and B.[33]

Conclusions

The objective of this work was to theoretically fingerprint the photophysical properties of four bare firefly bioluminophores. The control of the color of firefly bioluminescence would increase the efficiency of existent applications, and would open the way for the new applications for this system. However, it is difficult to understand how interactions with active site molecules can modulate the color of light emitted by the bioluminophore. Thus, we have calculated the theoretical photophysical properties of bare bioluminophores, in order to better understand what are the effects exerted by intermolecular interactions.

Our calculations have demonstrated that anionic bioluminophores have higher wavelength maxima and transition efficiencies than neutral bioluminophores. These features were attributed to π–π conjugation effects and higher HOMO(x)/LUMO(x) overlap, especially in the connection region between the two moieties of the anionic bioluminophores.

Upon excitation, the polarization of the anionic species decreases due to charge delocalization towards the full molecular structure. In the case of neutral species, in the ground state each moiety corresponds to a pole of opposite charge in regard to the other moiety. Upon excitation, the charge

difference between the poles increases significantly, which increases the dipolar moment of these bioluminophores.

Orbital delocalization can be seen for all bioluminophores upon excitation. However, this delocalization is more easily seen for anionic species.

Acknowledgements

Financial support from Fundação para a Ciência e Tecnologia (FCT, Lisbon) (Programa Operacional Temático Factores de Competitividade (COMPETE) e comparticipado pelo Fundo Comunitário Europeu (FEDER) (project PTDC/QUI/71366/2006) is acknowledged. A PhD grant to Luís Pinto da Silva (SFRH/BD/76612/2011), attributed by FCT, is also acknowledged.

Notes and references

1 S. M. Marques and J. C. G. Esteves da Silva, Firefly bioluminescence: a mechanistic approach of luciferase catalyzed reactions, *IUBMB Life*, 2009, **61**, 3523.
2 V. R. Viviani, F. G. Arnoldi, A. J. Neto, T. L. Oehlmeyer, E. J. Bechara and Y. Ohmiya, The structural origin and biological function of pH-sensitivity in firefly luciferases, *Photochem. Photobiol. Sci.*, 2008, **7**, 159.
3 L. Pinto da Silva and J. C. G. Esteves da Silva, Computational Studies of the Luciferase Light-Emitting Product: Oxyluciferin, *J. Chem. Theor. Comput.*, 2011, **7**, 809.
4 L. Pinto da Silva and J. C. G. Esteves da Silva, Firefly chemiluminescence and bioluminescence: efficient generation of excited states, *ChemPhysChem*, 2012, **13**, 2257.
5 M. Matsumoto, Advanced chemistry of dioxetane-based chemiluminescent substrates originating from bioluminescence, *J. Photochem. Photobiol., C*, 2004, **5**, 27.
6 I. Navizet, Y. J. Liu, N. Ferré, D. Roca-Sanjuán and R. Lindh, The chemistry of bioluminescence: an analysis of chemical functionalities, *ChemPhysChem*, 2011, **12**, 3064.
7 S. P. Schmidt and G. B. Schuster, Dioxethanone chemiluminescence by chemically-initiated electron exchange pathway – efficient generation of excited singlet-states, *J. Am. Chem. Soc.*, 1978, **100**, 1966.
8 H. Isobe, Y. Takano, M. Okumura, S. Kuramitsu and K. Yamaguchi, Mechanistic insights in charge-transfer-induced luminescence of 1,2-dioxetanones with a substituent of low oxidation potential, *J. Am. Chem. Soc.*, 2005, **127**, 8667.
9 L. Yue, Y. J. Liu and W. H. Fang, Mechanistic insight into the chemiluminescent decomposition of firefly dioxetanone, *J. Am. Chem. Soc.*, 2012, **134**, 11632.
10 L. Pinto da Silva and J. C. G. Esteves da Silva, Interstate crossing-induced chemiexcitation as the reason for the chemiluminescence of dioxetanones, *ChemPhysChem*, 2013, **14**, 1071.
11 Y. Ando, K. Niwa, N. Yamada, T. Enomoto, T. Irie, H. Kubota, Y. Ohmiya and H. Akiyama, Firefly bioluminescence quantum yield and colour change by pH-sensitive green emission, *Nat. Photonics*, 2008, **2**, 44.
12 K. Niwa, Y. Ichino, S. Kumata, Y. Nakajima, Y. Hiraishi, D. Kato, V. R. Viviani and Y. Ohmiya, Quantum Yields and Kinetics of the Firefly Bioluminescence Reaction of Beetle Luciferases, *Photochem. Photobiol.*, 2010, **86**, 1046.
13 A. Roda, M. Guardigli, P. Pasini and M. Mirasole, Bioluminescence and chemiluminescence in drug screening, *Anal. Bioanal. Chem.*, 2003, **377**, 826.
14 A. Roda, P. Pasini, M. Mirasoli, E. Michelini and M. Guardigli, Biotechnological applications of bioluminescence and chemiluminescence, *Trends Biotechnol.*, 2004, **22**, 295.
15 A. Roda and M. Guardigli, Analytical chemiluminescence and bioluminescence: latest achievements and new horizons, *Anal. Bioanal. Chem.*, 2012, **402**, 69.
16 V. Villalobos, S. Naik and D. Piwnica-Worms, Current state of imaging protein-protein interactions in vivo with genetically encoded reporters, *Annu. Rev. Biomed. Eng.*, 2007, **9**, 321.
17 J. Brogan, F. Li, W. Li, Z. He, Q. Huang and C. Y. Li, Imaging molecular pathways: reporter geners, *Radiat. Res.*, 2012, **177**, 508.
18 H. Takakura, K. Sasakura, T. Ueno, Y. Urano, T. Terai, K. Hanaoka, T. Tsuboi and T. Nagano, Development of Luciferin Analogues Bearing an Amino Group and Their Application as BRET Donors, *Chem.–Asian. J.*, 2010, **5**, 2053.
19 M. K. So, C. Xu, A. M. Loening, S. S. Ganbhir and J. Rao, Self-illuminating quantum dot conjugates for in vivo imaging, *Nat. Biotechnol.*, 2006, **24**, 339.
20 N. Ma, A. F. Marshall and J. Rao, *J. Am. Chem. Soc.*, 2010, **132**, 6884.
21 B. R. Branchini, J. C. Rosenberg, D. M. Ablamsky, K. P. Taylor, T. L. Southworth and S. J. Linder, Sequential bioluminescence resonance energy transfer-fluororescence resonance energy transfer-based ratiometric protease assays with fusion proteins of firefly luciferase and red fluorescent protein, *Anal. Biochem.*, 2011, **414**, 239.
22 L. Pinto da Silva and J. C. G. Esteves da Silva, TD-DFT/Molecular Mechanics Study of the Photinus pyralis Bioluminescence system, *J. Phys. Chem. B*, 2012, **116**, 2008.
23 L. Pinto da Silva and J. C. G. Esteves da Silva, Study on the Effects of Intermolecular Interactions on Firefly Multicolor Bioluminescence, *ChemPhysChem*, 2011, **12**, 3002.
24 L. Pinto da Silva and J. C. G. Esteves da Silva, Computational Investigation of the Effect of pH on the Color of Firefly Bioluminescence by DFT, *ChemPhysChem*, 2011, **12**, 951.
25 C. I. Song and Y. M. Rhee, Dynamics on the electronically excited state surface of the bioluminescent firefly luciferase-oxyluciferin system, *J. Am. Chem. Soc.*, 2011, **133**, 12040.
26 P. Naumov, Y. Ozawa, K. Ohkubo and S. Fukuzumi, Structure and spectroscopy of oxyluciferin, the light

emitter of the firefly bioluminescence, *J. Am. Chem. Soc.*, 2009, **131**, 11590.

27 T. Hirano, Y. Hasumi, K. Ohtsuka, S. Maki, H. Niwa, M. Yamaji and D. Hashizume, Spectroscopic studies of the light-color modulation mechanism of firefly (beetle) bioluminescence, *J. Am. Chem. Soc.*, 2009, **131**, 2385.

28 C. G. Min, A. M. Ren, J. F. Guo, L. Y. Zou, J. D. Goddard and C. C. Sun, Theoretical investigation on the origin of yellow-green firefly bioluminescence by time-dependent density functional theory, *ChemPhysChem*, 2010, **11**, 2199.

29 B. F. Milne, M. A. Marques and F. Nogueira, Fragment molecular orbital investigation of the role of AMP protonation in firefly luciferase pH-sensitivity, *Phys. Chem. Chem. Phys.*, 2010, **12**, 14285.

30 L. Pinto da Silva and J. C. G. Esteves da Silva, Theoretical Modulation of the Color of Light Emitted by Firefly Oxyluciferin, *J. Comput. Chem.*, 2011, **32**, 2654.

31 K. Stochkel, C. N. Hansen, J. Houmoller, L. M. Nielsen, M. Linares, P. Norman, F. Nogueira, O. V. Maltsev, L. Hintermann, S. B. Nielsen, P. Naumov and B. F. Milne, On the influence of water on the electronic structure of firefly oxyluciferin anions from absorption spectroscopy of bare and monohydrated ions in vacuo, *J. Am. Chem. Soc.*, 2013, **135**, 6485.

32 D. Cai, M. A. Marques and F. Nogueira, Accurate color tuning of firefly chromophore by modulation of local polarization electrostatic fields, *J. Phys. Chem. B*, 2010, **115**, 329.

33 D. Cai, M. A. L. Marques, B. F. Milne and F. Nogueira, Bioheterojunction Effect on Fluorescence Origin and Efficiency Improvement of Firefly Chromophores, *J. Phys. Chem. Lett.*, 2010, **1**, 2781.

34 I. Navizet, D. Roca-Sanjuán, L. Yue, Y. J. Liu, N. Ferré and R. Lindh, Are the bio- and chemiluminescence states of the firefly oxyluciferin the same as the fluorescence state?, *Photochem. Photobiol.*, 2013, **89**, 319.

35 M. J. Frisch, *et al.*, *Gaussian 09, Revision A.02*, Gaussian, Inc., Wallingford CT, 2009.

36 C. Adamo and V. Barone, Toward reliable density functional methods without adjustable parameters: The PBE0 model, *J. Chem. Phys.*, 1999, **110**, 6158.

37 L. Pinto da Silva and J. C. G. Esteves da Silva, Analysis of the performance of DFT functionals in the study of light emission by oxyluciferin analogs, *Int. J. Quantum Chem.*, 2013, **113**, 45.

38 D. Jacquemin, E. A. Perpète, I. Ciofini and C. Adamo, Assessment of the omega B97 family for excited-state calculations, *Theor. Chem. Acc.*, 2011, **128**, 127.

39 D. Jacquemin, V. Wathelet, E. A. Perpète and C. Adamo, Extensive TD-DFT Benchmark: Singlet-Excited States of Organic Molecules, *J. Chem. Theor. Comput.*, 2009, **5**, 2420.

40 Y. Zhao and D. G. Truhlar, Density functional for spectroscopy: No long-range self-interaction error, good performance for Rydberg and charge-transfer states, and better performance on average than B3LYP for ground states, *J. Phys. Chem. A*, 2006, **110**, 13126.

41 Y. Zhao and D. G. Truhlar, Density functionals with broad applicability in chemistry, *Acc. Chem. Res.*, 2008, **41**, 157.

42 C. C. Woodroofe, P. L. Meisnheimer, D. H. Klaubert, Y. Kovic, J. C. Rosenberg, C. E. Behney, T. L. Southworth and B. R. Branchini, Novel Heterocyclic Analogues of Firefly Luciferin, *Biochemistry*, 2012, **51**, 9807–9813.

43 N. R. Conley, A. Dragulescu-Andrasi, J. Rao and W. E. Moerner, A Selenium Analogue of Firefly D-Luciferin with Red-Shifted Bioluminescence Emission, *Angew. Chem., Int. Ed.*, 2012, **51**, 3350.

44 S. F. Chen, Y. J. Liu, I. Navizet, N. Ferré, W. H. Fang and R. Lindh, Systematic Theoretical Investigation on the Light Emitter of Firefly, *J. Chem. Theor. Comput.*, 2011, **7**, 798.

45 B. R. Branchini, M. H. Murtiashaw, R. A. Magyar, N. C. Portier, M. C. Ruggiero and J. G. Stroh, Yellow-Green and red firefly bioluminescence from 5,5-dimethyloxyluciferin, *J. Am. Chem. Soc.*, 2002, **124**, 2112.

46 P. Naumov and M. Kochunnoonny, Spectral-structural effects of the keto-enol-enolate and phenol-phenolate equilibria of oxyluciferin, *J. Am. Chem. Soc.*, 2010, **132**, 11566.

47 K. M. Solntsev, S. P. Laptenok and P. Naumov, Photoinduced dynamics of oxyluciferin analogues: unusual enol "super" photoacidity and evidence for keto-enol isomerization, *J. Am. Chem. Soc.*, 2012, **134**, 16452.

48 L. Pinto da Silva, R. Simkovitch, D. Huppert and J. C. G. Esteves da Silva, Oxyluciferin Photoacidity: The Missing Element for Solving the Keto-Enol Mystery?, *ChemPhysChem*, 2013, DOI: 10.1002/cphc.201300402.

49 A. R. Allouche, Gabedit-A Graphical User Interface for Computational Chemistry Softwares, *J. Comput. Chem.*, 2011, **32**, 174.

Chapter 6 – Characterization of $OxyLH_2$ and Related Compounds as Photoacids

6.1. Characterization of the Photoprotolytic Cycle of $OxyLH_2$, D-LH_2 and L

Article 20

Comparative study of the photoprotolytic cycle reactions of D-luciferin and oxyluciferin
Yuval Erez, Itay Presiado, Rinat Gepshtein, Luís Pinto da Silva, Joaquim C.G. Esteves da Silva and Dan Huppert
J. Phys. Chem. A **2012**, *116*, 7452-7461.

Luís Pinto da Silva was responsible for writing the Introduction and Summary sections of this paper, under the supervision of Professors Joaquim Esteves da Silva and Dan Huppert, and was involved in the discussion of the obtained results.

THE JOURNAL OF PHYSICAL CHEMISTRY A
Article
pubs.acs.org/JPCA

Comparative Study of the Photoprotolytic Reactions of D-Luciferin and Oxyluciferin

Yuval Erez,[†] Itay Presiado,[†] Rinat Gepshtein,[†] Luís Pinto da Silva,[‡] Joaquim C. G. Esteves da Silva,[‡] and Dan Huppert*,[†]

[†]Raymond and Beverly Sackler Faculty of Exact Sciences, School of Chemistry, Tel Aviv University, Tel Aviv 69978, Israel

[‡]Centro de Investigação em Química, Departamento de Quimica, Faculdade de Ciencias da Universidade do Porto R. Campo Alegre 687, 4169-007 Porto, Portugal

Supporting Information

ABSTRACT: Optical steady-state and time-resolved spectroscopic methods were used to study the photoprotolytic reaction of oxyluciferin, the active bioluminescence chromophore of the firefly's luciferase-catalyzed reaction. We found that like D-luciferin, the substrate of the firefly bioluminescence reaction, oxyluciferin is a photoacid with pK_a* value of ~0.5, whereas the excited-state proton transfer (ESPT) rate coefficient is 2.2×10^{10} s^{-1}, which is somewhat slower than that of D-luciferin. The kinetic isotope effect (KIE) on the fluorescence decay of oxyluciferin is 2.5 ± 0.1, the same value as that of D-luciferin. Both chromophores undergo fluorescence quenching in solutions with a pH value below 3.

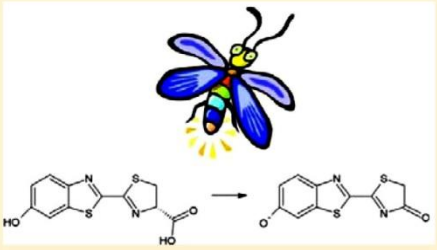

INTRODUCTION

Bioluminescence is a light-emitting phenomenon that occurs in living organisms, in which an excited-state product is formed in an enzyme-catalyzed reaction.[1−3] This enzyme is always termed luciferase, independently of the organism in which it is found.[4,5] The most studied bioluminescent system is that of the North American firefly, *Photinus pyralis*.[1−3,6] Firefly luciferase (Luc, EC 1.13.12.7) catalyzes a two-step reaction: first, the formation of an adenylyl intermediate (LH_2-AMP), by reaction of D-luciferin with adenosine-5′-triphosphate (ATP); second, the oxidation of LH_2-AMP. These latter reactions results in the formation of oxyluciferin in a singlet excited state.[1,6] The decay of the bioluminophore to the ground state is accompanied by emission of green light (~562 nm, at basic pH).[2,7−9]

Oxyluciferin, shown in Scheme 1, is usually thought to exist in one of six chemical forms, by means of a quadruple chemical equilibrium (deprotonation of the two hydroxyl groups, and neutral and anionic keto−enol tautomerism of the thiazole ring).[10−13] However, due to the instability of this chromophore in basic solutions, little is known about its spectroscopic and structural properties. In fact, it was only recently that the identities of the species that emit in solution and in Luc active site were discovered. The work of Naumov et al. revealed that oxyluciferin exists in solution in its enol form, whereas theoretical studies have determined that the bioluminescence emitter is anionic keto-form oxyluciferin.[10,12,14,15]

Scheme 1. Oxyluciferin

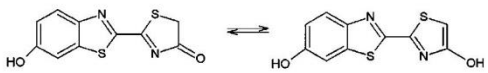

Previous studies have demonstrated that different factors can affect both the emission energy and the chemical equilibrium of oxyluciferin. Both experimental and theoretical studies have demonstrated that solvent polarity and various intermolecular interactions can modulate the emission wavelength of oxyluciferin, without the need of considering different species.[13,16−21] Also, several authors have demonstrated that the chemical equilibrium presented by oxyluciferin can be modulated by pH, solvent polarity and intermolecular interaction.[10−13,22]

Despite the difficulties of studying the spectroscopic properties of oxyluciferin, it was found that its absorption spectrum has a band at ~420 nm for basic pH, and at ~380 nm for acid-neutral pH.[10,22] The emission spectrum was found to be characterized by a peak at ~550 nm.[10] Decreasing the polarity of the solvent leads to a blue-shift of both the absorption and emission maximum.

D-Luciferin (Scheme 2), besides being one of the substrates of the bioluminescence reaction, is one of the most useful analogues of oxyluciferin due to its similar spectroscopic properties and higher stability. The absorption spectrum of this molecule is characterized by a maximum at ~330 nm in acidic solution and it is red-shifted at basic pH (~390 nm).[23−30] The emission spectrum of D-luciferin has a maximum at ~530 nm over the studied pH range 3−10. However, a decrease in the polarity of the solvent uncovers an emission band with a

Received: February 27, 2012
Revised: June 12, 2012
Published: June 14, 2012

Scheme 2. D-Luciferin

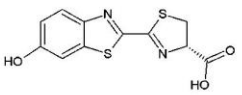

maximum at ~450 nm.[23−30] The red shift with increasing pH and polarity of the solvent is attributed to the deprotonation of the benzothiazole hydroxyl group.[23−30] In strongly acidic solutions an emission band at ~590 nm is found, which corresponds to the protonation of one of the nitrogen heteroatoms.[23−27]

In the current study we used time-integrated steady-state spectroscopy and time-resolved emission techniques to study the photoprotolytic reactions oxyluciferin undergoes. We then compared the obtained results with those of D-luciferin. We found that like D-luciferin, oxyluciferin is a photoacid, with a somewhat lower ESPT rate coefficient of 2.2×10^{10} s^{-1} (compared to 3.2×10^{10} s^{-1} of D-luciferin). Oxyluciferin, as does D-luciferin, undergo fluorescence quenching stemming either from geminate recombination with the proton or from excess protons in acidic media, where pH < 3.

EXPERIMENTAL SECTION

(4*S*)-2-(6-Hydroxybenzothiazole-2-yl)-4,5-dihydrothiazole-4-carboxylic acid (D-luciferin) 99.5% was purchased from Iris Biotech (Germany). HCl (1N) was purchased from Aldrich. Chemically synthesized oxyluciferin was obtained from 2-cyano-6-hydroxybenzothiazole and ethyl thioglycolate.[22,31] The parent compound 2-cyano-6-hydroxybenzothiazole was obtained from 2-cyano-6-methoxybenzothiazole (Aldrich, Steinheim, Germany).[22,31] For transient measurements the sample concentrations were between 2×10^{-4} and 2×10^{-5} M. Deionized water had a resistance of >10 MΩ. Methanol of analytical grade was purchased from Fluka. All chemicals were used without further purification.

The fluorescence up-conversion technique was employed in this study to measure the time-resolved emission of oxyluciferin at room temperature. The laser used for the fluorescence up-conversion was a cavity dumped Ti:Sapphire femtosecond laser, Mira, Coherent, which provides short, 150 fs, pulses at around 800 nm. The cavity dumper operated with a relatively low repetition rate of 800 kHz. The up-conversion system (FOG-100, CDP, Russia) operated at 800 kHz. The samples were excited by pulses of ~8 mW on average at the SHG frequency. The time response of the up-conversion system is evaluated by measuring the relatively strong Raman−Stokes line of water shifted by 3600 cm^{-1}. It was found that the fwhm of the signal is 300 fs. Samples were placed in a rotating optical cell to avoid degradation.

We used the time-correlated single-photon counting (TCSPC) technique to measure the time-resolved emission of oxyluciferin and D-luciferin. For sample excitations we used a cavity dumped Ti:Sapphire femtosecond laser, Mira, Coherent, which provides short, 80 fs, pulses. The TCSPC detection system is based on a Hamamatsu 3809U, photomultiplier and Edinburgh Instruments TCC 900 computer module for TCSPC. The overall instrumental response was about 40 ps (fwhm). The excitation pulse energy was reduced to about 10 pJ by neutral density filters.

SUMMARY OF PREVIOUS TIME-RESOLVED RESULTS OF D-LUCIFERIN

In previous papers we studied the photophysics and photochemistry of D-luciferin in water and water−methanol mixtures.[23−27] We found that D-luciferin is a photoacid. Photoacids are weak acids in their ground-state and much stronger acids in their first electronically excited state.[23−27,32−44] Usually, acidity is increased by more than seven pK_a units upon excitation. For a ground-state pK_a value of ~7, one expects an excited-state value of pK_a* ≤ 0. The rate of intermolecular ESPT to the solvent varies exponentially with the pK_a* value in the range 0.5−3. For pK_a* = 1, the expected rate coefficient is $\sim 5 \times 10^9$ s^{-1}, which is much higher than the radiative rate coefficient for an allowed transition, i.e., $k_r \sim 10^8$ s^{-1}. We found that D-luciferin is a strong photoacid with pK_a* of approximately 0, its ESPT rate coefficient is 3.2×10^{10} s^{-1}, and the kinetic isotope effect (KIE) on its fluorescence decay is ~2.5. The deprotonated form undergoes an effective fluorescence quenching by excess protons in aqueous solution. Scheme 3 describes the complex photoprotolytic reactions that

Scheme 3. Photoprotolytic Cycle of D-Luciferin and Oxyluciferin

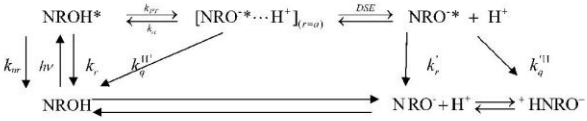

D-luciferin undergoes upon photoexcitation of the ground-state neutral protonated form, designated as NROH in the scheme. Upon excitation of the NROH form ESPT takes place to form the NRO^-*. The proton geminate recombination (reverse reaction) leads to ground-state NROH (k_q^{H+} in scheme 3). About half of the excited-state proton transfer events end up by fluorescence quenching whereas in the other events the proton is further removed from the NRO^-* molecules by a proton diffusion to the bulk (designated as DSE arrow in the scheme). The complexity of this reaction lies in the effective geminate recombination with the proton that leads to fluorescence quenching of the deprotonated form, NRO^-. There are two nitrogen atoms in the heterocyclic backbone of D-luciferin that can function as potential photobases. Upon excitation, these nitrogens may increase their basicity, so that they may snatch a proton from a nearby water molecule or react with a diffusing proton that was transferred to the solvent and form $^+HNRO^-$ that emits at 590 nm.

RESULTS

Steady State. Figure 1 shows the time-integrated steady-state excitation and emission spectra of oxyluciferin and D-luciferin in slightly acidic H_2O and D_2O solutions (pH ~ 6), respectively. The absorption maximum of the protonated NROH* form of D-luciferin and oxyluciferin are positioned at ~330 and 370 nm, respectively. The position of the NROH* emission band of both molecules is about the same (440 nm), whereas the position of the NRO^-* emission band of oxyluciferin (band maximum at 550 nm) is red-shifted with respect to that of D-luciferin by ~17 nm. The fluorescence intensity ratio $I^f_{NROH*}/I^f_{NROH^-*}$ is higher for oxyluciferin. This is an indication that D-luciferin is a stronger photoacid, provided that the radiative decay rates of both the NROH* and the

dx.doi.org/10.1021/jp301910p | J. Phys. Chem. A 2012, 116, 7452−7461

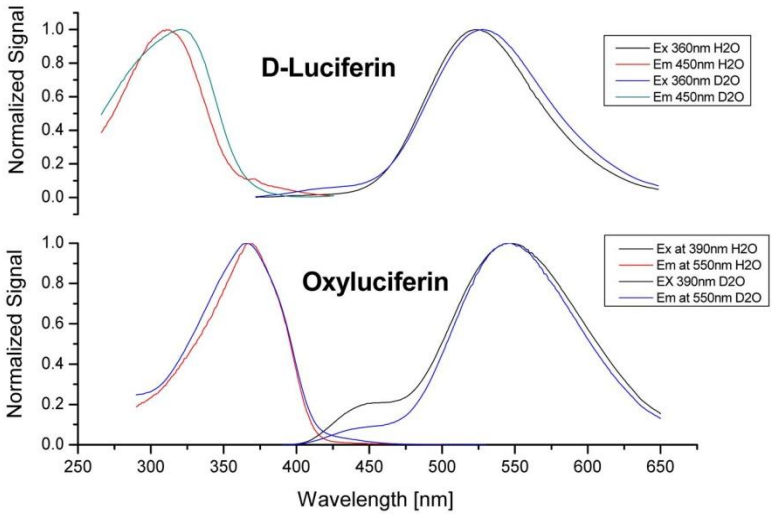

Figure 1. Time-integrated steady-state excitation and emission spectra in slightly acidic H_2O and D_2O solution (pH ~ 6), respectively, of (a) oxyluciferin and (b) D-luciferin.

NRO^{-}* forms of both D-luciferin and oxyluciferin are the same. The reality, however, is more complex, as will be shown by the time-resolved measurements. The absorption spectra of oxyluciferin in H_2O at several pH values are given in Figure s1d in the Supporting Information. At pH = 5 the absorption spectrum in the spectral range of 330−500 nm consists of two bands with peaks at 370 and 420 nm, which overlap to a great extent. At lower pH the intensity of the 420 nm band decreases, whereas that of the ~370 nm band increases. Two isosbestic points, at ~397 and 324 nm, are clearly seen. When the sample is excited at 374 nm, the emission spectrum consists of two bands; a weak band at 440 nm and a stronger one at 550 nm. Upon excitation at 420 nm, there is only a single band at ~550 nm, which is similar to the 550 nm band appearing when samples are excited in acidic solution at 370 nm.

Time-Resolved Emission. *Time-Correlated-Single-Photon-Counting Measurements.* Figures 2 and s1a in the Supporting Information show on linear and semilogarithmic scales the time-resolved emission of oxyluciferin in water at several wavelengths measured by the TCSPC technique, which is a highly sensitive method with a good signal-to-noise ratio and a wide dynamic range. The time resolution of this technique, however, is limited to ~20 ps and the full width half-maximum of the instrument's response function (IRF) is ~40 ps.

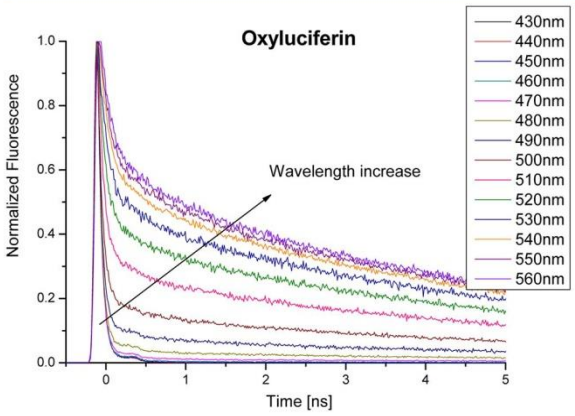

Figure 2. TCSPC time-resolved emission of oxyluciferin in water at several wavelengths.

As seen in the figures, the protonated NROH* form's signals measured at $\lambda \leq 470$ nm decay fast, whereas the signals at $\lambda \geq 510$ nm, mainly attributed to the NRO^{-}* species, have a bimodal decay curve with a short and long time decay components. Parts b and c of Figure s1 (Supporting Information) show biexponential fits of the fluorescence signals shown in Figures 2 and s1a (Supporting Information). The parameters of these fittings are given in Table s1 (Supporting Information).

Kinetic Isotope Effect. Figures 3 and s2 (Supporting Information) show on linear and semilogarithmic scales the time-resolved emission of oxyluciferin in both H_2O and D_2O, where in each panel the two signals are compared at a selected wavelength. The decay rate of the main fluorescence decay component at $\lambda \leq 470$ nm attributed to the protonated form is fast, and it is slower in D_2O than in H_2O. We therefore assign this fast decay component to ESPT to the solvent. In previous studies on ESPT processes of photoacids, we found that the kinetic isotope effect (KIE) is around 3 for photoacids with pK_a^* > 0.4, and this value reduces the stronger the photoacid. For D-luciferin we found that the KIE = 2.5 ± 0.1. Using a multistretched exponential decay function to fit the data, we found that the short-time decay component of oxyluciferin is 47 ± 5 ps and 118 ± 10 ps in H_2O and D_2O, respectively. The KIE value for oxyluciferin is therefore 2.5 ± 0.2, a figure that closely resembles that of D-luciferin. The values of the fitting parameters of the time-resolved emission of the signals for oxyluciferin in H_2O and D_2O at several wavelengths are given in Tables s1 and s2 (Supporting Information), respectively. Tables s3 and s4 (Supporting Information) provide the fitting parameters for D-luciferin in H_2O and D_2O, respectively. Detailed description of the fitting procedure is given in the Supporting Information.

The oxyluciferin signals at $\lambda \leq 500$ nm could be reasonably fitted by a large component (≥0.9) with a lifetime of 47 and

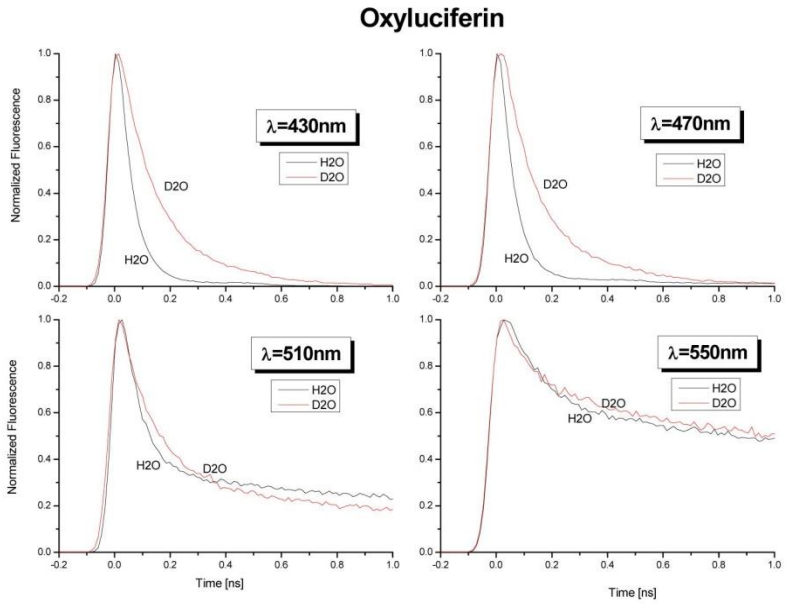

Figure 3. Time-resolved emission of oxyluciferin in both H_2O and D_2O.

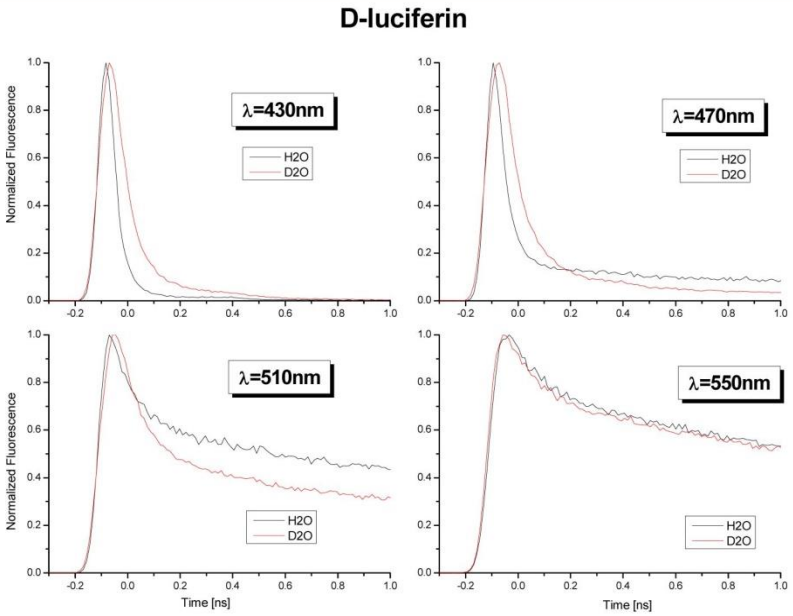

Figure 4. Time-resolved emission of D-luciferin in both H_2O and D_2O at pH ~ 6, excited by 150 fs pulses at 385 nm.

118 ps in H_2O (Table s1, Supporting Information) and D_2O (Table s2, Supporting Information) respectively. A long-time minor component (<0.1) of 5.2 ns in H_2O and 8.2 in D_2O is present in all the short wavelength measurements. At 460 nm, the amplitude of the long-time decay component is only 0.003. However, as the monitored wavelength becomes longer, the amplitude of this component also increases. Similar parameters were found for the fit of the D-luciferin signals. At $\lambda \geq 510$ nm the oxyluciferin signals have a relatively fast decay component of 0.13 ns in H_2O and 0.18 ns in D_2O with an amplitude of about 0.5 at 540 nm, followed by a long component, of 3.8 and 4.6 ns in H_2O and D_2O respectively. We attribute the short component at long wavelengths, $\lambda \geq 510$ nm to the irreversible recombination of the nitrogen atoms of the thiazole rings with the proton. The long lifetime is due to the radiative decay process of oxyluciferin in these solvents.

Figures 4 and s3 show on linear and semilogarithmic scales the time-resolved emission of D-luciferin in both H_2O and D_2O at pH ~ 6, excited by 150 fs pulses at 385 nm. In each panel the two signals are compared at a given wavelength, in much the same way as the signals of oxyluciferin are given in Figure 3. At $\lambda \leq 470$ nm the signal's decay curve mainly consists of a short-

time component, which exhibits a distinctive KIE. The decay time of the short component is 30 ± 5 ps in H_2O and 75 ± 10 ps in D_2O. We reported similar results in a previous article.[23] The decay times of D-luciferin in both H_2O and D_2O are 1.6 times shorter than those of oxyluciferin. At $\lambda \geq 510$ nm the fluorescence decay is bimodal, much like oxyluciferin. It has a short time decay component of ~100 ps and a relative amplitude of 0.5 at $\lambda \geq 530$ nm, which is the peak of the NRO^-* band. As in the case of oxyluciferin, the time constant of the long-time component of the fluorescence decay of the NRO^-* band varies with the solvent, $\tau_{H_2O} \simeq 3.9$ ns and $\tau_{D_2O} \simeq 4.6$ ns. The KIE is therefore 1.18, a considerably lower value than that of oxyluciferin (1.6). The lifetime of the NRO^-* form in both H_2O and D_2O is shorter than in oxyluciferin.

Parts a and b of Figure s4 (Supporting Information) show on linear and semilogarithmic scales the time-resolved emission signals of both D-luciferin and oxyluciferin in D_2O. In each panel the two signals are shown in a given wavelength. At $\lambda \leq 470$ nm the fluorescence decay of the ROH* of D-luciferin is much shorter than that of oxyluciferin. At 550 nm the decay times of the short components of both molecules have roughly the same value around 100 ps, whereas the time constant of the long component is 8.2 and 4.6 ns for oxyluciferin and D-luciferin, respectively.

To summarize this subsection, the D-luciferin ESPT rate constant in water, $k_{PT} = 3.2 \times 10^{10}$ s^{-1} is somewhat larger than that of oxyluciferin $k_{PT} = 2.2 \times 10^{10}$ s^{-1}. Both compounds have the same KIE of 2.5 when the solvent is replaced by D_2O. The emission of the NRO^- deprotonated form has a lifetime of 3.8 ns for D-luciferin and 5.2 ns for oxyluciferin. Both D-luciferin's and oxyluciferin's NRO^- time-resolved emission is bimodal with a short component decay time of about 130 ps and an amplitude of about 0.35.

Up-Conversion Fluorescence Measurements. Figures 5 and s5 show the fluorescence up-conversion signals of oxyluciferin

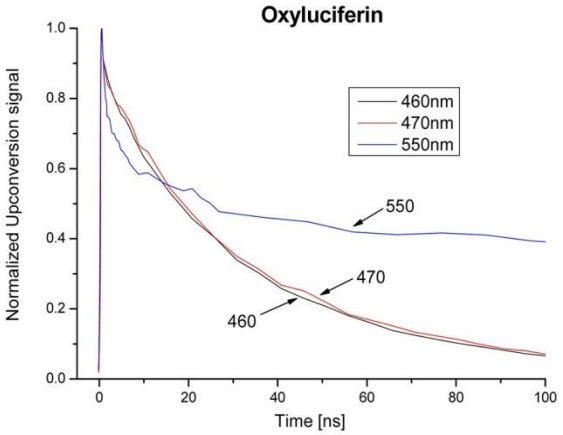

Figure 5. Fluorescence up-conversion signals of oxyluciferin at several wavelengths.

at several wavelengths. The time resolution of the up-conversion technique is approximately 100 times better than that of the TCSPC technique. The full width half-maximum of the IRF is ~300 fs compared with ~45 ps of the TCSPC. The up-conversion technique is about 3 orders of magnitude less sensitive than TCSPC, and consequently, the signal-to-noise ratio and the dynamic range are also smaller than TCSPC.

The signals have a short component of a few picoseconds followed by a longer nonexponential component. The average decay time of the long component is ~45 ps, which is comparable to the value obtained from the TCSPC signal of 47 ps, attributed to the ESPT rate to the solvent. The up-conversion signal measured at 550 nm does not have a rise component, as expected due to the NRO^-* creation reaction, i.e., NROH* → NRO^-* + H^+. The TCSPC signals measured at $\lambda \geq 530$ nm, and whose time resolution is much lower, also do not have a rise component. We suggest that this is due to an efficient nonradiative process, assisted by protons first transferred to the solvent and then recombined with the NRO^-* on the nitrogen site via a solvent bridge. The nitrogen atom is a mild base in the electronic ground state of heterocyclic compounds, and a much stronger base in the excited state. We therefore suggest that the nonexponential decay curve of the NRO^-* is due to an excited-state recombination process with the proton, NRO^-* + H^+ → NROH(g). A similar finding was reported and a similar explanation was offered previously in our study on the photophysics and photochemistry of D-luciferin.[23]

Figure 6a shows the fluorescence up-conversion signals of D-luciferin in water measured at several wavelengths. As seen in the figure, the average decay times of the D-luciferin signals are shorter than those of oxyluciferin. Figure 6b shows the oxyluciferin and D-luciferin signals measured at 470 nm. As seen in this figure, the oxyluciferin signal's decay time is longer than that of D-luciferin. At $\lambda \geq 530$ nm, the fluorescence up-conversion signal of D-luciferin (shown in Figure 6a) has a distinct rise component, whereas the oxyluciferin signal at long wavelengths does not (Figure 5). We consider the cause of this difference to be the faster proton-assisted quenching rate of oxyluciferin.

Time-Resolved Spectra of Oxyluciferin and D-Luciferin. Figure 7 shows the constructed normalized time-resolved emission spectra of oxyluciferin and D-luciferin in H_2O at several times in the range 50 fs to 1 ns. We constructed the spectra as follows. We assumed that at 2 ps the spectrum mainly consists of the NROH* emission and a smaller contribution from the NRO^-*. The shapes of the NROH* and NRO^-* emission bands at 2 ps are assumed to be roughly the same as those measured with the steady-state fluorometer. This assumption somewhat distorts the constructed spectra because it does not fully account for spectral shifts associated with solvation dynamics. Fortunately, the spectral shifts in the case of both chromophores are relatively small. This is shown in Figure 2, where the time-resolved fluorescence signals of the oxyluciferin NROH* band (430–470 nm) are nearly identical. When the change in solvent reorganization energy is low, the time-dependent band shift is small and the approximation is justified. The spectra shown in the figure were constructed from the time-resolved emission signals of the chromophores in water, and sampled in 10 nm intervals in the spectral range 430–560 nm. As seen in the figure, the NROH* band intensity diminishes with time. The time-resolved spectra of both chromophores have similar time dependence and spectral behavior. The intensity of the NROH* band decreases over time, whereas that of the NRO^-* band increases. The rates at which the NROH* decreases and the NRO^-* increases are similar. We therefore conclude that oxyluciferin and D-luciferin undergo ESPT to the solvent. Figures s6–s8 (Supporting

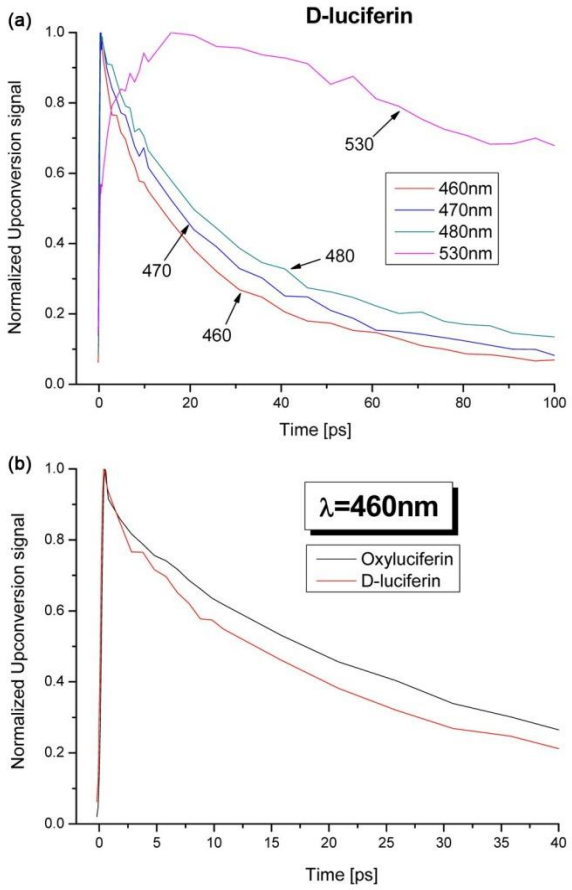

Figure 6. (a) Fluorescence up-conversion signals of D-luciferin in water measured at several wavelengths. (b) Fluorescence up-conversion signals of oxyluciferin and D-luciferin in water measured at 460 nm.

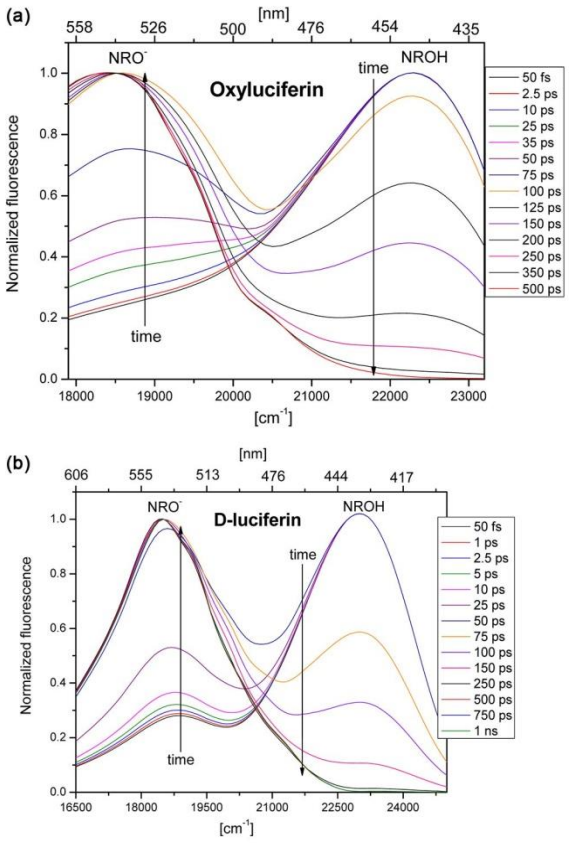

Figure 7. Normalized time-resolved emission spectra constructed from TCSPC signals: (a) oxyluciferin in H_2O; (b) D-luciferin in H_2O.

Information) show the time-resolved spectra of D-luciferin in H_2O and of oxyluciferin in both H_2O and D_2O. As expected, the rate of ESPT in D_2O is slower by a factor of 2.5 than in H_2O. A good criterion to the fit quality is the constructed steady-state spectra by time integration of the time-resolved spectra. This is shown in Figures s6c, s7c, and s8c in the Supporting Information. The figures show the steady-state emission spectra of oxyluciferin and D-luciferin in H_2O and also oxyluciferin in D_2O measured by a fluorometer against the constructed steady state by time integration of the time-resolved spectra. As seen in the figures, the constructed steady state qualitatively fits the measured spectra. We are unable to identify a new band that can be assigned to the keto/enol equilibrium that may take place on the thiazole ring.

Acid Effect. Figure 8 shows the time-resolved TCSPC emission signals of the NROH* of oxyluciferin at 440 nm and the NRO^-* at 540 nm in several acidic aqueous solutions. The NROH* signals are almost invariant under change of the acid concentration (Figure 8a), whereas the decay of NRO^-* signals varies with the concentration of the acid such that the higher its concentration the faster the decay rate. A similar acid effect was previously observed for D-luciferin. The excess protons in the solution react with the NRO^-* to form NROH(g). This reaction is diffusion-controlled, where the proton diffusion constant, $D_{H^+} \approx 10^{-4}$ cm^2/s, and the diffusion-controlled reaction rate coefficient, $k_D = 5 \times 10^{10}$ M^{-1} s^{-1}, for a reaction between the proton cation and the NRO^-* species anion. Thus, an acid concentration of 10 mM reduces the long decay time component of the NRO^-* from 5.2 ns to ~2 ns.

To summarize the acid effect, for both D-luciferin and oxyluciferin the main fluorescence band assigned to the NRO^- form is quenched when acid is added to aqueous solution, the quenching rate is diffusion controlled.

Methanol–Water Mixtures. Figure 9 shows the time-resolved emission of the NROH* (440 nm) and NRO^-* (540 nm) forms of oxyluciferin in several water–methanol mixtures. The signals of the NROH* are strongly dependent on the methanol concentration. In almost pure methanol (~99%) the decay time is rather long, i.e., 1.6 ns, whereas in a mixture of 95% water (by volume) the decay time is 47 ps. Similar dependence on the water–methanol mixture's composition is shared by many photoacids. For strong and weak photoacids whose $pK_a^* \geq 0$ the ESPT rate in methanol is 100 times slower than in water. Thus, an ESPT process with a time constant of 50 ps in water is expected to take 5 ns in methanol, which is about the same as the radiative lifetime of an allowed transition from a ground-state singlet state to an excited singlet state. According to the Marcus model, which relates the rate coefficient of a reaction and its free energy, the rate coefficient of reactions where $\Delta G > 0$ scales approximately exponentially

dx.doi.org/10.1021/jp301910p | J. Phys. Chem. A 2012, 116, 7452–7461

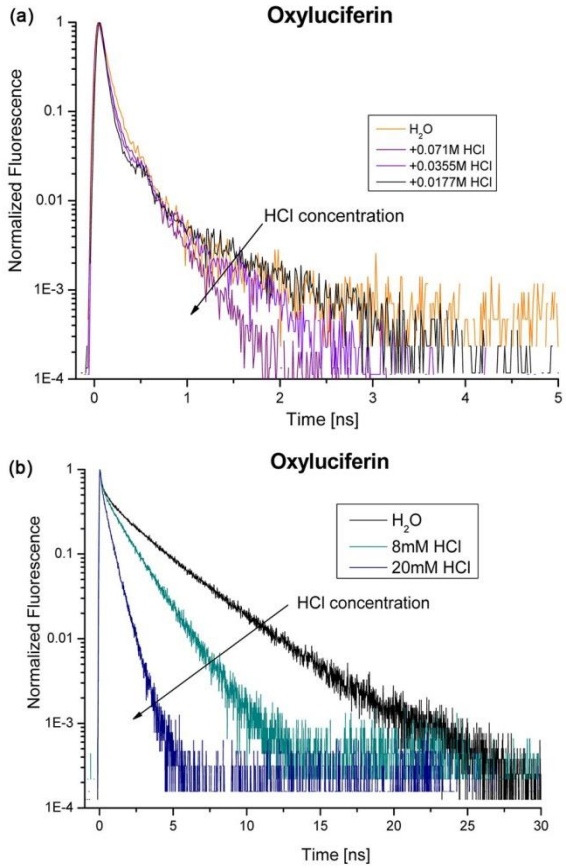

Figure 8. Time-resolved TCSPC emission signals of oxyluciferin in several acidic aqueous solutions measured at (a) 440 nm and (b) 540 nm.

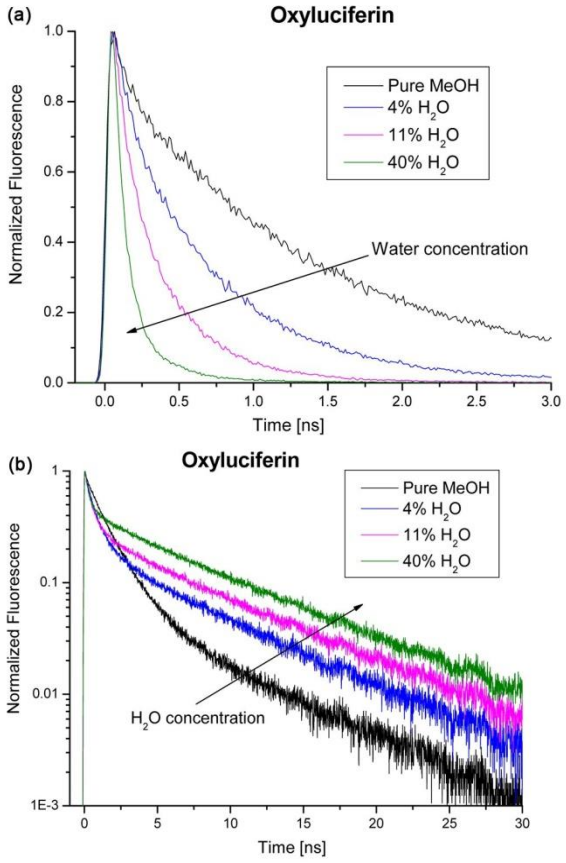

Figure 9. Time-resolved emission of oxyluciferin in several water–methanol mixtures: (a) NROH* (440 nm) form; (b) NRO^{-}* (540 nm) forms.

with the pK_a* value. For a weak photoacid with pK_a* value of ~1.5, the ESPT rate coefficient in water is ~10^9 s^{-1}. In these instances the radiative rate is much faster than the ESPT rate in methanol (10^7 s^{-1}), and thus the efficiency of the ESPT process is very low. The steady-state fluorescence spectrum of weak photoacids in methanol exhibits mainly the emission band of the protonated form and only ~1% of the deprotonated form, whereas in water both the protonated and deprotonated forms' emission bands appear.

The TCSPC signals shown in Figure 9b are bimodal and can be fitted by short and long decay components. The amplitude of the short decay component in water–methanol mixtures decreases as the water concentration increases. The decay time is independent of the mixture's composition. The lifetime of the long-time decay component is almost independent of the mixture's composition, as its value in neat water and neat methanol (and every volumetric ratio in between) is nearly the same. In neat methanol the amplitude of the short time decay component of the TCSPC signal at 540 nm is ~0.98. We attribute the short-time component of the 540 nm signal to the NROH* emission, whereas the long-time decay component, whose amplitude is 0.02, to the NRO^{-}* band. The 1.6 ns decay of the signal at 440 nm is similar to the decay time of the major component of the 540 nm signal.

Figure s9 in theSupporting Information shows the steady-state emission spectrum and the excitation of oxyluciferin in methanol. The emission spectrum consists of only the NROH band with a band maximum at ~445 nm. For D-luciferin, we found that it is capable in the excited state to transfer a proton in neat methanol and thus the steady-state spectrum consists of a strong NROH band and a weak NRO^{-} band.[24]

The emission spectrum of oxyluciferin in methanol consists of only the NROH* band, whereas in water the emission bands of both forms appear in the spectrum upon excitation of the ground-state NROH (Figure 1). Similar dependence of the time-resolved emission on the water–methanol mixture's composition was previously reported in our study on D-luciferin. The decay time of the NROH* band decreases the more aqueous the mixture becomes. However, even in pure methanol two bands appear in the D-luciferin emission spectrum, and the decay time of the NROH* is ~400 ps, indicating that ESPT does indeed take place. We therefore conclude that between these two homologous molecules D-luciferin is the stronger photoacid. This conclusion is also backed by the larger ESPT rate coefficient of D-luciferin in water of 3.3 × 10^{10} s^{-1} compared to 2.1 × 10^{10} s^{-1} of oxyluciferin.

Basic Solution. Figure 10 shows the steady-state excitation and emission spectra of oxyluciferin and D-luciferin in aqueous

dx.doi.org/10.1021/jp301910p | J. Phys. Chem. A 2012, 116, 7452–7461

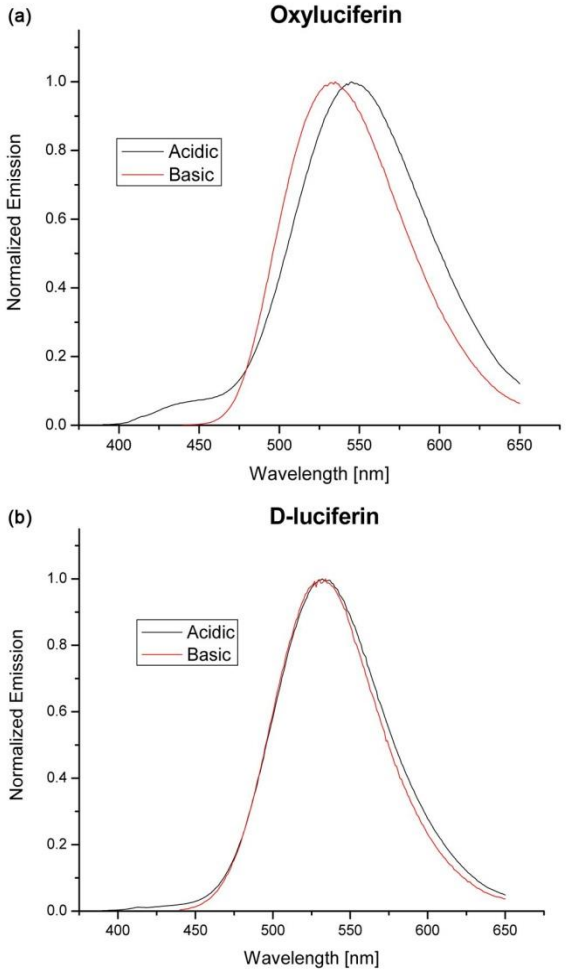

Figure 10. Steady-state excitation and emission spectra in aqueous acidic (pH ~ 4.5) and basic (pH ~ 9) solutions of (a) oxyluciferin and (b) D-luciferin.

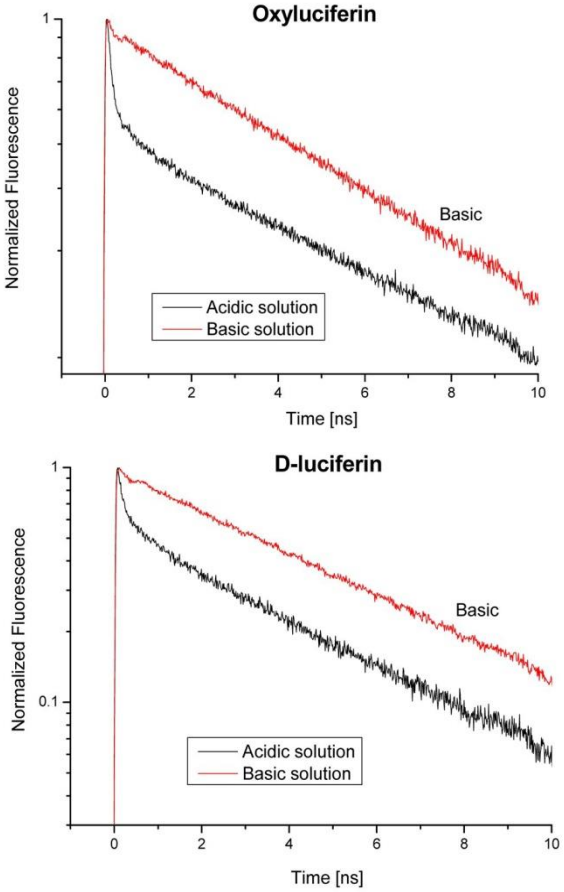

Figure 11. Time-resolved emission of the deprotonated NRO^{-}* form in both acidic (pH ~ 4.5) and basic (pH ~ 9) aqueous solutions of (a) oxiluciferin and (b) D-luciferin.

acidic (pH ~ 4.5) and basic (pH ~ 9) solutions, respectively. The oxyluciferin and D-luciferin spectra in the acidic solutions, where the molecules were excited at their NROH form's absorption band, are composed of two bands: a weak NROH* band and a strong NRO^{-}* band. The position of the peak of the NRO^{-}* band of oxyluciferin in basic solution is at ~540 nm, whereas its peak position upon excitation of the NROH form is at ~550 nm. The emissions of the NRO^{-}* of D-luciferin in both basic and acidic solutions are almost identical in their shapes and positions. We are unaware of previous reports on large changes in the position of the emission band of oxyluciferin as a function of the pH value of the solution. We are not yet certain of the origin of this strong pH effect on the NRO^{-}* band's position, though we suspect it is related to the tautomerization of the thiazole ring (Scheme 2) or to a second ionization of the excited-state species.[12]

Figure 11 shows the time-resolved emission of the deprotonated NRO^{-}* form of oxyluciferin and D-luciferin in both acidic and basic aqueous solutions, respectively. The TCSPC NRO^{-}* signals (measured at the peak of the emission band) of both oxyluciferin and D-luciferin in acidic solutions consist of a fast decaying component and a slow one. In basic solution the amplitude of the short component of the NRO^{-}* signal of both D-luciferin and oxyluciferin is smaller than 0.05, whereas in acidic solution its value is ~0.35. As aforesaid, we attribute the short component to fluorescence quenching by the geminate recombination with the proton probably occurring at one of the nitrogen atoms. In basic solutions, recombination does not occur because a proton is not transferred to the solution to begin with.

a. **Main Findings.** The ground-state pK_a measured for a 30% methanol in water rich methanol mixtures by absorption is ~7.
b. The steady-state emission measurements clearly show that when the NROH form is excited the spectrum consists of a dual emission band. The bands are assigned to the NROH* and NRO^{-}* forms.
c. The decay time of the time-resolved emission signal of the NROH* form is ~45 ps in H_2O and ~120 ps in D_2O.
d. The TCSPC signals of the NRO^{-}* measured at long wavelengths are bimodal with a short time decay component, whose average lifetime is about 0.2 ns, and a long decay time of about 5.2 and 8.2 ns in H_2O and D_2O, respectively, for the long component.

dx.doi.org/10.1021/jp301910p | J. Phys. Chem. A 2012, 116, 7452−7461

e. In acidic aqueous solutions the time-resolved TCSPC emission signals of the NROH* form are only slightly affected at an acid concentration of up to 20 mM, whereas the decay time of the long component of the NRO^-* decay decreases linearly with the acid concentration. The strong acid effect on the NRO^-* emission lifetime is attributed to recombination with the proton that leads to a ground-state NROH (g).
f. The ESPT rate of photoacids with $pK_a^* \geq 0.5$ in methanol is slower than in water by a factor of 100 or more. This is also true for oxyluciferin, a mild photoacid that is incapable of transferring a proton to methanol. D-Luciferin, however, is a stronger photoacid that can also transfer a proton to methanol.

DISCUSSION

The experimental results clearly show that like D-luciferin, oxyluciferin is a photoacid. In the ground state it is a weak acid with pK_a value of ~7, whereas in the electronically excited state it becomes a much stronger acid. We estimate the pK_a^* value to be approximately 0.5, which is roughly the pK_a^* of 2N68DS.

The ESPT rate coefficient of oxyluciferin in H_2O is 2.2×10^{10} s^{-1}, which is slightly lower than that of D-luciferin, i.e., 3.2×10^{10} s^{-1}.

The molecular backbone of both compounds is very similar. The difference lies in that the D-luciferin thiazole moiety is bonded to a carboxylic group, whereas the same moiety in oxyluciferin can present a ketonic or enolic functional group (Schemes 1 and 2). The pK_a^* values of 2N, its sulfonate derivatives, and cyano derivatives are smaller by about 7 orders of magnitude than their pKa values. 2N has a pK_a^* value of ~2.7 and that of 2N68DS is 0.5, whereas cyanonaphthols are even stronger with negative pK_a^* values, e.g., 5,8-dicyano-2-naphthol whose pK_a^* value is ~−4. Calculations have shown that the main indication to a photoacid's strength is the excited-state energy of the deprotonated form with respect to that of the protonated form. The more electron withdrawing functional groups bonded to the aromatic rings there are, the lower the energy of the deprotonated form and the stronger the photoacid, thus delocalizing the effective charge of the hydroxylate group and the overall energy of the deprotonated form.

D-Luciferin and oxyluciferin are different from other photoacids, because there is a large fluorescence quenching of the deprotonated NRO^-* form, when the molecule is excited from the ground-state NROH form, and the NRO^-* is the product of the photoprotolytic process (Scheme 3).

In general, photoacids can be divided into two groups, reversible and irreversible photoacids. For reversible photoacids, the second step in the photoprotolytic process, after a forward reaction, in which a proton is transferred to the solvent, is a diffusion-assisted geminate recombination of the deprotonated form with the proton to reform the excited protonated form of the photoacid. Irreversible photoacids, which undergo geminate recombination, however, decay to the ground state and therefore the fluorescence of the deprotonated form of an irreversible photoacid is weaker than that of a reversible one. In acidic solution (pH ≤ 3) the steady-state emission band intensity of the deprotonated form decreases linearly with the acid concentration. The time-resolved fluorescence decay curve on a semilogarithmic scale, of a deprotonated form of an irreversible photoacid is concave in solutions where the pH level is in the range 4−7. The concave shape is explained by the diffusion-assisted irreversible geminate recombination reaction with the proton. The amplitude of the fast component, seen in the NRO^- fluorescence decay of both D-luciferin and oxyluciferin is much larger than expected from a regular irreversible photoacid such as 1-naphthol and its sulfonate derivatives. The amplitude of the fast component in the emission of the RO^-* of 1N4S for example, is much smaller than those of both luciferin compounds. We therefore attribute this fast quenching process of the luciferins to the irreversible geminate recombination of the proton with the nitrogen of the thiazole ring, leading to an efficient fluorescence quenching. This reaction is efficient because it is probably assisted by a water bridge forming a proton wire between the hydroxyl group and the nitrogen.

SUMMARY

Oxyluciferin is the active chromophore of the bioluminescence luciferase enzyme-catalyzed reaction taking place in fireflies, for which D-luciferin acts as a substrate. These two compounds (shown in Schemes 1 and 2) are photoacids. The photoacidic functional group is the hydroxyl at position six on the 6-hydroxybenzothiazole moiety. On the thiazole, D-luciferin has a carboxylic group where oxyluciferin is in either a ketone or enol form. In the current study, we compare the photophysical and photochemical properties of both compounds. For this purpose, both time-resolved TCSPC and fluorescence up-conversion techniques were used. Both compounds are weak acids in their electronic ground state with a pK_a value of ~7. In the excited state, the acidity of both molecules increases by more than seven pK_a units. The rate coefficient of the ESPT to the solvent is high, i.e., 3.3×10^{10} and 2.1×10^{10} s^{-1} for D-luciferin and oxyluciferin, respectively. There is a strong KIE on both molecules' fluorescence decays of 2.5 ± 0.1. Fluorescence of both molecules' NRO^-* form is unusually quenched when excited from their NROH form (Scheme 3). The fluorescence decay of the NRO^-* form is bimodal with a minor component of 100 ps and an amplitude of 0.35 followed by a major component of 3.8 and 5.2 ns for D-luciferin and oxyluciferin, respectively. The fluorescence decay of the NRO^-* form of both compounds, when the molecules are in a basic solution and excited from their NRO^- form, is nearly exponential. We attribute the fast fluorescence quenching rate to the geminate recombination of the proton with NRO^-* at a nitrogen atom site that leads to the formation of the ground-state zwitterion $^+HNRO^-$.

ASSOCIATED CONTENT

Supporting Information

Time-resolved TCSPC and fluorescence up-conversion emission figures on semilogarithmic scale. Data fitting procedure and tables of fitting parameters. Time-resolved spectra of oxyluciferin in H_2O, D_2O, and methanol. This information is available free of charge via the Internet at http://pubs.acs.org

AUTHOR INFORMATION

Corresponding Author

*E-mail: huppert@tulip.tau.ac.il. Tel: 972-3-6407012. Fax: 972-3-6407491.

Notes

The authors declare no competing financial interest.

■ ACKNOWLEDGMENTS

This work was supported by grants from the Israel Science Foundation and from the James-Franck German-Israeli Program in Laser-Matter Interaction. Financial support from Fundação para a Ciência e Tecnologia (FCT, Lisbon) (Programa Operacional Temático Factores de Competitividade (COMPETE) e comparticipado pelo Fundo Comunitário Europeu (FEDER) (Project PTDC/QUI/71366/2006) is acknowledged. A Ph.D. grant to Luís Pinto da Silva (SFRH \76612\2011), attributed by FCT, is also acknowledged.

■ REFERENCES

(1) Marques, S. M.; Esteves da Silva, J. C. G. *IUBMB Life* **2009**, *61*, 6−17.
(2) Pinto da Silva, L.; Esteves da Silva, J. C. G. *J. Chem. Theory Comput.* **2011**, *7*, 809−817.
(3) Leitão, J. M.; Esteves da Silva, J. C. G. *J. Photochem. Photobiol. B* **2010**, *101*, 1−8.
(4) Viviani, V. R. *Cell. Mol. Life Sci.* **2002**, *59*, 1833−1850.
(5) Viviani, V. R.; Arnoldi, F. G.; Neto, A. J.; Oehlmeyer, T. L.; Bechara, E. J.; Ohmiya, Y. *Photochem. Photobiol. Sci.* **2008**, *7*, 159−169.
(6) Fraga, H. *Photochem. Photobiol. Sci.* **2008**, *7*, 145−158.
(7) Hosseinkhani, S. *Cell. Mol. Life Sci.* **2011**, *68*, 1167−1182.
(8) Navizet, I.; Liu, Y. J.; Ferré, N.; Roca-Sanjuán, D.; Lindh, R. *ChemPhysChem* **2011**, *12*, 3064−3076.
(9) Hasegawa, J. Y.; Fujimoto, K. J.; Nakatsuji, H. *ChemPhysChem* **2011**, *12*, 3106−3115.
(10) Naumov, P.; Ozawa, Y.; Ohkubo, K.; Fukuzumi, S. *J. Am. Chem. Soc.* **2009**, *131*, 11590−11605.
(11) Naumov, P.; Kochynnoonny, M. *J. Am. Chem. Soc.* **2010**, *132*, 11566−11579.
(12) Pinto da Silva, L.; Esteves da Silva, J. C. G. *ChemPhysChem* **2011**, *12*, 951−960.
(13) Hirano, T.; Hasumi, Y.; Ohtsuka, K.; Maki, S.; Niwa, H.; Yamaji, M.; Hashizume, D. *J. Am. Chem. Soc.* **2009**, *131*, 2385−2396.
(14) Chen, S. F.; Liu, Y. J.; Navizet, I.; Ferré, N.; Fang, W. H.; Lindh, R. *J. Chem. Theory Comput.* **2011**, *7*, 798−803.
(15) Song, C.; Rhee, Y. M. *J. Am. Chem. Soc.* **2011**, *133*, 12040−12049.
(16) Pinto da Silva, L.; Esteves da Silva, J. C. G. *J. Comput. Chem.* **2011**, *32*, 2654−2663.
(17) Pinto da Silva, L.; Esteves da Silva, J. C. G. *ChemPhysChem* **2011**, *12*, 3002−3008.
(18) Pinto da Silva, L.; Esteves da Silva, J. C. G. *J. Phys. Chem. B* **2012**, *116*, 2008−2013.
(19) Tagami, A.; Ishibashi, N.; Kato, D.; Taguchi, N.; Mochizuki, Y.; Watanabe, H.; Ito, M.; Tanaka, S. *Chem. Phys. Lett.* **2009**, *472*, 118−123.
(20) Milne, B. F.; Marques, M. A.; Nogueira, F. *Phys. Chem. Chem. Phys.* **2010**, *12*, 14285−14293.
(21) Nakatani, N.; Hasegawa, J. Y.; Nakatsuji, H. *J. Am. Chem. Soc.* **2007**, *129*, 8756−8765.
(22) Esteves da Silva, J. C. G.; Magalhães, J. M. C. S.; Fontes, R. *Tetrahedron Lett.* **2001**, *42*, 8173−8176.
(23) Erez, Y.; Huppert, D. *J. Phys. Chem. A* **2010**, *114*, 8075−8082.
(24) Presiado, I.; Erez, Y.; Huppert, D. *J. Phys. Chem. A* **2010**, *114*, 9471−9479.
(25) Presiado, I.; Erez, Y.; Huppert, D. *J. Phys. Chem. A* **2010**, *114*, 13337−13346.
(26) Erez, Y.; Presiado, I.; Gepshtein, R.; Huppert, D. *J. Phys. Chem. A* **2011**, *115*, 1617−1626.
(27) Presiado, I.; Gepshtein, R.; Erez, Y.; Huppert, D. *J. Phys. Chem. A* **2011**, *115*, 7591−7601.
(28) Morton, R. A.; Hopkins, T. A.; Seliger, H. H. *Biochemistry* **1969**, *8*, 1598−1607.
(29) Jung, J.; Chin, C. A.; Song, P. S. *J. Am. Chem. Soc.* **1976**, *98*, 3949−3954.
(30) Ando, Y.; Akiyama, H. *Jpn. J. Appl. Phys.* **2010**, *49*, 117002−117006.
(31) Ribeiro, C.; Esteves da Silva, J. C. G. *Photochem. Photobiol. Sci.* **2008**, *7*, 1085−1090.
(32) Ireland, J. E.; Wyatt, P. A. *Adv. Phys. Org. Chem.* **1976**, *12*, 131−221.
(33) (a) Gutman, M.; Nachliel, E. *Biochem. Biophys. Acta* **1990**, *1015*, 391−414. (b) Pines, E.; Huppert, D. *J. Phys. Chem.* **1983**, *87*, 4471−4478.
(34) Tolbert, L. M.; Solntsev, K. M. *Acc. Chem. Res.* **2002**, *35*, 19−27.
(35) Rini, M.; Magnes, B. Z.; Pines, E.; Nibbering, E.T. J. *Science* **2003**, *301*, 349−352.
(36) Mohammed, O. F.; Pines, D.; Dreyer, J.; Pines, E.; Nibbering, E. T. J. *Science* **2005**, *310*, 83−86.
(37) Tran-Thi, T. H.; Gustavsson, T.; Prayer, C.; Pommeret, S.; Hynes, J. T. *Chem. Phys. Lett.* **2000**, *329*, 421−430.
(38) Agmon, N. J. *Phys. Chem. A* **2005**, *109*, 13−35.
(39) Spry, D. B.; Fayer, M. D. *J. Chem. Phys.* **2008**, *128* (084508), 1−9.
(40) Siwick, B. J.; Cox, M. J.; Bakker, H. J. *J. Phys. Chem B* **2008**, *112*, 378−389.
(41) Mohammed, O. F.; Pines, D.; Nibbering, E. T. J.; Pines, E. *Agnew. Chem. Intern. Ed.* **2007**, *46*, 1458−1461.
(42) Mondal, S. K.; Sahu, K.; Sen, P.; Roy, D.; Ghosh, S.; Bhattacharyya, K. *Chem. Phys. Lett.* **2005**, *412*, 228−234.
(43) Prasun, M. K.; Samanta, A. *J. Phys. Chem. A* **2003**, *107*, 6334−6339.
(44) Bhattacharya, B.; Samanta, A. *J. Phys. Chem. B* **2008**, *112*, 10101−10106.

Article 21

Excited-state proton transfer of firefly dehydroluciferin
Itay Presiado, Yuval Erez, Ron Simkovitch, Shay Shomer, Rinat Gepshtein, Luís Pinto da Silva, Joaquim C.G. Esteves da Silva and Dan Huppert
J. Phys. Chem. A **2012**, *116*, 10770-10779.

Luís Pinto da Silva was responsible for writing the Introduction and Summary sections of this paper, under the supervision of Professors Joaquim Esteves da Silva and Dan Huppert, and was involved in the discussion of the obtained results.

THE JOURNAL OF PHYSICAL CHEMISTRY A
Article
pubs.acs.org/JPCA

Excited-State Proton Transfer of Firefly Dehydroluciferin

Itay Presiado,[†] Yuval Erez,[†] Ron Simkovitch,[†] Shay Shomer,[†] Rinat Gepshtein,[†] Luís Pinto da Silva,[‡] Joaquim C.G. Esteves da Silva,[‡] and Dan Huppert*[,†]

[†]Raymond and Beverly Sackler Faculty of Exact Sciences, School of Chemistry, Tel Aviv University, Tel Aviv 69978, Israel

[‡]Centro de Investigação em Química, Departamento de Quimica, Faculdade de Ciencias da Universidade do Porto, R. Campo Alegre 687 4169-007 Porto, Portugal

Supporting Information

ABSTRACT: Steady-state and time-resolved emission techniques were used to study the protolytic processes in the excited state of dehydroluciferin, a nonbioluminescent product of the firefly enzyme luciferase. We found that the ESPT rate coefficient is only 1.1×10^{10} s^{-1}, whereas those of D-luciferin and oxyluciferin are 3.7×10^{10} and 2.1×10^{10} s^{-1}, respectively. We measured the ESPT rate in water−methanol mixtures, and we found that the rate decreases nonlinearly as the methanol content in the mixture increases. The deprotonated form of dehydroluciferin has a bimodal decay with short- and long-time decay components, as was previously found for both D-luciferin and oxyluciferin. In weakly acidic aqueous solutions, the deprotonated form's emission is efficiently quenched. We attribute this observation to the ground-state protonation of the thiazole nitrogen, whose pK_a value is ~3.

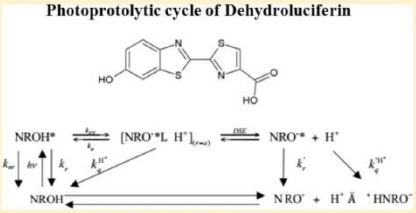

INTRODUCTION

Bioluminescence is an enzyme-catalyzed reaction, in which an excited-state product is formed and visible light is emitted.[1−3] This enzyme is always termed luciferase regardless of the organism in which it is found.[1−3] The most studied bioluminescence system is that of the fireflies due to their highly efficient luminescence.[1−4] Light is emitted by firefly oxyluciferin, which is formed due to a luciferase-catalyzed two-step reaction .[5,6]

Oxyluciferin (Scheme 1) is usually thought to exist in one of six chemical forms by means of a quadruple chemical equilibrium. However, several groups have demonstrated that oxyluciferin is formed in the anionic keto form during the bioluminescence reaction but exists in an enol form in solution.[7−10]

Scheme 1. Keto−Enol Tautomerism Equilibrium of Oxyluciferin

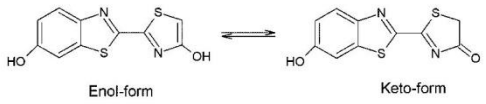

Despite the difficulties associated with the experimental study of oxyluciferin, it was found that its absorption spectrum has a band at ~440 nm for basic pH and one at ~370 at acidic-neutral pH.[10,11] The emission spectra were found to be characterized by a peak at ~550 nm at acidic-neutral pH and a peak at 540 nm at basic pH.[11] We have also found that oxyluciferin is a photoacid with an ESPT rate of 2.2×10^{10} s^{-1}. It also undergoes fluorescence quenching stemming either from geminate recombination with the proton or from excess protons in acidic media.[11]

D-Luciferin (Scheme 2) is one of the most useful analogues of the keto form of oxyluciferin, aside from being one of the substrates of the bioluminescence reaction. The absorption spectrum of this molecule is characterized by a maximum at ~330 nm in acidic solution, and it is red-shifted at basic pH (~390 nm).[11−16] The emission spectrum of D-luciferin has a maximum at ~530 nm over the studied pH range of 3−10.[11−16] However, a decrease in the polarity of the solvent uncovers an emission band with a maximum at ~450 nm.[11−16] The red shift with increasing pH and polarity of the solvent is attributed to the deprotonation of the benzothiazole hydroxyl group. In strongly acidic solutions, an emission band at ~590 nm is found, which corresponds to the protonation of one of the nitrogen heteroatoms. We have also found that D-luciferin is a photoacid with an ESPT rate of 3.7×10^{10} s^{-1}. It also undergoes fluorescence quenching stemming either from geminate recombination with the proton or from excess protons is acidic media.[11−16]

Scheme 2. Chemical Structures of D-Luciferin and L

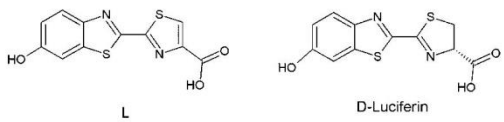

Received: September 5, 2012
Revised: October 10, 2012
Published: October 11, 2012

Firefly luciferase can also catalyze the formation of other nonbioluminescent products in dark lateral side reactions. In the presence of PP_i and dehydroluciferyladenylate (which is also produced in dark lateral reaction), luciferase can catalyze the formation of dehydroluciferin (L) (Scheme 2).[17−20] This molecule is an analogue of both oxyluciferin and D-luciferin. More importantly, while D-luciferin is more of an analogue of the keto form of oxyluciferin (due to the absence of a C═C double bond in the thiazole moiety), L is more of an analogue of the enol form of oxyluciferin (due to the presence of a C═C double bond in the thiazole moiety) (Scheme 2). This can be seen by the fact that at neutral-acidic pH, L has the same emission wavelength as oxyluciferin in aqueous solution (~550 nm).[21] Therefore, studying the spectroscopic properties and photoprotolytic cycle of this molecule can give us more insight into the spectroscopic properties of oxyluciferin in solution by bypassing the difficulties associated with experimenting with oxyluciferin itself. Moreover, the fact that luciferase can produce a fluorescent compound in a dark lateral reaction means that its bioluminescence reaction can affect the analysis of results obtained in spectroscopic studies of the luciferase−luciferin complex. Thus, there is the need for a more complete characterization of the photophysical properties and photoprotolytic cycle of L.

EXPERIMENTAL SECTION

(4S)-2-(6-Hydroxybenzothiazole-2-yl)-4,5-dihydrothiazole-4-carboxylic acid (D-luciferin) 99.5% was purchased from Iris Biotech (Germany). HCl (1 N) was purchased from Aldrich. Chemically synthesized oxyluciferin was obtained from 2-cyano-6-hydroxybenzothiazole and ethyl thioglycolate.[22] The parent compound 2-cyano-6-hydroxybenzothiazole was obtained from 2-cyano-6-methoxybenzothiazole (Aldrich, Steinheim, Germany).[8,20] L was chemically synthesized and purified as described previously.[20,22,23] For transient measurements, the sample concentrations were between 2×10^{-4} and 2×10^{-5} M. Deionized water had a resistance of >10 MΩ. Methanol of analytical grade was purchased from Fluka. All chemicals were used without further purification.

The fluorescence up-conversion technique was employed in this study to measure the time-resolved emission of L at room temperature. The laser used for the fluorescence up-conversion was a cavity-dumped Ti:Sapphire femtosecond laser, Mira, Coherent, which provides short, 150 fs, pulses at around 800 nm. The cavity dumper operated with a relatively low repetition rate of 800 kHz. The up-conversion system (FOG-100, CDP, Russia) operated at 800 kHz. The samples were excited by pulses of ~8 mW on average at the SHG frequency. The time response of the up-conversion system is evaluated by measuring the relatively strong Raman−Stokes line of water shifted by 3600 cm^{-1}. It was found that the fwhm of the signal is 300 fs. Samples were placed in a rotating optical cell to avoid degradation.

We used the time-correlated single-photon counting (TCSPC) technique to measure the time-resolved emission of L. The second harmonics (SHG) of the same laser described above, operating over the spectral range of 380−420 nm, was used to excite the photoacid samples. The TCSPC detection system is based on a Hamamatsu 3809U, photomultiplier, and Edinburgh Instruments TCC 900 computer module for TCSPC. The overall instrumental response was about 40 ps (fwhm). The excitation pulse energy was reduced to about 10 pJ by neutral density filters.

RESULTS

Figure 1 shows the excitation and fluorescence spectra of L in both H_2O and D_2O at slightly acidic samples (pH ≃ 6). The excitation spectrum was acquired at λ_{em} = 600 nm. For the emission spectrum, the sample was excited at 360 nm, and it consisted of a weak band with a peak at ~446 nm and a stronger band with a peak at ~550 nm. We attribute the two emission bands to the protonated NROH* and deprotonated NRO^-* forms of L, which, like D-luciferin and oxyluciferin (shown in Scheme 2), is a photoacid, and therefore, it undergoes a photoprotolytic process (shown in Scheme 3)

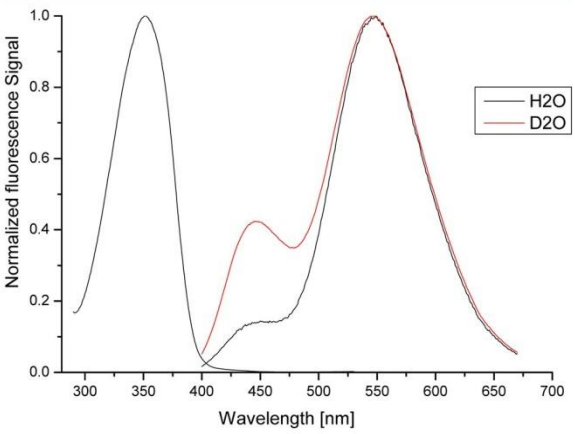

Figure 1. Excitation and fluorescence spectra of L in both H_2O and D_2O at slightly acidic samples (pH ≃ 6). The excitation spectrum was acquired at λ_{em} = 600 nm. For the emission spectrum, the sample was excited at 360 nm, and it consists of a weak band with a peak at ~446 nm and a stronger band with a peak at ~550 nm.

Scheme 3. Photoprotolytic Cycle of D-Luciferin, Oxyluciferin, and L

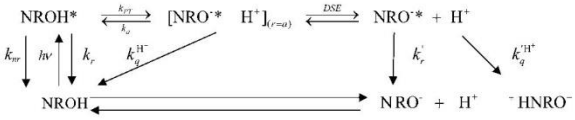

when the NROH form is electronically excited from its ground state. The NROH* form is a stronger acid than NROH. It transfers a proton to the solvent and becomes the deprotonated NRO^-* form within the excited-state lifetime. This ESPT process leads to the dual-band emission spectrum shown in Figure 1. The ESPT rate coefficient, k_{PT}, depends on the isotopic species that is transferred (H_3O^+/D_3O^+). The kinetic isotope effect (KIE) on k_{PT} for photoacids is usually around 3.[24] For both D-luciferin and oxyluciferin, we previously found a KIE value of ~2.5.[11] The steady-state emission is affected by the isotopic composition of the sample. The ratio between the intensities of the protonated and deprotonated forms of the bands in D_2O is higher than that in H_2O, as can be seen in Figure 1. We discuss the KIE in more detail later on.

Time-Resolved Emission. Figure 2 shows the fluorescence up-conversion time-resolved emission signal of L in aqueous solution. At $\lambda \leq 450$ nm, the signal consists of two components. The short-time component of about 1 ps and a relative amplitude of 0.2 at 440 nm is attributed to solvation dynamics,

dx.doi.org/10.1021/jp308818r | J. Phys. Chem. A 2012, 116, 10770−10779

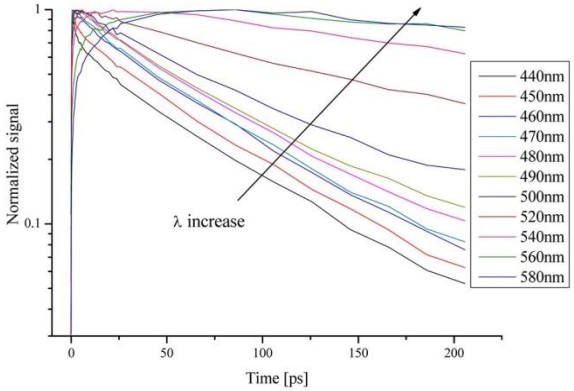

Figure 2. Fluorescence up-conversion time-resolved emission signal of L in aqueous solution.

which shifts the NROH* emission band to the red. The major component's decay is nonexponential with an average decay time of ~80 ps. At 460−490 nm, the short-time component disappears; therefore, the decay curve virtually consists of just the long-time component. A good fit to the nonexponential fluorescence up-conversion signals of the NROH* was obtained using a stretched exponent, $\exp[(-t/\tau)^{\alpha}]$, where $\alpha = 0.8$ and $\tau = 60$ ps. We attribute this component to the ESPT process of L. At $\lambda \geq 540$ nm, the signal consists of a distinctive rise component, followed by a long decay time. We attribute this emission signals to the formation of the excited deprotonated NRO^{-}* form by the photoprotolytic reaction described in Scheme 3.

Figures 3 and S1 in the SI show the time-resolved emission of L in aqueous solution detected at several wavelengths in the

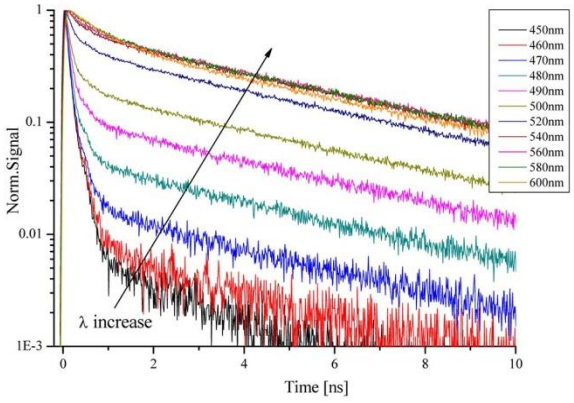

Figure 3. Time-resolved emission of L in aqueous solution detected at several wavelengths in the range of 450−600 nm on a semilogarithmic scale.

range of 450−600 nm on semilogarithmic and linear scales. The sample was excited by short ~150 fs laser pulses at ~387 nm. The excitation and detection of the time-resolved signal were carried out by the TCSPC technique, which has a wide dynamic range yet a limited time resolution of 20 ps because the instrument's response function (IRF) has a full width half-maximum (fwhm) of 40 ps. The signals in the range of 450−480 nm consist of a major decay component with an amplitude of 0.99 and a decay time constant of 88 ps and a longer minor decay component with a very small amplitude. The fast decay component arises from ESPT to the solvent. For D-luciferin and oxyluciferin, this time constant was significantly shorter, that is, 27 and 47 ps, respectively. We therefore conclude that the ESPT rate coefficients of D-luciferin, oxyluciferin, and L are 3.7×10^{10}, 2.1×10^{10}, and 1.1×10^{10} s^{-1}, respectively.

At $\lambda \geq 540$ nm, much of the signal arises from the emission of the deprotonated form, that is, the product of the photoprotolytic reaction. The TCSPC signal of L at these wavelengths could be divided into three time domains. The short-time domain from $t = 0$ until the signal's maximum is 100 ps in length. The rise of the signal is attributed to the formation of the NRO^{-}* form by the photoprotolytic reaction and the ~40 ps fwhm of the IRF. The second time domain stretches from the maximum to about $t = 1$ ns. It has a decay time of ~600 ps, and the intensity of the signal within this domain is reduced by about 35%. We attribute this component to ESPT from the hydroxyl group on the benzothiazole to a nitrogen on the thiazole ring via a water bridge made of one or two water molecules. Nitrogen in a heterocyclic ring is known to be a stronger base in the excited state.[25] It is also known that excited-state protonation of this nitrogen leads to fluorescence quenching. The time-resolved emission signals of both D-luciferin and oxyluciferin have similar fluorescence quenching intermediate time components. The long-time component of the time-resolved fluorescence decays exponentially with a time constant of 5.2 ns. This component is attributed to the radiative decay process of L. Similar radiative lifetimes exist for the fluorescence signals of both D-luciferin and oxyluciferin.[11]

Kinetic Isotope Effect. Figures 4 and S2 in the SI show on semilogarithmic and linear scales the time-resolved emission of L in both H_2O and D_2O. At $\lambda \leq 480$ nm, the TCSPC fluorescence decay signal provides the proton/deuteron transfer rate. At long wavelengths, the rise of the signal is indicative of the buildup of the deprotonated form's population. The NROH* and NRO^{-}* emission bands overlap at $\lambda > 520$ nm, and thus, TCSPC signals in that spectral region are the result of superposition of both emission bands. The time-resolved emission signal at frequency ν and time t is given by

$$I_F(\nu, t) = f_{NROH^*} \cdot g_{NROH^*}(\nu) \cdot F_{NROH^*}(t) + f_{NRO^{-}*} \cdot g_{NRO^{-}*}(\nu) \cdot F_{NRO^{-}*}(t) \quad (1)$$

where f_{NROH^*} and $f_{NRO^{-}*}$ are the oscillator strengths of the NROH* and NRO^{-}* emission bands, respectively, and $g_{NROH^*}(\nu)$ and $g_{NRO^{-}*}(\nu)$ are the line shape functions of the two bands. For simplicity, we assume that the line shapes of the two emission bands are constant in time. The time dependence of the NROH* band given in the term $F_{NROH^*}(t)$ is complex because the geminate recombination with the proton repopulates the NROH* state, and it causes the fluorescence decay curve to become nonexponential. The fluorescence decay of the NRO^{-}* of L, $F_{NRO^{-}*}(t)$, and other luciferins is complex because of the proton-assisted nonradiative process, that is, protonation of the heterocyclic nitrogen. The KIE on the time-resolved fluorescence of L and the two other luciferins at $\lambda \leq 480$ nm is relatively strong. We found a KIE value of 2.4 for L and 2.5 for D-luciferin and oxyluciferin. The structure of L (see Scheme 2) is simpler than that of oxyluciferin, which can exist in six different tautomers, where proton transfer can occur only from the two tautomers shown in Scheme 1. The reproducibility of the KIE values indicates that ESPT occurs

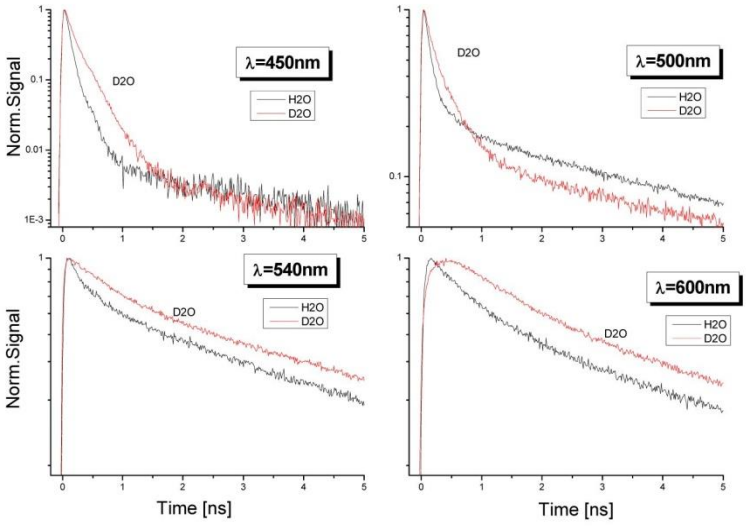

Figure 4. Time-resolved emission of L in both H_2O and D_2O on a semilogarithmic scale. At $\lambda \leq 480$ nm, the TCSPC fluorescence decay signal provides the proton/deuteron transfer rate.

from the hydroxyl group in L, where the hydroxyl is the only functional group capable of ESPT, but also in the other two luciferins. In the range of 490−530 nm, the relative amplitudes of the two bands rapidly change, from a large amplitude for the NROH* band and a small amplitude for the NRO^-* band at 490 nm to about equal amplitudes at ~520 nm. At $\lambda \geq 540$ nm, the relative amplitude of the NRO^-* signal is larger than that of the NROH*. In D_2O at 600 nm, the time-resolved signal clearly has a rise component stemming from the formation of the NRO^-* form via the photoprotolytic reaction. The formation time in D_2O is 2.5 times longer than that in H_2O. The biexponential fitting parameters to the TCSPC signals of L at various wavelengths in both H_2O and D_2O are given in Tables 1 and 2.

Table 1. Parameters of Time-Resolved Biexponential Analysis of Dehydroluciferin in H_2O

λ [nm]	τ_1 [ps]	b_1	τ_2 [ns]	b_2	χ^2
450	80	0.99	2.3	0.01	0.813
460	80	0.98	2.9	0.02	0.769
470	80	0.97	4.2	0.03	1.103
480	90	0.95	4.7	0.05	1.082
490	100	0.90	4.8	0.10	1.079
500	126	0.80	4.9	0.20	1.636
520	300	0.54	5.0	0.46	1.334
540	535	0.40	5.1	0.60	0.949
560	660	0.37	5.1	0.64	0.872
580	780	0.41	5.1	0.59	0.953
600	890	0.58	5.2	0.42	0.896

Comparing the Time-Resolved Emissions of the Three Luciferin Chromophores. In the past, we studied both D-luciferin and oxyluciferin with the same spectroscopic techniques.[11−16] In the current article, we wish to compare the steady-state and time-resolved spectra of the three compounds.

Figure 5a shows the time-resolved emission of the protonated forms of the three luciferins measured by the fluorescence up-conversion technique. As can be clearly seen, the decay time of NROH* of L is the longest. The decay time of D-luciferin is much shorter than L. As seen in Scheme 2, the two luciferins have similar structures. The difference lies in the thiazole ring, where the single bond of D-luciferin becomes a double C=C bond. This change accounts for the difference in the ESPT rates of a factor of 3.

Table 2. Time-Resolved Biexponential Analysis of Dehydroluciferin in D_2O

λ [nm]	τ_1 [ps]	b_1	τ_2 [ns]	b_2	χ^2
450	220	0.76	2.3	0.24	0.986
460	250	0.74	3.5	0.26	1.207
470	270	0.74	4.8	0.26	1.025
480	272	0.70	5.1	0.30	0.865
490	290	0.47	5.6	0.53	1.109
500	320	0.38	5.7	0.62	0.921
520	480	0.24	5.8	0.76	0.893
540	950	0.15	5.9	0.85	0.895
560	1300	0.27	6.0	0.73	0.801
580	1300	0.28	6.1	0.72	0.761

Figures 5b and S3 in the SI show the TCSPC signals of the three luciferin molecules on linear and semilogarithmic scales. At 450 nm, the time-resolved emission signal is greatly affected by the ESPT rate, whose time constants are 27, 47, and 88 ps for D-luciferin, oxyluciferin, and L, respectively. 2-Naphthol and 2-naphtholsulfonate derivatives are well-studied photoacids.[26] The ESPT rate from these molecules depends on the number of sulfonate groups and their positions in the molecule. For example, the ESPT time constants are 10 ns, 1 ns, and 40 ps for 2-naphthol, 2-naphthol-6-sulfonate, and 2-naphthol-6,8,-disulfonate, respectively. The differences in the ESPT rates can be explained by the Hamet relation and also by the Förster cycle. In the case of the three luciferins, the ESPT rates differ by much smaller values, and the reasons for them are yet unknown.

ESPT of L in Water−Methanol Mixtures. The photoacidity and the ESPT rate of photoacids with $pK_a^* \geq 0$ decrease

dx.doi.org/10.1021/jp308818r | J. Phys. Chem. A 2012, 116, 10770−10779

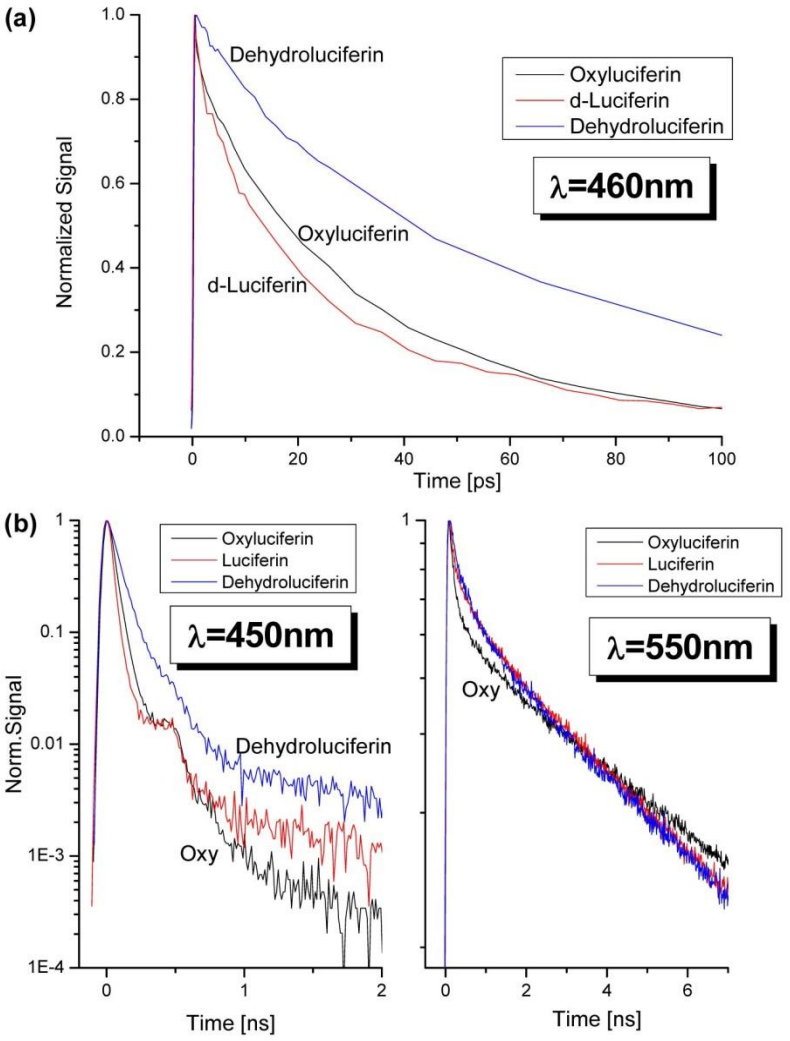

Figure 5. (a) Time-resolved emission of the protonated forms of the three luciferins measured by the fluorescence up-conversion technique. (b) TCSPC signals of the three luciferin molecules on a semilogarithmic scale.

by more than 2 orders of magnitude in methanol. The ESPT rates of L and 2-naphthol-6,8-disulfonate in water are 1.1×10^{10} and 2.0×10^{10} s^{-1}, respectively. On the basis of the free-energy relation between the ESPT rate and the pK_a*, we estimate the value of the latter to be 0.7 for L and 0.4 for 2-naphthol-6,8-disulfonate. 8-Hydroxypyrene-1,3,6-trisulfonate (HPTS) is a well-studied reversible photoacid with a pK_a* of ~1.3 and an ESPT rate coefficient of 10^{10} s^{-1} in water.[24] It cannot transfer a proton within the time frame of the excited state in neat methanol.

Figure 6 shows the steady-state emission spectra of L in several water−methanol mixtures. In pure methanol, the emission spectrum consists of only the NROH* emission band because the ESPT rate is slower than the radiative rate, which means that the efficiency of the ESPT process is very low. In a 10% aqueous solution of methanol (the lowest concentration of methanol in which L is soluble to an appreciable degree), the emission spectrum is composed of two emission bands. The weak band belongs to the NROH*

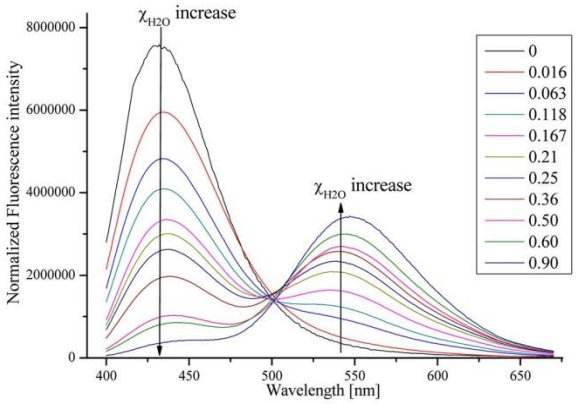

Figure 6. Steady-state emission spectra of L in several water−methanol mixtures.

form, whereas the strong band is that of the NRO^{-}* band. The less methanol there is in the mixture, the larger the intensity ratio becomes because the ESPT rate increases. This fluorescence intensity ratio is approximately given by the following expression:

$$I_{RO^{-}*}/I_{ROH*} \simeq \frac{k_{PT}}{k_F}\cdot\frac{k'_F}{k_F} \quad (2)$$

where k_F and k'_F are the reciprocals of the emission lifetimes of the NROH* and NRO^{-}* forms. It should be noted that k_F can be estimated from the emission of the NROH* form in the absence of an ESPT process by measuring the fluorescence decay in neat alcohols, where ESPT cannot occur. For the luciferins, the NRO^{-}* emission decay is not simply exponential with a rate coefficient k'_F because a proton-assisted quenching process take place, which further complicates the measurement of k_{PT} from the steady-state emission spectrum.

Figures 7 and S4 in the SI show on semilogarithmic and linear scales the time-resolved emission of L measured at 450 nm in water–methanol mixtures. As seen in the figures, the fluorescence decay rate of the NROH* form increases the higher the water content in the mixture. The decay of the signals shown in Figure 7 on a semilogarithmic scale is nearly exponential for more than 2 orders of magnitude for all of the mixtures that we measured. This implies that the geminate recombination taking place after proton transfer is irreversible. This is also verified in the time-resolved emission monitored at 550 nm, near the peak of the NRO^{-}* band. The decay of the NRO^{-}* signals in these mixtures is nonexponential, and their shape on a semilogarithmic scale is concave. This is due to the irreversible recombination process with the proton, which is characteristic for all luciferins that we studied, including L. Table 3 provides the decay times of the NROH* band in various water–methanol mixtures.

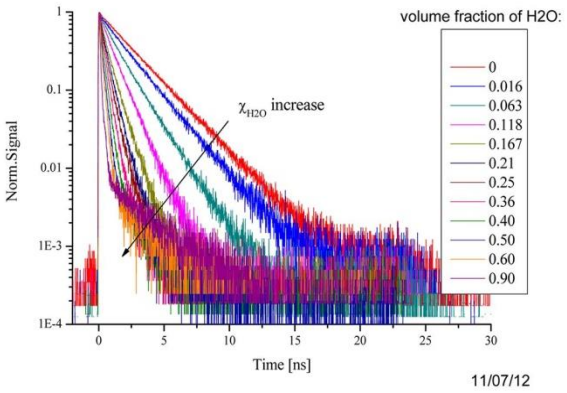

Figure 7. Time-resolved emission of L measured at 450 nm in water–methanol mixtures on a semilogarithmic scale. As seen in the figure, the fluorescence decay rate of the NROH* form increases the higher the water content in the mixture.

Acid Effect. For 1-naphthol and 1-naphtholsulfonate derivatives, which are simple irreversible photoacids carrying a hydroxyl group, addition of a strong mineral acid, such as HCl, leads to fluorescence quenching of the RO^{-}* emission by the reaction $RO^{-}* + H^{+} \rightarrow ROH*$.[27] This, we found, is also true for the luciferins.

Table 3. Average Lifetimes for Dehydroluciferin in MeOH/H_2O Mixtures; λ = 450 nm

volume fraction of H_2O	τ_{ave} [ns]
0	2.334
0.016	1.90
0.063	1.349
0.118	0.929
0.167	0.611
0.21	0.506
0.25	0.426
0.36	0.353
0.4	0.274
0.5	0.217
0.6	0.178
0.9	0.11

We conducted steady-state and time-resolved studies of L in the presence of HCl in the solution in concentrations ranging from 10^{-4} to 10^{-1} M. Figure 8 shows the steady-state emission spectra of L in 10% acidic aqueous solutions of methanol with acid concentrations in the range of 10^{-4} to 3×10^{-3} M. The intensity of both the NROH* and NRO^{-}* bands is reduced in the presence of HCl, although its effect is much stronger on the NRO^{-}* band than that on the NROH* band.

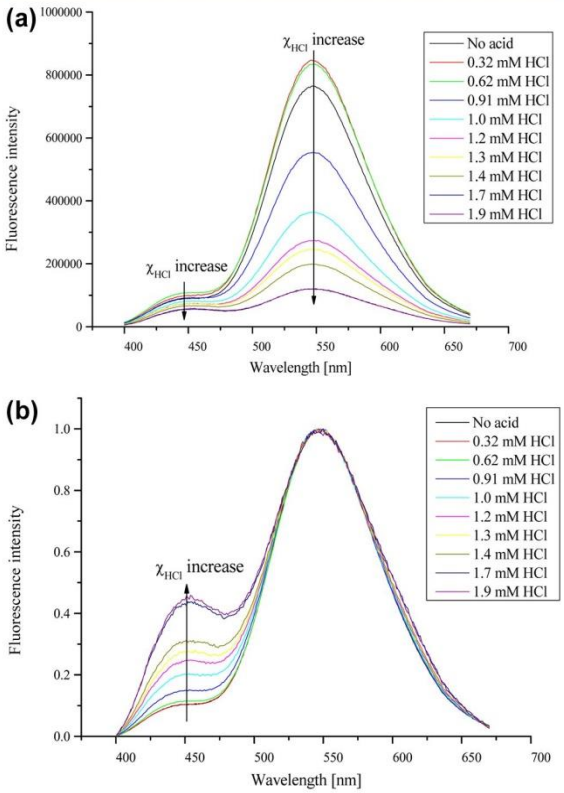

Figure 8. Steady-state emission spectra of L in acidic aqueous solutions with acid concentrations in the range of 10^{-4}–3×10^{-3} M; (a) non-normalized; (b) normalized.

Figure 9a shows the time-resolved emission of L measured at 550 nm near the peak of the NRO^{-}* emission band. The

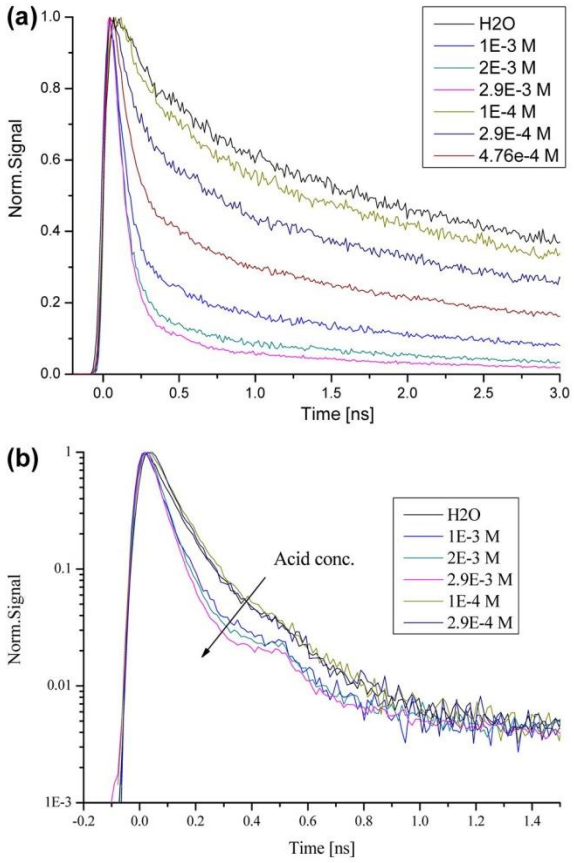

Figure 9. Time-resolved emission of L in various aqueous solutions of HCl measured at (a) 550 nm near the peak of the NRO^{-}* emission band and (b) 450 nm near the peak of the NROH* band.

fluorescence decay of the NRO^{-}* signal is bimodal with short- and long-time decay components. The amplitude of the short-time decay component increases with the acid concentration. The lifetime of this component decreases as the acid concentration increases. The lifetime of the long-time decay component is nearly invariant under change of the acid concentration in the range of 10^{-4}–10^{-3} M. At higher concentrations, the long decay time decreases as the acid concentration increases.

Figure 9b shows the time-resolved emission of L in the presence of HCl at the same concentrations as those shown in Figure 9a and measured at 450 nm, near the peak of the NROH* emission band. The decay of the NROH* signals is unaffected by the presence of HCl in the range of 10^{-5}–10^{-4} M. At higher concentrations, the fluorescence decay is shorter, that is, in neutral pH in water, the NROH* decay time is 90 ps, whereas in 1–10 mM, it is less than 50 ps. Table 4 provides the biexponential fitting parameters of both the NROH* and NRO^{-}* emission bands measured at 450 and 550 nm, respectively.

Main Findings. The main findings are as follows:

1. L is an irreversible photoacid with poor solubility in water.
2. The ESPT rate coefficient is 1.1×10^{10} s^{-1}, which is a value twice as small as that of oxyluciferin and three times smaller than that of D-luciferin.

Table 4. Biexponential Fits for Dehydroluciferin: Acid Effect

For λ = 450 nm				
C_{HCl}	a_1	τ_1 [ps]	a_2	τ_2 [ns]
no acid	0.996	80	0.004	3.0
1×10^{-4} M	0.95	85	0.05	2.9
2.9×10^{-4} M	0.95	75	0.05	2.9
1 mM	0.996	50	0.004	2.3
2 mM	0.996	<50	0.004	2.3
2.9 mM	0.996	<50	0.004	2.3
For λ = 550 nm				
C_{HCl}	a_1	τ_1 [ns]	a_2	τ_2 [ns]
no acid	0.33	0.35	0.67	0.42
1×10^{-4} M	0.4	0.28	0.6	4.2
2.9×10^{-4} M	0.54	0.23	0.46	3.9
4.75×10^{-4} M	0.71	0.13	0.29	3.5
1 mM	0.82	0.094	0.18	2.6
2 mM	0.90	0.094	0.10	2.0
2.9 mM	0.94	0.094	0.06	1.7

3. The KIE value is 2.4, which is similar to the value found in previous studies for D-luciferin and oxyluciferin.
4. In water–methanol mixtures, the ESPT rate decreases as the methanol content becomes higher. L cannot undergo ESPT in neat methanol.
5. Even in the presence of low excess proton concentration in the solution (milimolar), the steady-state fluorescence intensities of both the protonated and deprotonated forms are strongly suppressed. The time-resolved emission exhibits a large drop in the average decay time as well.

■ DISCUSSION AND DATA ANALYSIS

The results shown in Figures 1–5 clearly indicate that L, like the other two luciferin molecules that we previously studied, D-luciferin and oxyluciferin, is a photoacid. Photoacids are weak acids in the electronic ground state with pK_a's ranging from 9 to 4 and much stronger acids in the lowest excited electronic singlet state. Usually, the difference in the pK_a between the ground and excited states is higher than seven logarithmic units. The radiative lifetimes of the allowed transitions are about 10 ns or shorter. ESPT to the solvent occurs within this time window, and therefore, the ESPT rate coefficient is larger than 10^8 s^{-1}. After ESPT to water occurs, the solvated proton, the hydronium ion, may geminately recombine with the conjugate base of the photoacid to re-form the protonated form with the assistance of diffusion motion. For the luciferins, shown in Scheme 2, the nitrogen in the benzothiazole ring complicates the simple diffusion-assisted recombination process. The heteroatomic nitrogen is a stronger base in the excited state. It is also known that the recombination of the proton with the nitrogen leads to fluorescence quenching. In previous publications on the photophysics and photochemistry of the luciferins, we adopted an extended scheme that illustrates the elementary processes that the luciferins undergo upon photoexcitation (see Scheme 3).[11−16]

Upon photoexcitation of the ground-state neutral protonated form, designated as NROH in the scheme, ESPT to the solvent takes place and produces NRO^{-}* and a solvated proton. The proton geminate recombination (reverse reaction) leads to ground-state NROH (k_q^{H+} in Scheme 3). About half of the excited-state proton-transfer events end by fluorescence quenching, whereas in the other events, the proton is further

dx.doi.org/10.1021/jp308818r | J. Phys. Chem. A 2012, 116, 10770–10779

removed from the NRO^{-}* molecules by a proton diffusion to the bulk. The geminate proton can recombine with NRO^{-}* at longer times by diffusion-assisted reaction that can be mathematically formulated by the Debye−Smoluchowski equation (designated as the DSE arrow in the scheme). The complexity of this reaction lies in the effective geminate recombination with the proton that leads to fluorescence quenching of the deprotonated form, NRO^{-}. There are two nitrogen atoms in the heterocyclic backbone of the luciferins that can function as potential photobases. Upon excitation, these nitrogens may increase their basicity, so that they may snatch a proton from a nearby water molecule or react with a diffusing proton that was transferred to the solvent and form $^{+}HNRO^{-}$.

Water−Methanol Mixtures. In the previous section, we described the experimental results of L in water−methanol mixtures. In this section, we translate the fluorescence data to plots of ESPT rate coefficient versus the water−methanol mixtures' composition. The fluorescence decay of the protonated form increases the higher the water content in the mixture. As mentioned above, the decay curves of the NROH* form are nearly exponential. We obtained the ESPT rate coefficients from the average decay times, τ_{av}, by integrating the signals over time. Table 1 provides the values of τ_{av} obtained from the L signals from the various water−methanol mixtures. The longest decay time of the NROH* species, 2.33 ns, is obtained from the neat methanol solution. We assume that in pure methanol, the ESPT rate is much slower than $k_F \simeq 1/\tau_{av}^{meOH} = 4.15 \times 10^8\ s^{-1}$, where τ_{av}^{meOH} is the emission lifetime of the NROH* form in neat methanol in the absence of an ESPT process. To obtain the values of k_{PT} of L in water−methanol mixtures, we simply subtract the emission rate coefficient, k_F, from the fluorescence decay rate coefficient, $k = 1/\tau$, of the NROH* form in a water−methanol mixture of a given composition

$$k_{PT} = k - k_F \tag{3}$$

Figure 10 shows the plot of log k_{PT} versus the mole fraction of methanol in the mixture. The decrease in the value of k_{PT} with increasing mole fraction is nonlinear. Until an 0.8 mol fraction of methanol, the decrease in k_{PT} is moderate and almost linear. By this point, k_{PT} decreases by only a factor of 5. Upon further increase of the methanol concentration, k_{PT} drops sharply as the slope of the curve becomes steeper. At a water concentration of 0.015, the ESPT rate coefficient has a value of $\sim 10^8\ s^{-1}$. Similar dependence of the ESPT process on the water content of the mixture in water−methanol mixtures was previously found for photoacids with $pK_a^* \geq 0.4$. For stronger photoacids with $pK_a^* \leq 0$, we found that ESPT occurs even in neat methanol, where the k_{PT}^{meOH} value was equal to or higher than $2 \times 10^8\ s^{-1}$.

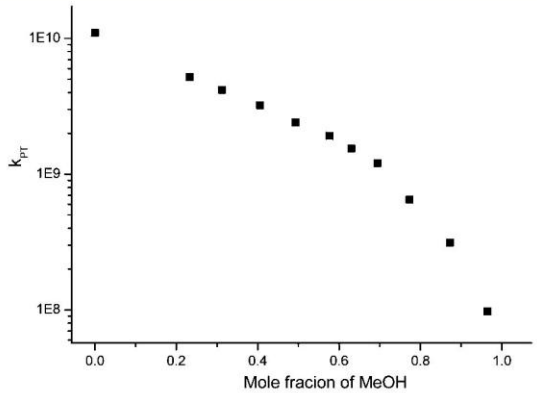

Figure 10. Plot of log k_{PT} versus the mole fraction of methanol in the mixture. Note that the decrease in the value of k_{PT} with increasing mole fraction is nonlinear.

Qualitative Explanation to the Acid Effect on L. In a previous study on D-luciferin,[11−16] the natural substrate of the firefly luciferase, in acidic solution, we found that at a pH level of about 1 (100 mM of HCl), the ground-state D-luciferin undergoes a protonation process. The emission spectrum of D-luciferin in a $c \geq 20$ mM acidic aqueous solution has a new emission band at 590 nm red-shifted with respect to the strongest emission band at 530 nm in a neutral aqueous solution. We attributed the new emission band to the zwitterion form designated as $^{+}HNRO^{-}$. The time-resolved emission signals show that the NRO^{-}* of the D-luciferin emission band at 530 nm and the zwitterion emission band at 590 are strongly quenched by a recombination process with an excess proton in an acidic aqueous solution. The recombination process is nearly diffusion-controlled, where $D_{H^+} = 0.9 \times 10^{-4}\ cm^2/s$. The diffusion-controlled rate coefficient is given by

$$k_D \cong 4\pi N' D_{H^+} R_D \tag{4a}$$

where $N' = N_A/1000$ and N_A is Avogadro's number. R_D is the Debye radius, which is given by the following expression:

$$R_D = \frac{ze^2}{4\pi\varepsilon_0 \varepsilon k_B T} \tag{4b}$$

where z is the ionic charge of the NRO^{-}* form, e is the electronic charge, ε_0 is the permittivity, ε is the dielectric constant of the solvent (for water, $\varepsilon = 78$), and k_BT is the thermal energy. The R_D value of luciferins is ~7 Å; hence, $k_{D_{H^+}} \simeq 5 \times 10^{10}\ M^{-1}\ s^{-1}$. In acidic samples, the second-order diffusion-controlled recombination rate coefficient is $k_{D_{H^+}}$, and the actual proton quenching rate of the NRO^{-}* fluorescence linearly depends on the product of this coefficient with the acid concentration. Figure S5 in the SI shows the time-resolved emission of the NRO^{-}* form of D-luciferin in aqueous solutions of 2, 3, and 4 mM HCl. The fluorescence decay time of the long-time component decreases as the acid concentration increases, whereas the short-time decay component is unaffected by this change. As opposed to the relatively mild acid effect on D-luciferin, the acid effect on the short-time component of L is much more pronounced, and it is already noticeable even at the low concentration of ~0.2 mM. Figure S6a in the SI shows the acid effect on the steady-state emission spectrum of D-luciferin. As seen in the figure, the fluorescence intensity of the NRO^{-}* band decreases as the acid concentration increases. While the fluorescence intensity of the NRO^{-}* band of D-luciferin decreases by a factor of 2, that of L decreases by a factor of 10 even at the low concentration of 2 mM. Addition of 2 mM HCl only affects the lifetime of the long-time component of the NRO^{-}* of D-luciferin. L, however, experiences the acid effect to a much greater extent as it impacts both the lifetime and amplitude of the short-time component, as can be seen in Figure 8b. At 1 mM, the pseudo-first-order reaction rate coefficient's value is $5 \times 10^7\ s^{-1}$, whereas k_F', the radiative rate coefficient, is 10 times larger, 2×10^8 ($\tau_{NRO^{-}*} = 5.2$ ns). We cannot therefore expect excess

dx.doi.org/10.1021/jp308818r | J. Phys. Chem. A 2012, 116, 10770−10779

protons at concentrations of up to 1 mM to have a significant effect on the fluorescence decays of both the NROH* and NRO^-* forms of L.

This explains what is seen in Figure 9b. The NROH* decay is not affected by the introduction of acid until its concentration reaches 1 mM. At neutral pH, the lifetime is 80 ps, and it drops to about 50 ps in the concentration range of 1−3 mM HCl. The steady-state and time-resolved emission spectra of the NRO^-* species, however, feel the effect of the acid from a concentration 10 times lower, that is, 0.2 mM. The intensity of the steady-state emission spectrum is reduced, and the decay profile of the time-resolved signal already changes from this low acid concentration. The amplitude of the short-time component increases from 0.2 in neutral pH solution to 0.9 in 3 mM HCl. The lifetime of the short-time decay component also decreases as the acid concentration increases. At 3 mM, the value of this lifetime is ∼100 ps, whereas in neutral pH, it is 500 ps. The lifetime of the long-time component of the NRO^-* band begins to be affected by the acid at concentrations higher than 1 mM, and the effect on this lifetime is in accord with what is expected from the diffusion-controlled reaction. We fit the time-resolved emission data from several solutions of varying acid concentrations with biexponential functions. The fitting parameters are given in Tables 2 and 3 for the NROH* and NRO^-* species, respectively.

The surprisingly strong acid effect on the NRO^-* band of L can be explained by the fact that the heterocyclic nitrogen atom in the benzothiazole ring is easily protonated by an excess proton in the ground state even at 2×10^{-4} M. When the $^+$HNROH species is excited, it undergoes ESPT to form the $^+HNRO^-$* form, which then undergoes a fast fluorescence quenching with a time constant of ∼100 ps. The change in the amplitude of the short-time component indicates that the protonation reaction of the heterocyclic nitrogen in the ground state depends on the acid concentration, as can be expected from the following chemical equilibrium: ($H^+ + NROH \overset{k_{eq}}{\rightleftarrows} {}^+HNROH$). The $^+$HNROH/NROH ratio increases the higher the acid concentration. Figure 11 shows the fluorescence intensity of the yellow emission band at ∼550 nm of both D-luciferin and L as a function of the acid concentration. The fluorescence intensity of L decreases sharply when the acid concentration approaches 1 mM. We attribute the large drop to the protonation of the nitrogen of the thiazole ring. We estimate that its pK_a is ∼3. This is accord with the findings of Haake et al.,[28] who measured the pK of thiazole and its derivatives. They found that its value is about 3. As mentioned above, we attribute the short-time component of the emission band at 550 nm to the $^+HNRO^-$* species, which is the product of the protolytic reaction when the reactant is $^+$HNROH*. At 4.7 mM, the protonation level is about 95%, as can be inferred from the fit to the time-resolved emission at 550 nm. The fluorescence intensity of the NRO^-* band of D-luciferin only mildly decreases with addition of acid and only at concentrations higher than 10 mM (see Figure 11). We are not yet certain as to why the NRO^-* fluorescence of L is much more sensitive to protonation of the nitrogen than D-luciferin and why the pK_a differs by more than one unit.

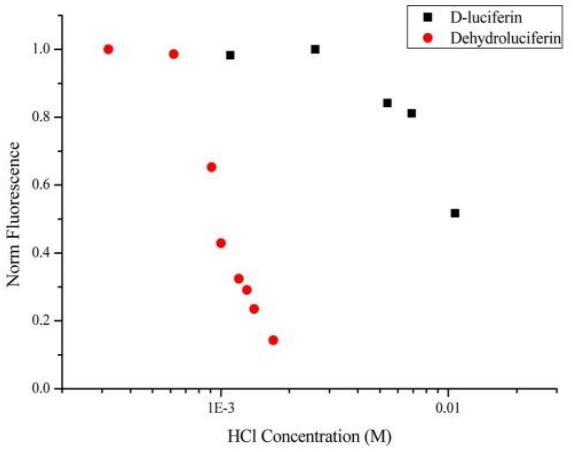

Figure 11. Steady-state spectra of the $^+HNRO^-$* emission band of both D-luciferin and dehyroluciferin in various HCl concentrations. Note how the relative fluorescence intensity changes as a function of the acid concentration.

SUMMARY

In the present work, we studied the photophysics and photochemistry of L, a nonbioluminescent chromophore of the firefly.

We found that L is a photoacid with an ESPT rate coefficient of 1.1×10^{10} s^{-1} and τ_{PT} = 88 ps. Previously, we found that D-luciferin and oxyluciferin transfer a proton to water with τ_{PT} values of 27 and 47 ps, respectively. D-Luciferin is a strong enough photoacid so as to transfer a proton to methanol. Only strong photoacids with pK_a* ≤ 0 can transfer a proton to aliphatic monols. After systematic study of the ESPT process of dehydroluciferin in water−methanol mixtures, we expectedly found that its ESPT rate decreases the higher the methanol content in the solution. The plot of the ESPT rate coefficient as a function of the mole ratio of methanol is nonlinear and similar in its shape to those of other photoacids, such as HPTS, 2-naphthol, and 5-cyano-2-naphthol. At a methanol mole ratio of 0.8, the ESPT rate decreases sharply by more than an order of magnitude as the methanol's mole ratio increases to 0.95.

We also conducted a study on the ESPT of L in aqueous solutions containing a strong acid. Surprisingly, a very strong acid effect on both the protonated and deprotonated forms' emissions was found. The steady-state fluorescence of both emission bands decreases as the acid concentration increases (see Figure 8). A significant decrease is noticeable even at concentrations as low as a few millimolars. At these low acid concentrations, the diffusion-controlled irreversible recombination reaction with a proton (NRO^-* + $H^+ \overset{k_D}{\rightarrow}$ NROH(g)) is ineffective because the pseudo-first-order rate coefficient is the product of k_D and the proton concentration, and because $k_D = 5 \times 10^{10}$ M^{-1} s^{-1} and the proton concentration is $\sim 10^{-3}$ M, its value is only $\sim 5 \times 10^7$ s^{-1}, which is four times smaller than the radiative rate coefficient, that is, 1.8×10^8 s^{-1}. The effective fluorescence quenching can be explained by ground-state protonation of the thiazole nitrogen. We found that the pK_a of this reaction for L is ∼3. This is accord with the findings of Haake et al.,[28] who measured the pK of thiazole and its derivatives. They found that its value is about 3. In a neutral aqueous solution, the deprotonated forms of the three luciferin molecules undergo an irreversible geminate recombination (fluorescence quenching by a proton) that is manifested by bimodal fluorescence decay curves at $\lambda \geq 540$ nm (see Scheme 2). The K_b of the nitrogen in the thiazole ring of L is probably

higher than those of the other two luciferins. The fluorescence of the $^{+}HNRO^{-}$* species, that is, the NRO^{-}* form protonated in its nitrogen site, is quenched within 100 ps. This leads us to conclude that the short-time decay component of the time-resolved fluorescence of the long wavelength band can be attributed to both $^{+}HNRO^{-}$* and NRO^{-}* forms. As the acid concentration rises, so does the amplitude of the short-time component, attributed to the $^{+}HNRO^{-}$* form. We also found that the fluorescence decay of the $^{+}HNROH$* species emitting at 450 nm is shorter than 50 ps, that is, shorter than that of the NROH*, whose lifetime is ~80 ps.

■ ASSOCIATED CONTENT

Supporting Information

Additional figures of dehydroluciferin on a linear scale, D-luciferin in acidic solution, dehydroluciferin in basic solution, and parameter tables of exponential fits to time-resolved data of dehydroluciferin. This material is available free of charge via the Internet at http://pubs.acs.org.

■ AUTHOR INFORMATION

Corresponding Author

*E-mail: huppert@tulip.tau.ac.il. Tel: 972-3-6407012. Fax: 972-3-6407491.

Notes

The authors declare no competing financial interest.

■ ACKNOWLEDGMENTS

This work was supported by grants from the Israel Science Foundation and from the James-Franck German−Israeli Program in Laser-Matter Interaction. Financial support from Fundação para a Ciência e Tecnologia (FCT, Lisbon) (Programa Operacional Temático Factores de Competitividade (COMPETE) e comparticipado pelo Fundo Comunitário Europeu (FEDER) (Project PTDC/QUI/71366/2006) is acknowledged. A Ph.D. grant to Luís Pinto da Silva (SFRH \76612\2011), attributed by FCT, is also acknowledged.

■ REFERENCES

(1) Marques, S. M.; Esteves da Silva, J. C. G. *IUBMB Life* **2009**, *61*, 6−17.
(2) Viviani, V. R.; Arnoldi, F. G.; Neto, A. J.; Oehlmeyer, T. L.; Bechara, E. J.; Ohmiya, Y. *Photochem. Photobiol. Sci.* **2008**, *7*, 159−169.
(3) Pinto da Silva, L.; Esteves da Silva, J. C. G. *ChemPhysChem* **2012**, *13*, 2257−2262.
(4) Pinto da Silva, L.; Esteves da Silva, J. C. G. *J. Chem. Theory Comput.* **2011**, *7*, 809−817.
(5) Pinto da Silva, L.; Esteves da Silva, J. C. G. *J. Phys. Chem. B* **2012**, *116*, 2008−2013.
(6) Pinto da Silva, L.; Esteves da Silva, J. C. G. *ChemPhysChem* **2011**, *12*, 3002−3008.
(7) Pinto da Silva, L.; Esteves da Silva, J. C. G. *ChemPhysChem* **2011**, *12*, 951−960.
(8) Esteves da Silva, J. C. G.; Magalhães, J. M. C. S.; Fontes, R. *Tetrahedron Lett.* **2001**, *42*, 8173−8176.
(9) Song, C.; Rhee, Y. M. *J. Am. Chem. Soc.* **2011**, *133*, 12040−12049.
(10) Naumov, P.; Ozawa, Y.; Ohkubo, K.; Fukuzumi, S. *J. Am. Chem. Soc.* **2009**, *131*, 11590−11605.
(11) Erez, Y.; Presiado, I.; Gepshtein, R.; Pinto da Silva, L.; Esteves da Silva, J. C. G.; Huppert, D. *J. Phys. Chem. A* **2012**, *116*, 7452−7461.
(12) Erez, Y.; Huppert, D. *J. Phys. Chem. A* **2010**, *114*, 8075−8082.
(13) Presiado, I.; Erez, Y.; Huppert, D. *J. Phys. Chem. A* **2010**, *114*, 9471−9479.
(14) Presiado, I.; Erez, Y.; Huppert, D. *J. Phys. Chem. A* **2010**, *114*, 13337−13346.
(15) Erez, Y.; Presiado, I.; Gepshtein, R.; Huppert, D. *J. Phys. Chem. A* **2011**, *115*, 1617−1626.
(16) Presiado, I.; Gepshtein, R.; Erez, Y.; Huppert, D. *J. Phys. Chem. A* **2011**, *115*, 7591−7601.
(17) Fontes, R.; Fernandes, D.; Peralta, F.; Fraga, H.; Maio, I.; Esteves da Silva, J. C. G. *FEBS J.* **2008**, *275*, 1500−1509.
(18) Fraga, H.; Fernandes, D.; Fontes, R.; Esteves da Silva, J. C. G. *FEBS J.* **2005**, *272*, 5206−5216.
(19) Ribeiro, C.; Esteves da Silva, J. C. G. *Photochem. Photobiol. Sci.* **2008**, *7*, 1085−1090.
(20) Pinto da Silva, L.; Esteves da Silva, J. C. G. *Photochem. Photobiol. Sci.* **2011**, *10*, 1039−1045.
(21) Fraga, H.; Esteves da Silva, J. C. G.; Fontes, R. *Tetrahedron Lett.* **2004**, *45*, 2117−2120.
(22) Fraga, H.; Esteves da Silva, J. C. G.; Fontes, R. *FEBS Lett.* **2003**, *543*, 37−41.
(23) Bowie, L. *J. Methods Enzymol.* **1978**, *57*, 15−28.
(24) Pines, E.; Huppert, D.; Agmon, N. *J. Chem. Phys.* **1988**, *88*, 5620−5630.
(25) Presiado, I.; Erez, Y.; Gepshtein, R.; Huppert, D. *J. Phys. Chem. C* **2009**, *113*, 20066−20075.
(26) Tolbert, L. M.; Solntsev, K. M. *Acc. Chem. Res.* **2002**, *35*, 19−27.
(27) Agmon, N.; Huppert, D.; Masad, A.; Pines, E. *J. Phys. Chem.* **1991**, *95*, 10407−10413.
(28) Haake, P.; Bausher, L. P. *J. Phys. Chem.* **1968**, *72*, 2213−2217.

6.2. Study of Deactivation Pathways for the Fluorescence of $OxyLH_2$, D-LH_2 and L

Article 22

Theoretical study of the efficient fluorescence quenching process of the firefly luciferin
Luís Pinto da Silva, Ron Simkovitch, Dan Huppert and Joaquim C.G. Esteves da Silva
J. Photochem. Photobiol. A: Chemistry **2013**, *266*, 47-54.

The theoretical calculations and the writing of the paper were performed by Luís Pinto da Silva, under the supervision of Professors Joaquim Esteves da Silva and Dan Huppert.

Journal of Photochemistry and Photobiology A: Chemistry 266 (2013) 47–54

Contents lists available at SciVerse ScienceDirect

Journal of Photochemistry and Photobiology A: Chemistry

journal homepage: www.elsevier.com/locate/jphotochem

Theoretical study of the efficient fluorescence quenching process of the firefly luciferin

Luís Pinto da Silva[a], Ron Simkovitch[b], Dan Huppert[b], Joaquim C.G. Esteves da Silva[a,*]

[a] Centro de Investigação em Química, Departamento de Química e Bioquímica, Faculdade de Ciências da Universidade do Porto, R. Campo Alegre 687, 4169-007 Porto, Portugal
[b] Raymond and Beverly Sackler Faculty of Exact Sciences, School of Chemistry, Tel Aviv University, Tel Aviv 69978, Israel

ARTICLE INFO

Article history:
Received 7 March 2013
Received in revised form 3 June 2013
Accepted 4 June 2013
Available online 14 June 2013

Keywords:
Fluorescence quenching
Firefly luciferin
Oxyluciferin derivatives
Intersystem crossing
Excited state proton transfer
Photoacids

ABSTRACT

The firefly oxyluciferin family of fluorophores has been attracting attention from the research community, due to their role on firefly bioluminescence. Moreover, this family exhibits a very efficient fluorescence quenching process. The elucidation of this process is very important, as it may occur inside of the luciferase active site, thereby decreasing the life time of bioluminescence. To this end we have used a computational approach to study the fluorescence quenching of firefly luciferin, the most studied member of the oxyluciferin family of fluorophores. We have found that the fluorescence quenching is due to the excited state protonation of the nitrogen heteroatom of the benzothiazole moiety. This protonation leads to a singlet to triplet intersystem crossing to triplet excited states, which explains the quenching of fluorescence.

1. Introduction

Hydrogen bonds and proton transfer reactions play important roles in many chemical, physical and biological processes [1–6]. Ground state hydrogen bonding is well studied, contrary to what happens in the excited state [6]. Nevertheless, this type of bonding can have important roles in excited state proton transfer (ESPT), on photochemistry and in fluorescence quenching processes, among others [7–11].

The acidity of many molecules which possess O–H groups increases after photoexcitation, which enables the study of proton-transfer involving hydrogen bonds in the excited state. This type of molecules are called photoacids [12,13]. A typical photoacid is a weak acid in the ground state with a pK_a in the range of 5–10. Also, the steady-state emission of the acidic form of a photoacid should have two emission bands: one attributed to an acidic form and another to a basic form (Scheme 1).

The oxyluciferin family of fluorophores has been receiving much attention from the research community, and it was found that oxyluciferin and a series of derivatives are photoacids [14–21]. This family of fluorophore has been receiving this kind of attention, as oxyluciferin is the light-emitting product of the firefly bioluminescence phenomenon [22–26]. Very interesting features of this phenomenon have triggered the development of new practical applications for this system in the pharmaceutical, biomedical and bioanalytical areas, among others [27–30].

Firefly oxyluciferin (Scheme 2) is thought to exist in one of six chemical forms due to a quadruple chemical equilibrium [31–33]. However, due to the instability of this chromophore in basic solutions, the complete characterization of its spectroscopic and structural properties have remained a challenge. D-Luciferin (Schemes 2 and 3) is one of the most useful derivatives of oxyluciferin due to similar spectroscopic properties and higher stability. It was found that D-luciferin is a photoacid with a $pK_a \approx 8$ (corresponding to the deprotonation of the hydroxyl-benzothiazole group) and a pK_a^* of approximately 0 [14,16–20]. When this molecule is photoexcited at pH < pK_a its absorption spectrum has a band at ~3.76 eV (corresponding to the carboxylate ion) [14,16–20]. The emission spectrum was found to be characterized by a peak at ~2.34 eV (corresponding to the emission of the doubly deprotonated D-luciferin dianion) [14,16–20]. The dianion is formed by ESPT involving the excited state carboxylate ion and solvent molecules (Scheme 4) [14,16–20].

One of the unique features of the photoprotolytic cycle of D-luciferin is a very large fluorescence quenching of the dianion species [14,16–20]. Experiment indicates that this quenching is due to a irreversible proton geminate recombination process with the fluorophore [14,16–20]. It was proposed that a solvent bridge composed of solvent molecules may form an efficient proton transporter, which connects the hydroxyl-benzothiazole group (the

* Corresponding author. Tel.: +351 226082869; fax: +351 226082959.
E-mail address: jcsilva@fc.up.pt (J.C.G. Esteves da Silva).

1010-6030/$ – see front matter © 2013 Elsevier B.V. All rights reserved.
http://dx.doi.org/10.1016/j.jphotochem.2013.06.001

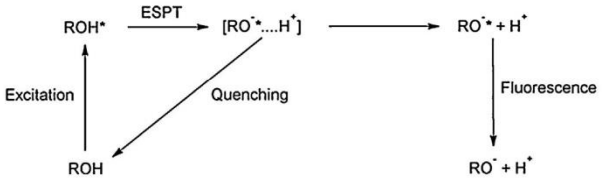

Scheme 1. General photoprotolytic cycle of a typical photoacid.

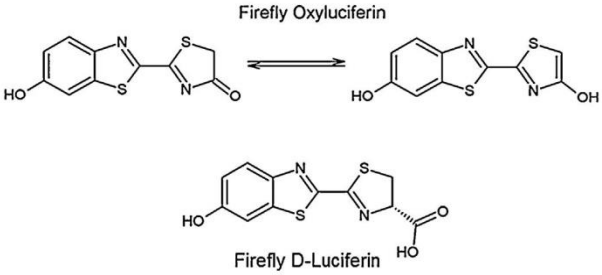

Scheme 2. Schematic representation of firefly oxyluciferin and D-luciferin.

proton donor) to one of the nitrogen heteroatoms, which could be photobases [14,16–20]. This efficient fluorescence quenching was also seen for other members of the oxyluciferin family of fluorophores (the same fluorescence quenching was even seen for oxyluciferin itself) [14,16–21].

Besides the intrinsic interest in the complete elucidation of the photoprotolytic cycle of D-luciferin, this type of study is even more important due to the role of oxyluciferin in firefly bioluminescence [27–30]. Thus, the clarification of the fluorescence quenching seen in the photoprotolytic cycle of this family of fluorophores is needed as it can also occur inside the luciferase active site, thereby decreasing the life time of bioluminescence. Given this, the objective of this work is to use a computational approach in the study of the efficient fluorescence quenching process observed for D-luciferin.

2. Computational methods

All the calculations were made by using the Gaussian 09 software package, specifically its density functional theory (DFT) based

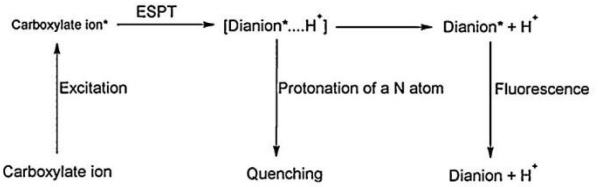

Scheme 4. Expected photoprotolytic cycle of firefly luciferin.

methods [34]. The ground state geometries of the luciferin species were obtained with the DFT PBE0 functional and the 6-31G(d) basis set (Scheme 3) [35]. Ground state relaxed coordinate scans were made in order to study the proton transfer reactions presented here, a strategy based on previous studies of proton transfer reactions [1,2]. Both geometry optimizations and relaxed coordinate scans were made *in vacuo*. The PBE0 functional was used due to good results in geometry optimizations of organic molecules [36–38].

The energies were re-evaluated at the CAM-B3LYP/6-31+G(d) with implicit solvent effects provided by the polarized continuum model (PCM, with parameters set for water) [39,40]. The excited state potential energy surfaces (PESs) were obtained by calculating the Franck–Condon curves by adding the time dependent (TD) CAM-B3LYP/6-31+G(d) vertical excitation energies [41]. Such strategy was already been successfully implemented to evaluate ESPT reactions [1,2,4,5,42,43]. The CAM-B3LYP and ωB97X-D functionals were used in order to get good estimates for possible charge transfer states [44,45].

3. Results and discussion

In order to see if our TD CAM-B3LYP/6-31+G(d)//PBE0/6-31G(d) reproduce well the absorption maxima of the luciferin species, we have calculated the absorption energies of both the carboxylate anion and dianion species (Scheme 3). The former molecule presented a theoretical absorption maximum of 3.91 eV, which differs only by 0.15 eV from the experimental value (~3.76 eV) [14,16–20]. The dianion species presented a calculated absorption maximum of 3.06 eV, which is only 0.12 eV lower than the experimental value (~3.18 eV) [14,16–20]. Thus, we can state that our theoretical approach presents results in line with experiment.

Three different partial charge schemes (Mulliken, NBO and ESP) were used in order to determine the atomic charges of N_b, N_t, O_1

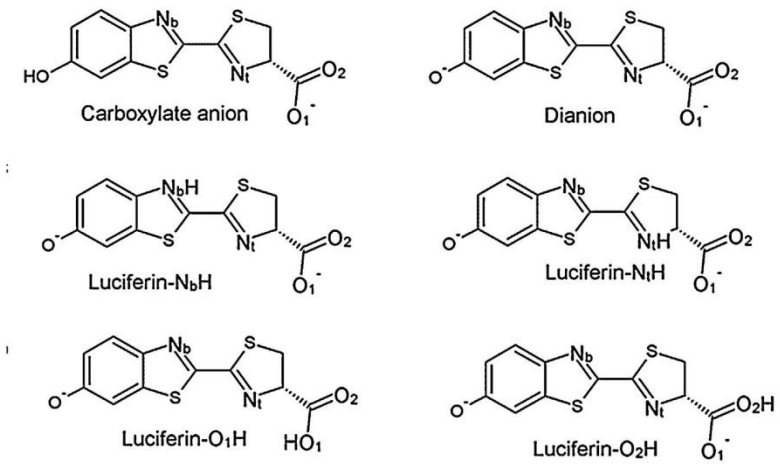

Scheme 3. Schematic representation of the six luciferin species studied in this work.

Table 1
Atomic charges of O_1, O_2, N_b and N_t of the luciferin dianion species, at both ground and excited states.

	Mulliken	ESP	NBO
Ground state			
O_1	−0.70	−0.86	−0.82
O_2	−0.69	−0.84	−0.82
N_b	−0.26	−0.47	−0.43
N_t	−0.18	−0.53	−0.49
Excited state			
O_1	−0.71	−0.86	−0.83
O_2	−0.69	−0.85	−0.83
N_b	−0.33	−0.60	−0.56
N_t	−0.29	−0.64	−0.59

and O_2 (Scheme 3) of the dianion species, in both the ground and excited states. This was made in order to analyze possible excited state proton acceptor atoms. The results are presented in Table 1. It can be seen that both O_1 and O_2 carry a higher negative atomic charge than all the other atoms analyzed, in the three different schemes. However, there is little difference in the charge of these atoms between the ground and excited states. The case is different for N_b and N_t. These two atoms have lower negative charges in the ground state than O_1 and O_2. However, in the excited state their negative charge increases between −0.07 and −0.14, which makes their charge more in line with the excited state atomic charges of O_1 and O_2. This is also in line with our previous assumption that N_b and N_t are stronger bases in the excited state than in the ground state [14,16–20]. In conclusion, these results indicate that by considering atomic charges only, O_1 and O_2 are the most likely excited state proton acceptors. However, N_b and N_t are also plausible candidates.

After these calculations, we have optimized the geometries of Luciferin-N_bH, Luciferin-N_tH, Luciferin-O_1H and Luciferin-O_2H as indicated in Section 2. Then, the ground state and the excited state Franck–Condon energies were re-calculated as indicated also in Section 2. The excited and ground state energies of Luciferin-O_1H were used as a reference, and the resulting relative energies are given in Table 2. It can be seen that in the ground state, Luciferin-N_tH is the most stable structure (with little difference for Luciferin-O_1H and Luciferin-O_2H), while Luciferin-N_bH is the most unstable structure. In the excited state, the situation is similar. However, Luciferin-N_tH is the most stable structure (with higher differences for Luciferin-O_1H and Luciferin-O_2H), while Luciferin-N_bH is not so unstable as compared with the other structures. Thus, the calculations performed so far indicate that Luciferin-N_tH is the most likely excited state proton acceptor. Nevertheless, it should be said that these stability calculations do not take into account the energetic of the proton transfer from the hydroxyl-benzothiazole group to any of these four atoms. So, their real relative stability may not be exactly as computed here.

Luciferin-N_tH presents a theoretical absorption maximum of 2.64 eV, which is associated with large oscillator strength of 1.0093. We have then performed a relaxed coordinate scan, in which we have increased the N_t—H distance from 1.03 to 1.28 Å. We have then re-evaluated the excited and ground state energies as indicated in the computational section methods. Excited and ground state Luciferin-N_tH energies were used as reference and the resulting curves are presented in Fig. 1a. It can be seen that the N_t—H dissociation reaction is very similar in both states, although being more unfavorable in the excited state. This is in line with the higher negative charge of N_t in the excited state. Fig. 1b and c present both the excited and ground state dissociation energies (when only ground state Luciferin-N_tH energy is used as reference) and the oscillator strength associated with each N_t—H bond length, respectively. These figures show that there is no interaction between the singlet ground and excited states, and there is no decline in the oscillator strength that can be associated with the protonation of the N_t atom, which can explain the efficient fluorescence quenching of firefly luciferin.

Table 2
Relative excited and ground state energies (kcal/mol) of Luciferin-N_bH, Luciferin-N_tH, Luciferin-O_1H and Luciferin-O_2H, with Luciferin-O_1H as reference.

	Ground state	Excited state
Luciferin-O_1H	0.0	0.0
Luciferin-O_2H	0.2	0.3
Luciferin-N_bH	14.7	6.1
Luciferin-N_tH	−0.3	−9.3

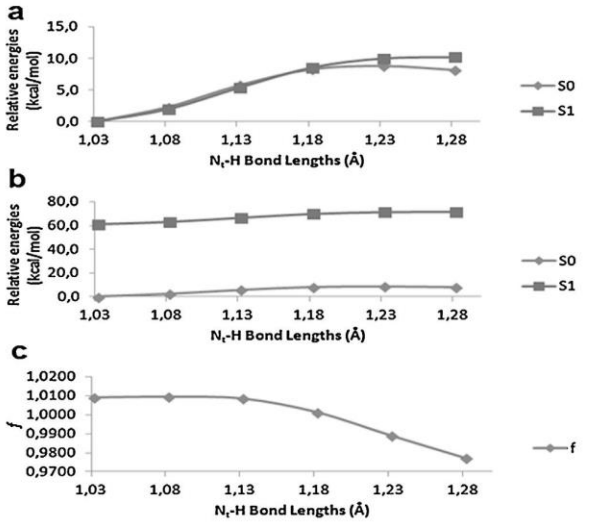

Fig. 1. (a) Comparison between the relative energies of singlet ground and excited states, when the energies of Luciferin-N_tH in both states were used as reference. (b) Comparison between the relative energies of singlet ground and excited states, when the energy of Luciferin-N_tH in the ground state was used as reference. (c) Oscillator strength of the singlet ground → excited state transition, as a function of the N_t—H bond length.

Given this results, we have calculated the triplet ground and excited states energies of the N_t—H bond, by CPCM-(CAM-B3LYP/6-31+G(d)) and CPCM-(TD CAM-B3LYP/6-31+G(d)) single point calculations in the singlet *in vacuo* PBE0/6-31G(d) structures. It is known that phosphorescence is much more easily quenched than fluorescence, so intersystem crossing from a singlet to a triplet state can account for the efficient fluorescence quenching of firefly luciferin [14,16–20]. The singlet/triplet excited and ground state energies are presented in Fig. 2 (with the energy of ground state Luciferin-N_tH as reference), as a function of the N_t—H bond length.

It can be seen that triplet states are not involved in a fluorescence quenching process involving N_t. The first and second triplet excited states are very close to each other in energy, but they are higher in energy than the first singlet excited state by 7.6–10.5 kcal/mol. This energy difference is too great for an intersystem crossing from the bright singlet excited state to the two dark triplet excited states.

After verifying that the fluorescence quenching process is not involved with the protonation of N_t, we have verified the possible role of the protonation of N_b. Although the fact that Luciferin-N_bH is the least stable species, the truth is that this efficient fluorescence quenching process was seen also for molecules of the oxyluciferin family that did not present a carboxylic group [14,16–20]. Therefore, the element responsible for this quenching mechanism must be present in all molecules of the natural oxyluciferin family of fluorophores, which is the case of N_b [14,16–20]. Moreover, as N_t, N_b is a stronger base upon photoexcitation than in the ground state

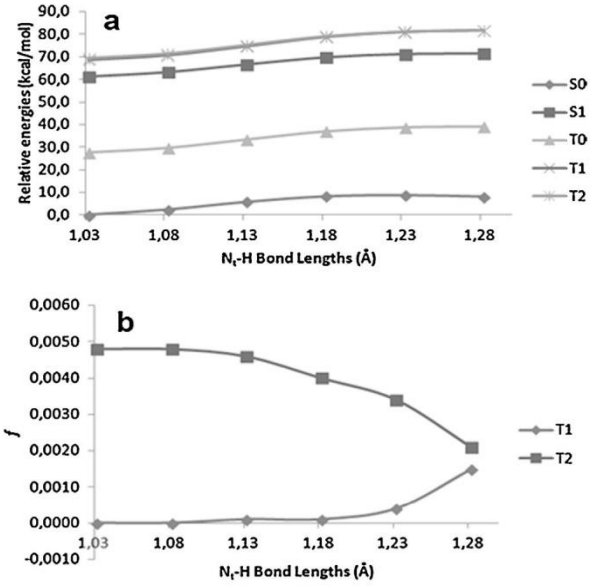

Fig. 2. (a) Comparison between the relative energies of singlet/triplet ground and excited states, when the energies of singlet ground state Luciferin-N_tH were used as reference. (c) Oscillator strength of the first and second triplet excited states, as a function of the N_t—H bond length.

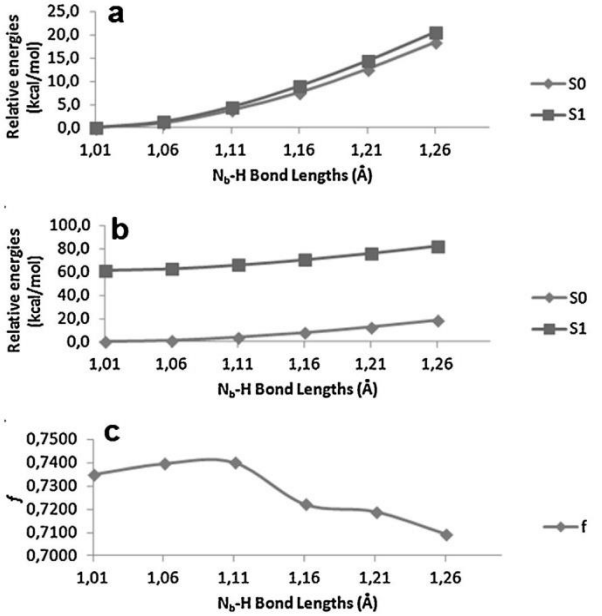

Fig. 3. (a) Comparison between the relative energies of singlet ground and excited states, when the energies of Luciferin-N_bH in both states were used as reference. (b) Comparison between the relative energies of singlet ground and excited states, when the energy of Luciferin-N_bH in the ground state was used as reference. (c) Oscillator strength of the singlet ground → excited state transition, as a function of the N_b—H bond length.

(Table 1). Also, the latter heteroatom is closer to the proton donor benzothiazole oxygen than N_t, which may facilitate the protonation of N_b.

Luciferin-N_bH has a theoretical absorption maximum of 2.64 eV, which is associated with an oscillator strength of 0.7351. We have then performed a relaxed coordinate scan, in which we have increased the N_b—H distance from 1.01 to 1.26 Å. We have then re-evaluated both the excited and ground states' energies as indicated in Section 2. Excited and ground state Luciferin-N_bH energies were used as reference and the resulting curves are presented in Fig. 3a. It can be seen that the N_b—H dissociation reaction is more unfavorable in the excited state, although being similar in both states. Fig. 3b and c shows the excited and ground state dissociation energies (when only ground state Luciferin-N_bH energy is used as reference) and the oscillator strength associated with each N_b—H bond length, respectively. These figures show that, as in the case of Luciferin-N_tH, no interaction between the singlet ground and excited states exists and a reduction in the oscillator strength can be observed. Therefore, the simple excited state protonation of N_bH cannot explain the efficient fluorescence quenching.

In view of these findings, we have also calculated the triplet ground and excited states energies of the N_b—H bond, by CPCM-(CAM-B3LYP/6-31+G(d)) and CPCM-(TD CAM-B3LYP/6-31+G(d)) single point calculations in the singlet *in vacuo* PBE0/6-31G(d) structures. The singlet/triplet excited and ground state energies are presented in Fig. 4 (with the energy of ground state Luciferin-N_bH as reference), as a function of the N_b—H bond length. The first and second excited states are not as close in energy as in the case of Luciferin-N_tH. Also, the second triplet excited state is also too high in energy than the first excited singlet state to afford intersystem crossing (energetic difference between 9.7 and 11.4 kcal/mol respectively). The first triplet state appears also not to be sufficiently close in energy to afford intersystem crossing (energetic difference between 5.7 and 5.8 kcal/mol). However, at this point the energetic difference between the first singlet and triplet excited states difference is low enough to allow us to conclude that no direct

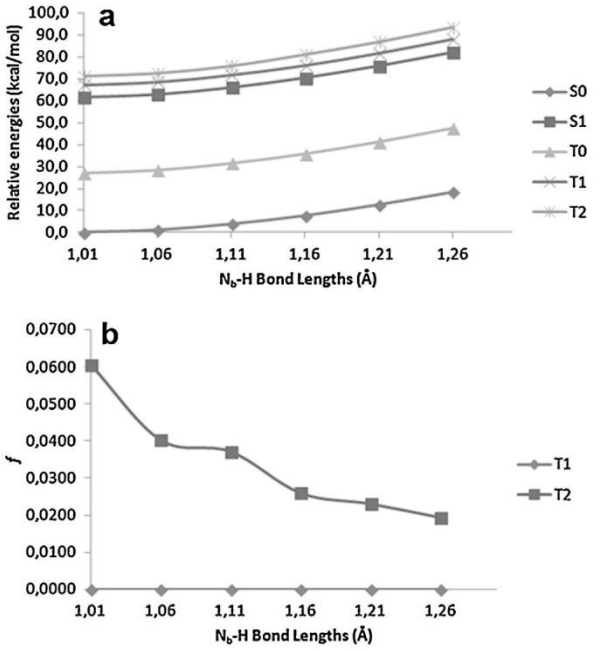

Fig. 4. (a) Comparison between the relative energies of singlet/triplet ground and excited states, when the energies of singlet ground state Luciferin-N_bH were used as reference. (b) Oscillator strength of the first and second triplet excited states, as a function of the N_b—H bond length.

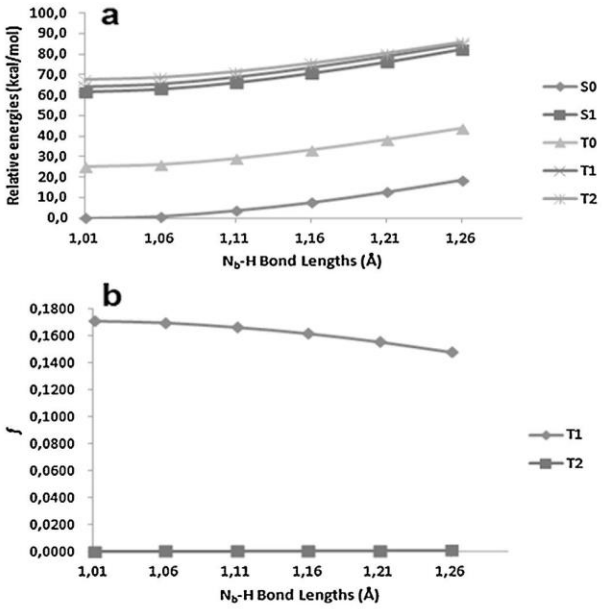

Fig. 5. (a) Comparison between the relative energies of singlet/triplet ground and excited states, when the energies of singlet ground state Luciferin-N_bH were used as reference. (b) Oscillator strength of the first and second triplet excited states, as a function of the N_b—H bond length. The singlet energies were obtained at singlet ground state relaxed N_b—H scan, while the triplet energies were obtained at triplet ground state relaxed N_b—H scan.

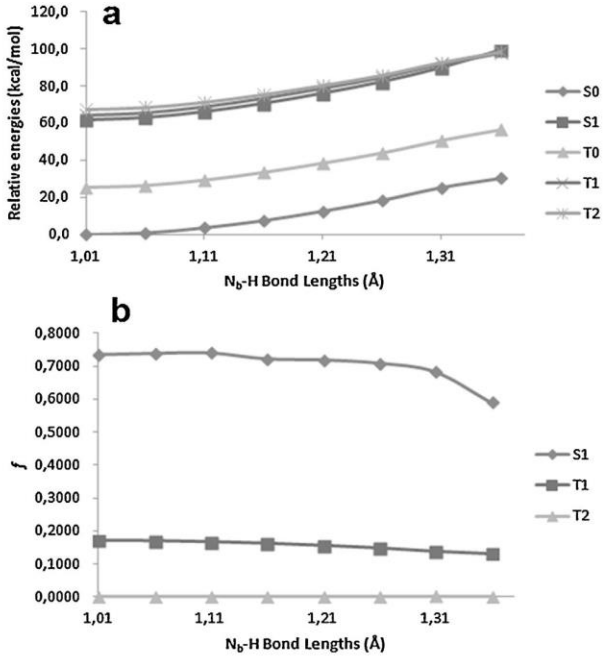

Fig. 6. (a) Comparison between the relative energies of singlet/triplet ground and excited states, when the energies of singlet ground state Luciferin-N_bH were used as reference. (b) Oscillator strength of the singlet and two triplet excited states, as a function of the N_b—H bond length. These energies were obtained at optimized Luciferin-N_bH structures, with the N_b—H bond fixed at the lengths indicated in the graphic.

interaction is seen, because of the approximations included in our calculation methodology.

In order to verify this hypothesis we have calculated the triplet ground state geometry of Luciferin-N_bH, at the *in vacuo* PBE0/6-31G(d) level of theory. Subsequently we have performed a N_b—H relaxed scan, from 1.01 to 1.26 Å. The first and second triplet excited state energies were re-calculated in single point calculations at the CPCM-(TD CAM-B3LYP/6-31+G(d)) level of theory. These results are given in Fig. 5. The ground and first singlet excited state energies are those of Fig. 4.

This new methodology of calculation indeed decreased the energy gap between the first singlet and first triplet (difference between 2.6 and 3.0 kcal/mol), and second triplet (difference between 3.7 and 5.9 kcal/mol) excited states. These energy differences indicate that in the protonation reaction of N_b, the first singlet excited state is indeed close in energy to the two triplet excited states. Moreover, these triplet states have much lower oscillator strengths than the first singlet excited state (Figs. 3c and 5b).

These new data are further evidence in support of singlet to triplet intersystem crossing as the mechanism for the efficient fluorescence quenching of firefly luciferin. Therefore, we have further improved our methodology of calculation in order to best assess this possibility. In order to do so, we have optimized the *in vacuo* geometry of Luciferin-N_bH at different N_b—H bond lengths (1.01–1.36 Å), at both the singlet and triplet ground states with the PBE0 functional and the 6-31G(d) basis set. The singlet/triplet ground and excited state energies were re-evaluated at the CPCM-(CAM-B3LYP/6-31+G(d)) and CPCM-(TD CAM-B3LYP/6-31+G(d)) level of theory. These data are shown in Fig. 6.

These new calculations indicate that singlet to triplet intersystem crossing is indeed the mechanism for the efficient fluorescence quenching of firefly luciferin. At N_b—H bond length of 1.36 Å, the first and second triplet excited states are lower in energy than the first singlet excited state by 1.4 and 0.8 kcal/mol, respectively. At N_b—H bond length of 1.01–1.31 Å these two triplet excited states are higher in energy than the first singlet excited state. This indicates that between N_b—H bond lengths of 1.31 and 1.36 Å there is a path for the transition of the singlet excited state to the two first triplet excited states. Moreover, it should be noted that the first and second triplet excited states differ in energy by only 0.6–3.2 kcal/mol in the bond stretching range of 1.01–1.36 Å. These small differences may allow for some internal conversion between the triplet states. Thus, these results indicate that during the excited state formation of Luciferin-N_bH, due to proton recombination, there is a path for the formation of dark or nearly dark triplet excited states (which can explain the efficient fluorescence quenching).

This intersystem crossing process is able to explain the efficient fluorescence quenching of firefly luciferin due to two reasons: first, as already stated in this manuscript, light emission from triplet states is much more easily quenched than emission from singlet states; second, as can be seen in Figs. 6–8b, the oscillator strengths of the triplet states are much smaller than that of the singlet excited state (the second triplet excited state is even a dark state).

In order to further confirm our proposed fluorescence quenching mechanism, we have re-evaluated the singlet/triplet ground and excited state energies at the CPCM-(CAM-B3LYP/aug-cc-pVDZ) and CPCM-(TD CAM-B3LYP/aug-cc-pVDZ) level of theory, by improving the basis set used. These data are shown in Fig. 7.

These new calculations are in line with the previous ones. At N_b—H bond length of 1.01–1.31 Å the two first triplet excited states are higher in energy than the first singlet excited state. At N_b—H bond length of 1.36 Å, the first triplet excited state is lower in energy than the first singlet excited state by 1.5 kcal/mol. The second triplet excited state has the same energy than the first singlet excited state. These results indicate that between N_b—H bond lengths of 1.31 and 1.36 Å there is a path for the transition of the singlet excited state to

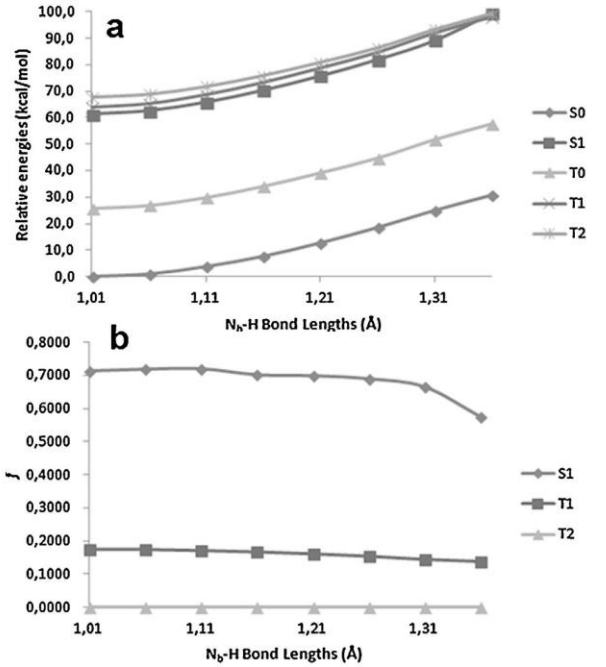

Fig. 7. (a) Comparison between the relative energies of singlet/triplet ground and excited states, when the energies of singlet ground state Luciferin-N_bH were used as reference. (b) Oscillator strength of the singlet and two triplet excited states, as a function of the N_b—H bond length. These energies were obtained at optimized Luciferin-N_bH structures, with the N_b—H bond fixed at the lengths indicated in the graphic. The calculations were made with the aug-cc-pVDZ basis set.

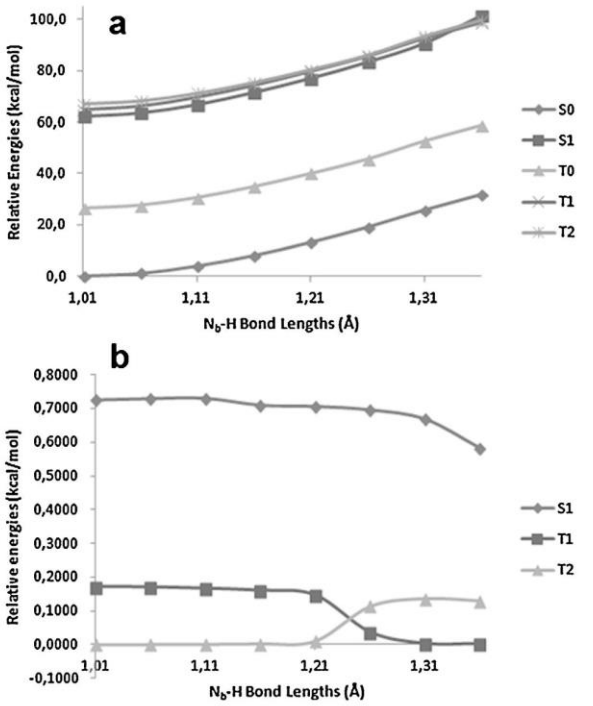

Fig. 8. (a) Comparison between the relative energies of singlet/triplet ground and excited states, when the energies of singlet ground state Luciferin-N_bH were used as reference. (b) Oscillator strength of the singlet and two triplet excited states, as a function of the N_b—H bond length. These energies were obtained at optimized Luciferin-N_bH structures, with the N_b—H bond fixed at the lengths indicated in the graphic. The calculations were made with the aug-cc-pVDZ basis set and the ωB97X-D functional.

the two first triplet excited states, and for some internal conversion between the triplet states. Moreover, as can be seen in Fig. 7, these two triplet states are dark or nearly dark excited states.

Further confirmation of our mechanism was provided by re-evaluation of the singlet/triplet ground and excited state energies, at the CPCM-(ωB97X-D/aug-cc-pVDZ) and CPCM-(TD ωB97X-D/aug-cc-pVDZ) level of theory. These data are shown in Fig. 8. As demonstrated by Figs. 6 and 7, these calculations also indicate that between N_b—H bond lengths of 1.31 and 1.36 Å there is a path for the transition of the singlet excited state to the two first triplet excited states, and for some internal conversion between the triplet states. Moreover, the two triplet excited states are still dark or nearly dark.

Despite all data here presented point to intersystem crossing as the reason behind the efficient fluorescence quenching mechanism of firefly luciferin, we are aware that some doubt may be cast to this results by the fact that the structural parameters of the triplet and singlet structures presented in Figs. 6–8 are different. To that end, we have tried to confirm the possibility of intersystem crossing between singlet and triplet excited states, with the same structural parameters. Given this we have used the STQN method, implemented in Gaussian 09, for locating transition structures [46]. This was done in order to obtain a transition structure between triplet and singlet ground state structures, at N_b—H bond length of 1.36 Å, with the QST2 option at the PBE0/3-21G(d) level of theory. The structure obtained was only used as a transition state input geometry for QST3 calculations at the PBE0/6-31G(d) level of theory. The resulting structure was then subjected to an Intrinsic Reaction Coordinate (IRC) calculation, from the transition structure to Luciferin-N_bH [47]. The energy differences between the first singlet and first and second triplet excited states are presented in Fig. 9a, at the CPCM-(TD-CAM-B3LYP/6-31+G(d)) level of theory, between N_b—H bond lengths of 1.247 and 1.366 Å. It can be seen that from the figure, that no intersystem crossing is found. However, with the increase in the N_b—H bond length there a decrease in the energy difference between the singlet and the triplet excited states. Thus, these data did not show a singlet/triplet crossing but showed us that it becomes more probable with the increase of the N_b—H bond length.

In order to pursue this line of thinking we have used triplet and singlet Luciferin-N_bH structures with N_b—H bond lengths of 1.40 Å, in a QST2 calculation at the PBE0/3-21G(d) level of theory. These structures along with the newly found transition structure, were used as input geometries in a QST3 calculation at the PBE0/6-31G(d), followed from a IRC calculation from the QST3 transition structure to Luciferin-N_bH. The energy differences between the first singlet and first and second triplet excited states are presented in Fig. 9b, at the CPCM-(TD-CAM-B3LYP/6-31+G(d)) level of theory, between N_b—H bond lengths of 1.181 and 1.403 Å. As in Fig. 9a, the energy differences between states decreases with increasing N_b—H bond length. More importantly, we can see that between N_b—H bond lengths of 1.181–1.349 Å, the first triplet excited state is higher in energy than the first singlet excited state. However, between 1.349 and 1.403 Å, the triplet state becomes lower in energy than the singlet excited state by 2.7 kcal/mol. This clearly points to a singlet/triplet intersystem crossing during the excited state protonation of Luciferin-N_bH. Moreover, the possibility of crossing was found when both triplet and singlet structures present the same structural parameters. Potential energy curves were drawn as in Figs. 4–6a (Fig. 9c), and the resulting curves are very similar to those other curves, while demonstrating the possibility for intersystem crossing. So, these new calculations further support our conclusion that it is an intersystem crossing process

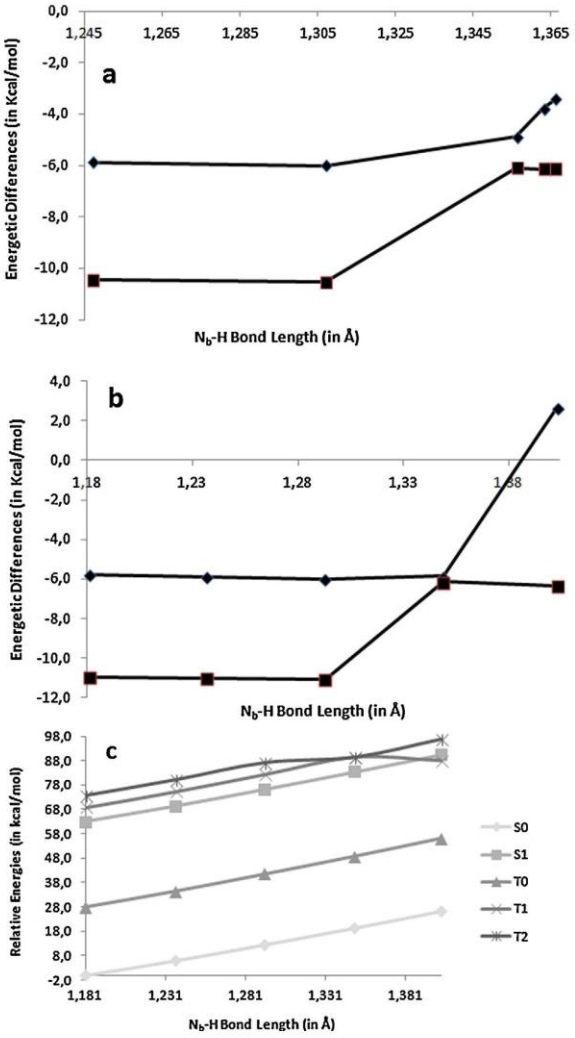

Fig. 9. (a) $\Delta E_{S1\text{-}T1}$ (♦) and $\Delta E_{S1\text{-}T2}$ (■) (in kcal/mol), at bond lengths of 1.247–1.366 Å. (b) $\Delta E_{S1\text{-}T1}$ (♦) and $\Delta E_{S1\text{-}T2}$ (■) (in kcal/mol), at bond lengths of 1.181–1.403 Å. These energies were obtained at IRC-obtained structures, with transition states obtained with the QST3 method at PBE0/6-31G(d) level of theory. The energy calculations were made with the 6-31+G(d) basis set and the CAM-B3LYP functional, in implicit water. (c) Comparison between the relative energies of singlet/triplet ground and excited states, when the energies of singlet ground state Luciferin-N_bH were used as reference.

that leads to the efficient fluorescence quenching mechanism of firefly luciferin.

4. Conclusion

In the present work, the efficient fluorescence quenching of firefly luciferin was studied by means of a time dependent density functional theory approach. This experimentally described efficient fluorescence quenching process was seen in the cases of firefly luciferin, dehydroluciferin and oxyluciferin (members of the oxyluciferin family of photoacids). This family of fluorophores has been attracting attention from researchers due to their role in the well-known and studied firefly bioluminescence. Therefore, the elucidation of this fluorescence quenching mechanism is needed as it may occur inside of the luciferase active site, thereby decreasing the efficiency of bioluminescence.

Our calculations have revealed that the fluorescence quenching is due to excited state protonation of the nitrogen heteroatom of the benzothiazole moiety. During this protonation reaction, there is a path from which the population of the first singlet excited state can cross over to triplet excited states. Light emission from triplet excited states is much more easily quenched than light emission from a singlet state. Moreover, the oscillator strengths of the triplet states are much lower than the one from the singlet excited state.

Acknowledgments

Financial support from Fundação para a Ciência e Tecnologia (FCT, Lisbon) (Programa Operacional Temático Factores de Competitividade (COMPETE) e comparticipado pelo Fundo Europeu (FEDER) (Project PTDC/QUI/71366/2006)) is acknowledged. A Ph.D. grant to Luís Pinto da Silva (SFRH/76612/2011), attributed by FCT, is also acknowledged. This work was also supported by grants from the Israel Science Foundation and from James-Franck German-Israeli Program in Laser-Matter Interaction.

Appendix A. Supplementary data

Supplementary data associated with this article can be found, in the online version, at http://dx.doi.org/10.1016/j.jphotochem.2013.06.001.

References

[1] M. Rosenberg, T.I. Sølling, Computational investigation of photo induced processes in alkyl nitrites and the product alkoxy radicals, Chemical Physics Letters 484 (2010) 113–118.
[2] N. Singla, P. Chowdhury, Role of hydrogen bonding in excited state intramolecular proton transfer of Indole-7-Carboxaldehyde: a theoretical and experimental study, Chemical Physics Letters 548 (2012) 71–79.
[3] Y.H. Liu, M.S. Mehata, J.Y. Liu, Excited-state proton transfer via hydrogen-bonded acetic acid (AcOH) wire for 6-hydroxyquinoline, The Journal of Physical Chemistry A 115 (2011) 19–24.
[4] B.K. Paul, S. Mahanta, R.B. Singh, N. Guchhait, A DFT-based theoretical study on the photophysics of 4-hydroxyacridine: single-water-mediated excited state proton transfer, The Journal of Physical Chemistry A 114 (2010) 2618–2627.
[5] S. Mahanta, B.K. Paul, R.B. Singh, N. Guchhait, Inequivalence of substitution pairs in hydroxynaphthaldehyde: a theoretical measurement by intramolecular hydrogen bond strength, aromaticity, and excited-state intramolecular proton transfer reaction, Journal of Computational Chemistry 32 (2011) 1–14.
[6] T. Kumpulainen, A.M. Brouwer, Excited-state proton transfer and ion pair formation in a Cinchona organocatalyst, Physical Chemistry Chemical Physics 14 (2012) 13019–13026.
[7] G.J. Zhao, K.L. Han, Ultrafast hydrogen bond strengthening of the photoexcited fluorenone in alcohols for facilitating the fluorescence quenching, The Journal of Physical Chemistry A 111 (2007) 9218–9223.
[8] P. Chowdhury, S. Panja, S. Chakravorti, Excited state prototropic activities in 2-hydroxy 1-naphthaldehyde, The Journal of Physical Chemistry A 107 (2003) 83–90.
[9] G.J. Zhao, K.L. Han, Effects of hydrogen bonding on tuning photochemistry: concerted hydrogen-bond strengthening and weakening, ChemPhysChem 9 (2008) 1842–1846.
[10] C. Kolano, J. Helbing, M. Kozinski, W. Sander, P. Hamm, Watching hydrogen-bond dynamics in a beta-turn by transient two-dimensional infrared spectroscopy, Nature 444 (2006) 469–472.
[11] D. Chandler, Physical chemistry - oil on troubled waters, Nature 445 (2007) 831–832.
[12] M.S. Baranov, K.A. Lukyanov, A.O. Borissova, J. Shamir, D. Kosenkov, L.V. Slipchenko, L.M. Tolbert, I.V. Yampolsky, K.M. Solntsev, Conformationally locked chromophores as models of excited-state proton transfer in fluorescent proteins, Journal of American Chemical Society 134 (2012) 6025–6032.
[13] I. Presiado, N. Karton-Lifshin, Y. Erez, R. Gepshtein, D. Shabat, D. Huppert, Ultrafast proton transfer of three novel quinone cyanine photoacids, The Journal of Physical Chemistry A 116 (2012) 7353–7363.
[14] Y. Erez, I. Presiado, R. Gepshtein, L. Pinto da Silva, J.C.G. Esteves da Silva, D. Huppert, Comparative study of the photoprotolytic reactions of D-luciferin and oxyluciferin, The Journal of Physical Chemistry A 116 (2012) 7452–7461.
[15] K.M. Solntsev, S.P. Laptenok, P. Naumov, Photoinduced dynamics of oxyluciferin analogues: unusual enol super photoacidity and evidence of keto-enol isomerization, Journal of American Chemical Society 134 (2012) 16452–16455.
[16] Y. Erez, D. Huppert, Excited-state intermolecular proton transfer of the Firefly's chromophore D-Luciferin, The Journal of Physical Chemistry A 114 (2010) 8075–8082.

[17] I. Presiado, Y. Erez, D. Huppert, Excited-state intermolecular proton transfer of the Firefly's chromophore D-Luciferin. 2. Water-methanol mixtures, The Journal of Physical Chemistry A 114 (2010) 9471–9479.
[18] I. Presiado, Y. Erez, D. Huppert, Excited-state intermolecular proton transfer of Firefly Luciferin III. Proton transfer to a mild base, The Journal of Physical Chemistry A 114 (2010) 13337–13346.
[19] Y. Erez, I. Presiado, R. Gepshtein, D. Huppert, Excited-state intermolecular proton transfer of firefly Luciferin IV. Temperature and pH dependence, The Journal of Physical Chemistry A 115 (2011) 1617–1626.
[20] I. Presiado, R. Gepshtein, Y. Erez, D. Huppert, Excited-state intermolecular proton transfer of Firefly Luciferin V. Direct proton transfer to fluoride and other mild bases, The Journal of Physical Chemistry A 115 (2011) 7591–7601.
[21] I. Presiado, Y. Erez, R. Simkovitch, S. Shomer, R. Gepshtein, L. Pinto da Silva, J.C.G. Esteves da Silva, D. Huppert, Excited-state proton transfer of firefly dehydroluciferin, The Journal of Physical Chemistry A 116 (2012) 10770–10779.
[22] L. Pinto da Silva, J.C.G. Esteves da Silva, Computational studies of the luciferase light-emitting product: oxyluciferin, Journal of Chemical Theory and Computation 7 (2011) 809–817.
[23] V.R. Viviani, F.G. Arnoldi, A.J. Neto, T.L. Oehlmeyer, E.J. Bechara, Y. Ohmiya, The structural origin and biological function of pH-sensitivity in firefly luciferases, Photochemical and Photobiological Sciences 7 (2008) 159–169.
[24] J.Y. Hasegawa, K.J. Fujimoto, H. Nakatsuji, Color tuning in photofunctional proteins, ChemPhysChem 12 (2011) 3106–3115.
[25] L. Pinto da Silva, J.C.G. Esteves da Silva, Firefly chemiluminescence and bioluminescence efficient generation of excited states, ChemPhysChem 13 (2012) 2257–2262.
[26] J. Vieira, L. Pinto da Silva, J.C.G. Esteves da Silva, Advances in the knowledge of light emission by firefly luciferin and oxyluciferin, Journal of Photochemistry and Photobiology B 117 (2012) 33–39.
[27] A. Roda, M. Guardigli, Analytical chemiluminescence and bioluminescence: latest achievements and new horizons, Analytical and Bioanalytical Chemistry 402 (2012) 69–76.
[28] S.M. Marques, F. Peralta, J.C.G. Esteves da Silva, Optimized chromatographic and bioluminescent methods for inorganic pyrophosphate based on its conversion to ATP by firefly luciferase, Talanta 77 (2009) 1497–1503.
[29] R. Alam, D.M. Fontaine, B.R. Branchini, M.M. Maye, Designing quantum rods for optimized energy transfer with firefly luciferase enzymes, Nano Letters 12 (2012) 3251–3256.
[30] L. Mezzanotte, I. Que, E. Kaijzel, B.R. Branchini, A. Roda, C. Lowik, Sensitive dual color in vivo bioluminescence imaging using a new red codon optimized firefly luciferase and a green click beetle luciferase, PloS ONE 6 (2011) e19277.
[31] L. Pinto da Silva, J.C.G. Esteves da Silva, Computational investigation of the effect of pH on the color of firefly bioluminescence by DFT, ChemPhysChem 12 (2011) 951–960.
[32] J.C.G. Esteves da Silva, J.M.C.S. Magalhães, R. Fontes, Identification of enzyme produced firefly oxyluciferin by reverse phase HPLC, Tetrahedron Letters 42 (2001) 8173–8176.
[33] P. Naumov, Y. Ozawa, K. Ohkubo, S. Fukuzumi, Structure and spectroscopy of oxyluciferin, the light emitter of the firefly bioluminescence, Journal of American Chemical Society 131 (2009) 11590–11605.
[34] M.J. Frisch, G.W. Trucks, H.B. Schlegel, G.E. Scuseria, M.A. Robb, J.R. Cheeseman, G. Scalmani, V. Barone, B. Mennucci, G.A. Petersson, H. Nakatsuji, M. Caricato, X. Li, H.P. Hratchian, A.F. Izmaylov, J. Bloino, G. Zheng, J.L. Sonnenberg, M. Hada, M. Ehara, K. Toyota, R. Fukuda, J. Hasegawa, M. Ishida, T. Nakajima, Y. Honda, O. Kitao, H. Nakai, T. Vreven, J.A. Montgomery Jr., J.E. Peralta, F. Ogliaro, M. Bearpark, J.J. Heyd, E. Brothers, K.N. Kudin, V.N. Staroverov, R. Kobayashi, J. Normand, K. Raghavachari, A. Rendell, J.C. Burant, S.S. Iyengar, J. Tomasi, M. Cossi, N. Rega, J.M. Millam, M. Klene, J.E. Knox, J.B. Cross, V. Bakken, C. Adamo, J. Jaramillo, R. Gomperts, R.E. Stratmann, O. Yazyev, A.J. Austin, R. Cammi, C. Pomelli, J.W. Ochterski, R.L. Martin, K. Morokuma, V.G. Zakrzewski, G.A. Voth, P. Salvador, J.J. Dannenberg, S. Dapprich, A.D. Daniels, O. Farkas, J.B. Foresman, J.V. Ortiz, J. Cioslowski, D.J. Fox, Gaussian 09, Revision A.02, Gaussian, Inc., Wallingford CT, 2009.
[35] C. Adamo, V. Barone, Toward reliable density functional methods without adjustable parameters: the PBE0 model, Journal of Chemical Physics 110 (1999) 6158–6169.
[36] D. Jacquemin, V. Wathelet, E.A. Perpète, C. Adamo, Extensive TD-DFT benchmark: singlet-excited states of organic molecules, Journal of Chemical Theory and Computation 5 (2009) 2420–2435.
[37] L. Pinto da Silva, J.C.G. Esteves da Silva, Analysis of the performance of DFT functionals in the study of light emission by oxyluciferin analogs, International Journal of Quantum Chemistry 113 (2012) 45–51.
[38] D. Jacquemin, E.A. Perpète, G.E. Scuseria, I. Ciofini, C. Adamo, TD-DFT performance for the visible absorption spectra of organic dyes: conventional versus long-range hybrids, Journal of Chemical Theory and Computation 4 (2008) 123–135.
[39] T. Yanai, D. Tew, N. Handy, A new hybrid exchange-correlation functional using the Coulomb-attenuating method (CAM-B3LYP), Chemical Physics Letters 393 (2004) 51–57.
[40] J. Tomasi, B. Mennucci, R. Cammi, Quantum mechanical continuum solvation models, Chemical Reviews 105 (2005) 2999–3093.
[41] F. Furche, R. Ahlrichs, Adiabatic time-dependent density functional methods for excited state properties, Journal of Chemical Physics 117 (2002) 7433–7447.
[42] R.B. Singh, S. Mahanta, N. Guchhait, Solvent dependent excited state spectral properties of 4-hydroxyacridine: evidence for only water mediated excited state proton transfer process, Journal of Photochemistry and Photobiology A 200 (2008) 325–333.
[43] R. Vivie-Riedle, V. De Waele, L. Kurtz, E. Riedle, Ultrafast excited-state proton transfer of 2-(2′-hydroxyphenyl)benzothiazole: theoretical analysis of the skeletal deformations and the active vibrational modes, The Journal of Physical Chemistry A 107 (2003) 10591–10599.
[44] C. Adamo, D. Jacquemin, The calculations of excited-state properties with time-dependent density functional theory, Chemical Society Reviews 42 (2013) 845–856.
[45] J.D. Chai, M. Head-Gordon, Long-range corrected hybrid density functionals with damped atom-atom dispersion corrections, Physical Chemistry Chemical Physics 10 (2008) 6615–6620.
[46] C. Peng, P.Y. Ayala, H.B. Schlegel, M.J. Frisch, Using redundant internal coordinates to optimize equilibrium geometries and transition states, Journal of Computational Chemistry 17 (1996) 49–56.
[47] H.P. Hratchian, H.B. Schlegel, Using Hessian updating to increase the efficiency of a Hessian based predictor-corrector reaction path following method, Journal of Chemical Theory and Computation 1 (2005) 61–69.

6.3. Study of the Nontraditional Enol Photoacidity of $OxyLH_2$ in Aqueous Solution

Article 23

Theoretical study of the nontraditional enol-based photoacidity of firefly oxyluciferin
Luís Pinto da Silva and Joaquim C.G. Esteves da Silva
ChemPhysChem **2015**, *16*, 455-464.

The theoretical calculations and the writing of the paper were performed by Luís Pinto da Silva, under the supervision of Professor Joaquim Esteves da Silva.

CHEMPHYSCHEM ARTICLES

ChemPubSoc Europe

DOI: 10.1002/cphc.201402533

Theoretical Study of the Nontraditional Enol-Based Photoacidity of Firefly Oxyluciferin

Luís Pinto da Silva and Joaquim C. G. Esteves da Silva*[a]

A theoretical analysis of the enol-based photoacidity of oxyluciferin in water is presented. The basis for this phenomenon is found to be the hydrogen-bonding network that involves the conjugated photobase of oxyluciferin. The hydrogen-bonding network involving the enolate thiazole moiety is stronger than that of the benzothiazole phenolate moiety. Therefore, enolate oxyluciferin should be stabilized versus the phenolate anion. This difference in strength is attributed to the fact that the thiazole moiety has more potential hydrogen-bond acceptors near the proton donor atom than the benzothiazole moiety. Moreover, the phenol-based excited-state proton transfer leads to a decrease in the hydrogen-bond acceptor potential of the thiazole atoms. The ground-state enol-based acidity of oxyluciferin is also studied. This phenomenon can be explained by stabilization of the enolate anion through strengthening of a bond between water and the nitrogen atom of the thiazole ring, in an enol-based proton-transfer-dependent way.

1. Introduction

Hydrogen bonding is an attractive interaction of fundamental importance in chemistry, biology and physics.[1–3] Given this, its nature is of great importance to the research community, and has been studied by using various experimental and computational methods.[4–6] Hydrogen bonding is important for molecular species in the excited state, for example, in excited-state proton transfer (ESPT), photochemistry, quenching processes, and so forth.[7–12]

The acidity of certain aromatic molecules can undergo significant changes upon photoexcitation.[13,14] Molecules that increase their acidity are termed photoacids, whereas so-called photobases increase their basicity. If the acidic and basic moieties exist in proximity within the same excited molecule, an intramolecular ESPT takes place. If not, the ESPT reaction is intermolecular, as in the case of ESPT to the solvent.

A typical photoacid is a weak acid in the ground state and a strong acid in the excited state. The typical photoprotolytic cycle of a photoacid is presented in Scheme 1. There is a long-standing interest in photoacidity because it allows the study of a vast array of photoinduced reactions (e.g. fast proton transfer, phototautomerism, photoisomerization, fluorescence quenching), and because it is a means of generating protons at a specified point in time.[13]

Firefly oxyluciferin (Figure 1) is the light-emitting product of the firefly bioluminescence reaction.[15–18] Interesting and advantageous features have made firefly bioluminescence a system of great importance in areas pivotal to human life, such as biomedicine, bioanalysis and pharmaceutical science.[19,20] Spectroscopic studies have demonstrated that oxyluciferin, along with a series of derivatives, is a photoacid.[21–25] The ground-state deprotonation of the enol group has been found to have a pK_a of 7.40, whereas upon photoexcitation its dissociation constant decreases to approximately 0.5.[21–23] It was also found that the ground-state enolate→enol dianion has a pK_a of 9.10.[23] The absorption spectrum of firefly oxyluciferin in water has a band at approximately 380 nm at acidic/neutral pH, and a band at approximately 420 nm at basic pH.[22,26] The emission spectrum is characterized by a peak at approximately 550 nm at acidic/neutral pH, and a peak at ap-

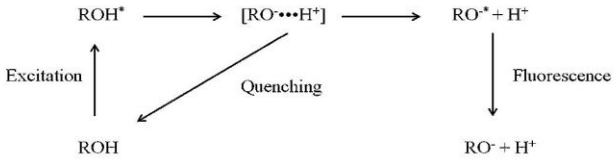

Scheme 1. Typical photoprotolytic cycle of a photoacid.

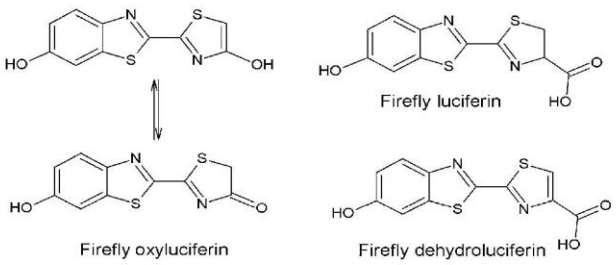

Figure 1. Structures of firefly oxyluciferin, luciferin and dehydroluciferin.

[a] Dr. L. Pinto da Silva, Prof. Dr. J. C. G. Esteves da Silva
Centro de Investigação em Química
Departamento de Química e Bioquímica
Faculdade de Ciências, Universidade do Porto
R. Campo Alegre 687, 4169-007 Porto (Portugal)
E-mail: jcsilva@fc.up.pt

Supporting Information for this article is available on the WWW under http://dx.doi.org/10.1002/cphc.201402533.

CHEMPHYSCHEM
ARTICLES
www.chemphyschem.org

proximately 540 nm at basic pH.[22,26] This pH-sensitive fluorescence was found to arise from π–π stacking oxyluciferin complexes. The ground-state deprotonation at pK_a 7.40 leads to changes in the conformation of these complexes, which affects the emission.[27] As well as the ESPT process itself and the pH-sensitive fluorescence, the study of the photoprotolytic cycle has uncovered several complex and unexpected photoinduced phenomena: efficient fluorescence quenching, slow photoinduced base-catalyzed tautomerism, and strong photoacidity of the enol group.[21–28]

Various experimental studies have concluded that in water, the enol form is more stable than the keto oxyluciferin species (Figure 1).[25,29,30] Therefore, oxyluciferin presents two possible proton-donating hydroxyl groups (Figure 1). It was thought that the hydroxyl group involved in the ESPT reaction was that of the benzothiazole moiety for two reasons. Firstly, luciferin and dehydroluciferin (two natural analogues of oxyluciferin; Figure 1) are also photoacids with similar pK_a/pK_a* values to oxyluciferin, and these molecules only contain a hydroxyl group on the benzothiazole moiety.[22,24] Secondly, photoacidity of an enol group in a five-membered ring is rare.[31] However, a comparative photophysical study of oxyluciferin and two analogues provided reliable evidence that the ESPT process occurs between the enol group and the solvent.[25] Thus, it is the enol group that causes oxyluciferin to be a photoacid.

The objective of his study was of characterize the nontraditional and rather exceptional enol-based photoacidity of oxyluciferin. This characterization is needed to better understand the photophysical properties and photoprotolytic cycle of oxyluciferin, and related analogues. Moreover, the characterization of the photolysis of this molecule provides insight into the rare phenomenon of enol-based photoacidity. To this end, we used a computational approach to perform a comparative study of the photoacidity of the benzothiazole and enol hydroxyl groups of oxyluciferin in water. In our opinion, such methodology is needed, as it allows direct and detailed information (down to the atomic level) on the oxyluciferin ground and excited states to be obtained, which cannot be provided directly by experimental methods.

2. Results and Discussion

2.1. Ground-State Acidity of the Enol Group

As well as being the photoacidic group in the excited state, the enol moiety of firefly oxyluciferin is also responsible for the ground state pK_a of 7.40.[21,27] Therefore, the first stage of this study was to investigate the higher ground-state acidity of this group, over the benzothiazole hydroxyl. In our opinion, these studies would help us to better understand the same process in the excited state. To this end, we have studied the proton-transfer process involving the two hydroxyl groups of the neutral enol species that is solvated by three explicit water molecules.

Figure 2 shows a representation of neutral enol species, and the corresponding anion that results from proton transfer to a solvent molecule. The energetic profiles of these proton-transfer reactions are presented in Figure 3a, and are relative to the S_0 energy of the corresponding neutral structure, with explicit water around the respective hydroxyl group. Our calculations indeed identify the enol functional group as responsible

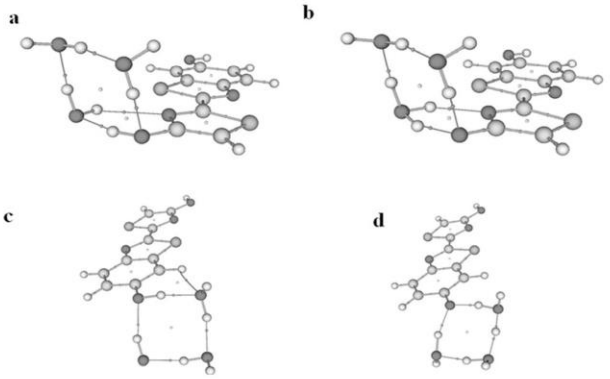

Figure 2. Representation (after QTAIM analysis) of ground-state neutral (a,c) and anionic (b,d) species of oxyluciferin, solvated at the thiazole (a,b) and benzothiazole (c,d) moieties.

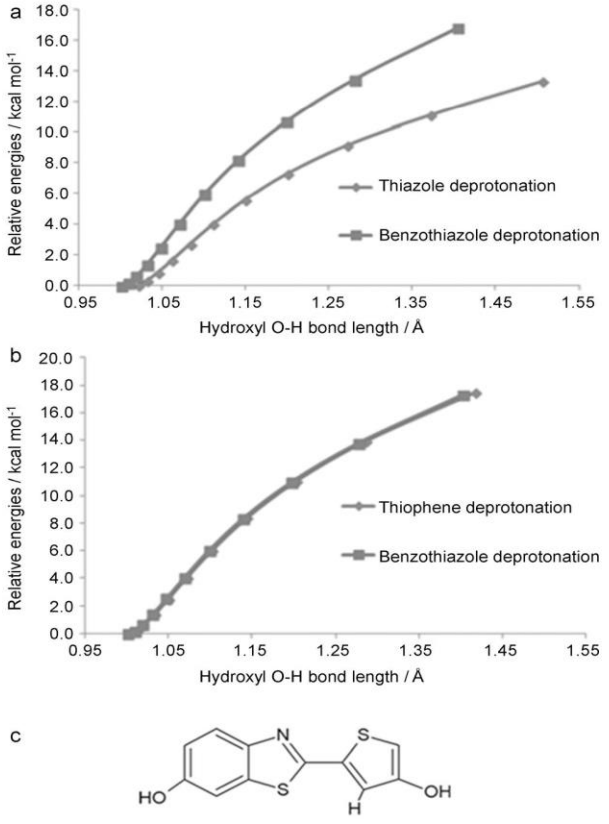

Figure 3. Relative energies of the deprotonation of thiazole/thiophene and benzothiazole moieties of a) oxyluciferin and b) an oxyluciferin analogue (c), as a function of hydroxyl O–H bond length [Å]. c) The oxyluciferin thiophene analogue, in which the thiazole nitrogen is replaced by a C–H group.

CHEMPHYSCHEM
ARTICLES
www.chemphyschem.org

for the acidity of neutral enolic oxyluciferin, as described previously in the literature.[21,27] The deprotonation of this group, and subsequent proton transfer to water, leads to an energy increase of only 13.3 kcal mol^{-1} (Figure 3a, "thiazole deprotonation" curve). A proton transfer from the benzothiazole hydroxyl group has an energetic cost of 16.8 kcal mol^{-1} (Figure 3a, "benzothiazole deprotonation" curve), 3.5 kcal mol^{-1} higher than the enol-based dissociation.

Figure 2 shows neutral oxyluciferin complexed with three water molecules at either the benzothiazole or thiazole hydroxyl groups, after quantum theory of atoms in molecules (QTAIM) analysis.[32] QTAIM is a model of electronic systems in which the principal features of molecular structures (atoms and bonds) are expressions of the system-observable electron-density distribution function. According to QTAIM, the molecular structure can be revealed by the stationary points of the electron density together with the gradients paths that originate and terminate at these points.

Visual analysis shows us that neutral oxyluciferin, when complexed at the thiazole moiety (Figure 2a), has three interactions with water molecules, acting as a hydrogen-bond donor in one interaction, and a hydrogen-bond acceptor in the other two (involving the thiazole nitrogen and thiazole hydroxyl oxygen). The number of interactions remains the same if the thiazole hydroxyl hydrogen is transferred to the solvent (Figure 2b). However, anionic oxyluciferin is the hydrogen-bond acceptor in all three interactions. The number of intermolecular interactions involving oxyluciferin is the same, when the solvated hydroxyl group is on the benzothiazole (Figure 2c). In this case, however, oxyluciferin is a hydrogen-bond donor in two interactions and an acceptor in only one. After deprotonation of this group, oxyluciferin is only involved in two interactions, acting as a hydrogen-bond acceptor in both (Figure 2d).

All intermolecular hydrogen-bond interactions between oxyluciferin and water molecules were characterized on basis of three QTAIM-derived parameters: the electron density $\rho(r)$, its Laplacian $\nabla^2\rho(r)$, and the energy density $H(r)$.[33–37] The low $\rho(r)$ values for all hydrogen bonds indicate that they are close-shell interactions, as expected.[33–37] $\nabla^2\rho(r)$ and $H(r)$ are used as indicators of the hydrogen bond strength.[38] Positive $\nabla^2\rho(r)$ and $H(r)$ values indicate weak hydrogen bonds, whereas medium-strength hydrogen bonds are characterized by positive $\nabla^2\rho(r)$ and negative $H(r)$ values. Strong hydrogen bonds are characterized by negative $\nabla^2\rho(r)$ and $H(r)$ values, as interactions with these characteristics are often classified as either covalent or partially covalent.[38–40]

The results of the QTAIM analysis for oxyluciferin solvated at the thiazole moiety are present in Table 1, and show that all hydrogen bonds involving the enolate anion are medium in strength. In the case of the neutral enol species, only the hydrogen bond between the enol hydrogen and the oxygen of the water molecule is medium in strength. The remaining hydrogen bonds are weak. The higher strength of the hydrogen bonds involving the enolate species should stabilize the anion relative to the neutral enol species.

The results of the QTAIM analysis for oxyluciferin solvated at the benzothiazole moiety are presented at Table 2. As in the case of thiazole-solvated oxyluciferin, only one of the hydrogen bonds involving the benzothiazole moiety of the neutral species is medium in strength. The other two are weak hydrogen bonds. In the case of the benzothiazolate anion, both hydrogen bonds are medium in strength. The increase in the strength of the hydrogen bonds should stabilize the anion/conjugate base over the neutral species/acid.

Table 1. QTAIM-derived $\rho(r)$, $\nabla^2\rho(r)$, and $H(r)$ values of the hydrogen bonds between neutral/enolate oxyluciferin and water molecules, in the ground state.

Hydrogen bonds	$\rho(r)$	$\nabla^2\rho(r)$	$H(r)$
neutral oxyluciferin H···O water	0.065	0.149	−0.015
neutral oxyluciferin N···H water	0.015	0.051	0.002
neutral oxyluciferin O···H water	0.033	0.115	0.000
anionic oxyluciferin O···H water	0.078	0.159	−0.024
anionic oxyluciferin N···H water	0.045	0.104	−0.007
anionic oxyluciferin O···H water	0.051	0.146	−0.007

Table 2. QTAIM-derived $\rho(r)$, $\nabla^2\rho(r)$, and $H(r)$ values of the hydrogen bonds between neutral/benzothiazole anionic oxyluciferin and water molecules, in the ground state.

Hydrogen bonds	$\rho(r)$	$\nabla^2\rho(r)$	$H(r)$
neutral oxyluciferin hydroxyl H···O water	0.053	0.145	−0.008
neutral oxyluciferin benzene H···O water	0.009	0.031	0.001
neutral oxyluciferin O···H water	0.035	0.120	0.000
anionic oxyluciferin O···H water	0.098	0.168	−0.040
anionic oxyluciferin O···H water	0.063	0.158	−0.014

The different number and strength of hydrogen bonds of anionic oxyluciferin solvated either at the benzothiazole or the thiazole moiety appears to provide an explanation for the enol-based acidity.[25] The enolate anion is involved in three medium-strength hydrogen bonds with water, whereas the benzothiazole anion is involved in two. The "extra" hydrogen bond of the enolate–water complex involves the thiazole nitrogen, which is in close proximity to the thiazole hydroxyl oxygen. In fact, these two heteroatoms are acceptors in a hydrogen bond with the same water molecule. The benzothiazole moiety possesses a similar nitrogen atom; however, it is farther away from the benzothiazole oxygen. Thus, it appears that the thiazole nitrogen atom, more so than the benzothiazole hydroxyl moiety, is the cause of the higher acidity of the enol group.[21,27]

To better support our hypothesis, we performed further calculations by creating an analogue of oxyluciferin (Figure 3c). This molecule has a C–H group instead of the thiazole nitrogen atom (i.e. a thiophene ring). We then modeled the ground-state proton-transfer reaction involving this molecule, by considering either the phenol or the enol group as the proton donor, using the methodology described above. The resulting energy curves are presented in Figure 3b.

This N→C–H substitution did not have a significant effect on the deprotonation of the phenol group. Deprotonation of this group led to an increase in energy of 17.4 kcal mol^{-1} (Fig-

CHEMPHYSCHEM
ARTICLES
www.chemphyschem.org

ure 3b), whereas in unmodified oxyluciferin the energy increase was 16.8 kcal mol^{-1} (Figure 3a). In contrast, the N→C–H substitution did affect enol deprotonation. In unmodified oxyluciferin, the energy increase was of 13.3 kcal mol^{-1} (Figure 3a). In the absence of the nitrogen atom, the final relative energy increased to 17.4 kcal mol^{-1}. Thus, these calculations indicate that in the absence of the nitrogen atom, the enol ceases to be the more acidic group; in this case, both the enol and phenol groups have similar acidity.

This was further supported by a QTAIM analysis of the ground state of the oxyluciferin analogue, solvated at either the benzothiazole or thiazole hydroxyl group (Figure 4, and

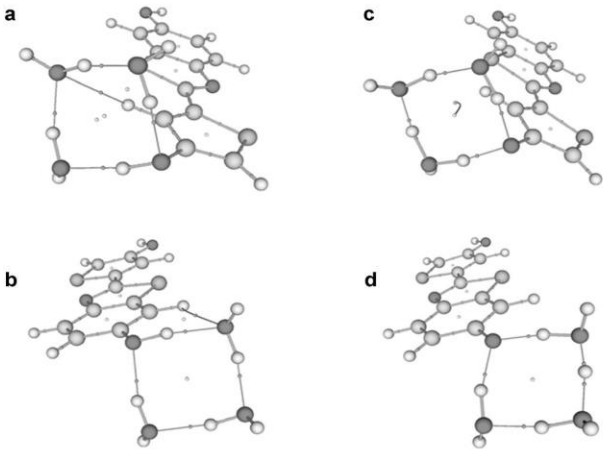

Figure 4. Representation (after QTAIM analysis) of ground-state neutral (a, b) and anionic (c, d) species of oxyluciferin thiophene analogue, solvated at the thiazole/thiophene (a, c) and benzothiazole (b, d) moieties.

Tables 3 and 4). Visual inspection of Figure 4 reveals that the neutral oxyluciferin analogue is involved in the same number of hydrogen bonds (three), when solvated either at the benzothiazole (Figure 4b) or thiazole (Figure 4a) moiety. This is in line with the results obtained for unmodified neutral oxyluciferin (Figure 2a and c). The results are also the same for the phenolate forms of unmodified oxyluciferin (Figure 2d) and the thiophene analogue (Figure 4d), which are involved in two hydrogen bonds. However, the absence of the thiazole nitrogen atom does affect the hydrogen-bond network involving the thiophene anionic moiety. In that oxyluciferin analogue,

Table 3. QTAIM-derived $\rho(r)$, $\nabla^2\rho(r)$, and $H(r)$ values of the hydrogen bonds between neutral/enolate oxyluciferin analogue and water molecules, in the ground state.

Hydrogen bonds	$\rho(r)$	$\nabla^2\rho(r)$	$H(r)$
neutral analogue H···O water	0.052	0.143	−0.008
neutral analogue thiophene ring C···H water	0.008	0.029	0.01
neutral analogue O···H hydrogen	0.034	0.115	0.000
anionic analogue O···H water	0.096	0.162	−0.038
anionic analogue O···H water	0.066	0.152	−0.016

Table 4. QTAIM-derived $\rho(r)$, $\nabla^2\rho(r)$, and $H(r)$ values of the hydrogen bonds between neutral/benzothiazole anionic oxyluciferin analogue and water molecules, in the ground state.

Hydrogen bonds	$\rho(r)$	$\nabla^2\rho(r)$	$H(r)$
neutral analogue hydroxyl H···O water	0.052	0.144	−0.008
neutral analogue benzene H···O water	0.009	0.031	0.001
neutral analogue O···H water	0.035	0.121	0.000
anionic analogue O···H water	0.100	0.167	−0.040
anionic analogue O···H water	0.064	0.158	−0.015

the thiophene moiety is only involved in two bonds (Figure 4c), whereas the enolate of unmodified oxyluciferin was involved in three hydrogen bonds (Figure 2b).

Analysis of the QTAIM-derived parameters indicates that both hydrogen bonds involving the enolate oxyluciferin derivative are medium in strength (Table 3), which was also indicated for the corresponding phenolate (Table 4). In contrast, the unmodified enolate is stabilized over the phenolate due to an extra hydrogen bond, arising from the presence of the thiazole nitrogen. Thus, these calculations support our explanation of the stronger acidity of the enol group, as the absence of the nitrogen in the thiophene analogue eliminates the stabilization of enolate oxyluciferin over the phenolate anion.

2.2. Photoacidity of the Enol Group within the Franck–Condon Approximation

Fundamental processes in photoacidity are electronic redistribution upon photoexcitation, proton dissociation and mobility, geminate recombination with the conjugated photobase, quenching, and excited-state decay.[13] In this study we focused on the electronic redistribution and proton dissociation processes, which we believe are more important for understanding the enol-based photoacidity of oxyluciferin, as these are the most specific regarding the identity of the photoacid functional group. To this end, we studied the ESPT process involving the two hydroxyl groups of the neutral enol species, when solvated by three explicit water molecules.

We initially believed the approach should include excited-state geometry optimizations to follow the ESPT reaction at the excited-state potential energy surface (PES). Such an approach should take into account the electronic redistribution and geometric relaxation that occurs after photoexcitation. However, performing such calculations on the ESPT is far from trivial. The choice of an effective reaction coordinate can be difficult, as the motion of the proton is accompanied by a significant electronic rearrangement and is normally coupled to other degrees of freedom, and is associated with problems related to classical or quantum treatment of its dynamics.[41–43]

An alternative approach is to calculate the Franck–Condon curves of the desired reaction. These curves can be obtained by modeling the desired reaction in the ground state, and then re-evaluating the PES by performing vertical excitation single-point energy calculations. This strategy can then be used to take into account the electronic redistribution resulting from photoexcitation, but not the geometry relaxation.

This strategy results from the notion that the absorption process can also provide valuable insight into the fluorescence properties of a molecule. It should be noted that the absorption spectrum often reflects the main features of the excited state, differing by a redshift that occurs due to geometry relaxation.[44–46] This approach has been used routinely with good results in the study of ESPT reactions,[28,47–52] and in the elucidation of other features of excited states.[53–60]

Given this reasoning, the potential Franck–Condon curves were obtained by performing vertical excitation calculations on the ground-state reactions (Figure 3a). Thus, the structures of Franck–Condon neutral enol oxyluciferin, and corresponding anions, are the same (Figure 2). The energetic profiles of these ESPT reactions, in terms of Franck–Condon potential curves, are presented in Figure 5a and are relative to the S_1 energy of the corresponding neutral structure, with explicit water around the respective hydroxyl group.

Our calculations indeed attribute the photoacidity of neutral enolic oxyluciferin to the enol moiety, as revealed by experiment.[25] The deprotonation of this group leads to an energy increase of only 7.0 kcal mol^{-1} (Figure 5a, "thiazole deprotonation" curve). ESPT from the benzothiazole hydroxyl group has an energetic cost of 12.5 kcal mol^{-1} (Figure 5a, "benzothiazole deprotonation" curve), 5.5 kcal mol^{-1} higher than the enol-based ESPT. It should be noted that whereas the Franck–Condon energies of both ESPT reactions increase with increasing hydroxyl O···H distance, the vertical excitation energies decrease in both cases (Figure 5b). Also, we note that although the energy of ESPT did not decrease with increasing hydroxyl O···H distance, as one would expect from a photoacid, in our opinion this is expected and not a source of concern. As mentioned, our approach only deals with electronic redistribution after photoexcitation. Therefore, this approach does not allow the system to fully relax with the subsequent steps of the ESPT reaction. Nevertheless, we have verified that the enol group is more photoacidic than the hydroxyl, as found experimentally.[25] Moreover, the Franck–Condon curves of both groups are more favorable than their ground-state counterparts (Figure S1 in the Supporting Information). Thus, our approach has provided us with a qualitatively accurate picture.

The Franck–Condon curves were also calculated for the ESPT reaction involving the oxyluciferin analogue. The resulting curves are presented in Figure 5c. The C–H substitution did not significantly affect the excited-state deprotonation of the phenol group. The deprotonation of this group led to an increase in energy of 13.0 kcal mol^{-1} (Figure 5c), whereas in the unmodified oxyluciferin, the energy increase was 12.5 kcal mol^{-1} (Figure 5a). In the enol-based ESPT, the energy increase of the analogue was 12.9 kcal mol^{-1}, whereas in modified oxyluciferin it was 7.0 kcal mol^{-1}. Thus, these calculations indicate that in the absence of the nitrogen atom, the enol group also ceases to be the more photoacidic group.

Figure S2 shows neutral oxyluciferin complexed with three water molecules at either the benzothiazole or thiazole hydroxyl groups, after QTAIM analysis (see also Tables S1 and S2).[32] It should be noted that the electron density used for this QTAIM analysis was that of the Franck–Condon state, and not of the ground state. As in the ground state, the enolate anion is involved in three medium-strength hydrogen bonds, whereas the phenolate anion is involved in only two hydrogen bonds of similar strength. Nevertheless, the results for the ground and Franck–Condon states are similar, although they might be expected to demonstrate that the acidity is greater in the latter state, which is not so surprising given that the geometry is the same for both states. Thus, this indicates that analyzing excited states with QTAIM, within the Franck–Condon approximation, does not give accurate results and so other approaches are needed to complement these findings.

According to Hynes and co-workers, the source of enhanced photoacidity of a given molecule relates to the anion in the ESPT reaction.[61] The anion is thus stabilized in the excited

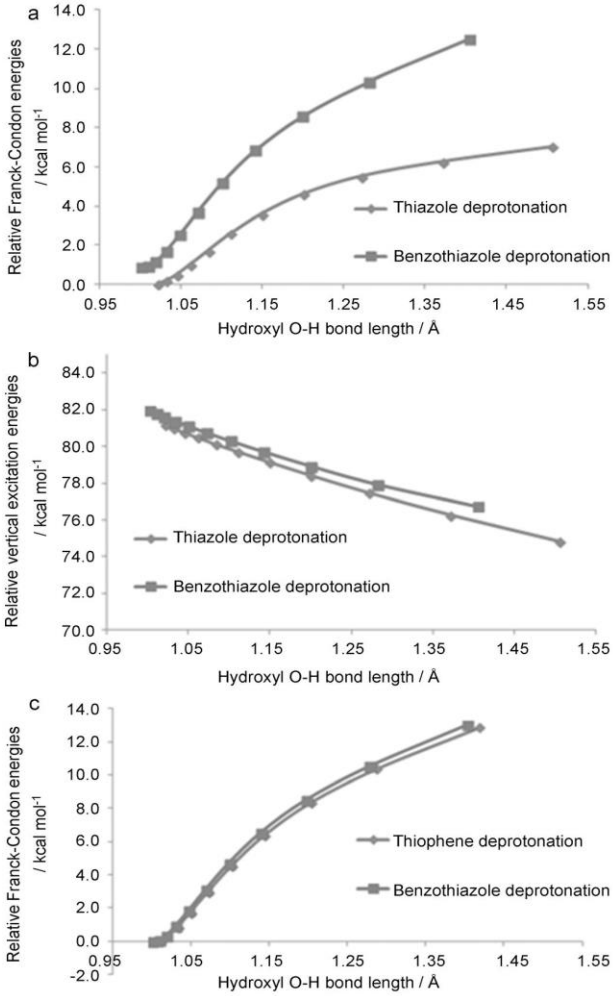

Figure 5. Relative Franck–Condon (a) and vertical excitation (b) energies of the deprotonation of thiazole and benzothiazole moieties of oxyluciferin, as a function of hydroxyl O–H bond length [Å]. c) Relative Franck–Condon energies of the deprotonation of thiophene and benzothiazole moieties of the oxyluciferin analogue, as a function of hydroxyl O–H bond length [Å].

state as photoinduced charge transfer rendered it a weaker base/proton acceptor in the excited state. Therefore, we measured the natural bond orbital (NBO) partial atomic charges of the deprotonated oxygen of both the benzothiazole and the enolate anion, at the ground and Franck–Condon states (Table 5). NBO charges can be obtained by performing an NBO analysis, which is an extension of a natural population analysis (NPA). NPA involves constructing natural atomic orbitals on each center, by dividing the electron density matrix into sub-

Table 5. NBO atomic charges of important oxyluciferin heteroatoms, during the ESPT reaction, at the ground and Franck–Condon states.

	Ground state	Excited state
thiazole O (anionic, solvated)	−0.871	−0.765
benzothiazole O (anionic, solvated)	−0.871	−0.794
thiazole N (neutral, solvated)[a]	−0.511	−0.588
thiazole N (anionic, solvated)[a]	−0.517	−0.591
thiazole N (neutral, solvated)[b]	−0.544	−0.629
thiazole N (anionic, solvated)[b]	−0.602	−0.688

[a] Solvated at the benzothiazole moiety. [b] Solvated at the enol moiety.

blocks with appropriate symmetry. The charge is then partitioned into these orbitals. In the NBO analysis, the NPA charge is further partitioned into core and bonding orbitals, lone pairs and Rydberg states. This type of charge scheme was found to yield good results when used to try to represent variations in pK_a.[62,63]

Indeed, the partial atomic charge of the oxygen atom decreased upon photoexcitation, which is consistent with the results of Hynes and co-workers.[61] If we compare the Franck–Condon charges, it is evident that the atomic charge of the deprotonated oxygen on both benzothiazole and thiazole is similar. Nevertheless, it is clear that the decrease in the negative partial charge of the benzothiazole oxygen is lower than at the thiazole. Thus, these results indicate that the deprotonated oxygen at the thiazole became the least powerful photobase, which is expected to stabilize the enolate anion over the phenolate.

We have also computed the NBO charges of the thiazole nitrogen atom, in the ground and Franck–Condon states, for thiazole-solvated neutral and anionic species (Table 5). This heteroatom was found to be important for the ground-state acidity of oxyluciferin, and can, therefore, also play a role in the corresponding excited-state process. It is evident that the thiazole nitrogen is a better hydrogen-bond acceptor in the Franck–Condon than in the ground state. Moreover, the negative charge of the thiazole nitrogen increases by −0.059 upon deprotonation of the enol group, thus increasing its photobasicity during ESPT. Thus, as in the ground state, it appears that hydrogen bonds involving the thiazole nitrogen should become stronger upon enol-based ESPT and, therefore, promote the enol-favored photoacidity of oxyluciferin.[25] However, it is still not clear if the increased photobasicity of the thiazole nitrogen occurs only in the enolate anion, and not in the benzothiazole anion. After all, this nitrogen atom also exists in the latter, and so in theory can also be involved in a hydrogen bond with the solvent. To test this hypothesis, we calculated the charge of the thiazole nitrogen, in the Franck–Condon state, in the neutral and anionic species of benzothiazole-solvated oxyluciferin (Table 5). The negative charge of the thiazole nitrogen also increases upon deprotonation of the phenol group. However, this increase is small (−0.003) compared with the increase found for the enol deprotonation reaction (−0.059). Therefore, these results do support the hypothesis that a hydrogen bond between water molecules and the thiazole nitrogen is stronger in the excited-state enolate anion than in the phenolate form of oxyluciferin.

2.3. Photoacidity of the Enol Group in the Emissive State

It should be noted that although our approach of studying the Franck–Condon state of oxyluciferin provides results that allows us to characterize the rare enol-based photoacidity of oxyluciferin, it is still an approximation. To obtain more accurate results, we tried to optimize, in the excited state, the transition state of the ESPT reactions between neutral enol oxyluciferin and one water molecule, placed either at the enol or phenol site. The obtained structures are presented in Figure 6a and b. These structures were confirmed to be transition states

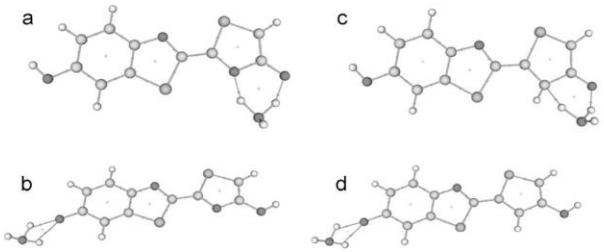

Figure 6. Representation (after QTAIM analysis) of the excited-state transition-state of enolate (a, c) and phenolate (b, d) ESPT reaction, of both unmodified (a, b) and N→C substituted (c, d) oxyluciferin.

of such reactions, by verifying that they present only one imaginary frequency with appropriate displacement vectors. The excited-state geometry optimizations were performed in vacuo at the CIS/6-31G(d) level of theory. The energies were recalculated at the TD CAM-B3LYP/6-311+G(d,p) level of theory, in implicit water.

We calculated that the transition state of the enol-based ESPT is 24.8 kcal mol^{-1} more stable than the transition state of the phenol-based ESPT. This indicates that the former reaction should be the more likely to occur, as has been found experimentally.[25] We also calculated the excited-state energy of these two structures, without the water molecules. Thus, these energy calculations refer only to the oxyluciferin moiety of the transition states. The enolate transition state was again more stable than the phenolate, in this case by only 2.3 kcal mol^{-1}. This indicates that the higher stabilization of the enolate transition state, compared to the phenolate, is mainly due to inter-

actions between oxyluciferin and the water molecule. To obtain more insight into these interactions, we analyzed these structures by QTAIM (Figure 6a and b).

Both transition states are involved in two intermolecular interactions with the water molecule. In the phenol-based ESPT, the phenolate oxygen accepts two hydrogen bonds from the hydronium cation. In the case of the enol-based ESPT, the situation is similar to that found in the ground and Franck–Condon states. The hydronium cation binds the enolate transition state by donating hydrogen bonds to both the thiazole nitrogen and oxygen atoms. The three QTAIM-derived parameters ($\rho(r)$, $\nabla^2\rho(r)$, and $H(r)$) are presented in Table 6 for all these

Table 6. QTAIM-derived $\rho(r)$, $\nabla^2\rho(r)$, and $H(r)$ values of the hydrogen bonds between excited-state oxyluciferin phenolate/enolate-based ESPT reaction transition-state and a water molecule, in the emissive state.

Hydrogen bonds	$\rho(r)$	$\nabla^2\rho(r)$	$H(r)$
enolate oxyluciferin enolic O···H water	0.095	0.130	−0.039
enolate oxyluciferin thiazole N···H water	0.104	0.031	−0.053
phenolate oxyluciferin phenolic O···H water	0.050	0.207	−0.002
phenolate oxyluciferin phenolic O···H water	0.050	0.207	−0.002

interactions. If we take into account the relationship between $\nabla^2\rho(r)$, and $H(r)$, the four studied hydrogen bonds can be characterized as medium in strength.[38–40] However, it should be noted that the $H(r)$ values of the phenolate transition state are only barely negative. In contrast, the negative $H(r)$ values for the enolate transition state are significant, and indicate that the hydrogen bonds present in the enol-based ESPT are stronger than those found in the phenolate transition state. Thus, the larger stabilization of the enolate transition state is attributed to stronger hydrogen bonds formed with the solvent.

The NBO charges were calculated for both phenolate and enolate transition states, which were divided into benzothiazole, thiazole and hydronium moieties (Table 7). The atomic

Table 7. NBO atomic charges of the oxyluciferin ESPT transition-state moieties and important heteroatoms, in the emissive state.

	Enolate	Phenolate
benzothiazole moiety	−0.154	−0.688
thiazole moiety	−0.526	−0.229
hydronium cation	0.682	0.917
thiazole N	−0.683	−0.585
phenolic O	–	−0.842
enolic O	−0.695	–

NBO charges for thiazole nitrogen (both structures), thiazole oxygen (enolate) and benzothiazole oxygen (phenolate) were also specified.

The phenolate transition state is more polar, with high charge separation between oxyluciferin and the hydronium cation. In the case of the enolate transition state, the charge is more delocalized over the entire structure. In agreement with the work of Hynes et al.,[61] the enolate oxygen is a weaker photobase than the phenolate oxygen, leading to stabilization of the enolate anion. Moreover, it is evident that the thiazole nitrogen is a better hydrogen-bond acceptor in the enolate transition state. This is important because, as can be seen in Figures 2 and 6a, this heteroatom is bound to the water molecule that abstracts the proton from the enol group. Our NBO analysis also demonstrates that the hydrogen bonds involving the enolate transition state are significantly polar, with a charge difference between the atoms of approximately 1.200. The charge difference between the atoms of the phenolate transition state, involved in the hydrogen bonds, is also significant ($\approx$1.400). However, in this case the oxyluciferin atom that accepts the two hydrogen bonds is the same (the phenolate oxygen). Therefore, this atom has to share its charge density with the two hydrogen atoms of the hydronium cation. Accordingly, the actual charge difference between each phenolate hydrogen bond should be much smaller than the one found for the enolate transition structure. This finding is in line with the results obtained from the QTAIM analysis, and can explain why the hydrogen bonds found in the enolate transition state are stronger than those present in the phenolate structure. Thus, as in the ground state, the presence of the thiazole nitrogen as a hydrogen-bond acceptor for the water molecule that abstracts the proton from the enol group is a determining factor for the enol-based photoacidity of oxyluciferin.

To provide further evidence for these conclusions, we have also calculated the transition state between the oxyluciferin analogue and one water molecule (Figure 6c and d). Our calculations demonstrated that the transition state of the enolate form of the thiophene analogue is more stable than the phenolate. This indicates that, as in the case of unmodified oxyluciferin, the photoacidity of this analogue is enol based.[25] However, the stabilization energy was found to be only 7.3 kcal mol^{-1}, which is 17.5 kcal mol^{-1} lower than that of unmodified oxyluciferin. Moreover, the energy difference between the oxyluciferins indicates that, without the water molecules, the phenolate is the most stable structure by 6.9 kcal mol^{-1}. Therefore, as in the case of unmodified oxyluciferin, the reason behind the enol-based photoacidity is the hydrogen bonding between the solvent and the thiazole moiety of the photoacid.

To obtain further information, we also analyzed these two structures by using QTAIM (Figure 6c and d). The three derived parameters—$\rho(r)$, $\nabla^2\rho(r)$, and $H(r)$—obtained for the intermolecular interactions, are listed in Table 8. As in the case of unmodified oxyluciferin, the phenolate form of the analogue is involved in two hydrogen bonds with the hydronium cation, with the phenolate oxygen as the acceptor in both cases. The enolate transition state is also involved in two hydrogen bonds with the hydronium cation. However, in this case the acceptors are the enolate oxygen and the carbon atom that replaces the ring nitrogen atom of oxyluciferin (Figure 6c). This is similar to that for the transition state of the unmodified enolate. The hydrogen bonds present in the phenolate were classified as medium in strength, according to the relationship between $\nabla^2\rho(r)$ and $H(r)$. The same classification was attributed to the bond between the enolate oxygen and the water molecule, of

Table 8. QTAIM-derived $\rho(r)$, $\nabla^2\rho(r)$, and $H(r)$ of the hydrogen bonds between excited-state phenolate/enolate-based ESPT reaction transition-state of oxyluciferin analogue and a water molecule, in the emissive state.

Hydrogen bonds	$\rho(r)$	$\nabla^2\rho(r)$	$H(r)$
enolate analogue enolic O···H water	0.080	0.141	−0.027
enolate analogue thiophene C···H water	0.077	−0.014	−0.034
phenolate analogue phenolic O···H water	0.052	0.207	−0.003
phenolate analogue phenolic O···H water	0.051	0.207	−0.003

the transition-state enolate. However, the negative values of both $\nabla^2\rho(r)$ and $H(r)$ indicate that the hydrogen bond involving the carbon atom (Figure 6c) is a strong interaction. Thus, the hydrogen-bonding network involving the enolate transition state is more stabilizing than that of the phenolate structure.

The NBO charges were also calculated for these two transition states (Table 9). The results are similar to those found for unmodified oxyluciferin (Table 7). Nevertheless, the difference between the two transition states is notable with respect to the NBO charge of the substituting carbon atom of the thiophene analogue. In the transition state, this atom carries a significant negative charge. However, when considering the phenolate transition state, the negative charge decreases to about half. Thus, this carbon atom is expected to be a much stronger hydrogen-bond acceptor in the enolate anion than in the phenolate. This is important to the photoacidity of this molecule, given the strength of the hydrogen bond involving this atom in the transition state of the enolate.

Table 9. NBO atomic charges of the oxyluciferin analogue ESPT transition-state moieties and important heteroatoms, in the emissive state.

	Enolate	Phenolate
benzothiazole moiety	−0.141	−0.781
thiophene moiety	−0.544	−0.130
hydronium cation	0.684	0.911
thiophene C	−0.603	−0.350
phenolic O	–	−0.853
enolic O	−0.711	–

Our calculations allow us to explain the enol-based photoacidity of oxyluciferin. The key to this phenomenon appears to be the hydrogen-bonding network formed between the conjugated photobase of the fluorophore, and the solvent. The hydrogen bonds between the enolate thiazole moiety and the solvent are stronger than those formed between the phenolate benzothiazole moiety and water. Thus, the enolate anion is stabilized over the phenolate species. The strength itself can be attributed to the high polarity of these interactions (NBO charge separation up to ≈1.200), and to the small hydrogen-bond lengths (≈1.69 Å for the phenolate transition state and ≈1.43 Å for the enolate structure). We attribute this increase in strength to the fact that the enolate anion has more effective hydrogen-bond acceptors (e.g. the nitrogen atom) near the proton donor atom, than the phenolate photobase. In the phenolate photobase, the same hydrogen-bond acceptor atom has to divide its charge density into two hydrogen bonds, thus decreasing the strength of both interactions. Given the higher number of hydrogen-bond acceptor atoms near the proton-donor site, this does not occur in the enolate anion. Moreover, the neutral→phenolate ESPT reaction decreases the hydrogen-bond acceptor potential of the thiazole nitrogen compared to the enolate anion, further destabilizing the phenolate photobase.

3. Conclusions

Firefly oxyluciferin is the active chromophore of the firefly bioluminescence reaction, which is produced in an excited state. This molecule was recently found to be a photoacid, involved in many complex and interesting photoinduced phenomena, including ESPT to the solvent, efficient fluorescence quenching, and pH-sensitive fluorescence. One such phenomenon was the unexpected and rare photoacidity of the stable enolic group.

In this manuscript we have presented our theoretical analysis of this enol-based photoacidity, by performing a comparative study of the ESPT reaction between oxyluciferin benzothiazole/thiazole moieties and water. We have found that the basis for such exceptional photoacidity is the hydrogen-bond network involving the conjugated photobase of oxyluciferin. Our calculations indicated that the bonds of this network that involve the anionic moiety vary in strength, when enol- or phenol-based ESPT are compared. The hydrogen bonds formed between the enolate thiazole moiety and water are stronger than those formed between the solvent and the phenolate benzothiazole moiety. Thus, the enolate anion is stabilized over phenolate in oxyluciferin. This increase in strength might be caused by the enolate anion presenting more hydrogen-bond acceptor atoms near to the proton donor atom, than the phenolate form of oxyluciferin. Moreover, the phenol-based ESPT reaction decreases the hydrogen-bond acceptor potential of these thiazole atoms.

In the course of this work we also studied the ground-state enol-based acidity of oxyluciferin, which was attributed to the presence of the thiazole nitrogen atom. The enolate anion is involved in three medium-strength hydrogen bonds with water, whereas the benzothiazole anion is only involved in two. The extra hydrogen bond of the enolate–water complex involves the thiazole nitrogen, which is in close proximity to the thiazole hydroxyl oxygen. In fact, these two heteroatoms are acceptors in a hydrogen bond with the same water molecule. Thus, this extra intermolecular interaction is expected to stabilize the ground-state enolate anion over the phenolate, and thereby explain the enol-based acidity.

Computational Details

Calculations were carried out by using the Gaussian 09 program package.[64] The ground-state geometries of oxyluciferin complexed with water molecules were optimized at the CAM-B3LYP/6-31G(d) level of theory.[65] Three specific water molecules were included in

the calculations within the Franck–Condon approximation, and one molecule was included in calculations of the emissive state. Vibrational frequency calculations, at the same level of theory, were made in order to ensure that the obtained structures were minima in their PES.

The proton transfer reactions were modeled by performing a relaxed PES scan, with geometry optimization at each point at the CAM-B3LYP/6-31G(d) level of theory. The ground-state PES was re-evaluated by performing single-point energy calculations at the CAM-B3LYP/6-311+G(d,p) level of theory. The excited-state PES was evaluated by calculating the Franck–Condon curves by obtaining the time-dependent CAM-B3LYP/6-311+G(d,p) vertical excitation energies.[66] Such a strategy was already used with success in other studies aiming to understand ESPT reactions.[28,47–52]

The excited-state transition-state structures were calculated in vacuo at the CIS/6-31G(d) level of theory.[67] Six excited states were considered for these calculations. The nature of these structures was assessed by performing vibrational analysis at the same level of theory.

CAM-B3LYP is a long-range corrected version of B3LYP by using the Coulomb-attenuating method.[65] This density functional was chosen because of good results obtained previously for $n\rightarrow\pi^*$, $\pi\rightarrow\pi^*$, charge transfer and Rydberg excited states.[68] The CIS method was chosen as previous works demonstrated that this method provides results that are comparable to those obtained with higher levels of theory (e.g. SAC-CI) for oxyluciferin.[69]

All single-point calculations were performed in implicit water, which was modeled by using the conductor-like polarizable continuum model.[70,71]

The excited-state transitions were calculated with the linear response approximation. Five states were calculated in the TD CAM-B3LYP/6-311+G(d,p) vertical excited-state energies.

The analysis of the intermolecular interactions between oxyluciferin and water molecules was performed by applying QTAIM theory.[32–37] The QTAIM tool can be used to identify the coordinates of critical points (CP) in which the gradient of electron density vanishes. The characteristics of CP derived from QTAIM analysis can be used as descriptors of different types of interactions.[32–37] Stable CPs can be divided into four categories: maxima in electron density almost always correspond to nuclei, and the minimum is a cage CP, bond CP and ring CP.[32–37] The QTAIM analysis was performed by using the Multiwfn code.[72]

Acknowledgements

Financial support from Fundação para a Ciência e Tecnologia (FCT), Lisbon [Programa Operacional Temático Factores de Competitividade (COMPETE) e comparticipado pelo Fundo Comunitário Europeu (FEDER, project PTDC/QUI/71366/2006)] is acknowledged. A Ph.D. grant to L.P.d.S. (SFRH/76612/2011), awarded by FCT, is also acknowledged.

Keywords: enols · excited-state proton transfer · hydrogen bonding · oxyluciferin · photoacidity

[1] N. Agmon, *Acc. Chem. Res.* **2012**, *45*, 63–73.
[2] D. D. Wang, G. J. Zhao, *Commun. Comput. Chem.* **2013**, *1*, 181–190.
[3] W. Hujo, S. Grimme, *Phys. Chem. Chem. Phys.* **2011**, *13*, 13942–13950.
[4] B. J. Miller, J. R. Lane, H. G. Kjaergaard, *Phys. Chem. Chem. Phys.* **2011**, *13*, 14183–14193.
[5] K. S. Kim, K. S. Oh, J. Y. Lee, *Proc. Natl. Acad. Sci. USA* **2000**, *97*, 6373–6378.
[6] P. Song, F. C. Ma, *Int. Rev. Phys. Chem.* **2013**, *32*, 589–609.
[7] T. Kumpulainen, A. M. Brouwer, *Phys. Chem. Chem. Phys.* **2012**, *14*, 13019–13026.
[8] G. J. Zhao, K. L. Han, *J. Phys. Chem. A* **2007**, *111*, 9218–9223.
[9] P. Chowdhury, S. Panja, S. Chakravorti, *J. Phys. Chem. A* **2003**, *107*, 83–90.
[10] G. J. Zhao, K. L. Han, *ChemPhysChem* **2008**, *9*, 1842–1846.
[11] C. Kolano, J. Helbing, M. Kozinski, W. Sander, P. Hamm, *Nature* **2006**, *444*, 469–472.
[12] D. Chandler, *Nature* **2007**, *445*, 831–832.
[13] N. Agmon, *J. Phys. Chem. A* **2005**, *109*, 13–35.
[14] L. M. Tolbert, K. M. Solntsev, *Acc. Chem. Res.* **2002**, *35*, 19–27.
[15] L. Pinto da Silva, J. C. G. Esteves da Silva, *ChemPhysChem* **2012**, *13*, 2257–2262.
[16] J. Vieira, L. Pinto da Silva, J. C. G. Esteves da Silva, *J. Photochem. Photobiol. B* **2012**, *117*, 33–39.
[17] S. Hosseinkhani, *Cell. Mol. Life Sci.* **2011**, *68*, 1167–1182.
[18] I. Navizet, Y. J. Liu, N. Ferré, D. Roca-Sanjuán, R. Lindh, *ChemPhysChem* **2011**, *12*, 3064–3076.
[19] S. Roura, C. Gálvez-Monón, A. Bayes-Genis, *J. Cell. Mol. Med.* **2013**, *17*, 693–703.
[20] A. Roda, M. Guardigli, *Anal. Bioanal. Chem.* **2012**, *402*, 69–76.
[21] L. Pinto da Silva, R. Simkovitch, D. Huppert, J. C. G. Esteves da Silva, *ChemPhysChem* **2013**, *14*, 3441–3446.
[22] Y. Erez, I. Presiado, R. Gepshtein, L. Pinto da Silva, J. C. G. Esteves da Silva, D. Huppert, *J. Phys. Chem. A* **2012**, *116*, 7452–7461.
[23] M. Rebarz, B. M. Kukovec, O. V. Maltsev, C. Ruckebusch, L. Hintermann, P. Naumov, M. Sliwa, *Chem. Sci.* **2013**, *4*, 3803–3809.
[24] I. Presiado, Y. Erez, R. Simkovitch, S. Shomer, R. Gepshtein, L. Pinto da Silva, J. C. G. Esteves da Silva, D. Huppert, *J. Phys. Chem. A* **2012**, *116*, 10770–10779.
[25] K. M. Solntsev, S. P. Laptenok, P. Naumov, *J. Am. Chem. Soc.* **2012**, *134*, 16452–16455.
[26] P. Naumov, Y. Ozawa, K. Ohkubo, S. Fukuzumi, *J. Am. Chem. Soc.* **2009**, *131*, 11590–11605.
[27] L. Pinto da Silva, R. Simkovitch, D. Huppert, J. C. G. Esteves da Silva, *ChemPhysChem* **2013**, *14*, 2711–2716.
[28] L. Pinto da Silva, R. Simkovitch, D. Huppert, J. C. G. Esteves da Silva, *J. Photochem. Photobiol. A* **2013**, *266*, 47–54.
[29] J. C. G. Esteves da Silva, J. M. C. S. Magalhães, R. Fontes, *Tetrahedron Lett.* **2001**, *42*, 8173–8176.
[30] N. Suzuki, M. Sato, K. Okada, T. Goto, *Tetrahedron* **1972**, *28*, 4065–4074.
[31] A. C. Weedon in *The Chemistry of Enols* (Ed.: Z. Rappoport), Wiley, New York, **1990**, chapter 9.
[32] R. F. W. Bader, *Acc. Chem. Res.* **1985**, *18*, 9–15.
[33] R. F. W. Bader, *Chem. Rev.* **1991**, *91*, 893–928.
[34] R. F. W. Bader, *J. Phys. Chem. A* **1998**, *102*, 7314–7323.
[35] S. Shaik, D. Danovich, W. Wu, P. C. Hiberty, *Nat. Chem.* **2009**, *1*, 443–449.
[36] H. S. Rzepa, *J. Chem. Theory Comput.* **2011**, *7*, 97–102.
[37] I. Vidal, S. Melchor, J. A. Dobado, *J. Phys. Chem. A* **2008**, *112*, 3414–3423.
[38] I. Rozas, I. Alkorta, J. Elguero, *J. Am. Chem. Soc.* **2000**, *122*, 11154–11161.
[39] S. Jenkins, I. Morrison, *Chem. Phys. Lett.* **2000**, *317*, 97–102.
[40] S. J. Grabowski, W. A. S. Sokalski, J. Leszczynski, *J. Phys. Chem. A* **2005**, *109*, 4331–4341.
[41] M. Savarese, P. A. Netti, C. Adamo, N. Rega, I. Ciofini, *J. Phys. Chem. B* **2013**, *117*, 16165–16173.
[42] M. T. Koper, *Phys. Chem. Chem. Phys.* **2013**, *15*, 1399–1407.
[43] B. Auer, L. E. Fernandez, S. Hammes-Schiffer, *J. Am. Chem. Soc.* **2011**, *133*, 8282–8292.
[44] B. F. Milne, M. A. Marques, F. Nogueira, *Phys. Chem. Chem. Phys.* **2010**, *12*, 14285–14293.
[45] D. Cai, M. A. Marques, F. Nogueira, *J. Phys. Chem. B* **2011**, *115*, 329–332.
[46] D. Cai, M. A. L. Marques, B. F. Milne, F. Nogueira, *J. Phys. Chem. Lett.* **2010**, *1*, 2781–2787.
[47] M. Rosenberg, T. I. Solling, *Chem. Phys. Lett.* **2010**, *484*, 113–118.

[48] N. Singla, P. Chowdhury, *Chem. Phys. Lett.* **2012**, *548*, 71 – 79.
[49] B. K. Paul, S. Mahanta, R. B. Singh, N. Guchhait, *J. Phys. Chem. A* **2010**, *114*, 2618 – 2627.
[50] S. Mahanta, B. K. Paul, R. B. Singh, N. Guchhait, *J. Comput. Chem.* **2011**, *32*, 1 – 14.
[51] R. B. Singh, S. Mahanta, N. Guchhait, *J. Photochem. Photobiol. A* **2008**, *200*, 325 – 333.
[52] R. de Vivie-Riedle, V. De Waele, L. Kurtz, E. Riedle, *J. Phys. Chem. A* **2003**, *107*, 10591 – 10599.
[53] L. Pinto da Silva, J. C. G. Esteves da Silva, *J. Comput. Chem.* **2011**, *32*, 2654 – 2663.
[54] K. Støchkel, C. N. Hansen, J. Houmøller, L. M. Nielsen, M. Linares, P. Norman, F. Nogueira, O. V. Maltsev, L. Hintermann, S. B. P. Naumov, B. F. Milne, *J. Am. Chem. Soc.* **2013**, *135*, 6485 – 6493.
[55] L. Pinto da Silva, J. C. G. Esteves da Silva, *Photochem. Photobiol. Sci.* **2013**, *12*, 2028 – 2035.
[56] L. Pinto da Silva, P. J. O. Ferreira, D. J. R. Duarte, M. S. Miranda, J. C. G. Esteves da Silva, *J. Phys. Chem. A* **2014**, *118*, 1511 – 1518.
[57] M. S. Miranda, L. Pinto da Silva, J. C. G. Esteves da Silva, *J. Phys. Org. Chem.* **2014**, *27*, 47 – 56.
[58] L. Pinto da Silva, J. C. G. Esteves da Silva, *J. Phys. Chem. B* **2014**, DOI: 10.1021/jp5036458.
[59] L. Pinto da Silva, M. S. Miranda, J. C. G. Esteves da Silva, *J. Photochem. Photobiol. A* **2014**, *278*, 9 – 13.
[60] D. Tuna, A. L. Sobolewski, W. Domcke, *J. Phys. Chem. B* **2014**, *118*, 976 – 985.
[61] J. T. Hynes, T. H. Tran-Thi, G. Granucci, *J. Photochem. Photobiol. A* **2002**, *154*, 3 – 11.
[62] K. C. Gross, P. G. Seybold, C. M. Hadad, *Int. J. Quantum Chem.* **2002**, *90*, 445 – 458.
[63] R. S. Vařeková, S. Geidl, C. M. Ionescu, O. Skřehota, M. Kudera, D. Sehnal, T. Bouchal, R. Abagyan, H. J. Huber, J. Koča, *J. Chem. Inf. Model.* **2011**, *51*, 1795 – 1806.
[64] Gaussian 09 (Revision A.02), M. J. Frisch, G. W. Trucks, H. B. Schlegel, G. E. Scuseria, M. A. Robb, J. R. Cheeseman, G. Scalmani, V. Barone, B. Mennucci, G. A. Petersson, H. Nakatsuji, M. Caricato, X. Li, H. P. Hratchian, A. F. Izmaylov, J. Bloino, G. Zheng, J. L. Sonnenberg, M. Hada, M. Ehara, K. Toyota, R. Fukuda, J. Hasegawa, M. Ishida, T. Nakajima, Y. Honda, O. Kitao, H. Nakai, T. Vreven, J. A. Montgomery, Jr., J. E. Peralta, F. Ogliaro, M. Bearpark, J. J. Heyd, E. Brothers, K. N. Kudin, V. N. Staroverov, R. Kobayashi, J. Normand, K. Raghavachari, A. Rendell, J. C. Burant, S. S. Iyengar, J. Tomasi, M. Cossi, N. Rega, J. M. Millam, M. Klene, J. E. Knox, J. B. Cross, V. Bakken, C. Adamo, J. Jaramillo, R. Gomperts, R. E. Stratmann, O. Yazyev, A. J. Austin, R. Cammi, C. Pomelli, J. W. Ochterski, R. L. Martin, K. Morokuma, V. G. Zakrzewski, G. A. Voth, P. Salvador, J. J. Dannenberg, S. Dapprich, A. D. Daniels, Ö. Farkas, J. B. Foresman, J. V. Ortiz, J. Cioslowski, D. J. Fox, Gaussian Inc., Wallingford CT, **2009**.
[65] T. Yanai, D. Tew, N. Handy, *Chem. Phys. Lett.* **2004**, *393*, 51 – 57.
[66] F. Furche, R. Ahlrichs, *J. Chem. Phys.* **2002**, *117*, 7433 – 7447.
[67] J. B. Foresman, M. Head-Gordon, J. A. Pople, M. J. Frisch, *J. Phys. Chem.* **1992**, *96*, 135 – 149.
[68] C. Adamo, D. Jacquemin, *Chem. Soc. Rev.* **2013**, *42*, 845 – 856.
[69] N. Nakatani, J. Y. Hasegawa, H. Nakatsuji, *J. Am. Chem. Soc.* **2007**, *129*, 8756 – 8765.
[70] V. Barone, M. Cossi, *J. Phys. Chem. A* **1998**, *102*, 1995 – 2001.
[71] M. Cossi, N. Rega, G. Scalmani, V. Barone, *J. Comput. Chem.* **2003**, *24*, 669 – 681.
[72] T. Lu, F. Chen, *J. Comput. Chem.* **2012**, *33*, 580 – 592.

Received: July 22, 2014
Revised: September 16, 2014
Published online on ■■ ■■, 2014

6.4. Study of the Involvement of π-π Stacked Complexes in the Photoprotolytic Cycle of $OxyLH_2$

Article 24

Theoretical photodynamic study of the photoprotolytic cycle of firefly oxyluciferin
Luís Pinto da Silva, Ron Simkovitch, Dan Huppert and Joaquim C.G. Esteves da Silva
ChemPhysChem **2014**, *14*, 2711-2716.

The theoretical calculations and the writing of the paper were performed by Luís Pinto da Silva, under the supervision of Professors Joaquim Esteves da Silva and Dan Huppert.

CHEMPHYSCHEM ARTICLES

ChemPubSoc Europe

DOI: 10.1002/cphc.201300330

Theoretical Photodynamic Study of the Photoprotolytic Cycle of Firefly Oxyluciferin

Luís Pinto da Silva,[a] Ron Simkovitch,[b] Dan Huppert,[b] and Joaquim C. G. Esteves da Silva*[a]

Firefly oxyluciferin presents a pH-sensitive fluorescence in aqueous solutions. Its fluorescence spectra are composed of two green peaks at different pH values, despite the enolate anion being the only emitter. A computational approach was used to further elucidate the photoprotolytic cycle of oxyluciferin and investigate its pH sensitivity. It was found that oxyluciferin forms π–π stacking complexes both in the ground and excited states, at basic and acidic/neutral pH. However, at different pH values, these complexes adopt a different conformation, which explains the lower energy of the emission at acidic/neutral pH, in comparison with the emission at basic pH.

1. Introduction

Firefly bioluminescence is a natural phenomenon, in which light is emitted in an enzyme-catalyzed chemical reaction.[1–5] The enzyme firefly luciferase catalyzes a two-step reaction, by which excited-state oxyluciferin is formed. This molecule is the light emitter of the bioluminescence reaction.[6–8] Oxyluciferin is formed in a singlet excited state due to the formation, and subsequent decomposition, of firefly dioxetanone. Several mechanisms have been proposed to explain the ability of dioxetanones to produce excited states: chemically initiated electron exchange luminescence (CIEEL), charge-transfer-induced luminescence (CTIL), gradually reversible charge-transfer-initiated luminescence (GRCTIL) and interstate crossing-induced chemiexcitation (ICIC).[9–12]

Oxyluciferin, as shown in Figure 1, is thought to exist in one of six chemical species, by means of a quadruple chemical equilibrium involving deprotonation of the hydroxyl groups and keto/enol conversion.[13–16] However, due to the instability of this chromophore in basic solutions, little is known about its spectroscopic and structural properties. Nevertheless, it is thought that under bioluminescence conditions, oxyluciferin exists in its anionic keto form, while in solution it exists as an enol species.[6–8,13–16]

More recently, oxyluciferin was found to be a photoacid.[14] The acidity of these molecules increases after photoexcitation, which enables the study of proton-transfer involving hydrogen bonds in the excited state. Moreover, a typical photoacid is a weak acid in the ground state with a pK_a in the range of 5–10. The steady-state emission of the acidic form of a photoacid should also have two emission bands: one attributed to an acidic form and another to a basic form.

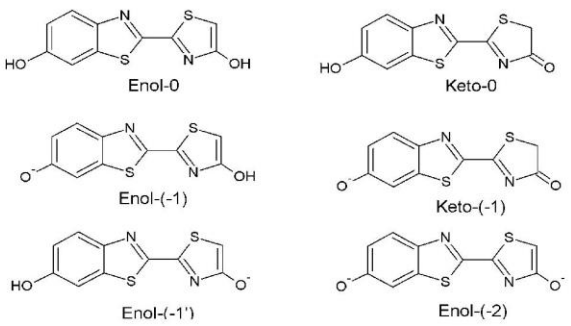

Figure 1. Representation of firefly oxyluciferin in its six different species.

It was found that oxyluciferin presents an absorption band at ~380 nm for acidic/neutral pH, and a band at ~420 nm for basic pH.[14] The first band corresponds to the neutral enol species, while the second band corresponds to its anion. After photoexcitation, the neutral enol species undergoes an excited-state proton transfer (ESPT) with the solvent, thus generating an excited-state anionic enol fluorophore.[14] This process occurs only for acidic/neutral pH and the emission spectrum presents a maximum at ~550 nm.[14] At basic pH, no ESPT occurs as oxyluciferin already lost a proton prior to photoexcitation. Similar to firefly luciferin and dehydroluciferin, oxyluciferin also presents a very effective fluorescence-quenching process.[14,17,18]

Recently, we measured the emission spectra of oxyluciferin in both aqueous acidic (pH~4.5) and basic solutions (pH~9).[14] As already mentioned, at acidic pH, where oxyluciferin is excited at its neutral form, the fluorescence spectrum is composed

[a] Dr. L. Pinto da Silva, Prof. Dr. J. C. G. Esteves da Silva
Centro de Investigação em Química (CIQ-UP)
Departamento de Química e Bioquímica
Faculdade de Ciências da Universidade do Porto
R. Campo Alegre 687 4169-007 Porto (Portugal)
E-mail: jcsilva@fc.up.pt

[b] Dr. R. Simkovitch, Prof. Dr. D. Huppert
Raymond and Beverly Sackler Faculty of Exact Sciences
School of Chemistry, Tel Aviv University
Tel Aviv 69978 (Israel)

Supporting information for this article is available on the WWW under http://dx.doi.org/10.1002/cphc.201300330.

CHEMPHYSCHEM
ARTICLES
www.chemphyschem.org

of two bands: a weak one corresponding to a neutral species and a strong one corresponding to an anionic-species emission. The green band at basic pH has a maximum at ~540 nm, whereas it presents a maximum at ~550 nm upon photoexcitation at acidic pH.[14] Moreover, experimental data indicate that the fluorescence of oxyluciferin in acidic solution consists of a fast decaying component and a slow one. In basic solutions, the amplitude of the short component of the anionic species signal is smaller than 0.05, whereas in acidic solutions, its value is ~0.35.[14] The longtime-component lifetime when excited at different pH is also different.[14] The difference in lifetime indicates that the emission stems from two different species.

Nevertheless, some care must be taken before attributing this pH-sensitive fluorescence to two different oxyluciferin fluorophores. Strong experimental evidence demonstrates that in aqueous solutions, only enol species are present, which discards the presence of keto species.[13–16] Recently, Naumov and co-workers experimentally demonstrated that the green fluorophore at acidic pH is enol-(−1′), which is consistent with our theoretical finding that in the excited state, the enol group is more acidic than the hydroxyl group of enol-form oxyluciferin.[6,16] Given this, in order for two different fluorophores to exist in the photoprotolytic cycle of oxyluciferin, enol-(−1) or enol-(−2) would have to be the emitters at basic pH. However, our earlier work only detected one pK_a (~7), while for enol-(−2), two deprotonations must have been seen.[14] The absence of enol-(−2) is consistent with our theoretical work, since we have found that this molecule is only formed at extreme pH values (~13–14), both in the ground and in the excited states.[6] Enol-(−1) could had been a possible emitter at basic pH, if the hydroxyl group was more acidic in the ground state than the enol group, contrary to what happens in the excited state.[6,16] However, our work has demonstrated that the enol group is more acidic than the hydroxyl group of enol-form oxyluciferin, both in the ground and in the excited states.[6]

Given this, it appears that enol-(−1′) is the sole fluorescence emitter in aqueous solution. Thus, the objective of the present work is to further elucidate this excited-state pH-sensitive fluorescence. To this end we will use a computational approach to study the enolate and neutral enol species in solution. In our opinion, a computational methodology is fundamental for the elucidation of this topic, as it allows us to obtain direct and detailed information (down to the atomic level) of the ground- and excited-state oxyluciferin species, which cannot be provided directly with an experimental approach.

2. Results and Discussion

Naumov and co-workers demonstrated that in the solid state, oxyluciferin exists as head-to-tail hydrogen-bonded enol-dimers.[15] This interaction between neutral enol species in the solid state leads us to question if oxyluciferin molecules still interact with each other in aqueous solution. It should be noted that despite enol-(−1′) being the sole fluorophore, it is formed in the excited state by two different pathways.[14,16] At acidic pH, enol-(−1′) is formed due to ESPT between enol-0 and solvent molecules after photoexcitation of the neutral enol species. At basic pH, enol-(−1′) is already formed in the ground state prior to excitation. Thus, if oxyluciferin molecules are interacting with each other, these different pathways may lead to changes in these interactions. These changes may account for the different pH-dependent fluorescence properties of enol-(−1′), as it was already demonstrated that the excited-state properties of oxyluciferin are sensitive to intermolecular interactions.[19–25]

We calculated the in vacuo ground-state geometries of enol-0 and enol-(−1′) (Tables S1 and S2 of the Supporting Information, SI, at the PBE0/cc-pVDZ level of theory). We then created two complexes, one composed of three enol-0 molecules and another of three enol-(−1′) molecules, in water boxes of 10 Å. These complexes were subjected to molecular-mechanics-based energy minimizations prior to dynamics simulations of 10, 100, 250, 500 and 1000 picoseconds.

Figure 2 shows the final frames of each of the five molecular dynamics simulations involving enol-0. It can be seen that in

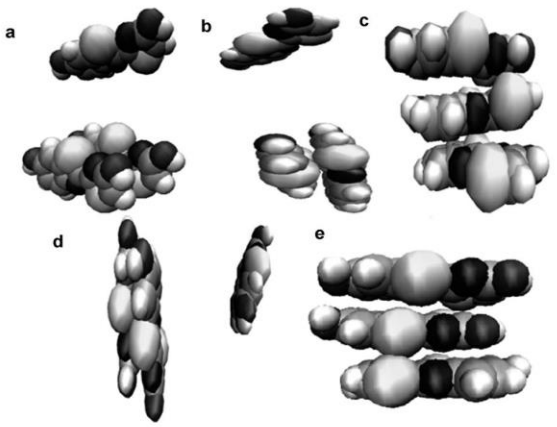

Figure 2. Ground-state enol-0 complexes at the final frame of molecular dynamic simulations of: 10 (a), 100 (b), 250 (c), 500 (d) and 1000 (e) picoseconds.

all frames, at least two oxyluciferin molecules are stacked one against the other (in the simulations of 250 and 1000 picoseconds, all three molecules are stacked one against the other). Given the structure of enol-0 (Figure 1) and this type of conformation, we suggest that at acidic pH (a condition at which enol-0 is predominant), the oxyluciferin molecules interact with each other by means of π–π stacking interactions.

Figure 3 presents the final frames of each of the five molecular dynamics simulations involving enol-(−1′). Similarly to enol-0, in every frame, two of the three oxyluciferin species form a molecular complex. Moreover, the third oxyluciferin molecule is close to the other two, in every frame, except for the final frame corresponding to the 1000 picoseconds molecular dynamics simulation (Figure 3d). These results were not expected by us, as due to the negative charge of enol-(−1′), we thought that these oxyluciferin complexes would not form due to elec-

CHEMPHYSCHEM
ARTICLES
www.chemphyschem.org

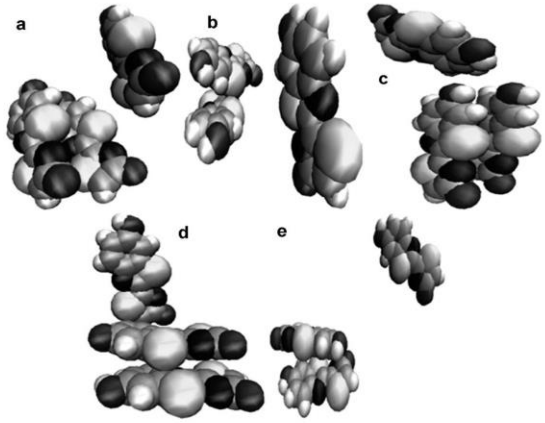

Figure 3. Ground-state enol-(−1′) complexes at the final frame of molecular dynamic simulations of: 10 (a), 100 (b), 250 (c), 500 (d) and 1000 (e) picoseconds.

Table 1. in vacuo ESP atomic charges of ground-state enol-0 and enol-(−1′) at the CAM-B3LYP/aug-cc-pVDZ level of theory.

	Enol-0	Enol-(−1′)
Benzothiazole moiety	−0.009	−0.208
Thiazole moiety	0.010	−0.793
Total	0.001	−1.001

trostatic repulsions. In Table 1 we can see the atomic ESP charges of enol-0 and enol-(−1′). We can see that a large part of the negative charge of enol-(−1′) resides in its thiazole moiety. Therefore, there should be at least a strong repulsion between the thiazole moieties of enol-(−1′) molecules. However, as can be seen in Figure 3, this moiety of the enol-(−1′) molecules that form the oxyluciferin complex are generally close to each other.

Thus, there must be some factor that decreases the importance of the electrostatic repulsions between the ground-state enol-(−1′) molecules. In the simulation regarding enol-(−1′), three Na^+ cations were added to the water box to neutralize the oxyluciferin–water complex. This was done because, experimentally, this complex corresponds to an aqueous solution at basic pH, to which sodium hydroxide was added to increase the pH of the solution.[14] It is possible that the presence of three cations interacting with the three enol-(−1′) anions decreases the electrostatic repulsion that exists between the oxyluciferin molecules.

To see the stability of these oxyluciferin complexes, we performed single-point *w*B97XD/cc-pVDZ in implicit water on structures containing the three oxyluciferin molecules, and on each one of the oxyluciferin molecules. This was made both for enol-0 and enol-(−1′). The energy of association was calculated as $\Delta E_{ass1} = E_{oxyluciferins} - (E_{oxyluciferin1} + E_{oxyluciferin2} + E_{oxyluciferin3})$ or $\Delta E_{ass2} = E_{oxyluciferins,Na\ ions} - (E_{oxyluciferin1} + E_{oxyluciferin2} + E_{oxyluciferin3} + E_{Na\ ions})$, in the case of enol-(−1′). This was made for the frames resulting from the molecular dynamics simulation of 100, 500 and 1000 picoseconds. The *w*B97XD density functional was used because it has an empirical dispersion correction term, contrary to CAM-B3LYP, and so can accurately predict π–π stacking interactions.[26] The cc-pVDZ basis set was used instead of aug-cc-pVDZ, which was used in the parameterization of oxyluciferin, due to the high number of atoms involved in the calculations. The results are present in Table 2.

Table 2. Energy of association of the three oxyluciferin molecules present in each simulation (ΔE_{ass1} and ΔE_{ass2}, in kcal mol^{-1}), calculated at the *w*B97XD/cc-pVDZ level of theory in implicit water.

	Enol-0 ΔE_{ass1}	Enol-(−1′) ΔE_{ass1}	ΔE_{ass2}
100 picoseconds	−12.7	−4.3	−29.1
500 picoseconds	−13.0	−68.3	−70.9
1000 picoseconds	−23.6	−8.5	−10.1

In Table 2, we can see that the enol-0 complexes are stable, especially when the three oxyluciferin molecules are stacked one against the other. These results are expected due to π–π stacking interactions between the oxyluciferins, and the neutrality of the system which indicates that no electrostatic repulsion should affect the interaction between the enol-0 molecules.

Contrary to what was expected were the results regarding enol-(−1′). Even considering that the three oxyluciferin molecules were all anions, and so should repulse each other, the values of both ΔE_{ass1} and ΔE_{ass2} were significantly negative (Table 2). Moreover, contrary to our hypothesis, above referred, these complexes can be very stable even when we do not consider the electrostatic interaction between oxyluciferins and Na^+ cations (Table 2, 1000 and 500 picoseconds). Therefore, it appears that π–π stacking interactions between enol-(−1′) molecules must be strong enough to compensate the electrostatic repulsive interaction between equal molecules. We can see that at 500 picoseconds, the ΔE_{ass1} is even more negative for enol-(−1′) than for enol-0. The interaction energy of aromatic complexes contains mainly four components: electrostatic, induction, dispersion and exchange repulsion.[27,28] As Enol-(−1′) molecules are anions, they can provide more electrons to be involved in dispersion interactions, which may explain the favourable interactions between these oxyluciferin molecules.[29] The significant effect of Na^+ on ΔE_{ass2} for enol-(−1′) at 100 picoseconds (Table 2), can be explained by the fact that the π–π stacking complex is still completely formed as can be seen in Figure 3b. This explanation is supported by the low ΔE_{ass1} (Table 2) of enol-(−1′) at 100 picoseconds.

Given these results, it appears that the most stable conformation for the three enol-0 molecules is a π–π stacking complex involving the three oxyluciferin molecules. For enol-(−1), it appears that the most stable conformation is when two oxyluciferin molecules are stacked one against the other, due to π–π stacking interactions, and one oxyluciferin molecule is nearby. This indicates that enol-(−1′) is formed from two starting conformations, at basic and acidic/neutral pH.[6,13–16] In the

CHEMPHYSCHEM
ARTICLES
www.chemphyschem.org

latter pH range, excited-state enol-(−1′) is formed after photoexcitation of the enol-0 present in the π–π stacking complex and ESPT-based deprotonation. At basic pH, excited-state enol-(−1′) is formed after photoexcitation of ground-state enol-(−1′) (present in a different π–π stacking complex than enol-0). Thus, this indicates that emitting enol-(−1′) may be formed in different conformations, depending on the pH, which may explain the pH-sensitive fluorescence in aqueous solutions without considering two different emitters.[6,13–16]

To verify this hypothesis, we have tried to obtain the conformations of excited-state enol-(−1′) in water at basic and acidic/neutral pH. To this end, we have used the most stable geometries of the three oxyluciferin molecules (Table 2, enol-0 and enol-(−1′)), as the initial structures for more simulations. The simulations were composed of 10000-steps energy minimizations and molecular dynamics of 500 picoseconds. The parameterized atomic charges were those of excited-state enol-(−1′) at the Franck–Condon state. Moreover, the hydrogen atoms of the enolic group of the three enol-0 molecules were withdrawn to simulate the formation of enol-(−1′) at acidic pH.

The most stable conformation of enol-0 was the final frame of the 1000 picoseconds molecular dynamics simulation. Therefore, it was the conformation used in the simulations regarding enol-(−1′) at acidic/neutral pH. The resulting conformation is presented in Figure 4a. The three oxyluciferin molecules still remained in a sort of π–π stacking complex after the simulations, despite the negative charge of each molecule. This complex presented an excitation energy of 2.35 eV, at the *w*B97XD/cc-pVDZ level of theory (Table 3). This value is consistent with the energy of a shoulder (2.36 eV) present in the absorption spectra of oxyluciferin in water.[15]

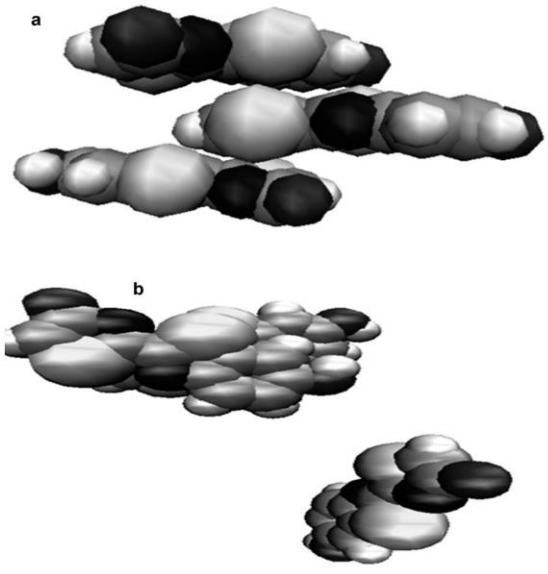

Figure 4. Excited-state conformation of enol-(−1′) complexes at acidic/neutral (a) and basic pH, after molecular dynamic simulations of 500 picoseconds.

Table 3. Excitation energies (E_{ex}, in eV) and wavelengths (λ_{ex}, in nm) of excited-state enol-(−1′) complexes at the Franck–Condon level at basic and acidic/neutral pH.

	E_{ex}	λ_{ex}
Acidic/neutral pH	2.35	528
Basic pH with Na^+ ions	2.60	476
Basic pH without Na^+ ions	2.60	476

The most stable conformation of enol-(−1′) was the final frame of the 500 picoseconds molecular dynamics simulation. The resulting conformation (excited-state enol-(1′) at basic pH) is presented in Figure 4b. In this case, only two of the enol-(1′) molecules are involved in a sort of π–π stacking complex. The three oxyluciferin molecules present an excitation energy of 2.60 eV, in the absence and presence of Na^+ cations (Table 3). Thus, this devalues the contribution of the cations to the excited-state properties of enol-(−1′). This computed value differs 0.35 eV from the experimental value of ~2.95 eV.[13] We do not think that this is a ssignificant difference given the approximations usually employed in this type of calculations.[30–32] Moreover, the experimental value of ~2.95 eV was obtained from a water (68%)/methanol (32%) mixture, while our calculations were made only on implicit water.[13]

The results obtained so far allow us to explain the pH-sensitive fluorescence of oxyluciferin by considering only a fluorescence emitter species.[14] Excited-state enol-(−1′) molecules present different conformations at acidic/neutral and basic pH (Figure 4). Also, these oxyluciferin molecules present similar excitation energies (2.35 versus 2.60 eV, at the *w*B97XD/cc-pVDZ level of theory), but different enough to look as if there are two different oxyluciferin species emitting in different pH ranges. These data model qualitatively what is seen experimentally.[14] These pH-sensitive excited-state conformations are due to differences in the π–π stacking complex formed between the ground state of oxyluciferin molecules in aqueous solution.

3. Conclusions

Experimental studies have demonstrated that firefly oxyluciferin presents different fluorescence maxima at acidic/neutral and basic pH. This indicates that two or more emitters may be responsible for the pH-sensitive fluorescence of oxyluciferin.

However, both theoretical and experimental data present in the literature indicate that the fluorescence emitted by oxyluciferin in water is due to its enolate species, irrespective of the pH. At acidic/neutral pH, neutral enol species are photoexcited and undergoe an ESPT process with water, leading to the formation of excited-state enolate anions. At basic pH, the enolate anion is formed in the ground state prior to photoexcitation, when (in the excited state) this molecule decays to the ground state with emission of light. However, no explanation is provided for the different emission maxima present in different pH ranges.

CHEMPHYSCHEM
ARTICLES
www.chemphyschem.org

We have employed a theoretical approach to study the photodynamics of the photoprotolytic cycle of oxyluciferin. We have found that both enol-0 and enol-(−1′) form ground-state π–π stacking complexes, both at acidic/neutral and basic pH. Nevertheless, due to the different charges of the oxyluciferin molecules, these complexes adopt different conformations, which results in different conformations of the excited-state π–π stacking complex of enol-(−1′) at acidic/neutral and basic pH. The different conformations lead to a more red-shifted band at acidic/neutral pH than at basic pH, when considering only one fluorescence emitter, namely, enol-(−1′).

Computational Section

The ground-state geometries of the species considered in this study were obtained with the PBE0 and the cc-pVDZ basis sets.[33] No solvent effects were considered in the geometry optimizations. The PBE0 density functional was used due to its good results in the calculations of geometries of organic molecules.[30,32,34]

To obtain complexes between oxyluciferin and an explicit solvent, a molecular mechanics methodology was used. TIP3P water molecules were added up to 10 Å by the LEAP module of the AMBER suite of programs.[35] We used this water-box size because we already successfully used water boxes up to 12 Å in previous theoretical studies of the interaction of firefly oxyluciferin with firefly luciferase.[19–21] Since luciferase–oxyluciferin complexes have many more atoms than the complexes presented here, we thought that we could reduce the size of the box without any decrease in the accuracy of the calculations. Three Na^+ cations were added to the complexes, corresponding to basic pH, to neutralize the charge of the complex. One phase of energy minimizations (10 000 steps) was performed by using the "not (just) another molecular dynamics" (program) NAMD molecular dynamic code with AMBER potential functions, parameters and file formats.[36] In this process, the particle mesh Ewalds method was used to include the long-range interactions.[37] All the minimizations steps were performed in an NVT ensemble, with a temperature of 298.15 K. Molecular dynamics simulations were performed with NAMD, on the energy-minimized systems. The integration step size was 2 femtoseconds, and all bonds involving water molecules were constrained.

The ground-state geometries of the studied molecules were used in their parameterization with the ANTECHAMBER module of AMBER and the general AMBER force field.[38] The charges of the ground-state molecules were derived by using the restrained electrostatic potential (RESP) method, at the CAM-B3LYP/aug-cc-pVDZ level of theory.[39] The CAM-B3LYP density functional was used due to its good results on organic molecules and for providing good estimates for charge-transfer states.[40,41] The excited-state charges of enol-(−1′) were derived by the RESP method by performing a single-point time-dependent *w*B97XD/aug-cc-pVDZ on the PBE0/cc-pVDZ-derived ground-state geometry.[42,43] This functional was used because at that point, π–π stacking interactions were proven to play a role in this fluorescence system. π–π stacking interactions can be modeled well by the *w*B97XD functional because it has an empirical dispersion correction term, contrary to the CAM-B3LYP method.[26]

Ground-state and excitation energies were calculated at the *w*B97XD/cc-pVDZ level of theory. The conductor-like polarized continuum model (CPCM) was used to simulate implicit water.[44] This functional was used as it can described well dispersion interactions and charge-transfer states.[26,41,43]

The excited-state properties of enol-(−1′) (charges and excitation energies) were computed at the Franck–Condon state, as the absorption spectrum often reflects the main features of light emission. In the case of firefly oxyluciferin, this approach was validated by four computational works.[21,45–47]

All calculations involving density functionals were performed with the Gaussian 09 program package.[48]

Acknowledgements

Financial support from the Fundação para a Ciência e Tecnologia (FCT, Lisbon) (Programa Operacional Temático Factores de Competitividade) (COMPETE) e comparticipado pelo Fundo Comunitário Europeu (FEDER) (Project PTDC/QUI/71366/2006) is acknowledged. A Ph.D. Grant to Luís Pinto da Silva (SFRH/76612/2011), attributed by FCT, is also acknowledged. This work was also supported by grants from the Israel Science Foundation and from the James-Franck German–Israeli Program in Laser-Matter Interaction.

Keywords: complexes · enolate species · firefly oxyluciferin · photoprotolytic cycle · pH-sensitive fluorescence

[1] S. M. Marques, J. C. G. Esteves da Silva, *IUBMB Life* **2009**, *61*, 6–17.
[2] L. Pinto da Silva, J. C. G. Esteves da Silva, *ChemPhysChem* **2012**, *13*, 2257–2262.
[3] I. Navizet, Y. J. Liu, N. Ferré, D. Roca-Sanjuán, R. Lindh, *ChemPhysChem* **2011**, *12*, 3064–3076.
[4] J. Vieira, L. Pinto da Silva, J. C. G. Esteves da Silva, *J. Photochem. Photobiol. B* **2012**, *117*, 33–39.
[5] L. Pinto da Silva, J. C. G. Esteves da Silva, *J. Chem. Theory Comput.* **2011**, *7*, 809–817.
[6] L. Pinto da Silva, J. C. G. Esteves da Silva, *ChemPhysChem* **2011**, *12*, 951–960.
[7] S. F. Chen, Y. J. Liu, I. Navizet, N. Ferré, W. H. Fang, R. Lindh, *J. Chem. Theory Comput.* **2011**, *7*, 798–803.
[8] C. I. Song, Y. M. Rhee, *J. Am. Chem. Soc.* **2011**, *133*, 12040–12049.
[9] J. A. Koo, S. P. Schmidt, G. B. Schuster, *Proc. Natl. Acad. Sci. USA* **1978**, *75*, 30–33.
[10] H. Isobe, Y. Takano, M. Okumura, S. Kuramistu, K. Yamaguchi, *J. Am. Chem. Soc.* **2005**, *127*, 8667–8679.
[11] L. Yue, Y. J. Liu, W. H. Fang, *J. Am. Chem. Soc.* **2012**, *134*, 11632–11639.
[12] L. Pinto da Silva, J. C. G. Esteves da Silva, *ChemPhysChem* **2013**, *14*, 1071–1079.
[13] J. C. G. Esteves da Silva, J. M. C. S. Magalhães, R. Fontes, *Tetrahedron Lett.* **2001**, *42*, 8173–8176.
[14] Y. Erez, I. Presiado, R. Gepshtein, L. Pinto da Silva, J. C. G. Esteves da Silva, D. Huppert, *J. Phys. Chem. A* **2012**, *116*, 7452–7461.
[15] P. Naumov, Y. Ozawa, K. Ohkubo, S. Kukuzumi, *J. Am. Chem. Soc.* **2009**, *131*, 11590–11605.

[16] K. M. Solntsev, S. P. Laptenok, P. Naumov, *J. Am. Chem. Soc.* **2012**, *134*, 16452 – 16455.
[17] Y. Erez, D. Huppert, *J. Phys. Chem. A* **2010**, *114*, 8075 – 8082.
[18] I. Presiado, Y. Erez, R. Simkovitch, S. Shomer, R. Gepshtein, L. Pinto da Silva, J. C. G. Esteves da Silva, D. Huppert, *J. Phys. Chem. A* **2012**, *116*, 10770 – 10779.
[19] L. Pinto da Silva, J. C. G. Esteves da Silva, *J. Phys. Chem. B* **2012**, *116*, 2008 – 2013.
[20] L. Pinto da Silva, J. C. G. Esteves da Silva, *ChemPhysChem* **2011**, *12*, 3002 – 3008.
[21] L. Pinto da Silva, J. C. G. Esteves da Silva, *J. Comput. Chem.* **2011**, *32*, 2654 – 2663.
[22] C. G. Min, A. M. Ren, J. F. Guo, Z. W. Li, L. Y. Zou, J. D. Goddard, J. K. Feng, *ChemPhysChem* **2010**, *11*, 251 – 259.
[23] C. G. Min, A. M. Ren, J. F. Guo, L. Y. Zou, J. D. Goddard, C. C. Sun, *ChemPhysChem* **2010**, *11*, 2199 – 2204.
[24] N. Nakatani, J. Y. Hasegawa, H. Nakatsuji, *J. Am. Chem. Soc.* **2007**, *129*, 8756 – 8765.
[25] A. Tagami, N. Ishibashi, D. Kato, N. Taguchi, Y. Mochizuki, H. Watanabe, M. Ito, S. Tanaka, *Chem. Phys. Lett.* **2009**, *472*, 118 – 123.
[26] L. M. da Costa, S. R. Stoyanov, S. Gusarov, X. Tan, M. R. Gray, J. M. Stryker, R. Tykwinski, J. W. M. Carneiro, P. R. Seidl, A. Kovalenko, *Energy Fuels* **2012**, *26*, 2727 – 2735.
[27] R. Podeszwa, R. Bukowski, K. Szalewicz, *J. Phys. Chem. A* **2006**, *110*, 10345 – 10354.
[28] M. O. Sinnokrot, C. D. Sherrill, *J. Am. Chem. Soc.* **2004**, *126*, 7690 – 7697.
[29] Z. Huang, H. Sun, H. Z. Y. Wang, F. Li, *J. Comput. Chem.* **2011**, *32*, 2055 – 2063.
[30] L. Pinto da Silva, J. C. G. Esteves da Silva, *Int. J. Quantum Chem.* **2013**, *113*, 45 – 51.
[31] M. R. Silva-Junior, M. Schreiber, S. P. Sauer, W. Thiel, *J. Chem. Phys.* **2008**, *129*, 104103 – 104114.
[32] D. Jacquemin, E. A. Perpète, I. Ciofini, C. Adamo, *Theor. Chem. Acc.* **2011**, *128*, 127 – 136.
[33] C. Adamo, V. Barone, *J. Chem. Phys.* **1999**, *110*, 6158 – 6169.
[34] D. Jacquemin, V. Wathelet, E. A. Perpète, C. Adamo, *J. Chem. Theory Comput.* **2009**, *5*, 2420 – 2435.
[35] D. A. Case, T. E. Cheatham, T. Darden, H. Gohlke, R. Luo, K. M. Merz, A. Onufriev, C. Simmelring, B. Wang, R. Wodds, *J. Comput. Chem.* **2005**, *26*, 1668 – 1688.
[36] J. C. Phillips, R. Braun, W. Wang, J. Gumbart, W. Tajkhorshid, E. Villa, C. Chipot, R. D. Skell, L. Kale, K. Schulten, *J. Comput. Chem.* **2005**, *26*, 1781 – 1802.
[37] U. Essmann, L. Perera, M. L. Berkowitz, T. Darden, H. Lee, L. G. Pedersen, *J. Chem. Phys.* **1995**, *103*, 8577 – 8593.
[38] J. M. Wang, R. M. Wolf, J. W. Caldwell, P. A. Kollman, D. A. Case, *J. Comput. Chem.* **2004**, *25*, 1157 – 1174.
[39] C. I. Bayly, P. Cieplak, W. D. Cornell, P. A. Kollman, *J. Phys. Chem.* **1993**, *97*, 10269 – 10280.
[40] T. Yanai, D. Tew, N. Handy, *Chem. Phys. Lett.* **2004**, *393*, 51 – 57.
[41] C. Adamo, D. Jacquemin, *Chem. Soc. Rev.* **2013**, *42*, 845 – 856.
[42] G. Scalmani, M. J. Frisch, B. Mennucci, J. Tomasi, R. Cammi, V. Barone, *J. Chem. Phys.* **2006**, *124*, 1 – 15.
[43] J.-D. Chain, M. Head-Gordon, *Phys. Chem. Chem. Phys.* **2008**, *10*, 6615 – 6620.
[44] M. Cossi, N. Rega, G. Scalmani, V. Barone, *J. Comput. Chem.* **2003**, *24*, 669 – 681.
[45] D. Cai, M. A. Marques, F. Nogueira, *J. Phys. Chem. B* **2011**, *115*, 329 – 332.
[46] B. F. Milne, M. A. Marques, F. Nogueira, *Phys. Chem. Chem. Phys.* **2010**, *12*, 14285 – 14293.
[47] D. Cai, M. A. L. Marques, B. F. Milne, F. Nogueira, *J. Phys. Chem. Lett.* **2010**, *1*, 2781 – 2787.
[48] Gaussian 09 (Revisian A.02), M. J. Frisch et al., Gaussian, Inc., Wallingford CT, **2009**.

Received: April 3, 2013
Revised: May 8, 2013
Published online on June 13, 2013

Article 25

Theoretical study of the effect of resonance on π-π stacked firefly oxyluciferin dimers
Luís Pinto da Silva, Margarida S. Miranda and Joaquim C.G. Esteves da Silva
J. Photochem. Photobiol. A: Chemistry **2014**, *278*, 9-13.

The theoretical calculations and the writing of the paper were performed by Luís Pinto da Silva, except the sections regarding the calculation of Nucleus Independent Chemical Shifts (NICS) values (which was performed by Margarida Miranda), under the supervision of Professor Joaquim Esteves da Silva.

Journal of Photochemistry and Photobiology A: Chemistry 278 (2014) 9–13

Contents lists available at ScienceDirect

Journal of Photochemistry and Photobiology A: Chemistry

journal homepage: www.elsevier.com/locate/jphotochem

Theoretical study of the effect of resonance on π–π stacked firefly oxyluciferin dimers

Luís Pinto da Silva[a], Margarida S. Miranda[b], Joaquim C.G. Esteves da Silva[a,*]

[a] Centro de Investigação em Química, Departamento de Química e Bioquímica, Faculdade de Ciências, Universidade do Porto, R. Campo Alegre 687, 4169-007 Porto, Portugal
[b] Centro de Geologia da Universidade do Porto, Faculdade de Ciências, Universidade do Porto, R. Campo Alegre, P-4169-007 Porto, Portugal

ARTICLE INFO

Article history:
Received 25 October 2013
Received in revised form
10 December 2013
Accepted 19 December 2013
Available online 2 January 2014

Keywords:
Oxyluciferin
Dimers
Resonance
π–π stacking
Aromaticity

ABSTRACT

Firefly oxyluciferin is a prime example in which π–π stacking interactions play an important role, by being the basis for the formation of sandwich-like oxyluciferin complexes. In the present study, we have used a theoretical methodology to further understand the effect of π–π stacking interactions in the properties of oxyluciferin molecule. More specifically, we have analysed the effect of resonance changes in oxyluciferin π–π stacking dimers. We have found that resonance changes have little effect on the ground state properties of the dimmers. More interestingly, by modulating the resonance of the dimmers we can obtain different transition energies and efficiencies. This results in changes in the degree of contributions made by the different orbital excitations that compose the excitation transition.

1. Introduction

Aromatic groups are easily found in nature, in a great variety of chemical systems: DNA, proteins, various types of drugs, supramolecular complexes, and so on [1–4]. Thus, the noncovalent interactions between those aromatic groups are expected to have a significant role on the organization and functions of the chemical systems referred above. These interactions are collectively termed π–π stacking, and have received considerable attention in recent years [5,6].

Studies of π–π stacking have indicated that the interplay between the interacting aromatic groups results in the establishment of dispersive van der Waals and electrostatic interactions [7].

π–π stacking aromatic complexes are generally found in one of the three possible types of structure: T-shaped, parallel-displaced and sandwich [7,8]. Rather recently, it was found that firefly oxyluciferin (Fig. 1) molecule forms sandwich-like π–π stacking complexes, in aqueous solutions [9]. The structure of the oxyluciferin complexes is pH-sensitive, by adopting different conformations at acidic/neutral and basic pH. More importantly, the different π–π stacking interactions at the oxyluciferin complexes are responsible for the pH-dependent fluorescence of this molecule [9–11].

In chemistry, resonance is a way of describing delocalized electrons within some molecules, which cannot be described by one single Lewis structure [12]. Such molecules are represented by several contributing structures, which are called resonance structures. Resonance among these structures signifies that the wavefunction is represented by the "mixing" of the contributing structures [12]. Resonance is also used to refer to an electron delocalization process. Noncovalent interactions between molecules may distort their electron cloud, thereby increasing or decreasing the electron delocalization of the compounds involved. Thus, these types of interactions may affect the resonance of a given molecule. We think that it is not a stretch to say that a molecule can present non-equal contributing structures in different solvents, due to the interaction of the molecule with different solvent molecules.

Aromaticity is a manifestation of resonance [13,14]. This phenomenon describes the way in which a conjugated ring of lone pairs, empty orbitals or unsaturated bonds shows a stronger stabilization than expected, which is associated with a resonance delocalized structure. Thus, we can say that the changes in resonance (as provoked by different intermolecular interactions) can affect the aromaticity of a molecule, and consequently the π–π stacking interactions that it can establish with other aromatic molecules. The aromatic character of a molecular system can be evaluated on the basis of the analysis of their magnetic properties,

* Corresponding author. Fax: +351 220 402 659.
E-mail address: jcsilva@fc.up.pt (J. C.G. Esteves da Silva).

1010-6030/$ – see front matter © 2013 Elsevier B.V. All rights reserved.
http://dx.doi.org/10.1016/j.jphotochem.2013.12.018

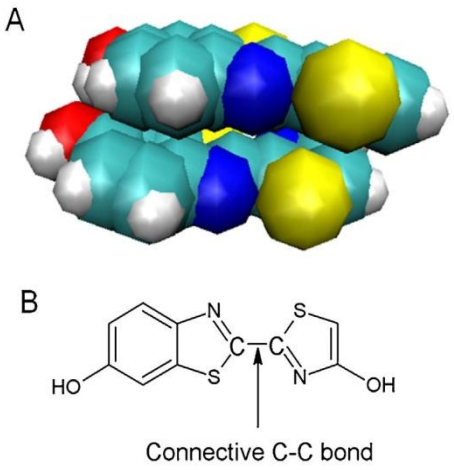

Fig. 1. (A) Representation of a firefly oxyluciferin sandwich-like dimer. (B) Schematic representation of a firefly oxyluciferin molecule, highlighting the connective C—C bond.

namely the observable effects of the circular ring current induced by applied external magnetic fields. For aromatic systems, these currents produce an induced magnetic field opposing the external one, a phenomenon which can be experimentally probed by the nuclear magnetic resonance (NMR) chemical shifts measured at each nucleus. This concept has been generalized and converted into a useful aromaticity index. This methodology involves the calculation of the chemical shifts not just at every nucleus but at any point in the space in the vicinity of molecules, leading to what is now described as Nucleus Independent Chemical Shifts (NICS). These are just the negative of the isotropic component of the chemical shielding tensor evaluated at the specific points. NICS is further described in Section 2 and in the first paragraph of Section 3.1.

Given the importance of intermolecular interactions (including π–π stacking ones) in the fluorescence of firefly oxyluciferin, the objective of the present study is to analyse the effects that changes in resonance of oxyluciferin can have in the oxyluciferin π–π stacking sandwich-like complexes. To this end, four firefly oxyluciferin dimers, in a π–π stacking sandwich-like conformation, were created. The oxyluciferin species used in this study was the neutral enolic one, as it was already demonstrated that this is the species involved in the sandwich-like π–π stacking complexes [9]. The length of connective benzothiazole-thiazole carbon is different in all dimers (Fig. 1), in order to affect the electron delocalization between the moieties, and consequently the resonance structures of oxyluciferin.

All calculations were made *in vacuo*, as our focus in this study was to see the effect of controlled changes in the resonance on the properties of π–π stacking dimers. Addition of explicit/implicit solvation models to the calculations would only result in perturbations on our system, which would be very difficult to disentangle, and so would impair our analyses of the sole effect of resonance changes on the dimmers.

2. Methods

Calculations were carried out using the Gaussian 09 program package [15]. The ground state geometries of the sole and dimmerized oxyluciferin molecules were determined at the *w*B97XD/6-311G(d,p) level of theory [16]. Subsequent vibrational frequency calculations, at the same level of theory, were made in order to ensure that the obtained geometries were indeed minimal in their potential energy surface. No structure presented an imaginary frequency, except the oxyluciferin dimer with a C—C bond length of 1.35 Å. However, this frequency was disregarded as it was residual (frequency of $-26.7\,cm^{-1}$ with an infrared intensity of 0.4695).

Table 1
Isotropic (σ_{iso}) and out-of-plane (σ_{ZZ}) components of the chemical shielding tensor measured at the centre (0) and 1.0 Å above the centre (+1) of the phenol ring (all values in ppm).

Bond length (Å)	NICS(0)		NICS(+1)	
	σ_{iso}	σ_{ZZ}	σ_{iso}	σ_{ZZ}
1.35	−10.03	−11.54	−10.55	−25.43
1.40	−10.14	−11.55	−10.63	−25.68
1.46	−10.25	−11.55	−10.71	−25.91
1.50	−10.32	−11.56	−10.76	−26.06

The properties of the electronically singlet excited states were calculated with time-dependent *w*B97XD/6-311G(d,p) single point calculations on the ground state geometries, within the vertical approximation. The *w*B97XD was used due to good performance for valence, Rydberg and charge transfer excited states [17]. Moreover, this functional has an empirical dispersion correction term, which allows it to correctly model π–π stacking interactions.

The aromatic character of the oxyluciferin rings was analysed in terms of the NICS parameters [26]. Traditionally the NICS values are calculated at the geometric centre of the rings and also, on order to account for the fact that the (aromatic) ring planes are nodal planes of the π-electron system, at a point 1.0 Å above it [18,19,26]. Another important component of the chemical shielding tensor to analyse is the out-of-plane component (conventionally along the Z direction, thus designated by σ_{ZZ}) which has been argued to better reflect the effects of the π-electron density, thus being presumably a better aromaticity index [20]. These calculations have being performed using the Gauge-Independent Atomic Orbital (GIAO) method implemented in the Gaussian 09 code, with the CAM-B3LYP/6-311G(d,p) wavefunctions at the *w*B97XD/6-311G(d,p) optimized geometries [21–26].

3. Results and discussion

3.1. Study of sole firefly oxyluciferin molecules

First, we have investigated the aromatic character of the rings composing sole firefly oxyluciferin (phenolic, thiazole, enolic-thiazole rings) with different C—C bond lengths. Changes in the aromaticity of the rings, due to the lengths of the C—C bond, will show that we have succeeded in changing the resonance of sole oxyluciferin molecules, as aromaticity is a manifestation of resonance.

Such properties can be adequately analysed in terms of the so called Nucleus Independent Chemical Shifts (NICS) parameters, as initially proposed by Schleyer and co-workers, involving the calculation of the isotropic component of the chemical shielding tensor at arbitrary points in the space within a molecule [26]. The NICS values are conventionally reported as the negative of the relevant tensor components, negative values indicating aromatic character. We thus choose to calculate both the isotropic and the out-of-plane components of the chemical shielding tensor, denoted respectively as σ_{iso} and σ_{ZZ}, evaluated at the ring centres and 1.0 Å above as a convenient way of characterizing aromaticity. The results are collected in Tables 1–3.

It could be anticipated that the thiazole rings should have some aromatic character due to the fact that these rings do indeed obey Huckel $(4n+2)$ rule. In fact, a simple electron count reveals that the thiazole rings have six π electrons, thus being π isoelectronic to the aromatic phenol. From the results in Tables 1–3 we can observe that

Table 2
Isotropic (σ_{iso}) and out-of-plane (σ_{ZZ}) components of the chemical shielding tensor measured at the centre (0) and 1.0 Å above the centre (+1) of the thiazole ring (all values in ppm).

Bond length (Å)	NICS(0)		NICS(+1)	
	σ_{iso}	σ_{ZZ}	σ_{iso}	σ_{ZZ}
1.35	−8.52	−22.73	−8.46	−17.19
1.40	−8.65	−22.74	−8.57	−17.54
1.46	−8.78	−22.76	−8.65	−17.84
1.50	−8.87	−22.78	−8.70	−18.01

Table 3
Isotropic (σ_{iso}) and out-of-plane (σ_{ZZ}) components of the chemical shielding tensor measured at the centre (0) and 1.0 Å above the centre (+1) of the enolic-thiazole ring (all values in ppm).

Bond length (Å)	NICS(0)		NICS(+1)	
	σ_{iso}	σ_{ZZ}	σ_{iso}	σ_{ZZ}
1.35	−11.16	−24.12	−9.17	−20.30
1.40	−11.35	−24.12	−9.32	−20.78
1.46	−11.53	−24.14	−9.45	−21.20
1.50	−11.66	−24.18	−9.53	−21.45

the phenol and the two five membered (thiazole) rings have negative NICS values which confirm the aromatic character of the rings. However, the first thiazole ring presents lower aromaticity than the second due to the fact that the first is benzoannelated and thus two π electrons are shared with the phenol ring decreasing the π electron density in the thiazole ring. Either components σ_{iso} and σ_{ZZ} measured at the centre and above the centre of the rings show an increase in the aromatic character with increasing C—C bond length (from 1.35 to 1.50 Å). Thus, in our opinion, these data indicates that we have successfully affected the resonance of oxyluciferin by modulating the connective C—C bond length.

We have also calculated the ESP atomic charges of the oxyluciferin molecules, with the four different C—C bond lengths. The data is collected in Table 4. With a C—C bond length of 1.35 Å, oxyluciferin presents a low dipole moment of 2.48 Debye. The negative charge is localized in the benzothiazole moiety, while the positive charge is localized in the enolic-thiazole one. At a C—C bond length of 1.40 Å, the dipole moment is slightly lower (2.47 Debye). This occurs due to a decrease of both negative and positive charges localized in both moieties. The trend of lower dipole moments and positive/negative charges localized on the two moieties is also seen (even more easily) in the oxyluciferin molecules with C—C bond lengths of 1.46 and 1.50 Å. Thus, the localization of charge is also affected by modulating the length of the connective C—C bond.

3.2. Study of firefly oxyluciferin dimers

We have calculated the relative energies of the four dimers, with the dimer with connective C—C bond lengths of 1.35 Å as reference. The dimer with a C—C bond length of 1.46 Å is the most stable (with a relative energy of −10.4 kcal/mol), while the dimer with the bond length of 1.50 Å is second most stable (relative energy of −9.0 kcal/mol). The dimer with bond length of 1.40 Å is the third most stable (relative energy of −7.8 kcal/mol), while the dimer with the shorter C—C bond length is the least stable complex.

We have also calculated the stabilization energy obtained by dimer formation, by using the following equation (being oxy the reference to the sole oxyluciferin molecules that constitute the dimers):

$$\Delta E_{stab} = E_{Dimer} - (E_{oxy1} + E_{oxy2})$$

The resulting ΔE_{stab} are presented in Table 5. We can see that the formation of dimers is indeed favourable for all bond lengths, with a nearly constant ΔE_{stab} of ∼−24 kcal/mol. This shows that oxyluciferin molecules are significantly stabilized by π–π stacking interaction formed with one another [9]. Moreover, we see that changes in the resonance of the dimers, has little to no effect in the stabilization energy obtained by dimer formation.

We have calculated the dipole–dipole interaction energies classically, by using the calculated dipolar moment of bare oxyluciferin and the distance between the two molecules that form the dimers. The obtained energies were -7.04×10^{-20}, -6.99×10^{-20}, -6.87×10^{-20} and -6.82×10^{-20} J, which correspond to dimers with C—C bond length of 1.35, 1.40, 1.46 and 1.50 Å respectively. This is in line with the trend that associates the dipolar moments with the C—C bond length: the higher the C—C bond length, the lower is the dipolar moment of oxyluciferin (Tables 4 and 6). The discovery that the dipole–dipole interaction energy decreases with increasing C—C bond length, as the computed ΔE_{stab}, indicates that the decrease in the dipolar moment may have a role in the slight destabilization of the dimers with increasing C—C bond length. We have calculated the dipole–dipole interaction energies (V, in J) by using the following equation, in which μ refers to the dipolar moment, ε_0 to the permittivity of free space and r to the distance between dipoles:

$$V = -\frac{2\mu^2}{4\varepsilon_0 r^3}$$

The ESP atomic charges were also calculated for each oxyluciferin molecule involved in the dimers. The results are presented in Table 6. As in the case of the stabilization energy, the changes in the resonance have little to no effect in the charge localization in the oxyluciferin molecules. The dipole moments of the dimers do decrease with increasing C—C bond length, but these changes are small (4.94–4.87 Debye). The localization of the positive/negative charges of oxyluciferin molecules is also basically not affected by resonance changes.

The major interest in firefly oxyluciferin research is to study its excited state properties, due to the capability of this molecule of exhibiting fluorescence, chemiluminescence and bioluminescence [27–29]. Thus, we have calculated the excitation transitions of the

Table 5
Stabilization energy obtained by dimer formation (ΔE_{stab}, in kcal/mol).

Bond length (Å)	ΔE_{stab} (kcal/mol)
1.35	−23.9
1.40	−23.9
1.46	−23.8
1.50	−23.7

Table 4
ESP atomic charges of the two moieties of sole oxyluciferin, at difference C—C bond lengths, and dipole moment.

Bond length (Å)	Benzothiazole	Enolic-thiazole	Dipole moment
1.35	−0.023	0.024	2.48
1.40	−0.021	0.022	2.47
1.46	−0.018	0.019	2.45
1.50	−0.016	0.017	2.44

Table 6
ESP atomic charges of the two oxyluciferin molecules of the four dimers, each with different C—C bond lengths, and dipole moment.

Bond length (Å)	Oxyluciferin1	Oxyluciferin2	Dipole moment (Debye)
1.35	−0.031	0.032	4.94
1.40	−0.031	0.032	4.90
1.46	−0.030	0.030	4.89
1.50	−0.033	0.032	4.87

Table 7
Excitation energies (E_{ex}, eV) and oscillator strength (f) presented by the four dimers, each with different C—C bond lengths. All these excitations correspond to $S_0 \rightarrow S_2$ transitions.

Bond length (Å)	E_{ex}	f
1.35	3.76	0.9287
1.40	3.91	0.9046
1.46	4.06	0.8671
1.50	4.17	0.8339

four dimers, in order to see what is the effect exerted by resonance changes (and consequently by changes in π–π stacking interaction) in the excited state properties of firefly oxyluciferin.

While the three excited state processes referred above (fluorescence, chemiluminescence and bioluminescence) correspond to light emission, the study of the excitation of the molecule can provide unique insight into its excited state properties. It should be noted that the absorption spectrum often reflects the main excited state features, with a difference of a red-shift that occurs after relaxation [29–35]. Moreover, some researchers have already demonstrated that the light-emitting state in firefly chemi/bioluminescence and fluorescence is the same, either within the enzyme or *in vacuo* [35].

In Table 7 are presented the excitation energies and the oscillator strength of the bright state for each dimer. From this table, we can see that the C—C bond length affects both excited state properties. The energy of the transition increases greatly with increasing bond length. Between the excitation energies of the dimers with C—C bond lengths of 1.35 and 1.50 Å there is a difference of 0.41 eV, which is equivalent to ~33 nm. Thus, changes in resonance have a non-negligible impact on the excitation energies of oxyluciferin dimers.

The excitation energies are not the only excited state parameter that is affected by modulation of the resonance. The value of the oscillator strength, a measure of the transition efficiency, also varies with modification of the C—C bond length. From Table 7, we can see that the efficiency of the excitation transition is higher with lower C—C bond lengths.

In order to better understand these results, we have studied in further detail the excitation transitions of the four dimers (Table 8). The excitation of all dimers consists on $S_0 \rightarrow S_2$ transitions. In the dimer with a C—C bond length of 1.35 Å, this transition consists on HOMO(−1) → LUMO, HOMO(−1) → LUMO(+1), HOMO → LUMO and HOMO → LUMO(+1) excitations. The more important excitations are HOMO(−1) → LUMO (38.9%) and HOMO → LUMO(+1) (42.3%). The two remaining excitations correspond only to 10.3% of the $S_0 \rightarrow S_2$ transition.

The dimer with a C—C bond length of 1.40 Å presents the same type of excitations. However, the contribution of some of the excitations to the $S_0 \rightarrow S_2$ transition is different. The HOMO → LUMO(+1) excitation now corresponds only to 39.9% of the transition, a decrease of 2.5% when in comparison with the value obtained for the dimer with a C—C bond length of 1.35 Å. The HOMO(−1) → LUMO(+1) and HOMO → LUMO excitations are now slightly more important (11.8%), while the contribution of HOMO(−1) → LUMO is basically the same.

Besides the same excitations found in other dimers, the dimer with C—C bond length of 1.46 Å presents also a HOMO(−2) → LUMO excitation (2.1%). The importance of HOMO → LUMO(+1) (37.4%) and HOMO(−1) → LUMO (37.7%) continue to decrease. For the contrary, the importance HOMO(−1) → LUMO(+1) (6.6%) and HOMO → LUMO (7.5%) continue to increase.

The dimer with C—C bond length of 1.50 Å presents the same five excitations, described in the above paragraph. As in line with the other dimers, the increase in C—C bond length leads to decreased contributions by HOMO → LUMO(+1) (35.9%) and HOMO(−1) → LUMO (35.7%), while HOMO(−1) → LUMO(+1) (7.6%) and HOMO → LUMO (8.6%) continuously become more important. In this case, the contribution of the HOMO(−2) → LUMO excitation (2.4%) also increases.

Given these results, it appears that from the five types of excitations that can constitute the $S_0 \rightarrow S_2$ transition of oxyluciferin dimers, the HOMO → LUMO(+1) and HOMO(−1) → LUMO are the ones that lead to a more efficient and less energetic transition. This conclusion is supported by the finding that the increase in the excitation energies, and decrease of the oscillator strengths, are associated to decreased contributions from these excitations to the bright $S_0 \rightarrow S_2$ transition. By its turn, HOMO(−1) → LUMO(+1) and HOMO → LUMO do not have the same capacity of the latter referred excitations, as their increased contribution was not able to prevent the decrease in the oscillator strength and increase in the excitation energies.

The ESP atomic charges were also calculated for each oxyluciferin molecule involved in the dimers in the excited state, along with the results obtained for the ground state. The results are presented in Table S4. We have not found any correlation between the degree of charge transfer and the value of excitation dimers, in function of the C—C bond length.

Table 8
Contributions (%) of the orbital excitations to the $S_0 \rightarrow S_2$ transitions of the four dimers, each with different C—C bond lengths.

Excitations	Bond length (Å)			
	1.35	1.40	1.46	1.50
HOMO(−2) → LUMO			2.1	2.4
HOMO(−1) → LUMO	38.9	38.8	37.4	35.9
HOMO(−1) → LUMO(+1)	5.5	5.9	6.6	7.6
HOMO → LUMO	4.8	5.9	7.5	8.6
HOMO → LUMO(+1)	42.3	39.9	37.7	35.7

4. Conclusions

π–π stacking interactions between aromatic groups are found widespread in chemical systems. So, the study of this type of noncovalent interaction is becoming more important in order to understand the conformations and properties of the systems above referred.

One particular system in which π–π stacking interactions are important is that of firefly oxyluciferin. This molecule forms complexes with molecules of its own species due to these noncovalent interactions. Moreover, the modulation of the π–π stacking interactions, that allow for the formation of the complexes, has a major role on its fluorescence properties (being responsible for the pH-sensitivity of oxyluciferin fluorescence).

In order to better understand π–π stacking interactions in general, and in the firefly oxyluciferin system in particular, we have studied the effect of resonance changes in the properties of firefly oxyluciferin sandwich-like dimers. Changes in resonance were achieved by modulating the length of the C—C bond that connects the benzothiazole and the thiazole moieties.

Changes in resonance have little to no effect in ground state properties of the dimers. The stabilization energy provided by dimerization is nearly the same for all dimmers, as well as charge localization and the dipole moment. Nevertheless, changes in the resonance have a great effect on the excited state properties of oxyluciferin dimmers.

The excitation energies of the dimers increase with increasing C—C bond length. The length of this bond has a different effect on the oscillator strength, as with increasing length the efficiency of the excited state transition is lower.

Further analysis of the dimers excited state transitions revealed that this effect is related to changes in the contributions by orbital excitations. Dimers with lower excitation energy and higher oscillator strength present transitions with higher contributions from HOMO → LUMO(+1) and HOMO(−1) → LUMO excitations. With increasing C—C bond length, the contributions of these excitations decrease, while the contributions of HOMO(−1) → LUMO(+1) and HOMO → LUMO increase.

Acknowledgments

Financial support from Fundação para a Ciência e a Tecnologia (FCT, Lisbon), Programa Operacional Temático Factores de Competitividade (COMPETE) e comparticipado pelo Fundo Comunitário Europeu (FEDER) (Project PTDC/QUI/71366/2006) is acknowledged. A PhD Grant to Luís Pinto da Silva (SFRH/BD/76612/2011) from Fundação para a Ciência e Tecnologia (FCT, Lisbon) is acknowledged. Margarida Miranda thanks FCT for the financial support under the frame of the Ciência 2008 program.

Appendix A. Supplementary data

Supplementary material related to this article can be found, in the online version, at http://dx.doi.org/10.1016/j.jphotochem.2013.12.018.

References

[1] M.O. Sinnokrot, C.D. Sherrill, J. Phys. Chem. A 110 (2006) 10656–10668.
[2] C.A. Hunter, J.K.M. Sanders, J. Am. Chem. Soc. 112 (1990) 5525–5534.
[3] E.C. Lee, D. Kim, P. Jurecka, P. Tarakeshwar, P. Hobza, K.S. Kim, J. Phys. Chem. A 111 (2007) 3446–3457.
[4] S.K. Burley, G.A. Petsko, Science 229 (1985) 23–28.
[5] R.K. Raju, J.W.G. Bloom, S.E. Wheeler, J. Chem. Theory Comput. 9 (2013) 3479–3490.
[6] K.L. Copeland, G.S. Tschumper, J. Chem. Theory Comput. 8 (2012) 4279–4284.
[7] C.F.R.A.C. Lima, M.A.A. Rocha, L.R. Gomes, J.N. Low, A.M.S. Silva, L.M.N.B.F. Santos, Chem. Eur. J. 18 (2012) 8934–8943.
[8] S.E. Wheeler, Acc. Chem. Res. 46 (2013) 1029–1038.
[9] L. Pinto da Silva, R. Simkovitch, D. Huppert, J.C.G. Esteves da Silva, ChemPhysChem 14 (2013) 2711–2716.
[10] L. Pinto da Silva, R. Simkovitch, D. Huppert, J.C.G. Esteves da Silva, ChemPhysChem (2013), http://dx.doi.org/10.1002/cphc.201300402.
[11] Y. Erez, I. Presiado, R. Gepshtein, L. Pinto da Silva, J.C.G. Esteves da Silva, D. Huppert, J. Phys. Chem. A 116 (2012) 7452–7461.
[12] P. Muller, Pure Appl. Chem. 66 (1994) 1077–1184.
[13] P.R. Schleyer, Chem. Rev. 105 (2005) 3433–3435.
[14] A.T. Balaban, P.R. Schleyer, H.S. Rzepa, Chem. Rev. 105 (2005) 3436–3447.
[15] M.J. Frisch, et al., Gaussian 09, Revision A.02, Gaussian, Inc., Wallingford, CT, 2009.
[16] J.D. Chai, M. Head-Gordon, Phys. Chem. Chem. Phys. 10 (2008) 6615–6620.
[17] C. Adamo, D. Jacquemin, Chem. Soc. Rev. 42 (2013) 845–856.
[18] P.R. Schleyer, H. Jiao, N.J.R.E. Hommes, V.G. Malkin, O. Malkina, J. Am. Chem. Soc. 119 (1997) 12669–12670.
[19] P.R. Schleyer, M. Manoharan, Z.X. Wan, B. Kiran, H. Jiao, R. Puchta, N.J.R.E. Hommes, Org. Lett. 3 (2011) 2465–2468.
[20] J.A. Pople, J. Chem. Phys. 24 (1956) 1111–1117.
[21] R. McWeeny, Phys. Rev. 126 (1961) 1028–1034.
[22] R. Ditchfield, Mol. Phys. 27 (1974) 789–807.
[23] J.L. Dodds, R. Mc Weeny, A.J. Sadlej, Mol. Phys. 41 (1980) 1419–1430.
[24] K. Wolinski, J.F. Hilton, P. Pulay, J. Am. Chem. Soc. 112 (1990) 8251–8260.
[25] T. Yanai, D. Tew, N. Handy, Chem. Phys. Lett. 393 (2004) 51–57.
[26] P.R. Schleyer, C. Maerker, A. Dransfeld, H. Jiao, N.J.R.R. Hommes, J. Am. Chem. Soc. 118 (1996) 6317–6318.
[27] J. Vieira, L. Pinto da Silva, J.C.G. Esteves da Silva, J. Photochem. Photobiol. B 117 (2012) 33–39.
[28] L. Pinto da Silva, J.C.G. Esteves da Silva, ChemPhysChem 13 (2012) 2257–2262.
[29] L. Pinto da Silva, J.C.G. Esteves da Silva, J. Chem. Theory Comput. 7 (2011) 809–817.
[30] B.F. Milne, M.A. Marques, F. Nogueira, Phys. Chem. Chem. Phys. 12 (2010) 14283–14285.
[31] L. Pinto da Silva, J.C.G. Esteves da Silva, J. Comput. Chem. 32 (2011) 2654–2663.
[32] K. Stochkel, C.N. Hansen, J. Houmoller, L.M. Nielsen, M. Linares, P. Norman, F. Nogueira, O.V. Maltsev, L. Hintermann, S.B. Nielsen, P. Naumov, B.F. Milne, J. Am. Chem. Soc. 135 (2013) 6485–6493.
[33] D. Cai, M.A. Marques, F. Nogueira, J. Phys. Chem. B 115 (2010) 329–332.
[34] L. Pinto da Silva, J.C.G. Esteves da Silva, Photochem. Photobiol. Sci. (2013), http://dx.doi.org/10.1039/C3P P50203A.
[35] Navizet, D. Roca-Sanjuán, L. Yue, Y.J. Liu, N. Ferré, R. Lindh, Photochem. Photobiol. 89 (2013) 319–325.

Article 26

A theoretical analysis of the potential role of π-π stacking interactions in the photoprotolytic cycle of firefly luciferin

Luís Pinto da Silva and Joaquim C.G. Esteves da Silva

ChemPhysChem **2014**, *15*, 3761-3767.

The theoretical calculations and the writing of the paper were performed by Luís Pinto da Silva, under the supervision of Professor Joaquim Esteves da Silva.

CHEMPHYSCHEM ARTICLES

ChemPubSoc Europe

DOI: 10.1002/cphc.201402558

A Theoretical Analysis of the Potential Role of π–π Stacking Interactions in the Photoprotolytic Cycle of Firefly Luciferin

Luís Pinto da Silva and Joaquim C. G. Esteves da Silva*[a]

Firefly oxyluciferin is a photoacid that presents a pH-sensitive fluorescence, which results from pH-dependent changes on the conformation of self-aggregated π–π stacking complexes. Luciferin is a derivative of oxyluciferin with very similar fluorescence and photoacidic properties. This similarity indicates that luciferin is also expected to be able to form π–π stacking complexes, but no pH-sensitive fluorescence is found for this compound. Here, a theoretical approach is used to rationalize this finding. We have found that luciferin only forms π–π stacking complexes in the ground state at acidic pH. At basic pH and in the excited state, luciferin is present as a dianion. This species is not able to self-aggregate, owing to repulsive electrostatic interactions. Thus, this emissive species is not subject to π–π stacking interactions; this explains its pH-insensitive fluorescence.

1. Introduction

Proton transfer is a fundamental process with an important role in chemistry and biology.[1,2] Prime examples are keto–enol tautomerism, proton transport, and protein relay systems in membrane-spanning proteins and enzymes.[3,4] A special class of compounds involved in proton-transfer processes is represented by heterocyclic aromatic molecules.[5,6] These molecules are known to undergo significant changes in their acidity upon photoexcitation.[7] Molecules that increase their acidity are termed photoacids, whereas photobases increase their basicity. The excited-state proton transfer (ESPT) can be intramolecular if the acidic and basic moieties coexist in the same molecule, or intermolecular (e.g. ESPT to the solvent).[8]

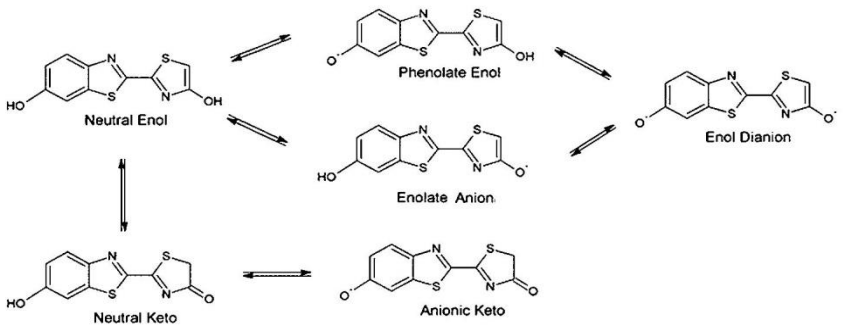

Scheme 1. Chemical equilibria of firefly oxyluciferin.

The firefly oxyluciferin (Scheme 1) family of fluorophores is a particular example of photoacids capable of ESPT to the solvent.[9] Up to now, the study of this family of photoacids has revealed many interesting, complex, and unexpected phenomena stemming from ESPT: efficient fluorescence quenching, photoacidity from an enol group, and photo-induced base-catalyzed keto–enol tautomerism.[9–12]

The most well-studied and well-known examples of this family are firefly oxyluciferin and luciferin (Scheme 1 and Scheme 2).[9,10] Both molecules are also key molecules in firefly bioluminescence. Bioluminescence can be characterized as light-emission occurring in a living organism, and is due to an enzyme-catalyzed chemical reaction.[13,14] In fireflies, this process is a two-step reaction catalyzed by the luciferase enzyme. In the first step, firefly luciferin reacts with adenosine-5′-triphosphate-Mg^{2+} (ATP-Mg^{2+}), which results in the formation of an adenylyl intermediate. The second step consists of the oxidation of this intermediate. The last step generates firefly oxyluciferin, which is formed directly in the singlet excited state.[15,16] Thus, this fluorophore is the bioluminescence emitter, decaying to the ground state with green to red emission (2.34 to 2.00 eV).

[a] Dr. L. Pinto da Silva, Prof. Dr. J. C. G. Esteves da Silva
Centro de Investigação em Química (CIQ-UP)
Departamento de Química e Bioquímica
Faculdade de Ciências, Universidade do Porto
R. Campo Alegre 697, 4169-007 Porto (Portugal)
E-mail: jcsilva@fc.up.pt

Supporting Information for this article is available on the WWW under http://dx.doi.org/10.1002/cphc.201402558.

CHEMPHYSCHEM
ARTICLES
www.chemphyschem.org

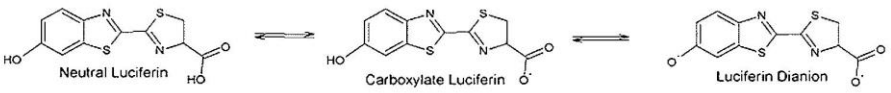

Scheme 2. Chemical equilibria of firefly luciferin.

This system presents some useful characteristics, namely ATP-dependence and high quantum yield, which have triggered the development of numerous applications in the pharmaceutical, biomedical, and bioanalytical fields.[17–19] In order to optimize these applications of firefly bioluminescence and to develop new ones, it is necessary to fully understand this system. One of the research topics that attracts the most attention is the elucidation of the color tuning mechanism of firefly oxyluciferin.[20–24] This fluorophore is able to emit green to red light both in firefly bioluminescence and in solution.[20–24] Until now, no definitive consensus has been reached, but the available evidence indicates that the color is modulated by an electrostatic field generated by intermolecular interactions formed between oxyluciferin and nearby molecules.[25–32] Nevertheless, the complete elucidation of this topic is impaired by doubt regarding the identity of the light emitter. In solution and in the solid phase the enol species are predominant.[33,34] Some studies point out that in the bioluminescence reaction only the anionic keto species is needed to obtain the green to red light emission.[35,36] However, recent studies have provided evidence to support the formation of the oxyluciferin enolate anion, which results from ESPT from the neutral keto species to nearby adenosine-5′-monophosphate (AMP).[12,25] Thus, it appears that ESPT may play a key role in firefly bioluminescence.

One of the objectives of our group is to understand ESPT stemming from oxyluciferin by characterizing the photoprotolytic cycle of this molecule and its derivatives in aqueous solution.[9–11,25,37,38] Measurements in aqueous solution, under both acidic (pH $\approx$ 4.5) and basic (pH $\approx$ 9) conditions, revealed pH-sensitive fluorescence for oxyluciferin.[10] At acidic pH, the emission peaks at 2.25 eV, whereas at basic pH, the emission shifts to 2.30 eV.[10] Moreover, experimental measurements indicate that the fluorescence of oxyluciferin at acidic pH consists of both a fast decaying component and a slow one. In basic solution, the amplitude of the short-time component of the anionic species signal is less than 0.05, whereas in acidic solution its value is approximately 0.35.[10] The longtime-component lifetime is also different if the compound is excited at different pH.[10] The difference in lifetime and emission peaks indicates that the fluorescence at acidic and basic pH stems from two species. However, there is some evidence that indicates that the emission only stems from one species. Strong experimental findings demonstrate that only neutral and anionic enol species are present in aqueous solution.[33,34,39] More recently, Naumov and co-workers have proved that the light emitter at acidic pH is the enolate-anion species.[12] Thus, in order for two different fluorophores to exist in the photoprotolytic cycle of this photoacid, the phenolate or dianion enol would have to be the emitters at basic pH. However, in our work we only detected one pK_a value, whereas two would have been necessary to account for the two deprotonations needed to form the dianion enol.[10] The phenolate enol could have been a possible emitter at basic pH if the hydroxyl group was more acidic in the ground state than the enol group. However, our theoretical work has indicated that the enol group is more acidic than the hydroxyl group both in the ground and excited states.[40] Therefore, the pH-sensitive fluorescence should be explained considering only the enolate anion. In our opinion, this statement is supported by both experimental and theoretical results that indicate that the oxyluciferin fluorescence emitter is the enolate anion. Various studies have demonstrated that, at acidic pH, the fluorophore is the enolate anion due to photoexcitation of the neutral enol and subsequent ESPT.[10,12,33] At basic pH, the emitter should be formed after ground-state deprotonation of the neutral enol, which is followed by photoexcitation of the anion. Theoretical studies have indicated that this anion species is the enolate anion.[40]

More recently we have employed a computational approach in order to clarify the pH-sensitive fluorescence and photoprotolytic cycle of oxyluciferin in aqueous solution.[38] We have found that both the neutral enol and enolate anion forms of oxyluciferin are able to form π–π stacking complexes in the ground state. However, the complexes present different conformations due to the different charges of these two oxyluciferin species. Therefore, on photoexcitation, the resulting excited-state enolate-anion species will be formed in different π–π stacking arrangements, which depend on the pH. Even considering only one emitter, the enolate anion, the different conformations lead to a more red-shifted band at acidic/neutral pH than at basic pH. Therefore, we ascribed the pH-sensitive fluorescence to different geometries of π–π stacking complexes.[38]

Notably, this pH-sensitive fluorescence was not found for firefly luciferin.[10] As already mentioned, luciferin is a member of the oxyluciferin family of photoacids, with very similar photoacidic and fluorescence properties to those of oxyluciferin itself.[9,10,41] Nevertheless, the fluorescence of luciferin peaks at 2.34 eV, irrespective of the pH, and this corresponds to the luciferin dianion.[10,41,42] However, given its great structural similarity with oxyluciferin, luciferin can also be expected to be involved in the formation of π–π stacking complexes. So, this leads to the following question: is luciferin unable to form π–π stacking complexes, or are the π–π stacking interactions unable to modulate its fluorescence?

Thus, the objective of the present manuscript is to answer this question. We think that the elucidation of this topic is needed in order to understand the photoprotolytic cycle of these photoacids, and to gain a better grasp on the role of π–π stacking interactions in the fluorescence of aromatic molecules. To this end, we have used a computational approach to study firefly luciferin in aqueous solution. This approach is based on molecular dynamics (MD) simulations and quantum mechanical (QM) calculations. MD simulations allow us to

CHEMPHYSCHEM
ARTICLES
www.chemphyschem.org

assess the possibility of the formation of π–π stacking complexes by taking into account the dynamics of the luciferin–water system. QM calculations can be used to obtain direct and detailed information (down to the atomic level) of the ground and excited-state luciferin species, which cannot be provided directly using experimental methodology.

2. Results and Discussion

The luciferin dianion species is known to be the sole fluorophore in water over the entire pH range (Scheme 2).[9,10,41,42] Nevertheless, this species is formed from two different pathways that depend on the pH. At acidic pH, the dominant ground-state species is the carboxylate luciferin (Scheme 2). Upon photoexcitation, this molecule undergoes ESPT with the solvent, and this generates the luciferin dianion. At basic pH, the dianion is already formed in the ground state prior to photoexcitation.[9,10,41,42] This situation is very similar to that found for oxyluciferin, in which we found neutral enol and enolate-anion species instead of carboxylate and dianionic anions.

In order to try to model the photoprotolytic cycle, we created two complexes. One was composed of three carboxylate luciferin ground-state species in a water box up to 12 Å, and the other was composed of three luciferin ground-state dianions in a similar water box. The first complex was built in order to obtain the conformation of luciferin at acidic pH prior to photoexcitation, whereas the second complex was expected to model luciferin at basic pH. Both complexes were subjected to 30000 steps of energy minimizations prior to MD simulations of 1 ns.

The three luciferin molecules in each complex are presented in Figure 1 as obtained in the final frame of the MD simulation.

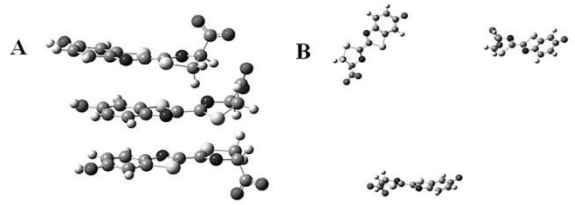

Figure 1. Ground-state A) carboxylate-anion and B) luciferin-dianion complexes at the final frame of MD simulations of 1 ns.

As shown in Figure 1, the carboxylate luciferin is capable of forming a sandwich-like π–π stacking complex, very similar to the one found for oxyluciferin (more specifically for the ground-state neutral enol).[38]

We then tried to assess the association energy of this π–π stacking complex by using Equation (1).

$$\Delta E_{ass\_water} = E_{complex} - (E_{luciferin1} + E_{luciferin2} + E_{luciferin3}) + BSSE + \Delta E_{solv} \quad (1)$$

where $\Delta E_{ass\ water}$ refers to the association energy of the complex in water, $E_{complex}$ is the energy of the complex, and $E_{luciferinx}$ refers to the energy of each one of the luciferin molecules by itself. The basis set superposition error (BSSE) was obtained by the counterpoise method.[43,44] The BSSE arises from the overlap of the basis functions of the atoms of interacting molecules as they approach one another. The complex can thus be artificially stabilized as a monomer by utilizing extra basis functions from another monomer to describe its electron distribution. As the counterpoise method can only be used in vacuo, $E_{complex}$ and $E_{lucferinX}$ were calculated in the gas phase. ΔE_{solv} is a term added to the equation in an attempt to add the solvent effects to $\Delta E_{ass\ water}$, and consists of Equation (2).

$$\Delta E_{solv} = \Delta E_{complex} - (\Delta E_{luciferin1} + \Delta E_{luciferin2} + \Delta E_{luciferin3}) \quad (2)$$

Each ΔE term consists of the difference between the energy of a structure in implicit water and that of the same structure in the gas phase. We also used Equation (3) to obtain this energy in the gas phase. The results are presented in Table 1.

$$\Delta E_{ass\_vacuo} = E_{complex} - (E_{luciferin1} + \Delta E_{luciferin2} + \Delta E_{luciferin3}) + BSSE \quad (3)$$

Table 1. Energy of association of the three oxyluciferin molecules in water and in the gas phase ($\Delta E_{ass\ water}$ and $\Delta E_{ass\ vacuo}$ in kcal mol^{-1}), the BSSE (in kcal mol^{-1}) and solvation energy (ΔE_{solv} in kcal mol^{-1}), calculated at the *w*B97XD/cc-pVDZ level of theory.

Water		Gas phase	
$\Delta E_{ass\ water}$	−26.4	$\Delta E_{ass\ vacuo}$	183.1
BSSE	90.0	BSSE	90.0
ΔE_{solv}	−209.5		

These results show that basis set superposition does indeed overly stabilize the π–π stacking complex by a significant 90 kcal mol^{-1}. It can also be seen that this complex is indeed stabilized in water by 26.4 kcal mol^{-1}, but is unstable in the gas phase. This large destabilization in vacuo is not unexpected. Each carboxylate luciferin is an anionic molecule, and this complex of three negative molecules should therefore generate significant repulsive electrostatic interactions. In water, stabilization is achieved due to solvent effects (ΔE_{solv} of −209.5 kcal mol^{-1}). This is in line with previous studies of π interactions, in which it was determined that solvents such as water maximize complementary electrostatics and minimize repulsive electrostatic interactions.[45]

Water also induces stabilization by further polarizing the luciferin molecules in the π–π stacking complex. In Table 2 the atomic Mulliken charges of each luciferin molecule (divided into the benzothiazole and carboxylic thiazole moieties) in the complex are presented, both in water and in the gas phase. It can be seen that in both media luciferin is a polar molecule with the negative charge density localized mainly on the carboxylic thiazole moiety. However, in the gas phase the benzo-

CHEMPHYSCHEM
ARTICLES
www.chemphyschem.org

Table 2. Atomic Mulliken charges of the benzothiazole and carboxylic thiazole moieties of the ground-state luciferin complexes in water at the *w*B97XD/cc-pVDZ level of theory. The in vacuo values are given in parentheses.

Carboxylate luciferin	Benzothiazole	Carboxylic thiazole
luciferin1	−0.003 (−0.136)	−1.029 (−0.992)
luciferin2	−0.011 (−0.104)	−0.947 (−0.951)
luciferin3	−0.003 (−0.097)	−1.029 (−1.022)
Luciferin dianion	**Benzothiazole**	**Carboxylic thiazole**
luciferin1	−0.938 (−0.944)	−1.061 (−1.057)
luciferin2	−0.886 (−0.897)	−1.112 (−1.103)
luciferin3	−0.931 (−0.966)	−1.068 (−1.031)

thiazole moiety still presents negative Mulliken charges of about −0.112. In water, the negative charge on this moiety is only about −0.006. Thus, even if the molecule is already polarized in both media, significant polarization still occurs on solvation. The interaction energy of π–π stacking complexes contains primarily four components: electrostatic, induction, dispersion, and exchange repulsion.[46,47] Induction and dispersion forces are attractive interactions that result from a permanent multipole or instantaneous dipole, respectively, and an induced dipole. Thus, if water increases the dipole moment of the carboxylate luciferin, it is expected that the attraction generated by induction and dispersion interactions will increase.

We also calculated the vertical excitation energy of the carboxylate luciferin π–π stacking complex in implicit water (Table 3). The computed value was 3.80 eV, which is well in line with the experimental value of 3.76 eV.[10,41] We also calculated the vertical excitation energy of each carboxylate species in order to evaluate the effect that π–π stacking has on the excited state properties of luciferin. Only one luciferin molecule presented a vertical excitation identical to that presented by the complex. The other two molecules presented significantly blue-shifted excitation energies (by 0.22 and 0.36 eV). This means that besides stabilizing the complex in the ground state, π–π stacking also stabilizes the Franck–Condon state. Although all the isolated luciferin molecules present excitation energies close to the experimental value, it is the complex that agrees best with the experiment.

Table 3. Vertical excitation energies (E_{ex}) of the ground state of the luciferin carboxylate and dianion species at the TD *w*B97XD/cc-pVDZ level of theory.

Carboxylate luciferin	E_{ex} [eV]
complex	3.80
luciferin1	3.98
luciferin2	3.80
luciferin3	4.12
Dianion luciferin	**E_{ex} [eV]**
complex	3.14
luciferin1	3.10
luciferin2	3.14
luciferin3	3.33

In Figure 1 the three ground-state luciferin dianions are presented in a water box. This is the complex corresponding to basic pH. Contrary to the case of the carboxylate luciferin and of oxyluciferin, the luciferin dianion is clearly not capable of generating π–π stacking complexes.[38] In fact, the dianion species are separated by more than 11 Å. This inability of forming π–π stacking complexes can be attributed to the double negative charge possessed by each molecule, which should generate repulsive electrostatic interactions that are impossible to overcome. Moreover, as seen in Table 2, the deprotonation of the hydroxyl group significantly reduces the polarization of the luciferin species (thereby reducing the possibility of potential dipole–dipole interactions).

We also calculated the vertical excitation of the three luciferin molecules together, and also of each one by itself (Table 3). As expected, the calculated vertical excitation energies are very similar to each other because the luciferin molecules should only interact with each other by long-range repulsive electrostatic interactions. Moreover, the vertical excitation energy of the three luciferin molecules (3.14 eV) is in line with the experimental value of 3.35 eV.[9,10,41]

The results presented so far indicate that at acidic pH, ground-state luciferin is present as a π–π stacking complex composed of the carboxylate luciferin species. At basic pH, the complex is disrupted by further deprotonation of luciferin, which generates the dianion species. The formation of the dianion increases the repulsive electrostatic interaction, and causes depolarization of this species, which makes the formation of π–π stacking complex unfavorable.

The next step in this study was to obtain stable conformations of the excited-state luciferin dianion in aqueous solution at basic and acidic pH. To this end, we used the geometries of the three luciferin species at basic and acidic pH (carboxylate and dianion species, Figure 1), as the initial structures for further MD simulations of 1 ns. The parameterized atomic charges were those of the dianion species at the Franck–Condon state. The Franck–Condon state was chosen in order to better compare these results with those obtained for the study of the pH-sensitive fluorescence of oxyluciferin, in which the same approach was used.[38] Moreover, the absorption spectrum often reflects the main excited-state features, with a difference that occurs due to geometry relaxation.[48,49] The strategy of using the Franck–Condon state to obtain information regarding the emissive state is routinely used with good results in a variety of topics.[50–60] The hydrogen atoms of the hydroxyl group of the three carboxylate luciferin anions were withdrawn in order to simulate the formation of the dianion species at acidic pH.[38]

The resulting conformations of the Franck–Condon luciferin dianion at acidic and basic pH are presented in Figure 2. Interestingly, at acidic pH the π–π stacking complex formed by the carboxylate luciferin species was disrupted by deprotonation of the luciferin dianion (Figure 2 A). In fact, one of the three luciferin molecules was about 24 Å away from the other two molecules in the final frame of the calculation. The other two

CHEMPHYSCHEM
ARTICLES
www.chemphyschem.org

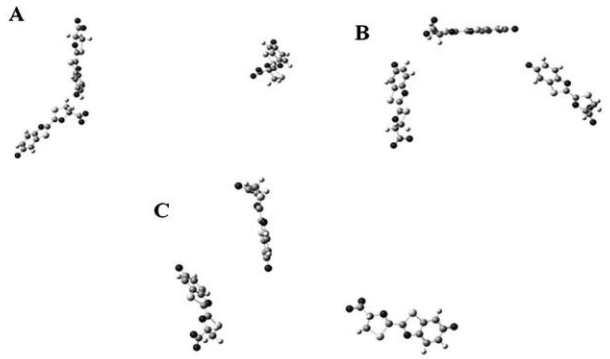

Figure 2. Excited-state luciferin-dianion complexes at acidic pH at the final frame of MD simulations of A) 1 ns and B) 1.5 ns, and C) at basic pH at the final frame of MD simulations of 1 ns.

were close together in a T-displaced conformation, not in a π–π stacking dimer. This behavior is different from that seen for oxyluciferin at acidic pH, at which oxyluciferin was found to be present in a disordered π–π stacking complex.[38] We attribute this inability of the luciferin dianion to form π–π stacking complexes to the significant repulsive electrostatic interaction between the molecules (given the double negative charge of each dianion) and the depolarization resulting from the carboxylate→dianion conversion (Table 2). Also, these molecules are known to become less polarized upon excitation.[60,61]

Despite not forming a π–π stacking complex, the two luciferin molecules present in the T-displaced conformation are close enough to exert a significant effect on each other's excited-state properties. In order to see if this conformation was maintained or if was only a transitory state resulting from the fact that the initial conformation was a π–π stacking complex, we subjected to this luciferin–water complex to another MD simulation of 500 ps. The resulting conformation of the three luciferin dianions is presented in Figure 2B. It can be seen that with a longer simulation time, the T-displaced conformation ceased to exist and all of the luciferin molecules were distant from each other.

The conformation of the Franck–Condon luciferin dianion at basic pH is presented in Figure 2C. As in the ground state (Figure 2B), the luciferin molecules were not involved in a π–π stacking complex. In fact, they were not close to each other. This is not in line with the results found for oxyluciferin, which was present as a π–π stacking complex at basic pH in the ground and excited states.[38]

The results presented so far have demonstrated that luciferin is only able to form ground-state π–π stacking complexes at acidic pH, under which conditions it takes the form of the carboxylate luciferin anion. The complex is able to form due to solvent effects, which are thought to maximize complementary electrostatics and minimize repulsive electrostatic interactions.[45] At basic pH in the ground state, and in the excited state, under which conditions luciferin is found as the dianion species, this molecule is not able to form π–π stacking complexes. This can be attributed to the deprotonation of the hydroxyl group, which increases the negative charge of each luciferin molecule to two. This is expected to increase the repulsive electrostatic interactions between the luciferin molecules to a point at which they cannot be overcome by solvent effects. Also, the deprotonation of this group reduces the polarization of luciferin, as this results in the molecule having a negative charge at each extreme of its scaffold. This depolarization is also expected to affect the dipole–dipole interactions between the luciferin molecules present in solution.

The calculated excitation energies of the luciferin dianion at acidic (both at 1 and 1.5 ns of MD simulation) and basic pH are presented in Table 4. The vertical excitation of each luciferin molecule by itself is also presented in the same table.

Table 4. Vertical excitation energies (E_{ex}) of the Franck–Condon states of the luciferin dianion species at the final frame of the MD simulation of 1 ns (presented in Figure 2A,C), at the TD *w*B97XD/cc-pVDZ level of theory.

Luciferin dianion (acidic pH)	E_{ex}[a] [eV]
complex	3.05 (3.16)
luciferin1	3.22 (3.02)
luciferin2	3.25 (3.24)
luciferin3	3.05 (3.17)
Luciferin dianion (basic pH)	**E_{ex}[a] [eV]**
complex	3.12
luciferin1	3.00
luciferin2	3.21
luciferin3	3.13

[a] The values in parentheses are the excitation energies of the luciferin dianion species at the final frame of the MD simulation of 1.5 ns (presented in Figure 2B).

The excitation energies of the three complexes are all similar to each other, with differences of only 0.04 to 0.12 eV. For oxyluciferin differences of 0.25 eV were found at acidic and basic pH.[38] Also, the difference between the vertical excitation energies of the luciferin complexes and the average of the energies of each luciferin molecule is not very significant (between 0.01 and 0.13 eV). This finding indicates that the interactions between the luciferin molecules (expected to be long-range electrostatic) do not significantly affect the vertical energy of the complexes.

All of these findings support the pH-insensitivity of luciferin in aqueous solution.[10] Even if photoexcited at acidic pH from a π–π stacking complex, luciferin emits light as a dianion that only interacts with other luciferin molecules by long-range electrostatic interactions. This is in stark contrast with oxyluciferin. The oxyluciferin fluorescence emitter, the enolate anion, emits light in π–π stacking complexes at both acidic and basic pH, but the conformation of the complexes is dependent on the pH. These different structures result in different π–π stacking interactions between the oxyluciferin, and lead to different emission wavelengths that depend on the pH.[38] In conclusion, our results indicate that luciferin only forms π–π stacking complexes in the ground state at acidic pH. Thus, this type of com-

CHEMPHYSCHEM
ARTICLES
www.chemphyschem.org

plex and the resulting π–π stacking interactions do not have a significant effect on the photophysical properties and photoprotolytic cycle of luciferin. Moreover, these findings further support that the oxyluciferin π–π stacking complexes are the basis for the pH-sensitive fluorescence of this fluorophore.[10,38]

3. Conclusions

Time-resolved measurements have revealed that the fluorescence of firefly oxyluciferin in aqueous solution is pH sensitive. At acidic pH the emission peaks at 2.25 eV, whereas at basic pH it shifts to 2.30 eV. Our recent theoretical study explained this feature by demonstrating that oxyluciferin is able to form self-aggregated π–π stacking complexes in both the ground and the excited state, and at acidic and basic pH. However, the conformations of these complexes are different at basic and acidic pH, and this leads to different types of π–π stacking interactions between the oxyluciferin molecules. The pH-dependent changes in these intermolecular interactions are then able to modulate the emission, thus generating pH-sensitive fluorescence.

Firefly luciferin is a derivative of oxyluciferin with very similar fluorescence properties. This similarity indicates that luciferin should also be able to form π–π stacking complexes. However, no pH-sensitive fluorescence has been observed for this molecule. Thus, a question arises: is luciferin not able to form π–π stacking complexes, or are the π–π stacking interactions not able to modulate its fluorescence? The objective of this manuscript was to answer this question.

We employed a theoretical approach based on MD simulations and QM calculations to study the photodynamics of the photoprotolytic cycle of luciferin. We have found that this molecule is only able to form π–π stacking complexes in the ground state at acidic pH, under which conditions it is present as a carboxylate anion. At basic pH and in the excited state this molecule is present as a dianion. This further deprotonation of luciferin is expected to increase the repulsive electrostatic interactions to a level at which the formation of π–π stacking complexes is not possible. Thus, in the excited state luciferin is not subjected to π–π stacking interactions, but only to long-range repulsive electrostatic interactions, and so presents a very similar fluorescence peak over the entire pH range.

Theoretical Section

The ground-state geometries of luciferin species were obtained with the PBE0 functional and the cc-pVDZ basis set with no solvent effects.[62] This functional was used due to its good results in the calculations of geometries of organic molecules.[63–65]

Stable luciferin–water complexes were obtained by means of molecular-mechanics-based methods. TIP3P water molecules were added up to 12 Å by the LEAP module of the AMBER suite of programs.[66] We used this water-box size due to good results in previous theoretical studies of the interaction of firefly luciferin, dehydroluciferin, and oxyluciferin with firefly luciferase and/or with water molecules.[29,32,63] Six Na^+ cations were added to the complexes at basic pH, thereby neutralizing the charge of the complex. This was carried out in order to simulate the frequent addition of NaOH to aqueous solution in order to increase the pH of the solution. This approach was also used in our recent study of the photoprotolytic cycle of oxyluciferin in water.[38] One phase of energy minimizations (30 000 steps) was performed by using the Not (just) Another Molecular Dynamics (program) (NAMD) MD code with AMBER potential functions, parameters, and file formats.[67] In this process, the particle mesh Ewalds method was used to include the long-range interactions.[68] Nonbonded interactions were considered with 14 Å cutoffs. The integration step size was 2 fs, and all bonds involving hydrogen and heavy atoms were constrained. All steps were performed in a NVT ensemble with a temperature of 298.15 K.

The ground-state geometries of the studied molecules were used in their parameterization with the ANTECHAMBER module of AMBER and the general AMBER force field.[69] The charges of the ground-state molecules were derived by using the restrained electrostatic potential (RESP) method at the *w*B97XD/aug-cc-pVDZ level of theory.[70] The Franck–Condon charges of luciferin were parameterized with the RESP method by performing single-point time-dependent (TD) *w*B97XD/aug-cc-pVDZ calculations on the PBE0/cc-pVDZ geometries.[71]

The ground state and vertical excitation energies of luciferin, after MD simulations, were calculated at the *w*B97XD/cc-pVDZ level of theory (TD *w*B97XD/cc-pVDZ for the Franck–Condon states). The conductor-like polarized continuum model (CPCM) was used to simulate implicit water.[72] We used this density functional due to good results in local $n\rightarrow\pi^*$ and $\pi\rightarrow\pi^*$, charge transfer and Rydberg excited states.[73] Moreover, *w*B97XD was designed with an empirical dispersion correction term, which is needed for a correct modelling of π interactions.[70]

All QM calculations were performed with the Gaussian 09 program package.[74]

Acknowledgements

Financial support from Fundação para Ciência e Tecnologia (FCT, Lisbon) (Programa Operacional Temático Factores de Competitividade ;COMPETE) e comparticipado pelo Fundo Comunitário Europeu (FEDER; Project PTDC/QUI/71366/2006) is acknowledged. A Ph.D. grant to L.P.d.S. (SFRH/76612/2011), attributed by FCT, is also acknowledged.

Keywords: fluorescence · oxyluciferin · photoacidity · photoprotolytic cycle · pi interactions

[1] M. A. Lill, V. Helms, *Proc. Natl. Acad. Sci. USA* **2002**, *99*, 2778–2781.
[2] G. Mathias, D. Marx, *Proc. Natl. Acad. Sci. USA* **2007**, *104*, 6980–6985.
[3] S. J. Formosinho, L. G. Arnaut, *J. Photochem. Photobiol. A* **1993**, *75*, 21–48.
[4] A. H. Zewail, *Pure Appl. Chem.* **2000**, *72*, 2219–2231.
[5] J. Waluk, *Acc. Chem. Res.* **2003**, *36*, 832–838.
[6] S. Mente, M. Maroncelli, *J. Phys. Chem. A* **1998**, *102*, 3860–3876.
[7] N. Agmon, *J. Phys. Chem. A* **2005**, *109*, 13–35.
[8] T. Förster, *Pure Appl. Chem.* **1970**, *24*, 443–450.
[9] L. Pinto da Silva, R. Simkovitch, D. Huppert, J. C. G. Esteves da Silva, *ChemPhysChem* **2013**, *14*, 3441–3446.
[10] Y. Erez, I. Presiado, R. Gepshtein, L. Pinto da Silva, J. C. G. Esteves da Silva, D. Huppert, *J. Phys. Chem. A* **2012**, *116*, 7452–7461.
[11] L. Pinto da Silva, R. Sinkovitch, D. Huppert, J. C. G. Esteves da Silva, *J. Photochem. Photobiol. A* **2013**, *266*, 47–54.

[12] K. M. Solntsev, S. P. Laptenok, P. Naumov, *J. Am. Chem. Soc.* **2012**, *134*, 16452 – 16455.
[13] T. Wilson, J. W. Hastings, *Annu. Rev. Cell Dev. Biol.* **1998**, *14*, 197 – 230.
[14] V. R. Viviani, *Cell. Mol. Life Sci.* **2002**, *59*, 1833 – 1850.
[15] H. Fraga, *Photochem. Photobiol. Sci.* **2008**, *7*, 146 – 158.
[16] S. M. Marques, J. C. G. Esteves da Silva, *IUBMB Life* **2009**, *61*, 6 – 17.
[17] A. Roda, M. Guardigli, *Anal. Bioanal. Chem.* **2012**, *402*, 69 – 76.
[18] A. Roda, M. Guardigli, E. Michelini, M. Mirasoli, *Anal. Bioanal. Chem.* **2009**, *393*, 109 – 123.
[19] K. Hochgräfe, E. M. Mandelkow, *Mol. Neurobiol.* **2013**, *47*, 868 – 882.
[20] J. Vieira, L. Pinto da Silva, J. C. G. Esteves da Silva, *J. Photochem. Photobiol. B* **2012**, *117*, 33 – 39.
[21] S. Hosseinkhani, *Cell. Mol. Life Sci.* **2011**, *68*, 1167 – 1182.
[22] L. Pinto da Silva, J. C. G. Esteves da Silva, *J. Chem. Theory Comput.* **2011**, *7*, 809 – 817.
[23] J. Y. Hasegawa, K. J. Fujimoto, H. Nakatsuji, *ChemPhysChem* **2011**, *12*, 3106 – 3115.
[24] V. R. Viviani, F. G. C. Arnoldi, A. J. S. Neto, T. L. Oehlmeyer, E. J. H. Bechara, Y. Ohmiya, *Photochem. Photobiol. Sci.* **2008**, *7*, 159 – 169.
[25] L. Pinto da Silva, J. C. G. Esteves da Silva, *J. Phys. Chem. B* **2014**, DOI: 10.1021/jp5036458.
[26] D. Cai, M. A. Marques, F. Nogueira, *J. Phys. Chem. B* **2013**, *117*, 13725 – 13730.
[27] N. Nakatani, J. Y. Hasegawa, H. Nakatsuji, *J. Am. Chem. Soc.* **2007**, *129*, 8756 – 8765.
[28] I. Navizet, Y. J. Liu, N. Ferré, H. Y. Xiao, W. H. Fang, R. Lindh, *J. Am. Chem. Soc.* **2010**, *132*, 706 – 712.
[29] L. Pinto da Silva, J. C. G. Esteves da Silva, *ChemPhysChem* **2011**, *12*, 3002 – 3008.
[30] C. G. Min, A. M. Ren, J. F. Guo, L. Y. Zou, J. D. Goddard, C. C. Sun, *ChemPhysChem* **2010**, *11*, 2199 – 2204.
[31] Y. Wang, Y. Hayamizu, H. Akiyama, *J. Phys. Chem. B* **2014**, *118*, 2070 – 2076.
[32] L. Pinto da Silva, J. C. G. Esteves da Silva, *J. Phys. Chem. B* **2012**, *116*, 2008 – 2013.
[33] J. C. G. Esteves da Silva, J. M. C. S. Magalhães, R. Fontes, *Tetrahedron Lett.* **2001**, *42*, 8173 – 8176.
[34] P. Naumov, Y. Ozawa, K. Ohkubo, S. Fukuzumi, *J. Am. Chem. Soc.* **2009**, *131*, 11590 – 11605.
[35] V. R. Viviani, D. R. Neves, D. T. Amaral, R. A. Prado, T. Matsuhashi, T. Hirano, *Biochemistry* **2014**, DOI: 10.1021/bi500160m.
[36] B. R. Branchini, M. H. Murtiashaw, R. A. Magyar, N. C. Portier, M. C. Ruggiero, J. G. Stroh, *J. Am. Chem. Soc.* **2002**, *124*, 2112 – 2113.
[37] I. Presiado, Y. Erez, R. Simkovitch, S. Shomer, R. Gepshtein, L. Pinto da Silva, J. C. G. Esteve da Silva, D. Huppert, *J. Phys. Chem. A* **2012**, *116*, 10770 – 10779.
[38] L. Pinto da Silva, R. Simkovitch, D. Huppert, J. C. G. Esteves da Silva, *ChemPhysChem* **2013**, *14*, 2711 – 2716.
[39] O. V. Maltsev, L. Yue, M. Rebarz, L. Hintermann, M. Sliwa, C. Ruckebusch, L. Pejov, Y. J. Liu, P. Naumov, *Chem. Eur. J.* **2014**, DOI. 10.1002/chem.201400210.
[40] L. Pinto da Silva, J. C. G. Esteves da Silva, *ChemPhysChem* **2011**, *12*, 951 – 960.
[41] Y. Erez, D. Huppert, *J. Phys. Chem. A* **2010**, *114*, 8075 – 8082.
[42] Y. Erez, I. Presiado, R. Gepshtein, D. Huppert, *J. Phys. Chem. A* **2011**, *115*, 1617 – 1626.
[43] S. F. Boys, F. Bernardi, *Mol. Phys.* **1970**, *19*, 553 – 566.
[44] S. Simon, M. Duran, J. J. Dannenberg, *J. Chem. Phys.* **1996**, *105*, 11024 – 11031.
[45] C. R. Martinez, B. L. Iverson, *Chem. Sci.* **2012**, *3*, 2191 – 2201.
[46] R. Podeszwa, R. Bukowski, K. Szalewicz, *J. Phys. Chem. A* **2006**, *110*, 10345 – 10354.
[47] M. O. Sinnokrot, C. D. Sherrill, *J. Am. Chem. Soc.* **2004**, *126*, 7690 – 7697.
[48] B. F. Milne, M. A. Marques, F. Nogueira, *Phys. Chem. Chem. Phys.* **2010**, *12*, 14285 – 14293.
[49] D. Cai, M. A. L. Marques, B. F. Milnes, F. Nogueira, *J. Phys. Chem. Lett.* **2010**, *1*, 2781 – 2787.
[50] D. Cai, M. A. Marques, F. Nogueira, *J. Phys. Chem. B* **2011**, *115*, 329 – 332.
[51] L. Pinto da Silva, P. J. O. Ferreia, D. J. R. Duarte, M. S. Miranda, J. C. G. Esteves da Silva, *J. Phys. Chem. A* **2014**, *118*, 1511 – 1518.
[52] M. S. Miranda, L. Pinto da Silva, J. C. G. Esteves da Silva, *J. Phys. Org. Chem.* **2014**, *27*, 47 – 56.
[53] K. Støchkel, C. N. Hansen, J. Houmøller, L. M. Nielsen, M. Linares, P. Norman, F. Nogueira, O. V. Maltsev, L. Hintermann, S. B. Nielsen, P. Naumov, B. F. Milne, *J. Am. Chem. Soc.* **2013**, *135*, 6485 – 6493.
[54] M. Rosenberg, T. I. Solling, *Chem. Phys. Lett.* **2010**, *484*, 113 – 118.
[55] N. Singla, P. Chowdhury, *Chem. Phys. Lett.* **2012**, *548*, 71 – 79.
[56] B. K. Paul, S. Mahanta, R. B. Singh, N. Guchhait, *J. Phys. Chem. A* **2010**, *114*, 2618 – 2627.
[57] S. Mahanta, B. K. Paul, R. B. Singh, N. Guchhait, *J. Comput. Chem.* **2011**, *32*, 1 – 14.
[58] R. B. Singh, S. Mahanta, N. Guchhait, *J. Photochem. Photobiol. A* **2008**, *200*, 325 – 333.
[59] R. de Vivie-Riedle, V. De Waele, L. Kurtz, E. Riedle, *J. Phys. Chem. A* **2003**, *107*, 10591 – 10599.
[60] L. Pinto da Silva, J. C. G. Esteves da Silva, *Photochem. Photobiol. Sci.* **2013**, *12*, 2028 – 2035.
[61] L. Pinto da Silva, J. C. G. Esteves da Silva, *Chem. Phys. Lett.* **2014**, *608*, 45 – 49.
[62] C. Adamo, V. Barone, *J. Chem. Phys.* **1999**, *110*, 6158 – 6169.
[63] L. Pinto da Silva, J. C. G. Esteves da Silva, *Int. J. Quantum Chem.* **2013**, *113*, 45 – 51.
[64] D. Jacquemin, E. A. Perpète, I. Ciofini, C. Adamo, *Theor. Chem. Acc.* **2011**, *128*, 127 – 136.
[65] D. Jacquemin, V. Wathelet, E. A. Perpète, C. Adamo, *J. Chem. Theory Comput.* **2009**, *5*, 2420 – 2435.
[66] D. A. Case, T. E. Cheatham, T. Darden, H. Gohlke, R. Luo, K. M. Merz, A. Onufriev, C. Simmelring, B. Wang, R. Woods, *J. Comput. Chem.* **2005**, *26*, 1668 – 1688.
[67] J. C. Phillips, R. Braun, W. Wang, J. Gumbart, W. Tajkhorshid, E. Villa, C. Chipot, R. D. Skell, L. Kale, K. Schulten, *J. Comput. Chem.* **2005**, *26*, 1781 – 1802.
[68] U. Essmann, L. Perera, M. L. Berkowitz, T. Darden, H. Lee, L. G. Pedersen, *J. Chem. Phys.* **1995**, *103*, 8577 – 8593.
[69] J. M. Wang, R. M. Wolf, J. W. Caldwell, P. A. Kollman, D. A. Case, *J. Comput. Chem.* **2004**, *25*, 1157 – 1174.
[70] J. D. Chai, M. Head-Gordon, *Phys. Chem. Chem. Phys.* **2008**, *10*, 6615 – 6620.
[71] G. Scalmani, M. J. Frisch, B. Mennucci, J. Tomasi, R. Cammi, V. Barone, *J. Chem. Phys.* **2006**, *124*, 094107 .
[72] M. Cossi, N. Rega, G. Scalmani, V. Barone, *J. Comput. Chem.* **2003**, *24*, 669 – 681.
[73] C. Adamo, D. Jacquemin, *Chem. Soc. Rev.* **2013**, *42*, 845 – 856.
[74] Gaussian 09 (Revision A.02), M. J. Frisch et al., Gaussian Inc., Wallingford, CT, **2009**.

Received: August 1, 2014
Published online on September 18, 2014

6.5. Study of the Possible Involvement of Enolate $OxyLH_2$ in Firefly Bioluminescence as a Light Emitter

Article 27

Efficient firefly chemi/bioluminescence: evidence for chemiexcitation resulting from the decomposition of a neutral firefly dioxetanone molecule
Luís Pinto da Silva, A. Joel M. Santos and Joaquim C.G. Esteves da Silva
J. Phys. Chem. A **2013**, *117*, 94-100.

The theoretical calculations were performed by Luís Pinto da Silva, while the experimental studies were performed by both Luís Pinto da Silva and Joel Santos. The writing of the paper was performed by Luís Pinto da Silva. This work was made under the supervision of Professor Joaquim Esteves da Silva.

THE JOURNAL OF PHYSICAL CHEMISTRY A
Article
pubs.acs.org/JPCA

Efficient Firefly Chemi/Bioluminescence: Evidence for Chemiexcitation Resulting from the Decomposition of a Neutral Firefly Dioxetanone Molecule

Luís Pinto da Silva, A. Joel M. Santos, and Joaquim C. G. Esteves da Silva*

Centro de Investigação em Química, Departamento de Química e Bioquímica, Faculdade de Ciências da Universidade do Porto, R. Campo Alegre 687, 4169-007 Porto, Portugal

Supporting Information

ABSTRACT: Both experimental and theoretical methodologies were employed in order to study the possibility of excited state oxyluciferin being formed as the result of the decomposition of a neutral dioxetanone. Excitation measurements in water (at different pH values) and in methanol, along with computational calculations, demonstrated that the hydroxyl-benzothiazole group of firefly dioxetanone and six oxyluciferin analogues is only deprotonated in conditions not in line with the firefly bioluminescence reaction. Thus, a new mechanism involving a neutral firefly dioxetanone must be presented in order to explain the chemiexcitation of oxyluciferin. It was also studied for the first time the interaction between a molecule involved in the bioluminescence reaction (neutral firefly dioxetanone) and the real second conformation of firefly luciferase.

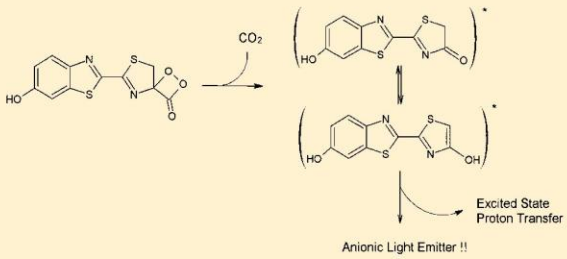

INTRODUCTION

Chemiluminescence is the emission of energy with limited emission of heat, as the result of a chemical reaction.[1] When this phenomenon occurs in a living organism, due to enzyme-catalyzed reaction, it is termed bioluminescence.[2−7] Both phenomena are gaining numeral practical applications in the fields of pharmaceutical, biomedical, and bioanalytical analysis, among others.[8−12]

The most important chemi/bioluminescence system is that of the fireflies, due to very high quantum yields (~40−60%).[13,14] Firefly luciferase catalyzes a two-step reaction: first, D-luciferin (D-LH_2) reacts with adenosine-5′-triphosphate-Mg^{2+} (ATP-Mg^{2+}), leading to the generation of an adenylyl intermediate (D-LH_2-AMP); in the second step, D-LH_2-AMP is oxidized in the presence of molecular oxygen (O_2), which results in the formation of oxyluciferin ($OxyLH_2$), adenosine-5′-monophosphate (AMP), and carbon dioxide (CO_2).[2−7,15,16] $OxyLH_2$ is thought to be formed in its anionic keto-form, in a singlet excited state, decaying to the ground state with emission of visible light[17−19] (Scheme 1).

It was demonstrated that $OxyLH_2$ is produced in a singlet excited state due to the formation and subsequent decomposition of firefly dioxetanone (FiDiox)[1−7] (Scheme 1). The efficient chemiexcitation is then thought to occur due to crossing points between the singlet ground and excited potential energy surfaces on the reaction coordinate.[20,21] The efficiency of bioluminescence is then described in terms of quantum yield, which is controlled by the efficiency of the chemical reaction, the efficiency of crossing to the excited state, and the efficiency of the fluorescence of the excited state product.[1−7]

FiDiox is supposed to have a deprotonated benzothiazole hydroxyl group, both because $OxyLH_2$ is formed in an anionic form and due to energetic reasons. The deprotonation of this hydroxyl group is expected to lower the energy barrier of FiDiox decomposition to values more appropriated to a favorable reaction.[3,20−23] Also, this deprotonated electron-donating hydroxyl-benzothiazole moiety is expected to explain the efficient formation of singlet excited state products. Several authors have proposed mechanisms in which the deprotonation of the hydroxyl-benzothiazole moiety trigger charge transfer phenomena, which are responsible for the efficient singlet excitation.[3,20,23−25]

Very recently we have studied the binding of D-LH_2-AMP and two other adenylates to *Luciola cruciata* luciferase.[26] Our calculations have indicated that the hydroxyl-benzothiazole group of these adenylates is indeed protonated in the active site of this enzyme. Also, there is experimental data that indicates that, in the ground state, the hydroxyl-benzothiazole group of D-LH_2 and $OxyLH_2$ is only deprotonated in water (dielectric constant of 78) at basic pH (pH ≈ 7−10) and not in less polar solvents or at acidic pH.[27−31]

Given that the active site of an enzyme (luciferase included) is characterized by a dielectric constant of 2.5−4, the bioluminescence reaction can occur in a pH range of ~5−

Received: October 24, 2012
Revised: December 14, 2012
Published: December 17, 2012

dx.doi.org/10.1021/jp311711p | J. Phys. Chem. A 2013, 117, 94−100

The Journal of Physical Chemistry A Article

Scheme 1. Schematic Representation of the Firefly Bioluminescence Reaction; X Can Either Represent a Protonated or Deprotonated −OH Group

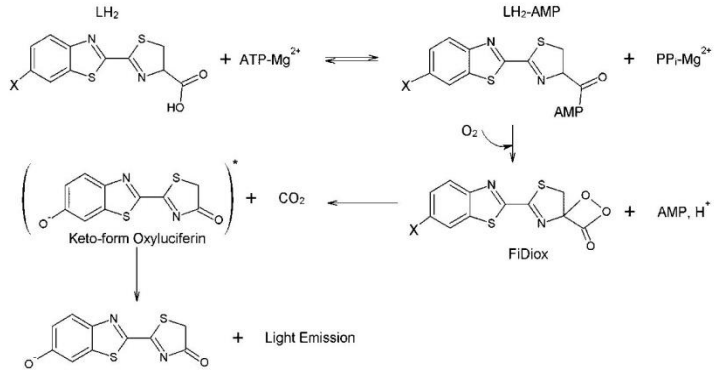

8,[2,15,32] and the hydroxyl-benzothiazole group of ground state D-LH_2, D-LH_2-AMP, and OxyLH_2 appear to be protonated in these conditions,[26−31] it is strange that the deprotonation of the same group in FiDiox can occur in the same conditions. It should be noted that the computational studies, in which was stated that the deprotonation of the hydroxyl-group was needed for an efficient bioluminescence, have only studied FiDiox outside of the enzymatic microenvironment.[20−23] Thus, they have ignored the geometric restraints imposed by the enzyme, and all types of intermolecular interactions that can occur between FiDiox and active site molecules. Moreover, we can not forget that an enzyme is a biological catalyst, so its job is to increase the rate of the chemical reactions that it catalyzes. So, any claim of the necessity of a deprotonated hydroxyl-group for an efficient firefly bioluminescence unsupported by studies inside the enzymatic environment is not a reliable one. Moreover, we cannot forget that it was computationally demonstrated that, during the decomposition of neutral FiDiox, there is a path for singlet excitation.[20]

Even the evidence that excited state OxyLH_2 is produced in its anionic form[17−19] is not a determinant factor for the necessity of a deprotonated hydroxyl-group. More recently, it has being demonstrated that OxyLH_2 and analogues are very strong photoacids.[30,31,33−37] Thus, OxyLH_2 can be chemiexcited from a neutral FiDiox and then undergo an excited state proton transfer (ESPT) process with active site molecules, in order to lose a proton and form an excited state anionic species.

Thus, and taking all these evidence into consideration, the objective of this work is to consider the possibility of the efficient firefly bioluminescence being a result of the decomposition of a neutral FiDiox. First, we will study the excitation spectra of six OxyLH_2 analogues, in various conditions of polarity and pH, in order to demonstrate that the hydroxyl-benzothiazole group cannot be deprotonated in the ground state, in conditions similar to that found in the bioluminescence reaction. Also, we will computationally verify if the deprotonation of the hydroxyl-benzothiazole group of FiDiox is similar to that experimentally verified for some of the six OxyLH_2 analogues studied here. Finally, we will be the first to study the interaction between neutral FiDiox and the active site of the newly found second catalytic conformation of *Photinus pyralis* luciferase.[41]

MATERIAL AND METHODS

Materials. The OxyLH_2 analogues studied in this article were D-LH_2, L-LH_2, dehydroLH_2 (L), L-6′methoxiLH_2 (L-MOLH_2), D-6′ethylLH_2 (D-ELH_2), and D-5,5-dimethylLH_2 (D-DMLH_2) (Chart 1). D-LH_2 and D-ELH_2 were purchased from

Chart 1. Schematic Representation of the Six OxyLH_2 Analogues

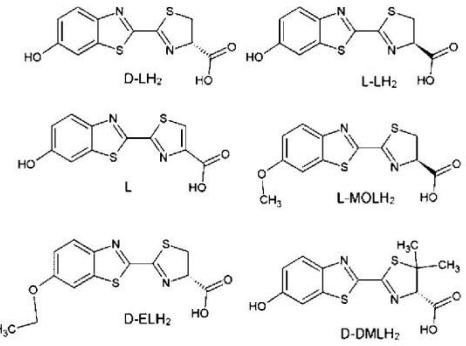

Sigma, as well as HEPES (4-(-2-hydroxyethyl)-1-piperazineethanesulfonic acid) and MES (2-(*N*-morpholino)-ethanesulfonic acid). HEPES buffer was used for basic pH, while MES was used for acid pH values. The pH values were adjusted by the addition of NaOH and HCl. In pH values below 3, the buffer effect was provided by the addition of the strong acid HCl. L, L-LH_2, L-MOLH_2, and D-DMLH_2 were synthesized and purified as described previously and were stocked in aqueous solutions.[38−42] Isocratic grade methanol was purchased from Merck. Sample used in absorption measurements that contained methanol, contained also 2−10% of water, due to the fact that the fluorophores were already dissolved in this solvent. The samples were prepared in deoxygenized solvents, in an inert atmosphere, in order to ensure that the fluorophores were stable.

Excitation Spectroscopy. Excitation spectra were recorded with a Horiba Jovin Yvon Fluoromax 4 TCSPC with an integration time of 0.1 s, using slit widths of 5 nm for excitation monochromators. The emission wavelengths used, in pH range 0.68−10.0 and water and methanol, were 530 nm for D-LH_2, L-LH_2, and D-DMLH_2, 550 nm for L, and 440 nm for L-MOLH_2 and D-ELH_2. Quartz cells, with a volume of 800 μL,

dx.doi.org/10.1021/jp311711p | J. Phys. Chem. A 2013, 117, 94−100

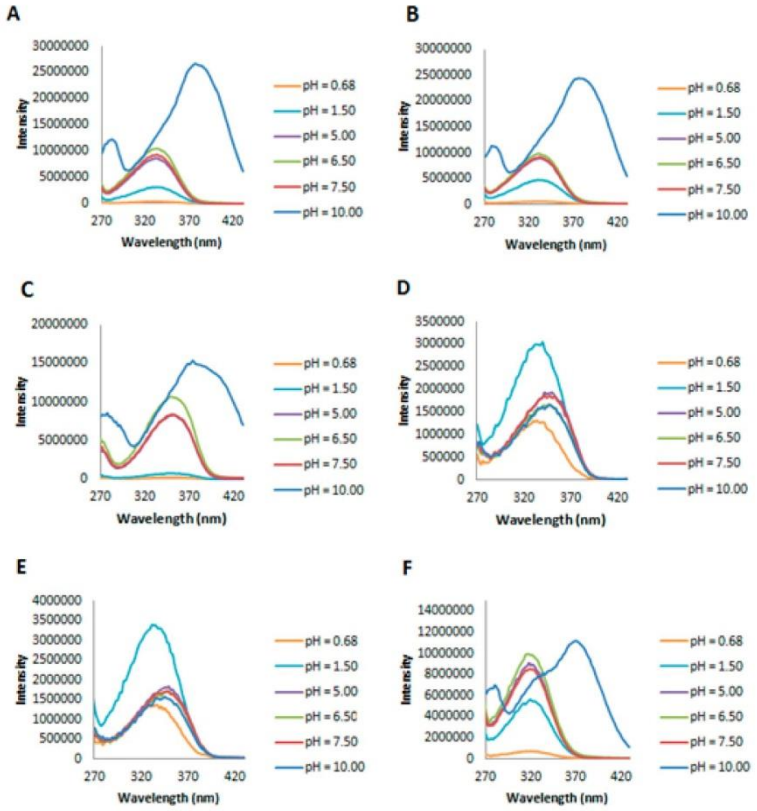

Figure 1. Excitation spectra of D-LH_2 (A), L-LH_2 (B), L (C), L-$MOLH_2$ (D), D-ELH_2 (E), and D-$DMLH_2$ (F), in various pH values.

were used. The fluorophores were studied at the concentration of 10 μM.

Computational Methods. Ground state geometry optimizations and frequency calculations were performed at the mPWKCIS/6-31G(d,p) level of theory, while the energies were recalculated at the mPWKCIS/6-31+G(d,p) level of theory.[44] The geometry optimizations were performed in vacuo. Some energies were recalculated with implicit solvent effects, by using the conductor-like polarized continuum model (CPCM) and the UAKS radii.[45]

We have used the mPWKCIS functional in geometry optimizations calculations due to good results in the optimizations of other dioxetanones.[46−48] The 6-31G(d,p) basis set was used in geometry optimizations due to its previous use in the geometry optimization of anionic and neutral FiDiox.[20]

The PDB structure 4G37 (*Photinus pyralis* luciferase trapped in the second catalytic conformation) was used as a starting structure in the study of the interaction of neutral FiDiox with luciferase.[43] Hydrogen atoms were added to the 4G37 structure by the MolProbity web server.[49] From the resulting structures were withdrawn the ligand DLSA and active site molecules Ala348, Arg218, Asp422, Gln448, Gly/341/339/316/315, His245, Lys443, Phe247, Ser 314/347, Thr343, Tyr340, and Wat772. These molecules were chosen due to their proximity to FiDiox and to their presence on previous studies of firefly bioluminescence.[19,26,43,50−57] The ligand DLSA was transformed in neutral FiDiox and AMP with the aid of the Avogadro software.[58] An initial guess for the geometry of this complex was obtained with the geometry optimization function of Avogadro.[58] Further geometry calculations were obtained with our own N-layered integrated molecular orbital and molecular mechanics (ONIOM) method.[59] Neutral FiDiox was included in the high layer, in which was used the mPWKCIS/6-31G(d,p) level of theory, while AMP and the remaining active site molecules were included in the low layer (in which the Dreiding force field was used).[60]

All the theoretical calculations were performed with the Gaussian03 software package.[61]

■ RESULTS AND DISCUSSION

Effect of the pH on the Excitation Measurements. Figure 1 and Table S1, Supporting Information, refer to the absorption of $OxyLH_2$ analogues at various values of pH.

Analyses of the excitation spectra (and Table S1, Supporting Information) demonstrate that L, L-$MOLH_2$, and D-ELH_2 present the longer wavelength maxima, while D-$DMLH_2$ presents the lower (pH 0.68−7.50). However, at pH 10.0, the excitation maxima of L, D-$DMLH_2$, D-LH_2, and L-LH_2 suffer from an accentuated red-shift. This phenomenon is expected to be caused by deprotonation of the benzothiazole oxygen, which is supported by the fact that the two molecules that do not present this red-shift cannot undergo this deprotonation (L-$MOLH_2$ and D-ELH_2, Chart 1). Naumov and co-worker have already demonstrated the importance of deprotonated benzothiazole oxygen for a more red-shift emission and excitation.[28] These results are in line with previous experimental studies of D-LH_2 and L.[29−31,33−36] These data

dx.doi.org/10.1021/jp311711p | J. Phys. Chem. A 2013, 117, 94−100

clearly indicate that, even in a polar environment as water, the hydroxyl-benzothiazole group of this type of molecule is not easily deprotonated in the ground state. In fact, only at basic pH (pH of 10) it is seen a red-shift associated with that deprotonation.[29−31,33−36] This was also seen for oxyluciferin.[30] As we know that the bioluminescence reaction also occurs at acidic pH (pH ≈ 5−6),[2,15] it appears to be very difficult to believe that an anionic FiDiox molecule is involved in the chemiexcitation of $OxyLH_2$. As for the higher excitation intensity of the deprotonated form, when in comparison with the protonated form, Naumov and co-worker have shown that, for an oxyluciferin derivative, the absorbance is higher with higher pH and wavelength.[28] Thus, a higher absorbance of the deprotonated form, could explain the higher excitation intensities.

Considering previous and present results,[29−31,33−36] these LH_2 molecules should be an anionic species in the ground state during nearly all the pH range (the carboxylic group has a pK_a ≈ 3). In the ground state, in the pH range of ∼8−10, the hydroxyl-benzothiazole group is also deprotonated. Thus, these results indicate that the ground state deprotonation of the hydroxyl-benzothiazole group of FiDiox should only occur at basic pH. However, the bioluminescence reaction is known to occur at both acidic and basic pH.[2,15,30,31,33−37] Therefore, it appears that the deprotonation of the hydroxyl-benzothiazole group of FiDiox does not occur at the same conditions of the firefly bioluminescence reaction.

Effect of the Polarity on the Excitation Measurements. Figure 2 and Table S2, Supporting Information, refer to the excitation of $OxyLH_2$ analogues in water and methanol. Despite the important information provided by the measurements in aqueous solutions at various pH values, the active site of firefly luciferase is expected to be much less polar than an aqueous solution.[32,50,52] Therefore, measurements in a less polar environment were needed.

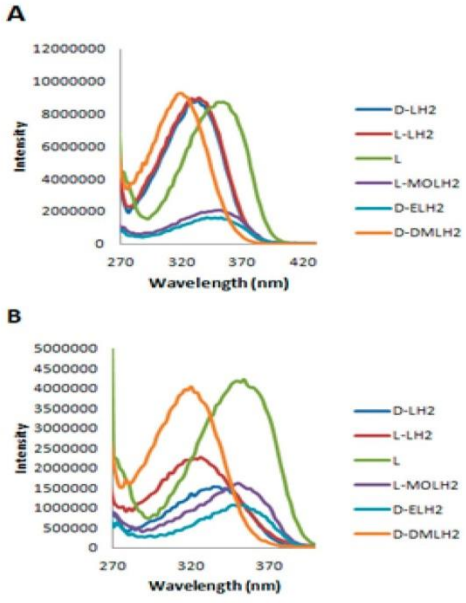

Figure 2. Excitation spectra in water (A) and methanol (B).

Analyses of the excitation spectra (and Table S2, Supporting Information) demonstrate that L, L-$MOLH_2$, and D-ELH_2 present the longer wavelength maxima. Also, the wavelength maxima (Table S2, Supporting Information) indicate that the hydroxyl-benzothiazole group is protonated in two different solvents. Moreover, it can also be seen that the polarity of the solvent does not have a relevant effect in the excitation spectra of these analogues, as the wavelength maxima are basically the same in the two solvents.

The results here presented indicate that not even in environments of lower polarity it can be observed the deprotonation of the hydroxyl-benzothiazole group. This further indicates that it is more likely that the hydroxyl-benzothiazole group of FiDiox is protonated inside of the active site of firefly luciferase. This is in line with the protonated state of D-LH_2-AMP and two other adenylates inside of *Luciola cruciata* luciferase.[26] Moreover, it is also in line with the experimental data regarding LH_2 and $OxyLH_2$.[27−31] Finally, this is in line with the possibility advanced by Naumov and co-workers, which is that the light emitter of *Cypridina* luminescence is chemiexcited from a neutral dioxetanone.[62]

Computational Study of the Ground State Deprotonation of Neutral FiDiox. In order to see if the deprotonation of the hydroxyl-benzothiazole group of neutral FiDiox can be comparable to the deprotonation of the same group in the six $OxyLH_2$ derivatives referred above, we have optimized the geometry of neutral FiDiox, D-LH_2, L, and D-$DMLH_2$ at the mPWKCIS/6-31G(d,p) level of theory. A relaxed coordinate scan was made in order to see the energetics of the O−H bond elongation of the hydroxyl group of these four molecules. The energies were re-evaluated at the mPWKCIS/6-31+G(d,p) level of theory. These single-point calculations were performed in implicit water, methanol, and with a dielectric constant of 4 (Figure 3) in order to simulate the hydrophobic environment of the luciferase active site.

It can be seen that the behavior of the O−H bond elongation of neutral FiDiox is very similar to that presented by the other three molecules, in the three different implicit environments. Moreover, we can see that, with decreasing polarity, the higher the energy needed for O−H bond elongations. Thus, these calculations indicate that the hydroxyl-benzothiazole group of neutral FiDiox behaves similarly to the ones present in the $OxyLH_2$ derivatives, which indicates that the probability of being an anionic FiDiox molecule to chemiexcited $OxyLH_2$ is apparently very low.

Interaction of Neutral FiDiox with *Photinus pyralis* Luciferase. Rather recently it was demonstrated by crystallography experiments, that firefly luciferase can adopt two very different conformations for the adenylation and oxidative steps, due to ∼140 °C terminal domain rotation.[43] This discovery clashes with previous assumptions that the conformation of the active site, during the two steps of the bioluminescence reaction, was very similar.[19,26,50−57] Therefore, despite numerous computational studies, apparently there is no study performed in the real conformation of the luciferase active site, at the oxidative step. In order to fill this gap in the existent literature, we have studied the interaction of FiDiox with active site molecules of this conformation and see the effect exerted by them in the geometric and charge parameters of FiDiox when compared with its in vacuo structure (Figure 4).

In Chart 2 are identified the different moieties analyzed in this subsection. In Table 1 are presented the atomic Mulliken charges of the $OxyLH_2$, CO_2, and Diox moieties, at the

dx.doi.org/10.1021/jp311711p | J. Phys. Chem. A 2013, 117, 94−100

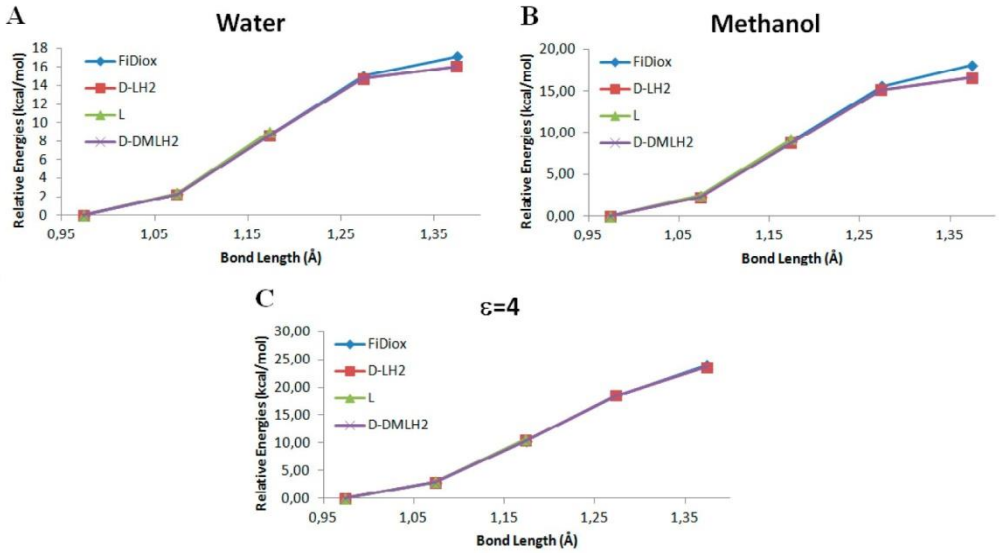

Figure 3. Relative energies of FiDiox, D-LH_2, L, and D-$DMLH_2$ at different hydroxyl O−H bond lengths (in Å) in implicit water (A), methanol (B), and with a dielectric constant (ε) of 4.

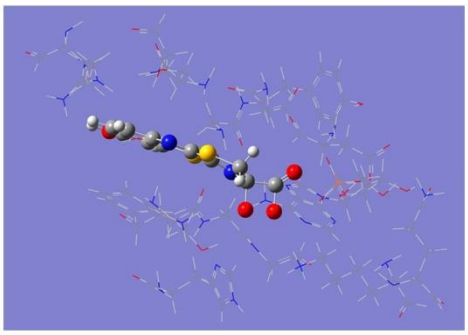

Figure 4. Neutral FiDiox interacting with active site molecules of the second conformation of *Photinus pyralis* luciferase.

Chart 2. Schematic Representation of Neutral FiDiox, and the Dioxetanone (Diox), $OxyLH_2$, and CO_2 Moieties

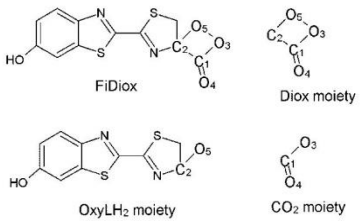

Table 1. Atomic Mulliken Charges of Diox, $OxyLH_2$, and CO_2 Moieties of in Vacuo FiDiox and Neutral FiDiox Optimized with Active Site Molecules (FiDiox-Luc)

	in vacuo FiDiox	FiDiox-Luc
Diox	−0.17	−0.27
$OxyLH_2$	0.05	0.04
CO_2	−0.05	−0.04

mPWKCIS/6-31+G(d,p) level of theory. These in vacuo single-point calculations only included the FiDiox molecules and not the active site molecules. It can be seen that the two FiDiox molecules present different charge distribution. The in vacuo $OxyLH_2$ moiety is positive by 0.05, while the CO_2 moiety is negative by −0.05. In the case of the FiDiox molecule, which resulted from the optimization calculation with active site molecules, the $OxyLH_2$ moiety is positive by 0.04, while the CO_2 moiety is negative by −0.04. In the case of the Diox moiety, it can be seen that it is negative in both cases, but more negative (by 0.10) in the case of the FiDiox that resulted from the geometry optimization with active site molecules.

In Table 2 are presented the atomic Mulliken charges of the atoms that constitute the Diox moiety. It can be seen that both

Table 2. Atomic Mulliken Charges of O_5, C_2, C_1, O_3, and O_4 of in Vacuo FiDiox and Neutral FiDiox Optimized with Active Site Molecules (FiDiox-Luc)

in vacuo FiDiox		FiDiox-Luc	
O_5	−0.13	O_5	−0.12
C_2	0.01	C_2	−0.11
C_1	0.40	C_1	0.41
O_3	−0.10	O_3	−0.10
O_4	−0.35	O_4	−0.35

O_5 and O_3 are negative atoms, with very similar charges, in both cases. The negative charge of O_4 is the same in both cases. In the case of C_1, there is a very small increase in its positive charge in the FiDiox that resulted from the geometry optimization with active site molecules, when compared with the in vacuo FiDiox. In the case of C_2, there is a large increase of negative charge when we compare the FiDiox that resulted from the geometry optimization with active site molecules with the in vacuo FiDiox.

In Table 3 are presented the geometric parameters of the Diox moiety. It can be seen that only negligible differences between the geometries of the Diox moieties of FiDiox. In

dx.doi.org/10.1021/jp311711p | J. Phys. Chem. A 2013, 117, 94−100

Table 3. Bond Lengths (in Å) and Angles and Dihedral (in deg) of the Diox Moiety of in Vacuo FiDiox and Neutral FiDiox Optimized with Active Site Molecules (FiDiox-Luc)

	in vacuo FiDiox	FiDiox-Luc
O_5-O_3	1.53	1.53
C_2-C_1	1.54	1.54
C_2-O_5	1.48	1.48
C_1-O_3	1.38	1.38
$O_5-C_2-C_1$	86.38	86.26
$O_3-C_1-C_2$	93.23	93.25
$O_5-C_2-C_1-O_3$	−0.38	−0.53

Figure 5, there is a visual comparison between the in vacuo FiDiox and the FiDiox that resulted from the geometry

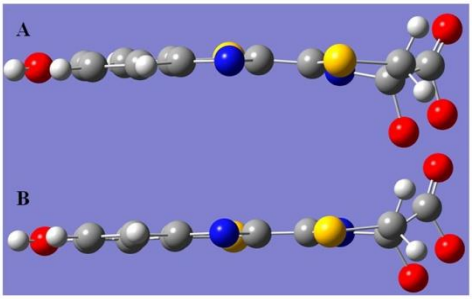

Figure 5. Structures of neutral FiDiox when optimized with active site molecules (A) and in vacuo FiDiox.

optimization with active site molecules, in which we can see that the geometry $OxyLH_2$ moiety was affected by interaction with active site molecules.

CONCLUSIONS

The possibility of $OxyLH_2$ being chemiexcited from the decomposition of a neutral FiDiox molecule was studied by means of both experimental and theoretical means.

Excitations measurements of six $OxyLH_2$ derivatives, in aqueous solutions of different pH values and in methanol, demonstrated that the hydroxyl-benzothiazole group is only deprotonated in water at basic pH. Theoretical calculations demonstrated that the hydroxyl-benzothiazole group of FiDiox has the same behavior as that of the same group in the above referred six $OxyLH_2$ analogues. The findings that this functional group is only deprotonated in polar environments ($\varepsilon \approx 78$) and at basic pH, while the bioluminescence reaction occurs in hydrophobic environments ($\varepsilon \approx 2.5-4$) and in a wide range of pH (~5−8), indicates that there is no possibility of existing an anionic FiDiox molecule in active site of firefly luciferase. Thus, our results indicate that chemiexcitation must occur from the decomposition of a neutral FiDiox molecule, as it is thought to occur in the case of *Cypridina* luminescence.[62] Anionic $OxyLH_2$ can then be formed by an ESPT process with an active site molecule, which can be expected due to numerous reports of the strong photoacidity of this type of molecules. These findings uncovered a brand new chemiexcitation mechanism for anionic $OxyLH_2$ formation.

In this work, it was also computationally studied for the first time the interaction between a molecule involved in the bioluminescence reaction, with the active site of the real conformation of luciferase for the oxidative step. Neutral FiDiox geometry was optimized with active site molecules of this conformation, and the effect exerted by these active site molecules on its geometric and charge density parameters was evaluated (by comparing the results with those obtained for in vacuo FiDiox).

Efforts are being made in order to study the decomposition reaction of neutral FiDiox in the active site of the real second conformation of firefly luciferase and to find a proton acceptor for the ESPT process between excited state $OxyLH_2$ and an active site molecule.

ASSOCIATED CONTENT

Supporting Information

Excitation wavelength maxima of the six $OxyLH_2$ derivatives and Cartesian coordinates of important molecules. This material is available free of charge via the Internet at http://pubs.acs.org.

AUTHOR INFORMATION

Corresponding Author

*Tel: 351 226082869. Fax: 351 226082959. E-mail: jcsilva@fc.up.pt.

Notes

The authors declare no competing financial interest.

ACKNOWLEDGMENTS

Financial support from Fundação para a Ciência e Tecnologia (FCT, Lisbon) (Programa Operacional Temático Factores de Competitividade (COMPETE) e comparticipado pelo Fundo Comunitário Europeu (FEDER)) (Project PTDC/QUI/71366/2006) is acknowledged. A Ph.D. Grant to L.P.d.S. (SFRH/BD/76612/2011), attributed by FCT, is also acknowledged.

REFERENCES

(1) Matsumoto, M. *J. Photochem. Photobiol., C* **2004**, *5*, 27.
(2) Pinto da Silva, L.; Esteves da Silva, J. C. G. *ChemPhysChem* **2012**, *13*, 2257.
(3) Navizet, I.; Liu, Y. J.; Ferre, N.; Roca-Sanjuan, D.; Lindh, R. *ChemPhysChem* **2011**, *12*, 3064.
(4) McCapra, F. *Acc. Chem. Res.* **1976**, *9*, 201.
(5) Hosseinkhani, S. *Cell. Mol. Life Sci.* **2011**, *68*, 1167.
(6) Wood, K. V. *Photochem. Photobiol.* **1995**, *62*, 662.
(7) Fraga, H. *Photochem. Photobiol. Sci.* **2008**, *7*, 146.
(8) Doyle, T. C.; Burns, S. M.; Contag, C. H. *Cell. Microbiol.* **2004**, *6*, 303.
(9) Luker, K. E.; Luker, G. D. *Antiviral Res.* **2008**, *78*, 179.
(10) Branchini, B. R.; Southworth, T. R.; Khattak, N. F.; Michelini, E.; Roda, A. *Anal. Biochem.* **2005**, *345*, 140.
(11) Fan, F.; Wood, K. V. *Assay Drug Dev. Technol.* **2007**, *5*, 127.
(12) Roda, A.; Guardigli, M. *Anal. Bioanal. Chem.* **2012**, *402*, 69.
(13) Ando, Y.; Niwa, K.; Yamada, N.; Enomot, T.; Irie, T.; Kubota, H.; Ohmiya, Y.; Akiyama, H. *Nat. Photonics* **2008**, *2*, 44.
(14) Niwa, K.; Ichino, Y.; Kumata, S.; Nakajima, Y.; Hiraishi, Y.; Kato, D.; Viviani, V. R.; Ohmiya, Y. *Photochem. Photobiol.* **2010**, *86*, 1046.
(15) Marques, S. M.; Esteves da Silva, J. C. G. *IUBMB Life* **2009**, *61*, 6.
(16) Pinto da Silva, L.; Esteves da Silva, J. C. G. *J. Chem. Theory Comput.* **2011**, *7*, 809.
(17) Pinto da Silva, L.; Esteves da Silva, J. C. G. *ChemPhysChem* **2011**, *12*, 951.
(18) Chen, S. F.; Liu, Y. J.; Navizet, I.; Ferre, N.; Fang, W. H.; Lindh, R. *J. Chem. Theory Comput.* **2011**, *7*, 798.
(19) Song, C. I.; Rhee, Y. M. *J. Am. Chem. Soc.* **2011**, *133*, 12040.

(20) Yue, L.; Liu, Y. J.; Fang, W. H. *J. Am. Chem. Soc.* **2012**, *134*, 11632.
(21) Chung, L.; Hayashi, S.; Lundberg, L.; Nakatsu, T.; Kato, H.; Morokuma, K. *J. Am. Chem. Soc.* **2008**, *130*, 12880.
(22) Liu, F.; Liu, Y.; De Vico, L.; Lindh, R. *J. Am. Chem. Soc.* **2009**, *484*, 69.
(23) Isobe, H.; Takano, Y.; Okumura, M.; Kuramitsu, S.; Yamaguchi, K. *J. Am. Chem. Soc.* **2005**, *127*, 8667.
(24) Koo, J. Y.; Schuster, G. B. *J. Am. Chem. Soc.* **1978**, *100*, 4496.
(25) Tanimura, M.; Watanabe, N.; Ijuin, H. K.; Matsumoto, M. *J. Org. Chem.* **2011**, *76*, 902.
(26) Pinto da Silva, L.; Vieira, J.; Esteves da Silva, J. C. G. *Chem. Phys. Lett.* **2012**, *543*, 137.
(27) Naumov, P.; Ozawa, L.; Ohkubo, S.; Fukuzumi, S. *J. Am. Chem. Soc.* **2009**, *131*, 11590.
(28) Naumov, P.; Kochunnoonny, M. *J. Am. Chem. Soc.* **2010**, *132*, 11566.
(29) Ando, Y.; Akiyama, H. *Jpn. J. Appl. Phys.* **2012**, *49*, 117002.
(30) Erez, Y.; Presiado, I.; Gepshtein, R.; Pinto da Silva, L.; Esteves da Silva, J. C. G.; Huppert, D. *J. Phys. Chem. A* **2012**, *116*, 7452.
(31) Presiado, I.; Erez, Y.; Huppert, D. *J. Phys. Chem. A* **2010**, *114*, 9471.
(32) Siegbahn, P. J. *J. Am. Chem. Soc.* **1998**, *120*, 8417.
(33) Erez, Y.; Huppert, D. *J. Phys. Chem. A* **2010**, *114*, 8075.
(34) Erez, Y.; Presiado, I.; Gepshtein, R.; Huppert, D. *J. Phys. Chem. A* **2011**, *115*, 1617.
(35) Presiado, I.; Gepshtein, R.; Erez, Y.; Huppert, D. *J. Phys. Chem. A* **2011**, *115*, 7591.
(36) Presiado, I.; Erez, Y.; Simkovitch, R.; Shomer, S.; Gepshtein, R.; Pinto da Silva, L.; Esteves da Silva, J. C. G.; Huppert, D. *J. Phys. Chem. A* **2012**, *116*, 10770.
(37) Solntsev, K. M.; Laptenok, S. P.; Naumov, P. *J. Am. Chem. Soc.* **2012**, *134*, 16452−16455.
(38) Fraga, H.; Esteves da Silva, J. C. G.; Fontes, R. *FEBS Lett.* **2003**, *543*, 37.
(39) Pinto da Silva, L.; Esteves da Silva, J. C. G. *Photochem. Photobiol. Sci.* **2011**, *10*, 1039.
(40) Fraga, H.; Fernandes, D.; Novotny, J.; Fontes, R.; Esteves da Silva, J. C. G. *ChemBioChem* **2006**, *7*, 929.
(41) White, E. H.; Whorter, H.; Field, G. F.; McElroy, W. D. *J. Org. Chem.* **1965**, *30*, 2344.
(42) Branchini, B. R.; Murtiashaw, M. H.; Magyar, R. A.; Portier, N. C.; Ruggier, M. C.; Stroh, J. G. *J. Am. Chem. Soc.* **2002**, *124*, 2112.
(43) Sundlov, J. A.; Fontaine, D. M.; Southworth, T. L.; Branchini, B. R.; Gulick, A. M. *Biochemistry* **2012**, *51*, 6493.
(44) Adamo, C.; Barone, V. *J. Chem. Phys.* **1998**, *108*, 664.
(45) Barone, V.; Cossi, M. *J. Phys. Chem. A* **1998**, *102*, 1995.
(46) Pinto da Silva, L.; Esteves da Silva, J. C. G. *J. Comput. Chem.* **2012**, *33*, 2118.
(47) Pinto da Silva, L.; Esteves da Silva, J. C. G. *J. Comput. Chem.* **2012**, *33*, 2127.
(48) Pinto da Silva, L.; Esteves da Silva, J. C. G. *ScienceJet* **2012**, *1*, 29.
(49) Chen, V. B.; Arendall, W. B., III.; Headd, J. J.; Keedy, D. A.; Immormino, R. M.; Kapral, G. J.; Murray, L. W.; Richardson, J. S.; Richardson, D. C. *Acta Crystallogr., Sect. D: Biol. Crystallogr.* **2010**, *66*, 12.
(50) Pinto da Silva, L.; Esteves da Silva, J. C. G. *ChemPhysChem* **2011**, *12*, 3002.
(51) Pinto da Silva, L.; Esteves da Silva, J. C. G. *J. Comput. Chem.* **2011**, *32*, 2654.
(52) Pinto da Silva, L.; Esteves da Silva, J. C. G. *J. Phys. Chem. B* **2012**, *116*, 2008.
(53) Milne, B. F.; Marques, M. A.; Nogueira, F. *Phys. Chem. Chem. Phys.* **2010**, *12*, 14285.
(54) Min, C. G.; Ren, A. M.; Guo, J. F.; Zou, L. Y.; Goddard, J. D.; Sun, C. C. *ChemPhysChem* **2010**, *11*, 2199.
(55) Navizet, I.; Liu, Y. J.; Ferré, N.; Xiao, H. Y.; Fang, W. H.; Lindh, R. *J. Am. Chem. Soc.* **2010**, *132*, 706.
(56) Nakatani, N.; Hasegawa, J. Y.; Nakatsuji, H. *J. Am. Chem. Soc.* **2007**, *129*, 8756.
(57) Tagami, A.; Ishibashi, N.; Kato, D.; Taguchi, N.; Mochizuki, Y.; Watanabe, H.; Ito, M.; Tanaka, S. *Chem. Phys. Lett.* **2009**, *472*, 118.
(58) *Avogadro*: An open-source molecular builder and visualization tool, version 1.0.0. http://avogadro.openmolecules.net/ (accessed 10.02.11).
(59) Vreven, T.; Morokuma, K.; Farkas, O.; Schlegel, H. B.; Frisch, M. J. *J. Comput. Chem.* **2003**, *24*, 760.
(60) Mayo, S. L.; Olafson, B. D.; Goddard, W. A. *J. Phys. Chem.* **1990**, *94*, 8897.
(61) Frisch, M. J.; et al. *Gaussian 03*, revision C.02; Gaussian Inc.: Wallingford, CT, 2004.
(62) Naumov, P.; Wu, C.; Liu, Y. J.; Ohmiya, Y. *Photochem. Photobiol. Sci.* **2012**, *11*, 1151.

Article 28

Chemiexcitation induced proton transfer: enolate oxyluciferin as the firefly bioluminophore

Luís Pinto da Silva and Joaquim C.G. Esteves da Silva

J. Phys. Chem. B **2015**, *119*, 2140-2148.

The theoretical calculations and the writing of the paper were performed by Luís Pinto da Silva, under the supervision of Professor Joaquim Esteves da Silva.

THE JOURNAL OF PHYSICAL CHEMISTRY B
Article
pubs.acs.org/JPCB

Chemiexcitation Induced Proton Transfer: Enolate Oxyluciferin as the Firefly Bioluminophore

Luís Pinto da Silva and Joaquim C. G. Esteves da Silva*

Centro de Investigação em Química, Departamento de Química e Bioquímica, Faculdade de Ciências da Universidade do Porto, R. Campo Alegre 687, 4169-007 Porto, Portugal

Supporting Information

ABSTRACT: Firefly bioluminescence is a phenomenon that attracts attention from the research community because of complex challenges for fundamental investigation, as well as diverse opportunities for practical application. Here we have studied the potential deprotonation of firefly oxyluciferin by using a theoretical approach in an enzymatic-like micro-environment in chemiexcited proton transfer involving adenosine 5′-monophosphate. We have uncovered a reaction route that links the evidence that the light-emitter is an anionic molecule while it is chemiexcited in its neutral form. Moreover, the results indicated that the anionic bioluminophore is the enolate anion and not the ketonic one. Further calculations supported this identification of the light-emitter: the spectrum of resulting enolate anion covers the entire yellow-green/red bioluminescence range, which is in line with the experimental findings regarding firefly multicolor bioluminescence.

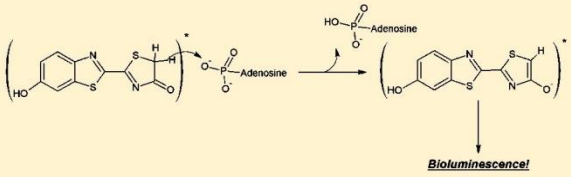

INTRODUCTION

Proton transfer is a very common and fundamental chemical process that plays an important role in a wide variety of chemical and biological phenomena.[1−4] Prime examples are keto−enol tautomerism, proton transport, and proton relay system in membrane-spanning proteins and in enzymes (respectively).[5−7] A special class of compounds presenting proton transfer is represented by heterocyclic aromatic molecules.[8−10] These molecules undergo a dramatic change in their acidity upon electronic excitation.[11] Photoacids increase their acidity, while photobases increase their basicity. Intramolecular excited state proton transfer (ESPT) is observed when the acidic and basic moieties coexist within the same excited state molecules.[12,13] The ESPT process can also be intermolecular, as in the case of proton transfer to a solvent molecule.

Scheme 1. Representation of Firefly Oxyluciferin and Two Natural Analogues

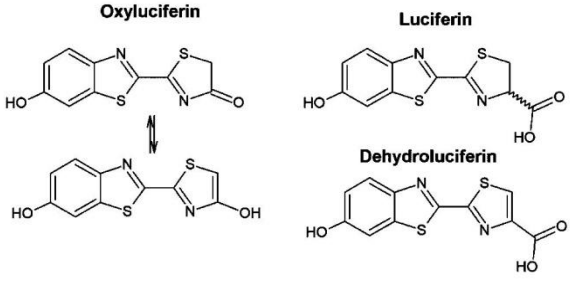

The oxyluciferin (Scheme 1) family of fluorophores is an example of photoacids involved in intermolecular ESPT with the solvent.[14−18] The study of this class of compounds revealed many interesting, complex, and unexpected photoinduced phenomena (stemming from ESPT): efficient fluorescence quenching, strong photoacidity of an enol group, and photoinduced base-catalyzed keto → enol tautomerism.[14−18]

Oxyluciferin also attracts attention from the research community by being the light-emitter of the firefly bioluminescence reaction.[19,20] Bioluminescence is light-emission occurring in a living organism due to enzyme-catalyzed chemical reaction. Firefly bioluminescence is a two-step reaction (Scheme 2): the luciferin molecule reacts with adenosine 5′-triphosphate-Mg^{2+} (ATP-Mg^{2+}), thus resulting in the formation of an adenylyl intermediate; the second step is the oxidation of this latter intermediate in the presence of molecular oxygen, generating oxyluciferin, adenosine 5′-monophosphate (AMP), and carbon dioxide.[21,22] The generated oxyluciferin is already formed in a singlet excited state, which decays to the ground state with emission of visible light.[23,24] Both computational and experimental studies have appointed the keto anion as the light-emitting species.[19−24] However, no experimental study has ever supported these results in a definitive manner. Useful features of this light-emitting system (as ATP-dependence, high quantum yield, low background noise, high speed of reaction, among others) have triggered the

Special Issue: Photoinduced Proton Transfer in Chemistry and Biology Symposium

Received: April 14, 2014
Revised: June 11, 2014
Published: June 13, 2014

dx.doi.org/10.1021/jp5036458 | J. Phys. Chem. B 2015, 119, 2140−2148

Scheme 2. Representation of the Firefly Bioluminescence Reaction

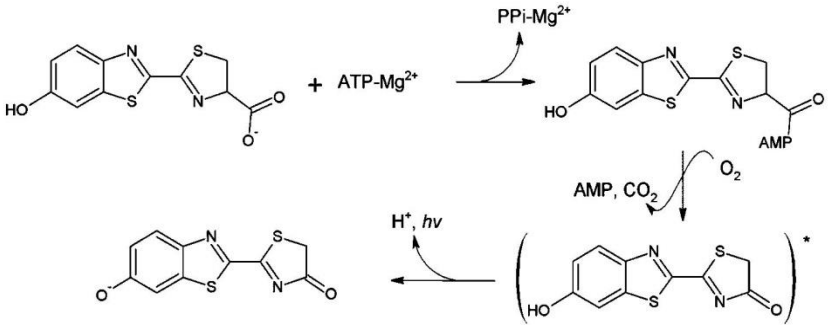

Scheme 3. Representation of the Formation and Subsequent Decomposition of Firefly Dioxetanone

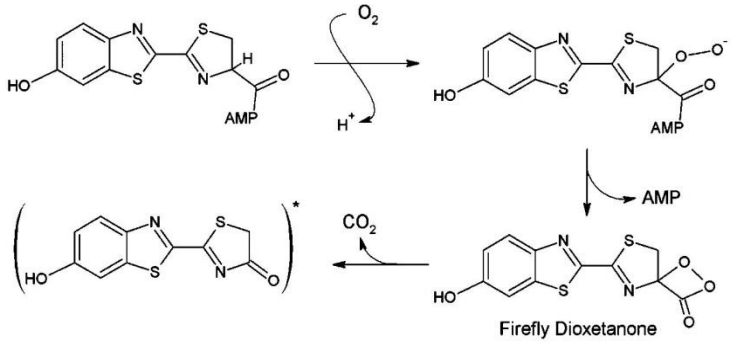

development of numerous applications in pharmaceutical, biomedical, and bioanalytical areas.[25−28]

It was demonstrated that oxyluciferin is produced in a singlet excited state because of the formation and decomposition of firefly dioxetanone (Scheme 3).[23,24] The efficient chemiexcitation is thought to occur because of crossings between the singlet ground and excited states surfaces in the decomposition reaction coordinate. Firefly dioxetanone is supposed to have a deprotonated benzothiazole hydroxyl group due to three main reasons: oxyluciferin is expected to be formed in an anionic form; the deprotonation of the hydroxyl group is expected to lower the energy barrier of the decomposition reaction to more favorable values; the deprotonated hydroxyl group is expected to trigger charge/electron transfers that are responsible for efficient singlet chemiexcitation.[23,24] However, recent findings have contradicted the expected ground state deprotonation of firefly dioxetanone.[14−18,29,30] Experimental data have demonstrated that the hydroxyl group of both luciferin and oxyluciferin only is deprotonated in water (dielectric constant of ∼80) at basic pH (pH ∼7−10) and not in less polar solvents or at acidic pH.[14−18] Theoretical calculations indicated that the hydroxyl group of firefly dioxetanone has the same behavior as that of same group in six oxyluciferin derivatives.[29]

Given these results and that an enzymatic active site is generally characterized by a dielectric constant of 2.5−4 [31,32] and that the bioluminescence reaction can occur in a pH range of ∼5−8,[19−24] it appears unlikely that the hydroxyl group of dioxetanone is deprotonated in this light-emitting reaction. Another recent experimental study, in which the absorption of oxyluciferin was measured inside the firefly luciferase active site, supported this idea. The measurements indicated a higher fraction of neutral species even in basic solutions.[30] Moreover, it was found that oxyluciferin in the enzymatic pocket is less sensitive than the bare luminophore to changes of pH in solution.[30]

The results indicating the protonated state of firefly dioxetanone in the enzymatic active site pocket may appear contradicting in regard to the studies that claim that a deprotonated hydroxyl group is needed for an efficient chemiexcitation.[23,24] However, it should be noted that these conclusions are mostly supported on computational works, which have only studied firefly dioxetanone outside the enzymatic microenvironment. Thus, they have ignored the geometric constraints imposed by the enzyme and all types of intermolecular interactions occurring between dioxetanone and active site molecules. Moreover, it was also computationally demonstrated that a path for singlet chemiexcitation exists during the decomposition of a neutral firefly dioxetanone.[33] Also, Naumov and co-workers have found that the light-emitter of *Cypridina* luminescence is chemiexcited from a neutral dioxetanone.[34] The fact that oxyluciferin is expected to be anionic when emitting bioluminescence can then be attributed to an ESPT process between this photoacid and an active site molecule after chemiexcitation, based on its documented photoacidity.[14−18] It should be noted that only anionic oxyluciferin species present emission wavelength compatible with bioluminescence.[35,36]

There is also uncertainty regarding the identity of the anionic species in this ESPT process. The decomposition of dioxetanone leads to the formation of oxyluciferin in its keto species (Scheme 3).[23,24] This indicates that the ESPT process should involve the benzothiazole hydroxyl group, thus

dx.doi.org/10.1021/jp5036458 | J. Phys. Chem. B 2015, 119, 2140−2148

generating an excited state anionic keto molecule. However, Naumov and co-workers have found that keto oxyluciferin can be converted in the enolate anion in solvents of low polarity and in the presence of base.[18] Given this, they have stated that the same reaction may occur in the active site of luciferin with AMP as the proton acceptor, given its proximity to oxyluciferin and its double negative charge.[18,37,38]

The main aim of this work is to clarify the possibility of anionic oxyluciferin generation by ESPT after chemiexcitation, in an enzymatic-like microenvironment, by means of a quantum mechanics/molecular mechanics (QM/MM) approach. For this purpose, the excited state potential energy surface of the proton transfer from oxyluciferin to AMP was calculated and characterized. The resulting anionic oxyluciferin structure was then studied in order to verify if its excited state properties are in line with experimental bioluminescence data.

METHODOLOGY

The proton transfer reaction between oxyluciferin and AMP was modeled by using a QM/MM approach, by using the "our own *N*-layered integrated molecular orbital and molecular mechanics" (ONIOM) method with an electrostatic embedding scheme and the link atom approach.[39,40] ONIOM models large molecular systems by defining two or three layers that are treated at different levels of accuracy. The high layer, treated with the most accurate method, was composed of neutral keto oxyluciferin and the phosphate group of AMP. The remaining AMP molecule was treated with the less accurate methods in the low layer.

Geometry optimizations were performed at the M06/6-31G(d) and UFF force field level of theory at the high and low layer, respectively.[41,42] Frequency calculations were performed at the same level of theory in order to verify the number of imaginary frequencies of the targeted structure. The proton transfer reaction was modeled by performing a relaxed potential energy surface (PES) scan, with geometry optimization at each point, at the ONIOM(M06/6-31G(d)/UFF) level of theory.

The ground state PES was re-evaluated by performing single point energy calculations at the ONIOM(M06/6-311+G(d,p)/UFF) level of theory. The excited state PES was evaluated by calculating the Franck−Condon curves by obtaining the time-dependent (TD) M06/6-311+G(d,p) vertical excitation energies.[43] Such strategy was already used with success in other studies aiming to understand ESPT reactions.[17,44−49] Nevertheless, with this approach it is not taken in consideration the geometric relaxation that occurs in the excited state. Given this, we have also modeled the ESPT reaction by performing excited state geometry optimizations. However, performing such description of the excited state PES is far from trivial. It is difficult to choose an effective reaction coordinate since the proton motion is accompanied by a significant electronic rearrangement and normally coupled to other degrees of freedom, besides the problems related to classical or quantum treatment of its dynamics.[50−53]

So we have replaced AMP in the excited state geometry optimizations by the carbonate ion. As AMP, the latter molecule is a dianion resulting from deprotonation of two oxygen atoms. Thus, CO_3^{2-} is a similar proton acceptor as AMP, with the benefit of being a much smaller molecule, thereby decreasing the number of degrees of freedom involved in the calculations.

The excited state PES of the ESPT reaction was obtained by performing an intrinsic reaction coordinate (IRC) calculation, in which the transition state is connected to the reactants and products.[54] These calculations were performed at the CIS/6-31G(d) level of theory.[55]

M06 was the chosen functional given good results in molecular geometry prediction and its recommendation for a combination of main-group thermochemistry, kinetics, and noncovalent interactions.[41,56] The CIS method was chosen, as previous results demonstrated that this method provided results regarding oxyluciferin comparable with ones obtained with higher levels of theory (as when using SAC-CI).[57] Moreover, the CIS method is able to analytically determine force constants needed for IRC and transition state determination, while TD-DFT methods are only able to obtain them by numerical differentiation.

After modeling of the ESPT reaction, the resulting anionic oxyluciferin structure was studied without both protonated AMP and the carbonate ion. The properties of the electronically excited states were calculated by TD M06/6-311+G(d,p) single point calculations on the ground and excited states structures within the vertical approximation. While bioluminescence is a light-emitting phenomenon, the absorption process can also provide valuable insight into the excited state properties of bioluminescence molecules. It should be noted that the absorption spectrum often reflects the main excited state features and that this approach was already used both experimentally and theoretically.[58−65] The electrostatic enzymatic microenvironmental effects on the excited state properties were taken into account through application of an external electric field.[66]

All calculations were performed in implicit diethyl ether, which was modeled by the conductor-like polarizable continuum model.[67,68] This nonpolar solvent was chosen because its dielectric constant (4.24) is in line with the dielectric constant values used to describe the bulk effect of a protein environment.[31,32]

All calculations were performed with the Gaussian 09 electronic structure program package.[69]

RESULTS AND DISCUSSION

The proton transfer reaction, obtained within the vertical excitation approach, was modeled by decreasing the distance between an oxygen atom from AMP and a hydrogen atom from oxyluciferin, from 2.04 to 1.00 Å, by performing a relaxed coordinate scan. The energies of the excited and ground states were then re-evaluated as described in the section Methodology. The resulting curves are presented in Figure 1, as a function of oxyluciferin C−H bond length. In Scheme 4 is presented the reaction mechanism of the proton transfer reaction. Ground frequency calculations indicate that the structures with C−H bond lengths of 1.11 and 2.04 Å are minima in their potential energy surface, while the structure with bond length of 1.30 Å is a transition state involved in the proton transfer reaction (imaginary frequency of −1720.07 cm^{-1} with an infrared intensity of 1971.09).

This reaction occurs mainly because of changes in three reaction coordinates: AMP oxygen−thiazole hydrogen (O−H), oxyluciferin thiazole carbon−hydrogen (C−H), and AMP oxygen−thiazole carbon (O−C). In Figure 2 are presented the lengths of O−H, C−H, and O−C during the proton transfer reaction, with either AMP or the carbonate ion as proton acceptors. As expected, the length of O−H decreases steadily during the reaction (more linearly in the oxyluciferin−AMP reaction than in oxyluciferin−carbonate). However, this

dx.doi.org/10.1021/jp5036458 | J. Phys. Chem. B 2015, 119, 2140−2148

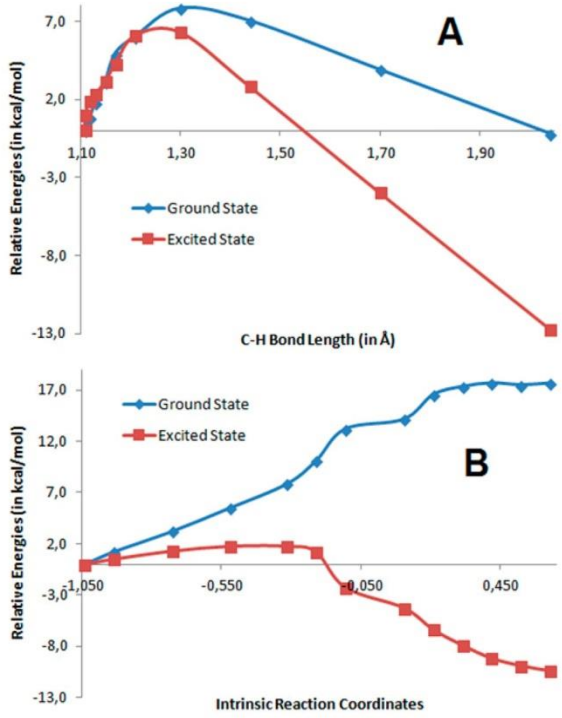

Figure 1. (A) Potential energy curves, as a function of the C−H bond length, of the proton transfer reaction between neutral keto oxyluciferin and AMP (both in the ground and excited states). (B) Potential energy curves, as a function of intrinsic reaction coordinate, of the proton transfer reaction between neutral keto oxyluciferin and carbonate ion (both in the ground and excited states).

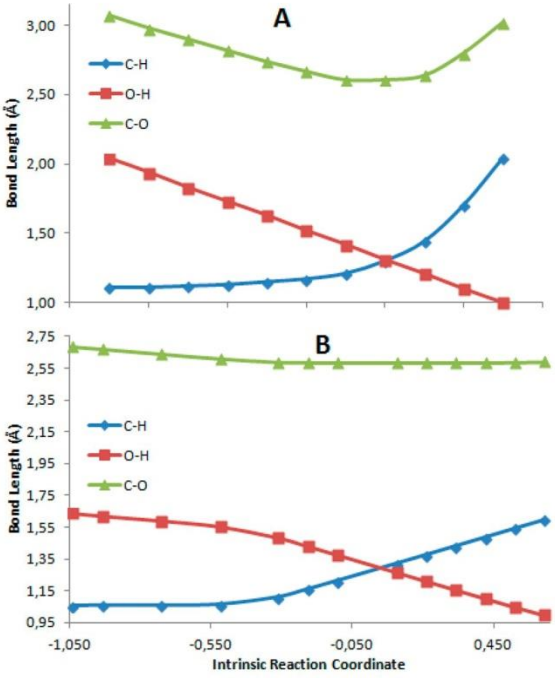

Figure 2. Changes in reaction coordinates of the proton transfer reaction between neutral keto oxyluciferin and AMP (A) or the carbonate ion (B).

decrease is not accompanied in a first phase by an increase in the C−H length in the oxyluciferin−AMP reaction. The calculated data indicate that the proton transfer reaction first proceeds by O−C decreasing distance, thus decreasing the O−H length. Only near the transition state is when the C−H length starts to decrease and the proton is really transferred to the AMP oxygen, which leads to an increase in O−C to values close to the initial ones. In the case of the oxyluciferin−carbonate reaction, the C−O reaction coordinate has a smaller importance in the ESPT mechanism. By analysis of Figure 2B, the oxyluciferin−carbonate reaction occurs mainly by proton

Scheme 4. Representation of the Chemiexcited Proton Transfer Reaction between Neutral Keto Oxyluciferin and the Carbonate Ion or AMP

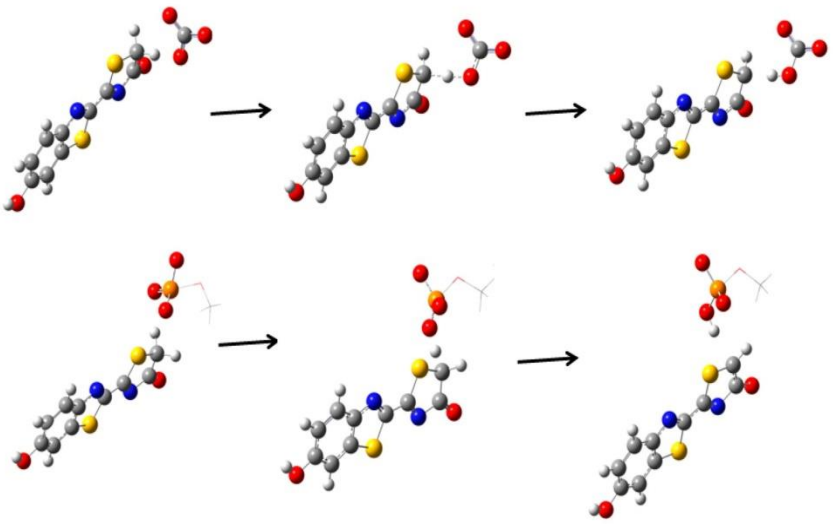

dx.doi.org/10.1021/jp5036458 | J. Phys. Chem. B 2015, 119, 2140−2148

motion and not by the approximation of the proton acceptor moiety.

The potential energy curves of oxyluciferin−AMP ESPT confirm the photoacidity of the thiazole C−H group. Despite the energy barrier of the ground state reaction being only of 7.8 kcal/mol, the final structure is only more stable than the reactant complex by 0.2 kcal/mol. This low energetic difference indicates that the reaction is not likely. For the contrary, this is a likely to occur excited state reaction. The energy barrier decreases from 7.8 to 6.3 kcal/mol. More importantly, the final structure of the reaction (in which AMP is protonated) is more stable than the reactant complex by 12.7 kcal/mol.

The study of the ESPT between neutral oxyluciferin and the carbonate ion (Scheme 4), within the vertical emission approach, also confirmed the photoacidity of the thiazole C−H group. The resulting PES curves are presented in Figure 1, as a function of the reaction's intrinsic coordinates. In the ground state it can be seen that the reaction is not likely, as the energy increases continually from 0.0 to 17.6 kcal/mol. For the contrary, the excited state enolate formation is clearly favorable. The activation barrier is only of 1.8 kcal/mol, while the product complex is more stable than the reactant one by 10.4 kcal/mol.

Thus, our calculations indicate that the photoacid character of oxyluciferin is indeed important in the firefly bioluminescence reaction, as the anionic bioluminophore can be formed by chemiexcitation induced ESPT with AMP. Moreover, it appears that the light-emitter is not the anionic keto species as expected but the enolate anion.[19−24] It should be noted that the hypothesis that an anionic enol species is the firefly light-emitter was recently reproposed, although only on a speculative basis.[14,18] Also, the fact the excited state proton transfer reaction has a low energy barrier, and that the product complex is significantly more stable than the reactant structure, explains why no neutral emissive species was detected despite oxyluciferin being chemiexcited in a neutral form.[30]

Wang and co-workers studied the bioluminescence spectra of the firefly system and have found either red (610 nm/2.03 eV) or yellow-green emission (560 nm/2.21 eV), depending on the pH value.[30] Moreover, they have found that the red emission component was present in the whole pH range, with similar intensity. For the contrary, the yellow-green emission intensity changed with pH.[30] These results are in line with the findings of Ando et al, who have proposed that the pH-dependent multicolor bioluminescence originates by changes in the intensity of the yellow-green component intensity.[70] At more basic pH values, the intensity of this component increases and dominates the bioluminescence spectrum. When the pH decreases, the intensity of the yellow-green emission also decreases, thus allowing the detection of the red emission.[70] Several theoretical studies on pH dependent behavior of firefly bioluminescence verified that the electrostatic interactions between oxyluciferin and active site molecules change in function of pH.[71−74] It should be noted that hydrogen bonding was also found to be important in the color tuning mechanism. Rather recently it was found that addition of a single water molecule to a bare ion caused a 0.23 eV blue-shift in the transition.[60]

Given all of these studies, one can expect that the yellow-green emission component of the bioluminophore is susceptible to changes in electrostatic interactions, while the red component is insensitive to it. Therefore, in order to be the bioluminophore, the enolate species should present these excited state features. To support this proposal, we have withdrawn this molecule from the anionic oxyluciferin−protonated AMP and oxyluciferin−protonated carbonate ion complexes and subjected it to calculations under the influence of an external electric field. Emissive properties of protein fluorescence are thought to be modulated mainly by changes in local electrostatic interaction between the luminophore and the protein microenvironment (which can be interpreted as an internal Stark effect).[66,75−79] An external Stark effect can be seen as result from the electrostatic field from polar solvent molecules. Nogueira and co-workers have stated that if one takes into account the protein cavity field (responsible for inducing the internal Stark shift) together with an existing external field (as the electrostatic field from polar solvent molecules), the entire environmental electrostatic interactions can be regarded as an effective external electric field imposed on the luminophore.[66] Thus, this reasoning allows us to study the excited state properties of the enolate species molecule in implicit diethyl ether and model the electrostatic micro-environmental effects through an effective electric field (an approach already used with good results).[66] The electric fields were projected on the x, y, and z directions with respect to the oxyluciferin molecule, with a magnitude of ±160 mV/Å in intervals of 40 mV/Å.[66,78,79]

The results of the vertical excitation calculations, regarding the enolate ion withdrawn from the anionic oxyluciferin−protonated AMP, under the effect of an external electric field are presented in Tables S5−S7 in Supporting Information. The results of the vertical emission calculations, regarding the enolate ion withdrawn from the anionic oxyluciferin−protonated carbonate ion, under the effect of an external electric field are presented in Tables 1−3. We have found that

Table 1. Emission Energies (E_{em}) and Oscillator Strength (f) of the Main Excited State Transition of Enolate Oxyluciferin When Subjected to an External Electric Field Applied in the x Orientation

magnitude (mV/Å)	E_{em} (eV)	f
−160	2.34	0.3208
−120	2.30	0.3102
−80	2.25	0.3037
−40	2.20	0.2987
0	2.16	0.2960
40	2.11	0.2950
80	2.06	0.2955
120	2.02	0.2970
160	1.97	0.2985

in all calculations the enolate species present two bright states, with an average difference between them of 1.64 eV. Thus, as in line with bioluminescence data, the spectrum of the enolate species presents two components.[30,70] However, the most blue-shifted state is too high in energy to be a state involved in firefly bioluminescence spectrum and to be populated by dioxetanone decomposition. So we state that only the most red-shifted state of this bioluminophore is of interest in the present situation, and it is the one to be characterized in the following paragraphs.

In Table 1 are presented the results of the calculations in which oxyluciferin is under the effect of an electric field projected on the x direction. The energy and intensity of the excited state are affected significantly by the electric field. The projection of a field of magnitude between 0 and +160 mV/Å increases the energy by 0.19 eV, while the projection of a field

dx.doi.org/10.1021/jp5036458 | J. Phys. Chem. B 2015, 119, 2140−2148

of magnitude between 0 and −160 mV/Å decreases the energy by the same amount. It should be noted that the projection of an external field with a magnitude between −160 and +160 mV/Å covers both the red and yellow-green emission characteristic of firefly bioluminescence.

In Table 2 are presented the results of the calculations in which oxyluciferin is under the effect of an electric field projected on the *y* direction.The energy of the excited state is less affected by changes in the electric field. By its turn, the intensity of this transition is similar to the one found when the electric field is projected in the *x* direction. The results of the calculations in which oxyluciferin is under the effect of an electric field projected on the *z* direction are presented in Table 3. The energy of the excited state is insensitive to the magnitude of the electric field, as well as its intensity.

Table 2. Emission Energies (E_{em}) and Oscillator Strength (f) of the Main Excited State Transition of Enolate Oxyluciferin When Subjected to an External Electric Field Applied in the *y* Orientation

magnitude (mV/Å)	E_{em} (eV)	f
−160	2.19	0.3188
−120	2.18	0.3129
−80	2.17	0.3078
−40	2.16	0.3019
0	2.16	0.2960
40	2.15	0.2901
80	2.14	0.2841
120	2.13	0.2789
160	2.12	0.2729

Table 3. Emission Energies (E_{em}) and Oscillator Strength (f) of the Main Excited State Transition of Enolate Oxyluciferin When Subjected to an External Electric Field Applied in the *z* Orientation

magnitude (mV/Å)	E_{em} (eV)	f
−160	2.15	0.2936
−120	2.15	0.2943
−80	2.15	0.2948
−40	2.15	0.2954
0	2.16	0.2960
40	2.16	0.2965
80	2.16	0.2970
120	2.16	0.2973
160	2.16	0.2977

The Franck−Condon state of the enolate ion is affected differently by a projected field than the emissive state (Tables S5−S7). In Table S5 are presented the results of the calculations in which oxyluciferin is under the effect of an electric field projected on the *x* direction. The intensity of this state is nearly insensitive to the magnitude of electric field. However, its energy is affected significantly by the electric field. The projection of a field of magnitude between 0 and +160 mV/Å increases the energy by 0.23 eV, while the projection of a field of magnitude between 0 and −160 mV/Å decreases the energy by 0.24 eV. In Table S6 are presented the results of the calculations in which oxyluciferin is under the effect of an electric field projected on the y direction. The energy and intensity of the excited state are much less affected by changes in the electric field. The results of the calculations in which oxyluciferin is under the effect of an electric field projected on the *z* direction are presented in Table S7.The results are similar to the one found when the field is projected in the *y* direction, as the intensity and energy of the Franck−Condon state are insensitive to field modulation.

The analysis referred above further supported the role of the enolate anion as a bioluminescence emitter. This ion is indeed sensitive to electrostatic interactions, here modulated by an external field.[66,71−74] Furthermore, the modulation of the field allowed us to cover the whole range of the yellow-green/red emission that is characteristic of firefly bioluminescence.[30,70] Also, the intensity of the red-shifted emission of the enolate anion is lower than the one presented by more yellow-green shifted emission, as in line with the work of Ando et al.[70] Thus, the enolate anion appears to be in line with previous characterization of firefly bioluminescence.[30,66,70−74] Even the emission intensity here calculated, somewhat lower than calculated in previous studies, can be explained by a recent study in which it was found that the luciferase enzyme increases the fluorescence efficiency of oxyluciferin.[74,79]

Nevertheless, we do not think that the present findings fully exclude the ketone form as the light-emitter. First, it is known that an oxyluciferin analogue locked in the keto form was able to emit both yellow-green and red bioluminescence, thus indicating the existence of a pathway for chemiexcitation formation of anionic keto oxyluciferin.[80] Also, the works of Wang and Ando showed us that the yellow-green and red emissions coexist, with the former component's intensity being sensitive to external perturbations.[30,70] However, by subjecting the enolate ion to a electric field, we were not able to simulate this coexistence. We were able to obtain yellow-green and red emissions not by intensity modulation but by shifts in the emission wavelength. In conclusion, our calculations indicate that excited state enolate ion is expected to be formed during the bioluminescence reaction and to be able to emit yellow-green and red emission, thus being a component of the color tuning mechanism.

■ CONCLUSION

In this article, we have presented our theoretical analysis on a possible chemiexcited proton transfer involving firefly oxyluciferin and its role on multicolor bioluminescence. First, we have studied the proton transfer between neutral keto oxyluciferin and AMP or carbonate ion via a QM/MM approach. We have found a route for the formation of an anionic bioluminophore, based on the photoacidic character of oxyluciferin, from a neutral excited bioluminophore. The resulting anion from the chemiexcited proton transfer was the enolate anion, which indicated that this species is a light-emitter product. This route allows us to link the evidence that the light-emitter is an anionic molecule while it is chemiexcited in its neutral form.

Further calculations were made in order to study the excited state properties of the enolate anion. The Stark effect is able to unify the color shift of a fluorophore by internal and external fields, thus allowing the study of excited state properties as a function of an electrostatic field. These calculations demonstrated that the enolate anion, in enzymatic-like microenvironment, can cover the entire yellow-green/red range of firefly bioluminescence. Thus, these results further support the notion of the enolate anion as a bioluminophore.

dx.doi.org/10.1021/jp5036458 | J. Phys. Chem. B 2015, 119, 2140−2148

■ ASSOCIATED CONTENT

Supporting Information

Cartesian coordinates of neutral keto oxyluciferin complexed with AMP and carbonate ion; bond lengths; excitation energies and intensities of enolate oxyluciferin when subjected to an electrostatic field. This material is available free of charge via the Internet at http://pubs.acs.org.

■ AUTHOR INFORMATION

Corresponding Author

*E-mail: jcsilva@fc.up.pt. Phone: 351 226082869. Fax: 351 226082959.

Notes

The authors declare no competing financial interest.

■ ACKNOWLEDGMENTS

Financial support from Fundação para a Ciência e Tecnologia (FCT, Lisbon) (Programa Operacional Temático Factores de Competitividade (COMPETE) and Fundo Comunitário Europeu (FEDER) (Project PTDC/QUI/71366/2006) is acknowledged. A Ph.D. grant to Luís Pinto da Silva (Grant SFRH/76612/2011) from FCT is also acknowledged.

■ REFERENCES

(1) Tuckerman, M. E.; Marx, D.; Parrinello, M. The nature and transport mechanism of hydrated hydroxide ions in aqueous solution. *Nature* **2002**, *417*, 925−929.
(2) Mohammed, O. F.; Pines, D.; Nibbering, E. T. J.; Pines, E. Base-induced solvent switches in acid-base reactions. *Angew. Chem., Int. Ed.* **2007**, *46*, 1458−1461.
(3) Lill, M. A.; Helms, V. Proton shuttle in green fluorescent protein studied by dynamic simulations. *Proc. Natl. Acad. Sci. U.S.A.* **2002**, *99*, 2778−2781.
(4) Mathias, G.; Marx, D. Structures and spectral signatures of protonated water networks in bacteriorhodopsin. *Proc. Natl. Acad. Sci. U.S.A.* **2007**, *104*, 6980−6985.
(5) Formosinho, S. J.; Arnaut, L. G. Excited-state proton-transfer reactions. 2. Intramolecular reactions. *J. Photochem. Photobiol., A* **1993**, *75*, 21−48.
(6) Gebicki, J.; Bally, T. Spontaneous hydrogen atom transfer on ionization: Characterization of enol radical cations in cryogenic matrices. *Acc. Chem. Res.* **1997**, *30*, 447−485.
(7) Zewail, A. H. Femtochemistry. Past, present, and future. *Pure Appl. Chem.* **2000**, *72*, 2219−2231.
(8) Gordon, M. S. Hydrogen transfer in 7-azaindole. *J. Phys. Chem.* **1996**, *100*, 3974−3979.
(9) Mente, S.; Maroncelli, M. Solvation and the excited-state tautomerization of 7-azaindole and 1-azacarbazole: Computer simulations in water and alcohol solvents. *J. Phys. Chem. A* **1998**, *102*, 3860−3876.
(10) Waluk, J. Hydrogen-bonding-induced phenomena in bifunctional heteroazaaromatics. *Acc. Chem. Res.* **2003**, *36*, 832−838.
(11) Agmon, N. Elementary steps in excited-state proton transfer. *J. Phys. Chem. A* **2005**, *109*, 13−35.
(12) Förster, T. Diabatic and adiabatic processes in photochemistry. *Pure Appl. Chem.* **1970**, *24*, 443−450.
(13) Douhal, A.; Lahmani, F.; Zewail, A. H. Proton-transfer reaction dynamics. *Chem. Phys. Lett.* **1996**, *207*, 477−498.
(14) Pinto da Silva, L.; Simkovitch, R.; Huppert, D.; Esteves da Silva, J. C. G. Oxyluciferin photoacidity: the missing element for solving the keto−enol mystery? *ChemPhysChem* **2013**, *14*, 3441−3446.
(15) Pinto da Silva, L.; Simkovitch, R.; Huppert, D.; Esteves da Silva, J. C. G. Theoretical photodynamic study of the photoprotolytic cycle of firefly oxyluciferin. *ChemPhysChem* **2013**, *14*, 2711−2716.
(16) Erez, Y.; Presiado, I.; Gepshtein, R.; Pinto da Silva, L.; Esteves da Silva, J. C. G.; Huppert, D. Comparative study of the photoprotolytic reactions of D-luciferin and oxyluciferin. *J. Phys. Chem. A* **2012**, *116*, 7452−7461.
(17) Pinto da Silva, L.; Simkovitch, R.; Huppert, D.; Esteves da Silva, J. C. G. Theoretical study of the efficient fluorescence quenching process of the firefly luciferin. *J. Photochem. Photobiol., A* **2013**, *266*, 47−54.
(18) Solntsev, K. M.; Laptenok, S. P.; Naumov, P. Photoinduced dynamics of oxyluciferin analogues: unusual enol "super" photoacidity and evidence for keto−enol isomerization. *J. Am. Chem. Soc.* **2012**, *134*, 16452−16455.
(19) Vieira, J.; Pinto da Silva, L.; Esteves da Silva, J. C. G. Advances in the knowledge of light emission by firefly luciferin and oxyluciferin. *J. Photochem. Photobiol., B* **2012**, *117*, 33−39.
(20) Pinto da Silva, L.; Esteves da Silva, J. C. G. Computational studies of the luciferase light-emitting product: oxyluciferin. *J. Chem. Theory Comput.* **2011**, *7*, 809−817.
(21) Marques, S. M.; Esteves da Silva, J. C. G. Firefly bioluminescence: a mechanistic approach of luciferase catalyzed reactions. *IUBMB Life* **2009**, *61*, 6−17.
(22) Hosseinkhani, S. Molecular enigma of multicolor bioluminescence of firefly luciferase. *Cell. Mol. Life Sci.* **2011**, *68*, 1167−1182.
(23) Pinto da Silva, L.; Esteves da Silva, J. C. G. Firefly chemiluminescence and bioluminescence: efficient generation of excited states. *ChemPhysChem* **2012**, *13*, 2257−2262.
(24) Navizet, I.; Liu, Y. J.; Ferré, N.; Roca-Sanjuán, D.; Lindh, R. The chemistry of bioluminescence: an analysis of chemical functionalities. *ChemPhysChem* **2011**, *12*, 3064−3076.
(25) Roda, A.; Guardigli, M. Analytical chemiluminescence and bioluminescence: latest achievements and new horizons. *Anal. Bioanal. Chem.* **2012**, *402*, 69−76.
(26) Fazzina, R.; Lombardini, L.; Mezzanotte, L.; Roda, A.; Hrelia, P.; Pession, A.; Tonelli, R. Generation and characterization of bioluminescent xenograft mouse models of MLL-related acute leukemis and in vivo evaluation of luciferase-targeting siRNA nanoparticles. *Int. J. Oncol.* **2012**, *41*, 621−628.
(27) Roda, A.; Cevenini, L.; Michelini, E.; Branchini, B. R. A portable bioluminescence engineered cell-based biosensor for on-site applications. *Biosens. Bioelectron.* **2011**, *26*, 3647−3653.
(28) Marques, S. M.; Peralta, F.; Esteves da Silva, J. C. G. Optimized chromatographic and bioluminescente methods for inorganic pyrophosphate based on its conversion to ATP by firefly luciferirase. *Talanta* **2009**, *77*, 1497−1503.
(29) Pinto da Silva, L.; Santos, A. J.; Esteves da Silva, J. C. G. Efficient firefly chemi/bioluminescence: evidence for chemiexcitation resulting from the decomposition of a neutral firefly dioxetanone molecule. *J. Phys. Chem. A* **2013**, *117*, 94−100.
(30) Wang, Y.; Hayamizu, Y.; Akiyama, H. Spectroscopic study of firefly oxyluciferin in an enzymatic environment on the basis of stability monitoring. *J. Phys. Chem. B* **2014**, *118*, 2070−2076.
(31) Simonson, T.; Brooks, C. L. Charge screening and the dielectric constant of proteins: Insights from molecular dynamics. *J. Am. Chem. Soc.* **1996**, *118*, 8452−8458.
(32) Gilson, M. K.; Honig, B. H. The dielectric-constant of a folded protein. *Biopolymers* **1986**, *25*, 2097−2119.
(33) Yue, L.; Liu, Y. J.; Fang, W. H. Mechanistic insight into the chemiluminescent decomposition of firefly dioxetanone. *J. Am. Chem. Soc.* **2012**, *134*, 11632−11639.
(34) Naumov, P.; Wu, C.; Liu, Y. J.; Ohmiya, Y. Spectrochemisty and artificial color modulation of Cypridina luminescence: indirect evidence for chemiexcitation of a neutral dioxetanone and emission from a neutral amide. *Photochem. Photobiol. Sci.* **2012**, *11*, 1151−1155.
(35) Naumov, P.; Ozawa, Y.; Ohkubo, K.; Fukuzumi, S. Structure and spectroscopy of oxyluciferin, the light emitter of the firefly bioluminescence. *J. Am. Chem. Soc.* **2009**, *131*, 11590−11605.
(36) Naumov, P.; Kochunnoonny, M. Spectral−structural effects of the keto−enol−enolate and phenol−phenolate equilibria of oxyluciferin. *J. Am. Chem. Soc.* **2010**, *132*, 11566−11579.

Anemonia majano. *Proc. Natl. Acad. Sci. U.S.A.* **2005**, *102*, 12712−12717.
(76) Ai, H. W.; Olenych, S. G.; Wong, P.; Davidson, M. W.; Campbell, R. E. Hue-shifted monomeric variants of *Clavularia* cyan fluorescent protein: identification of the molecular determinants of color and applications in fluorescence imaging. *BMC Biol.* **2008**, *6*, 13.
(77) Lockhart, D. J.; Kim, P. S. Internal Stark effect measurement of the electric field at the amino terminus of an alpha-helix. *Science* **1992**, *257*, 947−951.
(78) Manas, E. S.; Wright, W. W.; Sharp, K. A.; Friedrich, J.; Vanderkooi, J. M. The influence of protein environment on the low temperature electronic spectroscopic of Zn-substituted cytochrome *c*. *J. Phys. Chem. B* **2000**, *104*, 6932−6941.
(79) Pinto da Silva, L.; Esteves da Silva, J. C. G. Quantum/molecular mechanics study of firefly bioluminescence on luciferase oxidative conformation. *Chem. Phys. Lett.* **2014**, *608*, 45−49.
(80) Branchini, B. R.; Murtiashaw, M. H.; Magyar, R. A.; Portier, N. C.; Ruggiero, M. C.; Stroh, J. G. Yellow-green and red firefly bioluminescence from 5,5-dimethyloxyluciferin. *J. Am. Chem. Soc.* **2002**, *124*, 2112−2113.

Chapter 7 – Conclusions and Future Perspectives

Several conclusions can be withdrawn from this project, which the author of this Thesis hope can be used for developing new applications for the firefly bioluminescent system, or increase the efficiency of existent ones

7.1. Conclusions from the Study of the Flash Profile of Firefly Bioluminescence

Our first conclusion is that while L and L-LH_2 present a significant inhibitory power towards D-LH_2, they should not play any role on firefly bioluminescence as they cannot be formed from the bioluminescent substrate in oxidation and isomerism reactions.

The role of L-AMP in the flash profile was also further clarified. It was previously known that this compound is a tight-binding competitive inhibitor of D-LH_2. Now we predict L-AMP to be also a competitive inhibitor of LH_2-AMP, given that these adenylates present very similar binding mechanisms and affinity to luciferase. Moreover, we predict that this similarity prevents any attempt to decrease the affinity of L-AMP to luciferase by mutating the enzyme, as decreasing the binding of this adenylate would also decrease that of LH_2-AMP thereby decreasing the emission of light.

7.2. Conclusions from the Study of the Formation Mechanism of Firefly Dioxetanone

While being accepted by more than forty years, the carbanion mechanism for the formation of firefly dioxetanone has been questioned recently as it is problematic that a singlet dioxetanone is formed from inactivated triplet oxygen in a spin forbidden process. This lead to the proposal of two new reaction mechanisms: a radical and a single electron-transfer one. Our theoretical work has supported this paradigm shift, by demonstrating that there is no factor that would cause any specific interaction between the thiazole moiety of a LH_2-AMP carbanion and molecular oxygen. Moreover, our work indicates that such specific interaction is indeed possible between LH_2-AMP and •OOH radicals. Moreover, we have found the evidence for a radical-based mechanism in the chemiluminescent reaction between D-LH_2 and superoxide anion.

7.3. Conclusions from the Characterization of the Decomposition Reaction of Dioxetanone Molecules and the Subsequent Chemiexcitation Step

Our theoretical work has attributed a concerted mechanism for the decomposition reaction of simple dioxetanones. This mechanism has the advantage of being in line with experimental findings, as it can explain the high triplet/singlet product ratio (due to intersystem crossings between the ground singlet and triplet states) and the inefficient light emission of these molecules (as the singlet excited state is only populated by intersystem crossing from a triplet state). Moreover, we have presented evidence that excludes the involvement of a biradical intermediate in the peroxide bond breaking step, as this bond is a charge-shifted one (or even covalent depleted) and the two oxygen atoms are not equivalent (thereby preventing a homolytic cleavage). This finding was supported by the fact that when these two oxygen atoms are equivalent, as in the case of dioxetanedione, a biradical stepwise mechanism was indeed identified.

These findings allowed us to propose the Interstate Crossing-Induced Chemiexcitation mechanism as the reason for the chemiluminescence of dioxetanone molecules. Charge-transfer processes are needed to reach a transition state, in the vicinity of which direct population of excited states is possible. In the case of simple dioxetanones, this excited state population is mainly done by singlet/triplet intersystem crossings, thereby explaining the high triplet/singlet product ratio.

7.4. Conclusions from the Study of the Color Tuning Mechanism of the Bioluminescent Luciferase-OxyLH_2 System

We have found that the multicolor bioluminescence originated by the firefly system is the result of the electrostatic field formed by the intermolecular interactions between OxyLH_2 and the molecules of the luciferase active site. More specifically, the emission wavelength is determined by blue-shifting ionic interactions with AMP, red-shifting π-π stacking interactions with a phenylalanine residue, and red/blue-shifting hydrogen bonds with water molecules.

Our results also predicted that the fluorescence intensity of OxyLH_2 is controlled by the HOMO(x)/LUMO(x) orbital overlapping, particularly at the C-C bond that connects the two moieties of the light emitter. It was also found that a red-shift of the emission

can be obtained by a higher charge delocalization upon excitation, and by higher π-π conjugation between the two moieties of the bioluminophore.

7.5. Conclusions from the Characterization of $OxyLH_2$ and Related Compounds as Photoacids

We have characterized for the first time $OxyLH_2$ and related compounds (D-LH_2 and L) as photoacids, that is, they are able to donate a proton to the solvent via an excited state proton transfer (ESPT) reaction. In the excited state, $OxyLH_2$, D-LH_2 and L have pK_a^*'s of about ~0.5, which are significantly lower than their ground state pK_a's (~7-8). We have found that D-LH_2 presents a more efficient ESPT process (a rate coefficient of $3.2x10^{10}$ s^{-1}) than $OxyLH_2$ ($2.2x10^{10}$ s^{-1}) and L ($1.1x10^{10}$ s^{-1}). However, none of these molecules can be considered as particularly strong photoacids, as the ESPT reaction is inhibited in less polar solvents (as methanol), in the absence of base.

A very interesting finding was that $OxyLH_2$ emits a proton in the ESPT reaction from its enol group, given that photoacidity of an enol group in a five-membered ring is rare. We have found that in $OxyLH_2$ this is possible due to the presence of a hydrogen bond acceptor (the thiazole nitrogen) near the enol group, which allows the stabilization of the enolate anion over the phenolate one.

Another characteristic of the photoprotolytic cycle of $OxyLH_2$ and related compounds is an efficient fluorescence quenching process, which we have attributed to the protonation of the nitrogen heteroatom of the benzothiazole moiety. This protonation leads to a singlet to triplet intersystem crossing, which can explain the fluorescence quenching.

Contrary to D-LH_2 and L, $OxyLH_2$ presents a shift in the fluorescence wavelength maximum (550 to 540 nm) in aqueous solution when the pH changes from acidic (pH~4.5) to basic (pH~9). The explanation for this phenomenon is that $OxyLH_2$ forms π-π stacking complexes both in the ground and excited states, at basic and acidic pH. However, at different pH values, these complexes adopt a different conformation, which explains the higher emission wavelength maximum at acidic pH. Such π-π stacking complexes are absence in the emissive state of D-LH_2 in any pH range, which is in line with its lack of pH-sensitive fluorescence.

More important is the discovery of how the photoacidity of $OxyLH_2$ can play a role on firefly bioluminescence. Our finding that firefly dioxetanone must be protonated inside firefly luciferase indicates that excited state $OxyLH_2$ must be formed in a neutral

state. However, as the yellow-green-red emission associated with firefly bioluminescence can only be from an anionic light emitter, neutral excited state OxyLH_2 must donate a proton via an ESPT reaction inside luciferase active site. Our calculations demonstrated that OxyLH_2 can indeed donate a proton to AMP via an ESPT reaction, giving origin to the excited state enolate species. Moreover, we have found that this species is indeed sensitive to variations on the electrostatic field, and as the result, its emission spectrum can cover the entire yellow-green-red bioluminescence range. Thus, enolate OxyLH_2 appears to have a significant role on firefly bioluminescence.

7.6. Future Perspectives

The finding that there is no obvious difference between the binding mode of L-AMP and LH_2-AMP to firefly luciferase prevents the decrease of the inhibitory power of the former adenylate by mutating the enzyme, as it would also affect the binding of the latter intermediate. However, impairing the role of L-AMP in the flash profile can still be possible if one “mutates” the structure of D-LH_2 in order to prevent the LH_2-AMP to L-AMP oxidation side-reaction. This can be made by changing the hydrogen atoms present in the thiazole moiety of D-LH_2 (except that bound to the C_4 carbon).

While our results indicate that the carbanion mechanism for the formation of firefly dioxetanone is not feasible, and we do have results that support the radical-based mechanism, we do not have any evidence that excludes the single electron-transfer one. Thus, it is essential to verify if inside the luciferase active site, LH_2-AMP can only formed a radical (compatible only with the radical mechanism) or a carbanion (compatible only with the single electron transfer mechanism).

While our work have already reasonably characterized the decomposition reaction of simple dioxetanones, the next step should be to increase the structural complexity of these molecules, and analyze the effect of electron withdrawing and donating substituents on the decomposition and chemiexcitation steps.

Another development that can be based on our work is the design of new bioluminescent substrates that originate a more red-shifted and intense light emission. This can be achieved by increasing the length of the bond chains that connect the benzothiazole and thiazole moieties of D-LH_2 with C=C double bonds, thereby increasing the π-π conjugation. The elimination of the benzothiazole nitrogen should be investigated in order to prevent the efficient fluorescence quenching process associated with its protonation.

The finding that enolate $OxyLH_2$, and not only the anionic keto species, may have a significant role on firefly bioluminescence, has rekindled the keto-enol conundrum. Thus, the fluorescence emission of $OxyLH_2$ and analogs (restrained to its keto and enol forms) must be measured inside firefly luciferase active site, in order to determine if the resulting ESPT reaction results in a phenolate-keto or in an enolate species.

References

1. E.N. Harvey, *A history of luminescence: from the earliest times until 1900*. Dover Phoenix, New York 1957.
2. C.V Stevani, W.J. Baader, The chemiluminescent peroxyoxalate system, *Quim. Nova* **1999**, *22*, 715-723.
3. M.M. Rauhut, Chemiluminescence from concerted peroxide decomposition reactions, *Acc. Chem. Res.* **1968**, *2*, 80-87.
4. E.N. Harvey, Studies on bioluminescence. VIII: the mechanism of the production of light during the oxidation of *Pyrogallol. J. Biol. Chem.* **1917**, *31*, 311-336.
5. V.R. Viviani, F.G.C. Arnoldi, A.J.S. Neto, T.L. Oehlmeyer, E.J.H. Bechara, Y. Ohmiya, The structural origin and biological function of pH-sensitivity in firefly luciferases, *Photochem. Photobiol. Sci.* **2008**, *7*, 159-169.
6. A.D. Carlson, J. Copeland, Communication in insects. 1. Flash communication in fireflies, *Q. Rev. Biol.* **1985**, *60*, 415-436.
7. R.E. Young, Oceanic Bioluminescence: an overview of general functions, *Bull. Mar. Sci.* **1983**, *33*, 829-845.
8. R. De Cock, E. Matthysen, Aposematism and bioluminescence: experimental evidence from glow-worm larvae (*Coleoptera: Lampyridae*), *Evol. Ecol.* **1999**, *13*, 619-639.
9. T. Wilson, J.W. Hastings, Bioluminescence, *Annu. Rev. Cell. Dev. Biol.* **1998**, *14*, 197-230.
10. F. Fan, K.V. Wood, Bioluminescent assays for high-throughput screening, *Assay Drug Dev. Technol.* **2007**, *5*, 127-136.
11. B.R. Branchini, T.L. Southworth, N.F. Khattak, E. Michelini, A. Roda, Red- and green-emitting firefly luciferase mutants for bioluminescent reporter applications, *Anal. Biochem.* **2005**, *345*, 140-148.
12. A. Roda, M. Guardigli, Analytical chemiluminescence and bioluminescence: latest achievements and new horizons, *Anal. Bioanal. Chem.* **2012**, *402*, 69-76.
13. V.R. Viviani, The origin, diversity, and structure function relationships of insect luciferase, *Cell. Mol. Life Sci.* **2002**, *59*, 1833-1850.

14. Y. Ando, K. Niwa, N. Yamada, T. Enomot, T. Irie, H. Kubota, Y. Ohmiya, H. Akiyama, Firefly bioluminescence quantum yield and colour change by pH-sensitive green emission, *Nat. Photonics* **2008**, *2*, 44-47.
15. K. Niwa, Y. Ichino, S. Kumata, Y. Nakajima, Y. Hiraishi, D. Kato, V.R. Viviani, Y. Ohmiya, Quantum Yields and Kinetics of the Firefly Bioluminescence Reaction of Beetle Luciferases, *Photochem. Photobiol.* **2010**, *86*, 1046-1049.
16. H. Suzuki, Y. Kawarabayasi, J. Kondo, T. Abe, K. Nishikawa, S. Kimura, T. Hashimoto, T. Yamamoto, Structure and regulation of rat long-chain acyl-CoA synthetase, *J. Biol. Chem.* **1990**, *265*, 8681-8685.
17. P.C. Babbitt, G.L. Kenyon, B.M. Martin, H. Charest, M. Sylvestre, J.D. Scholten, K.H. Chang, P.H. Liang, D. Dunaway-Mariano, Ancestry of the 4-chlorobenzoate dehalogenase – analysis of amino-acid-sequence identities among families of acyl-adenyl ligases, enoyl-CoA hydratases isomerases, and acyl-CoA thioesterases, *Biochemistry* **1992**, *31*, 5594-5604.
18. W.D. McElroy, The energy source for bioluminescence in an isolated system, *Proc. Natl. Acad. Sci. U.S.A.* **1947**, *33*, 342-345.
19. W.D. McElroy, Properties of the reaction utilizing adenosinetriphosphate for bioluminescence, *J. Biol. Chem.* **1951**, *191*, 547-557.
20. T. Nakatsu, S. Ichiyama, J. Hiratake, A. Saldanha, N. Kobashi, K. Sakata, H. Kato, Structural basis for the spectral difference in luciferase bioluminescence, *Nature* **2006**, *440*, 372-376.
21. B.R. Branchini, M.H. Murtiashow, R.A. Magyar, S.M. Anderson, The role of lysine 529, a conserved residue of the acyl-adenylate-forming enzyme superfamily, in firefly luciferase, *Biochemistry* **2000**, *39*, 5433-5440.
22. S.M. Marques, J.C.G. Esteves da Silva, Firefly bioluminescence: a mechanistic approach of luciferase catalyzed reactions, *IUBMB Life* **2009**, *61*, 6-17.
23. H. Fraga, J.C.G. Esteves da Silva, R. Fontes, Identification of luciferyl adenylate and luciferyl coenzyme A synthesized by firefly luciferase, *ChemBioChem* **2004**, *5*, 110-115.
24. S. Inouye, Firefly luciferase: an adenylate-forming enzyme for multicatalytic functions, *Cell. Mol. Life Sci.* **2010**, *67*, 387-404.

25. I. Navizet, Y.J. Liu, N. Ferré, D. Roca-Sanjuán, R. Lindh, The Chemistry of bioluminescence: an analysis of chemical functionalities, *ChemPhysChem* **2011**, *12*, 3064-3076.
26. J.A. Sundlov, D.M. Fontaine, T.L. Southworth, B.R. Branchini, A.M. Gulick, Crystal structure of firefly luciferase in a second catalytic conformation supports a domain alternation mechanism, *Biochemistry* **2012**, *51*, 6493-6495.
27. D.M. Mofford, G.R. Reddy, S.C. Miller, Latent luciferase activity in the fruit fly revealed by a synthetic luciferin, *Proc. Natl. Acad. Sci. U.S.A.* **2014**, *111*, 4443-4448.
28. J.M.M. Leitão, J.C.G. Esteves da Silva, Firefly luciferase inhibition, *J. Photochem. Photobiol. B: Biology* **2010**, *101*, 1-8.
29. H. Fraga, D. Fernandes, R. Fontes, J.C.G. Esteves da Silva, Coenzyme A affects firefly luciferase luminescence because it acts as a substrate and not as an allosteric effector, *FEBS J.* **2005**, *272*, 5206-5216.
30. C. Ribeiro, J.C.G. Esteves da Silva, Kinetics of inhibition of firefly luciferase by oxyluciferin and dehydroluciferyl-adenylate, *Photochem. Photobiol. Sci.* **2008**, *7*, 1085-1090.
31. L. Pinto da Silva, J.C.G. Esteves da Silva, Kinetics of inhibition of firefly luciferase by dehydroluciferyl-coenzyme A, dehydroluciferin and l-luciferin, *Photochem. Photobiol. Sci.* **2011**, *10*, 1039-1045.
32. H. Fraga, D. Fernandes, J. Novotny, R. Fontes, J.C.G. Esteves da Silva, Firefly luciferase produces hydrogen peroxide as a coproduct in dehydroluciferyl adenylate formation, *ChemBioChem* **2006**, *7*, 929-935.
33. W.D. McElroy, M. DeLuca, J. Travis, Molecular uniformity in biological catalyses, *Science* **1967**, *156*, 150-160.
34. K.H. Chang, H. Xiang, D. Dunaway-Mariano, Acyl-adenylate motif of the acyl-adenylate/thioester-forming enzyme superfamily: A site-directed mutagenesis study with the Pseudomonas sp. Strain CBS3 4-chlorobenzoate:coenzyme A ligase. *Biochemistry* **1997**, *36*, 15650-15659.
35. Y. Oba, M. Ojika, S. Inouye, Firefly luciferase is a bifunctional enzyme: ATP-dependent monooxygenase and a long chain fatty acyl-CoA synthetase. *FEBS Lett.* **2003**, *540*, 251-254.
36. M. Nakamura, S. Maki, Y. Amano, Y. Ohkita, K. Niwa, T. Hirano, Y. Ohmiya, H. Niwa, Firefly luciferase exhibits bimodal action depending on

the luciferin chirality, *Biochem. Biophys. Res. Commun.* **2005**, *331*, 471-475.

37. S. Hosseinkhani, Molecular enigma of multicolor bioluminescence of firefly luciferase, *Cell. Mol. Life Sci.* **2011**, *68*, 1167-1182.
38. L. Pinto da Silva, J.C.G. Esteves da Silva, Computational studies of the luciferase light-emitting product: oxyluciferin, *J. Chem. Theory Comput.* **2011**, *7*, 809-817.
39. E.H. White, E. Rapaport, H.H. Seliger, T.A. Hopkins, The chemi- and bioluminescence of firefly luciferin: An efficient chemical production of electronically excited states, *Bioorg. Chem.* **1971**, *1*, 92-122.
40. B.R. Branchini, M.H. Murtiashaw, R.A. Magyar, N.C. Portier, M.C. Ruggiero, J.G. Stroh, Yellow-green and red firefly bioluminescence from 5,5-dimethyloxyluciferin, *J. Am. Chem. Soc.* **2002**, *124*, 2112-2113.
41. L. Pinto da Silva, J.C.G. Esteves da Silva, Computational investigation of the effect of pH on the color of firefly bioluminescence by DFT, *ChemPhysChem* **2011**, *12*, 951-960.
42. S.F. Chen, Y.J. Liu, I. Navizet, N. Ferré, W.H. Fang, R. Lindh, Systematic Theoretical Investigation on the Light Emitter of Firefly, *J. Chem. Theory Comput.* **2011**, *7*, 798-803.
43. C.I. Song, Y.M. Rhee, Dynamics on the Electronically Excited State Surface of the Bioluminescent Firefly Luciferase-Oxyluciferin System, *J. Am. Chem. Soc.* **2011**, *133*, 12040-12049.
44. M. Mehrabi, S. Hosseinkhani, S. Ghobadi, Stabilization of firefly luciferase against thermal stress by osmolytes, *Int. J. Biol. Macromol.* **2008**, *43*, 187-191.
45. M.R. Ganjalikhany, B. Ranjar, S. Hosseinkhani, K. Khalifeh, L. Hassani, Roles of trehalose and magnesium sulfate on structural and functional stability of firefly luciferase, *J. Mol. Catal. B Enzym.* **2010**, *62*, 127-132.
46. M. Yousefi-Nejad, S. Hosseinkhani, K. Khajeh, B. Ranjbar, Expression, purification and immobilization of firefly luciferase on alkyl-substituted Sepharose 4B, *Enzyme Microb. Technol.* **2007**, *40*, 740-746.
47. T. Hirano, Y. Hasumi, K. Ohtsuka, S. Maki, H. Niwa, M. Yamaji, D. Hashizume, Spectroscopic Studies of the Light-Color Modulation Mechanism of Firefly (Beetle) Bioluminescence, *J. Am. Chem. Soc.* **2009**, *131*, 2385-2396.

48. I. Navizet, Y.J. Liu, N. Ferré, H.Y. Xiao, W.H. Fang, R. Lindh, Color-Tuning Mechanism of Firefly Investigated by Multi-Configurational Perturbation Method, *J. Am. Chem. Soc.* **2010**, *132*, 706-712.
49. L. Pinto da Silva, J.C.G. Esteves da Silva, Theoretical modulation of the color of light emitted by firefly oxyluciferin, *J. Comput. Chem.* **2011**, *32*, 2654-2663.
50. L. Pinto da Silva, J.C.G. Esteves da Silva, Study on the effects of intermolecular interactions on firefly multicolor bioluminescence, *ChemPhysChem* **2011**, *12*, 3002-3008.
51. J.M. Hawronskyj, J. Holah, ATP: A universal hygiene monitor, *Trends Food Sci. Tech.* **1997**, *8*, 79-84.
52. S.M. Marques, J.C.G. Esteves da Silva, An optimized luciferase bioluminescent assay for coenzyme A, *Anal. Bioanal. Chem.* **2008**, *391*, 2161-2168.
53. P. Nyrén, A. Lundin, Enzymatic method for continuous monitoring of inorganic pyrophosphate synthesis, *Anal. Biochem.* **1985**, *151*, 504-509.
54. V. Jansson, K. Jansson, An enzymatic cycling assay for adenosine 5'-monophosphate using adenylate kinase, nucleoside-diphosphate kinase, and firefly luciferase, *Anal. Biochem.* **2003**, *321*, 263-265.
55. N. Tai, J.C. Schmitz, T.M. Chen, M.B. O'Neill, E. Chu, Identification of a cis-acting element of human dihydrofolate reductase mRNA, *Biochem. Biophys. Res. Commun.* **2008**, *369*, 795-800.
56. K. Hilpert, R.E.W. Hancock, Use of luminescent bacteria for rapid screening and characterization for short cationic antimicrobial peptides synthesized on cellulose using peptide array technology, *Nat. Protocol* **2007**, *2*, 1652-1660.
57. K. Hirokawa, N. Kajiyama, S. Muarakami, Improved practiral usefulness of firefly luciferase gene chimerization and random mutagenesis, *Biochim. Biophys. Acta Protein Struct. Mol. Enzymol.* **2002**, *1597*, 271-279.
58. H. Fugii, K. Noda, Y. Asami, A. Kuroda, M. Sakata, A. Tokida, Increase in Bioluminescence intensity of firefly luciferase using genetic modification, *Anal. Biochem.* **2007**, *366*, 131-136.
59. N.N. Ugarova, L.Y. Brovko, Protein structure and bioluminescent spectra for firefly bioluminescence, *Luminescence* **2002**, *17*, 321-330.

60. H. Takakura, R. Kojima, Y. Urano, T. Terai, K. Hanaoka, T. Nagano, Aminoluciferins as functional bioluminogenic substrates of firefly luciferase, *Chem. Asian J.* **2011**, *6*, 1800-1810.
61. G.R. Reddy, W.C. Thompson, S.C. Miller, Robust light emission from cyclic alkylaminoluciferin substrates for firefly luciferase, *J. Am. Chem. Soc.* **2010**, *132*, 13586-13587.